Plasma Membrane-derived Vesicles: Composition and Function

Presented by

Ephraim Abrokwa Ansa-Addo

Thesis submitted in partial fulfilment of the requirement

for the degree of

DOCTOR OF PHILOSOPHY (Ph.D)

Director of Studies: Prof. Jameel M. Inal

Second Supervisor: Dr. Christopher Bax

Cellular and Molecular Immunology Research Centre (CMIRC)

School of Human Sciences, Faculty of Life Sciences

London Metropolitan University

26th November 2010

"The heights by which great men reached and kept were not attained by a sudden flight, but they, while their companions slept, they toiled upwards in the night."

Dedicated to my dearest grandfather – The late Mr Alfred Christian Kusi

Source: Henry Wadsworth Longfellow

"Every time we feel the passion of our visions and dreams, we awaken the creative spirit within us, and express the beauty and power of our true selves in the world."

Dedicated to my dad, the late Rev. Dr. Samuel F. Ansa-Addo

Source: Eleanor Roosevelt

PAGE NUMBERING AS ORIGINAL

CONTENTS

Acknowledgements

I start by saying thanks to God Almighty, for it would not be possible without His love and mercy. A special thanks to Prof. Jameel Inal, for his continuous support and for how he guided me throughout my entire studies. I should say that I am extremely fortunate to have had Prof Inal as my director of studies, because his style of supervision, his enthusiasm, intelligence, availability and demand for perfection, and most importantly the patience to listen to his students makes him a gold standard research advisor to have. The training and guidance I have received from Prof Inal will surely stand me in good stead in the future, for I have not only improved on skills including observation, written and verbal communication, and a keen eye for detail, but also I have learned to appreciate my own efforts without the need to be arrogant. Put simply, I have become a better person and acquired skills to potentially become a successful scientist. Special thanks to London Metropolitan University, for the privilege and opportunity to undertake my studies in such an institution.

I'll thank my family, my mum, Mrs. Mercy Ansa-Addo and siblings (Mavis, Rhodaline and family, Victoria and Fred, Stephen and Lucy) and Rosie Clegg for your continuous support. You were all present when I needed your support and did not disappoint. Mum, Vicky and Fred, thanks for ensuring that I always had plenty of food and money to last me every week. To all the members of CMIRC including, Samuel Antwi-Baffour, Dan Stratton, Sharad kholia, Samira Jorfi and Laura Towns. You are all wonderful individuals and have the potential to be successful scientists. Samira, you have greatly impressed me with you work ethic and I urge you to continue in this manner. I thank our collaborators at the Instituto Oswaldo Cruz, Rio, Brazil for the joy in working together. Working together with Dr. Igor Cestari and

Prof. Marcel Ramirez was a productive period full of interactions and intellectual growth. Big thanks to Dr. Sigrun Lange for the kind gifts of antibodies or chemical reagents, of which we may have run out of stock or simply did not have in our laboratory. I also thank Maria McCrossan of the London School of Hygiene and Tropical Medicine for the service provided to acquire images with the transmission electron microscope. Thanks to all the members of MRU, especially to Amara and Sumeet. We have been together from the beginning and it would be great to complete together. Amara you are like my sister in the laboratory, the one person I opened up to when I was down. Sumeet I will miss our discussions and your assertiveness, and congratulations with your baby.

To the members of IBCHN, especially to Katia, you are a star and I thank you for all the reagents and consumables, which you provided me with every time I was in need. Apart from that, our lunchtime discussions and daily laughs were very refreshing, and also good luck with your thesis and with the future. Ora Msika, I will probably be in trouble if your name is not mentioned in this thesis, but I would, because you deserve to be acknowledged. Thank you for your helpful comments during our discussions and for help with materials. You have been a breath of fresh air since you commenced your PhD studies. Your energy and enthusiasm in the laboratory is always nice to experience, plus you're are a great companion and I am sure that we'll keep in touch. To the members of IHRP, Dr. Ed Welbeck, Dr. Muyiwa, Yichen, Xaiobei, Kevin, you guys are brilliant and good luck for the future.

My special thanks go to all the technical staff both past and present. Each one of you played a vital role in making my studies successful. So thanks to Dr. Nicky

Barber, Vicky, Eric, Dr. Brigette, Sophie, Ruth, Hannah, Pramila, Alan, Dr. Phil Bailey and Vidler, John Morgan and Crowder, not forgetting you, Photis. Thank you all very much for your help, it was much appreciated. I cannot forget all the members of staff in the Faculty of Life Sciences who kept me focussed all the time with their encouragements. So thank you to Dr. Una Fairbrother, Sheelagh Heugh, Dr. Kenneth White, Dr. Chris Palmer and Dr. Nick Chatterton. Thanks also to the security staff who allowed me on various occasions to stay late so that I could complete my experiments. Finally, a special thanks to all members and worshippers at High Cross United Reformed Church. To Rev. Francis and Sandra Ackroyd, my family and I cannot thank you enough for the way you have supported us throughout. For in both good and bad times, you were there to lend your support, which as you are aware, is greatly appreciated. THANKS TO YOU ALL!!!

Abstract

Plasma membrane-derived vesicles (PMVs) are small, intact, membrane vesicles, which are released by most cells upon activation with various extracellular stimuli. This study identified that procedures used in the isolation of PMVs could be further improved by first sonicating (sonicating water-bath) samples prior to isolation of PMVs. Following water-sonication, centrifugation of cell-debris-free supernatants at 25,000 *g* for 2 h, yielded mostly PMVs with minimal contamination with exosomes.

Agents (Histamine, PMA, ATRA) currently used in differentiation therapy for the treatment of acute myelocytic leukaemia (AML), are reported here to induce the release of PMVs from various cells and to halt the overproliferation of THP-1 promonocytes *in vitro*. Further investigations with the TGF-β receptor antagonist, SB-431542, showed that this inhibition was due to TGF-β1 present on PMVs, which initiates TGF-β signalling.

This thesis also identified a novel host cell entry strategy involving PMVs, employed by *T. cruzi* during infection. *T. cruzi* metacyclic trypomastigotes trigger the release of PMVs through integrins, lipid raft microdomains and Ca^{2+} channels such as stretch-activated channels (SAC) from several cell types. Released PMVs bound to the surface of *T. cruzi* and abolished its complement-mediated lysis by inhibiting activation of the C3 convertase. These PMVs also carried TGF-β, which enhanced mammalian cell invasion by *T. cruzi* metacyclics. Furthermore, *T. cruzi*-elicited release of PMVs, results in damage to the host plasma membrane. Parasites take advantage of the resulting membrane breach to enter cells before lysosomal membrane repair. Together, these results postulate important functions for PMVs in both mammalian cells and pathogens.

Original Publications

This report is based on the following published articles, abstracts and public presentations. In addition some unpublished data are presented.

I. **Ansa-Addo, E.A., Cestari, I., Ramirez, M.I. and Inal, J.M. (2010)** *Trypanosoma cruzi* utilisation of host cell vesicle release aids invasion. *Submitted to Science.*

II. **Ansa-Addo, E.A., Lange, S., McCrossan, M.V and Inal, J.M. (2010)** Human Plasma Membrane-derived Vesicles halt proliferation and induce differentiation of THP-1 acute monocytic leukaemia cells. *Journal of Immunology* **185,** 5236-46.

III. **Cestari, I., Ansa-Addo, E.A., Inal, J.M and Ramirez, M.I. (2010)** A novel mechanism of immune evasion by *Trypanosoma cruzi* mediated by host plasma membrane-derived vesicles. *Submitted to Nat. Commun.*

IV. **Hind, E., Heugh, S., Ansa-Addo, E.A., Antwi-Bafour, S., Lange, S and Inal J.M. (2010)** Red cell PMVs, Plasma Membrane-derived Vesicles calling out for standards. *Biochem. Biophys. Res. Commun.* **399,** 465-9.

V. **Antwi-Baffour, S., Kholia, S., Aryee, Y.K., Ansa-Addo, E.A. Stratton, D., Lange, S and Inal J.M. (2010)** Human Plasma Membrane-derived Vesicles inhibit the phagocytosis of apoptotic cells – possible role in SLE. *Biochem. Biophys. Res. Commun.* **398,** 278-83.

VI. **Evans-Osses, I., Ansa-Addo, E.A., Inal, J.M and Ramirez, M.I. (2010)** Involvement of lectin pathway activation in the complement killing of *Giardia intestinalis. Biochem. Biophys. Res. Commun.* **395,** 382-6.

Published Abstracts

VII. **Ansa-Addo, E.A and Inal, J.M. (2010)** *T. cruzi* interference with host cell membrane integrity triggers the release of PMVs: A mechanism for entry into mammalian cells. *J. Immunol.* **184,** 137.1

VIII. **Ansa-Addo, E.A and Inal, J.M. (2010)** Plasma membrane-derived vesicles promote adhesion and differentiation of THP-1 monocytes in a TGF-β dependent manner. *J. Immunol.***184,** 35.15

IX. **Jorfi, S., Ansa-Addo, E.A., El dine, S and Inal, J.M. (2010)** Plasma membrane-derived Microvesicles (PMVs) released from apoptotic Jurkat cells express upregulated surface Fas and induce apoptosis in recipient viable cells. *J. Immunol.***184,** 89.45

X. **Ansa-Addo, E.A., Cestari, I.d.S., Pathak, P., Ramirez, M.I and Inal, J.M. (2009)** Monocytic THP-1 cells stimulated by normal human serum (NHS) release cytokine-bearing plasma membrane-derived vesicles (PMVs), and can be inhibited by methyl-beta-cyclodextrin, calpeptin and Rho-kinase inhibitor, Y-27632. *J. Immunol.* **182,** 98.27.

XI. **Cestari, I.d.S., Ansa-Addo, E.A., Pathak, P., Ramirez, M.I and Inal, J.M. (2008)** The intracellular *Trypanosoma cruzi* induces the release from monocytes of plasma membrane-derived microvesicles, which protect the parasite from host complement. *Mol. Immunol.* **45,** 4173.

Public Presentations

XII. **Ansa-Addo, E.A and Inal, J.M (2010)** *T. cruzi* interference with host cell membrane integrity, triggers the release of PMVs: A mechanism for entry into mammalian cells. Presented at the 97th Annual Meeting of the American Association of Immunologists (AAI) from 7-11th May 2010.

XIII. **Ansa-Addo, E.A and Inal, J.M (2010)** *T. cruzi* interference with host cell membrane integrity, triggers the release of PMVs: Another mechanism for entry into mammalian cells. Presented in the House of Parliament as part of the 2010 SET for Britain competition on 8th March 2010.

XIV. **Ansa-Addo, E.A and Inal, J.M (2010)** *Trypanosoma cruzi* exploits host cell repair mechanisms to invade. Presented at the 2nd Postgraduate Research Students Symposium held at London Metropolitan University on 5th February 2010 - awarded first prize for best presentation.

XV. **Cestari, I.d.S, Ansa-Addo, E.A., Inal, J.M and Ramirez, M.I. (2008)** *Trypanosoma cruzi* release plasma membrane-derived vesicles (PMVs) to avoid lysis by the complement. Presented at the 24th Annual Meeting of the Brazilian Society of Parasitology/35th Annual Meeting on Chagas disease research from 27-29th October 2008.

XVI. **Ansa-Addo, E.A and Inal, J.M (2008)** Plasma Membrane Vesicles inhibit proliferation of THP-1 cells and induce their terminal differentiation into macrophages. Presented at the 1st Postgraduate Research Students Symposium held at London Metropolitan University on 3rd July 2008 - awarded first prize for best presentation.

Abbreviations

ADP	Adenosine diphosphate
AEBSF	4-(2-Aminoethyl) benzenesulfonyl fluoride
AML	Acute myelocytic leukaemia
An V	Annexin V
APL	Acute promonocytic leukaemia
ATRA	all-*trans* retinoic acid
BDMA	Benzyl dimethylamine
BSA	Bovine serum albumin
C5a	Complement 5a protein
Calp	Calpeptin
$[Ca^{2+}]_i$	Intracellular calcium
CCL-1	Chemokine (C-C motif) ligand-1
CCR5	Chemokine receptor 5
CD4	Cluster of differentiation 4
Chlor	Chlorpromazine
CM	Cerebral malaria
ConA	Concanavalin A
CPT	Camptothecin
CXCR4	Chemokine receptor 4
DAF	Decay accelerating factor
DAPI	4',6-diamidino-2-phenylindole
DDSA	Dodecenyl succinic anhydride
DEAE-cellulose	Diethyaminoethyl cellulose
DMSO	Dimethyl sulfoxide
DNA	Deoxyribonucleic acid
DTT	Dithio threitol
ECM	Extracellular matrix
ECS	Extracellular space
EGTA	Ethylene glycol-bis (2-aminoethylether) N,N,N',N'-tetraacetic acid
ELISA	Enzyme Linked immunosorbent assay
ER	Endoplasmic reticulum
Exos	Exosomes
FACS	Fluorescent activated cell sorter
FasL	Fas ligand
FasR	Fas receptor
FGF-1	Fibroblast growth factor -1
Fili	Filipin
fmk	Fluoromethylketone
FSC	Forward scatter
g	G-force
Gal-3	Galectin-3
G-CSF	Granulocyte - colony stimulating factor
GsMTx-4	Grammostola spatulata mechanotoxin 4
HIV-1	Human immunodeficiency virus 1
Hsp	Heat-shock protein
HUVECs	Human umbilical vein endothelial cells
IL-1α	Interleukin-1 alpha
IL-1β	Interleukin-1 beta

IL-12	Interleukin 12
IL-13	Interleukin 13
IL-17E	Interleukin 17 E
ILV	Intraluminal vesicles
LAMP-1	Lysosome associated membrane protein 1
LIT	Liver infusion broth
L-tropic	Lymphotropic
MAC	Membrane attack complex
MALDI-TOF	Matrix-assisted laser desorption/ionization – Time of Flight
MAT	Myosin adenosine triphosphate
M-βCD	Methyl-β-cyclodextrin
MHC	Major histocompatibility complex
MIF	Macrophage inhibitory factor
MNA	Methyl nadic anhydride
MPs	Microparticles
mRNA	messenger Ribonucleic acid
MSC	Mechanosensitive channels
M-tropic	Macrophage-tropic
MVs	Microvesicles
MVBs	Multivesicular bodies
NHS	Normal human serum
NI	Non-Induced
PB	Peripheral blood
PBB	Permeabilisation buffer
PBMCs	Peripheral blood mononuclear cells
PBS	Phosphate buffered saline
PBS-T	Phosphate buffered saline – Tween 20
PC	Phosphatidylcholine
PE	Phosphatidylethanolamine
PEAM	Platelet expressed adhesion molecules
PFA	Paraformaldehyde
PI	Propidium iodide
PI3K	Phosphatidylinositol-3-kinases
PL	Phospholipid
PM	Plasma membrane
PMA	Phorbol-12-myristate-13-acetate
PMN	Polymorphonuclear neutrophils
PMSF	Phenylmethanesulfonyl Fluoride
PMVs	Plasma membrane-derived vesicles
PMP	Platelet microparticles
PPV	Parasitophorous vacuole
PS	Phosphatidylserine
PSGL-1	P-selectin glycoprotein ligand-1
RANTES	Regulated on activation normal T cell expressed and secreted
RBCs	Red Blood Cells
RGD	Arginine-Glycine-Aspartate
RNA	Ribonucleic acid
RT	Room temperature
SAC	Stretch activated calcium channel
SD	Standard deviation
SDS	Sodium dodecyl sulphate
SSC	Side scatter
SM	Sphingomyelin

TAU	Triatomine urine
TEMED	N, N, N-tetramethylethylenediamine
TF	Tissue factor
TFG-β1	Transforming growth factor β 1
TfR	Transferrin receptor
TTP	Thrombocytopenic purpura
TPA	Tissue plasminogen activator
v/v	Volume per volume
w/v	Weight per volume
Y-27	Y-27632
Z-DEVD-fmk	Benzyloxycarbonyl-Asp-Glu-Val-Asp (OMe) fluoromethylketone
Z-VAD-fmk	Benzyloxycarbonyl-Val-Ala-Asp (OMe) fluoromethylketone

1. Introduction

1.1 General overview of microvesicles

Microvesiculation is a ubiquitous cellular mechanism, which occurs as a result of exocytosis or direct release of vesicles from the cell surface membrane [1]. At every stage in the growth of multicellular organisms, homeostasis results in a subtle balance between proliferation and degeneration of the cell. The cells undergo differentiation, expansion, carry out specialised functions, and then undergo programmed cell death. Lastly they are cleared by phagocytosis [2]. At every stage, cells are challenged by various factors such as chemical (including apoptosis) or physical stress conditions, which lead to the release of submicron fragments termed microvesicles (MVs) from the surface of the plasma membrane. These are usually referred to as microparticles (MPs, between 0.1-1 μm) and those released through a process of exocytosis, termed exosomes (50-100 nm) [3]. MVs released from healthy viable cells are normally smaller in size compared to apoptotic bodies or blebs, which are derived from damaged cells and unlike them, do not contain damaged DNA. Released MVs contain numerous proteins and lipids characteristic of their parental cell and consist of membrane and cytoplasmic constituents [3;4].

As membranes of MVs engulf some cytoplasm during membrane shedding, others have reported the possibility that they also contain proteins derived from the parent cell cytoplasm as well as their mRNA [5,6] . Hitherto, MVs have been suggested to 'hijack' infectious particles (e.g., human immunodeficiency virus (HIV) or prions) from the cytoplasm [7-9] and even whole intact organelles such as mitochondria [10]. Microvesicles are released from many different cell types, but they all differ slightly in their composition, mainly depending on status and cell origin. This had led to the plethora of terms used to describe microvesicles in a host of reports. For example,

membrane MVs derived from activated blood platelets and other cell-types such as monocytes are generally referred to as microparticles (MPs) [11]. MVs released during tissue development from the basolateral membrane of cells that synthesize morphogens (and are carriers for these molecules) are called argosomes [12]. Membrane MVs released by activated human polymorphonuclear neutrophils (PMN) are described in the literature as ectosomes [13]. In this report microparticles and not exosomes will be referred to as Plasma Membrane-derived Vesicles (PMVs).

1.2. Plasma Membrane-derived Vesicles - what are they?

1.2.1. Definition and background

Briefly, PMVs can be defined as a heterogeneous population of small intact membrane vesicles derived from the cell surface membrane. They are involved in intercellular communication during inflammation and are subcellular elements for cell signalling [14;15]. These vesicles are released by virtually all types of cells upon activation and apoptosis and during growth, into the extracellular microenvironment (*in vivo*) or into culture supernatants (*in vitro*). However, depending upon origin, they may differ in size, biochemical composition and biological effects. During the process of PMV release, normal cell phospholipid (PL) asymmetry is lost and this leads to increased exposure of phosphatidylserine (PS^+) on the outer leaflet of the PMV membrane. This phenomenon is detected through binding assays with annexin V-FITC, a widely accepted method of identifying and quantifying PMVs by flow cytometry. Studies based on PMVs derived from platelets [16], monocytes [17] and endothelial cells [18] have been well documented, but more recently, extensive studies have been carried out on erythrocytes [19], neutrophils [20], granulocytes [21] and adipocytes [22].

PMVs were first reported in 1946 when Chargaff *et al.* recognised that a precipitable factor that accelerates thrombin generation, was present in platelet-free plasma [23] . However, it was not until 1967 that lipid-rich platelet cell membrane-derived fragments in platelet-free plasma were obtained by ultracentrifugation. Moreover, it was observed that the fragments were capable of generating thrombin. In the report, a linear relationship was shown between the amounts of platelet microparticles (PMP), referred to as "platelet dust", and the platelet count present in the original blood sample. It was also observed that in polycythaemic patients with high platelet counts, there were higher levels of PMP, but low levels in thrombocytopenic patients [24]. Even though the first reports on PMVs were based on PMP and suggested roles in blood clotting, their ubiquity, as proved in more recent findings, suggests a more general role in various aspects in cell regulation.

1.3. Mechanism of release

1.3.1. Induction of PMV release

The exact mechanism which results in membrane vesiculation has not yet been elucidated. However, many reports have attributed this to multiple mechanisms, which include both physiological and exogenous agents. It is important to realise that PMVs, otherwise known as MPs, are not artefacts as sometimes thought or the result of a random process, such as the disintegration of the plasma membrane of dying necrotic cells. Instead, it is an extremely well regulated process associated with different cells upon stimulation.

Exogenous stimuli such as epinephrine, adenosine diphosphate (ADP), collagen, thrombin with collagen, and calcium ionophore (A23187) have all been reported to

stimulate the release of PMVs [25]. In addition to these, sublytic concentrations of the complement membrane attack complex (C5b-9) and mechanical factors such as sheer stress are essential factors, which lead to the release of PMVs from various cells. In 2002, it was reported that stimulation of human umbilical vein endothelial cells (HUVECs) with various agents including phorbol myristate acetate (PMA), thrombin or tissue plasminogen activator (TPA), did not result in significant release of PS^+PMVs despite changes in cell morphology after activation [26]. However, an earlier study revealed that HUVECs release PS^+PMVs only after stimulation with the lytic complement complex C5b-9, a physiological agonist [27]. Others later reported that these cells release PS^+PMVs after stimulation with high concentrations of A23187 (10 μM) [28].

1.3.2 Biochemical basis of PMV formation: control of membrane phospholipid asymmetry

Cell membrane phospholipids are highly specific in terms of their composition and distribution in various eukaryotic cells. Most eukaryotic cells under normal physiological conditions have an asymmetric distribution of membrane phospholipids. The choline phospholipids, phosphatidylcholine (PC) and sphingomyelin (SM) are mainly localised on the outer leaflet of the plasma membrane, whereas the amino phospholipids, phosphatidylserine (PS) and phosphatidyl-ethanolamine (PE) are located in the inner layer. The perpetuation of this membrane asymmetry is very important and so it is regulated through a convoluted balance of transmembrane enzymes. The classic theory of plasma membrane blebbing and release of PMVs is based on transverse migration of

anionic phospholids such as PS from the inner leaflet to the outer leaflet of the plasma membrane [14;29].

Various cellular events such as apoptosis, necrosis and cell activation may lead to loss of cell asymmetry and exposure of PS on the outer cell leaflet. In blood platelets, PS exposure on the outer layer of the cell membrane may in turn result in a prothrombotic state [30;31]; however, PS exposure also promotes clearance of apoptotic cells and cell fragments by macrophages [32;33].

1.3.3 Enzymes involved in the production of PMVs

There are five main enzymes involved in regulation of the asymmetry of cell membrane phospholipids and implicated in the release of plasma membrane-derived vesicles: gelsolin (present only in platelets), aminophospholipid translocase, floppase, scramblase and calpain (**Fig. 1**) [14]. These enzymes are said to maintain a dynamic asymmetric membrane steady state and in doing this they allow movement of choline phospholipids to the outer leaflet of the cell membrane, while at the same time redirecting amino phospholipids to the inner leaflet. Increases in intracellular calcium levels cause irregularities in the steady state, which result in calpain-mediated rearrangement of the actin cytoskeleton [34], exposure of PS on the outer layer of the cell membrane [35], and eventual exposure on the outer membrane of released PMVs [36].

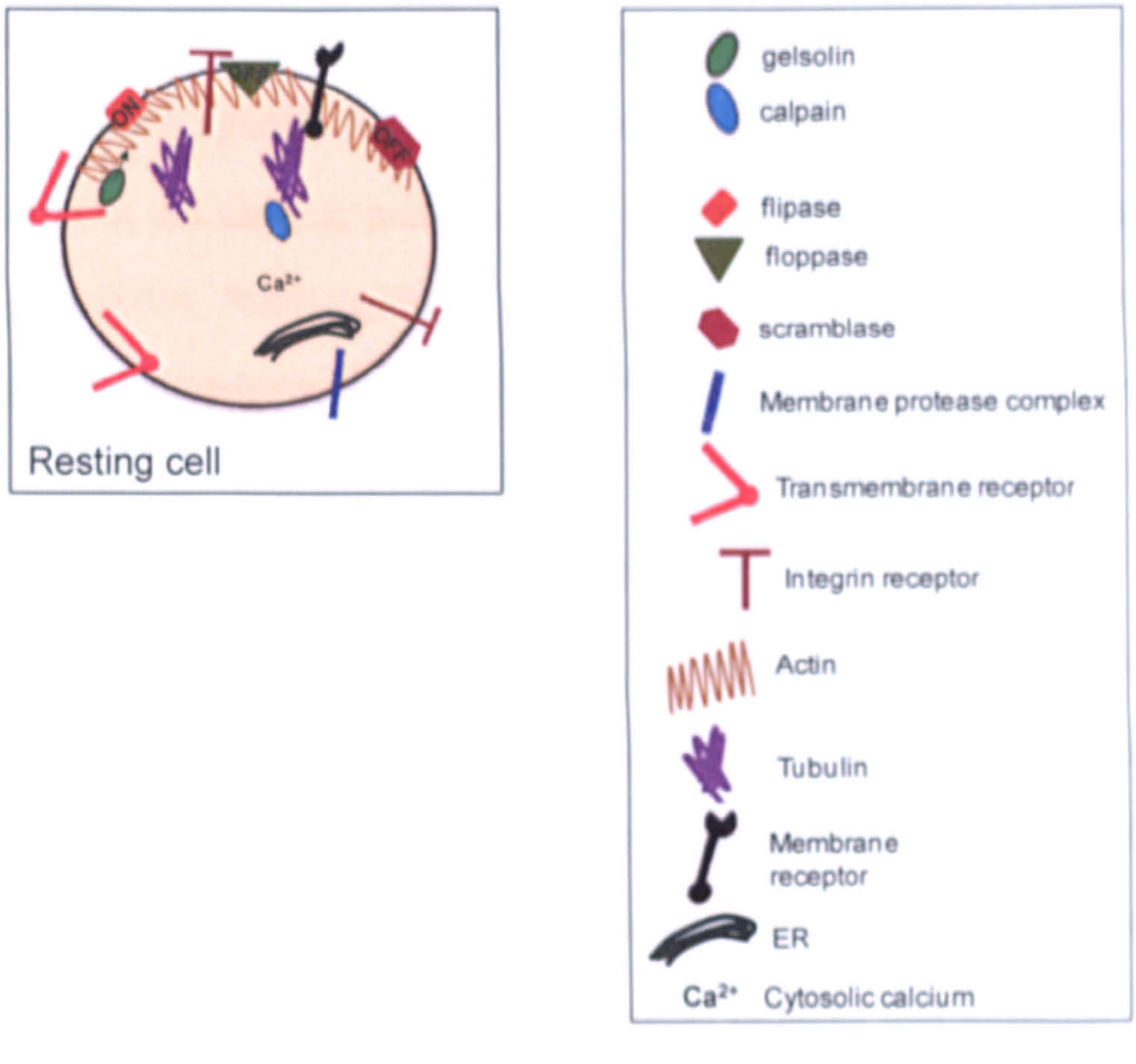

Figure 1 Schematic representation of a resting cell cytoskeleton

Calcium is stored in the endoplasmic reticulum (ER). When the cell is in the resting state, the enzyme, scramblase is inactive; Flipase, an ATP dependent translocases, is in the active state and transports PS and PE from outer leaflet of the PM to the inner layer, maintaining PS and PE inside. Floppase, also an ATP-dependent enzyme that contributes to maintaining the physiological asymmetry of the membrane is inactive under resting conditions.

1.3.3.1 Gelsolin

Increase in the concentration of intracellular calcium results in activation of gelsolin, an enzyme specific for PMV production in platelets (**Fig. 2A**). It functions by removing the capping proteins found at the ends of actin filaments of the platelet cytoskeleton. Rearrangement of the actin filament takes place and this allows cellular contractions to proceed once the capping proteins have been removed [37].

1.3.3.2 Aminophospholipid translocase

Under normal physiological conditions an inward-directed pump, aminophospholipid translocase or flipase [Mg^{2+}-and adenosine triphosphate (ATP)-dependent enzyme] is activated and controls the strict translocation of PS and PE against an electrochemical gradient, from the outer leaflet to the inner leaflet of the cell membrane. Each PS molecule transported requires one molecule of ATP, but the action of the flipase is inhibited by increases in intracellular calcium concentrations [38].

1.3.3.3 Floppase

Unlike flipase, floppase is less dependent on Mg^{2+}/ATP and is responsible for the transport of choline phospholipids (PC and sphingomyelin) from the inner layer to the outer layer of the plasma membrane; it is also activated by increases in intracellular calcium. Thus, the membrane asymmetry in resting cells is controlled by the cooperative action between flipase and floppase.

1.3.3.4 Scramblase

Increased intracellular calcium also activates the enzyme scramblase, which leads to collapse of the lipid asymmetry, and a free movement of phospholipids between both inner and outer leaflets of the cell membrane (**Fig. 2B**). Disruption of cell membrane asymmetry severely affects cell shape and the mechanical stability of the membrane. This results in a stable expression of PS on the outer leaflet followed by budding and release of PS^{+}PMVs [39;40] (**Fig. 2C**). Even though a high concentration of scramblase is present in platelet plasma membrane, an inherited defect occurs in Scott's syndrome (a rare autosomal recessive disorder of platelet coagulant activity), which provides a dramatic illustration of the biochemical processes underlying the physiological production of PMVs. The underlying defect is an inability to generate normal activity of the enzyme scramblase. This leads to a reduced expression of phosphatidylserine, and so also a reduction in the secretion of plasma membrane-derived vesicles. A defective scramblase means the ability to activate factor X and prothrombin is impaired; thus the disorder is associated with severe bleeding [41;42] .

1.3.3.5 Calpain

Influx of Ca^{2+} from extracellular sources and Ca^{2+} released by the endoplasmic reticulum (ER), causes activation of the enzyme, calpain, a cysteine proteinase of the papainase family (**Fig. 2A**). Calpain has several functions during the production of PMVs including cleavage of cytoskeletal actin filaments. This action leads to reorganization of the cytoskeleton, which facilitates shedding of PMVs. Other functions include activating apoptosis through procaspase 3 and BclxL. To confirm involvement of calpain in microvesicle release, calpeptin, a known inhibitor of calpain was shown to inhibit the release of PMVs from platelets [43]. In thrombotic

thrombocytopenic purpura (TTP) the presence of circulating calpain activity in the plasma is strongly associated with the release of platelet PMVs [44;45].

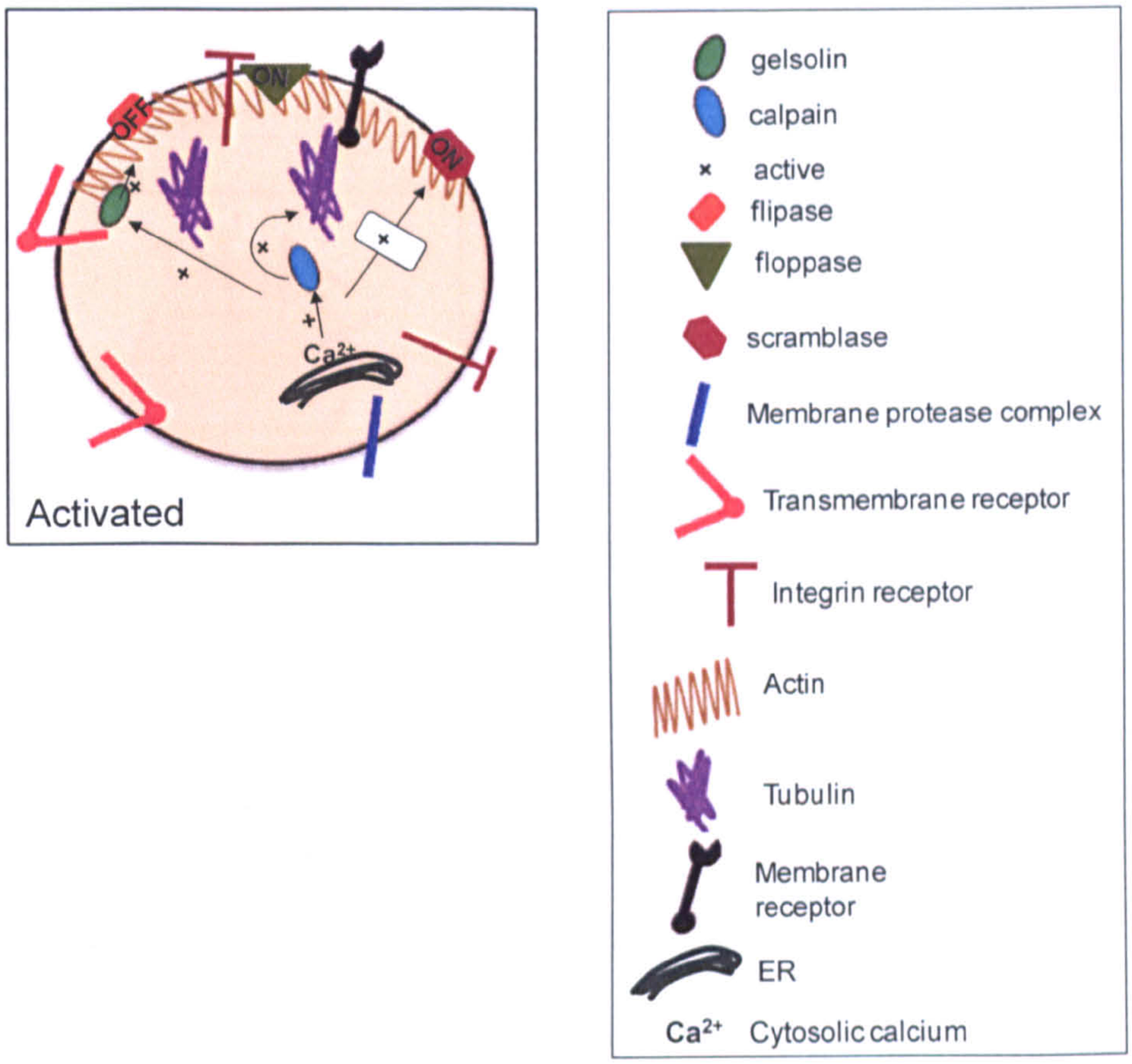

Figure 2A Initial responses following cell activation.

Increase in cytosolic calcium ions leads to the activation of calpain and gelsolin. Calpain activates another enzyme tubulin, and gelsolin cleaves the actin capping proteins leading to rearrangement of the long actin filaments. The increased cytoplasmic Ca^{2+} also leads to activation of scramblase and floppase and deactivation of flipase, by which point the asymmetry of phospholipids starts to become compromised.

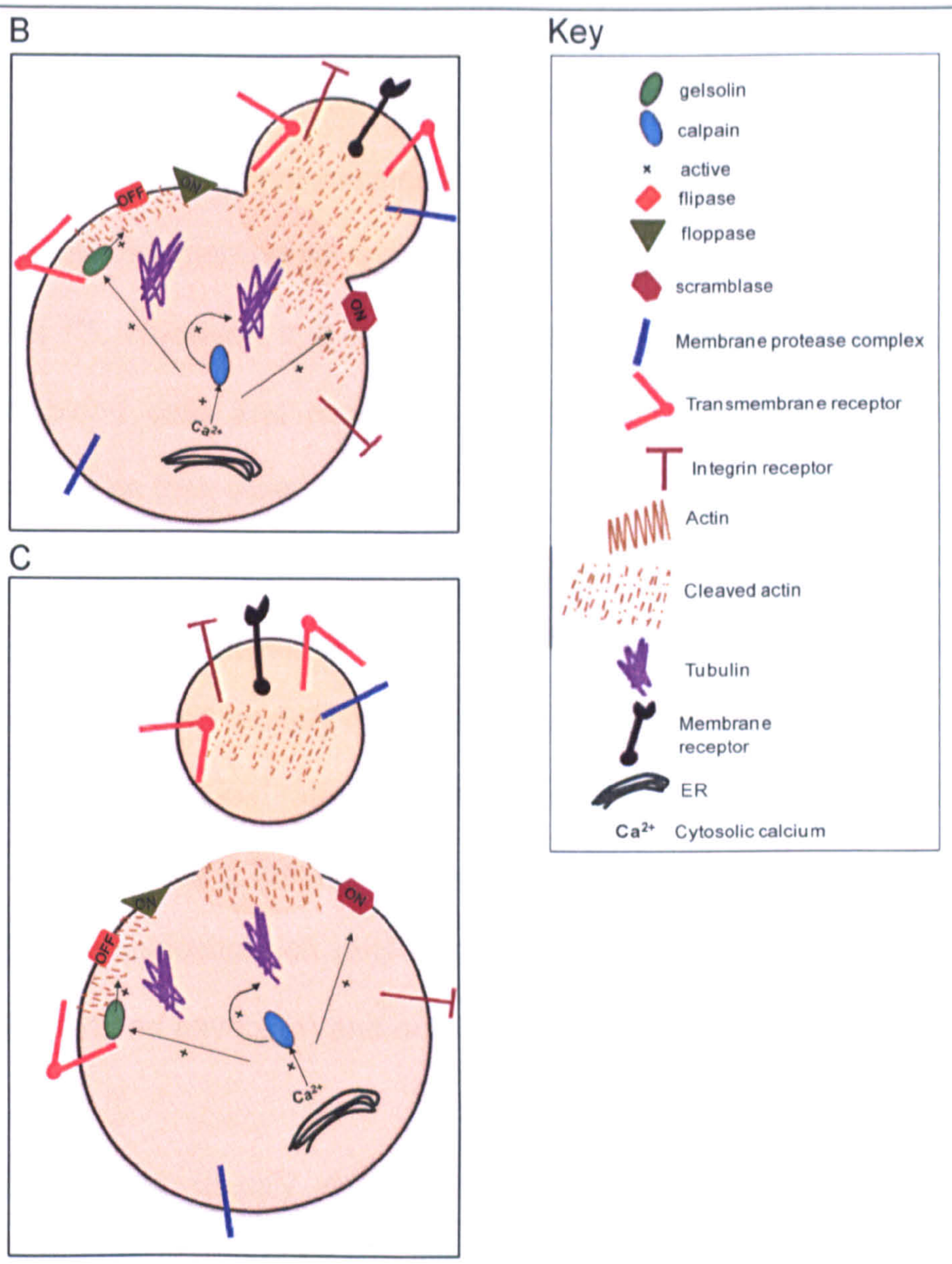

Figure 2 B and C. Activation of cell leads to cytoskeleton disruption and subsequent release of PMVs

Cleavage of the actin cytoskeleton leads to loss of cell asymmetry, followed by outward budding of the microvesicles from the surface membrane. Depending on the stimulus, specific proteins are localised within or on the surface of the budding vesicles before complete detachment from the original cell (B). Once released, PMVs exhibit protein profiling similar to the parent cell and some cleaved actin is inside the vesicles. The plasma membrane of the released vesicle also inverts so that PS normally expressed on the inner leaflet of the membrane would, in the PMVs be exposed on the outer leaflet (C).

1.3.3.6 Lipid rafts

It was first thought that translocation of PS from the inner leaflet to the outer leaflet of the plasma membrane represented the only mechanism leading to the release of PMVs [46]. However, it is now known that a significant number of PMVs released from blood cells and especially endothelial cells does not have accessible PS exposure on their outer leaflet [47;48].

Lipid rafts are specialised membrane domains enriched in certain lipid cholesterols and proteins and crudely regarded as an ordered region floating in a sea of poorly arranged lipids. Lipid rafts exist as three types: caveolae - specialised lipid rafts that carry out signalling functions, (glyco) sphingolipid-enriched membranes (GEM), and polyphosphoinositol rich rafts (PIP_2). They can also be subdivided into inside rafts (PIP_2 rich and caveolae) and outside rafts (GEM) [49].

Phospholipids usually contain unsaturated acyl chains whereas sphingolipids contain long, saturated acyl chains. Phospholipids tend to be loosely packaged in bilayers, because of their kinked acyl chains, which form liquid-disordered membranes that enable rapid lateral and rotational lipid movement. By contrast, sphingolipids are packed tightly into a bilayer, forming a quasi-gel phase, in which lipids have very little mobility. Cholesterol preferentially partitions with sphingolipid bilayers, and occupies the space between the acyl chains. The quasi-gel phase consequently alters to a much more fluid liquid-ordered conformation that floats in the liquid-disordered phospholipid phase, to form 'rafts'. The outer-leaflets of membrane rafts are connected to the inner leaflets, which are also enriched in cholesterol and phospholipids. Cholesterol plays an essential role for the stability of

lipid rafts, because rafts have specific interactions with the cytoskeleton and participate in constitutive signalling [50].

Recently, Simak and Gelderman (2006) hypothesized that lipid rafts may be shed in the form of PMVs from the plasma membrane. This was due to lipid raft observations in several PMV-like phenotypes released from endothelial cells [51] and other types of cells after activation with different stimuli [52]. The notion that PMVs are released from lipid raft domains was further enhanced in a report, which showed that clustering of platelet endothelial cell adhesion molecule-1 (PECAM-1, CD31) preceded the shedding of PMVs enriched in this molecule on the cell surface [53].

Initial characterisation of raft components took advantage of their insolubility in certain non-ionic detergents. This enabled their separation from glycerolipid-rich membranes. Using this biochemical approach, rafts were shown to selectively include some proteins and exclude others to varying degrees, which explains the difference in protein content within PMVs isolated from the same cell. When rafts join together as unit mobilities in the membrane plane, they can regulate the interaction of membrane-associated proteins. Because cholesterol is essential for the maintenance of the two membrane phases, extraction of cholesterol from the membrane results in the dispersal of lipid rafts. Hence, cholesterol can be thought of as the dynamic 'glue' that holds lipid rafts together. Cyclodextrin (natural cyclic oligosaccharides, which digests cholesterol) treatment periods must be limited because when applied to cells for several hours, the drug affects both the plasma membrane and the intracellular organelles connected to them. Nonetheless, a major property of rafts is that they can coalesce with other raft units, forming larger platforms. Further elucidation of the involvement of lipid rafts and other

microdomains will enhance our understanding of the mechanisms, which lead to the release of PMVs.

1.4 PMVs have a unique release mechanism

The release of PMVs is sometimes confused with other vesicles such as apoptotic bodies, formed during the process of apoptosis and exosomes, small vesicles released through exocytosis due to fusion of multivesicular bodies (MVBs) with the cell membrane. Some reports have concluded that the release of PMVs is distinct from both apoptotic bodies and exosomes [54].

1.4.1 Apoptotic bodies

Apoptosis can be defined very simply as programmed cell death, which occurs after sufficient cellular damage. This damage correlates with a distinct set of biochemical and physical changes involving the nucleus, cytoplasm and the plasma membrane. Cells round up (in the process losing contact with neighbouring cells) and shrink during early stages of apoptosis. In the cytoplasm, ER dilates causing the cisternae to swell and this forms vesicles and vacuoles. Nuclear chromatin starts to condense and aggregate into dense compact masses, which are degraded in the nucleus by endonucleases. The fragments can be analysed by the typical "DNA ladder" formation, observed when DNA is extracted (total or cytosolic) from cells and separated on an agarose gel. In this process degraded nucleus becomes convoluted and buds off into several fragments, which are referred to as apoptotic bodies [55]. Apoptotic bodies express PS on the outer leaflet, which facilitates their recognition and clearance by phagocytic cells (i.e. macrophages). Besides usually

carrying fragmented DNA, they are also easily distinguishable from PMVs by their larger mean diameter [56].

Exposure of PS on the outer leaflet of the plasma membrane is now generally accepted to correlate with deactivation of flipase and activation of scramblase, subsequently, leading to the release of PMVs. However, other observations suggest that the release of PMVs does not always follow exposure of PS. It is because the threshold of cytosolic Ca^{2+} required for formation of PMVs is higher than for exposure of PS at the outer leaflet [52]. Later, a topoisomerase I inhibitor, camptothecin (CPT), was shown to stimulate the release of PMVs from proapoptotic cultured HUVECs [26]. Interestingly, several phenotypically different PS^+PMVs were released from HUVECs treated with low concentrations of CPT before detection of PS on the cells or DNA degradation, which is the point of no return in apoptosis [57].

In addition, release of PMVs from the cells appeared to be limited, and it was not enhanced in the executive stage of apoptosis. Moreover, they also observed that CPT-induced release of PS^+PMVs was further enhanced by inhibition of myosin adenosine triphosphatase (MAT). Simply put, the use of a myosin light chain inhibitor failed to inhibit CPT-induced release of PMVs. Interestingly, staurosporin (a general kinase inhibitor) by itself caused a marked increase in the release of PS^+PMVs. These results contradict previous reports, which suggested that apoptotic blebbing is dependent on the activities of myosin adenosine triphosphatase and myosin light chain kinase [58]. However, it indicates that PS^+PMVs that are released at the early stage of proapoptotic stimulation are produced via a different mechanism than apoptotic blebbing, which result in the release of apoptotic bodies.

Nusbaum et al (2004), initially set about investigating the mechanism of apoptosis-dependent leukosialin (CD43) down-regulation during neutrophil apoptosis. However, they noticed that CD43 had been reported as the main sialoglycoprotein of the leukocyte plasma membrane with both adhesive and anti-adhesive properties [59]. Another report also suggested that CD43 expression levels decrease during the activation and adhesion of neutrophils due to proteolytic cleavage of the molecule [60]. In view of this, they decided to investigate the release of membrane vesicles during the apoptosis of neutrophils, in relation to the decreased expression of CD43. They found that decrease of CD43 was due to the molecule being removed from the surface of neutrophils through membrane blebbing, or the release of plasma membrane-derived vesicles after cell stimulation.

There are two signalling pathways for apoptosis - the extrinsic pathway of the caspases cascade and the intrinsic pathway of mitochondria cytochrome C release and apoptosome formation. Both pathways are present in neutrophils, but the use of the pan-caspase inhibitor, benzyloxycarbonyl-Val-Ala-Asp (OMe) fluoromethylketone (Z-VAD-fmk) and the specific caspase-3 inhibitor, benzyloxycarbonyl-Asp-Glu-Val-Asp (OMe) fluoromethylketone (Z-DEVD-fmk), did not inhibit PMN membrane blebbing, but down-regulated CD43 expression. It was concluded that PS-expression, membrane blebbing and CD43 decreased expression, result from distinct signalling mechanisms, which may occur independently of each other [61].

1.4.2 Exosomes

Exosomes have previously being described as a population of small membrane vesicles homogenous in size (50-90 nm) and shape, released by cells into the extracellular environment [62;63] . The release of exosomes was first described during the 1970s when Rose Johnstone and her group searching for an elusive amino acid transporter using immature sheep red blood cells, noticed that the cells were ejecting "tons of stuff" after binding to an antibody. In 1983, it was proposed that the release of exosomes might represent a mechanism for removing unwanted membrane proteins from reticulocytes. This was because many plasma membrane proteins were known to disappear during reticulocyte maturation to the final mature erythrocyte. An example is the transferrin receptor (TfR), which disappears as reticulocytes mature into erythrocytes [64,65]. However, several reports have shown that the process does extend to other mammalian cells – including dendritic cells [66], B cells, mast cells [67], T cells and several epithelial cell lines during maturation [68].

1.4.2.1 The endosomal pathway

All eukaryotic cells communicate with their environment by secreting proteins into the extracellular space and receiving signals such as cytokines, chemokines, or various nutrients [69] . The endosomal system consists of three main complex networks of membranes inside the cell, which assist during uptake and secretion. These include primary endocytic vesicles, early endosomes and multi-vesicular bodies (MVBs). Early endosomes located near the plasma membrane act as the first contact for primary endocytosed vesicles. Once endocytosed, these molecules are either directly recycled to the plasma membrane or targeted to MVBs (**Fig. 3A**). Intraluminal vesicles (ILVs) contained within MVBs are incorporated with proteins

sequestered to the limiting membrane of MVBs. This is achieved by invagination of the limiting MVB membrane, creating an enclosed compartment in which the lumen is topologically similar to normal cytoplasm [70;71].

Transmembrane proteins and receptors amongst other molecules are constantly targeted to internal vesicles of MVBs for lysosomal degradation. This process (degradation) occurs when MVBs fuse with the lysosomal membrane, releasing vesicles into the lysosome, where they are eventually degraded. The process is essential for cell removal of excessive membranes and transmembrane proteins, which are upregulated at the cell surface during activation.

Moreover, processing of these activated receptors into MVBs ensures that they are secluded from the cytosol and therefore inaccessible to their binding partners. Through this process cells are able to down regulate activated cell surface receptors, without the requirement of lysosomes [72]. It has been suggested that MVBs from dendritic cells act as a storage compartment for MHC class II molecules **(Fig. 3B)**.

However, not all the proteins are directed towards lysosomal degradation. Invaginated MVBs can also fuse directly with the plasma membrane, resulting in the release of ILVs into the extracellular environment as exosomes **(Fig. 3C)**. As depicted in figure 3, even after membrane internalization into early endosomes, the phosphorylated C-terminal docking site of epidermal growth factor receptor (EGFR) retains access to the cytosol where further possible signal transduction can occur.

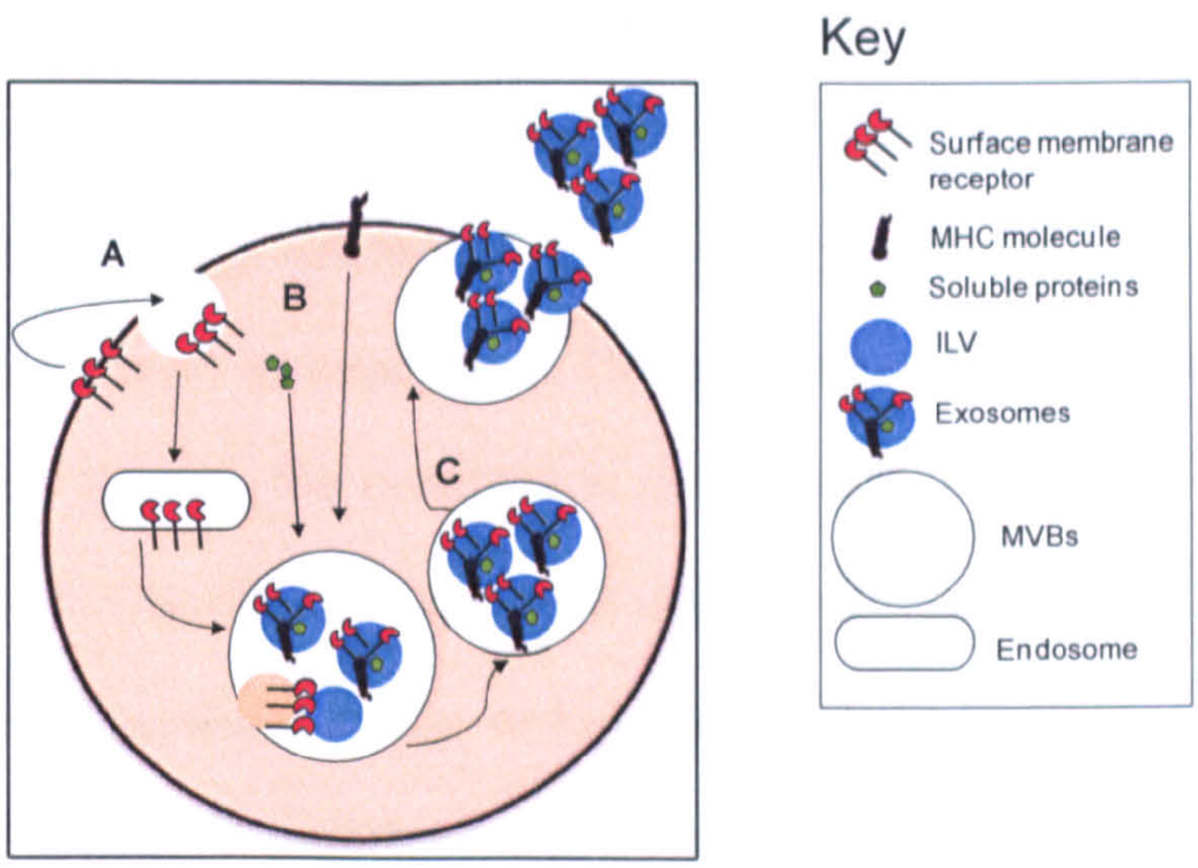

Figure 3 Different fates and functions of internalised vesicles.

(A) Cell surface membrane receptors such as the EGFR are internalised by endocytosis following ligand binding and activation of the host cell. The internalised receptor now carried within the endosome, is released into a Multivesicular body where they fuse with intraluminal vesicles (ILVs) to form exosomes. (B) MHC class molecules and some soluble proteins are also carried to the MVBs to be transported within exosomes (C) Multivesicular bodies can fuse with the plasma membrane and release internal cargo (exosomes) into the extracellular environment.

1.4.2.2 Exocytosis

Over the years, cells have implemented different mechanisms by which they release molecules into their extracellular environment. One of these, and possibly the most common, is the release of large biomolecules via the plasma membrane by a process known as exocytosis. The mechanism of exocytosis can be divided into two different modes, the constitutive (non-calcium-initiated) and the regulated (calcium-initiated). Constitutive exocytosis occurs within all cells either to release components of the extracellular matrix, or to allow newly synthesized proteins to be incorporated into the plasma membrane, following fusion with transport vesicles [73]. However, regulated exocytosis functions in neurological signalling, where vesicles released through the synapse (i.e. synaptic vesicles) induce nerve impulses, by fusing with the synaptic cleft membrane [74]. Another mechanism of exocytosis is fusion of multivesicular bodies with the plasma membrane, followed by release of their internal cargo into the extracellular environment.

1.4.2.3 Exosomes: structure and composition

Exosomes are more homogenous than PMVs, with sizes ranging from 30-100 nm in diameter. They have a density range from 1.13 g ml^{-1} (for B-cell derived exosomes) to 1.19 g ml^{-1} (for intestinal-cell-derived exosomes) and as confirmed by many groups, these vesicles carry protein biomarkers as in the original cell. They also share some common characteristics such as structure (lipid bilayer), size, density and general protein composition [75;76]. Some proteins can be found on the surface of the plasma membrane or in the cytoplasm of nearly all exosomes regardless of the cell type from which they were isolated. These are referred to as exosomal markers to help differentiate exosomes from other types of vesicles.

Particularly, these include surface molecules such as Major histocompatibility complex (MHC) class I and II molecules and tetraspanins – including CD9, CD63, CD81 and CD82, which represent the most abundant protein families present in exosomes. Tetraspanins have been described as a family of transmembrane proteins with four transmembrane domains and two different sizes of extracellular domains, which are defined by a number of conserved amino acids in the transmembrane domains. Although their exact function has not been clearly elucidated, they are said to interact with several other proteins, including integrins and MHC molecules [77;78]. Most exosomes also contain cytoplasmic proteins such as tubulin, actin, actin-binding proteins (which are components of the cytoskeleton), annexins and Rab proteins (involved in intracellular membrane fusion and transport).

Exosomes also contain molecules implicated in signal transduction such as protein kinases and heterotrimeric G-proteins, various metabolic enzymes (e.g. peroxidases, pyruvate, lipid kinases and enolase-1) and heat-shock proteins including Hsp70 and Hsp90. The latter are ubiquitous chaperone proteins, which are involved in antigen presentation, as they are able to bind antigenic peptides and participate in peptide loading onto MHC molecules [79] (Fig. 4). As this study is mainly about PMVs and not about exosomes, they will not be reviewed further.

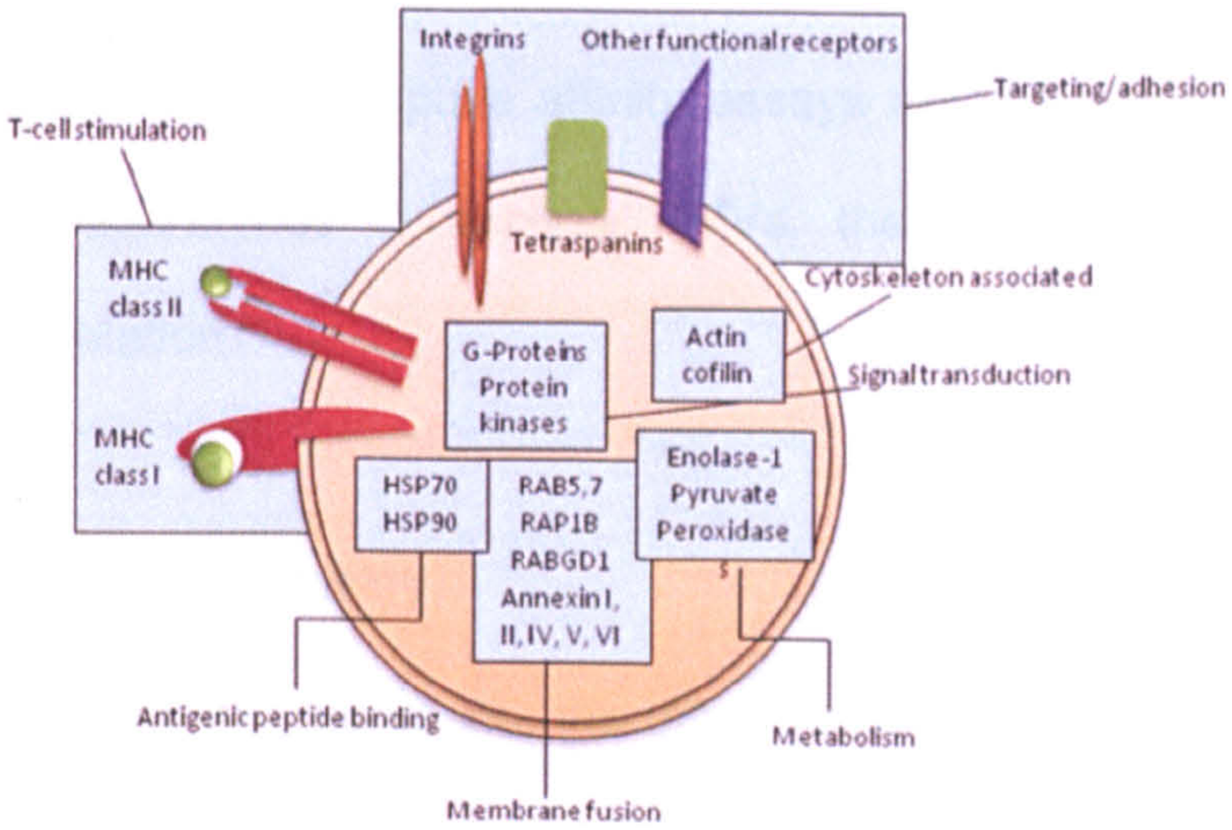

Figure 4 Schematic diagram of exosome produced by dendritic cells.

Exosome containing cytosolic proteins from the original cell and also various transmembrane proteins are exposed on the extracellular domain. Some known functions of the proteins depicted have been mentioned on the image.

1.5 Methods of PMV analysis

Investigators employ different methods to isolate and analyse PMVs. Although flow cytometer and microplate affinity assays are the most common methods used by most laboratories to analyse PMVs, there are problems associated with data interpretation.

1.5.1 Flow cytometry

Flow cytometry represents the most basic and common method for the analysis of PMVs. This is because it favours analysis of large numbers of PMVs up to the order of tens of thousands, and also provides information about their corpuscular characteristics, forward scatter parameter correlating with the size of PMVs and side scatter reflecting their granularity. On the flow cytometer, antibodies conjugated to three or even more antigens can be analysed on isolated PMVs. Similarly, accessibility of PS on the surface of PMVs can be detected using annexin V conjugated to fluorophores such as FITC or PE. Apart from the advantage of analysing large numbers of PMVs in a single isolated sample, flow cytometry also gives information about PMV characteristics and allows multiple antigen detection on a single isolated sample.

Although flow cytometry analysis is the method considered by many as the gold standard for analyses of PMVs, most commercial flow cytometers currently available are not able to accurately analyse smaller PMVs, which may be approximately 10-30 nm in diameter. Hence a population of smaller PMVs are normally missed out during analysis. Interestingly, most groups analyse PMVs using the forward scatter linear (FSC-H-Linear) and side scatter linear (SSC-H-linear) parameters on the flow

cytometer. However, we noticed using the Guava EasyCyte flow cytometer (Guava Technologies, UK) that with these settings only part of the samples are actually analysed. When set to FSC-Hlog and SSC-Hlog, all the samples are displayed and so can be accurately analysed (see result section 4.2.4). Also the fact that conventional flow cytometer instruments are normally very expensive and that they need a well-trained operator, together with a time consuming factor for analysis of samples, further highlights the advantage of flow machines like the Guava EasyCyte, which is easy to operate and interpret data, has a higher resolution, and easier to maintain .

1.5.2 Microplate Affinity Assays

Microplate affinity assays can be divided into two main types. The first and most commonly adapted for this type of assay is the Enzyme Linked Immunosorbent Assay (ELISA), designed using antibodies raised against PMV antigens to help capture or simply detect the PMVs. The other assay involves the use of annexin V in the presence of Ca^{2+} to help capture or detect PS^{+}PMVs, normally using a flow cytometer [80]. Annexin V is a calcium dependent phospholipid binding protein with a strong affinity for phosphatidylserine. In this study, all PMVs presented as PS^{+}PMVs were actually detected using a fluorophore-conjugated annexin V. Annexin V is also a protein naturally present in cells, and several groups have also identified by proteomics, the presence of annexin V inside isolated PMVs. It is possible that this endogenous form of annexin V can bind to PS exposed on PMVs, thus blocking their accessibility during analysis, although no such observations have yet been reported. The use of microplate based assays for PMV analysis has several advantages, such as the fact that they are more robust and can be developed more

easily into user-friendly, cost effective, clinical diagnostic/screening assays for analysis of high numbers of samples. Some disadvantages of this assay are that, unlike the flow cytometer, there is a lack of direct quantification of PMVs and also information about their size and granularity are not available. It is likely that only subsets of PMVs isolated are actually analysed as annexin V does not bind to all PS available, annexin V probably only binds to PMVs with accessible PS on their membrane surface.

1.6 Physiological roles of PMVs

We now know that PMVs as well as having beneficial roles on cells may also play significant roles in cell pathogenesis. In this section, important roles of PMVs in both *in vitro* and *in vivo* conditions will be discussed. First it is important to consider why cells may release these microvesicles into the extracellular microenvironment.

1.6.1 Why do cells release PMVs?

The study of PMVs in diseases has expanded our understanding of the process of microvesiculation or release of microvesicles, and helped eradicate any doubts as to whether PMVs are artefacts or not. Based on these, one might be tempted to speculate the rationale behind cellular release of PMVs. I propose that the biological effects of PMVs can be grouped into four main categories. Accordingly, PMVs may (i) function as mediators of cell-to-cell communication, (ii) play an integral part in host self-defence mechanisms, (iii) contribute directly or indirectly to pathogenic infections and finally (iv) represent a possible secretory pathway.

1.6.2 Role of PMVs as mediators of cell-to-cell communication

Many reports suggest that cells release PMVs in order to communicate with other cells through transfer of receptors, or simply to initiate signalling or cell contact. Recent reports also suggest roles in homeostasis [81] and thrombosis [82], angiogenesis [83], tumour metastasis [84], stem cell engraftment [85] and possibly many others. It is well known that cells communicate and exchange information among themselves through various mechanisms. Some of these include the use of secreted growth factors, cytokines, chemokines and small molecular mediators such as nucleotides, nitric oxide ions and bioactive lipids. Other mechanisms implemented, include the use of specialised adhesion molecules for cell-to-cell adhesion [86;87]. However, several investigators are now focusing on cell-to-cell communication by studying the involvement of PMVs and exosomes. These vesicles have been reported in many cases to contain numerous proteins and lipids similar to those present on the plasma membranes of parent cells. For several years this mechanism has been overlooked as a possible pathway by which cells may interact.

We now know that microvesicles in general encapsulate some cytoplasm, and thus cytosolic proteins, mRNA and microRNA (miRNA) during their release [5;6]. As mentioned earlier, cell-to-cell communication by PMVs can be in the form of direct cell stimulation resulting in activation of a signalling complex, transfer of surface receptors to local cells or delivering of proteins or mRNA to target cells. I will now focus on these few examples and elaborate on how investigators have elucidated the different ways in which PMVs interact with their microenvironment.

1.6.2.1 Role of PMVs in signal transduction

Proteomic studies have shown that PMVs carry numerous signalling proteins, including growth factors, cytokines, chemokines and bioactive lipids upon release from their parental cells [86]. Moreover, recent evidence suggests these biological signals can be transferred between different cell types [88,89]. Plasma membrane-derived vesicles can therefore be envisaged as a kind of signalling complex, with essential roles in cell contact and communication.

Morphogen-bearing PMVs referred to as 'argosomes' play essential roles during development, homeostasis and morphogenesis of multicellular organisms. For example, hedgehog morphogens (Hh^+) have been shown to be present on PMVs derived from activated T cells. Addition of these Hh^+ PMVs to human K562 pluripotent erythroleukaemic cells induced their differentiation towards the megakaryocytic lineage, as confirmed by the expression of $\alpha_{IIb}\beta_3$ integrin and CD42b, as well as inducing changes in the cell cycle [4]. It was previously shown that argosomes co-localize with Wingless proteins secreted by Wingless-producing cells and are transported through endosomes and finally released into the extracellular matrix, where they play crucial roles in tissue developmental signalling [90].

In addition, PMVs derived from platelets are well documented to activate certain signalling pathways in human cells. These PMVs have been shown to activate protein kinase C (PKC) in U-937 cells in addition to phosphatidylinositol-3-Kinase (PI3K), mitogen-activated protein kinase (MAPK) p42/44, p38 and c-jun NH_2-terminal kinase 1 (JNK1) [91]. Others showed that PMVs from platelets also induced phosphorylation of MAPKp42/44 and PI3K-Akt signalling pathways, in both normal

and malignant human haemopoietic cells [89]. The activation of MAPKp42/44 and Akt provides further molecular evidence that PMVs interact with target cells and activate several signalling cascades that increase cell proliferation and survival [92,93].

1.6.2.2 Transfer of surface receptors

The idea that PMVs can transfer receptors or proteins between cells was a phenomenal breakthrough, which was first studied in platelets. This work showed the transfer via PMVs of platelet-expressed adhesion molecules (PEAM) to haemopoietic cells, resulting in an increase of their ability to adhere to fibrinogen or endothelium [94]. These reports were supported by an earlier observation that platelet-derived PMVs could transfer the CD41 antigen ($\alpha_{IIb}\beta_3$ integrin) to endothelial cells [95].

Recently, it was proposed that a similar mechanism might be operating in tumour cells, as it was shown that PMVs isolated from activated platelets, transfer the antigen ($\alpha_{IIb}\beta_3$ integrin) to the surface of tumour cells. This transfer increased the adhesiveness of lung cancer cells to the endothelium and also increased their metastasis *in vivo* after injection into syngeneic mice [96]. Recently it was also shown that monocyte-derived PMVs are not only enriched in P-selectin glycoprotein ligand-1 (PSGL-1), but that they also express high levels of tissue factor (TF) [97]. This fuses with activated platelets and initiates coagulation after circulating through the peripheral blood. As platelets themselves do not secrete TF, other mechanism(s) must come into play to help explain how they acquire this receptor during coagulation. In previous studies, it was observed during co-culture of CD81-positive Jurkat T cells with CD81-negative U937 promonocytic cells that U937 cells became

positive for CD81, a tetraspan co-receptor involved in the activation of B and T cells. It was proposed that CD81 was carried on the surface of microvesicles released by Jurkat cells, and that the receptor was transferred to U937 cells. These cells were now able to produce an immune response during infection showing that the receptor had retained its function [98].

Receptor transfer via PMVs is not always good news for the recipient cell as various groups have already observed. PMVs isolated from culture supernatants of melanoma cells and epithelial ovarian cancer cells, were found to express Fas ligand (Fas-L) on the plasma membrane. This ligand normally stimulates apoptosis in T cells, which express the Fas receptor (Fas-R); hence removal allows the tumour cells to escape immunosurveillance [99-101].

Another report showed a mechanism by which HIV succeeds in sensitising certain types of cells to infection. The efficient infectivity of haemopoietic cells by HIV-1 is mainly dependent upon host expression of CD4 together with specific virus chemokine co-receptors, which mediate the cell surface binding of the virus and subsequently facilitates the transmission and propagation of HIV-1 [102;103]. The principal co-receptor for lymphotropic (L-tropic) HIV-1 strains or X4 viruses is the CXCR4 chemokine receptor and the macrophage-tropic (M-tropic) HIV-1 strains or R5 viruses, use the CCR5 chemokine receptor as co-receptors for entry into cells. The authors observed that individuals who are homozygous for a 32-base pair deletion in the CCR5 gene (Δ32/Δ32), which causes disruption in the expression of the CCR5 receptor, were in fact resistant to HIV infection [104]. HIV-1 primarily targets lympho/haemopoietic cells (macrophages, T-lymphocytes, megakaryocytes and dendritic cells), which express CD4 on their surface and either one or both of the

mentioned chemokine co-receptors. Moreover, there is mounting evidence that other types of cells including, endothelial cells [105], astrocytes [106], cardiomyocytes [107] and possibly renal cells [108] can be infected with HIV-1 strains and these could be important sources of the virus during chronic infections.

Until recently there was still debate about how these cells, which do not typically express HIV-related co-receptors on their surface become susceptible to infection by the virus. However, this can now be explained by the notion that PMVs released by cells, which are normally positive for these co-receptors can transfer the receptors to negative cells. Moreover, a recent report showed that PMVs derived from peripheral blood mononuclear cells (PBMCs) can transfer specific HIV-1 co-receptors onto endothelial cells during transendothelial migration, rendering these cells susceptible to HIV infection [109].

A similar mechanism showed that platelet-derived PMVs transfer CXCR4 receptor to CXCR4-null cells and sensitised them to HIV infection [110]. These results demonstrate that HIV-specific co-receptors are released on PMVs by various types of cells. These PMVs are transferred to cells, which were previously negative for the co-receptors rendering recipient cells susceptible to infection by the virus.

In 2005, pathological roles of released PMVs were reported in a study on cerebral malaria (CM). Evidence was presented, which showed the importance of the ATP-binding cassette transporter A1 (ABCA-1), a receptor, which regulates distribution of PS at the outer leaflet of the plasma membrane during the release of PMVs. In an experiment using *ABCA-1*$^{-/-}$ mice, it was observed that a reduction in the levels of released PMVs, offered a complete resistance to the development of cerebral

malaria by these mice. By contrast *ABCA-1*$^{+/+}$ mice released high numbers of PMVs and developed CM when infected by the parasite *Plasmodium berghei* ANKA. Furthermore, PMVs isolated from infected mice transferred the receptor to *ABAC-1*$^{-/-}$ mice causing infection by the parasite and development of CM [111].

1.6.2.3 Delivering of proteins, mRNA and mIRNA into target cells

Recent studies suggest that co-culturing of different cells result in the transfer of membrane and cytoplasmic components between the cultures [112]. During development, cells undergo certain functional and molecular changes, which often result in reprogramming of adult cells into pluripotent cells, a process known as epigenetic or nuclear reprogramming [113]. Although the mechanisms responsible are yet to be elucidated, various groups have reported the use of cell extracts to induce epigenetic changes in target cells co-cultured together. Extracts from embryonic stem cells (ESC), pluripotent cancerous cells or differentiated somatic cells like cardiomyocytes, have been found to reprogram, to some extent, terminally differentiated cells [114;115]. Likewise, the phenomenon was further demonstrated when permeabilised fibroblasts began to express various genes typical of lymphocytes, after being exposed to extracts from lymphocytic cells [116;117].

As previously mentioned, PMVs become enriched in various molecules, which are expressed in the cytoplasm of their parental cells during their secretion. Based on this notion, later studies described using a model of murine ESC-derived microvesicles, that, MVs may in fact, contribute to epigenetic reprogramming of target cells. Addition of ESC-derived MVs significantly improved the survival and expansion of murine haemopoietic stem and progenitor cell (HSPC) and

upregulated the expression of markers for early pluripotent and early haemopoietic stem cells. ESC-derived MVs also induced phosphorylation of MAPKp42/44 and serine-threonine kinase Akt. Furthermore, they observed that ESC-derived MVs were highly enriched in mRNA for various pluripotent transcription factors compared to parent cells, and this mRNA could be delivered to target cells and translated into corresponding proteins [5].

1.6.2.4 Transfer of HIV, prions and mitochondria

In addition to the HIV infection strategy involving transfer of co-receptors described earlier, another mechanism involving PMVs has been proposed, termed the 'Trojan horse mechanism', which elicits the direct transfer of HIV into cells [118].

A similar mechanism has been hypothesised for prion particle infection of cells. These infectious particles have been observed in platelet-derived PMVs and might therefore suggest a possible role for PMVs in their spread. However, further studies would be required to fully understand the extent to which PMVs as well as exosomes are implicated in the spread of other infectious agents [8].

A co-culture of human skin fibroblasts with A549 ρ° cells, a cell-line with the mitochondrial DNA (mtDNA) mutated and depleted so that the cells became incapable of aerobic respiration and growth, showed that the A549 ρ° cells acquired functional mitochondria from fibroblasts. These cells were able to propagate exponentially in a manner similar to the parental cell line with functional mitochondria [10]. This phenomenon of functional mitochondria transfer between cells possibly involves microvesicle (PMVs and exosomes) release.

1.6.3 Release of PMVs as part of a self-defence mechanism

1.6.3.1 Release of death signals via PMVs

Release of PMVs can be a defensive mechanism for host cells in response to stress, inflammation and tissue regeneration. It is well documented that cells shed PMVs enriched in death signals, including, Fas and caspases-1, which are deposited on the plasma membrane. Hence, they avoid passing the point of no return in terms of apoptosis. PMVs enriched in these signals can deliver death messages to nearby cells [119;120].

1.6.3.2 Escape from complement-mediated lysis

As well as avoiding apoptosis, some cells release PMVs as a mechanism to escape complement-mediated lysis. In the presence of sublytic complement, release of PMVs helps cells to escape from complement-mediated lysis, by removing the inserted, membrane attack complex (MAC) from the cell surface [121]. Various reviews suggest that cells release PS^{+}PMVs to prevent PS-induced phagocytosis of the cell. In preliminary work, PMV release from *T. cruzi* during culture and when stimulated with normal human serum, have also been examined (unpublished observations). One is therefore tempted to speculate that certain parasites might themselves release PMVs to either confer protection against complement lysis, or to aid their escape from macrophage phagocytosis, so facilitating their entry into cells.

1.6.4 PMVs contribute to Infection

As mentioned earlier, in addition to stimulating mammalian cells to secrete vesicles, parasites could themselves release PMVs although the reason(s) for this can only be speculated upon at present. In a recent study, we provided evidence that PMVs

isolated from THP-1 cells, Jurkat cells and HepG2 cells, fuse with *T. cruzi* and increased their invasion of Vero cells, HeLa cells and MCF-7 cells by evading complement lysis (**III.** Cestari I.d.S et al. 2010 - submitted).

Furthermore, PMVs isolated from the intestinal parasite, *Giardia intestinalis* (causative agent of diarrhoea) enhanced the parasite's attachment to endothelial cells (unpublished observations). The attachment of *Giardia intestinalis* to the microvilli of endothelial cells is necessary for the parasite to effectively establish infection [122]. It is important to emphasize that our data is the first to report possible contributions of PMVs during parasite infections.

1.6.5 Release of PMVs as a possible secretory pathway.

One of the fundamental properties of all living organisms is the separation of the interior compartment, including cytosol, from the surrounding environment by an amphipathic lipid bilayer termed the plasma membrane. In addition, eukaryotic cells possess a highly evolved endomembrane system, which allows the formation of organelles [123]. Organelles are enclosed subunits, which provide specialised surroundings for different biological processes. These include distribution of nutrients and metabolites, storage of materials, assembly and degradation of macromolecules and export of substances to the extracellular matrix.

Living organisms have developed essential processes such as intracellular transport and secretion, as well as endo- and exocytosis, in order to transport and exchange materials between organelles and the cell surroundings [124;125]. These mechanisms

are mediated by membrane vesicles (e.g. PMVs), which deliver their contents upon fusion with an acceptor membrane [126-128].

In eukaryotic cells, a number of specialised organelles assemble sequentially to form a network known as the conventional secretory pathway [129]. This is a highly regulated and specialised transport route directly involved in protein biogenesis, modification, sorting, quality control and secretion. The secretory route mediates transport of proteins, lipids and other molecules to intracellular organelles or directly to the plasma membrane where further export to the extracellular space occurs. However, an alternative route has been reported for some proteins, which are exported independent of this secretory pathway, known as the unconventional secretory pathway [130-132].

1.6.5.1 Conventional protein secretion

Conventional protein secretion is characterised by a complex secretory machinery, which begins when a signal recognition particle (SRP), binds to an N-terminal, hydrophobic, signal sequence of a nascent polypeptide chain, synthesized in the cytosol [133;134].

The complex is directed towards the membrane of the endoplasmic reticulum (ER) where SRP interacts with its cognate receptor [135;136]. The latter is an integral membrane protein, which consists of a large α- and smaller β-subunit [137]. Once bound, a sequence of activation processes results in release of SRP, followed by elongation and translocation of the polypeptide across the membrane to the lumen of the ER in a co-translational manner [138;139]. Once localised to the lumen, the polypeptide associates with ER resident chaperones, which ensure correct folding (a

quality control measure), before being packaged into membrane-coated transport vesicles, which are approximately 50 nm in diameter. The vesicles fuse with the Golgi apparatus to deliver their protein cargo, which are further packaged into specific vesicles and transported to the plasma membrane. Vesicle transportation is along a microtubular network by post-Golgi transport carriers, which fuse with the membrane and eventually release their content into the extracellular space [140;141].

Certain inhibitors can abolish this conventional secretory pathway involving the ER and the Golgi apparatus. The fungal metabolite brefeldin A (BFA), inhibits ADP-ribosylation factor 1 (ARF-1) recycling by disrupting the interaction of ARF with its guanine exchange factor (GEF). This impairs formation of COPI vesicles (transport intermediates involved in recycling of proteins from Golgi to ER) [142;143] and results in fusion of the cis- and medial-Golgi with ER. The drug monensin, irreversibly blocks transport from the trans-Golgi face leading to Golgi dilatation [144], which in turn disrupts the secretory pathway [145].

1.6.5.2 Unconventional protein export

In eukaryotic cells, protein export is mainly via the ER/Golgi dependent transport or classical secretory pathway. Soluble secreted proteins typified by having an N-terminal, hydrophobic, signal sequence, typically enter this pathway and are translocated across the ER to Golgi and eventually released into the extracellular space (see section 1.6.5.1). Despite lacking the classical N-terminal, hydrophobic, signal sequence, a number of secretory proteins can still be exported by cells. These proteins do not associate with the classical secretory pathway [131]. For example, interleukin-1β (IL-1β) and galectin-1 secretion was observed, despite the

absence of a functional ER/Golgi membrane translocation system [146;147]. These observations have resulted in the term unconventional protein export, to distinguish secretory processes that are independent of the classical ER/Golgi transport pathway.

As the phenomenon of unconventional protein export started to unravel, further characterisations uncovered common properties of these different proteins, which are functionally and structurally unrelated. For example, they do not contain a classical N-terminal, hydrophobic, signal sequence, they do not associate with the ER/Golgi membrane translocation machinery and they bear no ER/Golgi-dependent post-translational modifications e.g. N-linked glycosylation, despite carrying numerous consensus sites. Also, treatment with ER/Golgi transport inhibitors, such as BFA or monensin, does not affect their export into the extracellular space [148;149].

Later, others provided evidence that the release of FGF-2 is controlled by NF-κB mediated signalling and release of the non-classically exported protein, Engrailed, is regulated by post-translational modifications, such as phosphorylation [150;151]. Additionally, unconventional export of galectins is regulated during cell differentiation [152]. Together, these data indicate that unconventional secretion is not based on unspecific protein release caused by injury, or cell death as previously proposed [153]. Instead, it is a highly regulated process involving protein-based molecular machineries.

1.6.5.2.1 Current concepts of mechanisms of unconventional protein export

In general, the majority of unconventional secretory proteins are normally localised to the cytoplasm [131;154]. However, although, they share the properties mentioned in section 1.6.5.2, it is unlikely that their release into the extracellular space is via a common export pathway. Hitherto, four potential export mechanisms have been described in the literature to confer translocation of proteins lacking a classical N-terminal, hydrophobic, signal sequence into the extracellular environment [146].

The first model exemplified by the export of IL-1β [147], involves recruitment of endocytic membrane vesicles such as secretory lysosomes to the cell membrane. Under favourable conditions, lysosomal contents are translocated to the exterior of cells, when specialised, intracellular structures, such as lysosomes of cytotoxic T lymphocytes or melanosomes of melanocytes, fuse with the plasma membrane [155]. The second mechanism proposed, is characterised by direct translocation of leaderless proteins, using resident-protein mediated channels, such as adenosine triphosphate-binding cassette (ABC) transporters [156]. Non-classically exported proteins probably released by this mechanism, are the hydrophilic acylated surface protein B (HASPB) of *Leishmania* [157;158] and fibroblast growth factor 2 (FGF-2) [159].

The third mechanism involves fusion of multivesicular bodies (MVBs) with the plasma membrane. Multivesicular bodies carry exosomes, which are packaged with cargo molecules that are released into the extracellular space, upon fusion of MVBs with the plasma membrane [160]. Galectin-3 is an example of an unconventionally secreted protein exported via this route [161].

The fourth mechanism is characterised by shedding of plasma membrane-derived vesicles into the extracellular environment [1;2;162]. Vast arrays of proteins are translocated into the extracellular space, via this mechanism. Among these, the galectin family and other unconventionally exported proteins, not previously shown, are mediated through PMV release.

1.7 *Trypanosoma cruzi* Infection

Trypanosoma cruzi is a flagellated, intracellular, protozoan parasite of mammals and the causative agent of the debilitating Chagas disease in humans. Chagas disease is a chronic and incurable inflammatory condition, characterised by cardiomyopathy and digestive disorders, as reported in some cases [163;164]. The disease is said to affect approximately 16 to 18 million individuals in Latin America and to cause about 50,000 deaths per annum [165]. Invasion of mammalian cells is critical for survival of *T. cruzi* in the host; indeed, the ability to infect and replicate within a variety of cell types is an essential feature of the parasite's life cycle.

1.7.1 Mode of transmission

The sylvatic cycle naturally starts with transmission of trypomastigotes, from the bite of insect vectors of the *Reduviidae* family, to small, wild, vertebrate animals and back to insects. Cohabitation between humans and infected vectors or domestic animals, is the basis of transmission to humans. A bite from an infected insect, deposits 'excreta' containing infectious metacyclic trypomastigotes at the bite-site, which enters humans through a skin wound caused by scratching the contaminated site. Although considerable progress has been made in larger parts of Latin America, to control the natural transmission of the infection, the disease is still

present at endemic levels among the rural poor, who live in an open environment with many feral reservoir hosts [166]. The lack of an effective treatment for the chronic form means the disease still remains an important health issue in Latin America.

Even more serious is the ease with which transmissions from human-to-human can occur, through contact with contaminated blood, during pregnancy or blood transfusion [167]. Moreover, new means of transmission have been reported from contaminated food, even fruit juice and sharing of intravenous needles [168;169]. The latter means the disease has the potential to become an international threat and cases are now being seen in North America, Europe and Japan due to increasing human migration and mobility [170]. Recent reports show that insect vectors are developing resistance against current pesticides and also, new insect species are starting to spread the disease. The pool of wild animals from which insects would normally feed, has been reduced in recent years, due to environmental destruction [171].

1.7.2 Infection and replication

After invasion of mammalians cells, by metacyclic trypomastigote forms, the parasite undergoes at least three morphogenetic life cycles, before invading other cells such as macrophages, smooth and striated muscle cells, and fibroblasts. Metacyclic trypomastigotes (the extracellular non-dividing forms) and amastigotes (intracellular replicative forms) are found inside the cytoplasm of mammalian cells, whereas epimastigotes (non-infective forms) divide in the reduviid reservoir after blood feeding by insects. After invasion of mammalian cells, metacyclic trypomastigotes localise in a structure known as parasitophorous vacuole (PPV), formed during

invasion, when activated lysosomes migrate and fuse with the host plasma membrane, the resulting vacuole retaining the parasites. Trypomastigotes differentiate within these vacuoles, into amastigotes and replicate free in the cytosol. After continuous cycles of binary division, amastigotes differentiate back into highly motile trypomastigotes (blood forms) and are then released upon host-cell rupture [172].

Host cell entry by the parasite is a complex process with many factors involved [173]. Nonetheless, specific cell invasion strategies have been proposed. Entry into epithelial cells in a polarized manner via the basolateral membrane, where fibronectin and host cell receptors are associated is one strategy [174]. A recent report showed that intracellular lysosomes aid the entry of *T. cruzi* into cells. However, these entry mechanisms are still not very well clarified and so part of this thesis proposes a novel entry route involving release of plasma membrane-derived vesicles, by which *Trypanosoma cruzi* enters into mammalian cells.

1.8 Plasma membrane repair/resealing

1.8.1 Definition

In eukaryotic cells, survival depends on host maintenance of an intact plasma membrane (PM). A disruption in the PM of a eukaryotic cell interferes with its integrity, which if not resealed allows the unabated influx of potential toxins such as high Ca^{2+}, to flood into the cytoplasm of the damaged cell. Other vital ions and proteins could escape, thus, impairing normal cell function. If damage is left unrepaired, loss of PM integrity leads to cell death and also release of proteases that attack neighbouring cells [175] or induction of an inflammatory response [176].

In order to survive a breakage, most eukaryotic cells mount a rapid (within seconds) resealing response [177;178]. Such a response, also elicited by an influx of Ca^{2+}, results in the activation of a repair mechanism involving exocytosis of organelles such as lysosomes to the site of disruption [179]. Free-living amoebae such as *Physarum* and *Dictyostelium* regain normal function within seconds of being cut into half [180]. Also the sea urchin egg reseals to the point of preventing further Ca^{2+} entry within five seconds after inducing plasma membrane damage greater than 1000 μm^2. Once resealed, the wounded egg remains viable and could be fertilised [181].

1.8.2 Examples of resealing mechanisms

The biological significance of membrane resealing is primarily for survival of the damaged cell. Unrepaired damage leads to loss of cell constituents and subsequent death. Moreover, partially repaired damage is a feature of certain genetic diseases, most notably the muscular dystrophies. Recent reports suggest that some of the symptoms observed in muscle dystrophies might be due to plasma membrane damage. Amongst these, limb-girdle muscle dystrophy [182] is reported as a result of mutations in the gene encoding dysferlin, a 230 kD surface-bound protein essential for muscle PM repair [183;184]. In addition, cardiomyopathy was abrogated in mice treated with agents that elicit PM repair [185].

The first event in eukaryotic cell damage repair is the immediate resealing of the plasma membrane, to halt influx of Ca^{2+} and loss of cytoplasmic contents, albeit small (<1 μm in diameter) disruptions, are said to be passively repaired through thermodynamically driven lipid interactions [186]. Two highly conserved membrane fusion mechanisms have been described in nucleated cells for larger disruptions

(>10 μm^2). The first event mentioned earlier (see section 1.8.1), involves the rapid exocytosis of vesicles and fusion with the PM at the site of damage [187;188]. The second event described recently is reserved for PM disruptions larger than 1000 μm^2, caused for example by agents such as staurosporin or insertion of the complement MAC (both of which leads to release of PMVs). This mechanism referred to as the 'patch' hypothesis is activated by elevated Ca^{2+}, which stimulates vesicle-vesicle fusion, forming a larger vesicle that is literally added as a patch to the PM disruption site [177;189].

1.8.3 Organelles responsible for resealing

The exact mechanisms or identity of sealing organelles responsible for the PM repair is still unclear. However, the yolk granule is universally recognised as the sealing organelle responsible for repair in the sea urchin [181;190], but the lack of studies describing yolk granules in somatic cells, led leading investigators to look for alternative candidates. In view of this, lysosomes and enlargosomes were proposed.

1.8.3.1 Lysosomes and enlargosomes

The notion for proposing lysosomes as resealing organelles stems from the similarities with the yolk granule. Like yolk granules, lysosomes vesicle-vesicle fusion and vesicle-PM fusion activated by calcium-regulated exocytosis is required for patch formation [191]. Also like yolk granules of sea urchin eggs, lysosomes contain hydrolytic enzymes [192]. In addition, the role of lysosomes as resealing organelles was confirmed in a study, which showed that abating the activation of synaptotagmin (syt) VII, a broadly expressed lysosomal membrane protein and a member of the Ca^{2+}-binding protein family with antibodies or recombinant peptides

against the C2A domain of the protein, suppresses lysosomal exocytosis and reduces resealing [193;194]. Moreover, exocytosis of lysosomes and PM resealing were reduced in syt VII knockout mice [195]. However, these findings were challenged by reports, which argued that syt VII was not exclusively localised to lysosomes [196] and lysosomal exocytosis was actually enhanced in syt VII knockout mice-derived fibroblasts [197]. Furthermore, altering the morphology of lysosomes with vacuolin-1, a small molecule proposed to enlarge lysosome-derived and endosome-derived vacuoles, blocked Ca^{2+}-mediated lysosomal exocytosis, but membrane resealing continued unabated [198].

By contrast, exocytosis of enlargosomes was unaffected and so these were proposed as candidates for PM resealing [198;199]. However, this was not without controversy since enlargosomes, although distinct from lysosomes both morphologically and in their contents, are also widely distributed and are recruited to the PM following an increase in cytosolic Ca^{2+}. Also tetanus toxin, which is widely accepted as an inhibitor of PM resealing in somatic cells, failed to abrogate exocytosis of enlargosomes [200]. It is noteworthy, that the role of enlargosomes as resealing organelles is not well characterised. Thus, the specific organelle(s) responsible for PM resealing remains unknown and so perhaps, it would be incorrect to assume that PM repair is entirely regulated by a single specialised compartment. Instead, reflecting on the involvement of an array of organelles might be a closer concept since an increase in cytosolic Ca^{2+} might also perturb a variety of local responses.

Recently, a PM repair process has also been described in plants. Similar to animal cells, repair mechanisms in plant cells have been shown to respond to Ca^{2+} influx

resulting in cytoplasmic aggregation and rearrangement of the actin cytoskeleton [201].

1.9 Role of PMVs in disease

In addition to the aforementioned physiological functions of PMVs discussed, their participation in specific diseases is well documented. Hitherto, release of PMVs via activation of the ABCA-1 has been shown to enhance susceptibility to development of cerebral malaria [111]. Moreover, clinical studies revealed elevations in the levels of blood PMVs in diseases such as atherosclerosis and coronary disorders. Blood from patients with unstable angina or myocardial infarction had significant increases in PMV levels compared with stable angina or noncoronary defects [202]. Platelet-derived PMVs are elevated in patients with type 2 diabetes mellitus, but monocyte-derived PMVs were severely higher in patients with diabetic nephropathy, indicating possible vascular complications in diabetes [203;204].

In theory, all cell types can release PMVs, thus representing a physiological process in the cell's life. This implies that PMVs may have more pathophysiological roles than currently envisaged. Nonetheless, the progress already achieved in describing how PMV release influences diseases is encouraging. Amongst the conditions in which they have been shown to play a role are cardiovascular diseases [205], thrombus formation [206] and thrombosis, inflammation and rheumatoid disease [15], as well as in sickle cell anaemia, multiple sclerosis and even in pregnancy [52]. Later studies suggested that cancer metastasis is enhanced by contact with PMVs [96]. Indeed, PMVs have recently been shown to enhance angiogenesis [83], invasion and

metastasis of various cancers [207;208]. In this thesis, the effect of PMVs on the acute promonocytic cell line, THP-1, will also be investigated.

1.9.1 Acute Myeloid Leukaemia (AML)

Acute myeloid leukaemia represents a group of heterogeneous malignant clonal disorders, which occur due to genetic alterations of haemopoietic progenitor blasts. These genetic changes impair normal differentiation into erythrocytes, granulocytes and platelets, and lead to overproliferation of blasts due to an inability to respond to normal regulators of proliferation [209;210]. The overproliferation of blasts results in accumulation of non-functional cells termed myeloblasts, which if left untreated within a year of diagnosis, can lead to complications like fatal infection, severe bleeding and infiltration of vital organs [211].

According to epidemiological studies, AML is the most common myeloid leukaemia with approximately 11,000 cases diagnosed annually in the UK with a prevalence of 3.4 to 3.8 per 100,000 population, possibly rising to 17.9 per 100,000 adults aged between 65 years and over [212;213]. The median age at presentation of AML is 68-70 years and disease incidence is higher in males than in females and more in the white population than black. The disease is most often diagnosed in older adults than in children even though leukaemia is the most common malignancy of children aged 15 years and younger [212].

The incidence of AML is rapidly increasing in the elderly and it was suggested that this could be down to factors such as improvement in disease diagnosis and longer life expectancy, which results in increased exposure to environmental factors [214]. The exact aetiology of AML is not fully understood, as known risk factors are said to generally account for only a small number of observed cases [215]. Nonetheless, age, antecedent haematologic disease and genetic disorders have all been suggested as possible causes; as well as exposure to radiation, viruses and environmental (physical and chemical) factors [216,217].

1.9.2 Developmental therapeutics in AML

1.9.2.1 Inhibition of cell proliferation: targeting oncogene mutations

The understanding of the pathophysiology of AML has led to development of a host of potential targeted therapies. Drugs developed against the proliferation-promoting fms-like tyrosine kinase (FLT3) transmembrane enzyme, has been positive. Amongst these drugs, imatinib for example, has been successful in the treatment of chronic myeloid leukaemia and other diseases pathophysiologically based on the constitutive activation of the tyrosine kinase. The success of this drug spurred the search for similarly effective agents against AML [218].

1.9.2.2 Inhibition of signal transduction

Other therapies have focused on inhibiting signal transduction cascades, which involves cells receiving and transmitting signals systemically. Mutations in the RAS protein, a 21 kD guanine-nucleotide binding protein leads to autonomous growth, and this has been described in 10%-50% of AML patients. It was shown that farnesyl transferase inhibitors (FTI) abate growth of mutant RAS-transformed cell

lines. Successful phase I trials revealed that tipifarnib, the furthest FTI, was associated with responses in patients with advanced-stage AML. Despite disappointing phase II trials, the drug is still administered to chemotherapy-naïve AML patients [219].

1.9.2.3 Agents that promote cell differentiation

The discovery of cytarabine, a drug which causes differentiation of haemopoietic cells, in treatment of AML and the general notion that AML results from a combination of stem cell overproliferation as well as failure to differentiate, spurred the search for new differentiating agents and those that inhibit mitogenic signals [218]. Newer approaches including, differentiation therapy and apoptosis induction therapy were developed to treat overproliferating AML blast cells in acute leukaemia. The human monocytic leukaemic cell line, THP-1, differentiated after treatment with the retinoid, all-*trans*-retinoic acid (ATRA) *in vitro* [220].

Indeed, acute promyelocytic leukaemia (ALP), a subtype of AML, is currently treated using ATRA by specifically targeting neoplastic cells, leaving normal mature cells unaffected [221]. Other agonists which stimulate maturation of myeloid leukaemia cells include phorbol-12-myristate-13-acetate (PMA) [222], vitamin D_3 [223], calcium ionophore [224] and interferon gamma [225]. Recently, histamine was successfully used in a phase III clinical trial to inhibit proliferation of acute monocytic leukaemic cells, although the agonist did not induce myeloid differentiation [226]. All the agonists reported to induce differentiation of myeloid cells have been shown to stimulate the release of PMVs from several cell types [6;227]. Thus, part of this thesis will discuss the effect of PMVs on the acute monocytic cell line, THP-1.

2. Aims of the present study

During the last five years, research on microvesicles in general has intensified, with different functions having been elucidated. However, distinguishing between the various vesicles (exosomes and PMVs in particular) released by cells has proved very difficult and the rational for release of PMVs by different cells has only started to become unravelled.

Part of this study was designed to accomplish the following:

1. To isolate PMVs and characterise them effectively, distinguishing them from other vesicles by employing methods such as flow cytometry and electron microscopy.

2. To investigate the role of PMVs during the terminal differentiation of monocytic cells into macrophages, important for immune surveillance.

3. To investigate the possible role of PMVs during cellular invasion by intracellular pathogens such as bacteria and parasites.

Materials and Methods

3. Materials and Methods

3.1 Materials

3.1.1 Chemicals

AEBSF (Pefabloc)	Sigma-Aldrich
Acrylamide/Bisacrylamide	Sigma-Aldrich
Agar resin	Agar Scientific
Annexin V Alexa Fluor 488	Invitrogen
Annexin V reagent	R&D Systems
APS (Ammonium persulphate)	Sigma-Aldrich
ATRA (all-*trans*-retinoic acid)	Sigma-Aldrich
Bacitracin	Sigma-Aldrich
Barbituric acid	Sigma-Aldrich
BCA protein assay kit	Pierce Biosciences
BSA (Bovine serum albumin)	Sigma-Aldrich
BDMA (Benzyl dimethylamine)	Agar Scientific
Bromophenol blue	Fisher Scientific
Calcium chloride	Sigma-Aldrich
Calpeptin	Merck Biosciences
Chlorpromazine	Sigma-Aldrich
Concanavalin A	Sigma-Aldrich
Coomassie brilliant blue	BDH Limited, Poole, England
DAPI-VECTASHIELD	Vector Laboratories Inc, CA, USA
DDSA (Dodecenyl succinic anhydride)	Agar Scientific
DEAE- Cellulose	Sigma-Aldrich
DMSO (Dimethyl sulfoxide)	Sigma-Aldrich
DTT (Dithiothreitol)	Fisher Scientific
ECL WB Detection Reagent	SignaGen Laboratories
EGTA	Sigma-Aldrich
Equilibration buffer	Kind gift from IBCHN
Ethanol	Fisher Scientific
Fura-2-AM	Sigma-Aldrich
FBS (Foetal Bovine Serum)	Fisher Scientific
Filipin	Sigma-Aldrich
Gadolinium chloride	Reaction Product, Cheshire
Glacial acetic acid	Fisher Scientific
Glucose	Acros Organics
Glutaraldehyde	Agar Scientific
Glycerol	Sigma-Aldrich
Glycine	Sigma-Aldrich
Guava ViaCount reagent	Guava Technologies, UK
Guava Nexin reagent	Guava Technologies, UK
GsMTx-4	Peptides Int. Inc, USA
Haemin	Sigma-Aldrich
Halt Protease Cocktail	Pierce, Thermo-Scientific
HCl (Hydrochloric acid)	Fisher Scientific

HEPES	Sigma-Aldrich
Histamine	Sigma-Aldrich
Human FGF-1 ELISA kit	R&D Systems
Human Galectin 3 ELISA kit	R&D Systems
Human MIF ELISA kit	R&D Systems
Human TGF-β1 ELISA kit	R&D Systems
Human Cytokine Array kit	R&D Systems
Hybrid nitrocellulose membrane	Amersham Biosciences
Isopropanol	Sigma-Aldrich
Kanamycin	Sigma-Aldrich
Liver Infusion Broth	Becton, Dickinson and Co. USA
Magnesium chloride	Sigma-Aldrich
Methyl-β-cyclodextrin	Sigma-Aldrich
Methanol	Fisher Scientific
Milk powder	Marvel Original, Dublin
MNA (Methyl nadic anhydride)	Agar Scientific
Na_2HPO_4	BDH Lab supplies, England
Nifedipine	Sigma-Aldrich
NHS (Normal Human Serum)	Sigma-Aldrich
Osmium tetroxide	Agar Scientific
Paraformaldehyde	Sigma-Aldrich
PBS (Phosphate Buffered Saline)	Fisher Scientific
Penicillin / Streptomycin	Fisher Scientific
PKH26GL	Sigma-Aldrich
PKH67	Sigma-Aldrich
PMA (Phorbol-12-myristate-13-acetate)	Sigma-Aldrich
PMSF	Pierce, Thermo-Scientific
Ponceau S	Sigma-Aldrich
Potassium chloride	Sigma-Aldrich
Propidium iodide	Sigma-Aldrich
Propylene oxide	Agar Scientific
Protein molecular weight marker	BioRad
PSG (Phosphate solution + glucose)	CMIRC
PTA (Phosphotungstic acid)	Agar Scientific
R-18 (Octadecyl Rhodamine B Cl)	Invitrogen Molecular Probes
Rehydration buffer	Kind gift from IBCHN
Reynolds Lead Citrate stain	Agar Scientific
RGD (Arg, Gly, Asp)	Sigma-Aldrich
RGE (Arg, Gly, Ser)	Sigma-Aldrich
RPMI	Fisher Scientific
SB-431542	Sigma-Aldrich
SDS (Sodium dodecyl sulphate)	Sigma-Aldrich
Sodium azide	Avocado Research Chemicals
Sodium barbital	Sigma-Aldrich
Sodium cacodylate	Sigma-Aldrich
Sodium chloride	Sigma-Aldrich
Sodium hydroxide	Sigma-Aldrich
Sucrose	Sigma-Aldrich
TEMED	Sigma-Aldrich
Tris base	Sigma-Aldrich
Trichloroacetic acid	Fisher Scientific
Triton X-100	Sigma-Aldrich
Trypsin/EDTA solution	Sigma-Aldrich

Tryptose	Becton, Dickinson and Company
Tween 20	Sigma-Aldrich
Uranyl acetate	Agar Scientific
Verapamil	Sigma-Aldrich
Wheat germ agglutinin	Sigma-Aldrich
Wortmannin	Sigma-Aldrich
Y-27632	Calbiochem

3.1.2 Technical Devices

AMT Digital camera	Advanced Microscopy Tech.
Bacterial incubator	Heraeus Incubator
Cell culture flasks (75 cm^2)	Fisher Scientific
Centrifuge 5804 R	Eppendorf
Centrifuge 5810 R	Eppendorf
Cover glass (18 mm)	Fisher Scientific
Gel loading tips	Corning
Guava EasyCyte flow cytometer	Guava Technologies, UK
Fluorescence microscope (1X81)	Olympus Corporation, Germany
FLUOstar Omega plate reader	BMG Labtech, UK
Incubator Heraeus CO_2-Auto-Zero	Thermo Electron Corporation
Joel JEM-1200Electron microscope	Deben UK Ltd
Leica Ultracut R ultra microtome	Leica, Wien, Austria
Mini-PROTEAN 3-gel system	BioRad
Microcentrifuge 5417R	Eppendorf
Microplate (12-well)	Sigma-Aldrich
Microplate (24-well)	Sigma-Aldrich
Microplate (96-well)	Sigma-Aldrich
Nikon Inverted Microscope, TS100	Nikon Eclipse, Japan
pH-Meter 766 Calimatic	Jenway
Pioloform film copper grids	Agar Scientific
Roto-Shake Genie	Denley
Semi-dry transfer system	BioRad
Small volume tips	Sigma-Aldrich
Sorvall ultracentrifuge RC6	Thermo Electron Corporation
Sorvall T-865 rotor	Sorvall
F-20 micron rotor	Sorvall
SE-12 rotor	Sorvall
Sonicating waterbath	Townson & Mercer Ltd, Croydon
Spectrofluorimeter	Lambda Advanced Technology Ltd
UVP Chemiluminescence	UVP Bioimaging Systems, UK

3.1.3 Antibodies

Anti-Annexin V AlexaFluor 488	eBiosciences
Anti-CD11b PE	AbD Serotec
Anti-CD14 FITC	AbD Serotec
Anti-DC-SIGN FITC	AbD Serotec
Anti-LAMP-1 AlexaFluor 488	eBiosciences
Mouse anti-Actin	Kind gift Dr Sigrun Lange
Mouse anti-CD49d	AbD Serotec

Mouse anti-FGF-1	R&D Systems
Mouse anti-Galectin 3	R&D Systems
Mouse anti-MIF	R&D Systems
Mouse anti-TGF-β1	R&D Systems
Goat anti-CR1	Complement Technology
Goat anti-DAF	Complement Technology
Mouse anti-IgG FITC	AbD Serotec

3.2 Eukaryotic Cell lines

THP-1 cells (Human promonocytic cells) were used in most experiments as the source of plasma membrane-derived vesicles (PMVs). However, in some experiments, PMVs were isolated from Jurkat cells (Human T-cells), MCF-7 cells (Human breast cancer cells) and HepG2 cells (Human hepatocytes). HeLa cells (Human cervical cancer lines) were used for studies on *T. cruzi* invasion and in some experiments, PMVs isolated from these cells were utilised. Primary monocytes were also obtained from healthy donors.

Eukaryotic cell lines: THP-1 cells (ECACC; Ref No. 88081201)

Jurkat cells (ECACC; Ref No. 88042803)

MCF-7 cells (ECACC; Ref No. 86012803)

HepG2 cells (Received as a kind gift from Dr Kenneth White)

HeLa cells (Received as a kind gift Dr Una Fairbrother)

Vero cells (ECACC; Ref No. 84113001)

3.2.1 Eukaryotic Cell Culture Media: Cell Growth Medium (GM)

The RPMI 1640 supplemented growth medium was used to cultivate HeLa cells, HepG2, Jurkat cells, MCF-7 cells, THP-1, Vero cells. RPMI 1640 medium with phenol red, containing 2.05 mM glutamine was supplemented with 10% FBS (v/v) and 1% Penicillin / Streptomycin in 500 ml volumes and stored at 4°C.

Liver Infusion Tryptose Medium (LIT Medium)

Liver Infusion Tryptose medium was used to cultivate *T. cruzi*. The chemical components listed below were accurately weighed into a 1 L Duran bottle. The components were mixed with water and the pH adjusted to 7.3 with 4 M hydrochloric acid (HCl). The mixture was then autoclaved to sterilise before addition of heat-inactivated FBS (56°C, 30 min), glucose and haemin to a 1 L final volume. The final medium was filter sterilised through a 0.22 µm pore size membrane filter with a vacuum pump into autoclaved bottles and stored as 50 ml aliquots at 4°C.

LIT Medium:	5 g/l	Liver Infusion Broth (w/v)
	5 g/l	Tryptose (w/v)
	4 g/l	NaCl (w/v)
	0.4 g/l	KCl (w/v)
	8 g/l	Na_2HPO_4 (w/v)
		Millipore water
	2 g/l	Glucose (v/v)
	10 mg/l	Haemin (v/v)
	10%	Foetal bovine serum (v/v)

Medium was made to a 1 L final volume

3.3 Experimental Solutions- pH was either adjusted with 4 M HCl or 4 M NaOH

3.3.1 Mammalian cell freeze medium

20%	FBS (v/v)
10%	DMSO (v/v)
1%	Penicillin/Streptomycin (v/v)
69%	RPMI (v/v)

3.3.2 Parasite freeze medium

10%	FBS (heat-inactivated) (v/v)
2 g/l	Glucose (v/v)
10 mg/l	Haemin (v/v)
10%	DMSO (v/v)
80%	LIT medium

3.3.3 Triatomine urine (TAU) medium- pH 6.0

190 mM	NaCl,
17 mM	KCl,
2 mM	$CaCl_2$,
2 mM	$MgCl_2$,
8 mM	Na_3PO_4

Components were dissolved in Millipore water to 500 ml after adjusting pH with 4 M HCl.

3.3.4 TAU3AAG medium

10 mM	L-proline,
50 mM	L-glutamate,
2 mM	L-aspartate,
10 mM	Glucose
100 ml	TAU medium

3.3.5 PSG- pH 8.0

73 mM	NaCl
5 mM	Na_3PO_4
1%	Glucose (w/v)

Components were dissolved in 1 L Millipore water and stored at -20°C as 50 ml aliquots. pH was adjusted with 4 M HCl.

3.3.6 Lysis buffer- pH 7.4

100 mM	HEPES-KOH
2 mM	$CaCl_2$
0.2%	Triton X-100 (v/v)
10 mM	Protease inhibitor (AEBSF)
	Millipore water

Made up to 50 ml and stored as 1 ml aliquots at -20°C. pH was adjusted with 4 M HCl.

3.3.7 SDS-PAGE solutions

3.3.7.1 (4X) SDS Sample buffer- pH 6.8

200 mM	Tris-HCl
40%	Glycerol
2%	SDS (w/v)
0.2%	Bromophenol blue (w/v)
20 mM	DTT (added fresh on the day)
	Millipore water
	pH was adjusted using 4 M HCl solution

3.3.7.2 (1.5 M) Resolving buffer- pH 8.8

18.17 g Tris base
Dissolved in 100 ml deionised water and pH adjusted to 8.8

3.3.7.3 (0.5 M) Stacking buffer- pH 6.8

6.06 g Tris base
Dissolved in 100 ml deionised water and pH adjusted to 6.8

3.3.7.4 Resolving gel solution (12%)

2 ml	ddH_2O
1.25 ml	1.5 M Tris-HCl, pH 8.8
0.050 ml	10% SDS (w/v)
1.66 ml	Acrylamide/Bis 30% (w/v)
0.025 ml	10% APS (w/v)
0.0025 ml	TEMED

3.3.7.5 Stacking gel solution

1.53 ml	ddH_2O
0.625 ml	0.5 M Tris-HCl, pH 6.8
0.025 ml	10% SDS (w/v)
0.335 ml	Acrylamide/Bis 30% (w/v)
0.0125 ml	10 % APS (w/v)
0.0025 ml	TEMED

3.3.7.6 10X Electrophoresis running buffer (1L)

250 mM	Tris-HCl, pH 8.3
1925 mM	Glycine
50 ml	20% SDS (w/v)
950 ml	ddH_2O

3.3.7.7 Coomassie Brilliant Blue G-250

0.025%	Coomassie blue (w/v)
10%	Acetic acid (v/v)
90%	ddH_2O (v/v)

Mixed and filtered (Whatman number 1 paper)

3.3.7.8 Destain solution (500 ml)

35 ml	Acetic acid
25 ml	Methanol
440 ml	ddH_2O

3.3.7.9 Transfer buffer (10X)

250 mM	Tris base
1925 mM	Glycine
500 ml	ddH_2O

3.3.7.10 Sartoblot buffer (500 ml)

40 ml	Transfer buffer (1X)
100 ml	Methanol
360 ml	ddH_2O

3.3.7.11 Ponceau solution (0.25%)

0.25%	Ponceau S (w/v)
3%	Trichloroacetic acid (v/v)
	ddH_2O

3.3.7.12 Phosphate Buffered Saline (PBS) solution - 1L

140 mM	NaCl
2.7 mM	KCl
10 mM	Na_2HPO_4
1.8 mM	KH_2PO_4
	ddH_2O

3.3.7.13 Phosphate Buffered Saline – Tween 20 (PBS-T)

1 L	PBS
1 ml	Tween 20

3.3.7.14 Blocking buffer

6%	Milk powder (w/v)
100 ml	PBS-T

3.3.7.15 Antibody dilution buffer (WB)

3%	Milk powder (w/v)
100 ml	PBS-T

3.4 Permeabilisation Buffer (PBB)

0.5%	Tween 20 (v/v)
	PBS

3.5 Immunofluorescence antibody dilution buffers

3.5.1 Cell Dilution Medium

10%	FBS
1%	NaN_3 (w/v)
	PBS solution

3.5.2 Primary and secondary antibody dilution buffer

3%	BSA (w/v)
	PBS

3.5.3 Flow cytometry analysis buffer

3%	BSA (w/v)
1%	NaN_3 (w/v)
	PBS

3.5.4 Veronal buffer – pH 7.4

0.15 mM	$CaCl_2$
141 mM	NaCl
0.5 mM	$MgCl_2$
1.8 mM	Na Barbital
3.1 mM	Barbituric acid

All components dissolved in 500 ml of deionised water

3.6 Ringer's solution - pH 7.25

138 mM	NaCl
2.7 mM	KCl
1.06 mM	$MgCl_2.6H_2O$
1.8 mM	$CaCl_2$
12.4 mM	HEPES
5.6 mM	D-Glucose

All components dissolved in 500 ml deionised water

3.7 Annexin V binding buffer – pH 7.4

10 mM	HEPES/ NaOH
140 mM	NaCl
2.5 mM	$CaCl_2$

All components dissolved in 100 ml of deionised water

3.8 Methods

3.8.1 Maintaining cell lines

3.8.1.1 Non-adherent cell lines

Non-adherent Jurkat cells, THP-1 cells and primary monocytes were maintained in growth medium containing RPMI 1640 supplemented with 10% foetal bovine serum (FBS), 100 U/ml penicillin and 100 µg/ml streptomycin. In addition, cells were occasionally maintained for a week in growth medium supplemented with 1% kanamycin (Sigma-Aldrich) at 37°C in 5% CO_2 atmospheric conditions to inhibit mycoplasma contamination. The cells were split, depending on confluency every 3 to 5 days by washing twice with serum-free RPMI 1640. Simply, the cells were transferred into 50 ml centrifuge tubes and spun at 160 *g* for 5 min. Resulting supernatant was discarded and cells were gently resuspended in the remaining medium. Serum-free RPMI was added and cells were centrifuged as mentioned earlier. Resulting supernatant was discarded and cell pellets were resuspended in the appropriate volume of growth medium. Cells were then seeded in the desired dilution into new 75 cm^2 culture flasks. Cells were only cultured in medium supplemented with kanamycin for a week to avoid development of resistance to the antibiotic. Also, primary monocytes were used within a week of isolation.

3.8.1.2 Adherent cell lines

Adherent cells (MCF-7, HeLa and HepG2) were also maintained at 37°C with 5% CO_2, in RPMI growth medium. These cells were also split depending on confluency every 3 to 5 days. Cells were washed twice by changing GM with serum-free RPMI and addition of 0.25% (v/v) trypsin/EDTA in RPMI. After 10 min incubation at 37°C

with 5% CO_2, the flask was tapped several times to detach the cells and growth medium was added to inactivate the trypsin. The trypsin solution was removed by centrifugation at 200 *g* for 5 min followed by one wash in serum-free RPMI. Cell pellets were resuspended in the appropriate volume of GM and seeded in the desired dilution into new culture flasks. Exponentially growing cells with viability of 95% or higher was used in every experiment. The number of cells and viability were determined before the start of every experiment using the flow cytometer (ViaCount assay, Guava Technologies).

3.8.1.3 Isolation of peripheral blood monocytes

Human blood peripheral monocytes were purified from whole blood of healthy donors by centrifugation through a Hypaque-Ficoll (Amersham Biosciences) gradient. Venous blood was collected into EDTA-containing tubes and each 30 ml of blood sample was layered over a 20 ml solution of Ficoll-Hypaque. Sample was centrifuged at 500 *g* for 30 min and the mononuclear layer was removed by aspiration using a plastic Pasteur pipette. The purity of monocytes exceeded 95%, as determined by flow cytometry after staining the cells with fluorochrome-labelled antibody to CD14, and viability was greater than 97% as determined following staining with viacount assay dye (Guava ViaCount, Guava Technologies, UK). The cells were allowed to attach to the culture flask by maintaining in complete RPMI growth medium supplemented with 20% FBS and incubated overnight at 37°C in a 5% humidified, CO_2 incubator. Unattached cells were separated by centrifugation (200 *g* for 5 min) and cultured separately in 10% growth medium. Cultured monocytes were used three days after isolation for experiments.

3.8.1.4 Freezing of eukaryotic cells

To prepare frozen stocks for long-term storage, non-adherent cells grown to almost 100% confluency were washed twice (160 *g*, 5 min) with serum-free RPMI and cell number determined using Guava viacount as mentioned in section 3.8.1.2. Cells were carefully resuspended in freeze mix, transferred into cryo-vials (Greiner) at $1x10^7$ cells/ml in 1 ml volumes and immediately placed on ice. The cryo-vials were frozen at –80°C in special cryo boxes, which ensure a temperature decrease of 1°C per minute. For long-term storage the deep frozen cryo-vials were transferred to liquid nitrogen cell storage tanks. Adherent cells were also frozen by a similar procedure except that cells were first trypsinised to bring them into suspension, as described earlier. Suspended cells were washed by centrifugation at 200 *g* for 5 min. Cells were resuspended in the freeze mix and transferred into cryo-vials.

3.8.2 *Trypanosoma cruzi* culture

T. cruzi epimastigotes, strain X10/6, were cultured to exponential growth phase in liver infusion tryptose (LIT) liquid medium supplemented with 10% heat-inactivated FBS [228]. Parasites were split by centrifugation at 4,000 rpm for 10 min (A-4-62 swing-out rotor, using 5810R centrifuge, Eppendorf) and the resulting supernatant was discarded safely. Parasites were resuspended in serum-fresh LIT medium and washed by centrifuging as stated earlier. Parasite pellets were resuspended in fresh-LIT medium, transferred into 75 cm^2 flasks at desired dilutions and incubated at 28°C.

3.8.3 Freezing of *Trypanosoma cruzi* parasites

In order to freeze parasites for long-term storage, highly viable parasites were washed with LIT medium without serum and carefully resuspended in freeze mix. Parasites were transferred into cryo-vials at $1x10^7$ cells/ml and immediately placed on ice. Subsequent procedures for freezing were as described in section 3.8.1.4.

3.8.4 Thawing of cells

To defrost cells or parasites, cryo-vials were removed from liquid nitrogen and immediately thawed in a waterbath at 37°C. After cleaning the lid with 70% ethanol, the content was transferred to a 15 ml centrifuge tube containing 9 ml of fresh growth medium, prewarmed to 37°C and cells were sedimented by centrifugation at the appropriate speed (160 *g* or 200 *g*, 5 min for mammalian cells or 3,000 *g* for 5 min for parasites). To remove DMSO, the medium was discarded and the pellet was resuspended in fresh growth medium. The cells or parasites were then placed into culture flasks of the same size as had been used prior to freezing, and incubated at 37°C with 5% CO_2.

3.9 Biochemical Methods

3.9.1 Purification of microvesicles from conditioned medium

Plasma membrane-derived vesicles were isolated by a modification of a previously described method [229]. Conditioned medium from cells cultured with 10% FBS at 37°C and 5% CO_2, was centrifuged once at 200 *g* for 5 min to remove the cells. The supernatant was then centrifuged twice at 4,000 *g* for 30 min at 14°C to remove cell debris. Resultant supernatant was ultracentrifuged at 160,000 *g* for 2 h at 14°C. The isolated MV pellet was resuspended in sterile PBS and ultracentrifuged again at

160,000 *g* for 2 h at 14°C to remove proteins such as albumin possibly bound to the MV membrane surface. The MV pellet was resuspended in sterile PBS and quantified on a Guava EasyCyte flow cytometer using ExpressPlus software (Guava Technologies), or stained with Guava Nexin-FITC to determine surface PS expression. Isolated MVs were then used immediately or stored at -80°C for next day experiments. The above procedure is for isolation of both vesicle types (exosomes and PMVs) and so a slightly modified method, described below was used for isolation of more pure PMVs and exosomes.

3.9.2 Purification of Plasma Membrane-derived Vesicles from conditioned medium

Conditioned medium from cells cultured with 10% FBS at 37°C and 5% CO_2, was centrifuged once at 200 *g* for 5 min to remove the cells. The supernatant was then centrifuged at 4,000 *g* for 1 h to remove cell debris. The resultant supernatant was sonicated in a sonicating water-bath for 5 x 1 min prior to centrifugation in order to disperse aggregated exosomes. Supernatant was centrifuged at 25,000 *g* for 2 h to pellet PMVs. Pelleted PMVs were washed once by resuspending in sterile PBS and centrifuged again at 25,000 *g* for 2 h. The PMV pellet was resuspended in sterile PBS and quantified, or analysed for PS exposure as described under section 3.9.1. In some experiments, PMVs were isolated by reverse washing of the filter membrane, with PBS after filtration of debris-free supernatant through a 0.22 μm membrane.

3.9.3 Induction and purification of PMVs

In some experiments cells were washed twice at 200 *g* for 5 min and preincubated at 37°C in 5% CO_2 atmospheric conditions for 1 h. Cells were centrifuged in order to remove any background PMVs released during the preincubation step. Pelleted cells were resuspended in prewarmed RPMI (37°C) supplemented with 0.5 mM $CaCl_2$, and seeded into 24-well plates at $1x10^6$ cells/well in 1 ml reaction volumes. Cells were stimulated to microvesiculate by addition of the specific inducing agents being investigated and incubated at 37°C for 30 min with shaking. The reaction was stopped by placing on ice for 1 min and transferred into 1.5 ml microcentrifuge tubes. Cells were pelleted by low speed centrifugation at 200 *g* for 5 min and debris removed by twice centrifugating at 4,000 *g* for 30 min each time. Samples were sonicated in a sonicating water-bath for 5 x 1 min prior to centrifugation. PMVs were isolated from the resulting supernatant by centrifugation at 25,000 *g* for 2 h. This speed parameter was found to pellet PMVs without much contamination with aggregated exosomes; since PMVs are larger, they can be sedimented at 25,000 *g* leaving exosomes in the supernatant. PMVs isolated were resuspended in 200 µl of PBS and quantified by flow cytometry as described in section 3.9.1.

3.9.4 Isolation of PMVs and exosomes by the 'reverse filtration method'

Cells and cell debris-free culture supernatants were filtered through a 0.22 µm pore size membrane filter. After filtration of the supernatant, the membrane filter was reversed and PMVs bound to the surface were removed by washing with PBS. Isolated PMVs were pelleted by centrifugation at 25,000 *g* for 30 min and where exosomes were required, the resultant filtrate was ultracentrifuged at 160,000 *g* for 16 h, to pellet these vesicles.

3.9.5 Annexin labelling of PMVs and exosomes

Isolated PMVs or exosomes were resuspended in Annexin binding buffer and annexin-FITC (R&D Systems) was added or not (control) in a 200 µl final volume. Sample was then incubated at RT for 30 min with shaking and centrifuged at 25,000 *g* for 2 h to pellet PMVs or 160,000 *g* for 16 h to pellet exosomes. Samples were analysed immediately as directed by the manufacturer using the flow cytometer (Guava EasyCyte, Guava Technologies).

3.9.6 Cell treatments prior to induction of PMVs

Trypsinised HeLa cells and THP-1 cells were treated with various inhibiting agents, before the induction of PMV formation. Cells were washed and resuspended into prewarmed, serum-free RPMI 1640 supplemented with 0.5 mM $CaCl_2$. Cells were seeded in triplicate at $1x10^6$ cells/well into 12-well plates and the following agents were added at their required concentrations. The lipid raft inhibitors, methyl-β-cyclodextrin (MβCD) 5 mM, filipin 5 µg/ml and chlorpromazine 25 µg/ml), were added. Also L-type calcium ion channel blockers, Verapamil 200 µM, Nifedipine 200 µM and stretch-activated calcium channel blockers, GsMTx-4 20 µg/ml and $GdCl_3$ 200 µM were added and incubated at 37°C, 5% CO_2 for 45 min. In some experiments, the role of integrins was investigated, by pretreating HeLa or THP-1 cells with integrin receptor activation inhibitors, RGD peptide 100-500 µg/ml, control-peptide RGE 200 µg/ml and the antibody, monoclonal anti-mouse-CD49d (10 µg/ml) at 37°C, 5% CO_2 for 10 min prior to induction of PMVs with NHS.

The above experiment was repeated for HeLa and THP-1 cells, using *T. cruzi* as the inducing agent. In some experiments, semiconfluent HeLa cells were plated at

$2x10^5$ cells/well in GM into 12-well plates containing sterilized 18 mm round coverslips and incubated overnight at 37°C, 5% CO_2. Cells were washed the next day with serum-free RPMI and pre-treated with the agents mentioned earlier. In addition, THP-1 or HeLa cells, were also pre-treated at 37°C for 45 min with the calpain inhibitor, calpeptin (20 µM), the Rho-kinase inhibitor, Y-27632 (10 µM), which is important during apoptosis and Wortmannin (40 nM), a PI3K inhibitor). Cells were induced with 5:1 (parasites to cell) ratio or 5% NHS and the reaction was incubated at 37°C for 30 min with shaking.

3.9.6.1 Cell treatment prior to membrane resealing studies

To investigate the role of PMVs in damage repair mechanisms, trypsinised HeLa cells were preincubated with the lectins, concanavalin A (conA), 20 µg/ml for 10 min at RT and washed once by centrifugation at 200 *g* for 5 min prior to addition of parasites ($1x10^6$ at 37°C for 30 min). Cells were also preincubated with the agents mentioned in section 3.9.6, for 30 min. All chemical agents were washed-off prior to addition of parasites. Cells were fixed with 4% paraformaldehyde and labelled with anti-LAMP-1 AlexaFluor-488 as described under section 3.10.3. Labelled cells were analysed by flow cytometry using the ExpressPlus assay. In some experiments, semiconfluent HeLa cells treated as described above were examined by fluorescence microscopy for detection of secreted lysosomes.

3.9.6.2 Cell treatments prior to Infection experiments

HeLa cells were seeded into 12-well plates and incubated overnight prior to performing infection experiments. On the day of the experiment, culture medium

was changed twice with serum-free RPMI 1640 and cells were preincubated with various agents at the required concentrations. Semiconfluent HeLa cells were preincubated with the inhibiting agents mentioned under section 3.9.6 and cells were washed once by changing medium with fresh serum-free RPMI prior to addition of parasites.

3.9.7 Purification of metacyclic trypomastigote forms of *Trypanosoma cruzi*

Metacyclic trypomastigotes were obtained and purified, with slight modifications, according to the method of Sousa *et al* (1983) [230]. Briefly, epimastigotes ($5x10^8$ parasites/ml) in stationary phase were incubated in triatomine urine medium (TAU), for 2 h at 28°C. Parasites ($5x10^6$ parasites/ml) were then transferred and incubated in TAU3AAG medium, for 3 days at 28°C. In some experiments, epimastigotes left in late stationary phase also differentiated into metacyclic trypomastigotes in LIT medium. Metacyclic forms were identified under the light microscope and by DAPI-staining to observe the position of the nucleus and kinetoplast. These are arranged differently within epimastigotes and metacyclic trypomastigotes. Once confirmed, parasites were harvested by centrifugation (4,000 rpm, 10 min; A-4-62 swing-out rotor, using 5810R centrifuge, Eppendorf) and resuspended in phosphate saline solution with glucose (PSG). Metacyclic forms were purified using diethylaminoethyl (DEAE)-52-cellulose column. The metacyclic trypomastigotes obtained were recovered by centrifugation, resuspended in PSG and counted using a haemocytometer to determine the number.

3.9.8 *Trypanosoma cruzi* Invasion assay

Semiconfluent HeLa cells were infected *in vitro* with metacyclic trypomastigotes using a modification of a method described earlier (Cestari, personal communication). Round coverslips (18 mm) were placed into each well of a 12-well plate and sterilised overnight under UV-light. HeLa cells from the log phase were washed twice with RPMI 1640 by centrifugation as mentioned in section 3.8.1.2. Supernatant was discarded and cells were resuspended in RPMI without phenol red, but supplemented with 10% FBS and 1% pen/strep. Cells were seeded ($2x10^5$/well) into each well of the plate and incubated overnight at 37°C in a 5% CO_2 incubator.

After the overnight incubation, medium was removed and confluent cells were washed twice with RPMI 1640. Serum-free RPMI without phenol red was added to the wells and cells were infected by addition of pKH26GL-labelled, metacyclic trypomastigotes at a ratio of 5:1 parasites to cell in 1 ml final reaction volumes. Plates were incubated at 37°C, 5% CO_2 for 3 h. After 3 h invasion, medium was removed and the infected cells were washed three times by changing with sterile PBS. Cells were then fixed with 4% paraformaldehyde (PFA) at room temperature for 15 min and washed a further three times. The cell nucleus was stained with DAPI-VECTASHIELD with mounting medium and mounted onto microscopic slides by inversion of the coverslip so that the side with the attached cells came into contact with the DAPI-VECTASHIELD; infection was visualised by fluorescence or phase-contrast microscopy. The numbers of intracellular parasites were determined by counting at least 500 cells in duplicate coverslips. Also to check for superinfection

by the parasites, the numbers of infected cells were also counted. Data was normalised to 100 against control.

In other experiments, *T. cruzi* invasion assay was performed with semiconfluent Vero cells ($2x10^5$/well in duplicate) in the presence of PMVs ($5x10^5$/well) derived from THP-1, Jurkat, HepG2 and MCF-7 cell lines.

In order to investigate the role of TGF-β during *T. cruzi* invasion, assays were repeated with Vero cells in the presence of mouse anti-TGF-β1 antibodies (2.5 µg/ml or 10 µg/ml) or the TGF-β receptor antagonist, SB-431542 (10 µM).

3.9.9 Complement-mediated lysis assay

Normal human serum (NHS) was obtained from healthy donors, pooled and stored at -80°C for subsequent use. *T. cruzi* epimastigotes ($1x10^6$ in triplicate) resuspended in 100 µl of veronal buffer, were incubated with 100 µl of 25% NHS at 37°C for 10 min. The reaction was stopped after 10 min by addition of 800 µl of ice-cold veronal buffer and placed on ice for 1 min. *T. cruzi* samples were mixed with Trypan blue and viable parasites (not stained) were examined under the light microscope using a haemocytometer. In some experiments, *T. cruzi* metacyclic trypomastigotes ($1x10^6$ in triplicates) resuspended in 100 µl of veronal buffer, were incubated with 100 µl of 50% NHS in the presence or absence of THP-1 cell-derived PMVs ($1x10^6$/well) at 37°C for 60 min and quantified using a haemocytometer after mixing with Trypan blue.

3.9.10 Lysis Inhibition assay

T. cruzi ($1x10^6$ in triplicate) resuspended in 100 µl of veronal buffer, was incubated at 37°C for 10 min with NHS (25% or 50%) in the presence or absence of THP-1 cell-derived PMVs ($5x10^5$ or $1x10^6$/well). In some experiments, NHS was preincubated with PMVs at 37°C for 30 min prior to performing lysis assay.

3.9.11 R18- (Octadecyl rhodamine) labelling of PMVs and PMV-*T. cruzi* Interaction experiment

THP-1 cell-derived PMVs ($1x10^8$/ml) were resuspended in PBS and labelled with a solution of octadecyl rhodamine chloride (R18, 1.37 mM) by incubation with isolated PMVs at RT for 1 h in the dark with shaking. R18-labelled PMVs were separated from unincorporated R18 dye by ultracentrifugation at 100,000 *g* for 1 h followed by overnight dialysis in 14 kD dialysis tubes at 4°C in HEPES/NaCl buffer. The ratio of R18 to PMVs was estimated by measuring the fluorescence before and after removal of the unincorporated dye, and R18-labelled PMVs were suspended in veronal buffer. Purified *T. cruzi* metacyclic trypomastigotes ($5x10^5$ parasites) were resuspended in veronal buffer and incubated with the R18-labelled PMVs ($5x10^5$) in a 200 µl volume at 37°C for 10 min, followed by three washes at 4,000 rpm for 10 min with PBS. The parasites were fixed in 4% paraformaldehyde in PBS at RT for 15 min, followed by three washes with PBS. Fixed samples were mounted on slides using DAPI-VECTASHIELD with mountain medium (Vector Laboratories). Images were acquired using an Olympus IX81 inverted fluorescent microscope equipped with a monochromatic camera. Images were subsequently coloured using the Cell^M imaging software (Olympus Corp.).

3.9.12 Measurement of Intracellular calcium

THP-1 cells ($1x10^6$/ml) were washed twice with serum-free RPMI by centrifugation at 160 *g* for 5 min and incubated in 1 ml volumes with 2 mM Fura-2-AM at RT for 1 h in the dark with shaking. Labelled cells were washed a further three times with RPMI and resuspended in a physiological salt solution (PSS) containing 130 mM NaCl, 5 mM KCl, 1 mM $MgCl_2$ and 10 mM HEPES in the presence or absence of 1 mM $CaCl_2$ or 5 mM EGTA. Measurements were made before and after addition of *T. cruzi* epimastigotes or metacyclic trypomastigotes ($5x10^6$/ml) after 60 seconds with continual stirring, whilst monitoring fluorescence on a spectrofluorimeter upon excitation at 340 and 380 nm and measuring emission at 510 nm every second. Triton-X-100 (1%) was added after 150 seconds to measure the maximum fluorescence. Intracellular calcium was calculated using the equation: $[Ca^{2+}]_i$ = Kd[(R-Rmin)/(Rmax-R)x(Sf2/Sb2)] where Kd (dissociation constant) for Fura-2-AM is 224 nM. R is the ratio of the emission intensities measured at 505 nm on excitation at 340 and 380 nm. Rmin is the ratio of intensities obtained at zero intracellular Ca^{2+} (before the addition of 1% Triton X-100 to cells resuspended in buffer containing 5 mM EGTA) and Rmax is the ratio of emission intensities measured after lysing the cells with 1% Triton-X-100 thus allowing Fura-2 measurement in the maximum external calcium concentration of 1 mM. Sf2 is the emission intensities of free calcium measured at 380 nm [ratio of intensities measured after addition of 1% Triton-X-100 to cells resuspended in buffer containing with 5 mM EGTA (here, the calcium is free as it is bound to EGTA and not to Fura-2-AM)]. Sb2 is the emission intensities of bound calcium measured at 380 nm (ratio of maximum intensities measured after addition of 1% Triton X-100). All measurements were made at 37°C.

3.9.13 Growth Inhibition Assays

Human THP-1 cells or primary isolated monocytes in the exponential phase were washed twice with RPMI and resuspended in growth medium containing 5% FBS. Cells were seeded into 12-well plates at $1x10^5$ cells/well in triplicate. Different concentrations of PMVs were added to each well (except controls) and plates were incubated at 37°C for three days. On the days indicated, non-adherent cells were removed and counted by ViaCount assay on a Guava EasyCyte flow cytometer. In some experiments, cells were incubated with 30 µg PMVs alone, or in the presence of the TGF-β1 receptor antagonist, SB 431542 (10 µM). For other experiments, cells were treated with histamine (10 µM), ATRA (10 µM) and PMA (1 µM), and incubated at 37°C in a humidified atmosphere of 5% CO_2 for 3 days.

3.9.14 Differentiation Assay

Adherence of cells was determined following treatment with 30 µg of PMVs or heat-inactivated PMVs (65°C for 30 min). On the day of the experiment, $1x10^5$ cells/well were seeded into 12-well culture plates in triplicate. On each of the indicated days, the non-adherent cells were transferred into new plates and incubated at 37°C in a 5% CO_2 incubator. The wells were then washed twice with serum-free RPMI 1640 and the attached cells were released with trypsin/EDTA. The trypsinised cells, now in suspension were collected by centrifugation (200 *g*, 5 min), stained with ViaCount reagent and counted by flow cytometry.

To investigate differentiation, THP-1 cells were seeded into 24-well plates in triplicate. Cells were left untreated (control) or treated either with 30 µg PMVs or with PMA (1 µM) and incubated at 37°C in a humidified atmosphere of 5% CO_2 for

five days. After five days, cells still in suspension were removed and the plates were washed three times with RPMI 1640. Cells attached to the bottom of the plates were immuno-labelled at 4°C for 1 h with the antibodies, mouse anti-CD14-FITC, mouse anti-CD11b-PE or mouse anti-DC-SIGN-FITC with mouse-anti-IgG-FITC and mouse IgG-PE isotypes being used as controls. After three washes with PBS, cells were placed in PBS, 1% BSA and relative fluorescence determined using the FLUOstar Omega microplate reader.

3.9.15 Determination of Protein Concentration

The concentration of a protein solution was determined using the BCA Protein Assay Kit (Pierce, Thermo Scientific, UK). It uses a combination of the biuret reaction (reduction of Cu^{2+} ions to Cu^{+} ions by proteins in an alkaline medium) and the colorimetric detection of the Cu^{+} - cations by a bicinchoninic acid-containing colour reagent. Following the manufacturer's instructions, 10 µl of protein samples were diluted in double distilled water (ddH_2O; dilution 1:5) and added to 200 µl working solution consisting of a mixture of kit reagent A and reagent B (ratio 50:1 respectively). In parallel a dilution series of a 0.5 µg/µl BSA stock solution in ddH_2O were prepared and used as standard in later evaluation. Applied concentrations were 0, 62.5, 125, 250, 500, 750, 1,000, 1,500 and 2,000 µg/ml BSA in 500 µl ddH_2O. Volumes equal to samples were added to 200 µl of a mixture of kit reagent A and B (ratio 50:1) in a 96 well plate followed by incubation at 37°C for 30 min. After incubation at room temperature for 10 min to cool samples, A_{540} readings were taken on a FLUOstar Omega microplate reader. Protein concentrations of the unknown samples were determined by interpolation on a standard curve multiplied by a dilution of factor of 5.

3.9.16 Preparation of cell lysates

THP-1 cells ($1x10^7$) grown in culture flasks were sedimented by centrifugation (160 *g*, 5 min at 15°C). The pellet was washed once by careful resuspension in RPMI followed by centrifugation. After that, cells were counted using a haemocytometer and lysis was performed to give a protein concentration equivalent to $2x10^6$ cells/10 µl. If defined amounts of protein were required, the pellet was subjected to detergent based lysis followed by determination of total protein concentration using procedure for the BCA kit according to the procedure described under section 3.9.11. Briefly, cell lysis was performed by resuspension of the pellet in 0.2% Triton X-100 (w/v) containing protease inhibitor cocktail. To solubilise membrane proteins, samples were repeatedly pipetted and insoluble materials were sedimented by centrifugation (5,000 rpm, 5 min at 4°C, A-4-62 swing-out rotor, using 5810R centrifuge, Eppendorf). The total protein concentration was determined of the resultant supernatant and then subjected to SDS-PAGE analysis.

3.9.17 Sample preparation for SDS-Polyacrylamide Gel Electrophoresis (SDS-PAGE)

SDS sample buffer (4X) was added to samples in a ratio of 1:3 followed by incubation at 95°C for 4 min. Before loading the samples onto the gel, a centrifugation step was performed (2,000 *g*, 2 min) to collect all liquid at the bottom of the reaction microtube and loaded into the gel wells.

3.9.18 SDS-PAGE Protein Molecular Weight Standards

As a protein molecular weight standard, prestained Protein-Marker I (BioRad) was used. Prestained markers, ranging from 10 to 194 kD or 10 to 250 kD were used

when analysing gels by Western blot using the ECL detection system. Markers were applied by loading 5 µl into wells.

3.9.19 SDS-Polyacrylamide Gel Electrophoresis

To separate proteins, which were denatured by sodium dodecyl sulphate (SDS) according to their molecular masses, SDS polyacrylamide gel electrophoresis (SDS-PAGE) was performed as described (Laemmli, 1970) using the Mini PROTEAN III Electrophoresis System (Bio-Rad). Gels with dimensions of 102 x 73 mm and a thickness of 0.75 mm were cast between two glass plates by pouring freshly prepared 12% separating gel solution containing acrylamide/bisacrylamide into the gel cassette fixed in a casting frame. Unpolymerized separating gel solution was overlaid with H_2O-saturated butanol to achieve an even surface. After polymerization, H_2O-saturated butanol was poured off, washed twice with deionised water, and the excess water was blotted using a filter paper (Whatman 3 MM, Whatman AG). Then unpolymerized stacking gel was poured into the gel cassette and a plastic comb was inserted from the top, to form the loading wells in the stacking gel.

After polymerization, the gels were used immediately. To perform electrophoresis, the gel was placed into the electrode assembly device inside a clamping frame in the tank of the Mini PROTEAN III system. Electrophoresis running buffer was added to the inner and outer chambers of the tank and the plastic comb was carefully removed. Wells were washed with the running buffer to remove any free unpolymerized acrylamide/bisacrylamide. Samples were loaded into the wells of the stacking gel using extra long loading pipette tips. Electrophoretic separation was

performed at 150 V (constant voltage) until the bromophenol blue front of the SDS sample buffer reached the end of the resolving gel. Gels were either stained with Coomassie Brilliant Blue or transferred onto nitrocellulose membrane for Western blotting analysis.

3.9.20 Western Blotting Analysis

Proteins separated by SDS-PAGE were transferred to a Hybond C nitrocellulose membrane for further analysis using a semidry transfer device (Bio-Rad Sartoblot system). A Hybond C nitrocellulose membrane and two pieces of blotting paper (Whatman 3 MM, BioRad) were cut to the size of the separating gel. Blotting paper, nitrocellulose membrane and the sandwich-blotting cassette were equilibrated in Sartoblot buffer. One piece of blotting paper was placed on the cathode plate, and the nitrocellulose membrane was placed on top of the blotting paper. The gel was removed from between the sandwich-blotting cassette and placed on top of the membrane, and a second blotting paper was also placed on top of the gel. Having removed air bubbles, the anode plate, also dampened with the Sartoblot buffer was used to complete the sandwich. Electroblotting was carried at 15 V (constant voltage) for 1 h.

3.9.21 Reversible Ponceau Staining of Proteins

To verify successful protein transfer, hybond C nitrocellulose membranes were reversibly stained with Ponceau S solution (Serva Electrophoresis GmbH). The nitrocellulose membrane was incubated in 0.25% Ponceau S solution for 1 min. Subsequently, excessive Ponceau solution was washed away using deionised water until the protein bands became clearly visible. Marker bands were labelled using a

ball point pen and the membrane was completely destained following subsequent steps.

3.9.22 Immunochemical Protein Detection using the ECL System

Western blotting was performed as described above using hybond C nitrocellulose membrane (Amersham Biosciences). The membrane was incubated in blocking buffer for 1 h at room temperature or at 4°C, overnight, on a shaker. Following blocking, the membrane was rinsed with PBS-T and incubated with the primary antibody in the desired dilution for 1 h at room temperature on a shaker. Six 10 min washing steps with PBS-T were performed and the membrane was incubated with secondary goat-anti-rabbit IgG or goat-anti-mouse-IgG antibodies coupled to HRP in a 1:5000 dilution. After six 10 min washes with PBS-T on a shaker, visualization was performed using the enhanced chemiluminescence reagent system (ECL, Amersham Pharmacia). The ECL solutions (reagent A and B) were mixed at equal volumes and the membrane was incubated with the mixture for 1 min at room temperature and chemiluminescence was detected using UVP ChemiDoc-It system (UVP systems, UK).

3.10 Flow cytometry

The Guava flow cytometer allows complex biological studies such as cell counting and viability testing, white blood cell phenotyping, cytokine detection, cell activation marker analysis and other complex molecular analyses to be performed simultaneously. This saves time, but also generates accurate results, which comes much closer to mimicking the complex biological responses within the body. The Guava flow cytometer can be used to perform ten different assays; however, for

these studies only three assays were implemented. These were the ViaCount assay (for counting cells and determining viability), ExpressPlus assay (for cell activation marker analysis, cytokine expression, microvesicle analysis and studies on protein-protein interaction) and Nexin assay (for reporting apoptosis).

3.10.1 Cell counting and viability assessment

Cell number and viability were determined using the ViaCount assay, which distinguishes between viable and non-viable cells based on the differential permeabilities of two DNA-binding dyes in the Guava ViaCount reagent. The nuclear dye only stains nucleated cells, while the viability dye brightly stains dying or dead cells. This proprietary combination of dyes enables the Guava ViaCount assay to distinguish viable, apoptotic and dead cells. Cell debris is excluded from results based on negative staining with the nuclear dye.

3.10.2 Parasite labelling

T. cruzi (8.7 x 10^7 parasites) was labelled with the red membrane-dye, pKH26GL. Parasites, resuspended in sterile PBS were mixed in a 1:1 ratio with pKH26GL-dye (4 µM), which had been diluted in a diluent provided by the manufacturer to a 1 ml reaction volume. The mixture was incubated at RT for 5 min with shaking. After 5 min incubation, reaction was stopped by addition of an equal volume of BSA in PBS and incubated at RT for 1 min. Complete medium containing 10% FBS in RPMI was added and the mixture was centrifuged at 4,000 rpm for 10 min (A-4-62 swing-out rotor, using 5810R centrifuge, Eppendorf) to pellet parasites. Parasites were resuspended in PBS and centrifuged a further 4 times to wash away unbound dye, before addition to experiments.

3.10.3 Cell labelling

HeLa cells were labelled with Annexin V AlexaFluor 488 (Invitrogen), at RT for 15 min with shaking. Annexin V AlexaFluor 488 was diluted in a binding buffer (see section 3.7) and used at 10 µg/ml according to the manufacturer's instructions. Cells were washed three times with serum-free RPMI prior to experiments.

In some experiments, semiconfluent HeLa cells were labelled with anti-LAMP-1 AlexaFluor 488 (1 µg/10^6 cells) at 4°C for 1 h with shaking. Labelled cells were washed three times with serum-free RPMI prior to use in experiments. To study membrane repair mechanisms, HeLa cells were also labelled with 50 µg/ml of propidium iodide (PI) at RT for 1 min prior to fixation with 4% paraformaldehyde.

3.10.4 Immunofluorescence staining for cytokines

In order to determine the expression of cell activation markers as well as surface and intracellular cytokines by specific antibody staining, cells were processed according to the following protocol and analysed using flow cytometry. Cells were harvested, washed by centrifugation at 200 *g* for 5 min and total cell number and viability (usually >95%) was determined using ViaCount reagent (refer to 3.10.1). Cells were usually stained in eppendorf tubes and later transferred into a 96-well microtiter plate for analysis on the flow cytometer; however, they can also be stained in polystyrene round-bottom, 12 x 75 mm Falcon tubes.

Cell surface expression of TGF-β1, MIF, FGF-1 and Gal-3 molecules was analysed by flow cytometry (EasyCyte, Guava Technologies, UK). THP-1 cells (2 x 10^6) were washed twice (200 *g*, 5 min each) with PBS and resuspended in cold PBS containing 10% FBS and 1% NaN_3. Cells were incubated in the dark with primary

antibodies (2 µg/million cells, R&D systems, UK) against tested molecules at 4°C for 1 h with shaking. After three washes (400 *g*, 5 min), cells were stained with the isotype-matched controls (anti-mouse or anti-rabbit IgG-FITC, R&D systems) diluted 1:320 in PBS with 3% BSA and incubated with shaking, in the dark, at 4°C for 1 h. Cells were again washed three times with cold PBS, resuspended in 200 µl of PBS containing 3% BSA, 1% NaN_3 and analysed immediately using a flow cytometer and the ExpressPlus assay program.

For staining of intracellular cytokines, THP-1 cells ($2x10^6$/ reaction) in triplicate were resuspended in permeabilisation buffer (PBB) (0.5% Tween 20 in PBS) at room temperature for 20 min. Cells were permeabilised by washing three times with PB and incubated with 2 µg of primary antibodies at 4°C for 1 h in PBS with 10% FBS/ 1% NaN_3. Cells were washed three times and incubated with IgG-FITC-labelled secondary antibodies (4°C, 1 h), and again washed three times with PBS. Samples were resuspended in 200 µl each of PBS containing 3% BSA, 1% NaN_3 and analysed immediately by flow cytometry.

3.10.5 Immunofluorescence followed by induction of PMVs

To further investigate the notion that PMVs carry cytokines from the cell upon release, surface and intracellular immunostaining experiments were repeated in duplicate. Briefly, $1x10^7$ cells/reaction were washed as mentioned earlier and resuspended in PBS containing 10% FBS only. For intracellular staining, cells were first permeabilised with PBB at RT for 20 min. Cells were labelled with primary (10 µg/reaction) and secondary antibodies (1/320 dilution) according to steps described earlier. Antibody-labelled cells were resuspended in prewarmed PBS supplemented

with 2 mM $CaCl_2$ and stimulated to microvesiculate by addition of 10% NHS. After incubation at 37°C for 30 min, PMVs were isolated as described under section 3.9.2. Purified PMVs were analysed on the Guava EasyCyte flow cytometer for cytokines using appropriate antibodies and IgG-FITC as negative control.

3.11 Fluorescence microscopy

For fluorescent microscopy analysis, non-adherent cell samples were placed into 12-well plates containing coverslips by centrifugation (200 *g*, 5 min, with A-2-DWP rotor, using 5804R centrifuge, Eppendorf), and fixed with 4% paraformaldehyde at 37°C for 10 min. Plates were gently washed twice with PBS and coverslips were mounted on microscope slides with DAPI-VECTASHIELD medium (Vector Laboratories Inc. Burlingame, CA) for fixed cells and mounting medium (Agar Scientific, Essex, UK) for fixed PMVs. Images were collected using fluorescence microscope (1X81 motorized inverted fluorescence microscope, Olympus Corporation). Adherent cells, cultured on coverslips were fixed with 4% PFA and mounted on microscope slides with DAPI-VECTASHIELD medium.

3.12 Electron microscopy

3.12.1 Sample preparation for EM analysis

All processing steps were carried out in a fume cupboard, as hazardous chemicals were being used. THP-1 cells ($5x10^6$/ml, usually > 95% viability) were washed twice with RPMI and resuspended in fresh prewarmed (37°C) RPMI supplemented with 0.5 mM $CaCl_2$ in 15 ml centrifuge tubes. Cells were either stimulated or not (control) with 5% normal human serum (NHS) and incubated shaking in a waterbath (37°C, 30 min). After 30 min incubation, cells were fixed by the addition of 1 ml of 0.1 M

fixative solution (3% glutaraldehyde in 0.1 M sodium cacodylate buffer pH 7.2) and incubated at for 1 h. Fixed cells were harvested by low speed centrifugation (300 *g*, 5 min, with an A-4-62 swing-out rotor, using 5810R centrifuge, Eppendorf). Prior to post-fixation, pelleted cells were transferred into 1.5 ml microtubes and washed twice with 0.1 M sodium cacodylate buffer pH 7.2 using a microcentrifuge (300 *g*, 5 min). Samples were post-fixed by incubation at 0°C for 1 h in 1% osmium tetroxide solution (2% osmium tetroxide (Sigma-Aldrich) 1:1 0.2 M sodium cacodylate buffer), followed by three washes with deionised water and block stained by resuspending in 1% aqueous uranyl acetate (overnight on a rocker). They were then washed twice with deionised water and resuspended in 1% hot agarose. Cells were pelleted by centrifugation (5,000 *g*, 5 min) before the agarose solidifies.

When cool, the agarose embedded pellets were removed from the 1.5 ml microtubes and then cut into smaller pieces and placed into a 10 ml glass vial for subsequent processing. They were dehydrated in an ascending ethanol series (from 70% to 100% absolute ethanol, v/v, Sigma-Aldrich, 30 min each time) and washed twice (30 min each) with propylene oxide (Agar Scientific, Essex, UK). The propylene oxide was removed, and the pellets were infiltrated with a 1:1 mixture of propylene oxide: Agar resins (mixture of 4.8 g agar resin, 3.6 g MNA, 1.9 g DDSA and 0.2 g BDMA, Agar Scientific, Essex, UK) and left rocking overnight at room temperature. Infiltrated samples were changed twice with 100% agar resins (1 h, RT) and embedded in capsules using applicators. Finally these samples were polymerised at 60°C for 24 h.

In other experiments, pure isolated PMVs and exosomes were separately fixed and infiltrated with agar resin. The polymerised blocks were sent for cutting, staining, examination and image capture at the London School of Hygiene and Tropical Medicine (LSHTM), Electron Microscopy Unit. Ultra thin sections were cut on a Leica Ultracut R ultra microtome and picked up onto Pioloform film copper grids. The sections were then stained for 10 min in Reynolds Lead Citrate stain [231] before washing in ultrapure MilliQ water and examining on a Jeol JEM – 1200 Ex II Electron Microscope. Digital images were taken with a 1K, side mounted AMT Digital camera (Advanced Microscopy Techniques Corp. 3 Electronics Ave., Danvers, MA 01923 USA, supplied by Deben UK limited, IP30 9QS).

3.12.2 Negative staining

Pure isolated PMVs and exosome samples for Negative staining were also taken to the EM Unit at the LSHTM and stained with 2% aqueous uranyl acetate or 2% PTA (phosphotungstic acid) pH 6.8 + aqueous Bacitracin (300 µg/ ml diluted 1:10 in the negative stain acts as a spreading agent). Using fine tipped Watchmaker forceps to handle the 400 mesh copper grids with a pioloform support film (Grids and Pioloform powder from Agar Scientific Limited, Essex CM24 8DA), the grids were pre-treated with 1% aqueous Alcian Blue 8GX for 10 minutes before rinsing in MilliQ water. 5 µl of the sample (exosomes and PMVs) were placed on the grids for 1 min. This was then removed by touching the grid edge with a strip of filter paper and replaced with 5 µl of the stain for a further 1 min. The stain was then removed in the same way and the grid was allowed to air-dry, before examination on the Transmission Electron Microscope. Digital images were recorded using the AMT digital camera previously described for the examination of stained ultrathin sections.

3.13 Quantitation of cytokines by ELISA

PMVs were isolated from THP-1 cell-depleted conditioned media or from THP-1 cells stimulated with 10% NHS at 37°C for 30 min. The concentrations of TGF-β1, MIF, FGF-1 and Gal-3 were measured by using 30 µg of protein in ELISA kits (R&D Systems) according to the manufacturer's instructions. In some experiments, PMVs ($1x10^5$/ reaction), in triplicate, from THP-1, Jurkat and MCF-7 cells were lysed before measuring cytokine levels.

3.14 Human Cytokine Array (R&D Systems)

3.14.1 Principles of the assay

For this assay, the nitrocellulose membrane provided in duplicates with carefully selected capture antibodies spotted on it was used. The sample under investigation (i.e. serum, plasma or cell culture supernatants) was appropriately diluted and mixed with a cocktail of biotinylated detection antibodies and the sample/antibody mixture then incubated with the Human Cytokine Array. The cytokine/detection antibody complex then binds to its cognate immobilised capture antibody on the membrane, and any unbound material was removed by washing. Following the addition of Strepavidin-Horseradish Peroxidase and chemiluminescent detection reagents, light produced at each spot was in proportion to the amount of cytokine bound, which was measured using an absorbance plate reader.

3.14.2 Protocol

All reagents and samples used were brought to room temperature prior to use. Following the manufacturer's (R&D Systems) instructions, 2 ml of Array Buffer 4

(AB4) (block buffer, provided in kit) was pipetted into each well of a 4-well multi-dish and membrane containing the capture antibodies was placed into each well with the array number facing up. The membranes were incubated at RT for 1 h with shaking. Samples were prepared whilst membranes were incubating by adding 1 ml of each sample to 0.5 ml of AB4. To this mixture, 15 µl of reconstituted Cytokine Array Panel A Detection Antibody Cocktail was added, mixed and incubated at RT for 1 h. Array Buffer 4 was aspirated from the wells of the 4-well multi-dish and the sample/antibody mixture prepared earlier was added and incubated overnight at 4°C with shaking.

After overnight incubation, each membrane was carefully removed, placed into individual containers and washed three times with PBS wash buffer for 10 min on a rocking platform. The 4-well multi-dish was washed with deionised water and dried thoroughly. Strepavidin-HRP (provided in kit) was diluted in Array Buffer 5 (also provided in kit) 1/200 according to the manufacturer's instructions and 1.5 ml was added into each well of the 4-well multi-dish. After draining off excess buffer, membranes were returned from its wash container to the 4-well multi-dish containing the diluted Strepavidin-HRP. The dish was covered and incubated at RT for 30 min with shaking. After 30 min incubation, each membrane was washed as described earlier and incubated with chemiluminescent detection reagent. Excess reagent was blotted off the membrane onto absorbent paper and covered with a plastic wrap. After gently smoothing out air bubbles, wrapped membranes were examined using the UVP Chemi-Doc-it.

3.15 Correlation Analysis

For correlation analysis, experiments were carried out as described in sections 3.9.6, 3.9.6.1, 3.9.6.2 and 3.9.8. Data were plotted and analysed using GraphPad Prism.

3.16 Statistical Analysis

Statistical analysis for all data presented was performed by the unpaired *t*-test for repeated measures using GraphPad Prism version 5.00 for Windows (GraphPad Software, San Diego, USA). Statistical correlations between data values were also determined using GraphPad Prism software. Differences giving a value of $P < 0.05$ with confidence interval of 95% were considered statistically significant.

4. Flow cytometry analysis and characteristics of PMVs: how they differ from other vesicles

4.1 Introduction

The number of publications on plasma membrane-derived vesicles (PMVs) in recent times has increased exponentially, as many groups continue to investigate novel functions for these vesicles. However, the terminologies used by various researchers for describing these microvesicles, suggest that, some confusion still exists in differentiating between these PMVs, sometimes referred to as microparticles (MPs), and other vesicles released from cells. Different groups are isolating exosomes and referring to them as MPs, but a recent review article [1], shed further light on the difference between the two types of vesicles. Apart from the obvious size difference between PMVs and exosomes, one of the most distinguishing features, as discussed in the introduction of this thesis, is the peculiar cup-shaped phenotype of exosomes [232].

A report in 2002 [98], described the transfer of cell surface CD81, a coreceptor for B and T cells via MPs to acceptor U937 promonocytic cells. However, the centrifugation procedure used for MP purification probably accounts for a selection of the smallest microvesicles present in the preparation (30-90 nm), thus possibly containing mainly exosomes. They correctly discussed that the reduction of surface CD81 was due to endocytosis of the molecule and subsequent release through exosomes, via fusion of multivesicular bodies (MVBs) with the plasma membrane. However, they referred to these exosomes, as microparticles, a term generally used for PMVs. In this thesis, the term PMVs will be used when referring to vesicles, released by surface budding from the plasma membrane. The term exosomes will be used for vesicles, released through fusion of MVBs with the plasma membrane and MVs, when referring to both PMVs and exosomes. Experiments to be discussed

later in this thesis were designed to understand some of the mechanisms involved in the release of PMVs and possibly elucidate functions not previously described.

It was previously shown [121] that nucleated polymorphonuclear leukocytes (PML) were more able to recover from stimulation with sublytic complement than erythrocytes. Subsequent reports showed that the ability to resist complement-mediated lysis was due to removal of the membrane attack complex (MAC), from the cell surface [233-235]. Hitherto, it had been observed that stimulation of cells with sublytic complement resulted in an increase in cytosolic Ca^{2+} levels, which can be inhibited with EGTA [121]. Reports, which later followed mentioned that cells released PMVs after stimulation with C5b-9, a complex of proteins formed by the lytic pathway, during complement activation. This phenomenon, also observed in erythrocytes, has been proposed as a defense mechanism to protect cells from complement-mediated lysis [236;237].

The purpose of this study was partly to isolate PMVs effectively and to elucidate other distinguishing properties from exosomes. To achieve this, two independent experimental systems were used, namely, the characterisation of PMVs by flow cytometry and secondly, the investigation of their composition and function.

4.2 Characterisation of Plasma Membrane-derived Vesicles

4.2.1 Growth pattern of THP-1 monocytes

Initial experiments performed looked to determine the growth pattern of THP-1 cells in culture over a period of five days. This was pertinent, as most of the investigations

would require cells harvested from the exponential phase. This was already well established for the other cell lines under investigation, by the groups from which they were received as kind gifts. THP-1 cells were used in most experiments to characterise the structure and composition of PMVs. Their normal growth pattern in the presence of different amounts of serum was investigated.

Briefly, THP-1 cells ($1x10^5$/well) with >95% viability as determined by Guava ViaCount, were washed twice by centrifugation (160 *g* for 5 min), resuspended in the required amount of foetal bovine serum (FBS) and seeded into a 12-well plate in triplicate. The plate was incubated at 37°C in a 5% CO_2 humidified incubator for five days and the number of cells counted every day.

The result presented shows that cells grow better in higher amounts of FBS over the five-day period (**Fig. 4.1**). Perhaps what is more interesting is the fact that all the cells, regardless of growth condition doubled in numbers by day 3 and gradually decreased subsequently. Also, cells cultivated in higher amounts of FBS (5% and 10%) survived longer over the 5 day period, than those cultured in lower amounts (1% and 2%). This result suggests that THP-1 cells enter into an exponential phase on the third day of culture and have increased survival rate at serum concentrations between 5% and 10%. This experiment was repeated four times with very similar results. Knowing the growth patterns, exponentially growing cells were used for all subsequent experiments discussed in this report. Cell culture media used for isolation of PMVs were also collected from exponentially growing cells. PMVs were isolated according to the protocol described earlier (see materials and methods, section 3.9.1) and analysed using flow cytometry.

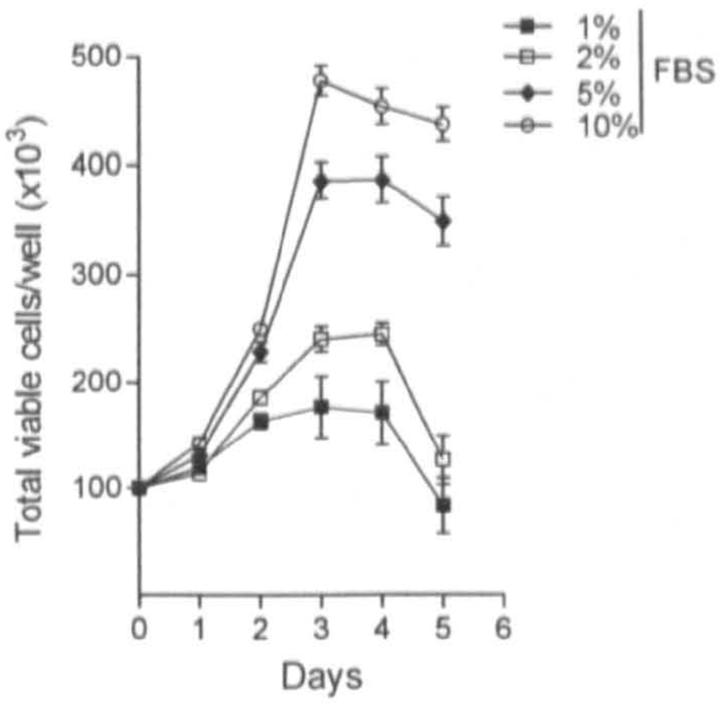

Figure 4.1 Growth pattern of THP-1 cells

THP-1 cells (1x10^5/well) were cultured in different amounts of FBS. Cells were seeded into 12-wells in triplicate and cell number was determined everyday using ViaCount reagent (ViaCount assay). Cells placed in 5% and 10% FBS show the quickest growth rate compared to ones in 1% and 2% FBS. Under all conditions cell number at least doubles by day 3. Values represent the means ± SD of triplicate experiments. This experiment was repeated four times with similar results.

4.2.2 Sublytic complement and the release of PMVs

Reports from several investigators have suggested that sublytic levels of complement can stimulate the release of PMVs from different cell types. In order to further enhance the procedure for isolating PMVs, experiments were set up to investigate the role of sublytic complement levels in the induction of these vesicles. THP-1 cells ($1x10^6$/well), resuspended in prewarmed (37°C) serum-free RPMI medium with 0.5 mM $CaCl_2$, were seeded in triplicate in a 24-well plate and stimulated with increasing concentrations of normal human serum (NHS; 2.5%, 5% and 10%) or 5% heat-inactivated (56°C for 1 h) NHS (NHS-HI). Wells containing cells only without NHS (non-induced, NI) were used as negative controls. Released PMVs, were isolated by differential centrifugation of THP-1 cell-depleted conditioned medium (see materials and methods, section 3.9.1) and analysed by flow cytometry.

Indeed, sublytic complement levels, in the form of NHS, induced release of PMVs. The number of PMVs released by the cells increased with higher amounts of NHS, suggesting a dose response. Not surprisingly, 5% NHS-HI failed to stimulate higher levels of PMVs (**Fig 4.2A**), as compared to native serum at the same concentration. Since PMVs are also released constitutively by various cells, there was a possibility that, the vesicles being detected in this experiment were sourced from the NHS. To show that PMVs isolated in this study were actually from cells and not sourced from NHS, human AB serum without cells was centrifuged in the same way as for conditioned medium from cells stimulated with NHS. PMVs were present in the cell-free AB serum, but at significantly lower levels than in the cell supernatants (**Fig. 4.2B**).

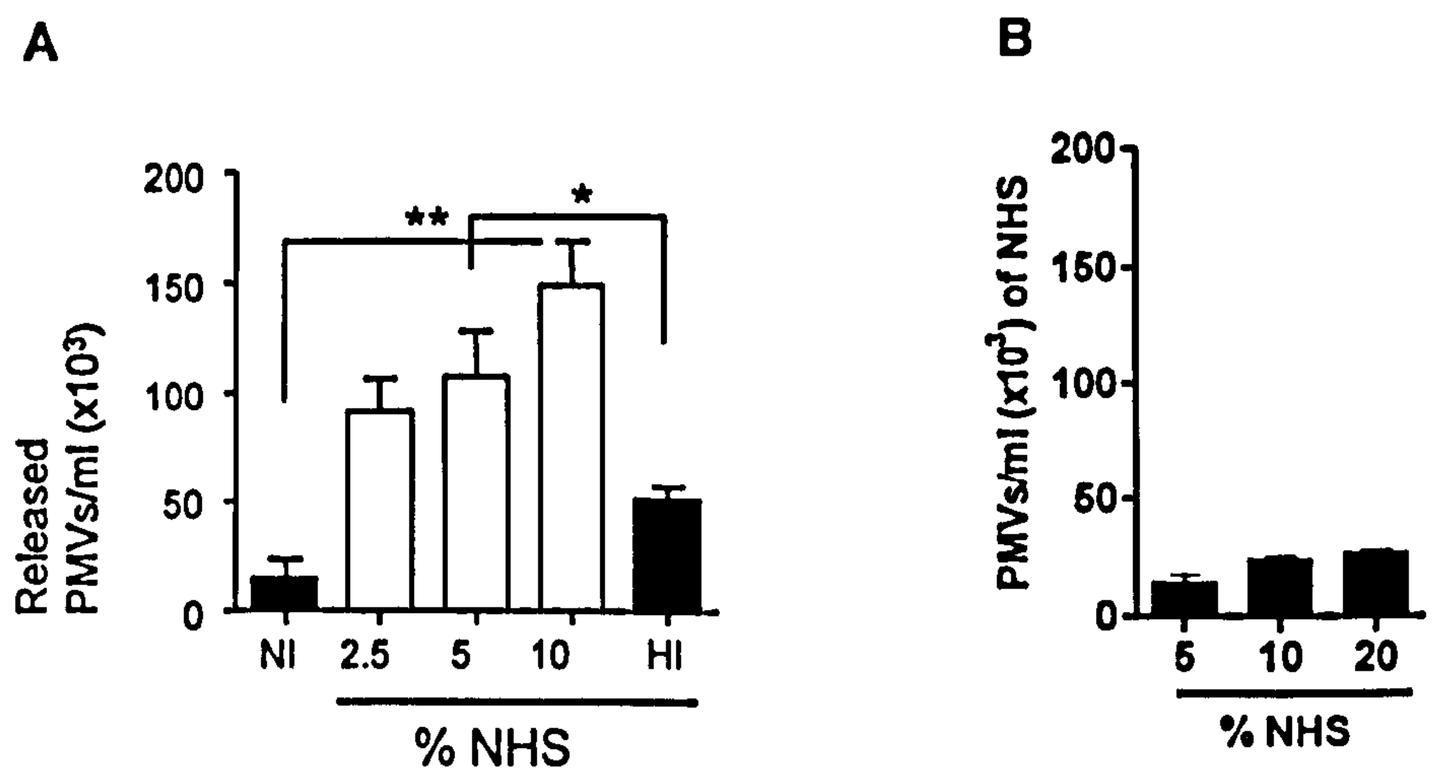

Figure 4.2 Sublytic complement levels can stimulate release of PMVs.

(A) THP-1 cells ($1x10^6$/well) in triplicate were left non-induced (NI) or stimulated at 37°C for 30 min with increasing amounts of NHS (2.5%, 5% and 10%) or with 5% heat-inactivated (56°C for 1 h) NHS (NHS-HI). (B) Addition of NHS (5%, 10% and 20%) to cell-free RPMI to quantify PMVs originally present in the serum. In both experiments, PMVs were isolated by differential centrifugation at 4,000 *g* and 25,000 *g* for 1 h and 2 h respectively. Values represent the means ± SD of a triplicate experiment. This experiment was repeated three times with similar results. $^{**}P < 0.01$, $^{*}P < 0.05$ were considered statistically significant.

4.2.3 Flow cytometry analysis and annexin V labelling of isolated PMVs

PMVs were isolated by differential centrifugation of THP-1 cell-depleted conditioned medium (described in materials and methods, section 3.9.1) and analysed by flow cytometry. The vesicles were identified by their size and granularity, as assessed by the logarithmic amplification of forward (FSC) and side scatter (SSC) signals, respectively (**Fig. 4.3A**). As indicated by the dot plot distribution, PMVs, localised within the R1 region, are heterogeneous in size and granularity.

Phosphatidylserine expression on the membrane surface indicates the loss of lipid membrane asymmetry, and this is the main characteristic of cells undergoing early apoptosis. However, during release of PMVs, the loss of cell asymmetry, results in inversion of the two membranes on the vesicles. PC and sphingomyelin carried on the outer leaflet are inverted inwards, while PE and PS in the inner leaflet are exposed on the external surface. Using flow cytometry, isolated PMVs from THP-1 cells and primary monocytes were found to express PS on the outer leaflet by staining with annexin V-FITC as described in section 3.9.5 (**Fig. 4.3B**). Annexin V (AnV) staining to detect PS exposure was repeated for PMVs isolated from other cell types and found to correspond with values reported here (not shown).

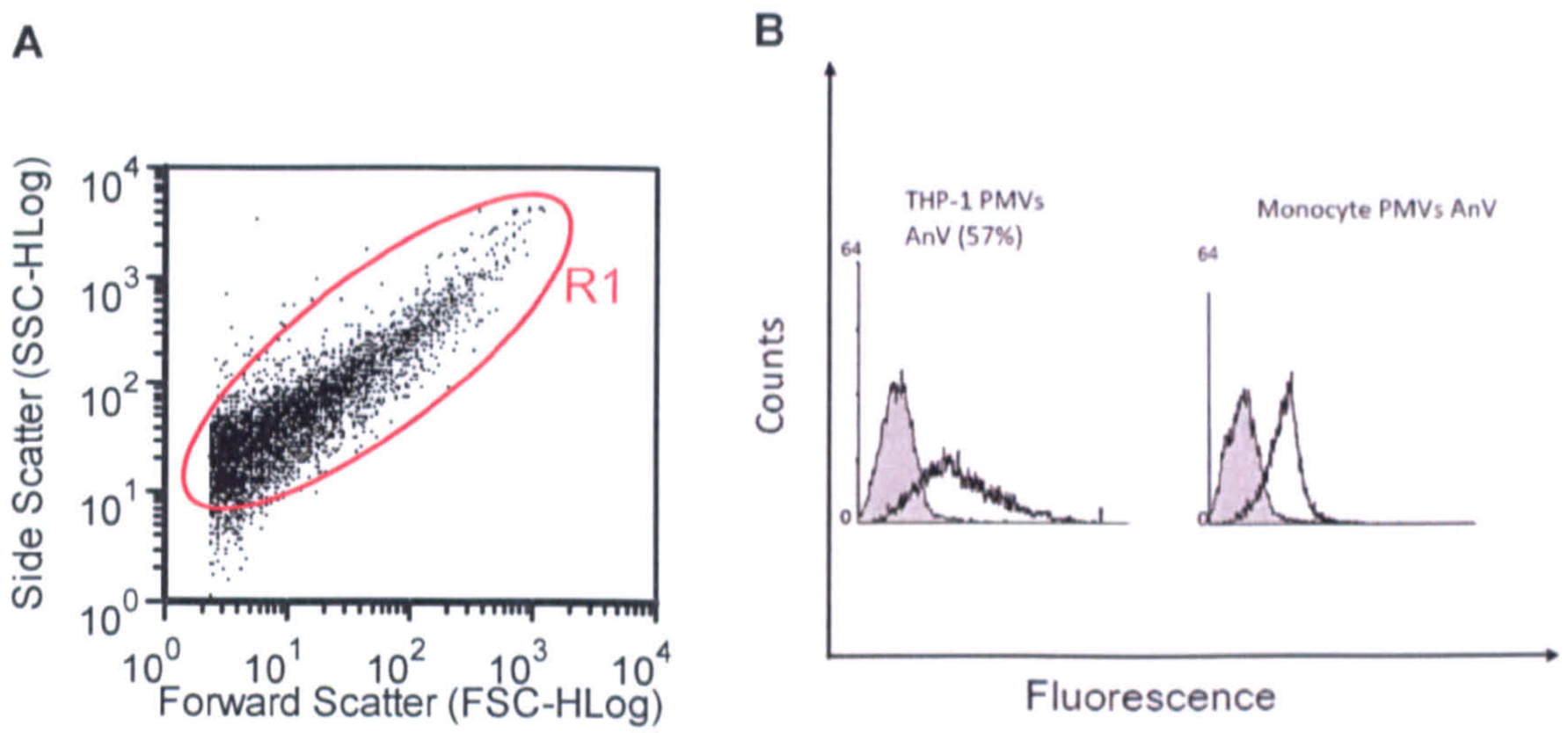

Figure 4.3 Flow cytometry of isolated PMVs.

(A) Representative dot plot distribution of PMVs on a flow cytometer. Plot shows forward scatter (size) and side scatter (granularity). PMVs are heterogeneous in size and the region, R1, represents the FSC/SSC scatter gate of the vesicles. (B) Isolated PMVs were analysed for PS expression by staining with annexin V (AnV)-FITC. The resulting histograms show approximately 57% of labelled PMVs from THP-1 cells and 54% from primary monocytes to be AnV-FITC positive. Unlabelled PMVs, shown in grey were used as negative controls. All experiments were repeated several times, with similar results.

4.2.4 Release of PMV is via a mechanism independent of apoptosis

Due to the expression of PS on the surface of PMVs, one might speculate that release of these vesicles, is simply a response to apoptosis. Also since apoptotic cells release PMVs themselves, it could be that the isolated vesicles are in fact apoptotic bodies. As mentioned earlier, apoptotic bodies express PS on the outer leaflet to help facilitate their recognition and clearance by phagocytic cells. Since Annexin V can also bind PS expressed by apoptotic bodies, experiments were performed to examine whether the release of PMVs was simply due to the onset of apoptosis, resulting in the release of apoptotic bodies. To investigate this, THP-1 cells ($1x10^6$/ml) in triplicate were seeded into a 24-well plate and stimulated with 5% NHS. Cells were collected at regular time intervals and stained for Annexin V-FITC binding and the percentage of cells undergoing apoptosis was also determined by flow cytometry. Supernatant was also collected at each time point and analysed for released PMVs.

Results showed that some cells undergo apoptosis during the release of PMVs, thus exposing higher levels of PS with time. However, the increase in PS exposure correlates with the release of PMVs; and this is at maximum after 20 min incubation. However, apoptosis remained at a low level and constant throughout the experiment (**Fig. 4.4A**). After 1 h stimulated cells were washed (160 *g*, 5 min) once with serum-free RPMI medium resuspended in fresh growth medium and incubated at 37°C. Cells were analysed after incubation for a further 30 min, 45 min and 60 min to detect apoptosis, through binding of annexin V-FITC to the plasma membrane together with analysis of released PMVs.

Strikingly, the levels of apoptosis, annexin V binding and release of PMVs, returned to control levels (time 0) (**Fig. 4.4B**). This means that the cells were not at the point of no return in terms of apoptosis and so the process was reversible. The release of PMVs is therefore via a mechanism different from apoptosis.

4.2.5 PMVs contain proteins characteristic of their parental cell.

A common property of PMVs is that they contain numerous proteins, lipids and cytoplasmic constituents, characteristic of their parental cell. PMVs were isolated from THP-1 cells and their protein profile compared with the original cell. Protein concentration of a THP-1 cell lysate (30 µg) or of isolated PMVs (after stimulation with 2.5%, 5% and 10% NHS), was measured with the BCA assay kit (Pierce) as described in section 3.9.11. Samples were prepared and subjected to SDS-PAGE analysis.

PMVs shared a similar protein profile with their parental cell (**Fig. 4.5A**). In addition, levels of actin, an important constituent of the membrane cytoskeleton, increased in the PMVs, as compared with parental cells. The presence of actin was identified by trypsin digestion of the band, after SDS-PAGE analysis and further assessment was performed by MALDI-TOF. Furthermore, actin levels also remained the same in the PMVs, even under increasing extracellular stimulus. In addition to MALDI-TOF analysis, presence of actin in PMVs was further confirmed by Western Blotting analysis. Complement regulatory proteins, decay accelerating factor (DAF) and complement receptor-1 (CR1), were also identified by Western Blotting in the isolated PMVs (**Fig. 4.5B**).

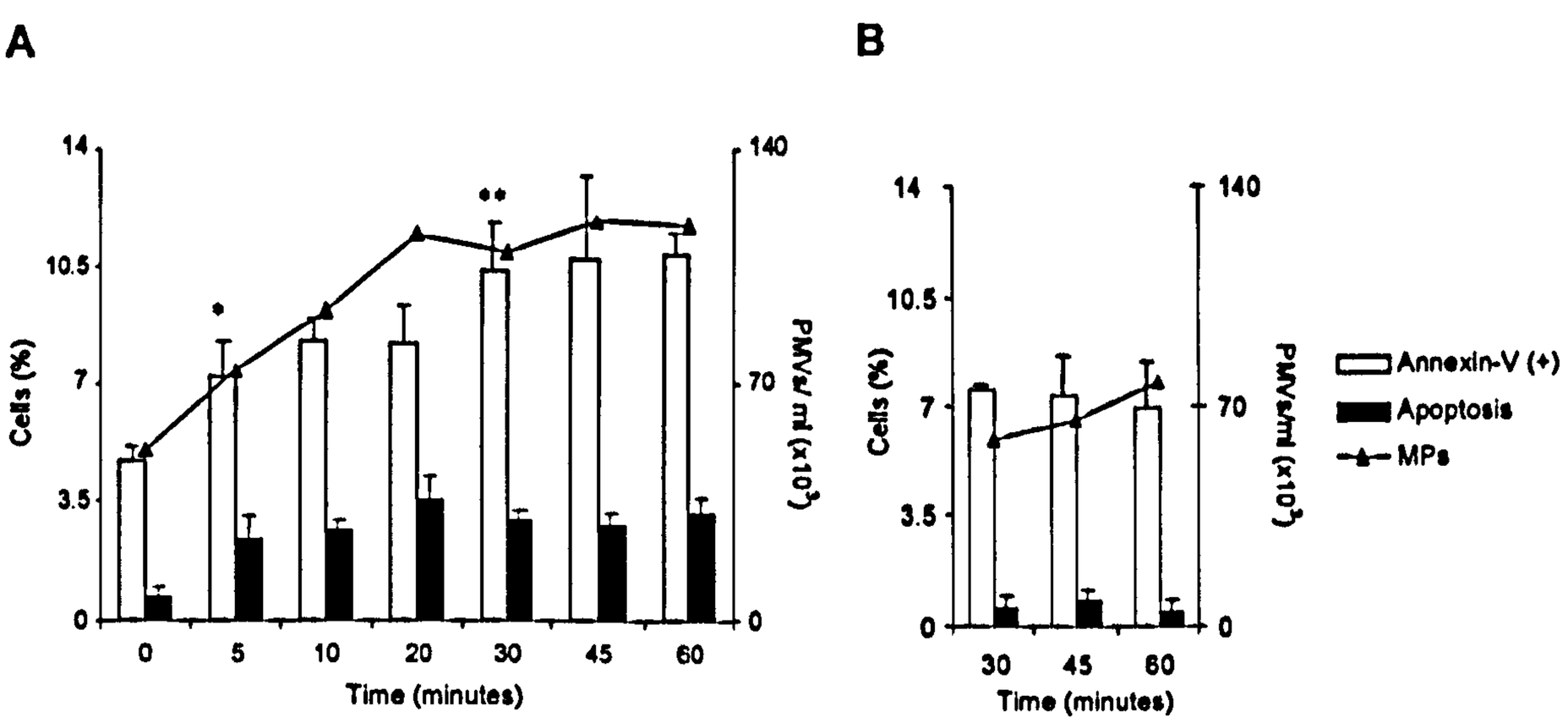

Figure 4.4 Release of PMVs is different from apoptosis.

Release of PMVs was not entirely dependent on cells undergoing apoptosis. (A) PS exposure on the cell surface as assessed by annexin V binding increases to significant levels after 30 min of stimulation without much change in levels of apoptosis (Nexin assay, Guava Technologies). A maximal number of PMVs (MPs) was released after 20 min and did not change up to 1 h incubation. (B) PS exposure and the number of PMVs released returned to normal levels when cells were suspended in fresh medium and incubated. Values shown are the means ± SD of two independent experiments performed in triplicate. $^{**}P < 0.01$; $^{*}P < 0.05$ were considered statistically significant.

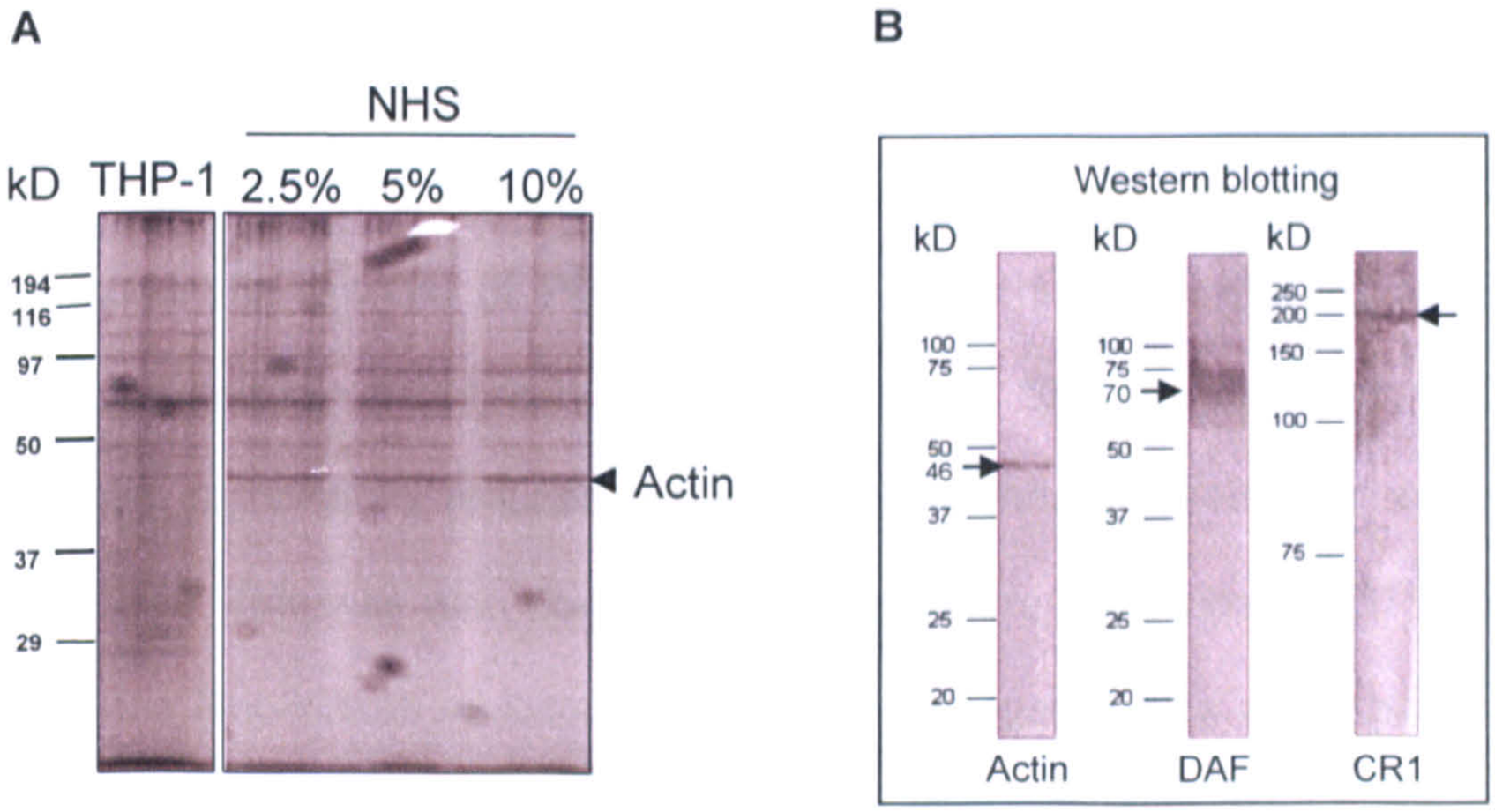

Figure 4.5 Protein profile of THP-1 cells and THP-1 cell derived PMVs.

(A) SDS-PAGE confirmed a similar protein profile for PMVs and the THP-1 cells from which they were isolated. A 46 kD band identified as actin by MALDI-TOF was present at higher levels in the PMVs after stimulation with NHS. (B) Western blot analysis confirmed the presence of actin, DAF (70 kD band) and CR1 (200 kD band) in isolated PMV lysates.

4.2.6 Different agents inhibit the release of PMVs in the presence of NHS

To further understand the mechanisms leading to the release of PMVs and so authenticate their origin, the next experiments concentrated on inhibiting their release. Different groups have reported the use of EGTA, a calcium chelator in reducing the amount of PMVs released by platelets. In this study, EGTA also inhibited release of PMVs in the cell-lines tested. Similarly, calpeptin, an inhibitor of calpain, significantly reduced the number of PMVs released after stimulation with 5% NHS. This was also observed after cells were preincubated (37°C for 45 min) with the Rho-kinase inhibitor, Y-27632. These agents, plus a combination of both, completely abrogated the release of PMVs after activation. EGTA, mentioned here to inhibit the release of PMVs, was used as a negative control (**Fig. 4.6A**).

Some reports have suggested that activation of raft domains could be associated with the release of PMVs, [238] and so in this study inhibitors of lipid rafts and endocytosis were also investigated. Pretreatment of THP-1 cells ($1x10^6$/well in triplicate) with 5 mM methyl-β-cyclodextrin (MβCD, the cholesterol-depleting agent) abrogated PMV release after induction of cells with NHS. However, filipin (the agent which sequesters cholesterol) and chlorpromazine (an inhibitor of endocytosis via clathrin-coated pits) actually caused slight increase in the amount of PMVs released by THP-1 cells. However, neither of these agents induced release of PMVs when used alone without normal human serum (**Fig. 4.6B**).

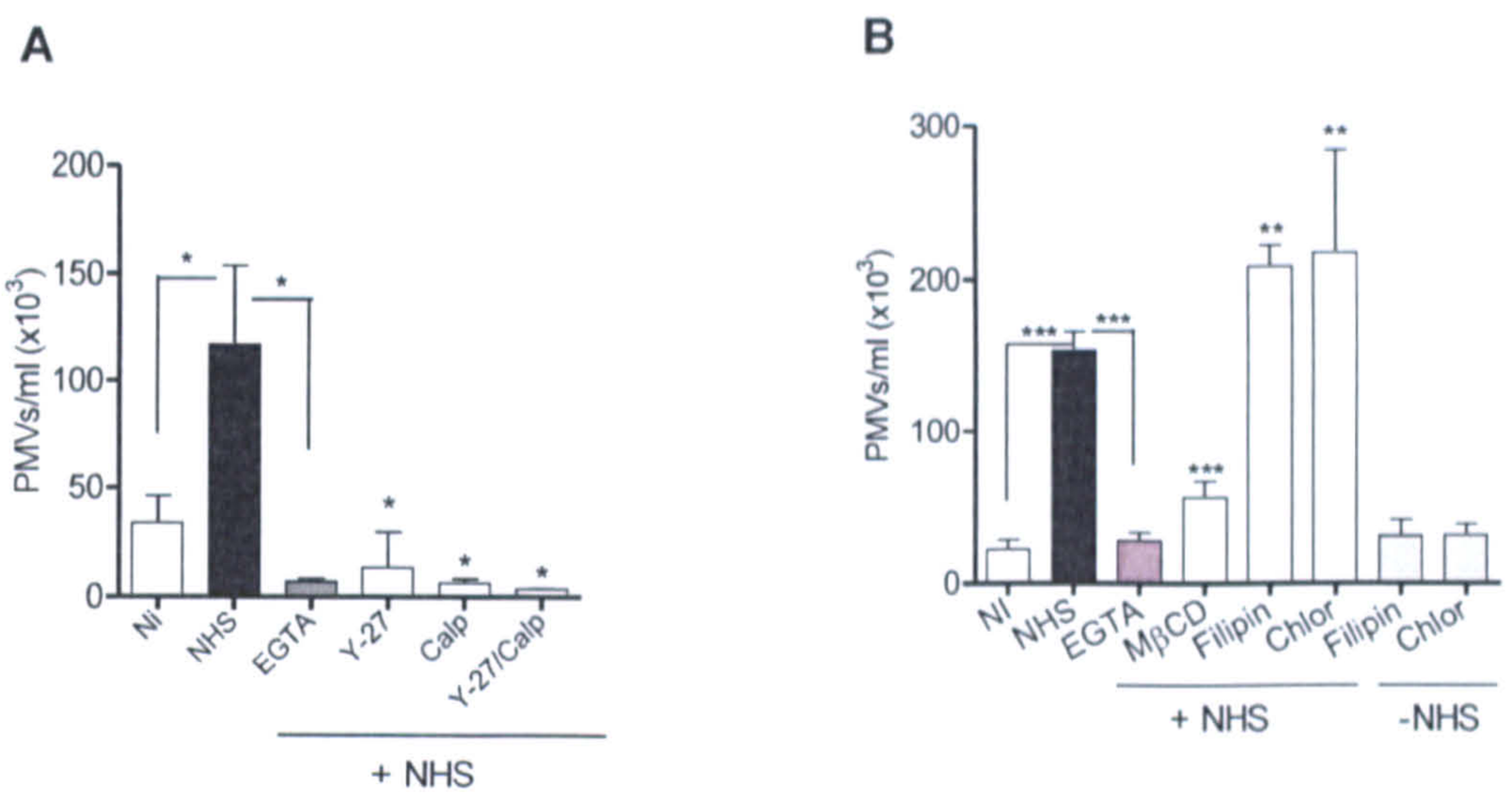

Figure 4.6 Inhibition of PMV release

(A) The release of PMVs is inhibited after preincubation (37°C, 45 min) of THP-1 cells ($1x10^6$/well) with Y-27632 (Y-27) (a Rho-kinase inhibitor, 10 μM), calpeptin, calp, (inhibitor of calpain, 20 μM) or with both. (B) THP-1 cells were also preincubated (37°C, 45 min) with the cholesterol-depleting agent, MβCD (5 mM), the cholesterol sequestering agent, filipin (5 μg/ml), or the endocytosis inhibitor, chlorpromazine, chlor, (25 μg/ml). Cells were stimulated by addition of 5% NHS and EGTA (5mM) was used as negative control. Data presented are mean ± SD of three independent experiments performed in triplicate. ***$P < 0.001$; **$P < 0.01$; *$P < 0.05$ were considered statistically significant.

4.2.7 Transmission electron microscopy (TEM) analysis of PMVs

To further support the protocols being used in the isolation of PMVs, THP-1 cells were prepared for transmission electron microscopy according to the method of Robert Durmashkin (personal communication). Images were taken at the London School of Hygiene and Tropical medicine (LSHTM). The objective was to be able to visualise release of the vesicles upon stimulation with NHS. Briefly, THP-1 cells left untreated (**Fig. 4.7A**) or stimulated with 5% NHS at 37°C for 30 min (**Fig. 4.7B**), were fixed immediately with glutaraldehyde and processed to Agar resin for transmission electron microscopy, according to the method described earlier (see section 3.12.1). Cells left untreated, had very few membrane protrusions or pseudopodia and a much smoother outer layer (**Fig. 4.7A and Inset**). However, cells activated with serum, showed increased disturbance on the plasma membrane, indicated by observation of more pseudopodia. Short arrows indicate PMVs detached from the plasma membrane (**Fig. 4.7B and Inset**).

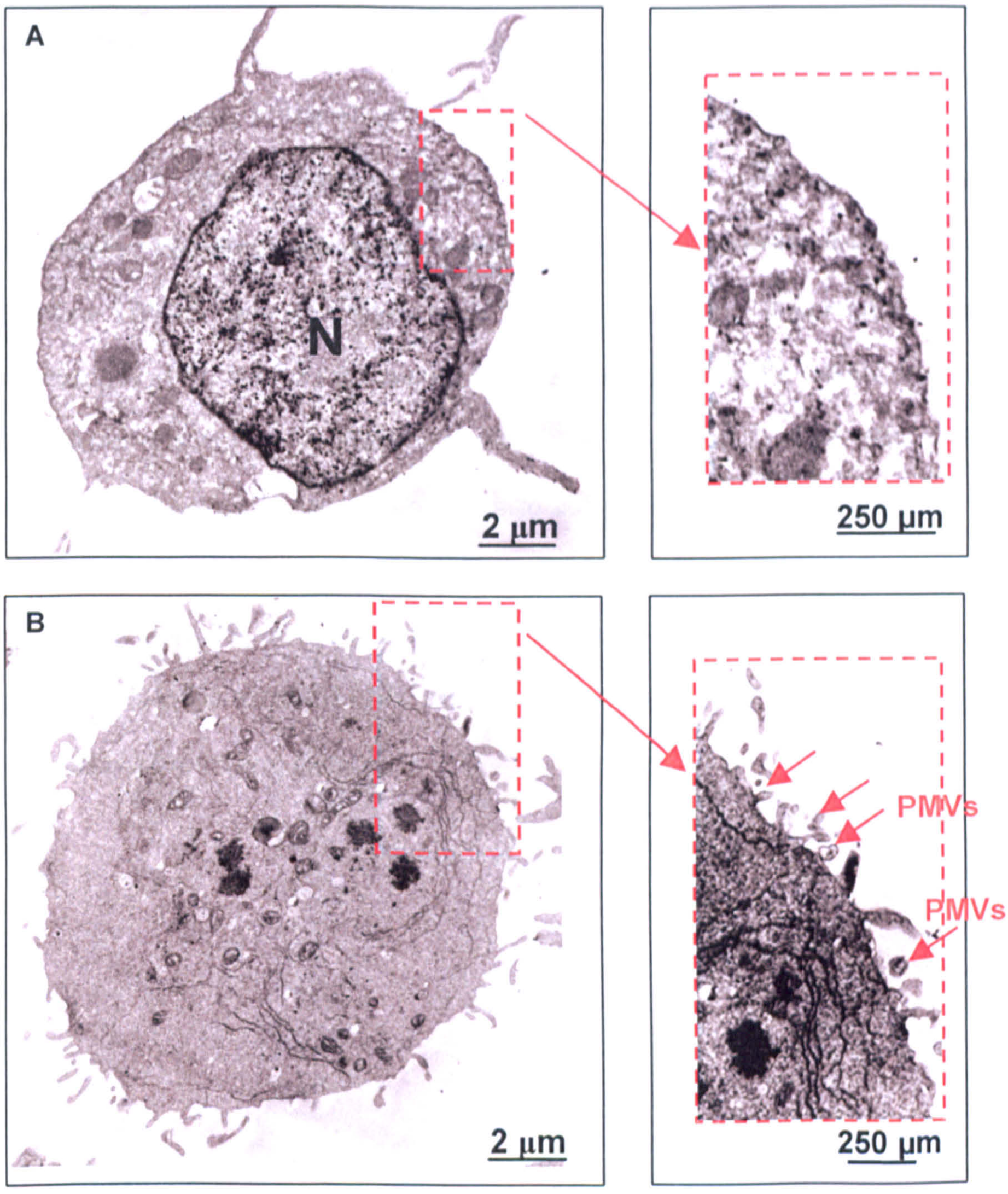

Figure 4.7 Electron microscopy analysis of PMVs

To observe the release of PMVs, THP-1 cells in RPMI were left non-induced (A) or stimulated with 5% NHS (B) and processed to Agar resin after fixation with 0.1 M fixative solution. Scale bar= 2 µm. Magnified images show details of released PMVs close to the cell (short arrows indicate released PMVs, scale bar= 500 nm). N represents the nucleus.

4.2.8 Cells release both PMVs and exosomes

Close examination of the electron microscopy images, showed that THP-1 cells, release both PMVs (indicated with red arrows) and exosomes (released by exocytosis, indicated with arrow heads), upon activation with NHS (**Fig. 4.8A**). Purified PMVs were also processed to agar resin and observed by electron microscopy (**Fig. 4.8A and Insets**). More evidence that cells release both PMVs and exosomes – inset; purified separately and processed to resin (**Fig. 4.8B and Inset**). The process of exocytosis was also observed after cell activation with NHS. Fusion of a multivesicular body (MVB) with the plasma membrane and release of exosomes from the intravesicular lumen was also observed (**Fig. 4.8C**), in which arrowheads show exosomes and the asterisk represents the intravesicular lumen of a fused MVB releasing exosomes.

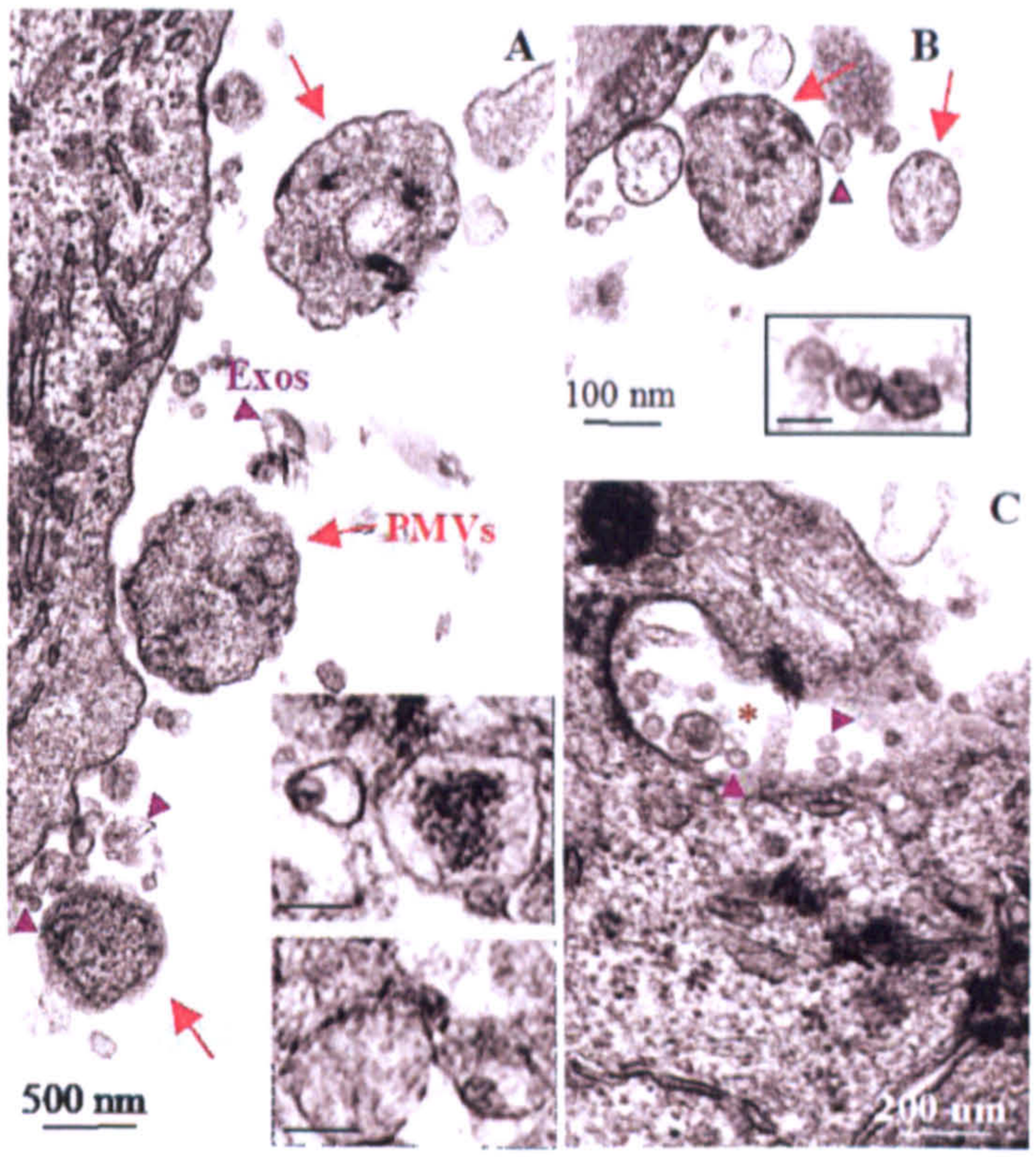

Figure 4.8 Release of PMVs by THP-1 cells

(A) THP-1 cells release both PMVs (red arrows) and exosomes (arrowheads) after stimulation - insets show purified PMVs. Scale bar= 100 nm. (B) Released PMVs (arrows) and exosomes (arrows heads) from activated cells – inset shows cup-shaped exosomes. Scale bar= 100 nm. (C) Fusion of MVBs with plasma membrane and release of exosomes (exocytosis). Asterisk indicates intravesicular lumen of fused MVB. Cells and purified microvesicles (PMVs and exosomes) were fixed with glutaraldehyde, and processed for electron microscopy. Bar = 200 nm.

4.3 Analysis of THP-1 cell-derived PMVs for presence of cytokines

Having confirmed that microvesicles displayed a protein profile similar to the parental cell, an attempt was made to investigate the specific cytokine content of the PMVs isolated from THP-1 cells. To achieve this, the Human cytokine array kit (R&D systems) was used following the manufacturer's instructions (see section 3.14). Briefly, PMVs ($3x10^7$) isolated from the culture medium of THP-1 cells were either lysed with 0.5% Triton X-100 plus protease inhibitor cocktail, or left unlysed and loaded onto a nitrocellulose membrane provided with the assay kit. After detection by chemiluminescence (UVP Bioimaging Systems, UK), spots representative of cytokines were observed on the membranes.

Low levels of the cytokines MIF, IL-12 and IL-13 were detected when PMVs were left unlysed (**Fig. 4.9 A**). However, levels were markedly increased when PMVs were lysed. Also a protein such as Serpin E1, which was not observed in the unlysed sample, was detected after lysis (**Fig. 4.9 B**). It is noteworthy that the increased intensity of the positive controls observed on the lysed PMV membrane, may be due to excess proteins caused by lysing the PMVs. Excess proteins might be binding to the capture antibodies for the positive controls on the membrane. Table 1, shows all cytokines, which could have possibly been present in the samples, however, only those in bold were actually detected.

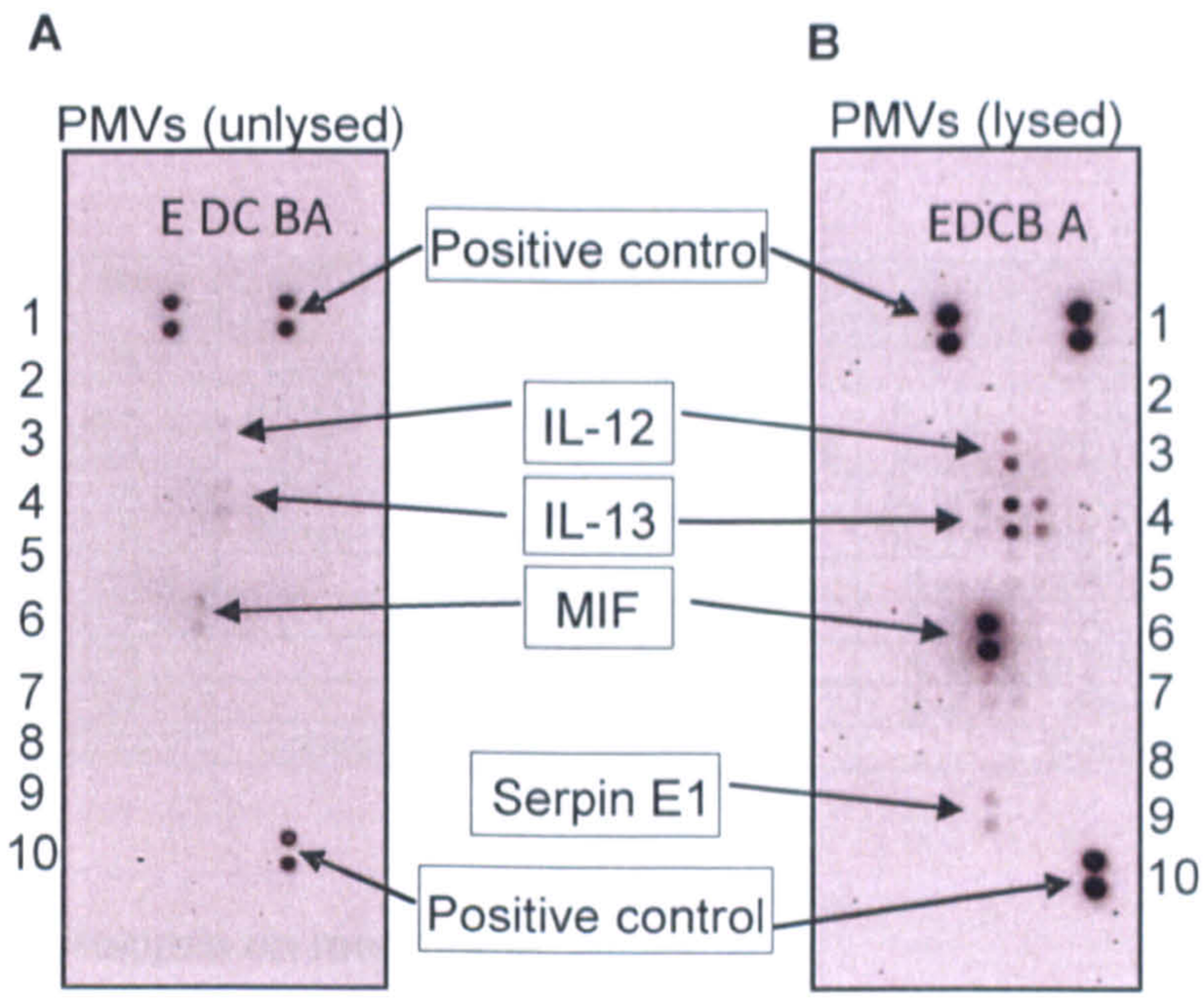

Figure 4.9 Cytokine measurement in PMVs lysed and unlysed from THP-1 cells

THP-1 cell-derived PMVs ($3x10^7$) were either left unlysed or lysed with 0.5% Triton X-100. Samples were loaded unto the membrane provided with the Human Cytokine Array kit and incubated overnight at 4°C. After several washes, membrane was incubated at RT for 30 min with Strepavidin-HRP (1:200 dilution), and after another three times washing, dots were detected by chemilumiscence. (A) Cytokine content of PMVs isolated from THP-1 cells detected without lysis. Only a few cytokines were detected with low spot intensities. (B) Level of detection increased after PMVs were lysed with 0.5% Triton X-100 plus protease inhibitor cocktail. More spots representative of cytokines were detected and the intensity of MIF, IL-12 and IL-13 detected in the unlysed sample were increased after lysis.

No.	E	D	C	B	A
1	Control	-	-	-	Control
2	RANTES	IL-32α	IL-10	IL-1α	C5α
3	SDF-1	P-10	**IL-12p70**	IL-1β	CD154
4	TNF-α	I-TAC	**IL-13**	**IL-1ra**	G-CSF
5	Strem-1	MCP-1	**IL-16**	**IL-12**	**GM-CSF**
6	-	**MIF**	IL-17	IL-4	GRO-α
7	-	**MP-1α**	**IL-17E**	IL-5	CCL1
8	-	MIP-1β	IL-23	**IL-6**	sICAM-1
9	-	**Serpin E1**	IL-27	IL-8	IFN-γ
10	Control				Control

Table 1. Cytokines on membrane

Table 1 shows cytokines potentially detectable on the membrane and highlighted in bold are the cytokines, which were actually detected in the PMVs.

4.4 Investigation of an effective method for the isolation of PMVs

4.4.1 Differential centrifugation also pellets aggregated exosomes

As shown on Fig. 4.8, and discussed in section 4.2.8, cells generally release both PMVs and exosomes when activated, and so developing a good isolation method, which distinguishes the two vesicle types is paramount. PMVs can be differentiated from exosomes based on a number of physical properties, such as the difference in size. Since exosomes are smaller than PMVs, differential centrifugation steps are generally employed in most laboratories to obtain particular vesicles. Another distinguishing feature is the level of surface PS expression analysed by annexin V binding. PMVs, due to their inverted plasma membrane during the process of release, express more PS on the outer leaflet. However, exosomes form clusters that amount to the size of PMVs and current centrifugation methods do not distinguish between the two.

After two centrifugations at 4,000 *g* for 30 min, annexin V positive PMVs were isolated by ultracentrifugation of supernatant depleted of debris, at 160,000 *g* for 2 h without prior water-sonication (**Fig. 4.10 A**). However, this also resulted in aggregated exosomes being pelleted together with the PMVs (**Fig. 4.10 B, white arrows**). This is consistent with an earlier report, which showed that exosomes form clusters by binding to other exosomal vesicles [230].

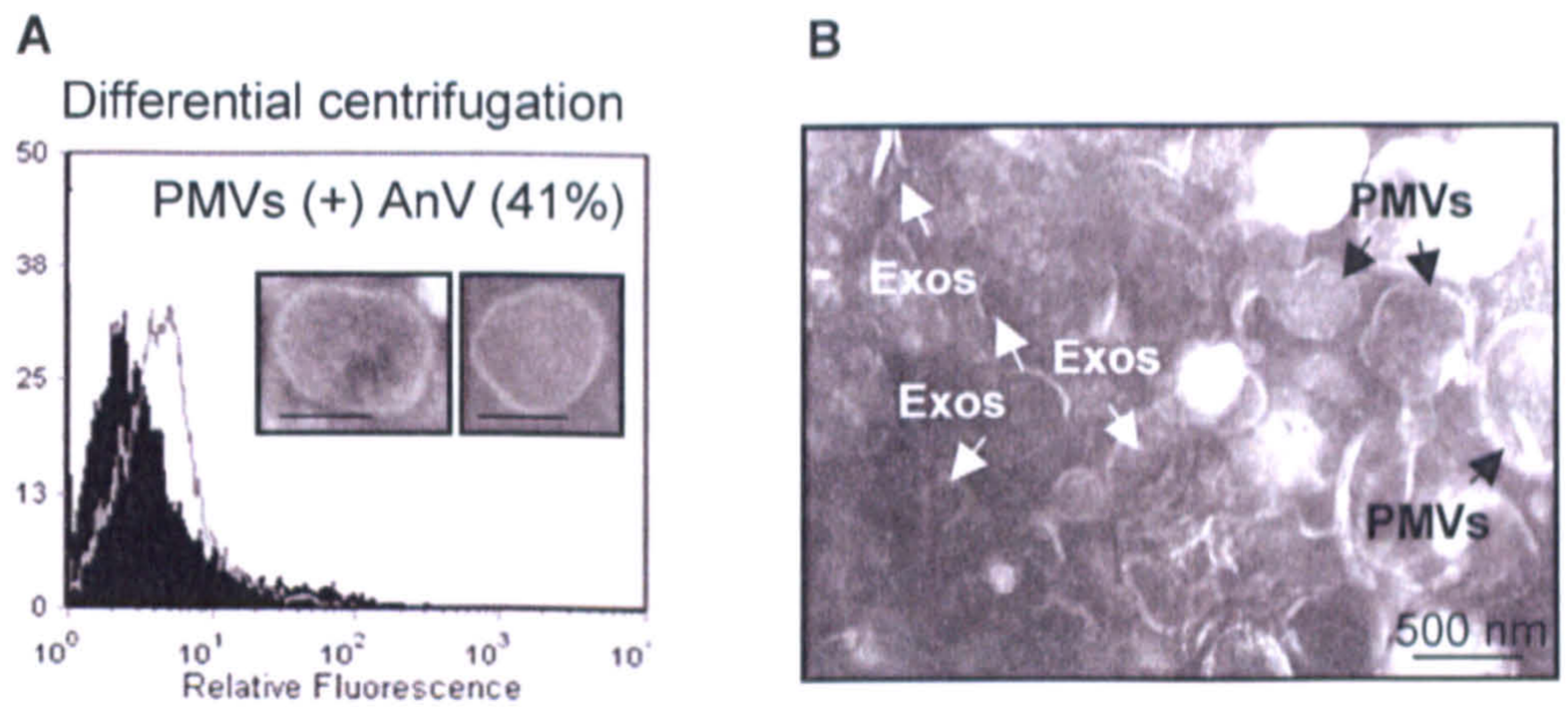

Figure 4.10 PMVs and aggregated exosomes pellet together upon centrifugation

(A) PMVs (inset) isolated by differential centrifugation from culture supernatants as described in 'materials and methods' showed 41% positive binding for annexin V-FITC, analysed by flow cytometry. (B) Ultracentrifugation of debris-free supernatants without prior sonication in a sonicating water-bath yielded PMVs (black arrows), but aggregated exosomes (white arrows) were also obtained in the fraction. Scale bar= 500 nm.

4.4.2 Sonication and filtration of supernatants minimises contamination of PMV samples with exosomes

In order to eliminate contamination of PMVs with aggregated exosomes, the procedure described in section 3.9.3 was performed. Cell-free culture supernatant was twice centrifuged at 4,000 *g* for 30 min to remove debris. Supernatant was water-sonicated (Towbin, sonicating waterbath, UK) for 5 x 1 min to separate any aggregated exosomes and filtered through a 0.22 µm membrane. It was postulated that exosomes ranging from 30 nm to 90 nm in size were small enough to pass through the membrane. However, PMVs, which normally range from 0.1 µm to 1 µm would be trapped and could be recovered by reversing the filter membrane and washing through with PBS.

Indeed, annexin V-FITC positive PMVs were isolated, with less exosome contamination after centrifugation of the retained PBS solution, at 25,000 *g* for 30 min (**Fig. 4.11 A**). To further characterise the difference between the two methods, the filtrate (PMVs-free supernatant) obtained after filtration through the 0.22 µm filters was ultracentrifuged (160,000 *g*, 16 h) to pellet exosomes (**Fig. 4.11 B**). Exosomes were less positive for PS (18%) after Annexin V staining, compared to PMVs recovered from the filter (47%). In both cases the isolated vesicles were fixed and negatively stained as described under materials and methods (see section 3.12.2) for electron microscopy examinations (**Fig. 4.11 and Insets**).

In a slightly modified method, the filtration step was eliminated. In this procedure, cell-free supernatant was centrifuged at 4,000 *g* for 1 h to remove debris. Skipping the filtration step, resultant supernatant was sonicated (5 x 1 min) in a sonicating

water bath prior to centrifugation at 25,000 *g* for 2 h. Electron microscopy images of more pure PMVs isolated by this procedure are presented (**Fig. 4.11 C**). Exosomes were isolated by ultracentrifugation at 160,000 *g* for 16 h after initial centrifugation at 25,000 *g* to pellet PMVs (**Fig. 4.11 D**).

This method was further supported in other work carried out in the lab (Pathak, P [2008] MSc project) looking at Lamp-1 and CR1 expression on exosomes. Lamp-1 was reported to be much more highly expressed on exosomes than on PMVs [240]. In the study, a mixture of exosomes and PMVs were applied to a 10-40% sucrose gradient, spun at 30,000 *g* for 1 h. The first six (1 ml) fractions were pooled (pool 1) and found to be highly positive for Lamp-1 expression after antibody labelling. In the same study it was shown that pool 2 fractions (7-11) were in contrast more positive for annexin V binding. This suggested that pool 1 fractions consist mainly of exosomes and pool 2 fractions mainly of PMVs. It was also found that pool 1 fractions were over 58% positive for CR1. However, after filtration through a 0.22 µm membrane, 28% of the filtrate was still positive for CR1. This number further increased after sonication of the pool 1 sample before filtration. This means smaller exosomes were able to pass through the membrane and still give positive detection of the receptor, but before sonication, aggregated exosomes were trapped on the membrane. Therefore, sonicating the sample separated aggregated exosomes, so that after filtration a higher percentage positive for CR1 was detected. The same experiment was carried out on pool 2 samples. Pool 2 was found to be 50% positive for CR1; however, only 7% remained positive after filtration. This value did not change after sonication of the sample suggesting that pool 2 fractions mainly contain PMVs, and these were trapped on the membrane during filtration.

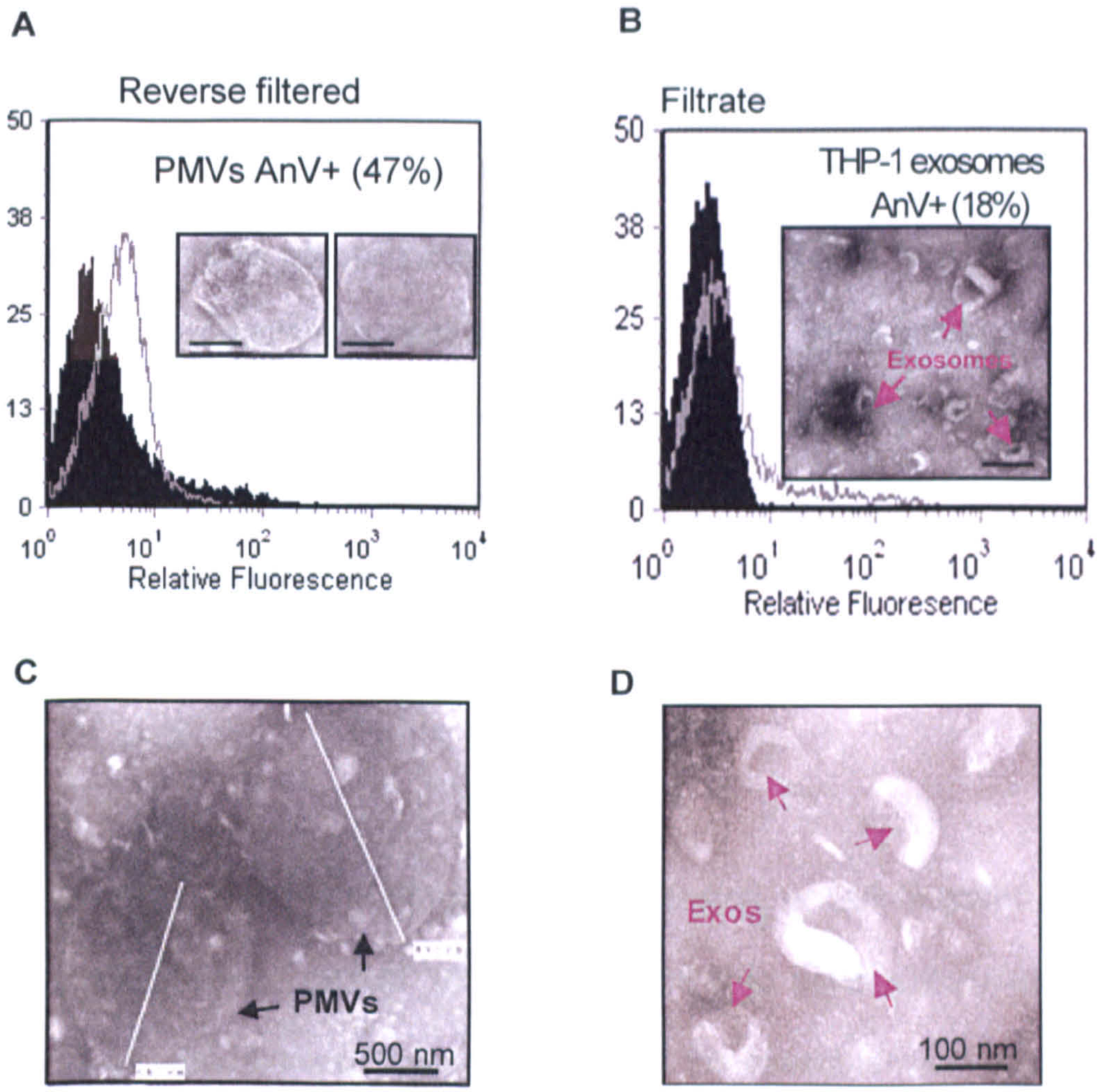

Figure 4.11 Enhancement of the PMVs isolation method

(A) Isolated microvesicles from reverse washing of the membrane filters were confirmed by EM as PMVs and were also PS positive after annexin V-FITC (47%) staining. (B) However, the filtrate was less positive (18%) for annexin V and EM analysis showed cup-shaped exosomes (insert). Scale bar= 100 nm (C) Images of more pure PMVs isolated after sonication of supernatant followed by centrifugation at 25,000 *g* for 2 h. Scale bar= 500 nm. (D) Exosomes isolated from PMV-free supernatant centrifuged at 25,000 *g* for 2 h.

4.4.3 Dot plot distribution of PMVs and exosomes on flow cytometer

Having successfully isolated PMVs and exosomes and characterised them by electron microscopy, further phenotypic differences were noted by flow cytometry analysis. PMVs have been well characterised previously by flow cytometry analysis, however, various groups have tried but so far failed to observe a typical dot plot distribution of exosomes. Debris-free supernatants sonicated in a sonicating water-bath to separate aggregated exosomes, were either filtered through a 0.22 µm membrane, or directly centrifuged at 25,000 *g* for 2 h to pellet PMVs. PMVs isolated after prior sonication of debris-free supernatant were confirmed by their distinct, heterogeneous forward and side scatter distributions by flow cytometry (**Fig. 4.12 A**).

Supernatant depleted of PMVs, either by filtration, or centrifugation at 25,000 *g* for 2 h, was ultracentrifuged at 160,000 *g* for 16 h to pellet exosomes. Using isolated PMVs as control, the dot plot distribution of the exosomes was interestingly distinct. The distribution of the vesicles was more homogeneous, as assessed by the logarithmic amplification of forward (FSC) and side scatter (SSC) signals. Distribution on the side scatter signal (y-axis) remained between 10^0 and 10^2, whilst, on the forward scatter axis, the distribution was detected between 10^0 and 10^1 (**Fig. 4.12 B**). These vesicles, smaller than PMVs and homogenous in size and granularity, fit the characteristics of exosomes. Based on this finding, the two vesicle preparations were mixed together and analysed on the flow cytometer. The dot plot showed two distinct scatterings (**Fig. 4.12 C**) almost like an overlaid image of figures 4.12 A and B. This result shows that exosomes have a particular dot plot distribution, distinct from PMVs that can be detected by flow cytometry analysis.

It must however be mentioned that the flow cytometer utilised here (Guava EasyCyte, Guava Technologies), has a far superior resolution compared to other models. This sensitivity could have aided in detecting the much smaller exosomes.

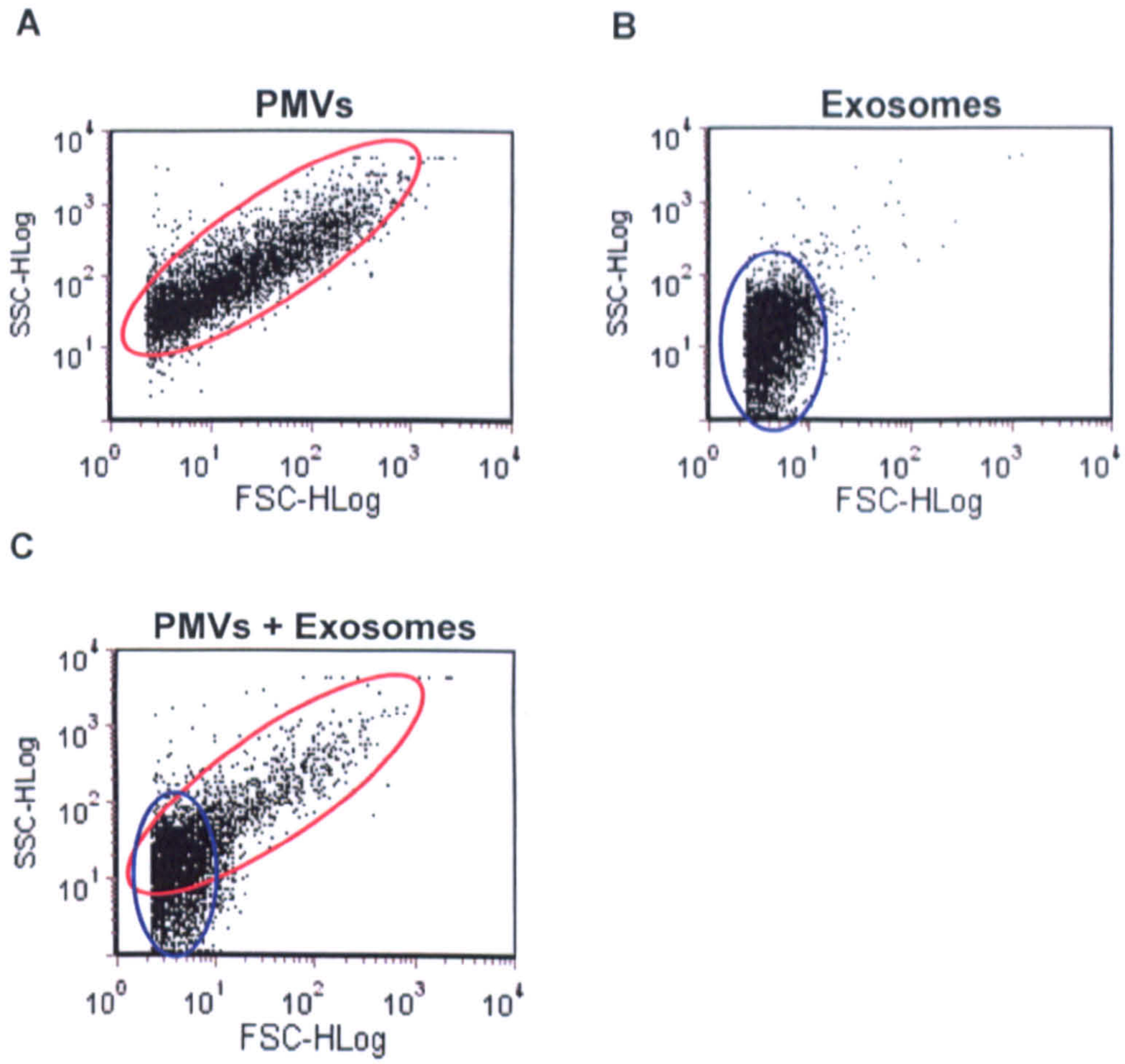

Figure 4.12 Flow cytometry differences between PMVs and Exosomes

PMVs and exosomes isolated and analysed by flow cytometry showing forward scatter (FSC-HLog), which refers to size, and side scatter (SSC-HLog), which shows granularity of the vesicles. (A) Dot plot distribution of PMVs isolated by reverse washing of filter membrane or direct centrifugation (25,000 *g* for 2 h) after flow cytometry analysis. (B) Exosomes isolated after ultracentrifugation at 14°C for 16 h of PMVs-free supernatant. Dot plots were homogenous in size and granularity. (C) Flow cytometer dot plot of a sample mixture containing both PMVs and exosomes.

4.4.4 Cytokines present in PMVs and exosomes

Since PMVs and exosomes can be isolated and readily distinguished by flow cytometry, it was decided to investigate any possible difference in the cytokines present in each vesicle type. After obtaining PMVs and exosomes via the sonication and filtration method, positive isolation of each vesicle was confirmed by flow cytometry and subjected to the following: PMVs and exosomes were analysed together or individually according to the manufacturer's instructions using the Human cytokine array kit (see materials and methods, section 3.14). A sample mixture of the two vesicles was positive for nine cytokines on the antibody-coated membrane (**Fig. 4.13 A and left membrane**). Analysis of PMVs alone was also positive for eight cytokines (**Fig. 4.13 A and middle membrane**). However, some cytokines, acute phase proteins/growth factors were not detected when exosomes alone were analysed (**Fig. 4.13 A and right membrane**). These include complement C5a, RANTES, G-CSF, IL-17E and IL-1ra. Table 2 shows the cytokines detected on the array after the assay.

Other cytokines thought to be important were investigated and quantified by ELISA (R&D Systems). These cytokines, transforming growth factor β1 (TGF-β1), macrophage migration inhibition factor (MIF), fibroblast growth factor 1 (FGF-1) and galectin-3 (Gal-3) were all found to be present in isolated PMVs. The levels of TGF-β1 and MIF (**Fig. 4.13 B and C**) were significantly higher in PMVs than exosomes. However, no significant difference was detected in the levels of FGF-1 and galectin-3, carried by the microvesicles (**Fig. 4.13 D and E**). Unfortunately none of the proteins measured here were uniquely found on only one vesicle type. This is thought to be due to the overlap in size between the two types of vesicles. Even with

an improved method for isolating the two vesicles, overlap in their sizes will always see one vesicle type contaminated with the other. However, it is noteworthy that such contamination is now minimal when debris-free supernatants are sonicated (sonicating water-bath, 5 x 1 min) prior to either filtering through a 0.22 µm membrane filter or by direct centrifugation (25,000 *g*, 2 h) for isolation of PMVs.

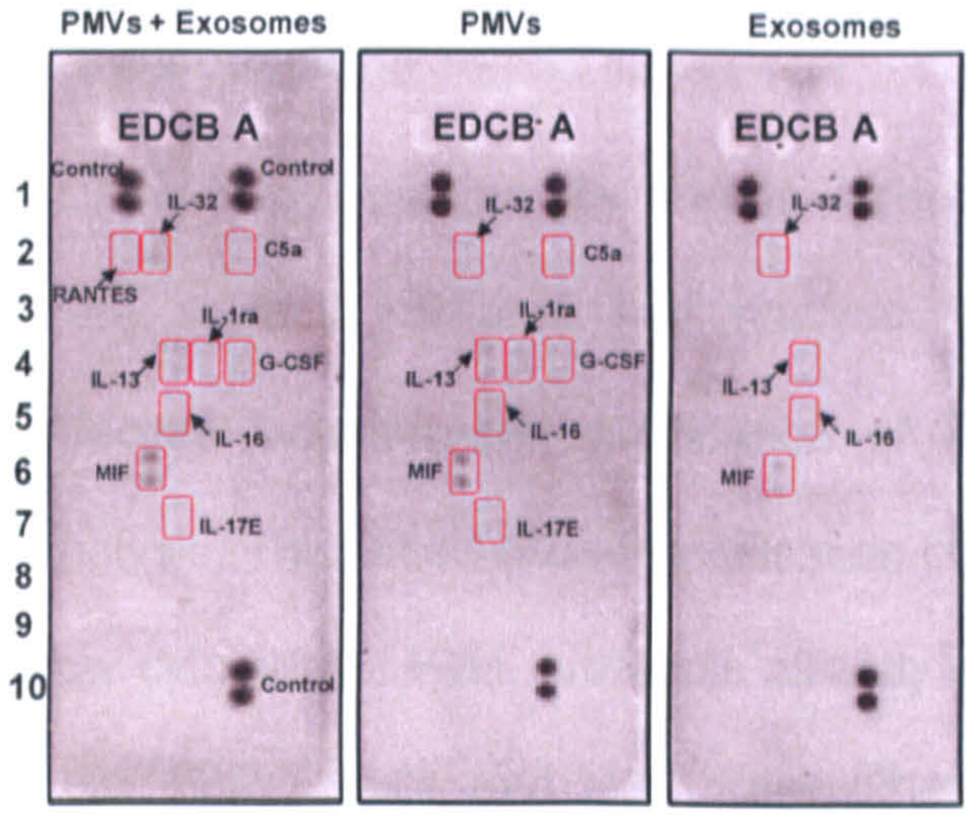

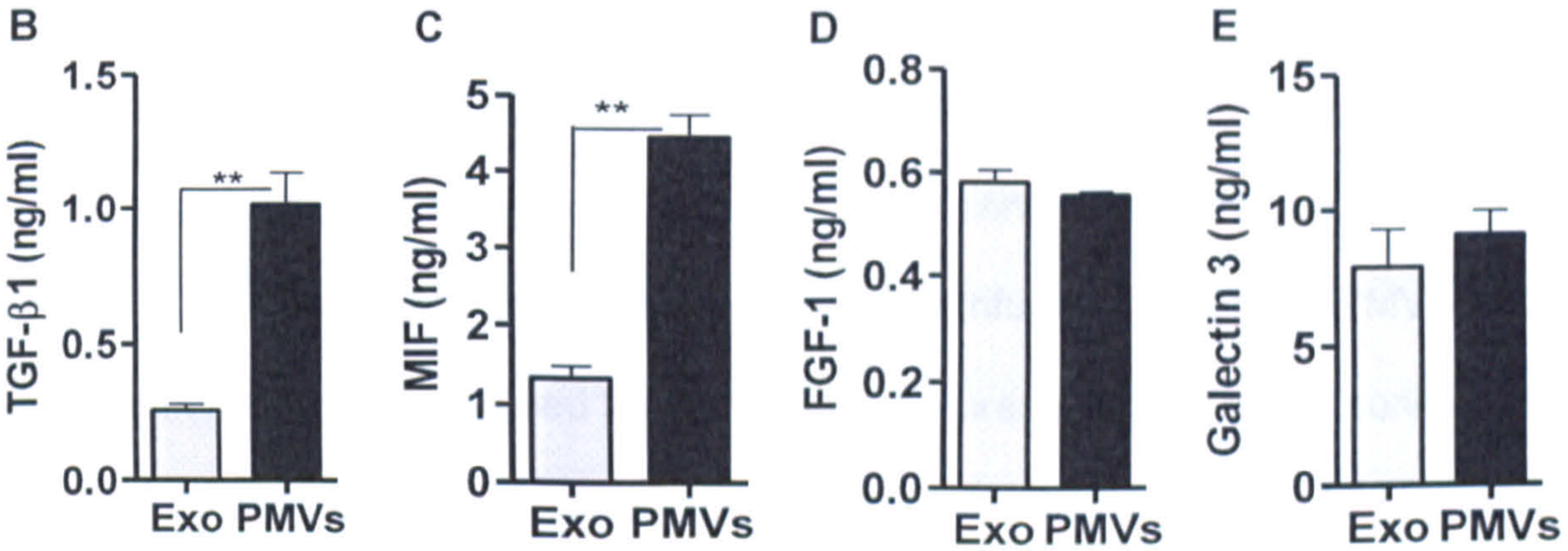

Figure 4.13 Cytokine analyses in PMVs and Exosomes

(A) Image of membrane showing positive detection of cytokines present in PMVs and exosomes. (B, C) ELISA analysis showed that TGF-β1 and MIF were present at about four fold higher levels in PMVs than exosomes. No difference was observed in the levels of FGF-1 and galectin-3 (D, E). Data represent mean ± SD of two independent experiments performed in triplicate. $^{**}P < 0.01$ was considered statistically significant.

No.	PMVs + Exosomes	PMVs	Exosomes
1	C5a	+	-
2	IL-32	+	+
3	RANTES	+	-
4	G-CSF	+	-
5	IL-1ra	+	-
6	IL-13	+	+
7	IL-16	+	+
8	MIF	+	+
9	IL-17E	+	-

Table 2. Tabulated summary of the cytokines detected in PMVs and how they differed from those in exosomes.

4.5 Discussion

In this study, plasma membrane-derived vesicles from various mammalian cells were correctly isolated and analysed by flow cytometry. Also procedures for effective isolation and purification of PMVs were carefully refined to enhance analysis. This aided clear identification of PMVs, distinct from exosomes by EM and flow cytometry. First, protocols already established, were adapted to isolate PMVs from THP-1 cells and later from other cell-lines. Normal human serum, which contains complement factors, was initially used to stimulate THP-1 cells to release PMVs. At the start of the study, PMVs released into the conditioned media after stimulation with NHS, were isolated by differential centrifugation, starting from 4,000 *g* for 1 h to 160,000 *g* for 2 h. However, these centrifugations pelleted PMVs greatly contaminated with aggregated exosomes. In the present study, prior sonication of debris-free supernatant separated aggregated exosomes and allowed isolation of much purer PMVs and exosomes. Isolation of PMVs was confirmed by screening through various tests, including positive binding of annexin V-FITC on the surface to confirm exposure of PS on the outer membrane leaflet and SDS-PAGE to confirm similar protein profile with parental cell.

Heat-inactivation (56˚C, 1 h) of NHS, confirmed that PMV release in the presence of serum was due to insertion of MAC. This is in agreement with a report which showed that microvesiculation from erythrocytes was caused by MAC present in human serum [241]. Isolated PMVs were correctly identified by flow cytometry, by positive detection of their phenotypic size and granularity based on forward and side scatter signals. Electron microscopy examinations, further confirmed the release of

PMVs from THP-1 cells. Careful examination of the EM images showed contamination of PMVs with exosomes, identified by their typical cup-shaped morphology [78]. The presence of exosomes in this preparation meant any findings, made for PMVs, might not be entirely true. Thus, a protocol was required to isolate PMVs with little or no contamination from exosomes.

A review of the literature showed that exosomes could not be detected on the flow cytometer and so the dot plot distribution for this type of vesicle remained unknown. The size of exosomes compared to PMVs, meant their detection and analysis on the flow cytometer has for many years eluded researchers. This might also be due to the fact that many commercially available flow cytometers do not have a high enough resolution to allow detection of these smaller vesicles. The possibility of detecting exosomes on the flow cytometer was thus investigated. Many investigators are still not sure of the particular type and so prefer to use the more general term, microvesicles, when referring to either vesicle.

Sonication of cell-free and debris-free supernatants in a sonicating water-bath for 5 x 1 min separated aggregated exosomes. Centrifugation at 25,000 *g* for 2 h pelleted PMVs, but exosomes remained in the resultant supernatant and were pelleted by ultracentrifugation at 160,000 *g* for 16 h. In another protocol used, cell-free and debris-free conditioned media were filtered through a 0.22 µm membrane. PMVs, which range from 0.1-1 µm in diameter, were accumulated on the membrane and later detached by 'reverse washing' with PBS, and pelleted by subsequent centrifugation at 25,000 *g* for 30 min. The filtrate containing smaller exosomes (50 to 100 nm in diameter) was ultracentrifuged at 160,000 *g* for 16 h. Electron microscopy

analysis showed pure PMVs, but also pure exosomes were isolated after sonication of the samples. Furthermore, flow cytometry analysis revealed a distinct dot plot distribution for exosomes, which was not previously reported.

Unlike the dot plot distribution of PMVs, which is normally detected between log 10^0 to 10^4 on both the forward and side scatter axis, due to their varying sizes and granularity, exosomes were depicted from 10^0 to 10^2 on the side scatter axis and between 10^0 and 10^1 on the forward scatter axis. This is because exosomes are much smaller than PMVs, and also more homogeneous in size. This result also shows that exosomes can be detected using a flow cytometer. More importantly, for the first time, exosomes can be distinguished from PMVs during sample analysis on the flow cytometer. Applying the now refined PMV isolation method, a dose response with NHS was measured for this type of vesicle after THP-1 cells were activated. More importantly, negligible levels of vesicles in the NHS itself showed that the source of quantified PMVs was largely that released by activated cells, rather than sourced in the serum.

As mentioned earlier, PS exposure on the membrane surface indicates the loss of lipid bilayer asymmetry, and this is mainly characteristic of cells undergoing apoptosis [242;243]. However, PMVs also express PS, which indicates an inversion of the inner and outer membrane leaflets. One might therefore ask whether release of PMVs is dependent on apoptosis, and that these vesicles are in fact apoptotic bodies. Data presented showed that although some PMVs are released during the process of apoptosis, the mechanism involved is independent of apoptosis. Proteins carried by these vesicles reflected that of the parental cell, when assessed by SDS-

PAGE, and Western Blotting revealed the presence of complement regulatory proteins, DAF and CR1, which are present in THP-1 cells.

In this study, blocking the influx of extracellular calcium with EGTA inhibited the NHS activated release of PMVs. Also, deactivation of calpain, with calpeptin, reduced the number of released PMVs and a similar reduction was detected after THP-1 cells were pretreated with the Rho-kinase inhibitor, Y-27632, before stimulation with NHS. These results confirm the involvement of calcium during the release of PMVs and also calpain, the enzyme that cleaves the actin cytoskeleton. It is noteworthy, that the degree of inhibition may depend on the cells being investigated. This is because unlike THP-1 cells, HeLa cells for example have been reported to have very low expression levels of ABCA-1 [244], a transporter protein involved on the release of PMVs. Activation of lipid raft domains was also found to be important as disruption of these sites, resulted in less PMVs being detected. However, more PMVs were detected when the process of endocytosis was blocked with chlorpromazine.

In agreement with previous reports, PMVs isolated were shown to carry a range of intracellular and extracellular cytokines, growth factors and acute phase proteins, possibly not carried by exosomes. Amongst these, RANTES, IL-17E and G-CSF were not detected in exosomes. Using ELISA, higher levels of TGF-β1 and MIF were measured in PMVs, compared to exosomes. No significant difference however, was detected in the levels of FGF-1 and Gal-3 carried by PMVs and exosomes. Even with all these carefully devised protocols to aid the effective isolation of PMVs,

overlap between the sizes of PMVs and exosomes, still interferes with designing protocols to purify one type of vesicle.

5. Human Plasma Membrane-derived Vesicles halt proliferation and induce differentiation of THP-1 acute monocytic leukaemic cells

5.1 Introduction

In this chapter the role of PMVs in promoting the terminal differentiation of human monocytic cells into macrophages will be discussed. The participation of released PMVs in various diseases has been extensively investigated. Elevations of PMVs have been observed in diseases such as cerebral malaria [245], diabetes mellitus [204;246], rheumatoid diseases [247] , thrombosis, multiple sclerosis and sickle cell anaemia [47;248;249]. Recently, the role of PMVs in abetting angiogenesis, invasion and metastasis of various cancers has also been reported [83,250]. Surprisingly, the role of PMVs in acute myeloid leukaemia has not yet been reported.

5.1.1 Acute myelogenous leukaemia and current therapeutics

Acute myelogenous leukaemia (AML) represents a group of heterogeneous clonal disorders, in which stem cells fail to differentiate and instead overproliferate resulting in accumulation of non-functional cells known as myeloblasts. The monoblastic subtype (AML-M5) of AML termed acute monocytic leukaemia from which the cell line THP-1 is derived represents about 9% of all adult AMLs. The notion that AML is a direct result of stem cell overproliferation and failure to differentiate resulted in the development of differentiation therapies to treat the disorder. This therapy offers the best treatment for monocytic leukaemia and works by inducing differentiation of leukaemic promonocytes into mature non-replicative cell types undergoing cell cycle arrest that eventually undergo apoptosis [251]. Retinoids such as all-*trans*-retinoic acid (ATRA) is currently in use for treatment of acute promyelocytic leukaemia (APL) [221] , a subtype of AML, by specifically targeting neoplastic cells, leaving normal mature cells unaffected. Other agonists such as PMA [222], vitamin D_3 [223], interferon-

γ [225] and calcium ionophore (A23187) [224] have been successfully used in differentiation therapy to treat myeloid leukaemia.

5.1.2 Release of PMVs induced by current agonists used in differentiation therapy

As mentioned earlier, the *in vitro* release of PMVs can be initiated by sublytic complement complexes and to some extent bacterial products such as fMet-Leu-Phe (fMLP) [252] and lipopolysaccharide (LPS) [253], providing cells have the cognate receptors. In addition, the agonists; calcium ionophore, PMA and ATRA used in differentiation therapy can also induce PMV release [6;227]. Moreover, the inflammatory mediator histamine, also used in differentiation therapy is shown in this report to stimulate PMV release from THP-1 cells. Since these agonists described as possible therapies for acute monocytic leukaemia, are also inducers of PMV release, we wondered whether PMVs themselves could induce cell cycle arrest/terminal differentiation (the hallmark of differentiation therapy) in THP-1 cells. This is appropriate since it was recently reported that microvesicles derived from neutrophils, termed ectosomes interfere with the maturation of immature dendritic cells [229] . Also the early success with ATRA in APL has not been followed up with new drugs and myeloid leukaemia cells may develop resistance to existing therapies [254;255].

In addition to the agonists mentioned, recombinant proteins such as TGF-β1 have also been shown to inhibit the proliferation of murine megakaryocyte precursors [256]. As aforementioned, PMVs upon release carry numerous membrane proteins, lipids and cytoplasmic constituents, characteristic of the parental cell and are able to

transmit such proteins between cells. Amongst these are cytokines, for example TGF-β1, a 25 kD multifunctional protein, found predominantly on platelet microvesicles [257], with pleiotrophic functions including the regulation of cell proliferation, differentiation, morphogenesis and phenotype expression [258-260], and increases in the expression of several extracellular matrix components including, fibronectin, proteoglycans and several types of collagen. Many cells are also induced to upregulate the expression of integrins or cell adhesion molecules [261]. Thus, a net increase in the extracellular matrix and cells' ability to adhere more effectively are due to TGF-β1. Hitherto, TGF-β1 has been shown to prevent myogenesis, haematopoiesis and to prevent adipocyte differentiation [262-264], while promoting the differentiation of intestinal epithelial cells [265]. Overall TGF-β1 plays a role in many physiological processes, such as proliferation, differentiation, migration and cell survival, which affect many biological processes, including wound healing, development, carcinogenesis and immune responses [256;260;266] .

5.1.3 Release of PMVs as an alternative to conventional secretory export

In eukaryotic cells, the vast majority of extracellular proteins (like TGF-β1), which possesses an N-terminal, signal or leader sequence, are localised to the lumen of the endoplasmic reticulum (ER) where they are packaged into transport vesicles and delivered to the Golgi apparatus. Fusion with the plasma membrane eventually results in release of transport vesicles into the extracellular space, a process referred to as classical/conventional protein secretion [129;267]. However, a number of secretory proteins lack the classical N-terminal, hydrophobic, signal sequence [147] and have been shown not to associate with the ER-Golgi membrane translocation machinery [130;131]. Furthermore, treatment with the ER-Golgi transport blocker,

brefeldin A, did not impair emergence of such molecules in the extracellular space [148]. These observations led to the term non-conventional protein secretion, to describe secretory processes that are independent of the classic ER-Golgi transport pathway.

Unlike TGF-β1, which has a signal sequence and can be transported via the conventional protein export, cytokines lacking a signal peptide cannot associate with the ER-Golgi transport machinery and are transported inside microvesicles [132;268;269]. Amongst these, epimorphin, FGF-1 and FGF-2, MIF and Gal-3 are all transported to the plasma membrane via the adenosine triphosphate cassette transport channel or by exocytosis of exosomes [270;271].

This study shows (figure 5.4 and 5.5) the presence in PMVs of leaderless cytokines MIF, FGF-1 and Gal-3. Although their specific function in PMVs and intercellular communication and possible induction of myeloid differentiation cannot be commented on, like TGF-β1, these cytokines have been reported to function during the differentiation of myeloid cells. For example, MIF was reported to induce the migration of monocytes into tissues, whilst changes in Gal-3 expression are important for myeloid cell differentiation into specific lineages [272;273].

The role of PMVs in intercellular communication is probably their most important. This is illustrated by studies carried out on melanoma patients suggesting the development of immunosuppression by tumours to be through their release of microvesicles, which promote the generation of suppressive myeloid cells, without

the need for cell-cell contact [274]. Another example of PMV-mediated intercellular communication is that of leukocyte PMVs transferring leukocyte antigens to endothelial cells, their resulting activation being associated with changes in phosphorylation of cellular proteins and cell adhesion molecules [275]. Looking at platelet-derived PMVs, they were shown to modulate monocyte-endothelial cell interaction and stimulate proliferation, survival and chemotaxis of haemopoietic cells [89].

In addition, PMVs containing the receptor EGFRvIII were found to merge with the plasma membrane of cancer cells lacking EGFRvIII, and transfer oncogenic activity, thus contributing to a horizontal propagation of oncogenes and their associated transforming phenotype among subsets of cancer cells [276]. Studies on the effect of TGF-β1 have shown it to inhibit the proliferation of various cell types *in vitro* [277]. This study describes for the first time, the presence of surface-bound TGF-β1 on PMVs. Given the important role TGF-β1 plays in the regulation of cellular proliferation, a series of experiments were set up to investigate whether growth regulation and differentiation of promonocytic leukaemia cells could be influenced by TGF-β1-bearing PMVs, released through the action of known differentiation therapeutics.

5.2 Agonists used in differentiation therapy to treat AML, induce release of PMVs and reduce cell proliferation

Histamine, PMA and ATRA, currently in use or under trial for differentiation therapy, are also potent inducers of microvesicles. Here, their *in vitro* effect on the growth rate of THP-1 cells, as well as PMV release potential was investigated. THP-1 cells

were resuspended in complete medium containing 5% FBS and seeded into 24-well plates at $1x10^5$ cells/well in triplicate. Cells were incubated for three days following treatment with PMA (1 μM), ATRA (10 μM) and histamine (10 μM) or left non-induced (NI). On the days indicated, cells were stained with Viacount reagent, a DNA-binding dye (Guava technologies, UK) and counted using the Viacount assay by flow cytometry (see materials and methods, section 3.10.1).

Addition of histamine, ATRA and PMA reduced the growth rate of THP-1 cells after 3 days, with marked reductions observed in wells treated with PMA (**Fig. 5.1 A**). This confirms the agonist's ability to limit proliferation of THP-1 promonocytes and hence their use in differentiation therapy as potential treatments for AML. Further analysis of their activation of PMV release confirmed previous observations made with ATRA and PMA [278;279]; however, histamine is shown for the first time as a potent inducer of PMV release (**Fig. 5.1 B**), with a dose-dependent response (**Fig. 5.1 C**). The decreasing proliferation levels observed with histamine, ATRA and PMA inversely correlated with levels of PMV release (**Fig. 5.1D**). Elsewhere, all three agonists were shown to cause marked elevations in cytosolic Ca^{2+} levels in THP-1 cells (see original publication, **II.** Ansa-Addo EA et al. (2010) *J Immunol.* **185,** 5236-46).

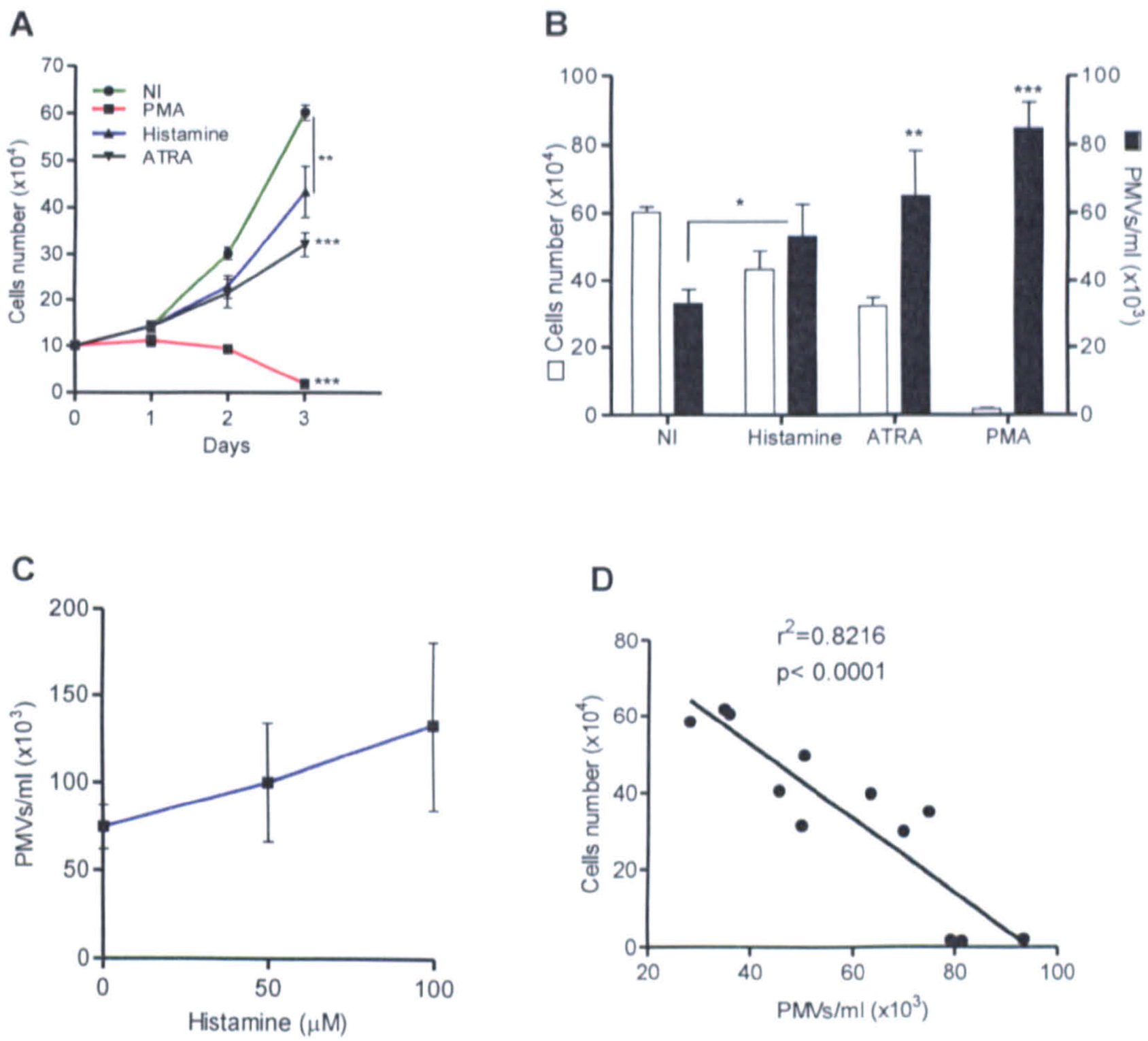

Figure 5.1 Histamine, ATRA and PMA induce PMV release, and limit cell proliferation.

(A) THP-1 cells ($1x10^5$/well) are seeded into 24-well plates in triplicate and left non-induced (NI) or incubated at 37°C for 3 days with 10 μM histamine, 10 μM ATRA and PMA (1 μM). On the days shown, cell numbers are determined using the viacount assay on the Guava EasyCyte flow cytometer following addition of the agonists. (B) To induce release of PMVs, THP-1 cells ($1x10^6$/well), are seeded in triplicate and incubated with 100 μM histamine, 100 μM ATRA and 10 μM PMA at 37°C for 30 min with shaking. The apparent inverse correlation between cell number and PMVs/ml released after treatment with the agonists is confirmed. (C) Dose response increase in PMVs/ml released after treating with increasing (50-100 μM) histamine concentrations. (D) Significant negative correlation between cell number on the third day following treatment with histamine/ATRA/PMA and released PMVs/ml after addition of these agonists. Data represents the mean ± SD of a single experiment performed in triplicate. ***$P < 0.001$, **$P < 0.01$, *$P < 0.05$ were considered to be statistically significant.

5.3 PMVs reduce the proliferation of THP-1 cells

Since the agonists used in differentiation therapy induced release of PMVs from THP-1 cells, it was decided to investigate the effect of adding PMVs separately to cells in culture. Growth inhibition and differentiation assays were set up as described earlier (see section 3.9.13 and 3.9.14). Briefly, THP-1 cells ($1x10^5$/well) were seeded in 1 ml volumes into 24-well plates with or without 10 µg/ml of PMVs, in triplicate. This amount was chosen as current estimates of microvesicle concentration in the peripheral blood of healthy individuals are 5-50 µg/ml. In another experiment, increasing amounts of PMVs (5-30 µg) was added to investigate the dose response. Plates were incubated at 37°C in a humidified atmosphere of 5% CO_2 for 3 days. On each of the days indicated, cells were stained with ViaCount reagent (Guava technologies, UK) and the number of viable and apoptotic cells (ACs)/well was determined using the ViaCount assay by flow cytometry.

After a lag phase of about 24 h, the increase in cell number of the cultures treated with PMVs, over the following 48 h, was markedly less than that of cells without added PMVs (**Fig. 5.2 A**). Neither the PMVs added, nor the ViaCount reagent used was cytotoxic to the cultures as the percentage of apoptosis was similar between untreated and PMVs-treated (**Fig. 5.2 A**) cells. This reduction in growth rate, in the presence of PMVs, was significant by day three (**Fig. 5.2 A**), with 10 µg providing a saturating amount (**Fig. 5.2 B**). Results obtained are similar to earlier observations made on addition of TGF-β1 to THP-1 cells [280] and by an autocrine/paracrine mechanism described in HL60 cells [281]. Further investigations (reported elsewhere)

confirmed that addition of PMVs facilitates exit from the cell cycle into cell arrest, G_0/G_1, compared to control (**II.** Ansa-Addo EA et al. 2010).

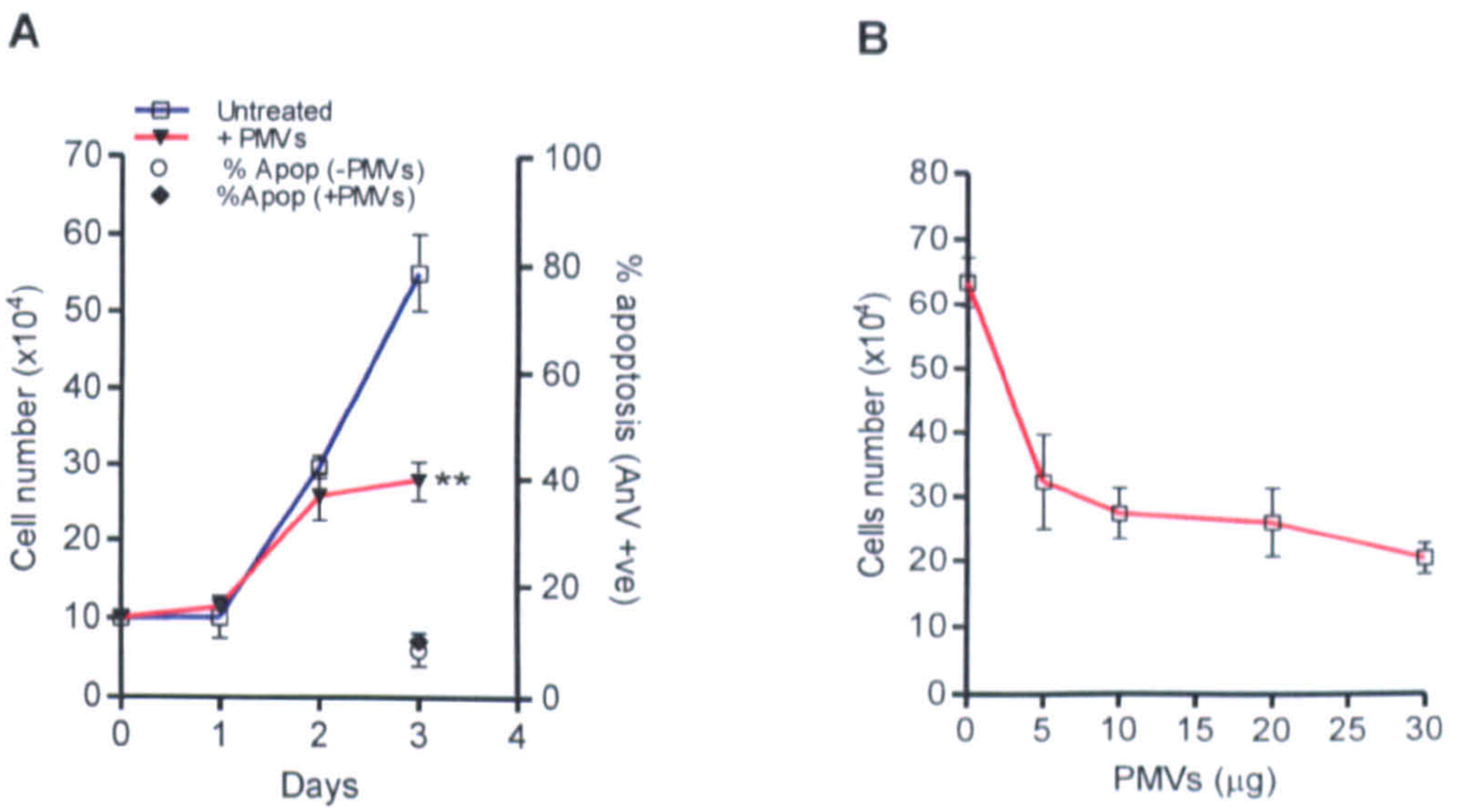

Figure 5.2 PMVs reduce the growth rate of THP-1 monocytes

(A) THP-1 cells were seeded at $1x10^5$ cells/well in triplicate in RPMI supplemented with 5% FBS. Wells were incubated without (open square) or with 10 μg PMVs (solid triangle). At 24 h intervals, cells were harvested and the number determined by flow cytometry. On day 3, the final day of the experiment, the percentage of apoptosis (Annexin V positive) was determined to be approximately 15% whether PMVs had (solid diamond) or not (open circle) been added. After 48 h the addition of PMVs appeared to have halted proliferation of cells (B) The number of viable cells, 3 days after exposing to PMVs, did not reduce substantially with amounts of PMVs ≥10 μg. Each point represents the mean ± SD of triplicate cultures performed several times with similar results. $^{**}P < 0.01$ was considered to be statistically significant.

5.4 PMVs alter cell morphology, increase adherence and induce terminal differentiation

When primary monocytes and THP-1 cells are cultured, they grow in suspension as round cells. However, in addition to the apparent exit from the cell cycle, distinct changes in cell morphology were observed within 24 h of addition of PMVs. The cells began to assume an irregular shape, which became more marked by day three. In order to examine changes in adherence, THP-1 cells were seeded into 24-well plates in RPMI containing 5% FBS, and left untreated or treated with either PMVs (30 µg) or equal amounts of heat-inactivated PMVs (65˚C for 30 min). On each of the days indicated, non-adherent cells were removed into new plates and reincubated at 37˚C in a 5% CO_2 incubator. The old plate was washed three times with RPMI and adherent cells were trypsinised for counting. Consistent with the increase in cell adhesion, membrane protrusions appeared by day 3 **(Fig. 5.3 A)** and increased numbers of cells attached to the culture plate **(Fig. 5.3 B, red bars)**. Cell adhesion was slightly reduced when heat-inactivated PMVs were used **(blue bars in Fig. 5.3 B)**, but only a few cells attached without any treatment **(black bars in Fig. 5.3 B)**.

These observations suggested that PMVs might be inducing the expression of a macrophage-like phenotype in the cells. To investigate this, THP-1 cells were treated with 30 µg of PMVs and after 5 days incubation, were found to have increased expression of CD14 **(Fig. 5.3 C)** and CD11b **(Fig. 5.3 D)** (typical for macrophages), but not DC-SIGN (dendritic cells) **(Fig. 5.3 E)**. Untreated cells expressed low levels of these surface receptors and PMA (1 µM) treated cells were used as a positive control for differentiation into macrophages **(Fig. 5.3 C-E)** [222].

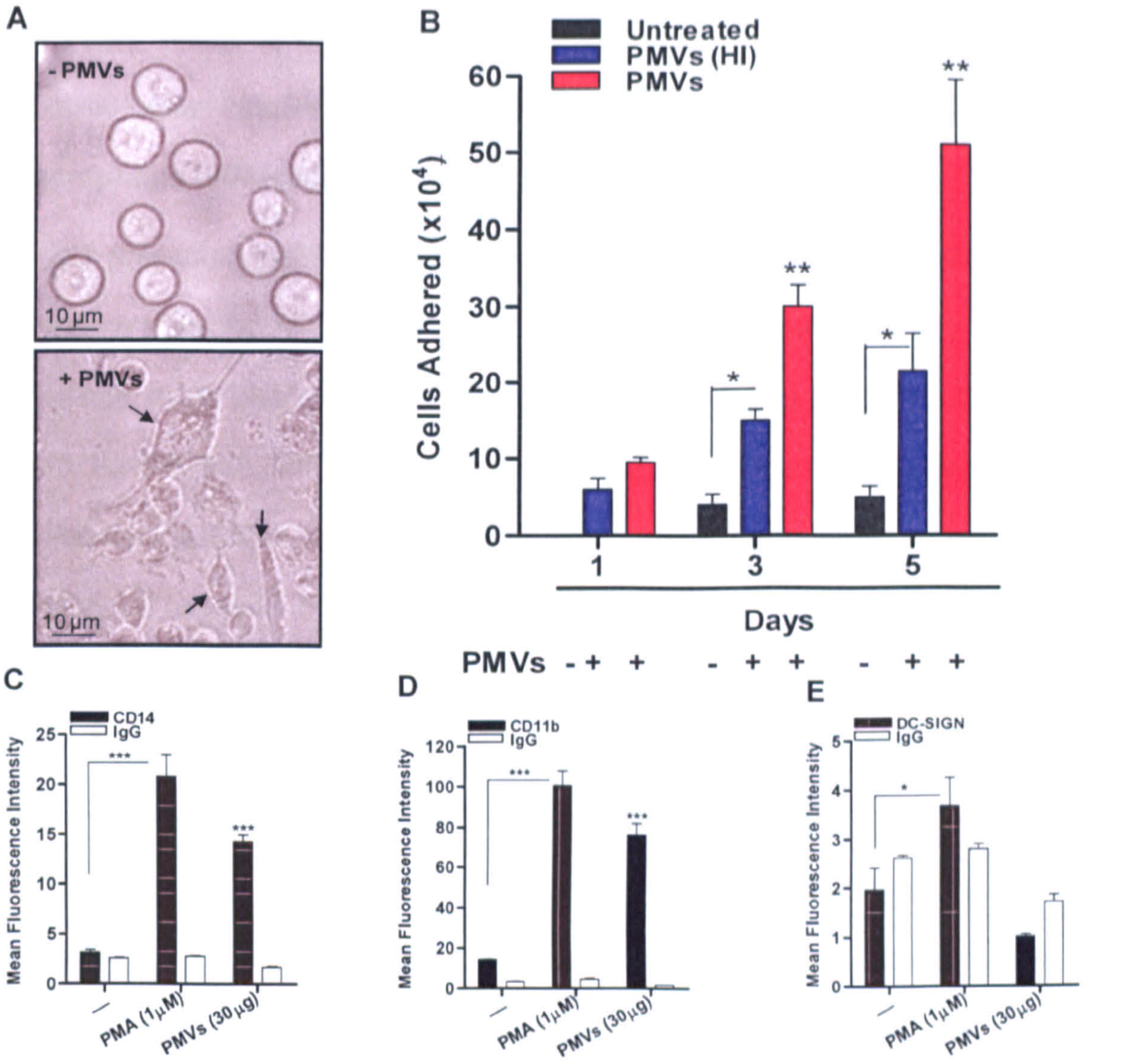

Figure 5.3 Addition of PMVs alters cell morphology, promotes adhesion and differentiation

(A) Human THP-1 cells ($1x10^5$/well) were seeded in triplicate into 24-well plates with or without PMVs. Cell morphology was assessed daily using an inverted light microscope. Arrows in cultures treated with PMVs, indicate attached cells with pseudopodia-like processes after five days incubation. Scale bar = 10 µm (control); 10 µm (treated). (B) Increased numbers of cells were found attached to the plates in PMV-treated wells (red bars). However, heat-inactivation (HI) at 65˚C for 30 min, reduced the number of attached cells (blue bars), but very few cells adhered to the culture plates in the absence of PMVs (black bars). (C-E) Mean fluorescence intensity, indicative of surface expression levels, showed cells treated with PMVs to be significantly positive for CD14 and CD11b, but not DC-SIGN, as compared to untreated control. PMA-treated cells used as a control for monocyte-derived macrophages, were also shown to be highly positive for CD14 and CD11b. Data represents the mean ± SD of two experiments performed in triplicate. ***$P < 0.001$, **$P < 0.01$, *$P < 0.05$ were considered to be statistically significant.

5.5 PMVs released from THP-1 monocytes carry extravesicular TGF-β1 and intravesicular cytokines, MIF, FGF-1 and Gal-3, involved in monocyte-to-macrophage differentiation

In data presented earlier (see section 4.3, table 1), isolated THP-1 PMVs applied to a human cytokine microarray (R&D systems) were shown to carry a range of cytokines, acute phase proteins and chemokines, including IL-12 p70, IL-13, I-TAC, IL-16, IL-17E, MIF, MIP-1 alpha and Serpin-E1. Given the wide range of cytokines carried by the PMVs, investigations focussed on TGF-β1, which if present on the surface of released PMVs, could potentially bind in an autocrine/paracrine-like manner to its cognate receptor on cells [282] and initiate myeloid differentiation [281]. Since TGF-β1 has a signal peptide, we also examined whether cytokines such as MIF, FGF-1 and Gal-3, which lack a signal sequence [268;283,284], are transported in PMVs. Although it had previously been shown that such leaderless cytokines are transported via a non-conventional secretory process [130], it is noteworthy that most of these studies are based on exosomes, which are released upon fusion of multivesicular bodies with the plasma membrane [285].

By flow cytometry (**Fig. 5.4 A**) THP-1 cells were noted to strongly express TGF-β1 (98%) on the surface. This has been described for the pro-peptide part of the large latent complex, often tethered to fibronectin in the extracellular matrix [286]. MIF (30%), FGF-1 (28%) and Gal-3 (17%) are expressed on the surface at lower levels (**Fig. 5.4 A**). Upon stimulation of these labelled cells with 10% NHS, the PMVs released showed expression of TGF-β1 (41%), but not of MIF (0.08%), FGF-1 (0%) and Gal-3 (0.34%) (**Fig. 5.4 B**). When the cells were permeabilised with 0.5%

Tween 20, there was an increased labelling of MIF (87%), FGF-1 (85%) and Gal-3 (92%) (**Fig. 5.4 C**), which implies their greater intracellular expression. Moreover, when these intracellular labelled cells were in turn stimulated to microvesiculate, the plots showing relative fluorescence in PMVs (**Fig. 5.4 D**), showed greater expression of MIF (24%), FGF-1 (22%) and Gal-3 (21%) than found on surface-labelled PMVs, in **Fig 5.4 B**, respectively, suggesting an intravesicular location for these leaderless cytokines in PMVs. Immunofluorescence microscopy further confirmed the extracellular and intracellular expression of TGF-β1, MIF, FGF-1 and Gal-3 on THP-1 cells (**Fig 5.5 A and B**). Furthermore, expression of these cytokines on THP-1 PMVs is confirmed (**Fig. 5.5 C and D**).

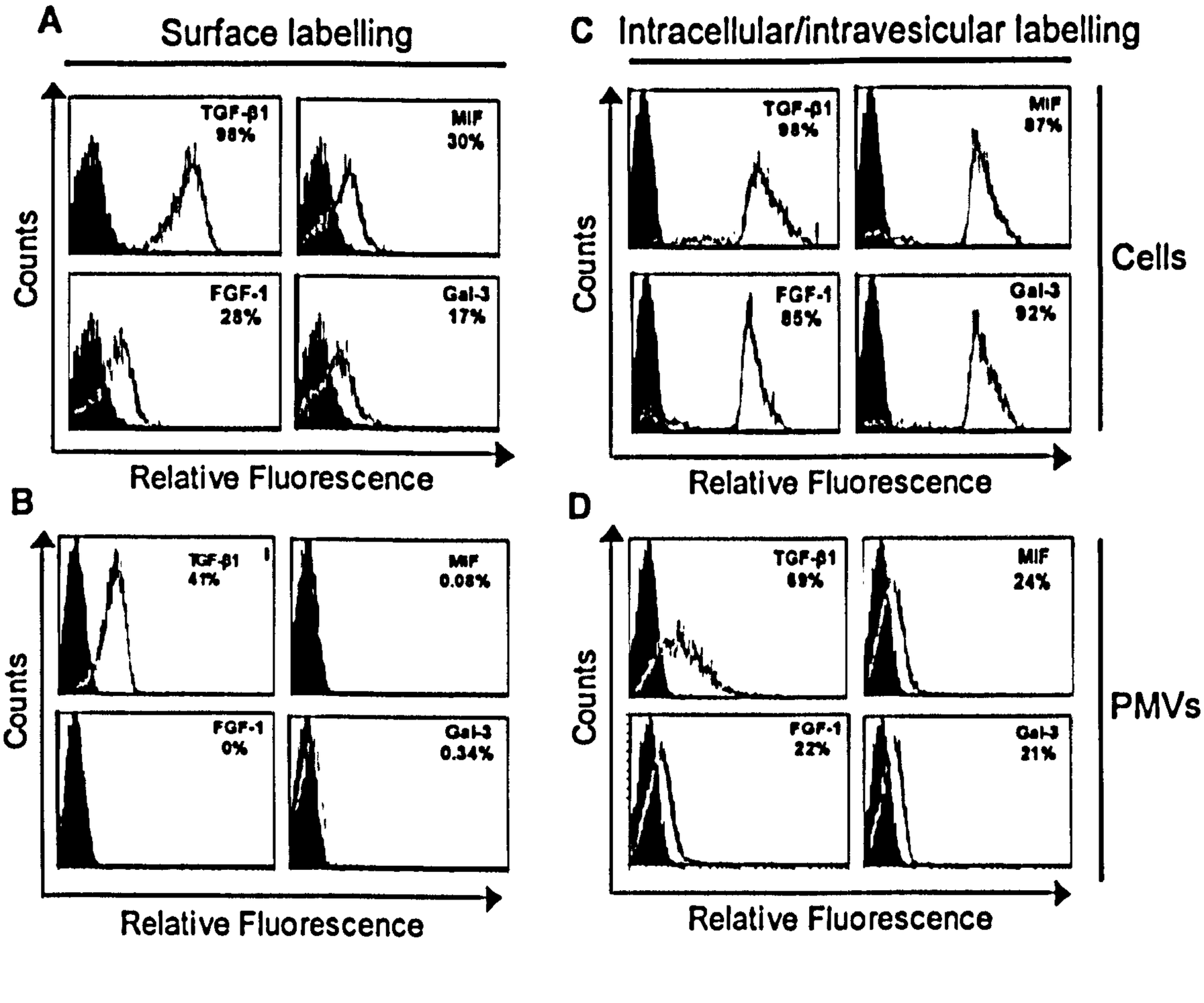

Figure 5.4 Flow cytometry analysis of PMVs for TGF-β1, MIF, FGF-1 and Gal-3.

(A) THP-1 cells ($2x10^6$) and of PMVs, (B) showing surface labelling with antibodies against TGF-β1, and cytokines, which lack a signal peptide (MIF, FGF-1 and Gal-3). Intracellular staining after cell permeabilisation with 0.5% Tween-20 for the aforementioned cytokines (C) and intravesicular staining of released PMVs (D).

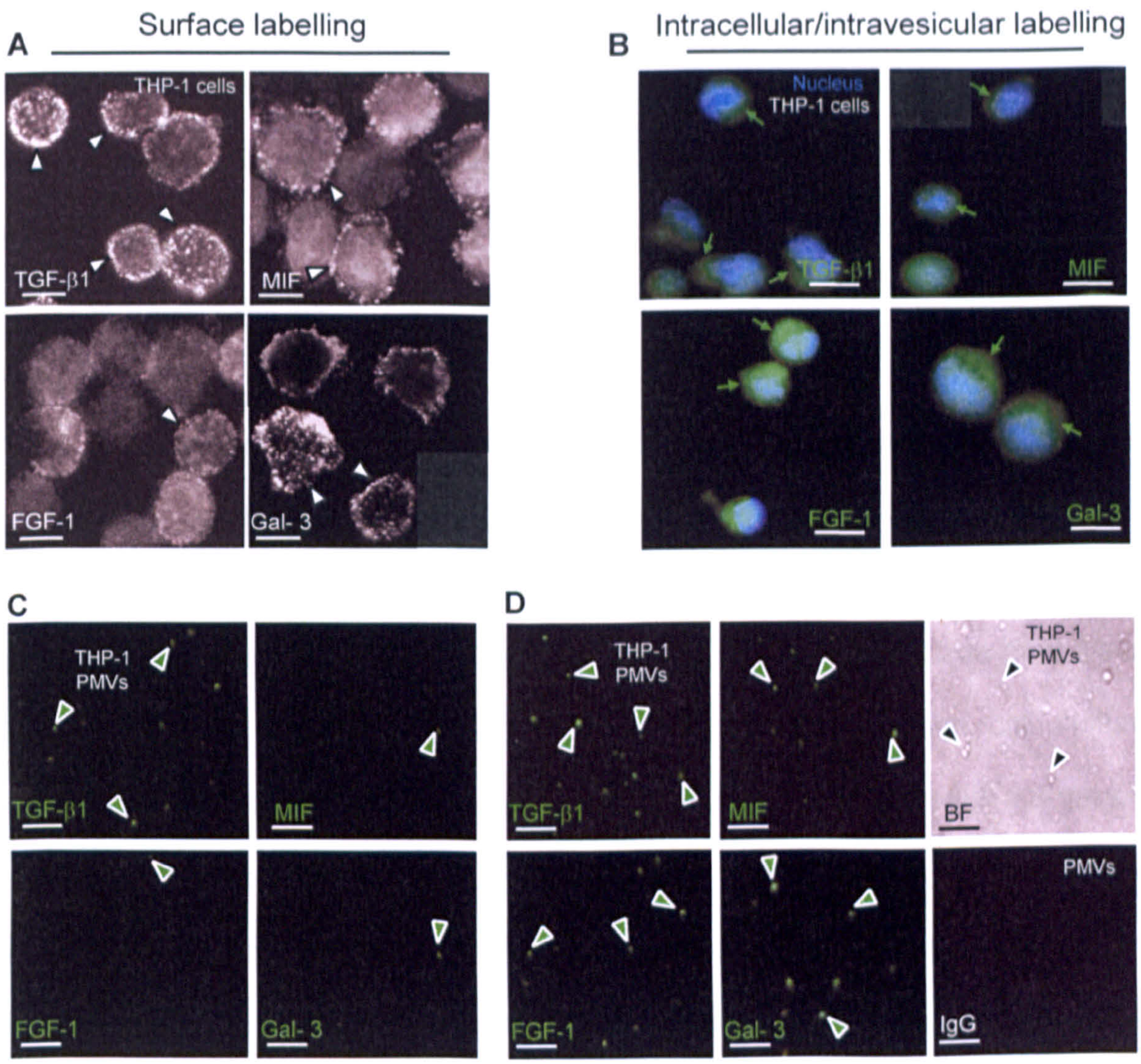

Figure 5.5 Extravesicular expression of TGF-β1 and intravesicular expression of MIF, FGF-1 and Gal-3 by immunofluorescence microscopy.

(A) Surface labelling of TGF-β1 on THP-1 cells, but low levels of MIF, FGF-1 and Gal-3 without prior cell permeabilisation. Arrow heads indicate the respective cytokine detected. (B) Permeabilisation of THP-1 cells ($2x10^6$) with PBS/0.5% Tween-20, the fixed cells were labelled with antibodies against TGF-β1, MIF, FGF-1 and Gal-3. Nucleus was stained with DAPI (blue) while FITC shows detection of the various cytokines (green arrows). Scale bar for A and B = 100 µm. (C) Surface labelling of TGF-β1 on THP-1-derived PMVs, but only low levels of MIF, FGF-1 and Gal-3 was detected. (D) PMVs isolated from permeabilised cells labelled with antibodies to TGF-β1, MIF, FGF-1 and Gal-3. BF (Bright Field), IgG (Isotype control), Scale bar for C and D = 20 µm.

Although no significant difference was observed in TGF-β1 levels, by ELISA, whether or not the PMVs were lysed (**Fig. 5.6 A**), by contrast, levels of MIF, FGF-1 and Gal-3, where significantly higher when PMVs were lysed before measurement (**Fig. 5.6 B-D**). This data supports the results shown in figure 5.4, and further confirms that TGF-β1 is predominantly expressed on the PMV surface, while MIF, FGF-1 and Gal-3 are mostly intravesicular.

When MIF was measured in PMV-depleted cell culture supernatant, we noticed that levels of MIF (**white bar in Fig. 5.6 E**) were lower as compared to those found in cell culture supernatant (including unlysed PMVs) (**blue bar in Fig. 5.6 E**). However, levels of MIF were significantly higher when measurements were made from lysed PMVs alone (**red bar in Fig. 5.6 E**). This suggests that when cell culture supernatant is used to measure the amount of secreted cytokines, levels are greatly underestimated because many cytokines are carried within intact PMVs. Microvesicles derived from monocytes were reported to induce apoptosis by delivering the apoptotic signal caspase 1, a leaderless protein to vascular smooth muscle cells (VSMCs). The same effect was not detected when monocyte cell culture supernatant depleted of microvesicles was added to VSMCs [287]. This further confirms that PMVs carry the majority of non-conventionally secreted proteins released into culture supernatants.

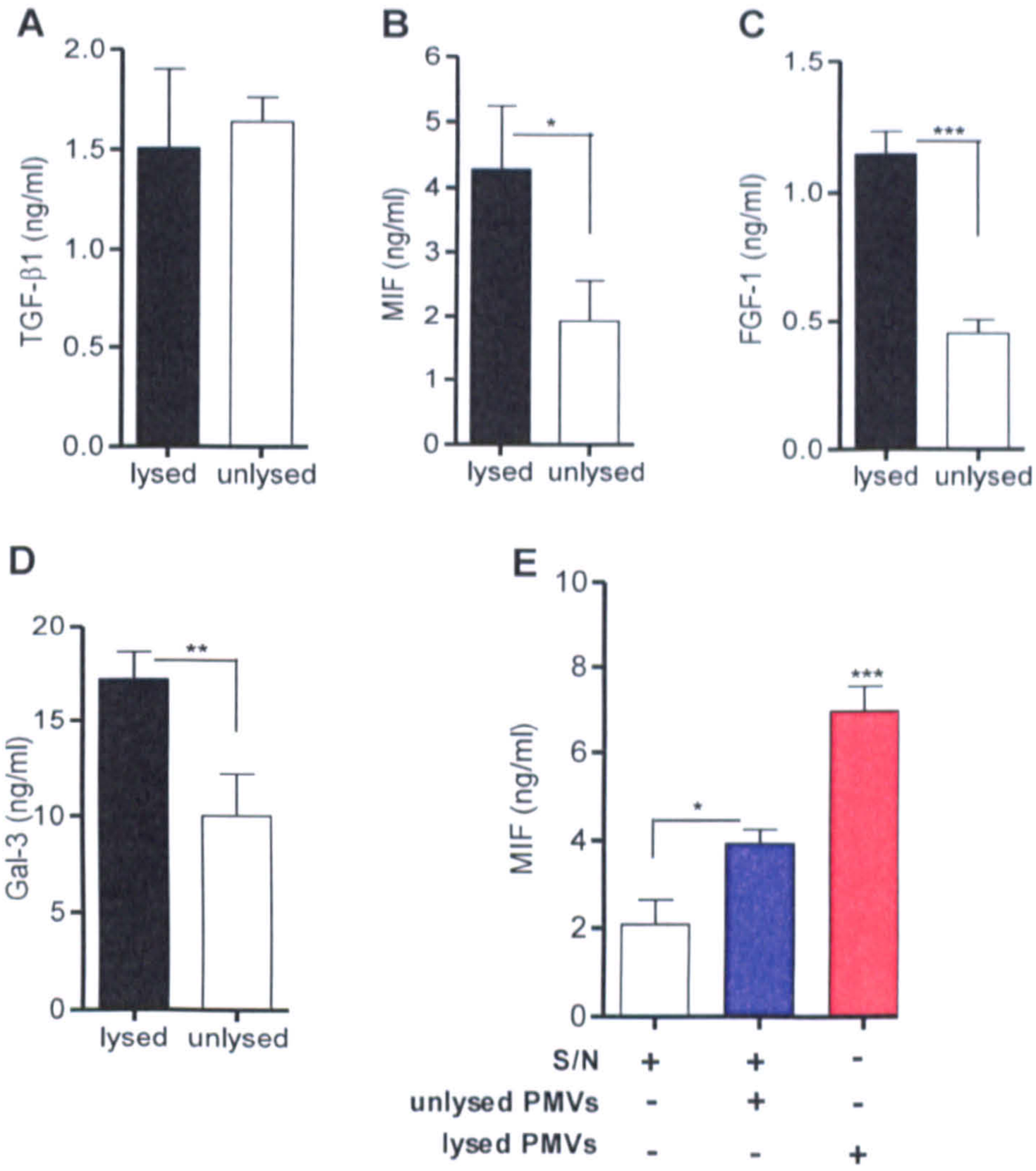

Figure 5.6 ELISA measurements of selected cytokines in lysed and intact PMVs released from THP-1 cells

PMVs (30 µg) from stimulated cells (10% NHS at 37°C for 30 min) were either lysed or left unlysed and cytokine levels measured. (A) There was no significant difference between TGF-β1 levels in lysed or intact PMVs. Increased levels of MIF (B), FGF-1 (C) and Gal-3 (D), however, were measured by ELISA after lysis of PMVs. (E) Shows ELISA measurement of MIF from cell culture supernatants with and without PMVs. Supernatant (S/N) with PMVs removed had low levels of MIF (white bar). However, in S/N plus PMVs, which is representative of a cell culture medium, higher concentrations of MIF were detected (blue bar). When PMVs were separated from the supernatant and lysed with 1% Triton X-100, significantly higher concentrations of MIF were detected (red bar). Data represents mean ± SD of two separate experiments performed in duplicate. ***$P < 0.001$; **$P < 0.01$; *$P < 0.05$ were considered statistically significant.

5.6 TGF-β1 carried by PMVs inhibits proliferation of THP-1 monocytes

It was further investigated whether the ability to inhibit the rate of cell growth was only characteristic of PMVs released from THP-1 cells. When PMVs from other cell lines, such as, MCF-7 (breast cancer), Jurkat (T cell) as well as those from THP-1 (monocytic leukaemia) were added to THP-1 cells, only those from Jurkat and THP-1 cells, which carried higher levels of TGF-β1 (**Fig. 5.7A**), significantly reduced proliferation (**Fig. 5.7 B**) a known pre-requisite for differentiation. By contrast, MCF-7 PMVs, which carry less TGF-β1, only reduced proliferation marginally compared to untreated control. This apparent correlation between levels of TGF-β1 and growth reduction, suggests the effect observed could be due to TGF-β1 present on the PMVs.

Involvement of TGF-β1 was confirmed by showing that the inhibition of growth rate of cultures treated with PMVs was restored to near control rates with 10 μM SB-431542 (**Fig. 5.7 C**), the specific inhibitor of TGF-β receptor kinase and the associated intracellular mediators such as Smad, both central to TGF-β1-mediated differentiation of myeloid cells [288]. Moreover, the specificity of SB-431542, in inhibiting TGF-β1 signalling, has also been demonstrated in experiments to inhibit the TGF-β1-dependent growth of HT-29 colon cancer cells [289].

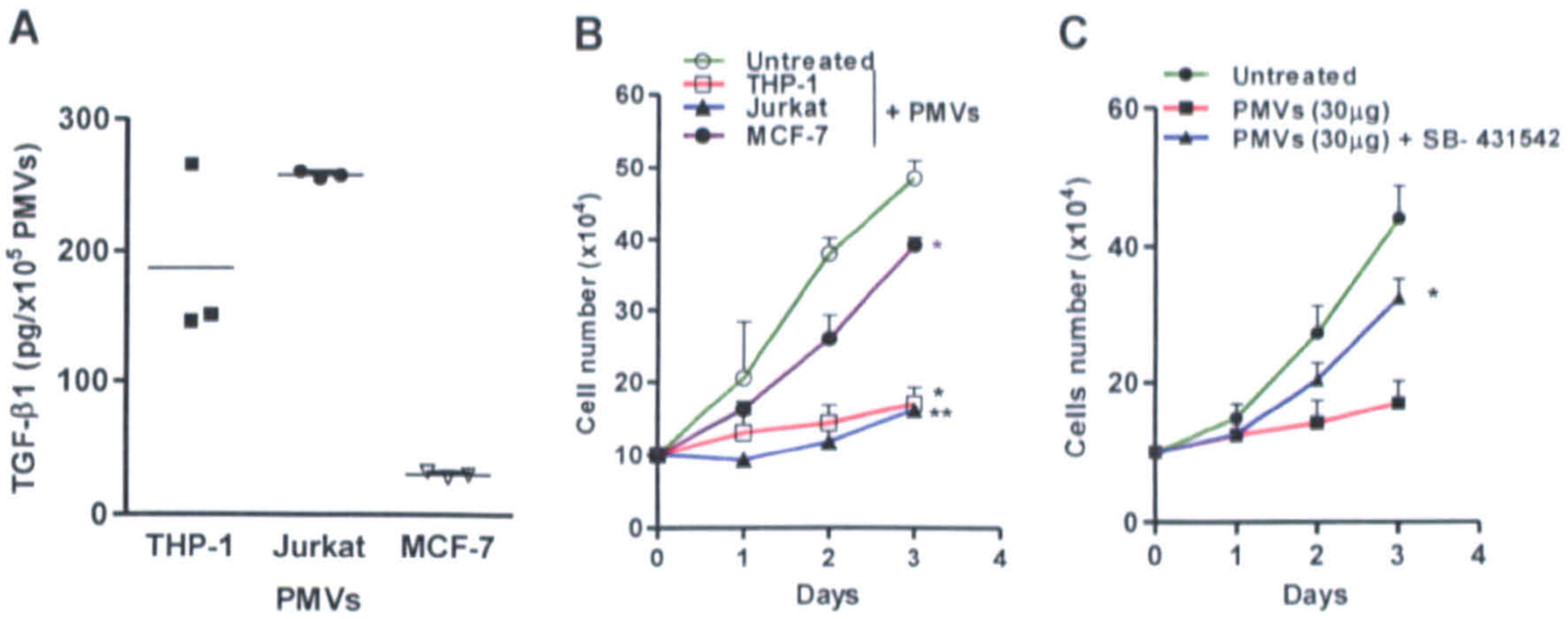

Figure 5.7 PMVs carry TGF-β1, which is responsible for the reduced rate of cell growth

(A) PMVs isolated from THP-1 and Jurkat cells, unlike those from MCF-7 cells, carry higher levels of TGF-β1, as measured by ELISA. (B) THP-1 cells ($1x10^5$/well) were left untreated or treated with PMVs (30 μg) isolated from THP-1, Jurkat or MCF-7 cell-lines. The cells were incubated at 37°C and quantified each day by flow cytometry. PMVs from THP-1 and Jurkat cells were more effective at reducing the growth rate than MCF-7 PMVs. (C) Addition of the TGF-β1 receptor antagonist, SB-431542 (10 μM), abolished the inhibitory effect of PMVs and restored the growth rate of the cells to almost control levels. Data represent mean ± SD of two separate experiments performed in triplicate. $^{**}P < 0.01$, $^{*}P < 0.05$ were considered to be statistically significant.

5.7 Discussion

The release of Plasma Membrane-derived Vesicles by various cells has been implicated in a wide range of biological activities in both *in vitro* and *in vivo* studies [290-292]. The most characterised function is that of intercellular communication [3,293]. For example, neutrophil-derived ectosomes have been found to interfere with the maturation of monocyte-derived dendritic cells [229]. Moreover, platelets were reported to transfer tissue factor to monocytes [16], but not to neutrophils [294] through the release of PMVs. In addition, erythrocyte-derived PMVs may transfer phosphatidylserine to nucleated cells and falsely mark them for clearance by phagocytosis [120].

The present study, demonstrated for the first time that PMVs (isolated from THP-1 cells) carry TGF-β1 on their membrane surface. These TGF-β1-bearing PMVs can modulate the growth rate of peripheral blood monocytes and their leukaemic counterparts *in vitro* without stimulating apoptosis. In addition, a dramatic change was observed in the morphology of PMV-treated cells. The cells became increasingly irregular in shape and had membrane extensions that resembled pseudopodia. An examination of several differentiation characteristics revealed that the cells that were completely attached to the culture plate following incubation with PMVs, also expressed typical markers of macrophages. Thus, the adherent cells expressed significantly higher levels of CD14 and CD11b, but not the dendritic cell specific marker DC-SIGN [295]. Data presented here also showed that PMVs isolated from Jurkat and THP-1 cells carrying high TGF-β1 (>200 pg/1x10^5 PMVs), caused significantly greater reductions in the growth rate of THP-1 cells, as compared to

PMVs from MCF-7 breast cancer cells expressing lower levels of TGF-β1 (~30 pg/1x10^5 PMVs).

Previously it was shown that recombinant TGF-β1 (rTGF-β1) could promote differentiation of human promonocytic leukaemic cells into macrophages [280]. The present results are in agreement, but go on to show that upon attachment of PMVs to THP-1 cells, which may, as in the case of contact (and fusion) of monocyte-derived PMVs with platelets be annexin V-mediated, the source of macrophage-inducing TGF-β1 is likely be that which is carried on PMVs. Although contact with or phagocytosis of apoptotic cells and PMVs by macrophages has been shown to release TGF-β1, at levels of 80 pg/ml [296] and 350 pg/ml [297] respectively, importantly, such release and autocrine-like action of TGF-β1 on the THP-1 cells, resulting in the observed reduction in proliferation (and consequent differentiation), is unlikely to have occurred in this study, as low TGF-β1-carrying MCF-7-derived PMVs were unable to elicit significant reductions in proliferation.

Several inhibitors of TGF-β1 signalling have been reported as potential therapeutics in cancer immunotherapy. Among these is the TGF-β receptor antagonist, SB-431542, shown to inhibit the ligand-dependent growth of HT-29 colon cancer cells [288]. It was also demonstrated to be a selective inhibitor of endogenous activin and TGF-β1 signalling, [298;299]. The involvement of TGF-β1 was demonstrated in this study by showing that 10 μM SB-431542 almost completely reversed the growth inhibition due to PMV-treatment of cells.

This study also confirmed that the leaderless, intracellular cytokines, MIF, FGF-1 and Gal-3, are present within PMVs, and thus secreted non-conventionally. As reported for TGF-β1, and described earlier, these leaderless cytokines have also been shown to play important roles during the differentiation of myeloid cells. It is noteworthy, that significant levels of non-conventionally secreted proteins released by cells may be carried within PMVs, and that these are not detected in culture supernatants. For example, significant levels of MIF were detected in lysed PMVs, compared to PMV-depleted supernatants. Whilst intravesicular cytokines and other proteins such as caspases [119] can be delivered to, and cause effects in recipient cells, this has not hitherto been shown for a surface-bound cytokine, as described herein, for TGF-β1.

The concept that surface TGF-β1 can stimulate TGF-β1-mediated signalling on cell-to-cell contact is not new and has been described in T cells. Regulatory T cells ($CD4^+CD25^+$) express active TGF-β1 [300], which interacts with receptor on effector cells thereby mediating immunosuppression [301]. Similarly, surface-bound, albeit latent TGF-β1, on the surface of colorectal cancer (CRC) cells has also been implicated in immunosuppression following cell-cell contact [302]. Although activation may occur through various mechanisms, upon cell contact, latent TGF-β1 may be activated by alpha V integrins, then mediating Smad signalling through the TGFβRI and TGFβRII receptors; mitogen activated protein kinase (MAPK) and PI3K/Akt pathways may also be modulated. This report shows that PMVs are released from cells stimulated through deposition with either sublytic complement or upon treatment with agents used in differentiation therapy, or that synergise with other such agents, to induce cell cycle arrest and promonocyte differentiation. When the

PMVs were added to the promonocytic leukaemia cell line THP-1, the cells were found to exit the cell cycle at G_0/G_1 and had the effect of promoting differentiation along the monocytic lineage to mature $CD14^+$ monocytes. To further ascertain the relative importance of PMV release after stimulation with ATRA, PMA or histamine, in terms of limiting proliferation, it would be interesting to stimulate promonocytic cell lines with these agents following pre-treatment with calpeptin, which specifically blocks calpain-mediated PMV release. In view of the need to expand the limited range of therapies in monocytic leukaemia, it might be prudent to look at other PMV-releasing agents as potential alternative drugs in differentiation therapy in AML.

Also, since addition of PMVs inhibited the growth rate of human peripheral blood monocytes, one could speculate that PMVs may be involved in terminal monocyte-macrophage differentiation during infection. This is supported by observations (reported in chapter 7) that *Salmonella enterica serovar typhimurium* (*S. typhi)* SL1-344 stimulates PMV release from THP-1 cells and induces differentiation. In other work, marked numbers of neutrophils, dendritic cells and macrophages where observed in mice chronically infected with *S. typhi* [303]. These *in vitro* findings support a model in which TGF-β1-bearing PMVs, released constitutively from monocytes, or in higher amounts during pathogen infections, support a possible autocrine/paracrine-like mechanism to significantly reduce proliferation of monocytes and induce terminal differentiation into macrophages. Moreover, these findings may provide insight into the mechanisms underlying the increased macrophage numbers measured during infections and therefore warrants further study.

6. *Trypanosoma cruzi*-elicited release of plasma membrane-derived vesicles, enhances their invasion of cells

6.1 Introduction

The procedures employed in the isolation and characterisation of PMVs, as well as their possible roles in promoting the differentiation of human monocytes into macrophages has so far been discussed. This role in promoting the terminal differentiation of promonocytic leukaemia cells seems at least in part, to be due to surface TGF-β1 carried by PMVs. Chapter six goes on to look at the process of cellular invasion by the intracellular protozoan parasite, *T. cruzi*, which is also part mediated by TGF-β1. The role of PMVs in inhibiting host complement is also explored.

6.1.1 Overview of the *Trypanosoma cruzi* parasite

The protozoan parasite, *Trypanosoma (T.) cruzi* is the aetiological agent of Chagas disease, which affects approximately 16 to 18 million individuals in Latin America, and causes about 50,000 deaths per annum [165]. During its life cycle, *T. cruzi* undergoes several morphological changes, and each stage has developed survival strategies against the hostile environment encountered in host cells [304].

The sylvatic cycle alternates between an insect vector and a vertebrate host. Epimastigotes (non-infective stage) residing in the mid-gut of the insect, move to the hindgut and differentiate into metacyclic trypomastigotes (vertebrate infective stage) ready for release. A single bite from the insect releases the parasites onto the host skin, which are then inoculated after scratching of the bite site. Once inside the host, the parasite has to evade the innate immune system and infect host cells in order to progress in its life cycle. Metacyclic trypomastigotes differentiate into amastigotes (multiplicative intracellular stage) and after several rounds of binary division,

differentiate into bloodstream trypomastigotes. These break out of the cell and infect other cells or circulate in the blood and are taken up by the insect vector, thus repeating the infectious cycle.

6.1.2 Human Complement System

The main barrier encountered by the parasite during infection of mammalian cells is the human complement system. This consists of 20 serum proteins, which are sequentially activated by specific proteins or carbohydrates expressed by invading pathogens. The complement system is part of the host's innate immune defense mechanism and once activated, forms a major barrier against infectious pathogens, resulting in their destruction [305].

The complement system is activated via three pathways, the classical, lectin and alternative pathways. The classical pathway (CP) is activated when C1q binds to the pathogen and activates its associated proteases C1r and C1s, leading to cleavage of the C2 and C4 components and generation of the C3 convertase (C4b2a). The lectin pathway is activated when pathogen carbohydrates are recognised by mannan-binding lectin (MBL), L-ficolins and H-ficolins. These proteins interact with the MBL-associated serine protease–2 (MASP-2), which then cleaves C2 and C4 to form the C3 convertase. Activation of the alternative pathway, involves direct binding of the C3b component to the pathogen and subsequent association with Factor B to form the C3 convertase (C3bBb) [305].

6.1.3 Mechanism of Infection

Recently, Cestari and Ramirez (2010) reported that metacyclic trypomastigotes of some *T. cruzi* strains are susceptible to complement-mediated lysis in human serum [306], suggesting that other extrinsic factors may contribute to immune evasion. Moreover, *T. cruzi* metacyclic trypomastigotes have to invade cells after evading the immune system and several parasite surface molecules have been described which participate in this process [307]. *T. cruzi*-elicited signals result in an increase in host cell cytosolic Ca^{2+}, which activates exocytosis of lysosomes to the plasma membrane. Parasites fuse with the lysosomes to form the parasitophorous vacuole (PPV), in which they reside and initiate their differentiation into amastigotes [308,309]. During infection of mammalian cells, *T. cruzi* is challenged by drastic physiological changes, which raises the question of whether previously unknown host factors are utilised by the parasite to evade the innate immune system.

The data presented in this section shows that addition of monocyte-derived PMVs enhanced *T. cruzi* invasion of mammalian cells. Moreover, PMVs isolated from several cell types including the T cell line, Jurkat, the hepatocyte, HepG2 and the breast cancer cell line, MCF-7, increased infection in a TGF-β dependent fashion. Subsequent experiments with our collaborators at the Instituto Oswaldo Cruz, Rio de Janeiro, Brazil showed that *T. cruzi* mediates the release of PMVs, which bind to the complement C3 convertase and inhibit its catalytic activity, thus diminishing complement-mediated killing of the parasite (Cestari et al, 2010- submitted).

6.2 *T. cruzi* metacyclic trypomastigotes stimulate the release of PMVs

Earlier reports have suggested that unlike the epimastigote, insect form, *T. cruzi* metacyclic trypomastigotes elicit an increase in host cytosolic Ca^{2+} during invasion. Also, since metacyclic trypomastigotes from the hind region of the insect vector, have the first contact with the host bloodstream during the early stages of infection, experiments were setup to investigate whether *T. cruzi* can stimulate the release of PMVs from mammalian cells. THP-1 cells were washed twice by centrifugation (160 *g*, 5 min) and resuspended in fresh RPMI supplemented with 2 mM $CaCl_2$. Cells were seeded into 12-well plates at $1x10^6$ cells/well in triplicate and incubated with epimastigotes or metacyclic trypomastigotes ($5x10^6$ parasites/well) at 37°C for 30 min, in the presence or absence of 5 mM EGTA. After incubation, supernatant was collected and released PMVs were isolated and analysed according to the method described in section 3.9.2.

Epimastigotes failed to stimulate PMV release from THP-1 cells (**Fig 6.1 A**). In contrast, metacyclic trypomastigotes induced a three-fold increase in PMV release compared to non-induced (NI) cells, and the mechanism involved is calcium-dependent, since the Ca^{2+}-chelating agent, EGTA, reduced the number of released vesicles to that of control. Moreover, metacyclic trypomastigotes induced a dose-dependent response in the release of PMVs (**Fig 6.1 B**) and further experiments with Fura-2AM-labelled THP-1 cells showed that infective trypomastigotes, but not epimastigotes induce a ten-fold increase in intracellular Ca^{2+} in the host cell (**Fig 6.1 C**).

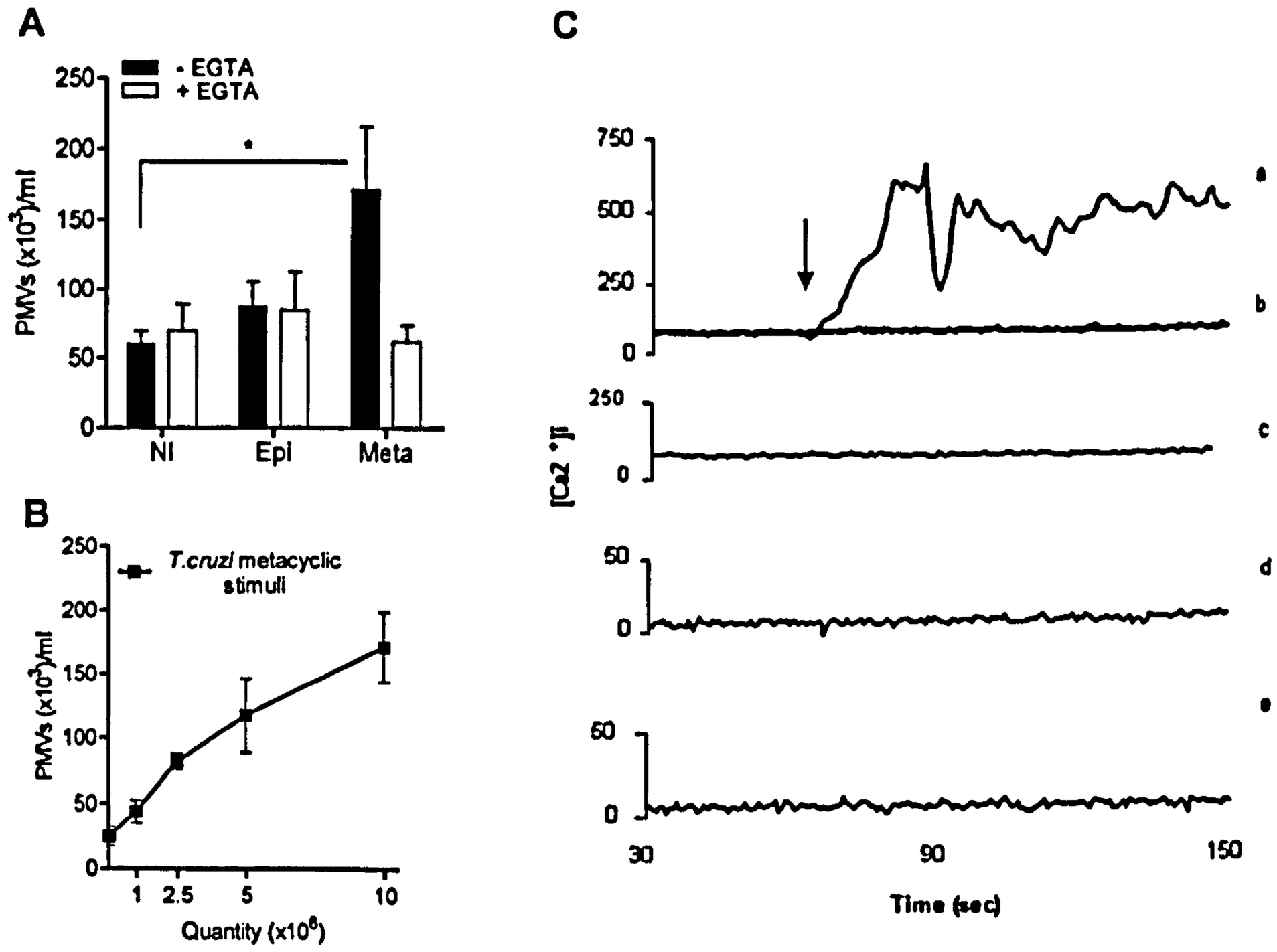

Figure 6.1 *T. cruzi* metacyclic trypomastigotes elicit a Ca^{2+} response to induce release of PMVs.

(A) *T. cruzi* metacyclic trypomastigotes, but not epimastigotes, stimulate THP-1 cells to release PMVs. Cells were incubated at 37°C for 30 min with parasites at a 1:5 (cells to parasites) ratio in triplicate 1 ml reactions. PMV release in the presence or absence or EGTA (5 mM) is isolated by differential centrifugation and analyses performed by flow cytometry. (B) Using increasing amounts of metacyclic trypomastigotes, PMV release is measured as a dose-dependent response. (C) Infective metacyclics induce an increase in cytosolic Ca^{2+} in THP-1 cells. Cells labelled with Fura-2AM are placed into a quartz crystal cuvette in a spectrophotofluorometer and stimulated with *T. cruzi* after 60 seconds (arrow): a) metacyclic trypomastigotes, b) epimastigotes, c) control (no parasites), d) metacyclic trypomastigotes with 5 mM EGTA e) epimastigotes with 5 mM EGTA. Data represents the mean ± SD of two individual experiments performed in triplicate. $^*P < 0.05$ was considered to be statistically significant.

6.3 THP-1 cell-derived PMVs enhance *T. cruzi* invasion, which is abolished after heat-treatment or trypsinisation of the vesicles

T. cruzi metacyclic trypomastigotes, but not epimastigote forms stimulate the release of PMVs from mammalian cells. The results presented in figure 6.1 raised more questions including, why was it metacyclic trypomastigotes and not epimastigotes, which stimulated the release of PMVs from THP-1 cells? Could these *T. cruzi*-induced PMVs be carrying extrinsic factors that might explain why trypomastigotes are infective as compared to epimastigotes? Indeed, the data presented earlier showed that THP-1 cell-derived PMVs, carry complement regulatory proteins such as decay accelerating factor (DAF) and complement receptor 1 (CR1) (see section 4.2.6, figure 4.6 B).

In order to answer these questions, experiments were set up to investigate the role of PMVs in *T. cruzi* infection. In chapter 5, data presented showed that PMVs might participate in the differentiation of monocytes into macrophages. Since *T. cruzi* can stimulate cells to release PMVs, the role of these vesicles during parasite invasion was investigated. Semi-confluent Vero cells seeded overnight into 12-well plates at $2x10^5$/well in triplicate, were preincubated with PMVs ($1x10^6$/well) at 37°C for 30 min. In some experiments, *T. cruzi* metacyclic trypomastigotes were preincubated with PMVs and washed extensively, prior to addition to cells. Parasites were also analysed by flow cytometry after incubating with PMVs for expression of annexin V, which is exposed on the surface of PMVs. The invasion assay was performed at 37°C for 3 h with metacyclic trypomastigotes or epimastigotes in a 5:1 (parasites to cell) ratio. To detect how the PMVs might be interacting with *T. cruzi*, a binding experiment was set up. Briefly, *T. cruzi* metacyclic trypomastigotes ($5x10^5$) were

incubated with or without R-18 labelled THP-1 cell-derived PMVs ($5x10^5$) at 37°C for 30 min. Parasites were washed three times by centrifugation at 4,000 rpm for 10 min with PBS. After washing, parasites were fixed by centrifugation on to coverslips and fixed with 4% formaldehyde. Coverslips were inverted on to microscope slides and stained with DAPI-VECTASHIELD containing mounting medium to stain the nucleus and kinetoplast, and images were acquired using the Olympus 1X81 fluorescence camera microscope as described in section 3.9.8.

Addition of THP-1 cell-derived PMVs significantly enhanced *T. cruzi* invasion of Vero cells (**Fig. 6.2 A**). However, epimastigotes, which are non-infective, failed to invade even in the presence of PMVs, thus, implying that the mechanism is also dependent on the infective stage of the parasite. Furthermore, invasion in the presence of PMVs was dose-dependent (**Fig. 6.2 B**) and the parasites acquired annexin V from the vesicles possibly suggesting binding/fusion between the two membranes (**Fig. 6.2 C**). Hitherto, incubation of R-18 labelled PMVs with *T. cruzi* showed the vesicles to bind to the surface membrane of the parasite (**Fig. 6.2 D**). Subsequent experiments carried out in the lab confirmed this binding interaction between PMVs and *T. cruzi*, as fusion of the two membranes [Cestari, I. (2009) Ph.D project]

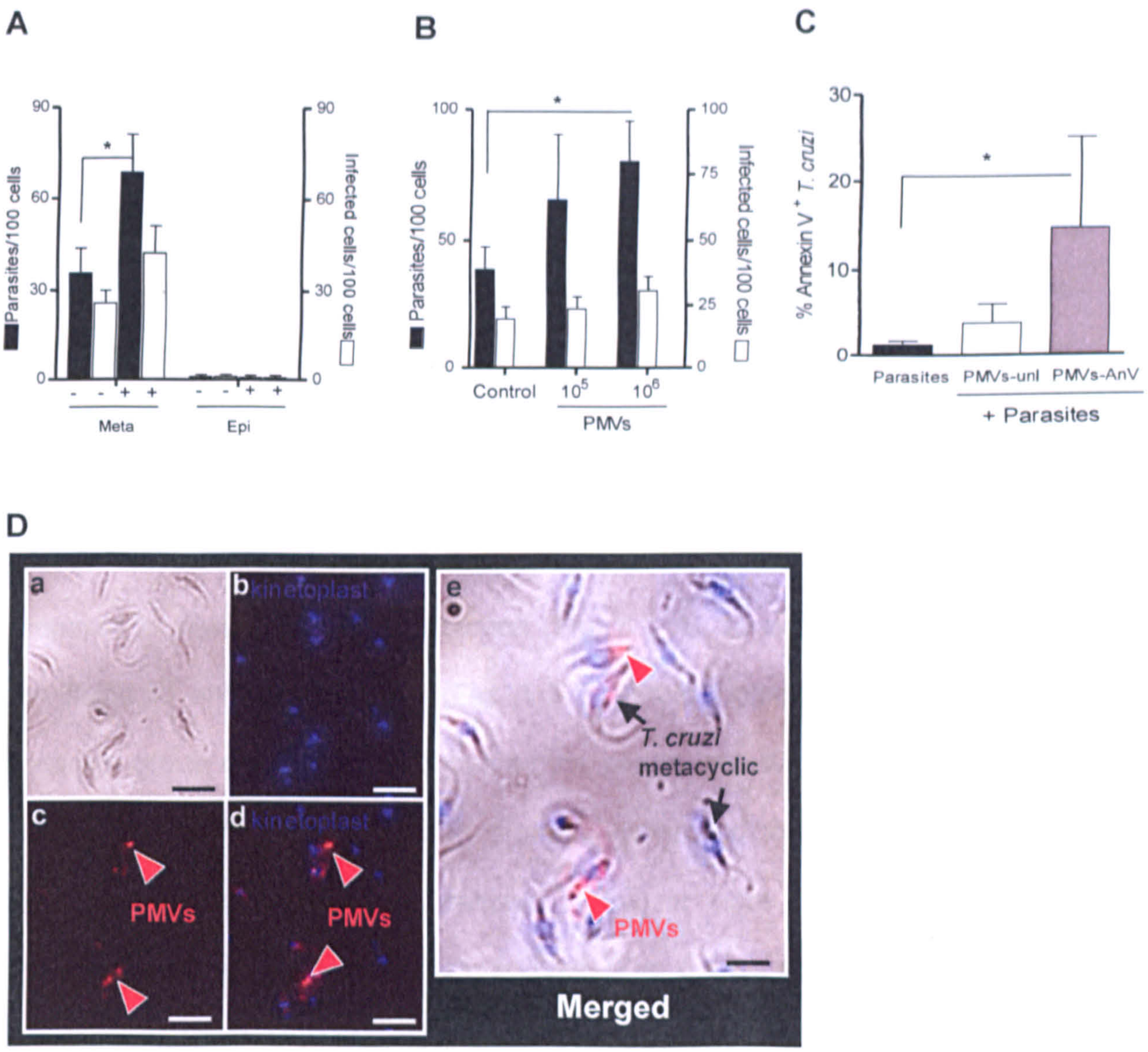

Figure 6.2 PMV enhancement of *T. cruzi* infection, is strain specific and dose-dependent

(A) Addition of THP-1 cell-derived PMVs, increase *T. cruzi* infection of Vero cells. However, only the infection of metacyclic trypomastigotes is enhanced, thus impling that the mechanism involved is stage specific. (B) Invasion of metacyclic trypomastigotes in the presence of PMVs is dose-dependent. (C) *T. cruzi* acquire annexin V from annexin-labelled PMVs following incubation at 37°C for 15 min, and five washes with PBS. (D) THP-1 cell-derived PMVs bind to the surface membrane of *T. cruzi*. (a) Brightfield image of *T. cruzi* metacyclic trypomastigotes. Scale bar = 100 µm. (b) *T. cruzi* stained with DAPI, blue fluorescence shows the parasite kinetoplasts. (c) R-18-labelled PMVs are shown in red. (d) Combined image of R-18-labelled PMVs and DAPI stained *T. cruzi*. (e) Fluorescence image showing that PMVs bind to the surface of *T. cruzi*. Arrows indicate parasites and arrowheads show the position of PMVs. Scale bar = 20 µm. Data represent the mean ± SD of two separate experiments performed in triplicate. $^{*}P < 0.05$ was considered to be statistically significant.

If PMVs enhance *T. cruzi* invasion, then it could be due to the molecule(s) they carry. In order to elucidate these, invasion experiments were repeated, but this time, isolated PMVs were either heat-inactivated (65°C for 1 h) or trypsinised (0.25% trypsin/EDTA) at 37°C for 10 min to remove all surface molecules prior to performing infection assays. THP-1 cell-derived PMVs (5x105) were also lysed by freezing at -80°C and thawing in a 37°C water bath repeatedly for at least 10 times. This PMV lysate was then incubated with Vero cells infected with *T. cruzi*.

Indeed, heat-inactivated PMVs failed to enhance *T. cruzi* invasion of Vero cells, compared to PMVs not heat-inactivated (**Fig. 6.3 A**). Likewise, trypsinised PMVs also failed to enhance invasion (**Fig. 6.3 B**), thus suggesting requirement of a protein or group of proteins produced by the parent cell. It is noteworthy, that the addition of PMVs does not only promote enhanced cell invasion, but also encourages superinfection (cells infected by two or more parasites) by *T. cruzi*, although, this was only detected at low levels (**Fig. 6.3 C**). After fixing and staining samples with DAPI-VECTASHIELD (Vector laboratories, CA, USA), intracellular trypomastigotes (**Fig. 6.3 D**) were detected after examination under a fluorescence microscope.

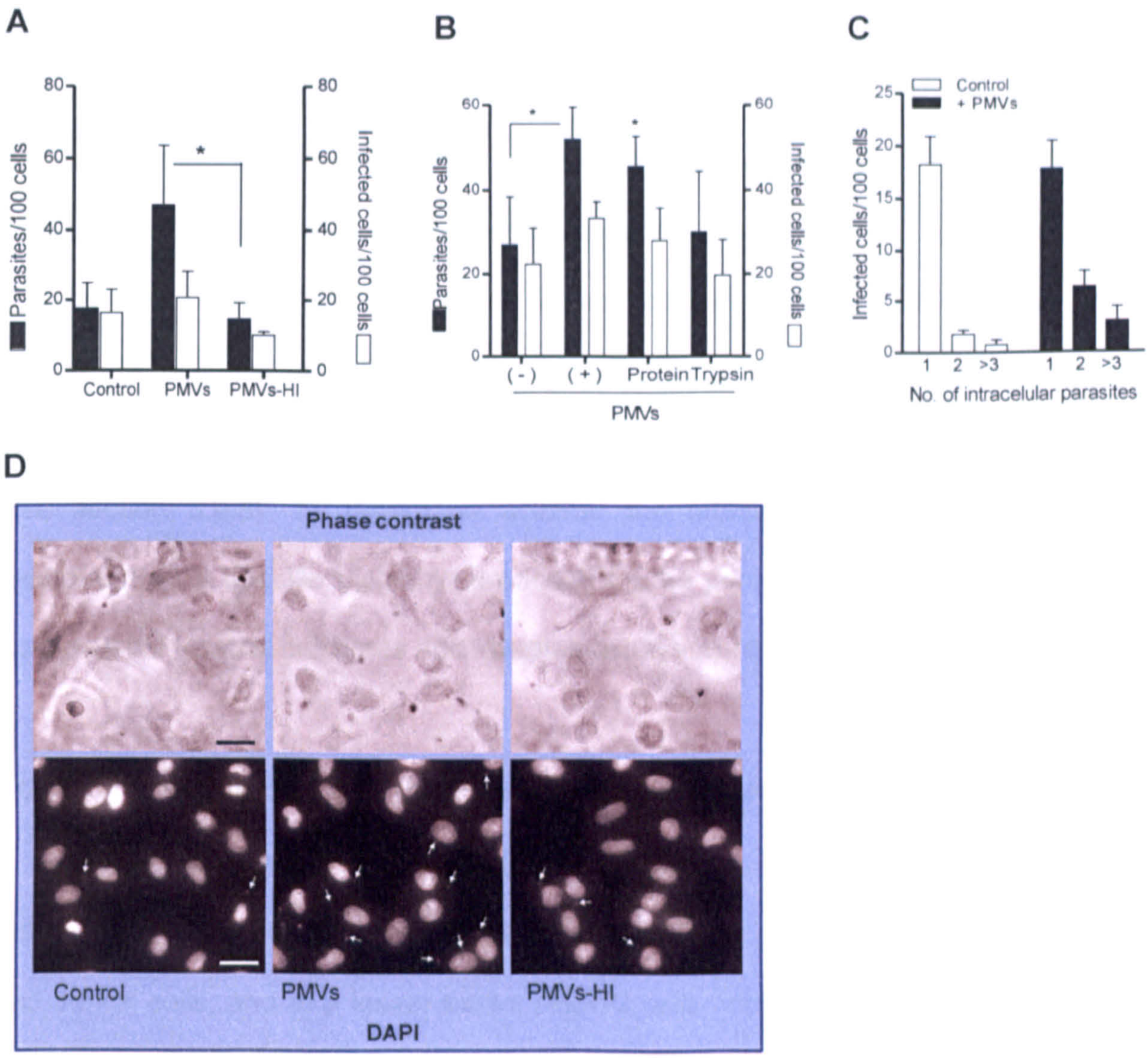

Figure 6.3 Surface molecules on PMVs participate in increasing infection

(A) Heat-inactivation of PMVs at 65°C for 1 h, (PMVs-HI) inhibits ability of the vesicles to enhance *T. cruzi* infection. PMVs, which have not been heat-inactivated significantly (PMVs), increase parasite infection. (B) Likewise, trypsinisation of PMVs to remove surface molecules, (Trypsin) affects the role of these vesicles in enhancing infection, since trypsinisation removes surface proteins such as TGF-β1, required for invasion. However, PMV lysate (Protein) obtained after continuous freeze thaw of the vesicles, enhanced parasite infection. (C) PMVs also encourage superinfection of cells, although, this occurred at lows. (D) Representative image of infected Vero cells without (control) or with PMVs, untreated or heat-inactivated (PMVs-HI). Data represent the mean ± SD of duplicate experiments performed in triplicate. $^{*}P < 0.05$ was considered to be statistically significant. Scale bar= 100 µm.

6.4 The enhanced invasion due to PMVs is independent of cell type and depends on TGF-β

The *in vivo* survival of *T. cruzi* metacyclic trypomastigotes depends on the successful infection of several cell types. Therefore experiments were setup to investigate whether THP-1 cell-derived PMVs could also enhance *T. cruzi* invasion of other cell lines. Accordingly, the breast cancer cell line, MCF-7 and the hepatocyte cell line, HepG2, were infected with a similar ratio of metacyclic trypomastigotes and invasion was performed as described in materials and methods (see section 3.9.8). To determine whether the effect of PMVs observed was dependent on a specific molecule produced by the parent cell, vesicles were also isolated from several cell types and invasion assays were performed with Vero cells.

Consistent with the data presented earlier, THP-1 cell-derived PMVs also enhanced *T. cruzi* invasion of MCF-7 (**Fig. 6.4 A**) and HepG2 cells (**Fig. 6.4 B**), thus, implying that the process is not eukaryotic cell specific. Moreover, PMVs derived from THP-1 and Jurkat cells, and to a lesser extent HepG2 cells, increased *T. cruzi* invasion of Vero cells (**Fig. 6.4 C**). Strikingly, the extent of invasion elicited by PMVs from the various cell lines, correlated with the level of TGF-β measured in the particular cell (**Fig. 6.4 D**). For example, Jurkat cell-derived PMVs, which bear the highest levels of TGF-β, enhance invasion the most. In contrast, MCF-7 cell-derived PMVs, which carried the least amount of TGF-β, failed to enhance cell entry by *T. cruzi*.

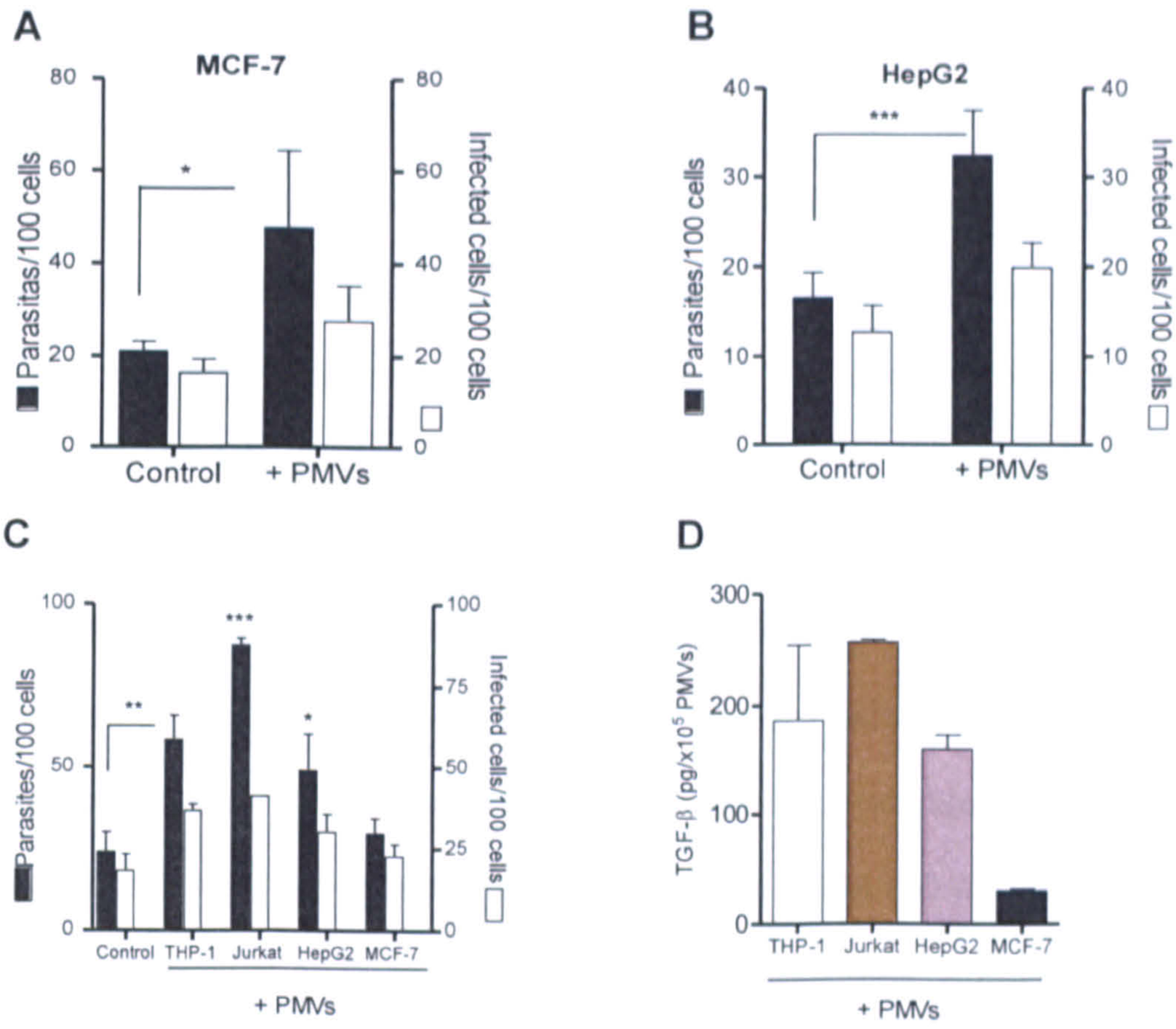

Figure 6.4 TGF-β-bearing PMVs enhance *T. cruzi* invasion of various cells

The effect of PMVs on cell invasion by *T. cruzi* is independent of the eukaryotic cell type being infected. To investigate, the breast cancer cell line, MCF-7 and hepatocyte cell line, HepG2, both $2x10^5$cells/well in duplicate, are infected with *T. cruzi* metacyclic trypomastigotes ($1x10^6$/well) in the presence or absence (control) of PMVs ($5x10^5$/well). Invasion is allowed to proceed at 37°C for 3 h and washed three times with PBS prior to fixing with 4% paraformaldehyde. After two further washes, coverslips with attached cells are inverted on microscope slides and subsequently fixed with DAPI-VECTASHIELD. Slides are examined by fluorescence microscopy. (A) THP-1 cell-derived PMVs increase MCF-7 cell invasion by *T. cruzi* metacyclic trypomastigotes. (B) Invasion of HepG2 cells by *T. cruzi* also increases after adding PMVs from THP-1 cells. (C) PMVs isolated from Jurkat and HepG2 cell lines enhance *T. cruzi* invasion of Vero cells. (D) The extent of invasion strikingly correlates with the levels of TGF-β carried within PMVs from the corresponding cell line. Data represent the mean ± SD of two independent experiments performed in duplicate. ***$P < 0.001$, **$P < 0.01$ and *$P < 0.05$ were considered to be statistically significant.

6.5 Inhibition of TGF-β activation, reduces PMV-mediated *T. cruzi* Invasion

The results described in section 6.4 implied that TGF-β might also be important in mediating *T. cruzi* invasion. Earlier, TGF-β-bearing PMVs were described to halt the proliferation of THP-1 promonocytic cells and induce their terminal differentiation into macrophages (see chapter 5 of this thesis). TGF-β is predominantly present on the surface of PMVs (see section 5.5), and so could be mediating its effect by binding to the surface of the parasite. To investigate this, parasites were preincubated with THP-1 cell-derived PMVs at 37°C for 30 min and invasion assays performed as described earlier. Semiconfluent Vero cells seeded into 12-well plates in duplicate were incubated with parasites (control) or preincubated with anti-TGF-β antibody or the TGF-β-receptor antagonist, SB-431542 (10 μM) at 37°C for 10 min prior to the addition of *T. cruzi* metacyclic trypomastigotes. Agents were washed off with serum-free RPMI prior to the addition of *T. cruzi* at 5:1 (parasites to cell) ratio and plate was incubated at 37°C for 3 h; after which excess parasites were aspirated and cells were washed three times with PBS. Infected cells were fixed with 4% paraformaldehyde and samples analysed as described earlier. Although the role of TGF-β in *T. cruzi* invasion is not novel, as the molecule was previously described to enhance invasion of several cell types by the parasite [310;311], the results herein gave a good indication that the PMV-mediated *T. cruzi* invasion is elicited through the TGF-β signalling pathway.

Increased *T. cruzi* invasion was measured in wells incubated with parasites only (**Fig 6.5 A**). By contrast *T. cruzi* invasion was reduced when cells were preincubated with mouse anti-TGF-β antibody, but not the control, α-ovalbumin. Surprisingly,

increasing the concentration of anti-TGF-β antibody did not elicit a dose-dependent inhibitory response (**FIg. 6.5 B**), implying that *T. cruzi* could employ other invasion strategies for entry. Nevertheless, the more specific TGF-β receptor antagonist, SB-431542 (SB), abrogated *T. cruzi* invasion to control levels (**FIg. 6.5 A**). Moreover, flow cytometry analysis showed that almost a third of the parasites became positive for TGF-β (30%) after incubation with PMVs (**Fig. 6.5 C, right**).

The PMVs used thus far in this study, had been separately isolated and invasion assays had been performed, by either preincubating the PMVs with parasites or directly with the cells. To further understand the mechanisms by which PMVs enhance *T. cruzi* invasion of mammalian cells, and to propose an *in vivo* model, it was paramount to investigate whether PMVs released from *T. cruzi*-induced THP-1 cells, could simultaneously enhance parasite invasion of neighbouring cells. This could emulate an *in vivo* mechanism whereby *T. cruzi* stimulates the release of PMVs from blood cells, and subsequently fuses with the vesicles to acquire TGF-β prior to infection.

Briefly, semiconfluent Vero cells ($2x10^5$cell/well) were incubated together with *T. cruzi* metacyclic trypomastigotes in a 5:1 (parasite to cell) ratio into all the wells in the lower chambers of a transwell plate. THP-1 cells ($1x10^6$/well) were either seeded alone or together with *T. cruzi* metacyclic trypomastigotes in the upper chamber. One well in the upper chamber contained only purified PMVs. One of the infection experiments was carried out in the presence of the TGF-β receptor antagonist, SB-431542. The plate was incubated at 37°C for 3 h and later washed and analysed as described earlier (see materials and methods, section 3.9.8).

Interestingly, when *T. cruzi* was added to the upper chamber, which contained only THP-1 cells, invasion of the parasites incubated together with Vero cells in the lower chamber was increased (**Fig. 6.5 D**). By contrast, having THP-1 cells alone in the upper chamber did not enhance invasion of the parasites incubated in the lower chamber with Vero cells. This result indicates that *T. cruzi*-mediated release of PMVs from cells, could simultaneously elicit an increase in host cell invasion by the parasite. Furthermore, preincubation of Vero cells with the TGF-β receptor antagonist, SB-431542 reversed the PMV-mediated enhancement of *T. cruzi* invasion (**Fig. 6.5 D**). Together, these results show that the increased *T. cruzi* infection, which is measured in the presence of PMVs, is due to TGF-β carried on the surface of the vesicles as previously shown in chapter 5 for the TGF-β-bearing PMVs stimilating monocyte THP-1 terminal differentiation.

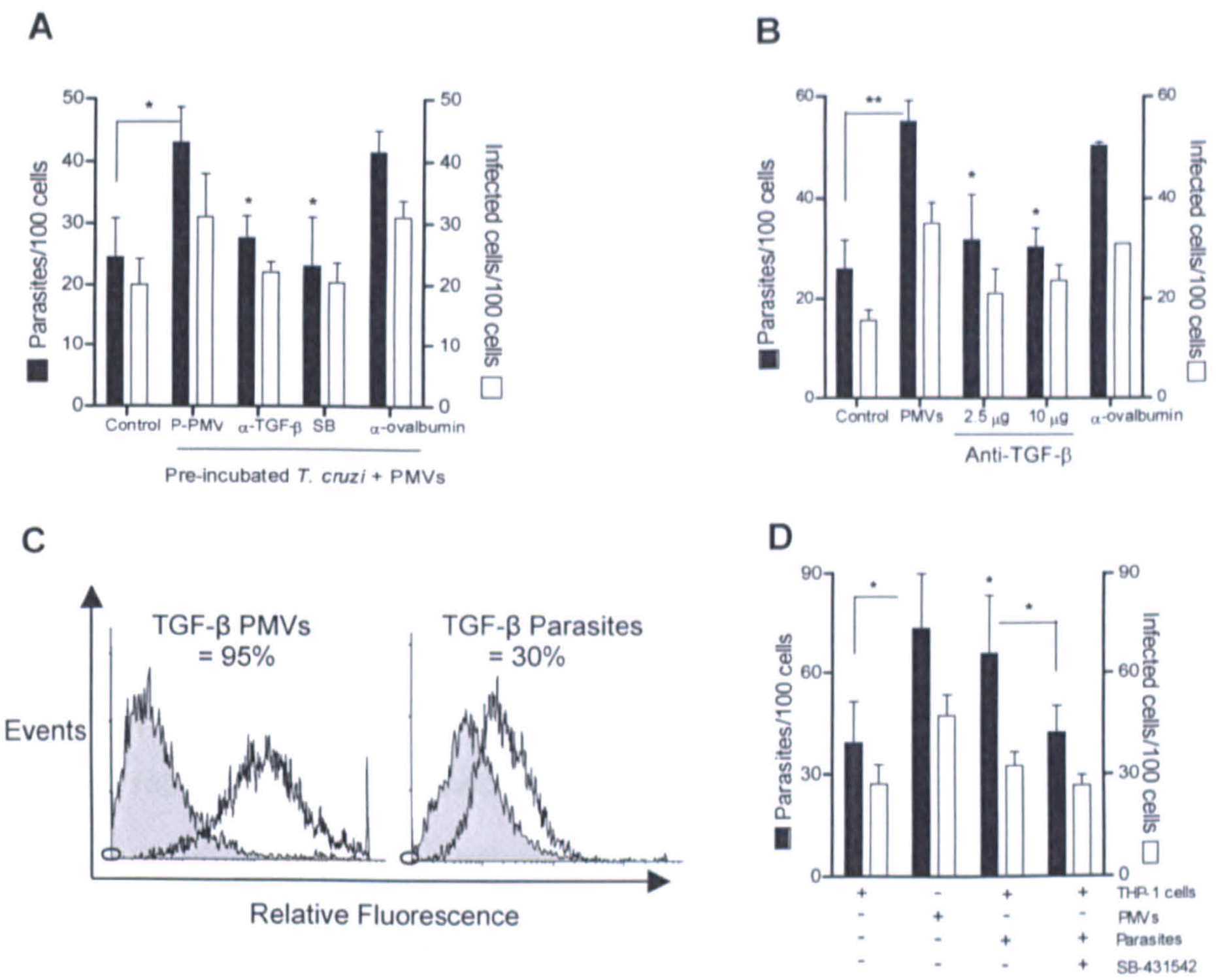

Figure 6.5 PMV enhancement of *T. cruzi* infection, utilises TGF-β on the surface of the vesicles

(A) Preincubation of Vero cells with mouse anti-TGF-β antibody (2.5 μg/ml) at 37°C for 10 min, significantly abrogates cell invasion by *T. cruzi* and a similar result is obtained when cells are incubated with SB, the TGF-β receptor antagonist, SB-431542 (10 μM). (B) Increasing the concentration of anti-TGF-β antibody to 10 μg/ml does not inhibit parasite invasion in a dose-dependent manner. (C) *T. cruzi* metacyclic trypomastigotes acquire TGF-β (30%) after their incubation with TGF-β-bearing PMVs (95%) as assessed by flow cytometry. (D) *T. cruzi*-stimulated PMV release can simultaneously induce an increase in parasite invasion of cells. Inhibition in the presence of the TGF-β receptor antagonist, SB-431542, shows that the mechanism is also via the TGF-β signalling pathway. Data represent the mean ± SD of two independent experiments performed in duplicate. $^{**}P < 0.01$ and $^{*}P < 0.05$ were considered to be statistically significant.

6.6 PMVs inhibit the complement-mediated lysis of *T. cruzi*

When *T. cruzi* is inoculated into mammals during the sylvatic cycle, it has to negotiate the lytic effect of the host complement system, in order to progress in its life cycle and establish an effective infection. Metacyclic trypomastigotes are well known to evade lysis by the host complement system prior to causing disease. Therefore, in order to further characterise the role of PMVs during mammalian cell invasion by *T. cruzi*, the effect of these vesicles on complement activity was investigated.

Since epimastigotes are highly susceptible to complement-mediated killing, lysis experiments were initially performed with this non-infectious stage. However, a recent report showed that metacyclic trypomastigotes of some *T. cruzi* strains are sensitive to complement-mediated killing [306] and so later experiments were performed with this infective stage in near physiological conditions (50% human serum). To investigate this, *T. cruzi* epimastigotes ($1x10^6$/microtube) in triplicate were incubated in 100 µl reaction volumes with 10% human serum at 37°C for 5 or 10 min, in the presence or absence of THP-1 cell-derived PMVs ($5x10^5$/100 µl). Placing microtubes on ice stopped the reaction and the percentage of lysed and unlysed parasites was determined by trypan blue exclusion and counted with the aid of a haemocytometer. As a control, epimastigotes were incubated with 10% heat-inactivated (56°C for 30 min) human serum. In some experiments, *T. cruzi* epimastigotes were incubated with 10% human serum in the presence of increasing numbers of PMVs and parasite lysis was determined as described in materials and methods (see section 3.9.9). And in another experiment, *T. cruzi* metacyclic

trypomastigotes ($1x10^6$/well in triplicate) were incubated with 50% NHS in the presence or absence of THP-1 cell-derived PMVs ($1x10^6$/well) at 37°C for 1 h in 100 µl reaction volumes.

Lysis assays showed that the presence of THP-1 cell-derived PMVs does indeed inhibit *T. cruzi* epimastigote killing by human serum (**Fig. 6.6 A**) and the process was dose-dependent (**Fig. 6.6 B**). By contrast, heat-inactivation (65°C for 1 h) of PMVs abolishes their protective effect against complement-mediated killing (**Fig. 6.6 B**). Experiments carried out in near physiological conditions (50% human serum) with infective parasites showed that, indeed, PMVs confer protection (up to two-fold increase in parasite survival) against complement-mediated lysis to *T. cruzi* metacyclic trypomastigotes (**Fig. 6.6 C**).

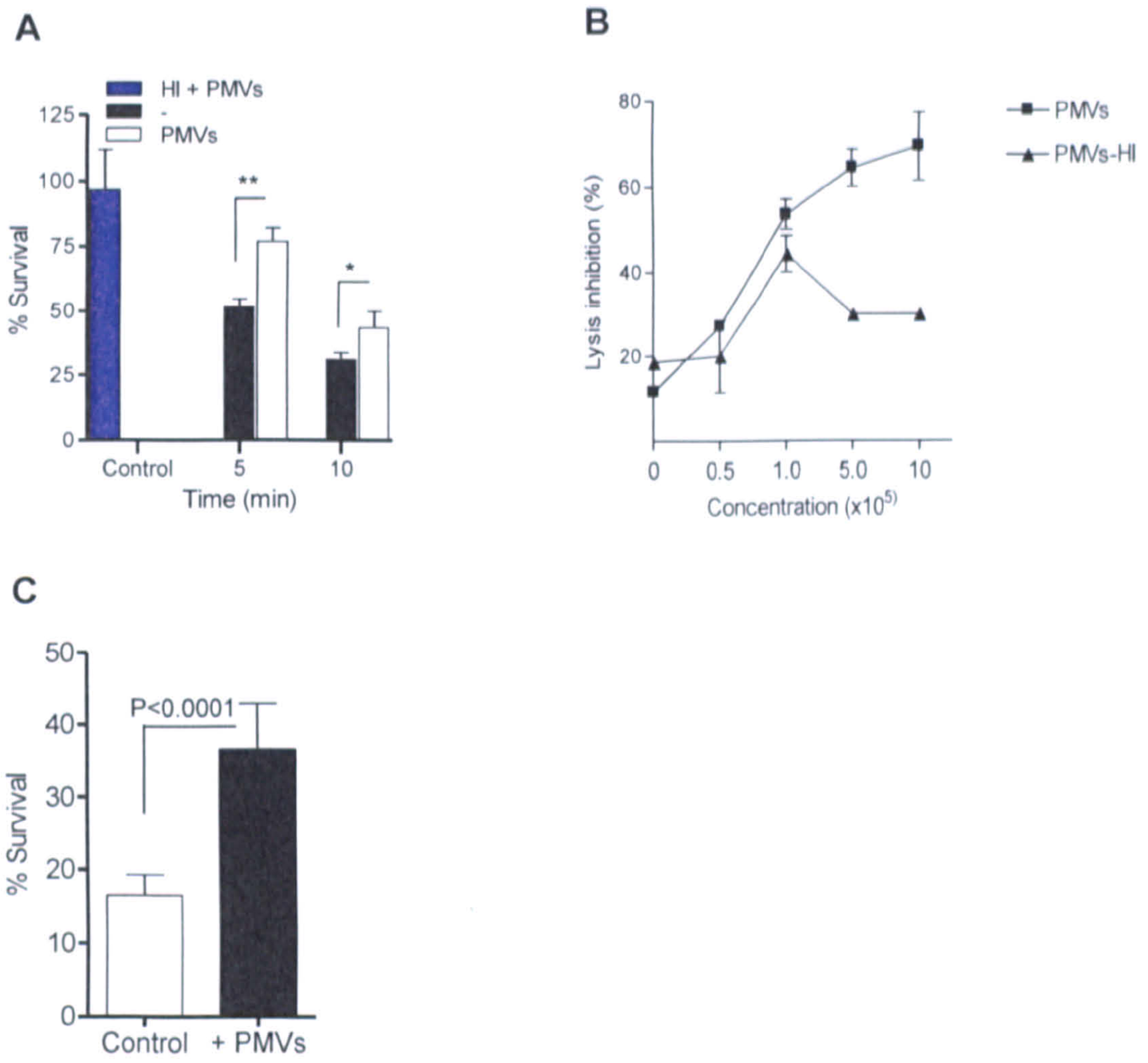

Figure 6.6 PMVs inhibit *T. cruzi* lysis by the complement system

(A) THP-1 cell-derived PMVs ($5x10^5$/microtube) protect epimastigotes ($1x10^6$/microtube in triplicate) against complement-mediated killing (white bars) using 10% human serum in 100 µl, as compared to parasites incubated without PMVs (black bars). Heat-inactivated (56°C for 30 min) human serum, which does not lyse epimastigotes, is used as a negative control. (B) Addition of increasing amounts of PMVs enhances parasite survival against complement-mediated killing. By contrast, heat-inactivated PMVs (65°C for 1 h) fail to confer protection against complement-mediated lysis of *T. cruzi*. (C) THP-1 cell-derived PMVs ($1x10^6$/well) also confer protection of *T. cruzi* metacyclic trypomastigotes ($1x10^6$/well in triplicate) against complement-mediated killing in 50% human serum. Data represent the mean ± SD of two independent experiments performed in duplicate. ***$P < 0.001$, **$P < 0.01$ and *$P < 0.05$ were considered to be statistically significant.

6.7 Discussion

The exact mechanism(s) involved in the invasion of mammalian cells by *T. cruzi* has not been completely elucidated, and so it continues to be a challenge for parasitologists across the globe. Although a mechanism that involves the recruitment of host cell lysosomes to the plasma membrane, and subsequent fusion with the invading *T. cruzi* metacyclic trypomastigote was described a decade ago [309], this entry strategy has recently been challenged by various investigators [312,313]. *T. cruzi* metacyclic trypomastigotes, unlike epimastigote forms, are able to negotiate activation of the complement system prior to invading and establishing infection [314;315]. However, the metacyclic trypomastigote stage of some *T. cruzi* strains was recently reported to be sensitive to complement-mediated lysis in human serum [306], suggesting that external factors might be contributing to parasite immune evasion.

In this chapter, a novel mechanism utilised by *T. cruzi* to evade the host innate immune system and to promote invasion is described. *T. cruzi* metacyclic trypomastigotes, but not epimastigotes (non-infective) induced from THP-1 cells, the release of PMVs in a Ca^{2+}-dependent and dose-dependent manner. These PMVs are then involved in inhibiting parasite lysis by the complement system and in aiding invasion of host cells. This observation is consistent with reports, which show that the levels of PMVs are elevated in diseased conditions and during stress [18;316;317]. Hitherto, increased plasma levels of PMVs have been observed during malaria infections [318], pregnancy [319], thrombosis [15] and cancer [320]. Experiments performed in our laboratory, together with other reports have shown that PMVs can be induced from peripheral blood mononuclear cells [321] (Cestari et al, 2010-submitted).

Here, I present evidence that the addition of PMVs, isolated from cell lines including THP-1, Jurkat and HepG2 cells enhanced *T. cruzi* invasion of Vero cells in a dose-dependent manner. Likewise, these PMVs increased parasite entry into other mammalian cells including MCF-7 and HepG2 cell lines. Although, *T. cruzi* is known to typically infect several cell types [322], their enhanced invasion observed here in the presence of PMVs, suggest that the effect of these vesicles is not dependent on the eukaryotic cell line. Moreover, the increased invasion observed with PMVs isolated from different cell lines, suggests that the mechanism is not absolutely dependent on the parent cell from which the vesicles were derived. Interestingly, the enhanced effect of PMVs on *T. cruzi* invasion of cells was abolished after heat-inactivation or trypsinisation of the vesicles, thus, suggesting the involvment of a molecule or molecules present inside the vesicles.

Further investigations revealed that the enhanced *T. cruzi* invasion in the presence of PMVs was due to TGF-β, carried on the surface of the vesicles. As described in chapter 4 of this thesis, a distinctive feature of PMVs is their ability to carry molecules from the parent cell, which is then utilised in intercellular communication. Consistently, I described in chapter 5 of this thesis that THP-1 cell-derived PMVs carry TGF-β on their surface and this inhibits the proliferation and induces differentiation of THP-1 promonocytes into macrophages. Moreover, TGF-β was proposed to enhance the invasion of epithelial and cardiac cells by *T. cruzi* [310;323], aid the intracellular cycle of the parasite [324] and to exacerbate the problem of fibrosis during acute and chronic Chagas disease [325]. Accordingly, treating cells with neutralising mouse anti-TGF-β antibodies, as well as with the more specific TGF-β-receptor antagonist, SB-431542, reduced *T. cruzi* invasion of cells.

Strikingly, PMVs derived from cell lines carrying increasing levels of TGF-β, correlated with their effect on invasion. Thus, PMVs derived from THP-1 and Jurkat cells, bearing higher levels of TGF-β (~180 and 280 pg/x10^5 PMVs respectively), enhanced *T. cruzi* invasion. By contrast, MCF-7 cell-derived PMVs, which carried low levels of TGF-β (~25 pg/x10^5 PMVs), failed to increase *T. cruzi* invasion of Vero cells. This further supports the observation that PMV-mediated, enhanced *T. cruzi* invasion, is due to TGF-β carried on the surface of the vesicles. Consistent with these findings, patients with chronic Chagas disease have been reported with elevated levels of circulating TGF-β [326].

In addition, mice with acute *T. cruzi* infections were shown to have increasing levels of TGF-β. This agrees with results obtained in our group, which showed that the levels of TGF-β-bearing PMVs increased within 24 h post-infection and remained persistent for several days. We found that PMVs derived from mice infected with *T. cruzi*, carried higher levels of TGF-β (~35-55 ng/ml of plasma) compared to non-infected (~35 ng/ml of plasma) (Cestari et al. 2010 - submitted). It is noteworthy that the addition of PMVs to cells broadly resulted in an increase in the number of invading parasites per cell, rather than an increase in the number of infected cells. Thus, I speculate that the initially invading *T. cruzi* carries PMVs to the host, which then activates a plethora of signalling pathways, rendering the cell more susceptible to infection by other parasites.

Data presented here also shows that PMVs before being utilised by *T. cruzi* for invasion, bind to the parasite surface and aid its immune evasion by inhibiting complement-mediated lysis. The survival of *T. cruzi* epimastigotes in human serum

was enhanced in the presence of PMVs.

Further investigations have revealed more information as to how PMVs inhibit the complement-mediated lysis of *T. cruzi*. PMVs have been shown to strongly inhibit the classical and lectin pathways by binding to the complement C3 convertase (C4b2a), a key complex in the complement cascade, on the surface of the parasite. This binding causes a delay in dissociation of the complex (C4b2a) and affects its activity by inhibiting C3 cleavage (Cestari et al. 2010 - submittd). Inhibiting the cleavage of C3 has several biological significance because, C3 is required for effective complement lysis by all the pathways, it is also important to generate the anaphylotoxins, C3a and C5a, essential during activation of host cell response against pathogens. C3 is also involved during the opsonisation of pathogens, for effective phogocytotic clearance. This finding is supported by an earlier report, which showed vesicles exposing phosphatidylserine inhibit activation of the complement system [327]. Together, these data suggest that PMVs inhibit the early clearance of *T. cruzi*, by inhibiting the activity of the complement system. PMVs bearing TGF-β, then elicit signals, which result in an increased uptake of parasites by the host cell.

7. *Trypanosoma cruzi* exploits host cell repair mechanisms to invade

7.1 Introduction

7.1.1 Mechanisms leading to mammalian cell invasion by pathogens

As mentioned in the introduction of this thesis, intracellular pathogens have to infect and replicate in mammalian cells, in order to survive. Therefore understanding the processes involved in their invasion is paramount, if effective treatments or possible cures are to be developed for diseases caused by these pathogens. In earlier work it was shown that *T. cruzi* could induce the release of PMVs from several cell types. The aim of the present work was to investigate the role of these PMVs in the invasion of the parasite. The question posed was: 'Why would *T. cruzi* induce the release of PMVs?' In order to investigate this, it was essential to understand the various mechanisms by which intracellular pathogens invade. Among some of these proposed mechanisms are activation of calcium ion channels, lipid raft microdomains, PI 3-kinase signalling and integrins. In addition to L-type calcium channels, this study also identified for the first time, the possible involvement of stretch-activated channels (SACs), via trp-C6 activation in the release of PMVs and mammalian cell invasion by *T. cruzi*.

7.1.2 Role of Calcium channels in pathogenic infection

The involvement of calcium ions and L-type calcium ion channels in the release of PMVs has been well investigated and established in the literature [14,328,329]. Stimulation of mammalian cells in the presence of the calcium chelator, EGTA, is known to inhibit release of PMVs. It was recently reported that blockage of L-type calcium channels (and therefore presumably the release of PMVs, although this was not mentioned) with the L-type calcium blockers, nifedipine or verapamil inhibits invasion of various cells by intracellular pathogens [330,331]. An increase in intracellular calcium levels, results in rearrangement of the actin cytoskeleton, followed by release of PMVs. In recent reports by various groups, the link between reorganization of host cell cytoskeleton and invasion by pathogens has been established as an important mechanism. A report by Zhou et al (1999) [332] showed that the bacteria, *S. typhi*, induces membrane ruffling and rearrangement of the actin cytoskeleton for entry into host cells. In this article, they proposed that the bacterial protein, SipA (an actin-binding protein), was required for actin cytoskeleton remodeling as its inhibition resulted in reduced internalisation of *S. typhi*.

A host of authors have emphasized the role of the cytoskeleton during the entry of pathogens into cells. Work in the late 1990s mentioned two mechanisms by which many pathogenic bacteria exploit host cell functions [333;334], including activation of signal transduction pathways and cytoskeleton rearrangements in order to invade. These mechanisms, the first known as the 'zipper' mechanism involves contact between bacterial surface molecules and cellular receptors. The second is a 'trigger' mechanism in which the bacteria send signals to the host cell to induce membrane ruffling and remodeling of the cytoskeleton, resulting in their uptake. Certain

pathogens, such as *Yersinia* species (spp) induce their uptake via the zipper mechanism, by directly binding to host cell integrins [335]. Others such as *Salmonella* and *Shigella* spp. use the so-called trigger mechanism whereby they engage the cell signalling machinery, by injecting bacterial proteins that directly activate cellular pathways leading to their uptake [336,337].

7.1.3 Mechanosensitive Ion channels

Most of the calcium channels reported to play a role in the rearrangement of the cytoskeleton are L-type channels. However, in addition to L-type calcium channels, we investigated the possible involvement of other channels, such as mechanosensitive channels (MSC) and focused on stretch-activated channels (SAC). Mechanosensitive channels (MSC) are ubiquitous ion channels, which serve many functions in cells and higher organisms. Since these channels have not been previously reported to function during the release of PMVs, we investigated their possible involvement. The release of PMVs is sometimes activated by the sheer stress sustained by the host cell in the presence of the inducing agent. Since stretch-activated channels are affected by stress, we investigated how abrogation of these channels might affect the release of PMVs.

Even though these reports are hugely important, recent findings have shown that cytoskeleton rearrangement is not the first initiating response when pathogens interact with host cell receptors. Some reports have implicated a role for host membrane cholesterol during the uptake of bacteria. It was shown that cholesterol plays an important role during the entry of *Mycobacteria* spp into macrophages [338;339]. These reports showed that depletion of cell plasma membrane cholesterol

with MβCD resulted in a reduction of *Mycobacterium (M.) bovis* uptake of approximately 85 to 90% by macrophages. In addition, cholesterol depletion also caused a reduction in the uptake of *M. tuberculosis*, by approximately 85%. Interestingly, this reduction in uptake was not so significant in other bacteria such as *Escherichia coli, Yersinia pseudotuberculosis* and *S. typhi*; hence, the process was thought to be specific only for mycobacterial entry. The idea that cholesterol aids uptake of pathogens into cells encouraged other researchers to investigate the involvement of lipid rafts in infection, since these domains contain the steroid metabolite [340].

7.1.4 Pathogens utilize lipid raft domains for cellular invasion

The cell's plasma membrane consists of small, heterogeneous and highly dynamic microdomains. These domains are mainly composed of phospholipids, (glyco)-sphingolipids and cholesterol. The size of rafts and their duration are uncertain, however, evidence indicates that the basic raft units are small (26–70 nm in diameter), accommodating only a few proteins. Estimates of the half-life range from milliseconds to minutes [341].

It is well established that pathogens in general must evade immune surveillance in order to succeed in causing disease [341]. However, since the signalling for innate and the adaptive immune responses is initiated in rafts, some pathogens have evolved mechanisms to sabotage this signalling by co-opting raft pathways that lead to proliferation and/or apoptosis of immune cells. Experimental evidence indicates that host rafts are exploited by some pathogens, to cross the plasma membrane and avoid degradation and subsequent antigen processing by target cells [342;343]. The

recruitment of rafts seems to be a general mechanism employed by microorganisms for infecting cells. For example, HIV-1 uses rafts for almost all of its life cycle events involving immune and non-immune cells: passage across host cell mucosa [344], infection production after entry of virus into host immune cells [345], subversion of host-cell signalling for evasion of immunity and replication of virus [346], exit of the virus from immune cells [347] and dispersal through the vascular system of the host [348].

Bacteria are also proposed to use host rafts for entry into cells [342,343]. Bacteria prefer raft sites for entry into cells, because these domains are known to function as sorting devices that distribute proteins to the apical side of epithelial cells [349], thus, making them more accessible for entry. Although, raft and non-raft domains are equally available on cells, pathogens gain two advantages by entering via these receptors [341]. The first is avoidance of the intracellular degradative pathway, which would otherwise lead to disintegration of the pathogen. The other is the ability to trigger cell signalling, which leads to membrane ruffling and actin cytoskeleton rearrangement, both of which are required for cellular entry. Put simply, by entering through raft domains, pathogens are able to hide from many of the immune system's effector mechanisms.

7.1.5 Integrins are involved in raft-mediated cell invasion

The interactions between rafts and integrins have long been established in the literature [350-352]. Integrins are heterodimeric cell surface receptors (glycoproteins), which mediate cell-cell and cell-extracellular matrix (ECM) interactions. Integrin binding induced by raft clustering is also said to modulate cytoskeleton

rearrangement [353], which leads one to speculate that PMVs may also be released during this binding interaction. Not surprisingly, the involvement of integrins in the entry process and intracellular replication of microbial pathogens is becoming increasingly evident. Cellular invasion by viruses and the uptake of a greater number of intracellular bacteria into host cells have been shown to utilize integrins and integrin-dependent signalling [354]. Host cell adhesion molecules have a role either to defend against microbial infection, or engage in the processes leading to pathological establishment. For this reason, many pathogens have evolved ways to adhere to cell adhesion molecules that mediate cell-cell and cell-ECM interactions [355]; these include integrins, immunoglobulin receptors and selectins.

For intracellular pathogens, cell adherence is an absolute requirement for uptake (invasion). The importance of integrins for the entry of bacterial pathogens into host cells has been extensively investigated [356-359]. It was shown that interaction between Ipa, a *Shigella flexneri* protein with α5β1 integrin is an important *Shigella* factor, which triggers reorganisation of the actin cytoskeleton and promotes entry of the bacteria into cells [360]. All the findings discussed in this section strongly lead one to speculate that the release of PMVs is as essential as the assembly of raft microdomains, cholesterol and activation of integrins during the entry of pathogens into mammalian cells.

7.1.6 Damage repair mechanism by lysosomes

To understand how *T. cruzi* induction of PMVs via the receptors and domains mentioned earlier would affect the host and therefore aid parasite uptake, it was pertinent to uncover how mammalian cells repair plasma membrane breakage.

A break in the plasma membrane of a eukaryotic cell interferes with its integrity and immediately compromises the essential role of this structure as a barrier, and this can cause death to the affected cell due to excess influx of substances such as Ca^{2+}. A calcium-dependent mechanism was proposed, which involves rapid resealing of the disruption, by exocytosis of activated lysosomes [179;194]. Influx of calcium through the breakage recruits lysosomes, which fuse together and patch-up the site of damage. This mechanism of wound repair has been reported in skeletal muscle cells, gut, skin and aortic endothelium cells [179]. Moreover, recent findings suggest the same mechanism can be used to explain processes by which cells repair larger surface lesions caused by pore-forming proteins, such as the complement MAC and the bacterial toxin streptolysin O (SLO) [361]. Furthermore, a recent report revealed a secret relationship between the repair of membrane damage by activated lysosomes and invasion of mammalian cells by *T. cruzi* [362].

In this review, *T. cruzi* invasion was significantly enhanced by disruption of host cell microfilaments [309], a process which results in release of PMVs. During *T. cruzi* invasion of fibroblasts, host cell lysosomes were shown to gradually accumulate at the parasite entry site and to progressively fuse with the plasma membrane as invasion proceeded. Subsequent studies demonstrated that fusion of host cell lysosomes with the plasma membrane is a prerequisite for entry of *T. cruzi* into several cell types, and that the process is activated by elevations in cytosolic Ca^{2+} levels stimulated by the parasite [363]. Here, I present evidence that the release of PMVs from cells induced by *T. cruzi*, causes damage to the integrity of the host plasma membrane, and parasites exploit the subsequent damage for entry before lysosomal repair.

However, these are not likely to be the only mechanisms involved in cell invasion. Indeed, several investigators have proposed a role for cytokines such TGF-β1 and Gal-3 during cell invasion by *T. cruzi* [310;311;364]. The release of PMVs is a process that follows depolymerization of the actin cytoskeleton, which is itself caused by activation of signalling cascades induced by increases in cytosolic Ca^{2+}. Increase of cytosolic Ca^{2+} concentration is in part caused by activation of host cell integrin receptors and lipid raft microdomains by microbial pathogens. For this reason experiments were designed to investigate the role of PMVs in the entry of microbial pathogens into cells, focusing mainly on *T. cruzi* infection. It is important to emphasise that this study is the first to report a possible link between release of PMVs and pathogenic invasion. This study also offers a possible explanation as to why it's essential for intracellular pathogens such as *T. cruzi*, to stimulate the release of PMVs from their host prior to infection.

7.2 Analysis of PMV cytokine content following induction with *Trypanosoma cruzi* and *Salmonella typhimurium*

The notion that different external stimuli, or in this study pathogens, can influence the sorting of specific proteins into PMVs by lipid rafts during their release was initially tested. In order to observe this, PMVs were isolated from THP-1 cells left non-induced (NI), or stimulated with either parasite or bacteria. Following the manufacturer's instructions, the human cytokine array was used to detect a range of cytokines, chemokines and acute phase proteins carried within released PMVs. Briefly, $3x10^7$ THP-1 cells were resuspended in prewarmed RPMI supplemented with $CaCl_2$ (see materials and methods). Cells were left unstimulated (non-induced, NI) or stimulated with a 10:1 ratio of either *T. cruzi* or *S. typhi* to cells, in a 30 ml final

reaction volume. After incubation at 37°C for 30 min, PMVs were isolated according to the method described under section 3.9.2.

Isolated PMVs were quantified on the flow cytometer and then lysed with 0.5% Triton X-100 containing protease inhibitors to precipitate membrane-bound and cytosolic proteins. Precipitated proteins were quantified using the BCA protein measurement kit (Pierce, UK) and 100 µg of protein was loaded onto respective membranes. After various incubations and washes, membranes were developed with an ECL solution and spot intensities were analysed using the image j software. Results obtained showed differences in the concentration of cytokines and also the type of cytokines detected. For example, compared to non-induced cells, some new cytokines and chemokines were detected after stimulation of cells with *T. cruzi* and *S. typhi*. Positive detection was assessed by the appearance of dots or an increase in dot intensity (**Fig 7.1 A**). The intensity of each dot was analysed and the percentage fold increase was calculated using non-induced (NI) values as standard. Generally most cytokines or chemokines were only detected after THP-1 cells were activated (**Fig 7.1 B**).

Interestingly, some cytokines were detected at varying concentrations depending on the stimulus for PMV release. This is observed with IL-1 receptor antagonist (IL-1ra), a naturally occurring protein that competitively binds to IL-1 receptor, thereby inhibiting its signalling activation in target cells. Whereas the levels in non-induced and *T. cruzi*-activated samples remained almost the same, levels after stimulation with *S. typhi* were significantly lower. A similar trend can be seen with MIF, an important constituent of the immune system that acts in coordination with

glucocorticoids to control inflammation and immunity. Moreover, some factors such as C5a and IL-1α were only detected after the cells were stimulated, and others including IL-32α and RANTES were only detected in PMVs after stimulation with *T. cruzi*.

Together, these results show that some proteins carried by PMVs, have been specifically cargoed to mediate specially required functions. As such, *T. cruzi* would stimulate the release of TGF-β-PMVs, which then confer *T. cruzi* protection against complement-mediated lysis (Cestari et al., 2010 submitted) and enhance its invasion of mammalian cells. Also, HIV mediates the release of $CXCR5^{+}$ PMVs, which transfer the receptor to non-CXCR5 expressing cells, rendering them susceptible to infection. In an ongoing study, we have observed that host cells infected with Coxsackie virus, undergo apoptosis and release higher levels of Fas-bearing PMVs. These PMVs spread the apoptosis signal to neighbouring cells and cause them to become apoptotic and subsequently, inhibit further infection by the virus.

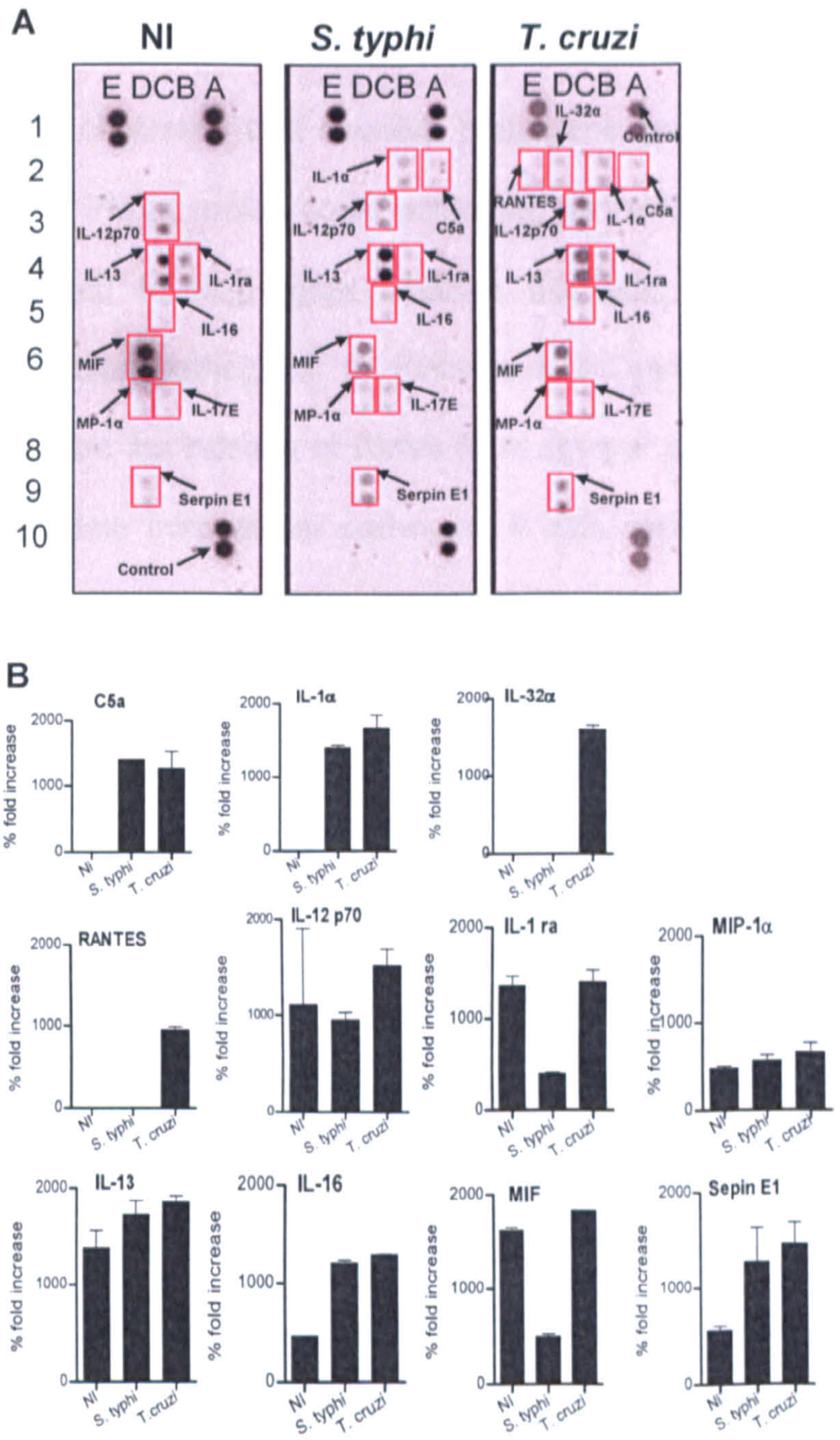

Figure 7.1 Cytokines, chemokines transported by pathogen stimulated THP-1 PMVs

(A) Membrane of human cytokine array showing dots representative of positive cytokine detection. A1, E1 and A10 are positive controls provided by the manufacturer. (B) Densitometry analyses of cytokines detected as positive. Each is represented as percentage fold increase using values from non-induced samples as standard. Analysis was done using image J densitometry software. Data represent mean ± SD of a single experiment performed in duplicate.

7.3 PMVs and cell invasion by intracellular pathogens

Having confirmed that invasive pathogens can stimulate the release of cytokine-bearing PMVs, which could potentially be used during invasion, experiments were conducted to investigate whether this was a characteristic, peculiar only to intracellular pathogens or pathogens in general. As aforementioned, *T. cruzi* stimulated the release of PMVs from several cell types. However, since *T. cruzi* is an obligate intracellular pathogen, it was asked whether the same phenomenon could be observed for a non-intracellular parasite such as, the blood-dwelling, extracellular *T. brucei*. Experiments were performed in triplicate, first to stimulate release of PMVs from THP-1 cells (results not shown) and later HeLa cells, which was subsequently used for all invasion experiments.

Indeed, *T. cruzi* induced the release of PMVs from HeLa cells and this was inhibited in the presence of EGTA. However, *T. brucei*, the extracellular pathogen failed to induce PMVs from HeLa cells (**Fig. 7.2 A**). Moreover, the process of vesiculation after *T. cruzi* activation of cells was dose dependent, as the number of released PMVs, increased with higher ratios of parasites to cells (**Fig. 7.2 B**). Based on these results it was speculated that all or most intracellular pathogens induce release of PMVs from their host, whilst most extracellular pathogens do not. To investigate this hypothesis, experiments were carried out using the food-borne pathogen, *S. typhi* (wild-type, strain SL1344) and its non-invasive form carrying a deletion in the SPI1 pathogenicity island. Also HeLa cells were stimulated in some experiments with *Giardia intestinalis* (syn. *G. lamblia, G. duodenalis*), a flagellated, unicellular, extracellular eukaryotic microorganism and the causative agent of various diarrheal diseases worldwide. The bacteria strains were kindly provided by Prof. Jay Hinton

(Institute of Food Research, Norwich Research Park, Norwich) and cultured in the Microbiology Research Unit until ready to use. *Giardia intestinalis* (GI) was kindly provided by Prof Marcel Ramirez of the Instituto Oswaldo Cruz, Rio, Brazil. Briefly, semiconfluent HeLa cells seeded in triplicate into 12-well plates were placed into RPMI supplemented with 0.5 mM $CaCl_2$ and stimulated with *S. typhi* 5:1 (bacteria to cell) ratio or *Giardia intestinalis*. In addition, *Giardia intestinalis* ($1x10^6$/well) in triplicate was stimulated with 5% NHS in the presence or absence of the calcium chelator, EGTA (5 mM). Plates were incubated at 37°C for 30 min and reaction was stopped by placing on ice for 1 min. Supernatant was collected and released PMVs were isolated and quantified according to the procedure described in section 3.9.3.

Results obtained showed that invasive *S. typhi*, wild-type strain, positively induced release of PMVs from HeLa cells compared to control (5% NHS). In contrast and as predicted, the non-invasive, mutant strain (SPI1) was unable to induce a release of PMVs (**Fig. 7.2 C**). Moreover, *Giardia intestinalis*, the extracellular parasite failed to stimulate the release of PMVs from either THP-1 cells (**Fig. 7.2 D**) or HeLa cells (**Fig. 7.2 E**). Surprisingly, *Giardia intestinalis* was able to release PMVs from itself when stimulated with 5% NHS (**Fig. 7.2 F**), and ongoing experiments are showing that these vesicles released by the parasite, enhance its attachment to the host epithelium prior to causing disease. Furthermore, the NHS-mediated release of PMVs from GI was dose dependent (**Fig. 7.2 G**) and the vesicles released were positive for annexin V (**Fig. 7.2 H**).

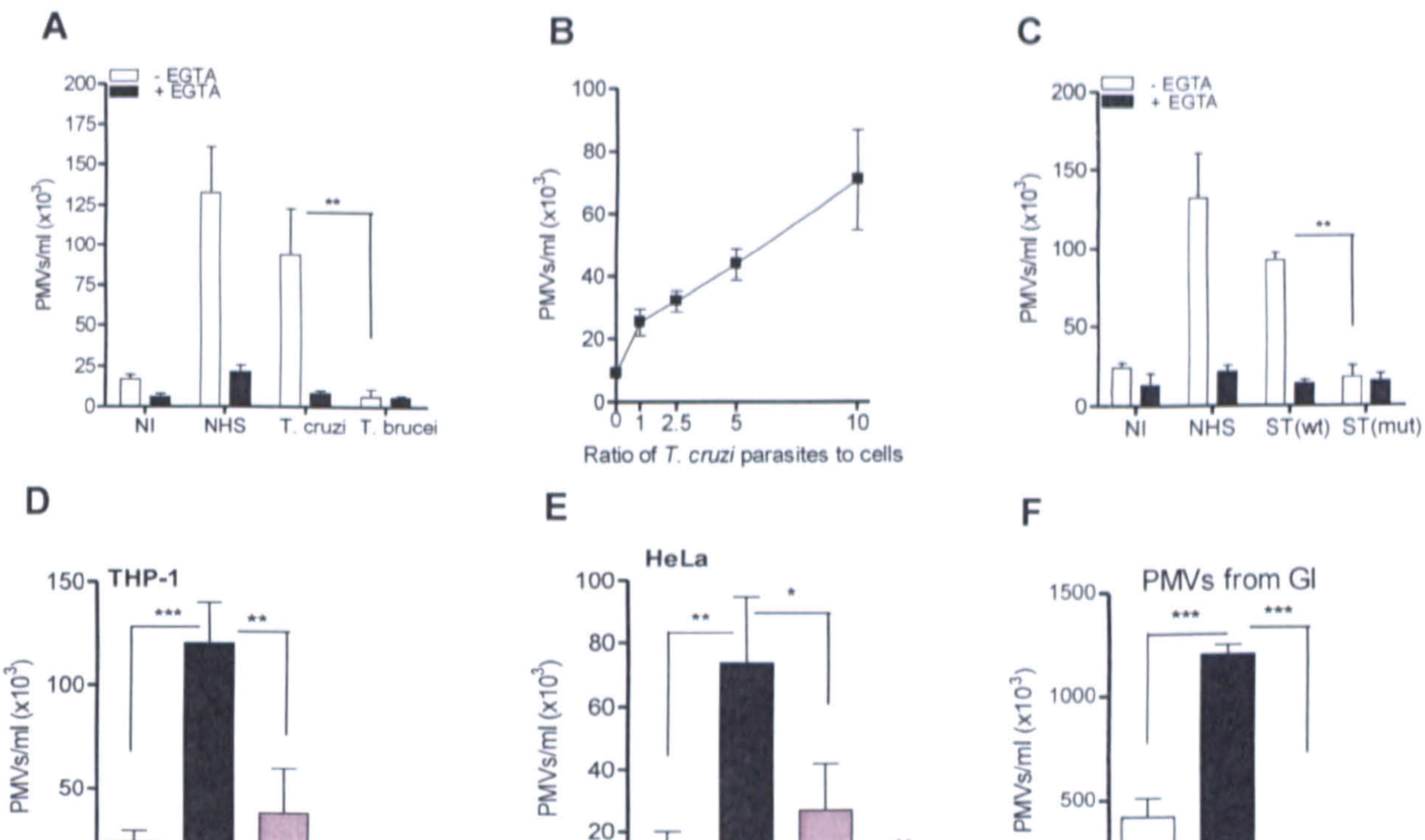

Figure 7.2 Intracellular pathogens induce release of PMVs, in contrast to non-intracellular pathogens.

(A) *T. cruzi*, an obligate intracellular parasite induces the release of PMVs from HeLa cells, but *T. brucei*, a non-intracellular pathogen does not. (B) The release of PMVs after stimulation of cells with *T. cruzi* is observed as dose dependent (C) The invasive *S. typhi* [wild type (wt), SP1344], also stimulates a significant number of PMVs from HeLa cells. In contrast, the knockout mutant (mut) strains (SPI1) is unable to induce the release of PMVs. (D) Stimulation of THP-1 cells ($1x10^6$/well) with *Giardia intestinalis* (GI) 5:1 (parasites to cell) ratio does not enhance the release PMVs. (E) Likewise GI does not mediate the release of PMVs from HeLa cells. (F) Surprisingly, GI releases PMVs from itself after stimulation with 5% NHS and this can be inhibited with calpeptin (20 μM). (G) NHS mediates the release of GI-PMVs in a dose-dependent response. (H) Moreover, the PMVs released by GI are 50% positive for annexin V after staining. Values represent the mean ± SD of triplicate experiments. All experiments were repeated more than three times with similar results. ***$P < 0.001$, **$P < 0.01$, *$P < 0.05$ were considered to be statistically significant.

7.3.1 Processes involved in *T. cruzi* induction of cell vesiculation

After establishing that intracellular pathogens such as *T. cruzi* and *S. typhi* are capable of inducing mammalian cells to release PMVs, in contrast to non-intracellular pathogens, it was decided to focus on *T. cruzi* and deduce by which mechanism(s) it causes cells to vesiculate. After reviewing the literature, involvement of four mechanisms were investigated. Firstly, there are reports that activation of calcium ion channels in turn activates cytoskeleton depolymerization, which aids the entry of pathogens into cells. Others have shown the involvement of cholesterol and lipid raft domains during bacterial and parasite entry into mammalian cells [339;365]. In these reports, the authors communicate how activation of raft domains by intracellular pathogens results in calcium influx and remodelling of the cytoskeleton. This result would lead one to speculate that PMVs are also released, because an increase in cytosolic Ca^{2+} would activate the enzyme, calpain, which in turn cleaves the cytoskeleton, leading to actin depolymerization and subsequent release of PMVs.

In addition, the role of integrins in cell invasion has been shown through inhibition experiments using the Arginine-Glycine-Aspartate (RGD) peptide and the anti-CD49d antibody [354]. Interestingly, integrins have also been reported to interact with raft domains through signalling, a mechanism also described to activate calcium channels and depolymerization of the cytoskeleton [350;351;366].

7.3.2 Calcium channels are important for PMV release and *T. cruzi* entry into mammalian cells

Having established that intracellular pathogens, particularly, *T. cruzi* can induce the release of PMVs from host cells, further studies were conducted to investigate whether this was through activation of calcium channels. Briefly, HeLa cells resuspended in prewarmed RPMI + $CaCl_2$ were seeded in triplicate into 24-well plates and preincubated for 45 min with the L-type calcium channel blockers, verapamil or nifedipine (200 µM) separately or together. In some wells, stretch-activated channel (SAC) blockers, gadolinium chloride ($GdCl_3$, 200 µM) or GsMTx-4 (20 µg/ml), a peptide component of the tarantula spider venom were preincubated with cells prior to stimulation with *T. cruzi* metacyclic (5:1 ratio of parasites to cells) or 5% NHS. After adding the inducing agents, reactions were incubated at 37°C for 30 min with shaking and PMVs released were isolated and analysed as described under materials and methods.

In the presence of verapamil and nifedipine, *T. cruzi* stimulation of PMVs was reduced compared to untreated cells (**Fig. 7.3 A**). Interestingly, a stronger reduction was observed when activation of SAC was blocked with $GdCl_3$ or GsMTX-4. (**Fig. 7.3 B**). Application of GsMTX-4 in invasion assays, reduced parasite entry into cells, compared to untreated cells (**Fig. 7.3 C**). Even more interesting was the failure of these agents to inhibit the release of PMVs when cells were stimulated with sublytic complement (**Fig. 7.3 D**). These results suggest that *T. cruzi* has to activate calcium channels in order to stimulate release of PMVs. As mentioned in section 4.2.3, PMV release in the presence of human serum is due to MAC insertion into host plasma

membrane. Host cells rid themselves of this complex by releasing MAC-bearing PMVs into the extracellular environment.

7.3.3 Lipid rafts are important for PMV release and *T. cruzi* entry into mammalian cells

Another mechanism utilised by *T. cruzi* for invasion is via activation of host lipid raft domains. Therefore the role of lipid rafts in the release of PMVs shown previously for THP-1 cells (see section 4.2.7) and whether *T. cruzi* requires activation of these domains for their entry into mammalian cells was investigated. Employing a similar protocol as described earlier, HeLa cells resuspended in RPMI containing $CaCl_2$ were preincubated with the cholesterol sequesting agents, methyl-β-cyclodextrin (MβCD, 5 mM), which disrupts cholesterol or the cholesterol binding agent, filipin (5 µg/ml) at 37°C for 45 min prior to addition of parasites or NHS. After incubation at 37°C for 30 min, released PMVs were isolated and quantified by flow cytometry.

For invasion assays, semiconfluent HeLa cells ($2x10^5$/well) seeded overnight into 12-well plates were preincubated with MβCD or filipin prior to addition of metacyclic *T. cruzi* and reaction was incubated at 37°C for 3 h. After 3 h incubation, plates were washed three times by changing the medium with sterile PBS to wash-off parasites that had not infected. Cells were fixed with 4% paraformaldehyde and washed a further three times with PBS. Coverslips with confluent cells were stained with DAPI-VECTASHIELD with mounting medium and inverted onto microscope slides.

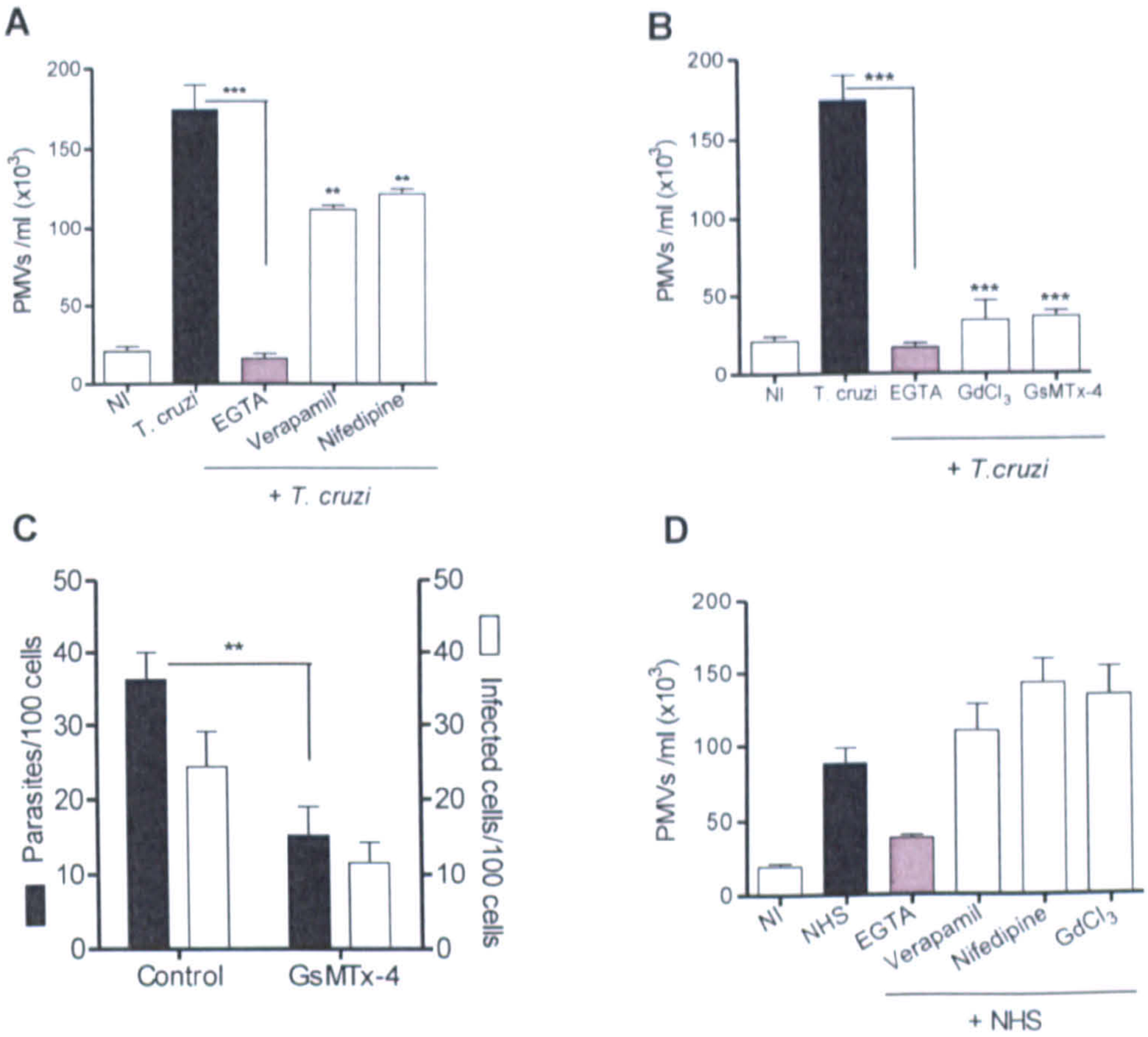

Figure 7.3 Inhibition of calcium channels inhibits the release of PMVs and reduces *T. cruzi* entry into mammalian cells

(A) Blocking the activation of L-type calcium channels with verapamil and nifedipine (200 μM each), caused a reduction in *T. cruzi*-stimulated release of PMVs. (B) A similar result was obtained after HeLa cells were preincubated (37°C, 45 min) with the stretch-activated channel blockers, $GdCl_3$ (200 μM) and GsMTx-4 (20 μg/ml) prior to the addition of metacyclic *T. cruzi*. (C) Inhibition of calcium channel activation, not only caused a reduction in the release of PMVs, but also more importantly, abrogated the entry of parasites. (D) No such inhibition was observed with these agents when HeLa cells were stimulated with NHS. Data represent the mean ± SD of three individual experiments performed in triplicate. ***P <0.001, **P <0.01 were considered statistically significant.

Invasion was examined by mounting slides on an inverted fluorescence microscope (Olympus Corp. UK). The results obtained showed that disruption of lipid rafts with MβCD significantly reduced *T. cruzi* stimulated release of PMVs (**Fig. 7.4 A**) and subsequently, abrogated parasite entry into cells. However, treatment with filipin failed to reduce parasite ingress into cells (**Fig. 7.4 B**). This might be due to the fact that filipin, unlike cyclodextrin, sequesters cholesterol but does not deplete disrupt the steroid. Moreover, unlike the failure of the calcium channel blockers to inhibit PMV release with NHS stimulation, disruption of lipid rafts with MβCD also reduced the release of PMVs when stimulated with serum (**Fig. 7.4 C**).

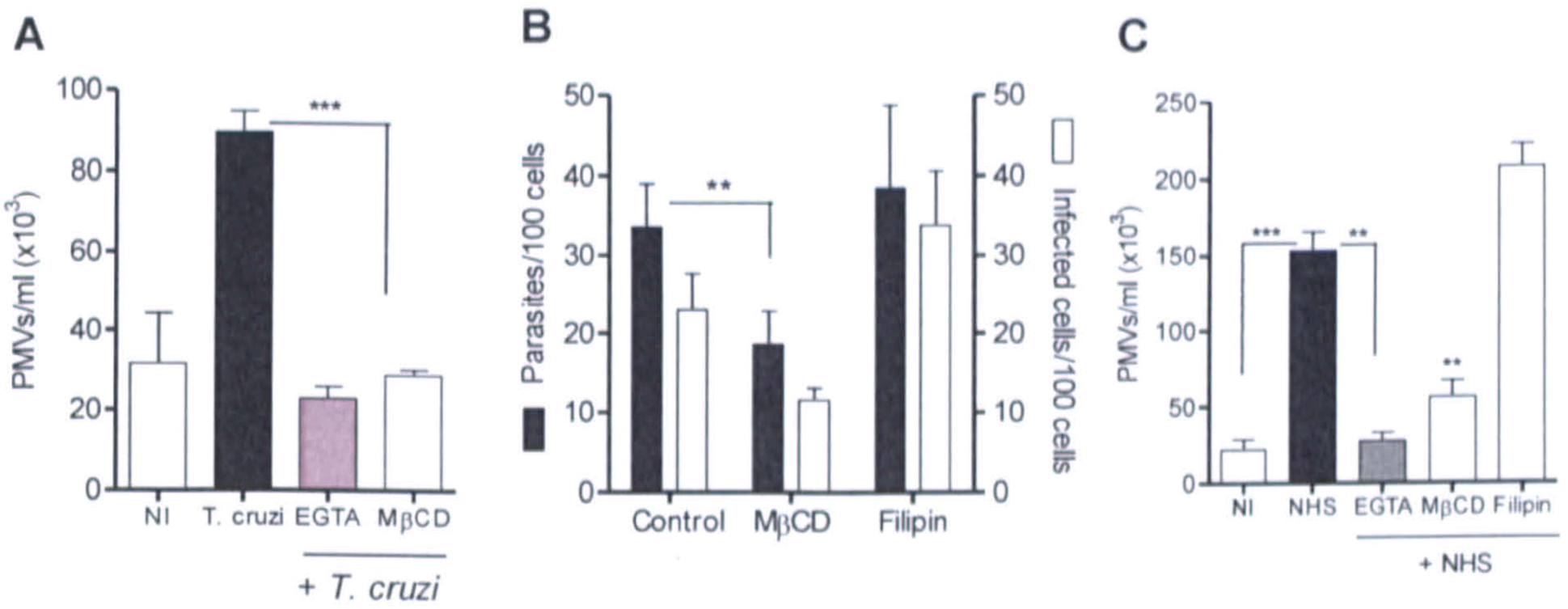

Figure 7.4 Blocking activation of raft domains inhibits the release of PMVs and reduces *T. cruzi* entry into mammalian cells

(A) Disruption of lipid rafts with MβCD (5 mM) caused a reduction in the release of PMVs after stimulation of HeLa cells with metacyclic *T. cruzi*. (B) MβCD was also found to reduce parasite entry into mammalian cells after analysing a 3 h invasion assay using an inverted fluorescence microscope (Olympus Corp. UK). Remarkably, no such inhibition was measured where cells had been pretreated with the cholesterol-sequestering agent, filipin (5 µg/ml). (C) Stimulation of PMVs by sublytic complement was also reduced after depletion of cholesterol domains with MβCD, but no reduction was detected in the presence of filipin. Data represent the mean ± SD of three individual experiments performed in triplicate. ***P <0.001, **P <0.01 were considered statistically significant.

7.3.4 Integrins are important for PMV release and *T. cruzi* entry into mammalian cells

In addition to calcium channels and lipid raft domains described earlier, integrins have also been reported to function during invasion of microbial pathogens into cells [367]. However, it has not yet been shown whether these signalling molecules participate in the mechanism of microvesiculation. Also the role of integrins in the invasion of mammalian cells by *T. cruzi*, has not been well characterised, albeit, studies have been carried out in various laboratories to suggest as such. Hitherto, it was shown that patients with mild Chagas disease have lower numbers of $CD49d^+$ expressing cells. By contrast $CD49d^+$ cells were much higher in patients who suffered from severe Chagas disease [368].

In the present study the role of integrins in the release of PMVs was investigated. Trypsinised HeLa cells ($1x10^6$/well) were resuspended in prewarmed RPMI with $CaCl_2$ and seeded into 24-well plates in triplicate. Cells were pretreated with the RGD peptide or the control peptide, RGE (200 µg/ml each). In the same experiment, activation of the integrin α4β1 (CD49d/CD29 or very late antigen-4, VLA-4), was blocked using the antibody, mouse anti-CD49d (10 µg/ml) and the plate was incubated at 37°C for 45 min prior to stimulation with *T. cruzi* metacyclic or NHS. Plasma membrane-derived vesicles were induced by incubation at 37°C for 30 min with shaking and vesicles were isolated according to the procedure described under section 3.9.2. Also, semiconfluent HeLa cells ($2x10^5$/well) in triplicate were infected with parasites ($1x10^6$/well), after pretreating with the integrin blockers mentioned above and invasion assays were performed at 37°C for 3 h.

In the presence of the RGD peptide or the anti-CD49d antibody, *T. cruzi* stimulation of PMVs was significantly reduced (**FIg. 7.5 A**). Invasion assays showed reductions in the number of invading parasites, in the presence of the RGD peptide, but not the control peptide, RGE (**FIg. 7.5 B**). Inhibition of *T. cruzi* invasion was measured as dose dependent and maximum reduction was measured with 500 µg/ml (**FIg. 7.5 C**). As observed for calcium channels, inhibiting the activation of integrins failed to abate release of PMVs when cells were stimulated with NHS (**FIg. 7.5 D**). Together these results present evidence that *T. cruzi* activation of these receptors/domains, is absolutely necessary to its induction of PMVs, and maybe more importantly its invasion into mammalian cells.

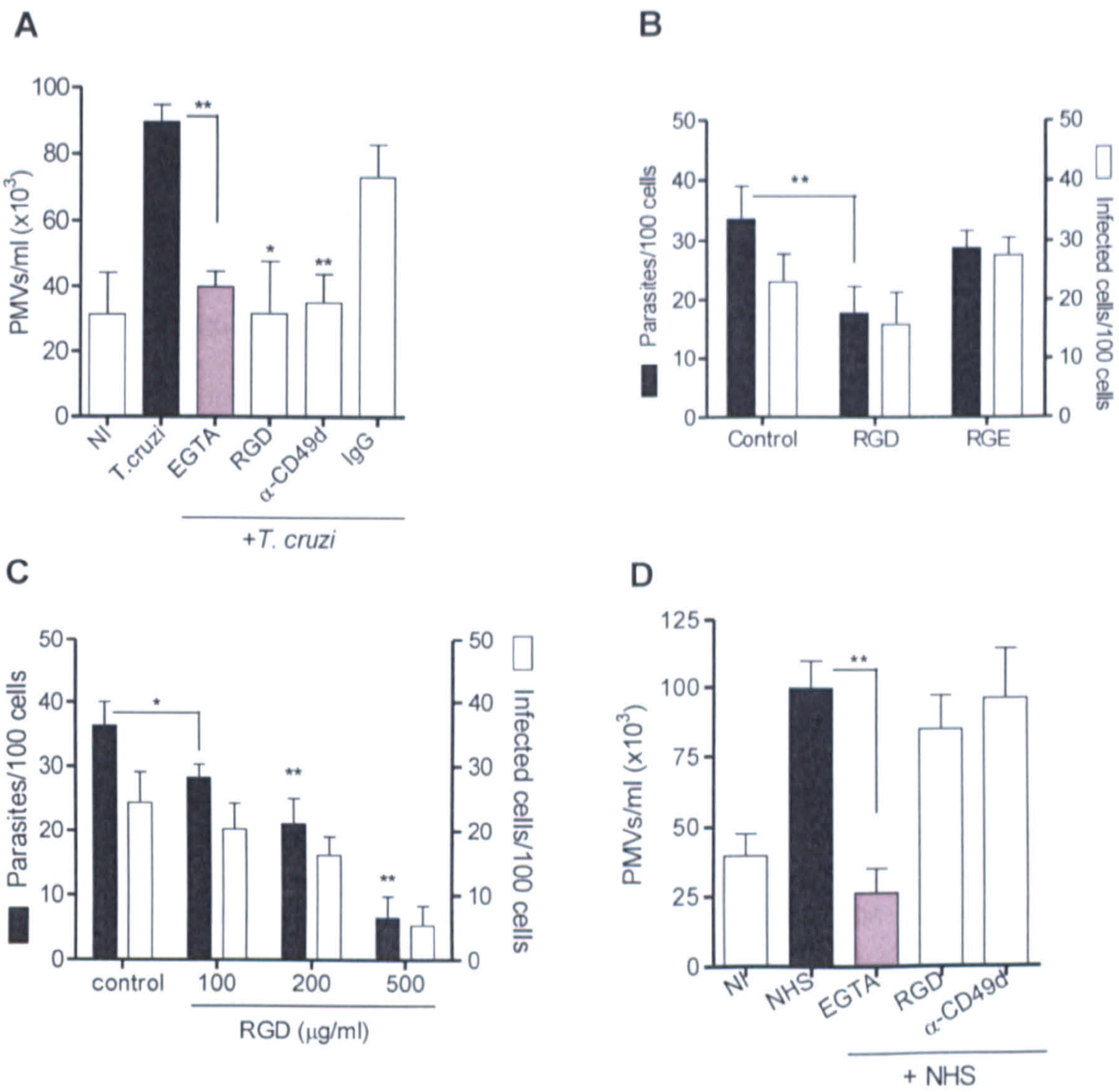

Figure 7.5 Blocking activation of integrins inhibits the release of PMVs and reduces *T. cruzi* entry into mammalian cells

(A) Pre-treatment of HeLa cells ($1x10^6$/ml) with RGD peptide or control RGE and the integrin α4β1 antibody, mouse anti-CD49d, reduced the number of released PMVs after stimulation with *T. cruzi*. PMVs were still released in the presence of the isotype mouse-IgG control. (B) Invasion into semiconfluent HeLa cells ($2x10^5$/well) by metacyclic *T. cruzi* was significantly reduced in the presence of the RGD peptide, but the control peptide, RGE, failed to inhibit entry of parasites. (C) Effect of RGD on *T. cruzi* entry into cells was dose dependent and maximum reduction was measured with 500 μg/ml. (D) In the presence of sublytic complement, blocking the activation of integrins with RGD peptide or mouse anti-CD49d antibody both failed to inhibit the release of PMVs. Data represent the mean ± SD of two independent experiments performed in triplicate. $^{**}P < 0.01$, $^{*}P < 0.05$ were considered statistically significant.

7.3.5 *T. cruzi* activation of the PI 3-Kinase pathway, induces release of PMVs and aids parasite entry into cells

The involvement of the PI 3-Kinase signalling pathway came to light after being reported to participate during the entry of *T. cruzi* into mammalian cells. In a recent report, it was shown that blocking activation of this pathway with wortmannin abated the entry of parasites into cells [308]. Since the authors of this report were not aware that *T. cruzi* can induce the release of PMVs from host cells, it was pertinent to investigate the effect, if any, that wortmannin treatment might elicit on parasite induction of these vesicles. In the presence of wortmannin, *T. cruzi* failed to induce release of PMVs from HeLa cells (**Fig. 7.6 A**) and its entry into these cells was also reduced (**Fig. 7.6 B**).

Interestingly, release of PMVs after stimulation with NHS also reduced after treating cells with wortmannin (**Fig. 7.6 C**). Under both conditions (*T. cruzi* or NHS), treatment of cells with calpeptin significantly abrogated the release of PMVs. This finding suggests that treatment of cells with wortmannin might be abolishing *T. cruzi* induction of PMVs from the host. Hence, another possible explanation for the reduced invasion observed after wortmannin treatment, might be due to inhibition of PMV release by the agent. Reduction in the release of PMVs asserts that the host cells sustain less damage, meaning plasma membrane integrity is not compromised for *T. cruzi* exploitation and subsequent entry.

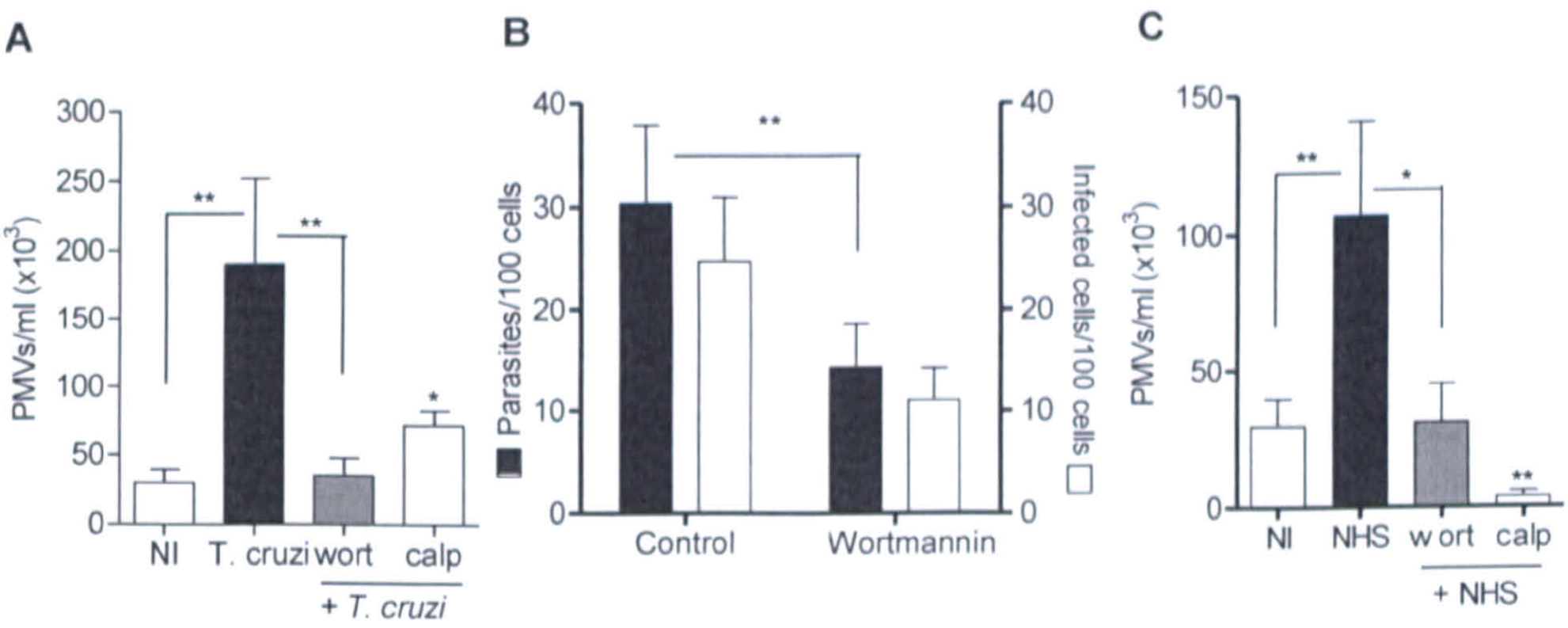

Figure 7.6 Blocking the activation of PI 3-Kinase reduces the release of PMVs and renders *T. cruzi* unable to infect.

(A) Pre-treatment of HeLa cells ($2x10^5$/well in triplicate) with wortmannin (40 nM) at 37°C for 45 min inhibites the release of PMVs after stimulation with parasites. Cells are treated with calpeptin (20 μM) as a positive control. (B) Pretreating HeLa cells with wortmannin significantly reduces *T. cruzi* invasion compared to control, without treatment. (C) Wortmannin treatment also inhibits PMV release after stimulation of cells with sublytic complement. Data represent the mean ± SD of three individual experiments performed in triplicate. $^{**}P < 0.01$, $^{*}P < 0.05$ were considered statistically significant.

Interestingly, agents, which reduced the release of PMVs, also caused marked reductions in the number of invading parasites. Although, some agents failed to inhibit release of PMVs after NHS stimulation, all the pathways investigated showed that inhibiting the activation of these receptors/domains, also reduced release of the vesicles, and perhaps more importantly, rendered *T. cruzi* unable to invade. Together these findings further confirm the suggestion that *T. cruzi* has to activate these receptors/domains, to induce the release of PMVs, thereby exploiting the resulting membrane damage for their ingress into cells. If release of PMVs induced by *T. cruzi* or NHS resulted in breach of plasma membrane integrity, which in the case of infection is exploited by the parasite for entry, then understanding how eukaryotic cells would normally repair damage to their plasma membrane is important since PMV release also occurs constitutively.

7.4 Release of PMVs induces plasma membrane damage and results in recruitment of lysosomes to the site of damage

As mentioned in section 7.1.6, damage to the plasma membrane allows the influx of calcium, which rapidly recruits lysosomes to the site of damage. These lysosomes fuse together and reseal the breakage, allowing the cell to survive and resume normal function. During the process of PMV release, the complete detachment of the vesicle from the parent cell could be envisaged as a damage, which would require resealing. This study investigated whether the release of PMVs results in damage to the plasma membrane, which then allows calcium influx and subsequent activation of lysosomal exocytosis to the site of damage.

7.4.1 Normal repair mechanism in eukaryotic cells

In eukaryotic cells membrane repair involves the rapid recruitment of lysosomes to the site of damage. The model below depicts a mechanism where the ubiquitous release of PMVs from a resting cell (**Fig. 7.7 A**), may result in a breakage to the plasma membrane when the vesicle is completely detached from the cell (**Fig. 7.7 B**). This allows the influx of calcium that activates the exocytosis of lysosomes, which fuse together and patch-up the damage, resulting in the transfer of internal membrane to the surface of the cell (**Fig. 7.7 C**). The involvement of lysosomes in the resealing process is confirmed by detection of the lysosome-specific protein, LAMP-1, using fluorescently labelled antibodies by flow cytometry or a fluorescent microscope (**Fig. 7.7 D**).

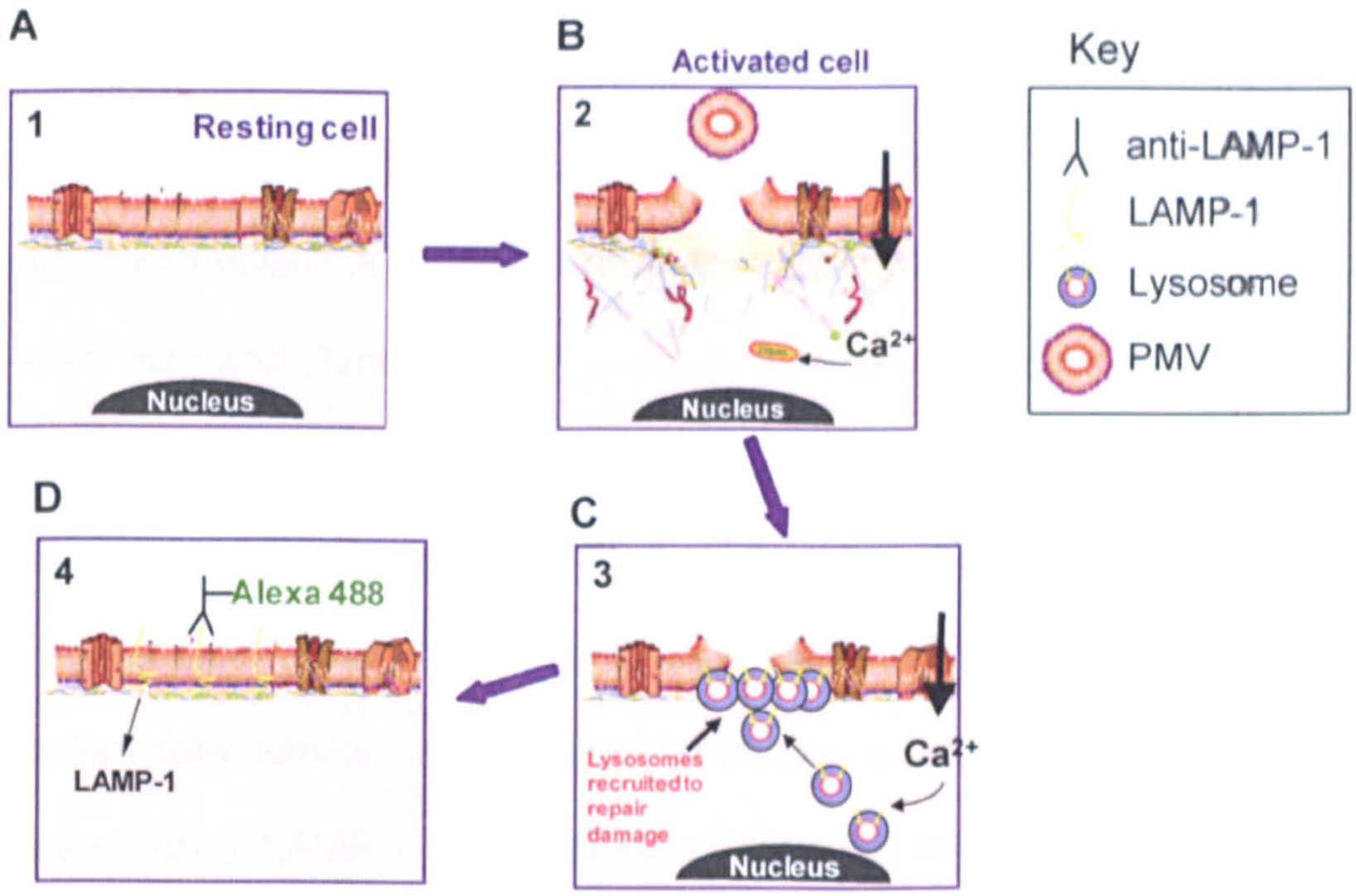

Figure 7.7 Normal membrane repair involving lysosomes

(A) An intact plasma membrane of a cell in the resting state. (B) The integrity of the membrane is compromised by damage to the cell caused by mechanisms such as the complete detachment of PMVs, physical or chemical damage. (C) Calcium influx through the resulting damage activates the exocytosis of lysosomes to the site of damage. (D) Lysosomes fuse together and patch-up the damage resulting in transfer of internal membrane and subsequently, expression of the lysosome specific marker, LAMP-1, to the surface. Detection of LAMP-1 using a fluorescein-conjugated antibody, which is then analysed by flow cytometry and fluorescence microscopy, is accepted as a measure of damage repair.

7.4.2 *T. cruzi* Induction of PMVs activates the exocytosis of lysosomes

To investigate whether *T. cruzi* induction of PMVs results in plasma membrane damage that requires repair, HeLa cells were trypsinised into suspension and seeded into 1.5 ml microcentrifuge tubes in triplicate. The cells were preincubated with concanavalin A (conA) at room temperature for 10 min or with calpeptin (37°C for 45 min) and stimulated (37°C for 30 min) to microvesiculate by the addition of *T. cruzi* (5:1 parasites to cells). To observe the involvement of lysosomes, the reaction was fixed after 30 min with PFA and labelled with anti-LAMP1-AlexaFlour-488 antibody before analysis on the flow cytometer. Moreover, semiconfluent HeLa cells treated with similar agents were analysed on the fluorescence microscope for expression of LAMP-1, which indicates the recruitment of lysosomes.

Indeed, stimulation of HeLa cells with *T. cruzi* in the absence of resealing inhibitors, resulted in the release of PMVs (**Fig. 7.8 A 1 and 2**) and the recruitment of lysosomes to the cell surface, seen here by the expression of higher LAMP-1 fluorescence (**Fig. 7.8 B 1-4**). However, preincubation of HeLa cells with calpeptin, an inhibitor of calpain, caused a marked reduction in the release of PMVs (**Fig. 7.8 C 1 and 2**), and LAMP-1 expression was severely ablated. This result suggested that by inhibiting the release of PMVs, the host cell plasma membrane sustains less damage leading to a significant reduction in LAMP-1 fluorescence (**Fig. 7.8 D 1-3**).

Interestingly, the release of PMVs from cells pretreated with conA, continued unabated and parasite attachment was slightly enhanced in the presence of this

agent (**Fig. 7.8 E 1 and 2**). However, the expression of LAMP-1 was significantly reduced, suggesting that lysosomal recruitment was abolished (**Fig. 7.8 F 1-3**). The aforementioned results suggest that in the presence of conA, the activation of lysosomal exocytosis is specifically inhibited. This result is in agreement with an earlier report, which described conA as a specific inhibitor of membrane resealing [369], but shows further that this agent has no inhibitory effect on the release of PMVs. Together, these results show that *T. cruzi* induction of PMVs causes breakage to the host plasma membrane, which parasites exploit for their ingression into cells before the exocytosis of lysosomes, which would have been concomitantly activated, reseals the damage.

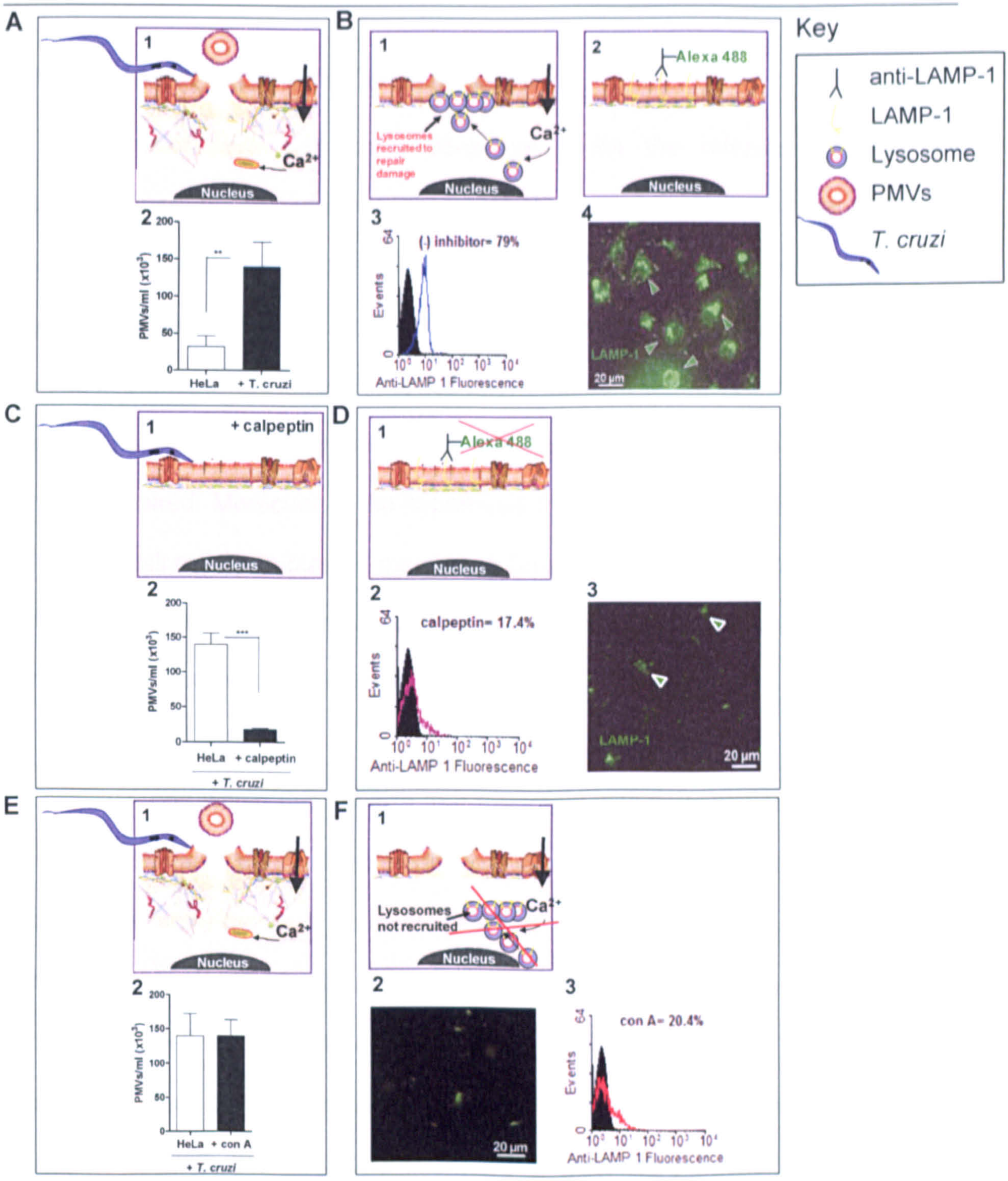

Figure 7.8 Release of PMVs activates the exocytosis of lysosomes

(A) Addition of *T. cruzi* activates the release of PMVs from HeLa cells, resulting in a breach of the plasma membrane (PM) (A1 and A2). (B) Breakage to the PM allows the influx of Ca^{2+} (B1), which recruits lysosomes (B1) to the site of damage. Repair is detected by the transfer of the lysosome specific protein, LAMP-1 to the surface (B2), which is analysed by immunofluorescence on the flow cytometer (B3) and microscope (B4). (C) In presence of the calpain inhibitor, calpeptin, *T. cruzi* fails to induce the release of PMVs (C1 and C2) and therefore less damage is sustained by the PM. (D) Less PMVs means less compromise to the integrity of the PM (D1) and so fewer lysosomes are recruited to the surface, resulting in less LAMP-1 fluorescence (D2 and D3). (E) Interestingly, in the presence of conA, membrane damage through *T. cruzi* induction of PMVs is unaffected (E1 and E2). However, low LAMP-1 fluorescence is detected (F2 and F3), suggesting that conA is a specific inhibitor of the resealing mechanism.

7.4.3 Release of PMVs aids *T.cruzi* invasion

If treatment of cells with conA does not inhibit the release of PMVs as aforementioned, but nonetheless, abrogates the lysosome-mediated mechanism of resealing/repair, then *T. cruzi*-induced damage in the presence of this agent should proceed unabated. It was postulated that if the activation of lysosomal exocytosis to the site of damage was indeed inhibited after treatment with conA, then the damage caused by the parasite due to release of PMVs should remain unrepaired or at least partially repaired. Moreover, if the hypothesis that complete PMV detachment from the parent cell results in plasma membrane breakage is accurate, then cells treated with conA should have increased susceptibility to *T. cruzi* invasion or at least parasite entry should proceed unabated.

By contrast, one would hypothesize that treatment with calpeptin should inhibit the release of PMVs so that *T. cruzi* mediated plasma membrane damage is abrogated and parasite entry blocked. To investigate this, semi-confluent HeLa cells cultured onto coverslips inside 12-well plates in triplicate, were treated or not (control) with either conA (RT for 10 min) or calpeptin at 37°C for 45 min. The agents were washed off prior to the addition of parasites and once added the reaction was incubated at 37°C, 5% CO_2 for 3 h. After 3 h, wells were washed three times by subsequent changes of PBS and fixed with 4% PFA at RT for 15 min. After three further washes, coverslips were inverted on microscope slides with DAPI-VECTASHIELD medium. In some experiments treated or untreated cells were stimulated with parasites for 30 min and fixed with 4% PFA. After washing off uninfected parasites, samples were labelled with annexin V Alexaflour-488 antibody to detect released PMVs and images were collected using fluorescence

microscope (1X81 motorized, inverted fluorescence microscope, Olympus Corporation).

Indeed, *T. cruzi* entry was significantly enhanced after HeLa cells were pretreated for ten minutes with conA. By contrast and in agreement with the hypothesis, treatment with calpeptin rendered the parasites unable to invade. Interestingly, pre-treatment of HeLa cells with conA for more than ten minutes (30 minutes), resulted in a marked reduction in the number of invading parasites (**Fig. 7.9 A**) and examination of microscopic images revealed a loss of cell cytoplasm (**Fig. 7.9 B**). PMVs isolated from this experiment were positive for PS as assessed by annexin V binding to the surface (**Fig. 7.9 C**). Moreover, treatment with conA resulted in superinfection of cells (multiple infections of individual cells) as envisaged. As such, there was a general increase in invasion; however, the number of cells infected by two or more parasites occurred at very low levels (**Fig. 7.9 D**). Untreated cells released PS^{+}PMVs as detected by positive annexin V binding and subsequent invasion of the parasite (**Fig. 7.9 E**). In the presence of calpeptin, no such release of PMVs was detected and parasites failed to invade (**Fig. 7.9 F**). Furthermore, treatment with conA allowed the release of PMVs to proceed unabated, but also parasite attachment and entry into cells was significantly enhanced (**Fig. 7.9 G**). Together, these results show that the release of PMVs causes damage to the plasma membrane, which parasites exploit for entry. Moreover, if the repair of damage is delayed, this could lead to complete loss of cell cytoplasm.

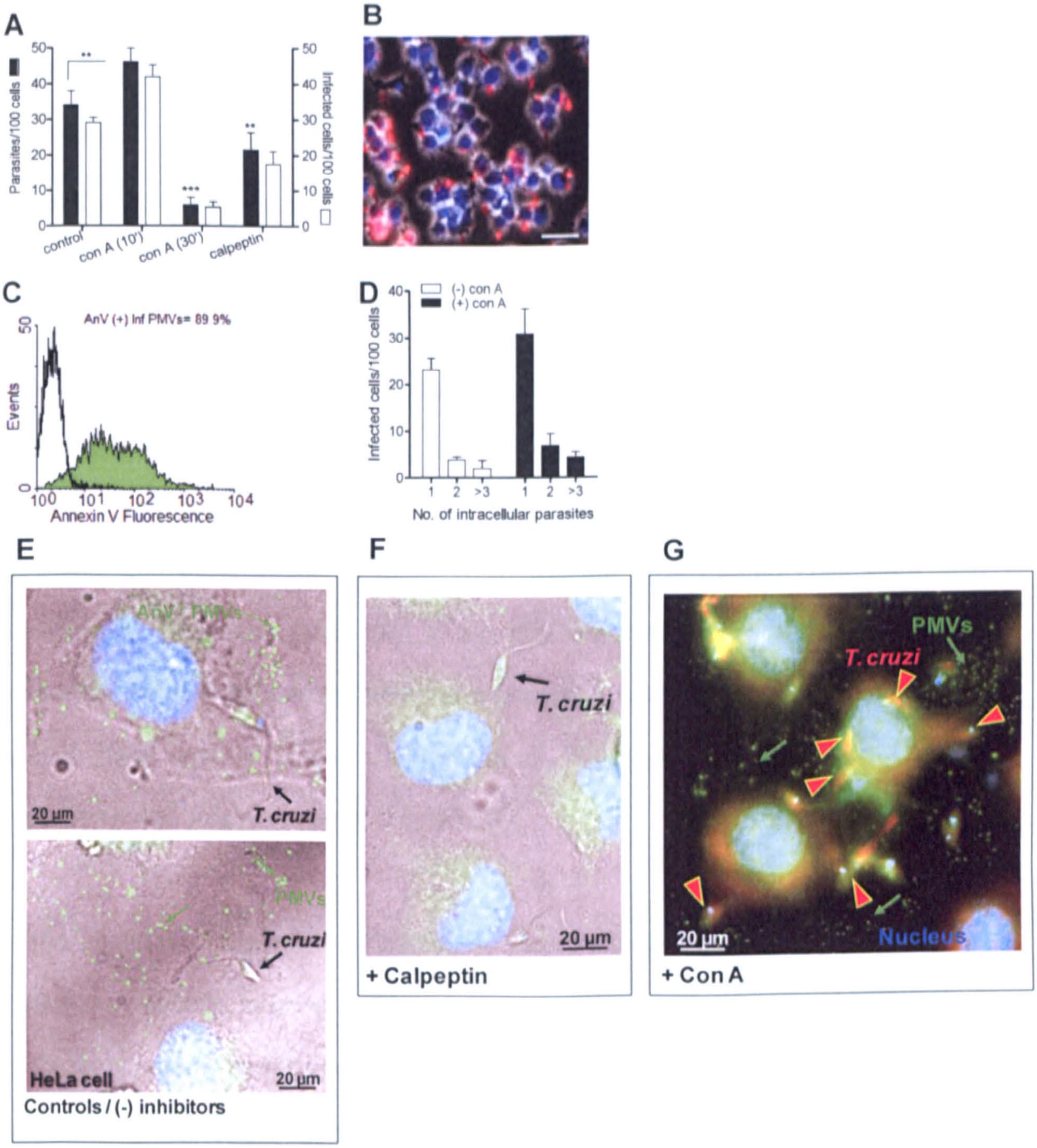

Figure 7.9 *T. cruzi* exploits host membrane damage for entry

(A) Inhibiting the exocytosis of lysosomes with conA, enhanced the entry of *T. cruzi* into HeLa cells, but by contrast, treatment with calpeptin severely abolishes the entry of parasites into cells. (B) Close examination revealed loss of cell cytoplasm after longer conA treatment. Scale bar = 100 µm (C) PMVs isolated from the invasion assay, were PS+ after binding with annexin V (D) Pretreatment (RT, 10 min) with conA (20 µg/ml) enhances the overall extent infection, and superinfection occurs at low levels. (E) Fluorescence microscopy images of cells infected with *T. cruzi* (black arrows) shortly after induction of PMVs (green arrows) in the absence of inhibitors. (F) Pretreatment (37°C, 45 min) with calpeptin (20 µM) inhibits the release of PMVs and subsequently, the entry of *T. cruzi* into cells. (G) By contrast, treatment with conA fails to inhibit the release of PMVs (green arrows), but instead, exacerbates the infection of HeLa cells by parasites (red arrowheads). All chemical agents were washed off twice with PBS prior to addition of parasites. Scale bar = 20 µm.

7.4.4 Release of PMVs is a required step for migration and fusion of lysosomes

Several reports have suggested that recruitment and fusion of lysosomes with the plasma membrane, is required to facilitate *T. cruzi* invasion of mammalian cells [309;370;371]. As aforementioned, the release of PMVs is a trigger for lysosomal exocytosis; however, further studies were conducted to elucidate other possibilities. The detection of *T. cruzi*-mediated surface expression of LAMP-1 (a measure of lysosomal exocytosis), described above for conA and calpeptin treated cells, was repeated with other inhibitors of microvesiculation. The treated cells were also labelled with propidium iodide (PI) to examine membrane repair. An uptake of PI shows an unrepaired plasma membrane breakage caused by parasites. Chemical agents were used to inhibit the release of PMVs and the effect on LAMP-1 expression was examined by flow cytometry.

In the absence of chemical inhibitors, *T. cruzi* induced the release of PMVs (**Fig. 7.10 A1**) from cells, causing damage to the host plasma membrane, which resulted in the subsequent recruitment of lysosomes to the site of damage (**Fig. 7.10 A2**) [LAMP-1 expression (93%), indicated by green fluorescence]. As such, the uptake of PI was low (**Fig. 7.10 A3**), meaning the damage has been repaired by the recruited lysosomes. The unabated release of PMVs meant that *T. cruzi* invasion of cells progressed after 3 h as expected (**Fig. 7.10 A4**). By contrast, treatment with $GdCl_3$ inhibited the release of PMVs (**Fig. 7.10 B1**) as previously observed and this abrogated LAMP-1 expression (**Fig. 7.10 B2**), meaning no lysosomal exocytosis. Strikingly, PI incorporation was significantly lower (**Fig.7.10 B3**), however, this was not due to damage resealing since lysosomal exocytosis was abrogated. Instead,

this implies that treatment with $GdCl_3$ reduced *T. cruzi* induction of PMVs so that the host plasma membrane integrity was more or less left intact, thus rendering the parasites unable to invade **(Fig. 7.10 B4)**.

As for $GdCl_3$, treatment with calpeptin also inhibited the release of PMVs **(Fig. 7.10 C1)** and abrogated lysosomal exocytosis **(Fig. 7.10 C2)**, thus confirming earlier observations. The low PI incorporation was again due to the lack of PMV release, rather than resealing by lysosomes **(Fig. 7.10 C3)**. As such, invasion experiments with calpeptin treated cells, showed a reduction in the number of intracellular parasites **(Fig. 7.10 C4)**. As observed with previous experiments, the release of PMVs continued unabated after the cells were treated with conA **(Fig. 7.10 D1)**. In agreement with earlier data, lysosomal exocytosis was inhibited **(Fig. 7.10 D2)** and increased levels of PI incorporated **(Fig. 7.10 D3)** into the cells, thus suggesting an unrepaired membrane damage. Subsequently, *T. cruzi* entry was not inhibited **(Fig. 7.10 D4)** since the cells had endured injury through the release of PMVs, which had not been repaired.

The activation of PI 3-Kinase has been shown to be an important step during *T. cruzi* invasion of cells, and so this study investigated whether inhibition of this kinase has any role during the release of PMVs and subsequent lysosomal exocytosis. Data presented here shows that treatment with wortmannin inhibited the release of PMVs **(Fig. 7.10 E1)** and subsequently abrogated the migration of lysosomes to the membrane surface **(Fig. 7.10 E2)**. Moreover, the incorporation of PI was low **(Fig. 7.10 E3)** and *T. cruzi* invasion of cells was reduced **(Fig. 7.10 E4)**, implying that the

host plasma membrane is intact. This is in agreement with other findings, which showed that wortmannin treatment abrogates *T. cruzi* entry, but goes to show that the reason for less invasion might be due to wortmannin inhibition of PMV release [308;312].

Treatment with RGD partially inhibited the release of PMVs (**Fig. 7.10 F1**) hence the slight increase in LAMP-1 fluorescence (**Fig. 7.10 F2**), although this was lower than untreated (control). As RGD only partially inhibited the release of PMVs, PI incorporation was slightly raised as compared to other inhibitors such as $GdCl_3$ or calpeptin (**Fig. 7.10 F3**). However, *T. cruzi* entry into HeLa cells was still inhibited (**Fig. 7.10 F4**). The control peptide RGE, failed to inhibit the release of PMVs as reported earlier (**Fig. 7.10 G1**). In the presence of this agent release of PMVs caused damage, which was repaired by recruited lysosomes (**Fig. 7.10 G2**). Here, the low PI uptake was due to lysosomal resealing and not the lack of PMV release (**Fig. 7.10 G3**). As expected, invasion experiments confirmed that *T. cruzi* entry was not abrogated in the presence of this agent (**Fig. 7.10 G4**). Another agent shown to inhibit the release of PMVs is Y-26732; however, in my hands it only partially inhibited *T. cruzi*-induced release of the vesicles (**Fig. 7.10 H1**). Moreover, increased LAMP-1 expression (**Fig. 7.10 H2**) was still detected and PI incorporation was significantly lower (**Fig. 7.10 H3**). This was surprising, as one would expect lower LAMP-1 expression due to lack of PMVs. However, it is worth noticing that the release of PMVs was only partially inhibited, hence the cells might have sustained more damage (in contrast to the other inhibitors $GdCl_3$, calpeptin and wortammin), which strongly reduced the PMV release. Furthermore, invasion experiments showed a reduction in the number of intracellular parasites (**Fig. 7.10 H4**), thus

implying that even with only a slight reduction in the release of PMVs cells were kept intact enough to avoid *T. cruzi* entry.

Together, these data imply that inhibition of PMV release means less damage is sustained by the host plasma membrane. Less damage means fewer lysosomes being required for resealing, as the host cell integrity is relatively intact. It is therefore conceivable that the release of PMVs induced by live parasites is a required step for migration and fusion of lysosomes during invasion of *T. cruzi* into mammalian cells. These findings agree with earlier studies, which showed that Ca^{2+} triggered actin cytoskeleton rearrangement caused by live parasites is a required step for migration and fusion of lysosomes during formation of the *T. cruzi*-containing vacuole [371].

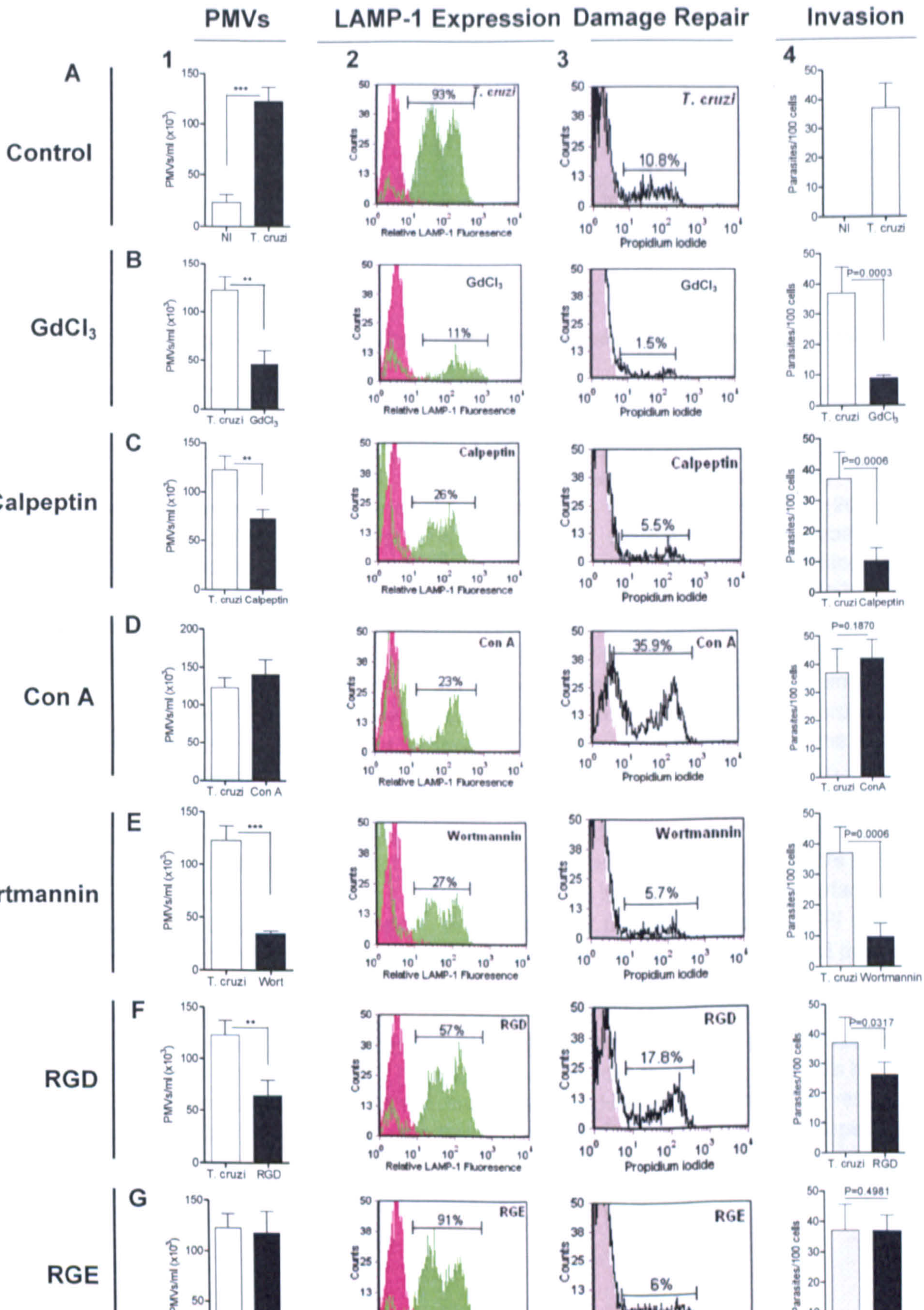
PMVs
LAMP-1 Expression
Damage Repair
Invasion
1
2
3
4
A
Control
B
GdCl3
C
Calpeptin
D
Con A
E
Wortmannin
F
RGD
G
RGE
PMVs/ml (x10³)
Parasites/100 cells
Counts
Relative LAMP-1 Fluorescence
Propidium Iodide
NI
T. cruzi
GdCl3
Calpeptin
Con A
Wort
RGD
RGE
ConA
***
**
93%
10.8%
11%
1.5%
26%
5.5%
23%
35.9%
27%
5.7%
57%
17.8%
91%
6%
P=0.0003
P=0.0006
P=0.1870
P=0.0317
P=0.4981

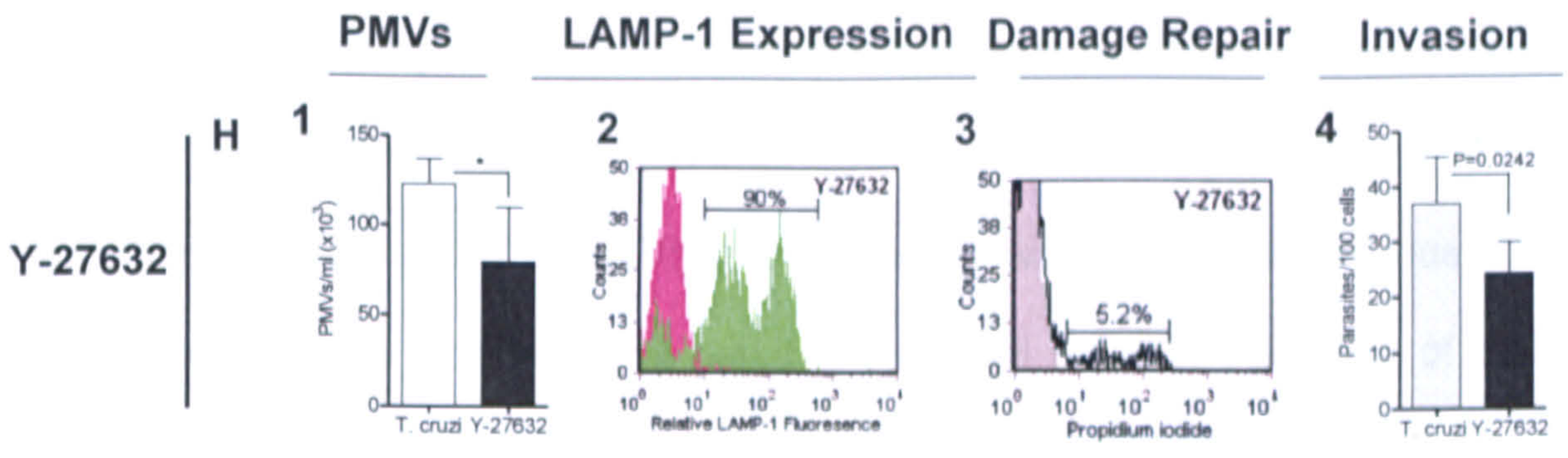

Figure 7.10 Inhibitors of PMVs release modulates lysosomal exocytosis and repair

(A1) In the absence of inhibitors, parasites induce the release of PMVs (black bar) compared to cells only (NI, non-induced, white bar). (A2) Lysosomes are recruited to the site of damage to reseal breach (increased green LAMP-1 fluorescence, 93%) thus the plasma membrane remains intact (A3, low PI incorporation). Untreated cells are infected by *T. cruzi* after 30 min invasion experiments performed at 37°C. (B1) Treatment with $GdCl_3$ (200 μM) inhibits the release of PMVs (black bar) and so lysosomes are not required for repair (B2, low LAMP-1 fluorescence, 11%), since the plasma membrane integrity remains intact (B3, PI, black line). (B4) In the presence of this agent, *T. cruzi* was rendered unable to invade. (C1-4) Similar result is obtained after calpeptin (20 μM) treatment. Like $GdCl_3$, calpeptin is a potent inhibitor of PMV release. (D1) Release of PMVs in the presence of conA continues unabated. (D2) However, migration of lysosomes to reseal the resulting damage is abrogated (23% LAMP-1 fluorescence), thus, leading to an increase in PI incorporation (35.9%) (D3). (D4) Parasite entry after treatment with conA was not affected by the agent. (E1) Wortmannin (Wort, 40 nM) treatment reduces the release of PMVs, thus also inhibits the migration of lysosomes (E2, 27% LAMP-1 fluorescence). (E3) The lack of PMV release means that the plasma membrane integrity remains intact, thus rendering *T. cruzi* unable to invade (E4). (F1) Incubation with RGD (200 μM) partially inhibits the release of PMVs so that the cell sustains some damage. (F2) Lysosomes respond by migrating to the surface, but only partially (57% LAMP-1 fluorescence), as indicated by the slight increase in PI uptake (17.8%) (F3). (F4) However, cell invasion by *T. cruzi* still reduces. (G1) The control peptide, RGE, does not inhibit the release of PMVs and so cells endure damage, which leads to the recruitment of lysosomes for repair (G2, 91% LAMP-1 fluorescence). (G3) This keeps the cells intact (low PI uptake, 6%), and renders *T. cruzi* unable to invade (G4). (H1) Treatment with the Rho-kinase inhibitor, Y-27632 (10 μM), partially blocks the release of PMVs but not migration of lysosomes (H2, 90% LAMP-1 fluorescence). (H3) There is thus little resultant damage (low PI uptake) and parasite entry is reduced (H4). Data represent two independent experiments performed in triplicate. ***$P < 0.001$, **$P < 0.01$, *$P < 0.05$ were considered to be statistically significant.

7.4.5 *T. cruzi* entry is facilitated by host release of PMVs and not due to externally added vesicles

In order to rule out the possibility that *T. cruzi* invasion was simply due to the presence of PMVs and not as a result of host cell release, the effect of adding purified PMVs was investigated. In data obtained from our laboratory, we observed that addition of PMVs from THP-1 or Jurkat cells enhanced *T. cruzi* invasion of several cell types both *in vitro* and *in vivo* (Cestari et al. 2010- submitted). In the present study HeLa cell-derived PMVs were investigated to see whether like THP-1 and Jurkat cell-derived PMVs, they could also enhance parasite entry. PMVs were isolated from the culture supernatant of HeLa cells according to the procedure described in section 3.9.2.

Semiconfluent HeLa cells ($2x10^5$/well) cultured overnight in triplicate in 12-well plates were washed three times with serum-free RPMI 1640. Cells were preincubated or not with various inhibitors of PMV release and with conA (an inhibitor of lysosomal migration) as previously mentioned and agents washed off. Serum-free RPMI 1640 was added to the cells and incubated together with PMVs ($1x10^6$/well) and parasites ($1x10^6$/well) in 1 ml reaction volumes. Invasion was allowed to proceed at 37°C for 3 h and later fixed with 4% PFA after several washes with PBS.

Addition of PMVs failed to enhance invasion, in contrast to the results described previously. In the absence of inhibitors, no significant difference was measured between untreated cells (control) and those containing PMVs (**Fig. 7.11 A**). When the cells were pretreated with $GdCl_3$, *T. cruzi* failed to invade and addition of HeLa

cell-derived PMVs failed to reverse the effect of the agent (**Fig. 7.11 B**). Similarly, addition of PMVs failed to reverse the inhibitory effect of Y-27632 (**Fig. 7.11 C**) and calpeptin (**Fig. 7.11 D**) on parasite entry.

The enhancement of invasion by PMVs, as reported previously was due to the presence of TGF-β on the vesicle surface. A correlation between the concentrations of TGF-β and infection was observed. Thus, Jurkat and THP-1 cell-derived PMVs, which had higher levels of TGF-β, significantly enhanced invasion. By contrast, HepG2 and MCF-7, which had lower levels of TGF-β only partially, increased infection (Cestari et al. 2010- submitted). Why the addition of PMVs to HeLa cells failed to enhance *T. cruzi* invasion is not clear, however, I speculate that this could be due to the fact that HeLa cells do not express connexin43 (Cx43) [372], a gap-junctional protein reported to mediate TGF-β signalling [373;374].

Furthermore, it was decided that if the exocytosis of lysosomes to the plasma membrane and its fusion with the invading parasite is the essential factor for *T. cruzi* invasion, then the abrogation of lysosomal migration with conA should result in a reduction of parasite entry. However, this was not the case as *T. cruzi* invasion of cells after treatment with conA continued unabated (see figures 7.9, 7.10D and 7.11E), and strikingly, the parasite still induced the release of PMVs prior to entering the cells. This confirms that the release of PMVs and not lysosomal migration is the important factor during *T. cruzi* entry into cells.

To further confirm this finding, HeLa cells were concomitantly treated with conA and Y-27632 (inhibitor of PMV release) to see if the effect of the two agents would counteract each other. As such, if *T. cruzi* entry into cells is not dependent on the release of PMVs, then treating cells with conA should counteract the effect of Y-27632 and parasite invasion should proceed unabated as observed previously with cells separately treated with conA. However, since the release of PMVs is an important step for effective *T. cruzi* invasion, its inhibition with Y-27632, prevented parasite entry even in the presence of conA (**Fig. 7.11 E**). To put simply, lysosomal exocytosis is not a required step for *T. cruzi* invasion of cells, since its abrogation with conA did not prevent parasite entry. In contrast, the release of PMVs is essential as this causes damage to the host plasma membrane, which *T. cruzi* then exploits for entry. Representative data of a typical invasion experiment, examined with an Olympus 1X81 motorized fluorescent microscope. The images acquired show brightfield, DAPI and TRITC (red) colour channels (**Fig 7.11 F**). Together, these data show that in addition to TGF-β reported previously, *T. cruzi* induction of PMVs from the host cell is a vital mechanism required for entry.

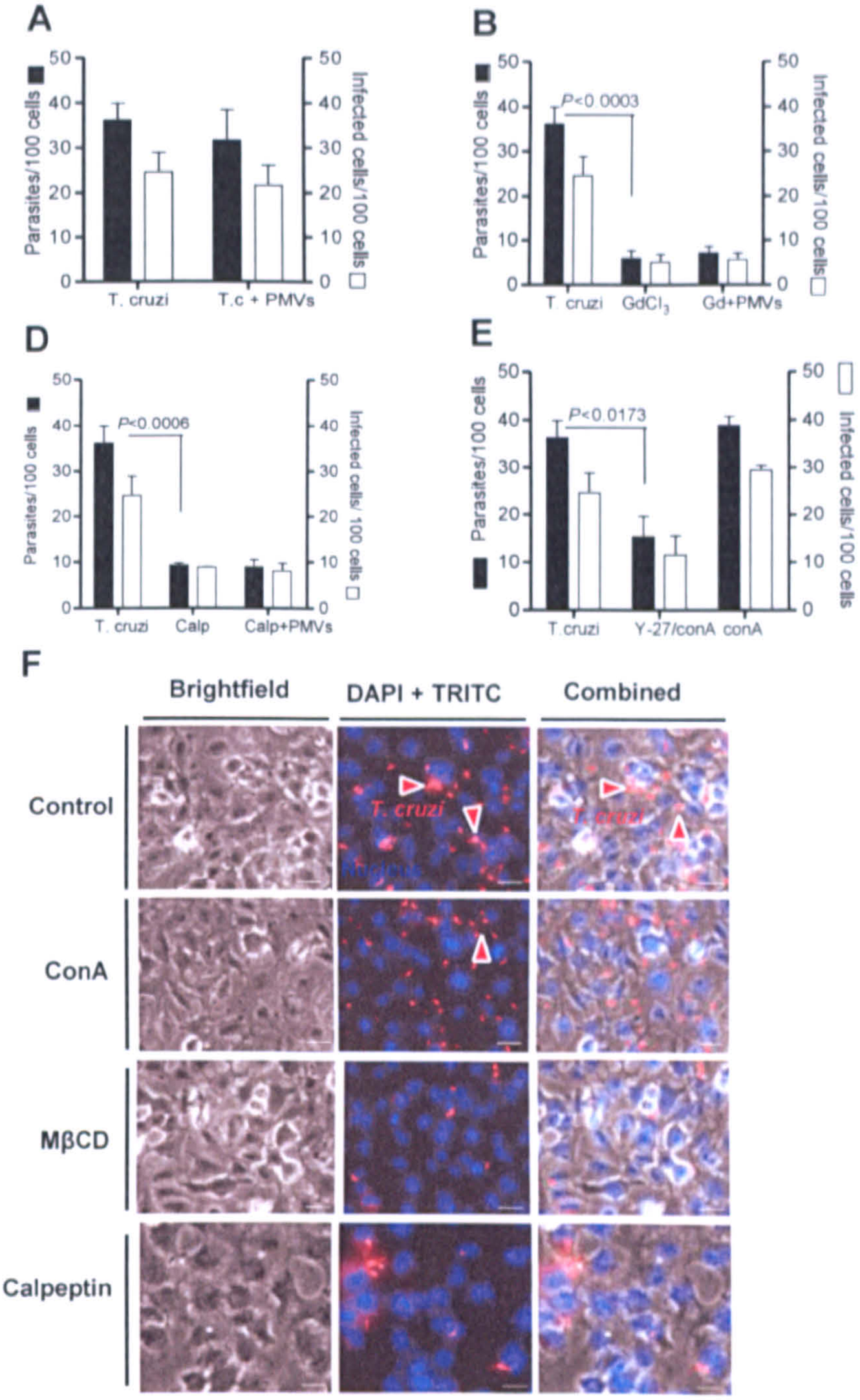

Figure 7.11 *T. cruzi* induction of PMVs is vital for entry into cells

(A) Addition of HeLa cell-derived PMVs ($1x10^6$/well) fails to enhance *T. cruzi* invasion of HeLa cells, compared to cells infected with parasites only. (B) Pretreatment (37°C for 30 min) with $GdCl_3$, (Gd, 200 μM) reduces the invasion of parasites, but addition of PMVs to cells pretreated with the agent fails to enhance infection. Similarly Y-27632, Y-27, 10 μM (C) and calpeptin, calp, 20 μM (D) treatments inhibit *T. cruzi* entry, but the addition of PMVs fails to reverse their effects. (E) Concomitant treatment with Y-27632 and conA reduces entry of parasites into cells, However, *T. cruzi* entry into HeLa cells continues unabated in the presence of conA only treatment. (F) Representative fluorescence images of *T. cruzi* invasion. HeLa cells were infected with *T. cruzi* metacyclic trypomastigotes in the presence or absence of inhibitors of PMV release and lysosomal exocytosis. Parasites are labelled with 4 μM pKH26 (red) and DAPI stained kinetoplast in blue. Scale bar = 100 μm. Values represent the mean ± SD of two independent experiments performed in duplicate. ***$P<$ 0.001, **$P<$ 0.01, *$P<$ 0.05 were considered to be statistically significant.

7.4.6 Correlation analysis

With so many reports suggesting that lysosomal exocytosis is a requirement for *T. cruzi* entry into mammalian cells, it was decided to graphically correlate all the findings discussed here for better comparison. How the release of PMVs affects the integrity of the host plasma membrane (PM) was compared. We noticed that PM integrity (measured by PI exclusion) is greatest when fewer PMVs are released. As PMV release increases, more PI is incorporated and host PM integrity is compromised (**Fig. 7.12 A**). A direct correlation was observed between the release of PMVs and the recruitment of lysosomes. Thus, when cells release fewer PMVs, only small numbers of lysosomes are recruited and as the release of PMVs increases to a maximum, exocytosis of lysosomes follow a similar trend (**Fig. 7.12 B**).

The release of PMVs directly corresponds with parasite invasion of mammalian cells, thus, further confirming that these two processes (PMV release and invasion) might be occurring concomitantly (**Fig 7.12 C**). Since the release of PMVs induced by parasites is a form of damage to the host plasma membrane, lysosomes would be recruited to reseal the membrane. However, sensing injury to the host plasma membrane, parasites exploit the resultant damage for entry before lysosomal resealing is complete. Probably, the ability of *T. cruzi* to fuse and reside in acidic lysosomes to form the parasitophorous vacuole (a characteristic peculiar only to this pathogen), was adopted through evolution, possibly, because the parasite constantly coincided with activated lysosomes during its exploitation of host plasma membrane damage for entry. A comparison of how PM integrity affects *T. cruzi*

invasion gave a negative correlation. This data showed that *T. cruzi* invasion was highest when host PM integrity was at its weakest. However, as PM integrity increases, host cytoskeleton becomes more intact and parasite entry is significantly reduced (**Fig. 7.12 D**).

Interestingly and as suggested by earlier findings, lysosomal exocytosis is not directly correlated to *T. cruzi* invasion. In this study, an increase in lysosomal exocytosis did not always enhance *T. cruzi* invasion into cells (**Fig. 7.12 E**). Moreover, an increase of lysosomal exocytosis inversely correlated with host cell PM integrity. Less damage to the PM integrity required recruitment of fewer lysosomes, whilst, more lysosomes are recruited when PM integrity is severely compromised (**Fig. 7.12 F**).

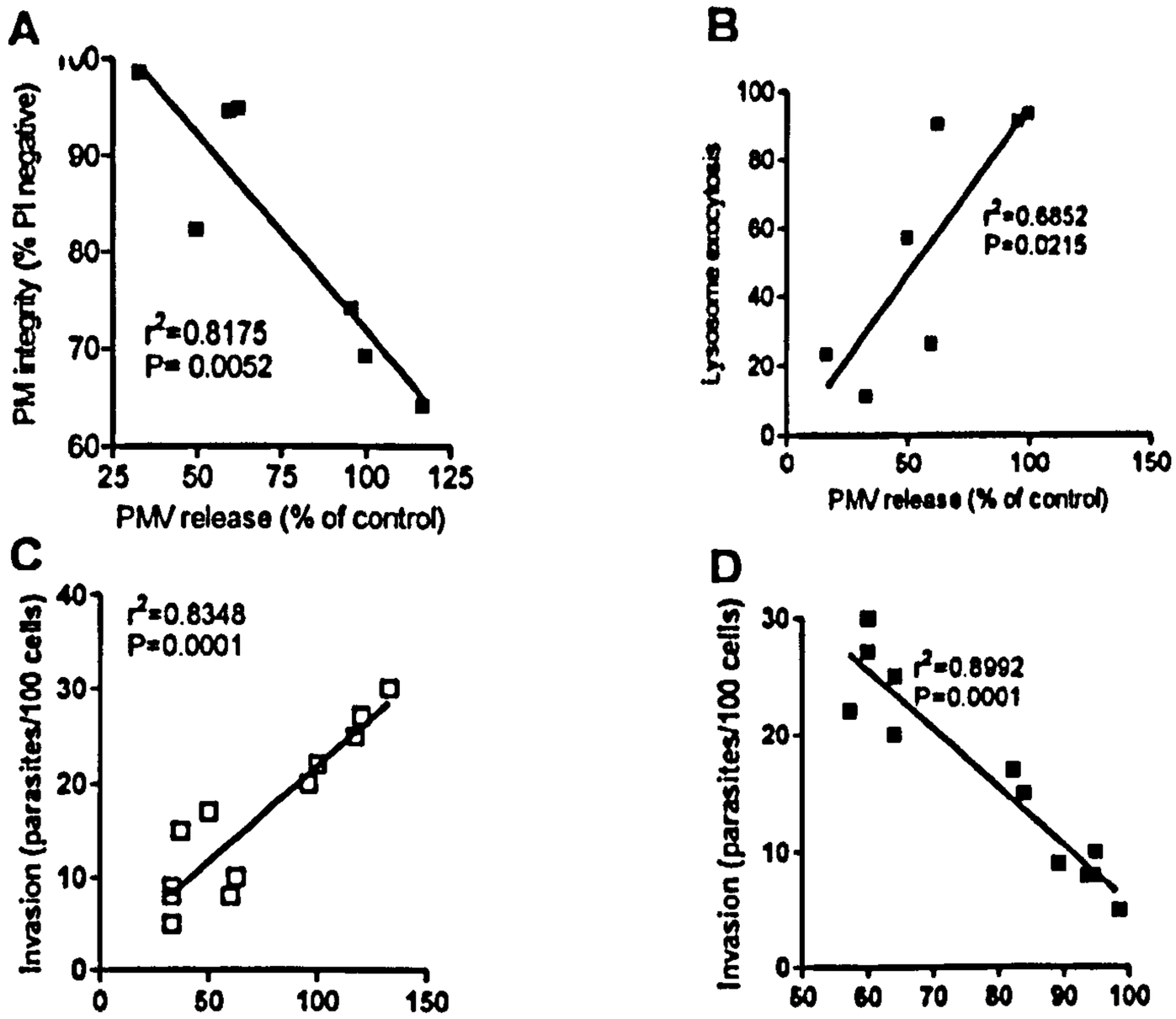

Figure 7.12 Correlation graphs comparing the relationship between PMV release, lysosomal exocytosis and invasion

(A) The release of PMVs induced by parasites negatively correlates with PM integrity. Host cell PM integrity is most intact when PMVs release is low. (B) The release of PMVs is directly proportional to lysosomal exocytosis. This means more lysosomes are recruited to the surface for repair, as cells endure more damage due to the release of PMVs. (C) Likewise the release of PMVs positively correlates with *T. cruzi* invasion. More parasites gain entry as host cell release of PMVs is augmented. (D) By contrast, PM integrity is inversely proportional to *T. cruzi* invasion. Simply, more parasites gain entry when host cell PM integrity is severely damaged. (E) Lysosomal exocytosis does not correlate with *T. cruzi* invasion. (F) More lysosomes are recruited when the host PM integrity is severely damaged. In contrast, fewer lysosomes are activated when PM integrity is relative intact.

7.5 Proposed model for *T. cruzi* entry into cells

The findings discussed here suggest that the release of PMVs represent another entry mechanism employed by *T. cruzi* during invasion. A model is therefore proposed where invasion involves parasite induction of PMVs from host cells (**Fig. 7.13**). When *T. cruzi* initially contacts mammalian cells, it elicits siganls through integrins, lipid raft domains or calcium channels, which results in the release of PMVs. Detachment of PMVs from the parent cell results in a breach of PM integrity and subsequent influx of Ca^{2+}. Calcium influx activates exocytosis of lysosomes to the site of damage, but *T. cruzi* concomitantly exploits the resultant damage before lysosomal repair can be instigated.

Activated lysosomes then fuse with *T. cruzi* to form the parasitophorous vacuole. Invaded parasites take residence within the vacuole and use the acidic environment to initiate their differentiation from metacyclics trypomastigotes into amastigotes. Parasites use a protein, Tc Tox, to break out of the vacuole and complete their differentiation into amastigotes in the cytoplasm [375]. Amastigotes replicate by binary division and after multiple replications, differentiate back into trypomastigotes and break out to infect other cells or are taken into the gut of biting insects.

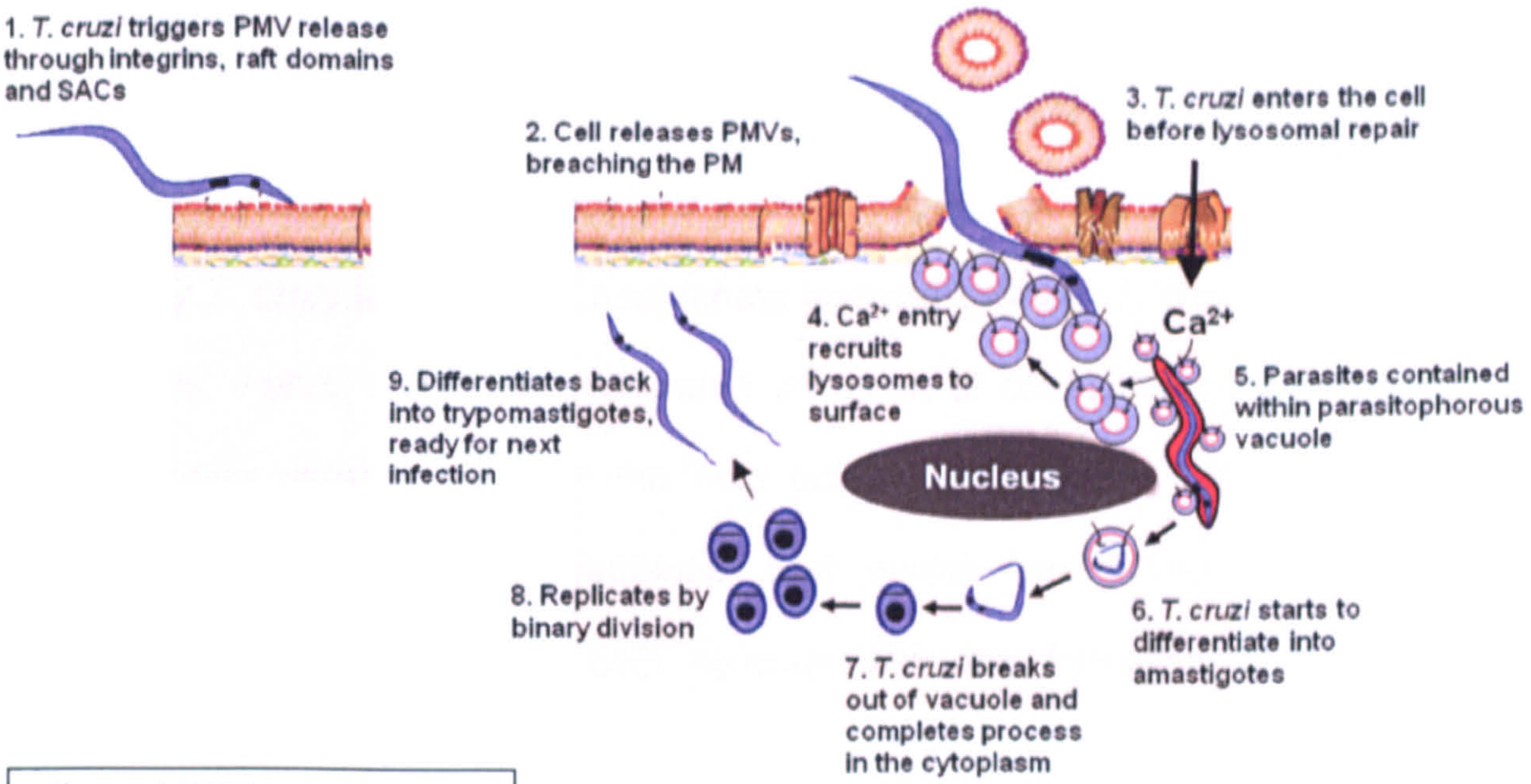

Figure 7.13 The PMV release mechanism of *T. cruzi* cell invasion

A resting cell releases PMVs resulting in a plasma membrane breach, after contact with *T. cruzi* through activation of calcium channels, integrins or lipid raft domains. Parasite entry occurs concomitantly with lysosomal exocytosis activated by Ca^{2+} influx. *T. cruzi* fuses with the parasitophorous vacuole and starts to differentiate into amastigotes, but it breaks out into the cytoplasm where it completes the process. After completing its differentiation into amastigotes, *T. cruzi* replicates by binary division and breaks out of the host cell after multiple replications. For ease of clarity, parasites are not drawn to scale.

7.6 Discussion

The role of PMVs in *T. cruzi* invasion of mammalian cells is currently unknown. Nonetheless, we recently reported a novel mechanism involving PMVs that is utilised by *T. cruzi* to evade the host innate immune system. *T. cruzi* induces from blood cells, PMVs, which are involved in inhibition of complement-mediated lysis and in aiding parasite invasion into host cells (Cestari et al. 2010- submitted). Infective *T. cruzi* metacyclic trypomastigotes exploit two distinct strategies for entering into host cells, and both coincide with the formation of a nascent parasitophorous vacuole in which the parasite transiently resides [312]. The first mechanism of invasion, described over a decade ago, involves exocytosis and fusion of lysosomes with the plasma membrane at the parasite attachment site [309]. A second mechanism, recently described, involves invagination of host plasma membrane and formation of a lysosome independent vacuole. This vacuole initially contains plasma membrane markers, but undergoes a late maturation process by fusing with recruited lysosomes [376].

In the present study, a novel mechanism is described, independent of lysosomes, which involves the early release of PMVs from host cells induced by *T. cruzi* during invasion. However, just like the mechanisms previously described, retention of the parasite and establishment of infection still requires activation and fusion of lysosomes to form the parasitophorous vacuole. It is shown that *T. cruzi* could induce the release of PMVs from several cell types *in vitro*, which carry various cytokines, chemokines and acute phase proteins. The expression levels of these cytokines varied according to whether cells were stimulated with other pathogens such as bacteria or whether, if left unstimulated, there was no expression. Levels of

cytokines such as IL-12 and IL-13 were previously reported to increase during *T. cruzi* invasion of mammalian cells [377;378]. Cytokines and acute phase proteins such as RANTES, MIF, IL-16 and Serpin E1 are also secreted during *T. cruzi* invasion of mammalian cells [379;380].

In addition, it is reported here that the intracellular pathogen *S. typhimurium* (wild-type) can also induce the release of PMVs. In contrast, *Giardia Intestinalis*, a flagellated, unicellular, extracellular pathogen, failed to stimulate the release of PMVs either from THP-1 or HeLa cells. However, *G. intestinalis*, itself released PMVs when stimulated with sublytic complement in a dose-dependent response and these vesicles were positive for exposure of phosphatidylserine after staining with annexin V-FITC. Moreover, the PMVs released after induction with *T. cruzi* was dose-dependent. By contrast non-intracellular pathogens such as *T. brucei* and a mutant *S. typhi* (strain SPI1) failed to induce host cells to release PMVs. Furthermore, results presented here have shown that *T. cruzi* epimastigote (non-invasive insect-dwelling stage) does not induce the release of PMVs. Although, they have been shown to play vital roles in cell-to-cell communication, export pathways and intercellular transfer of receptors, it is still unknown why cells release PMVs. It is possible they function during host immune defense as a signal for danger or a messenger activating the immune system, or as mentioned above, as inhibitors of *T. cruzi* complement-mediated lysis, whilst aiding entry of the parasite into cells.

This study showed that *T. cruzi* induction of PMVs is dependent on activation of integrin receptors, lipid raft microdomains and L-type calcium channels as blocking these receptors/domains with agents (RGD, MβCD, verapamil and nifedipine),

respectively abrogated release of the vesicles. It is also shown for the first time that stretch-activated calcium channels are involved in the release of PMVs.

Furthermore, blocking activation of these receptors/domains and thus, inhibiting the release of PMVs reduced *T. cruzi* entry into cells. Others have previously shown that inhibitors, which block activation of L-type calcium channels, integrins or lipid rafts, also reduce *T. cruzi* invasion into cells. The results of the present study are in agreement, but go on to show that in addition, SACs and PI 3-Kinases also participate in the release of PMVs and their abrogation reduces parasite invasion. Interestingly, blocking activation of these receptors failed to inhibit release of PMVs after stimulating cells with sublytic complement. Data presented also showed that PMV release is inhibited by wortmannin, a phosphatidyl-inositol$_3$ kinase inhibitor. Together, these show that PMV release is dependent on Ca^{2+}, and since their release can be inhibited by integrin, PI 3-Kinase and lipid raft inhibitors indicates that cell signalling pathways are involved in the processes leading to Ca^{2+} mobilisation from intracellular compartments.

It is well documented that plasma membrane damage caused by stress factors or by pore-forming complexes, can be rapidly resealed by lysosomes, which fuse together and patch-up the breakage [189;381]. The present study also showed that the release of PMVs induced by *T. cruzi* metacyclic forms resulted in damage to the host cell plasma membrane. This leads to a rise in cytosolic Ca^{2+} and subsequently activates the exocytosis of lysosomes to the site of damage. Rapid repair of the damage is necessary to prevent loss of internal contents and cell death.

After stimulating cells with *T. cruzi*, higher numbers of PMVs were detected and in the absence of inhibitors, increased fluorescence of the lysosome-specific marker, LAMP-1 was detected. An increase in LAMP-1 fluorescence indicates activation of lysosomal repair. As aforementioned, release of PMVs induced by parasites caused damage to the integrity of the host cell plasma membrane. If so then preventing release of PMVs should mean less damage to the plasma membrane and so LAMP-1 fluorescence should not increase. Indeed, cells treated with calpeptin failed to release PMVs after *T. cruzi* induction, and also reduced LAMP-1 fluorescence was detected. HeLa cells treated with conA also resulted in a reduction of LAMP-1 fluorescence, thus, indicating that lysosomal exocytosis was inhibited. Interestingly, *T. cruzi*-elicited PMV release continued unabated, implying that conA specifically abrogates lysosomal exocytosis as previously shown [369].

Invasion assays confirmed that conA does not affect PMV release since the number of invading parasites was similar or slightly higher when compared to untreated cells (control). However, long-term (RT for 30 min) treatment of the cells with conA resulted in loss of host cell cytoplasm and prevention of *T. cruzi* entry. By contrast, parasite invasion was significantly reduced in cells treated with calpeptin. This data further confirmed that the release of PMVs compromised host plasma membrane integrity, which *T. cruzi* exploits to enter cells. Hence, the absence of PMV release meant no damage was sustained by the host plasma membrane for exploitation by *T. cruzi*. It also affirms that *T. cruzi* invasion due to the loss of plasma membrane integrity is via a mechanism independent of lysosomal exocytosis as parasites still invaded even after blocking with conA. This implies that *T. cruzi* requirement of host cell PMV release for entry is more important than lysosomal recruitment. Others

have confirmed this and have speculated that Ca^{2+}-triggered cytoskeleton rearrangement (i.e. release of PMVs) induced by *T. cruzi* is a requirement for lysosome exocytosis [308;371]. However, recruitment and fusion of lysosomes during *T. cruzi* invasion to form the parasitophorous vacuole is important for parasite retention in the host in order to establish a successful infection [308].

Flow cytometry analysis summarised on figure 7.10, showed that the release of PMVs induced by parasites resulted in the recruitment of lysosomes, which repair the resultant damage and so less PI was incorporated. Furthermore, when PMV release was inhibited through the actions of $GdCl_3$, calpeptin, wortmannin and RGD, PI uptake was also less. However, this was not a result of damage repair, but the lack of damage due to abrogation of PMV release from host cells. It is noteworthy that parasite entry was unabated in the presence of conA, which unlike calpeptin and $GdCl_3$ does not inhibit PMV release. The procession of *T. cruzi* entry in the presence of conA, although lysosomal exocytosis was abolished (see also PI uptake on figure 7.10) confirms that parasite entry is not dependent on lysosomes. It is now known that the release of PMVs induced by *T. cruzi* results in loss of host cell integrity, and that without rapid repair by lysosomes, this causes complete membrane breakdown.

Although, the mechanism of invasion described here is independent of lysosomal exocytosis, host cell entry by *T. cruzi* metacyclic trypomastigotes is accomplished by exploiting a cellular wound repair mechanism involving Ca^{2+} regulated exocytosis of lysosomes [312]. This data is in agreement with an earlier report, which showed that

lysosomal exocytosis is not required for *T. cruzi* invasion, but for retaining the parasite inside the host in order to establish complete infection [308].

Finally, a model was proposed based on the data obtained from this study. Release of PMVs triggered by Ca^{2+} influx and induced by *T. cruzi* results in a breach of host cell plasma membrane integrity. Lysosomal exocytosis is activated by Ca^{2+} influx to the site of damage for repair. However, this occurs concomitantly with *T. cruzi* entry as parasites seek to take advantage of the resultant membrane breakage before the mandatory lysosomal repair.

8. General Discussion

8.1 PMVs: Isolation and characterisation

The process of microvesiculation by several cell types has been implicated in a wide range of biological activities, in both *in vitro* and *in vivo* studies [14]. The most characterised function is that of intercellular communication, reported for all isolated PMVs. In this thesis, PMVs and exosomes were isolated by methods developed within CMIRC, including filtration, water-sonication and differential centrifugation. Purified microvesicles were then characterised by flow cytometry and electron microscopy to confirm correct isolation. Released PMVs are shown to carry a range of cytokines, chemokines and acute phase proteins, which are both intravesicular and extravesicular. Cytokines present in each vesicle were identified using the human cytokine array kit and quantified by ELISA.

PMVs are released constitutively by cells in culture or from cells activated with various stimuli [382]. Several cell types released PMVs when induced with NHS. At the advent of microvesicle research, it was shown that erythrocytes escape from complement destruction by shedding PMVs in the presence of NHS [383]. Others followed up with work, which showed that insertion of C5b-9 caused release of PMVs from endothelial cells, PMN and platelets [27;121;236]. Here, the use of a C9-depleted human serum failed to induce the release of PMVs from THP-1 cells. Isolated PMVs were stained with annexin V-FITC to determine surface PS exposure and found to be 54% positive. The mechanisms leading to the release of PMVs require an increase in cytosolic Ca^{2+}, which in turn activates the enzyme, calpain, involved in detachment of vesicles from the parent cell [384]. Inhibition of PMV release with EGTA confirmed the involvement of calcium in the process. Likewise, the specific calpain inhibitor, calpeptin completely abrogated the release of PMVs

after stimulation of cells with either NHS or *T. cruzi* metacyclic trypomastigotes. In agreement with previous reports, the Rho-kinase inhibitor, Y-27632 also inhibited release of PMVs, thus confirming that the release of PMVs could sometimes be elicited during the process of apoptosis, although the two mechanisms (PMV release and apoptosis) are independently activated.

By contrast to non-induced THP-1 cells, which had a smooth surface membrane, activated cells displayed increased disturbance on the PM and the release of PMVs as observed by electron microscopy. In addition to PMVs, cells also released exosomes when MVBs fused with the plasma membrane [385]. Water-sonication of cell-free supernatants for 5 x 1 min prior to centrifugation separated aggregated exosomes and improved isolation of the two vesicle types with minimal contamination. Having devised a method for effective isolation of PMVs and exosomes, their dot plot distributions on the flow cytometer were compared and found to differ. Unlike PMVs which were heterogeneous, the distribution of exosomes was more homogeneous and clustered. This study is the first to identify the dot plot distribution of exosomes on the flow cytometer. Furthermore, PMVs and exosomes were found to carry similar proteins from the parental cell, although PMVs sometimes carried higher amounts of certain cytokines. For example, PMVs from THP-1 cells carried higher amounts of TGF-β1 and MIF than exosomes, but no difference was detected between levels of FGF-1 and Gal-3 in the two vesicle types.

8.2 PMVs: role of myeloid cell differentiation

The next investigations focused on the hypothesis that PMVs play significant roles during the differentiation of monocytes into macrophages. It was previously shown

that recombinant TGF-β1 could promote the differentiation of human promonocytic leukaemia cells into macrophages [280]. TGF-β1 has pleiotrophic functions including elevation in expression of several extracellular matrix components, such as fibronectin, proteoglycans and several types of collagen. In addition to these, many cells are also induced to up-regulate the expression of integrins or cell adhesion molecules [261]. Thus, a net increase in the extracellular matrix and cells' ability to adhere more effectively are due to TGF-β1. Transforming growth factor-β1 has been shown to prevent myogenesis, haematopoiesis and to prevent adipocyte differentiation, while promoting the differentiation of intestinal epithelial cells [262-265]. Overall TGF-β1 plays a role in many physiological processes, such as proliferation, differentiation, migration and cell survival, which affect many biological processes, including wound healing, development, carcinogenesis and immune responses [256;260;266]. In the last decade, numerous roles for PMVs have been reported *in vitro* and *in vivo*, and investigations to identify new functions are still ongoing.

The present study showed for the first time that PMVs carry TGF-β1 on their membrane surface, and that this surface-bound TGF-β1 can halt the proliferation of acute myelocytic cells without inducing apoptosis. In addition, a dramatic change in the morphology of PMV-treated cells was observed. The cells became increasingly irregular in shape and had membrane extensions that resembled pseudopodia. Further examinations revealed that cells, which attached to the culture plates after treatment with PMVs, also expressed typical markers of macrophages. These cells expressed significantly higher levels of CD14 and CD11b, but not the dendritic cell specific marker DC-SIGN [295]. Data obtained also showed that PMVs isolated from cells, which carry higher levels of TGF-β1 (≥ 200 pg TGF-β1/10^5 PMVs), caused

significantly greater reductions in the growth rate of THP-1 cells, as compared to PMVs from cells that expressed lower levels (~30 pg TGF-β1/10^5 PMVs).

8.2.1 PMV release: a possible secretory pathway

This study also confirmed the presence within PMVs of non-conventionally secreted proteins released into culture supernatants. Hitherto, MIF, FGF-1 and Gal-3 were confirmed within PMVs and like TGF-β1, these leaderless cytokines play essential roles in myeloid differentiation [2;272]. Significant levels of such cytokines lacking signal peptides may be carried within PMVs and these are not always detected in culture supernatants. Here, marked levels of MIF were measured in lysed PMVs, compared to PMV-depleted supernatant. Whilst intravesicular cytokines and other proteins such as caspases [287] can be delivered to, and cause effects in recipient cells, this has not been shown for a surface-bound cytokine, as described herein, for TGF-β1.

8.2.2 Agents used in the treatment of AML, also induce the release of PMVs

The present study also highlighted that PMA, histamine and ATRA, currently used in differentiation therapy for treatment of AML can stimulate release of PMVs. THP-1 cells treated with these agonists exited the cell cycle at G_0/G_1, and so stopped proliferating. Morphological changes similar to those noted with PMVs were observed in cells treated with such agonists. Others have shown PMA and ATRA to halt proliferation of myeloid cells and induce their differentiation [222,386]. This study is in agreement and speculates that the agonists mentioned here, may be inducing release of PMVs, which carry higher levels of the cytokines involved in myeloid

differentiation. Thus, it might be useful to look at other PMV-releasing agents as potential alternative drugs in differentiation therapy for treatment of AML.

8.3 Role of PMVs in pathogen invasion

In the past decade, studies on PMVs and their physiological functions have increased exponentially. Documented roles include receptor transfer, protein secretory routes and escape from death [132;292]. Simply put, PMV numbers are elevated in diseased states [291;320], a hint perhaps on the pathological importance of these vesicles. Surprisingly, the importance of PMVs has scarcely been associated with pathogenic infections, except for HIV which was reported to infect *CXCR5*$^{-/-}$ cells by transfer of the receptor from *CXCR5*$^{+/+}$ cells through microvesicles. Here, I also show that the addition of THP-1, Jurkat and to lesser extent HepG2 cell-derived PMVs could bind to the surface of *T. cruzi* metacyclic trypomastigotes and confer parasite protection against complement-mediated lysis so aiding parasite evasion of the host innate immune system. These vesicles also carried TGF-β1, which enhanced parasite invasion of Vero cells. Data obtained showed that PMVs from cells, which expressed higher levels of TGF-β1, correlates respectively with the level of invasion. This increased invasion was inhibited in the presence of the TGF-β receptor antagonist, SB-431542 and anti-TGF-β antibody.

8.3.1 *T. cruzi*-elicited signals lead to PMV release and invasion

Previous work reported that activation of calcium channels by pathogens increased cytosolic Ca^{2+}. Data presented in this study is in agreement, but shows further that this increased cytosolic Ca^{2+} resulted in the release of PMVs [227;328]. Inhibition of

these channels reduced invasion and replication of intracellular pathogens, such as, *T. gondii* and *T. cruzi*. Rearrangement of the cytoskeleton allows membrane ruffling and release of PMVs, and some bacteria utilised this process for their uptake into host cells [332]. In this study *S. typhi* SP-344 (wild-type) induced PMV release from HeLa cells, but not the SPI1 strain (mutant non-invasive form). This is in agreement with a report, which showed that wild-type *S. typhi* caused an increase in cytosolic Ca^{2+}, rearrangement of cytoskeleton and membrane ruffling, but not the mutant form [184].

Also, *T. cruzi* induced the release of PMVs from HeLa cells, but *T. brucei*, a non-intracellular pathogen failed to stimulate vesicle release. Use of MβCD, RGD peptide and wortmannin showed that induction of PMVs by *T. cruzi* was through activation of several receptors/domains, including lipid raft microdomains, integrins and PI 3-Kinase, all of which leads to an increase in cytosolic Ca^{2+}. Others confirmed this by showing that depletion of host membrane cholesterol with MβCD abolished the entry of *Mycobacteria* spp into cells [338,339]. Moreover, integrins have been reported as cellular routes of invasion for some bacterial pathogens [354]. Parasite activation of integrin signalling pathways was shown to interact with membrane raft domains, resulting in increased cytosolic Ca^{2+} [350]. In addition, PI 3-Kinase has been associated with *T. cruzi* entry into mammalian cells [376;387].

8.3.2 PMV release leads to activation of lysosomal exocytosis

Several reports have described the mechanisms by which eukaryotic cells repair PM damage following injury. Membrane repair/resealing is activated by influx of Ca^{2+}

through damage sites, which activates migration of specific organelles, including lysosomes to the site of damage [361;381]. The release of PMVs causes damage to the host plasma membrane, which *T. cruzi* exploits for entry before lysosomal repair. Abrogation of PMV release rendered parasites unable to invade. In agreement with others, data presented shows that *T. cruzi* entry into mammalian cells is independent of lysosomes. This is contrary to an earlier report, which proposed that *T. cruzi* entry requires recruitment of lysosomes to the plasma membrane [309]. However, it confirms that fusion of the parasite with lysosomes to form the parasitophorous vacuole is pertinent for the successful establishment of infection. This also agrees with work, which showed that abrogation of lysosomal exocytosis, although it did not reduce *T. cruzi* entry, abolished infection due to absence of the PPV, which is required for the retention of parasites and their subsequent differentiation into amastigotes [308;388]. It is therefore proposed that the release of PMVs from host plasma membrane is a mechanism, which must occur in order for *T. cruzi* to enter mammalian cells. A model is therefore described where the active movement and the application of force exerted by *T. cruzi* to gain entry into cells, causes activation of SAC, which allows the influx of calcium. This increased cytosolic Ca^{2+} causes cytoskeleton rearrangement that leds to the release of PMVs.

The mechanisms mentioned here are by no means the only routes employed by *T. cruzi* for entry into mammalian cells. *T. cruzi* entry into host cells is a complex process involving several factors. Other mechanisms described by others, include *T. cruzi* interaction with TGF-β receptors on the surface of host cells [310;311;389].

8.4 Summary and Concluding Remarks

In conclusion PMVs are now widely accepted as biological entities with vast physiological functions. They have been described in diseases including diabetes mellitus, rheumatoid arthritis, sickle cell anaemia, thrombosis, cancers and in angiogenesis. In addition, the role of PMVs in receptor transfer inspired studies on host cell invasion by such infectious agents as HIV and prions. This thesis provides further evidence to support PMVs as biological materials. Procedures for isolation of microvesicles (PMVs and exosomes) have been enhanced to minimise contamination with either vesicle type.

It also reports the possible involvement of PMVs in the differentiation of monocytes into macrophages during infection, and showed that current differentiation therapy agents used in the treatment of AML, stimulated release of PMVs. These PMVs carry on their membrane surface TGF-β1, and halted the proliferation of acute monocytic leukaemic cells, THP-1, and induced their terminal differentiation into macrophages. Furthermore, this work identified an invasion strategy employed by *T. cruzi* to enter mammalian cells. Released PMVs interact and bind to the surface of *T.cruzi* and prevent its complement-mediated lysis by inhibiting cleavage of the C3 convertase. After evading the innate immune system, *T. cruzi* induces the release of PMVs, which compromise the integrity of the host cell membrane. Parasites then exploit the resulting damage for entry before lysosomal repair.

References

References

1. Hugel B, Martinez MC, Kunzelmann C, Freyssinet JM. Membrane microparticles: two sides of the coin. Physiology.(Bethesda.) 2005;20:22-27.

2. Martinez MC, Tesse A, Zobairi F, Andriantsitohaina R. Shed membrane microparticles from circulating and vascular cells in regulating vascular function. Am.J.Physiol Heart Circ.Physiol 2005;288:H1004-H1009.

3. Ratajczak J, Wysoczynski M, Hayek F, Janowska-Wieczorek A, Ratajczak MZ. Membrane-derived microvesicles: important and underappreciated mediators of cell-to-cell communication. Leukemia 2006;20:1487-1495.

4. Martinez MC, Larbret F, Zobairi F et al. Transfer of differentiation signal by membrane microvesicles harboring hedgehog morphogens. Blood 2006;108:3012-3020.

5. Ratajczak J, Miekus K, Kucia M et al. Embryonic stem cell-derived microvesicles reprogram hematopoietic progenitors: evidence for horizontal transfer of mRNA and protein delivery. Leukemia 2006;20:847-856.

6. Baj-Krzyworzeka M, Szatanek R, Weglarczyk K et al. Tumour-derived microvesicles carry several surface determinants and mRNA of tumour cells and transfer some of these determinants to monocytes. Cancer Immunol.Immunother. 2006;55:808-818.

7. Pelchen-Matthews A, Raposo G, Marsh M. Endosomes, exosomes and Trojan viruses. Trends Microbiol. 2004;12:310-316.

8. Robertson C, Booth SA, Beniac DR et al. Cellular prion protein is released on exosomes from activated platelets. Blood 2006;107:3907-3911.

9. Bess JW, Jr., Gorelick RJ, Bosche WJ, Henderson LE, Arthur LO. Microvesicles are a source of contaminating cellular proteins found in purified HIV-1 preparations. Virology 1997;230:134-144.

10. Spees JL, Olson SD, Whitney MJ, Prockop DJ. Mitochondrial transfer between cells can rescue aerobic respiration. Proc.Natl.Acad.Sci.U.S.A 2006;103:1283-1288.

11. George JN, Thoi LL, McManus LM, Reimann TA. Isolation of human platelet membrane microparticles from plasma and serum. Blood 1982;60:834-840.

12. Greco V, Hannus M, Eaton S. Argosomes: a potential vehicle for the spread of morphogens through epithelia. Cell 2001;106:633-645.

13. Hess C, Sadallah S, Hefti A, Landmann R, Schifferli JA. Ectosomes released by human neutrophils are specialized functional units. J.Immunol. 1999;163:4564-4573.

14. Piccin A, Murphy WG, Smith OP. Circulating microparticles: pathophysiology and clinical implications. Blood Rev. 2007;21:157-171.

15. Distler JH, Pisetsky DS, Huber LC et al. Microparticles as regulators of inflammation: novel players of cellular crosstalk in the rheumatic diseases. Arthritis Rheum. 2005;52:3337-3348.

16. Scholz T, Temmler U, Krause S, Heptinstall S, Losche W. Transfer of tissue factor from platelets to monocytes: role of platelet-derived microvesicles and CD62P. Thromb.Haemost. 2002;88:1033-1038.

17. Satta N, Toti F, Feugeas O et al. Monocyte vesiculation is a possible mechanism for dissemination of membrane-associated procoagulant activities and adhesion molecules after stimulation by lipopolysaccharide. J.Immunol. 1994;153:3245-3255.

18. Combes V, Simon AC, Grau GE et al. In vitro generation of endothelial microparticles and possible prothrombotic activity in patients with lupus anticoagulant. J.Clin.Invest 1999;104:93-102.

19. Sadallah S, Eken C, Schifferli JA. Erythrocyte-derived ectosomes have immunosuppressive properties. J.Leukoc.Biol. 2008;84:1316-1325.

20. Gasser O, Hess C, Miot S et al. Characterisation and properties of ectosomes released by human polymorphonuclear neutrophils. Exp.Cell Res. 2003;285:243-257.

21. Pap E, Pallinger E, Pasztoi M, Falus A. Highlights of a new type of intercellular communication: microvesicle-based information transfer. Inflamm.Res. 2009;58:1-8.

22. Aoki N, Yokoyama R, Asai N et al. Adipocyte-Derived Microvesicles Are Associated with Multiple Angiogenic Factors and Induce Angiogenesis in Vivo and in Vitro. Endocrinology 2010

23. Chargaff E, West R. The biological significance of the thromboplastic protein of blood. J.Biol.Chem. 1946;166:189-197.

24. Wolf P. The nature and significance of platelet products in human plasma. Br.J.Haematol. 1967;13:269-288.

25. Horstman LL, Ahn YS. Platelet microparticles: a wide-angle perspective. Crit Rev.Oncol.Hematol. 1999;30:111-142.

26. Simak J, Holada K, Vostal JG. Release of annexin V-binding membrane microparticles from cultured human umbilical vein endothelial cells after treatment with camptothecin. BMC.Cell Biol. 2002;3:11.

27. Hamilton KK, Hattori R, Esmon CT, Sims PJ. Complement proteins C5b-9 induce vesiculation of the endothelial plasma membrane and expose catalytic surface for assembly of the prothrombinase enzyme complex. J.Biol.Chem. 1990;265:3809-3814.

28. Qu J, Adam J, Bloxham DM et al. Phosphatidylserine-dependent adhesion of T cells to endothelial cells. Biochim.Biophys.Acta 2000;1501:99-115.

29. Zwaal RF, Schroit AJ. Pathophysiologic implications of membrane phospholipid asymmetry in blood cells. Blood 1997;89:1121-1132.

30. Bevers EM, Comfurius P, van Rijn JL, Hemker HC, Zwaal RF. Generation of prothrombin-converting activity and the exposure of phosphatidylserine at the outer surface of platelets. Eur.J.Biochem. 1982;122:429-436.

31. Zwaal RF, Bevers EM. Platelet phospholipid asymmetry and its significance in hemostasis. Subcell.Biochem. 1983;9:299-334.

32. Khandelwal S, Saxena RK. A role of phosphatidylserine externalization in clearance of erythrocytes exposed to stress but not in eliminating aging populations of erythrocyte in mice. Exp.Gerontol. 2008;43:764-770.

33. Borisenko GG, Matsura T, Liu SX et al. Macrophage recognition of externalized phosphatidylserine and phagocytosis of apoptotic Jurkat cells--existence of a threshold. Arch.Biochem.Biophys. 2003;413:41-52.

34. Fox JE, Austin CD, Boyles JK, Steffen PK. Role of the membrane skeleton in preventing the shedding of procoagulant-rich microvesicles from the platelet plasma membrane. J.Cell Biol. 1990;111:483-493.

35. Diaz C, Schroit AJ. Role of translocases in the generation of phosphatidylserine asymmetry. J.Membr.Biol. 1996;151:1-9.

36. Connor J, Pak CH, Zwaal RF, Schroit AJ. Bidirectional transbilayer movement of phospholipid analogs in human red blood cells. Evidence for an ATP-dependent and protein-mediated process. J.Biol.Chem. 1992;267:19412-19417.

37. McLaughlin PJ, Gooch JT, Mannherz HG, Weeds AG. Structure of gelsolin segment 1-actin complex and the mechanism of filament severing. Nature 1993;364:685-692.

38. Seigneuret M, Devaux PF. ATP-dependent asymmetric distribution of spin-labeled phospholipids in the erythrocyte membrane: relation to shape changes. Proc.Natl.Acad.Sci.U.S.A 1984;81:3751-3755.

39. Williamson P, Bevers EM, Smeets EF et al. Continuous analysis of the mechanism of activated transbilayer lipid movement in platelets. Biochemistry 1995;34:10448-10455.

40. Zwaal RF, Comfurius P, Bevers EM. Mechanism and function of changes in membrane-phospholipid asymmetry in platelets and erythrocytes. Biochem.Soc.Trans. 1993;21:248-253.

41. Weiss HJ, Vicic WJ, Lages BA, Rogers J. Isolated deficiency of platelet procoagulant activity. Am.J.Med. 1979;67:206-213.

42. Zwaal RF, Comfurius P, Bevers EM. Scott syndrome, a bleeding disorder caused by defective scrambling of membrane phospholipids. Biochim.Biophys.Acta 2004;1636:119-128.

43. Basse F, Gaffet P, Bienvenue A. Correlation between inhibition of cytoskeleton proteolysis and anti-vesiculation effect of calpeptin during A23187-induced activation of human platelets: are vesicles shed by filopod fragmentation? Biochim.Biophys.Acta 1994;1190:217-224.

44. Murphy WG, Moore JC, Kelton JG. Calcium-dependent cysteine protease activity in the sera of patients with thrombotic thrombocytopenic purpura. Blood 1987;70:1683-1687.

45. Kelton JG, Warkentin TE, Hayward CP, Murphy WG, Moore JC. Calpain activity in patients with thrombotic thrombocytopenic purpura is associated with platelet microparticles. Blood 1992;80:2246-2251.

46. Horstman LL, Jy W, Jimenez JJ, Bidot C, Ahn YS. New horizons in the analysis of circulating cell-derived microparticles. Keio J.Med. 2004;53:210-230.

47. Shet AS, Aras O, Gupta K et al. Sickle blood contains tissue factor-positive microparticles derived from endothelial cells and monocytes. Blood 2003;102:2678-2683.

48. Simak J, Holada K, Risitano AM et al. Elevated circulating endothelial membrane microparticles in paroxysmal nocturnal haemoglobinuria. Br.J.Haematol. 2004;125:804-813.

49. Jacobson K, Dietrich C. Looking at lipid rafts? Trends Cell Biol. 1999;9:87-91.

50. Bodin S, Tronchere H, Payrastre B. Lipid rafts are critical membrane domains in blood platelet activation processes. Biochim.Biophys.Acta 2003;1610:247-257.

51. Jimenez JJ, Jy W, Mauro LM et al. Endothelial cells release phenotypically and quantitatively distinct microparticles in activation and apoptosis. Thromb.Res. 2003;109:175-180.

52. Simak J, Gelderman MP. Cell membrane microparticles in blood and blood products: potentially pathogenic agents and diagnostic markers. Transfus.Med.Rev. 2006;20:1-26.

53. Jy W, Jimenez JJ, Mauro LM et al. Agonist-induced capping of adhesion proteins and microparticle shedding in cultures of human renal microvascular endothelial cells. Endothelium 2002;9:179-189.

54. Muralidharan-Chari V, Clancy JW, Sedgwick A, Souza-Schorey C. Microvesicles: mediators of extracellular communication during cancer progression. J.Cell Sci. 2010;123:1603-1611.

55. Lawen A. Apoptosis-an introduction. Bioessays 2003;25:888-896.

56. Kulkarni GV, McCulloch CA. Serum deprivation induces apoptotic cell death in a subset of Balb/c 3T3 fibroblasts. J.Cell Sci. 1994;107 (Pt 5):1169-1179.

57. Nagata S. DNA degradation in development and programmed cell death. Annual Review of Immunology 2005;23:853-875.

58. Mills JC, Stone NL, Erhardt J, Pittman RN. Apoptotic membrane blebbing is regulated by myosin light chain phosphorylation. J.Cell Biol. 1998;140:627-636.

59. Ostberg JR, Barth RK, Frelinger JG. The Roman god Janus: a paradigm for the function of CD43. Immunol.Today 1998;19:546-550.

60. Bazil V, Strominger JL. CD43, the major sialoglycoprotein of human leukocytes, is proteolytically cleaved from the surface of stimulated lymphocytes and granulocytes. Proc.Natl.Acad.Sci.U.S.A 1993;90:3792-3796.

61. Nusbaum P, Laine C, Bouaouina M et al. Distinct signaling pathways are involved in leukosialin (CD43) down-regulation, membrane blebbing, and phospholipid scrambling during neutrophil apoptosis. J.Biol.Chem. 2005;280:5843-5853.

62. Raposo G, Nijman HW, Stoorvogel W et al. B lymphocytes secrete antigen-presenting vesicles. J.Exp.Med. 1996;183:1161-1172.

63. Zitvogel L, Regnault A, Lozier A et al. Eradication of established murine tumors using a novel cell-free vaccine: dendritic cell-derived exosomes. Nat.Med. 1998;4:594-600.

64. Pan BT, Johnstone RM. Fate of the transferrin receptor during maturation of sheep reticulocytes in vitro: selective externalization of the receptor. Cell 1983;33:967-978.

65. Johnstone RM. Exosomes biological significance: A concise review. Blood Cells Mol.Dis. 2006;36:315-321.

66. Thery C, Boussac M, Veron P et al. Proteomic analysis of dendritic cell-derived exosomes: a secreted subcellular compartment distinct from apoptotic vesicles. J.Immunol. 2001;166:7309-7318.

67. Skokos D, Botros HG, Demeure C et al. Mast cell-derived exosomes induce phenotypic and functional maturation of dendritic cells and elicit specific immune responses in vivo. J.Immunol. 2003;170:3037-3045.

68. Wolfers J, Lozier A, Raposo G et al. Tumor-derived exosomes are a source of shared tumor rejection antigens for CTL cross-priming. Nat.Med. 2001;7:297-303.

69. Keller S, Sanderson MP, Stoeck A, Altevogt P. Exosomes: from biogenesis and secretion to biological function. Immunol.Lett. 2006;107:102-108.

70. Thery C, Boussac M, Veron P et al. Proteomic analysis of dendritic cell-derived exosomes: a secreted subcellular compartment distinct from apoptotic vesicles. J.Immunol. 2001;166:7309-7318.

71. Vidal M, Mangeat P, Hoekstra D. Aggregation reroutes molecules from a recycling to a vesicle-mediated secretion pathway during reticulocyte maturation. J.Cell Sci. 1997;110 (Pt 16):1867-1877.

72. Ceresa BP, Schmid SL. Regulation of signal transduction by endocytosis. Curr.Opin.Cell Biol. 2000;12:204-210.

73. Mellman I. Membranes and sorting. Curr.Opin.Cell Biol. 1996;8:497-498.

74. Mellman I. Endocytosis and molecular sorting. Annu.Rev.Cell Dev.Biol. 1996;12:575-625.

75. McLellan AD. Exosome release by primary B cells. Crit Rev.Immunol. 2009;29:203-217.

76. Van NG, Raposo G, Candalh C et al. Intestinal epithelial cells secrete exosome-like vesicles. Gastroenterology 2001;121:337-349.

77. Escola JM, Kleijmeer MJ, Stoorvogel W et al. Selective enrichment of tetraspan proteins on the internal vesicles of multivesicular endosomes and on exosomes secreted by human B-lymphocytes. J.Biol.Chem. 1998;273:20121-20127.

78. Thery C, Zitvogel L, Amigorena S. Exosomes: composition, biogenesis and function. Nat.Rev.Immunol. 2002;2:569-579.

79. Buschow SI, van Balkom BW, Aalberts M et al. MHC class II-associated proteins in B-cell exosomes and potential functional implications for exosome biogenesis. Immunol.Cell Biol. 2010

80. Mallat Z, Hugel B, Ohan J et al. Shed membrane microparticles with procoagulant potential in human atherosclerotic plaques: a role for apoptosis in plaque thrombogenicity. Circulation 1999;99:348-353.

81. Nagal A, Sato T, Akimoto N, Ito A, Sumida M. Isolation and identification of histone H3 protein enriched in microvesicles secreted from cultured sebocytes. Endocrinology 2005;146:2593-2601.

82. Matzdorff AC, Berchner D, Kuhnel G et al. Relative and absolute changes of activated platelets, microparticles and platelet aggregates after activation in vitro. Haemostasis 1998;28:277-288.

83. Mostefai HA, Andriantsitohaina R, Martinez MC. Plasma membrane microparticles in angiogenesis: role in ischemic diseases and in cancer. Physiol Res. 2008;57:311-320.

84. Janowska-Wieczorek A, Marquez-Curtis LA, Wysoczynski M, Ratajczak MZ. Enhancing effect of platelet-derived microvesicles on the invasive potential of breast cancer cells. Transfusion 2006;46:1199-1209.

85. Majka M, Kijowski J, Lesko E et al. Evidence that platelet-derived microvesicles may transfer platelet-specific immunoreactive antigens to the surface of endothelial cells and CD34+ hematopoietic stem/ progenitor cells--implication for the pathogenesis of immune thrombocytopenias. Folia Histochem.Cytobiol. 2007;45:27-32.

86. Majka M, Janowska-Wieczorek A, Ratajczak J et al. Numerous growth factors, cytokines, and chemokines are secreted by human CD34(+) cells, myeloblasts, erythroblasts, and megakaryoblasts and regulate normal hematopoiesis in an autocrine/paracrine manner. Blood 2001;97:3075-3085.

87. Vandendries ER, Furie BC, Furie B. Role of P-selectin and PSGL-1 in coagulation and thrombosis. Thromb.Haemost. 2004;92:459-466.

88. Yuan A, Farber EL, Rapoport AL et al. Transfer of microRNAs by embryonic stem cell microvesicles. PLoS.One. 2009;4:e4722.

89. Baj-Krzyworzeka M, Majka M, Pratico D et al. Platelet-derived microparticles stimulate proliferation, survival, adhesion, and chemotaxis of hematopoietic cells. Exp.Hematol. 2002;30:450-459.

90. Greco V, Hannus M, Eaton S. Argosomes: a potential vehicle for the spread of morphogens through epithelia. Cell 2001;106:633-645.

91. Barry OP, Kazanietz MG, Pratico D, FitzGerald GA. Arachidonic acid in platelet microparticles up-regulates cyclooxygenase-2-dependent prostaglandin formation via a protein kinase C/mitogen-activated protein kinase-dependent pathway. J.Biol.Chem. 1999;274:7545-7556.

92. English D, Garcia JG, Brindley DN. Platelet-released phospholipids link haemostasis and angiogenesis. Cardiovasc.Res. 2001;49:588-599.

93. Morales-Ruiz M, Lee MJ, Zollner S et al. Sphingosine 1-phosphate activates Akt, nitric oxide production, and chemotaxis through a Gi protein/phosphoinositide 3-kinase pathway in endothelial cells. J.Biol.Chem. 2001;276:19672-19677.

94. Janowska-Wieczorek A, Majka M, Kijowski J et al. Platelet-derived microparticles bind to hematopoietic stem/progenitor cells and enhance their engraftment. Blood 2001;98:3143-3149.

95. Barry OP, Pratico D, Savani RC, FitzGerald GA. Modulation of monocyte-endothelial cell interactions by platelet microparticles. J.Clin.Invest 1998;102:136-144.

96. Janowska-Wieczorek A, Wysoczynski M, Kijowski J et al. Microvesicles derived from activated platelets induce metastasis and angiogenesis in lung cancer. Int.J.Cancer 2005;113:752-760.

97. Del C, I, Shrimpton CN, Thiagarajan P, Lopez JA. Tissue-factor-bearing microvesicles arise from lipid rafts and fuse with activated platelets to initiate coagulation. Blood 2005;106:1604-1611.

98. Fritzsching B, Schwer B, Kartenbeck J et al. Release and intercellular transfer of cell surface CD81 via microparticles. J.Immunol. 2002;169:5531-5537.

99. Andreola G, Rivoltini L, Castelli C et al. Induction of lymphocyte apoptosis by tumor cell secretion of FasL-bearing microvesicles. J.Exp.Med. 2002;195:1303-1316.

100. Abrahams VM, Straszewski SL, Kamsteeg M et al. Epithelial ovarian cancer cells secrete functional Fas ligand. Cancer Res. 2003;63:5573-5581.

101. Abrahams VM, Straszewski-Chavez SL, Guller S, Mor G. First trimester trophoblast cells secrete Fas ligand which induces immune cell apoptosis. Mol.Hum.Reprod. 2004;10:55-63.

102. Fauci AS. Host factors and the pathogenesis of HIV-induced disease. Nature 1996;384:529-534.

103. Berger EA, Murphy PM, Farber JM. Chemokine receptors as HIV-1 coreceptors: roles in viral entry, tropism, and disease. Annu.Rev.Immunol. 1999;17:657-700.

104. Samson M, Libert F, Doranz BJ et al. Resistance to HIV-1 infection in caucasian individuals bearing mutant alleles of the CCR-5 chemokine receptor gene. Nature 1996;382:722-725.

105. Edinger AL, Mankowski JL, Doranz BJ et al. CD4-independent, CCR5-dependent infection of brain capillary endothelial cells by a neurovirulent simian immunodeficiency virus strain. Proc.Natl.Acad.Sci.U.S.A 1997;94:14742-14747.

106. Khiati A, Chaloin O, Muller S, Tardieu M, Horellou P. Induction of monocyte chemoattractant protein-1 (MCP-1/CCL2) gene expression by human immunodeficiency virus-1 Tat in human astrocytes is CDK9 dependent. J.Neurovirol. 2010;16:150-167.

107. Eugenin EA, Morgello S, Klotman ME et al. Human immunodeficiency virus (HIV) infects human arterial smooth muscle cells in vivo and in vitro: implications for the pathogenesis of HIV-mediated vascular disease. Am.J.Pathol. 2008;172:1100-1111.

108. Segerer S, Mack M, Regele H, Kerjaschki D, Schlondorff D. Expression of the C-C chemokine receptor 5 in human kidney diseases. Kidney Int. 1999;56:52-64.

109. Mack M, Kleinschmidt A, Bruhl H et al. Transfer of the chemokine receptor CCR5 between cells by membrane-derived microparticles: a mechanism for cellular human immunodeficiency virus 1 infection. Nat.Med. 2000;6:769-775.

110. Majka M, Rozmyslowicz T, Honczarenko M et al. Biological significance of the expression of HIV-related chemokine coreceptors (CCR5 and CXCR4) and their ligands by human hematopoietic cell lines. Leukemia 2000;14:1821-1832.

111. Combes V, Coltel N, Alibert M et al. ABCA1 gene deletion protects against cerebral malaria: potential pathogenic role of microparticles in neuropathology. Am.J.Pathol. 2005;166:295-302.

112. Niu X, Gupta K, Yang JT, Shamblott MJ, Levchenko A. Physical transfer of membrane and cytoplasmic components as a general mechanism of cell-cell communication. J.Cell Sci. 2009;122:600-610.

113. Hochedlinger K, Plath K. Epigenetic reprogramming and induced pluripotency. Development 2009;136:509-523.

114. Taranger CK, Noer A, Sorensen AL et al. Induction of dedifferentiation, genomewide transcriptional programming, and epigenetic reprogramming by extracts of carcinoma and embryonic stem cells. Mol.Biol.Cell 2005;16:5719-5735.

115. Gaustad KG, Boquest AC, Anderson BE, Gerdes AM, Collas P. Differentiation of human adipose tissue stem cells using extracts of rat cardiomyocytes. Biochem.Biophys.Res.Commun. 2004;314:420-427.

116. Do JT, Scholer HR. Nuclei of embryonic stem cells reprogram somatic cells. Stem Cells 2004;22:941-949.

117. Landsverk HB, Hakelien AM, Kuntziger T et al. Reprogrammed gene expression in a somatic cell-free extract. EMBO Rep. 2002;3:384-389.

118. Gould SJ, Booth AM, Hildreth JE. The Trojan exosome hypothesis. Proc.Natl.Acad.Sci.U.S.A 2003;100:10592-10597.

119. Sarkar A, Mitra S, Mehta S, Raices R, Wewers MD. Monocyte derived microvesicles deliver a cell death message via encapsulated caspase-1. PLoS.One. 2009;4:e7140.

120. Liu R, Klich I, Ratajczak J, Ratajczak MZ, Zuba-Surma EK. Erythrocyte-derived microvesicles may transfer phosphatidylserine to the surface of nucleated cells and falsely 'mark' them as apoptotic. Eur.J.Haematol. 2009;83:220-229.

121. Morgan BP, Campbell AK. The recovery of human polymorphonuclear leucocytes from sublytic complement attack is mediated by changes in intracellular free calcium. Biochem.J. 1985;231:205-208.

122. Hansen WR, Fletcher DA. Tonic shock induces detachment of Giardia lamblia. PLoS.Negl.Trop.Dis. 2008;2:e169.

123. Palade G. Intracellular Aspects of the Process of Protein Synthesis. Science 1975;189:867.

124. Sollner TH. Regulated exocytosis and SNARE function (Review). Mol.Membr.Biol. 2003;20:209-220.

125. Stahl PD, Barbieri MA. Multivesicular bodies and multivesicular endosomes: the "ins and outs" of endosomal traffic. Sci.STKE. 2002;2002:e32.

126. Harter C, Wieland F. The secretory pathway: mechanisms of protein sorting and transport. Biochim.Biophys.Acta 1996;1286:75-93.

127. Rothman JE. Mechanisms of intracellular protein transport. Nature 1994;372:55-63.

128. Rothman JE, Wieland FT. Protein sorting by transport vesicles. Science 1996;272:227-234.

129. Lee MC, Miller EA, Goldberg J, Orci L, Schekman R. Bi-directional protein transport between the ER and Golgi. Annu.Rev.Cell Dev.Biol. 2004;20:87-123.

130. Cleves AE. Protein transports: the nonclassical ins and outs. Curr.Biol. 1997;7:R318-R320.

131. Nickel W. The mystery of nonclassical protein secretion. A current view on cargo proteins and potential export routes. Eur.J.Biochem. 2003;270:2109-2119.

132. Nickel W. Unconventional secretory routes: direct protein export across the plasma membrane of mammalian cells. Traffic. 2005;6:607-614.

133. Blobel G, Dobberstein B. Transfer of proteins across membranes. II. Reconstitution of functional rough microsomes from heterologous components. J.Cell Biol. 1975;67:852-862.

134. Walter P, Gilmore R, Blobel G. Protein translocation across the endoplasmic reticulum. Cell 1984;38:5-8.

135. Meyer DI, Krause E, Dobberstein B. Secretory protein translocation across membranes-the role of the "docking protein'. Nature 1982;297:647-650.

136. Rapoport TA. Transport of proteins across the endoplasmic reticulum membrane. Science 1992;258:931-936.

137. Tajima S, Lauffer L, Rath VL, Walter P. The signal recognition particle receptor is a complex that contains two distinct polypeptide chains. J.Cell Biol. 1986;103:1167-1178.

138. Brodsky JL. Translocation of proteins across the endoplasmic reticulum membrane. Int.Rev.Cytol. 1998;178:277-328.

139. Gilmore R. Protein translocation across the endoplasmic reticulum: a tunnel with toll booths at entry and exit. Cell 1993;75:589-592.

140. Hirschberg K, Miller CM, Ellenberg J et al. Kinetic analysis of secretory protein traffic and characterization of golgi to plasma membrane transport intermediates in living cells. J.Cell Biol. 1998;143:1485-1503.

141. Martin-Verdeaux S, Pombo I, Iannascoli B et al. Evidence of a role for Munc18-2 and microtubules in mast cell granule exocytosis. J.Cell Sci. 2003;116:325-334.

142. Mossessova E, Corpina RA, Goldberg J. Crystal structure of ARF1*Sec7 complexed with Brefeldin A and its implications for the guanine nucleotide exchange mechanism. Mol.Cell 2003;12:1403-1411.

143. Robineau S, Chabre M, Antonny B. Binding site of brefeldin A at the interface between the small G protein ADP-ribosylation factor 1 (ARF1) and the nucleotide-exchange factor Sec7 domain. Proc.Natl.Acad.Sci.U.S.A 2000;97:9913-9918.

144. Hashieh IA, Remy L, Mathieu S, Gerolami A. The effects of monensin on the transport of horseradish peroxidase into intracellular lumina in cultured rat hepatocytes. Hepatology 1989;10:61-65.

145. Tartakoff AM. Perturbation of vesicular traffic with the carboxylic ionophore monensin. Cell 1983;32:1026-1028.

146. Hughes RC. Secretion of the galectin family of mammalian carbohydrate-binding proteins. Biochim.Biophys.Acta 1999;1473:172-185.

147. Rubartelli A, Cozzolino F, Talio M, Sitia R. A novel secretory pathway for interleukin-1 beta, a protein lacking a signal sequence. EMBO J. 1990;9:1503-1510.

148. Florkiewicz RZ, Majack RA, Buechler RD, Florkiewicz E. Quantitative export of FGF-2 occurs through an alternative, energy-dependent, non-ER/Golgi pathway. J.Cell Physiol 1995;162:388-399.

149. Muesch A, Hartmann E, Rohde K et al. A novel pathway for secretory proteins? Trends Biochem.Sci. 1990;15:86-88.

150. Wakisaka N, Murono S, Yoshizaki T, Furukawa M, Pagano JS. Epstein-barr virus latent membrane protein 1 induces and causes release of fibroblast growth factor-2. Cancer Res. 2002;62:6337-6344.

151. Maizel A, Tassetto M, Filhol O et al. Engrailed homeoprotein secretion is a regulated process. Development 2002;129:3545-3553.

152. Lutomski D, Fouillit M, Bourin P et al. Externalization and binding of galectin-1 on cell surface of K562 cells upon erythroid differentiation. Glycobiology 1997;7:1193-1199.

153. McNeil PL, Muthukrishnan L, Warder E, D'Amore PA. Growth factors are released by mechanically wounded endothelial cells. J.Cell Biol. 1989;109:811-822.

154. Prudovsky I, Bagala C, Tarantini F et al. The intracellular translocation of the components of the fibroblast growth factor 1 release complex precedes their assembly prior to export. J.Cell Biol. 2002;158:201-208.

155. Stinchcombe J, Bossi G, Griffiths GM. Linking albinism and immunity: the secrets of secretory lysosomes. Science 2004;305:55-59.

156. Cleves AE, Kelly RB. Rehearsing the ABCs. Protein translocation. Curr.Biol. 1996;6:276-278.

157. Denny PW, Gokool S, Russell DG, Field MC, Smith DF. Acylation-dependent protein export in Leishmania. J.Biol.Chem. 2000;275:11017-11025.

158. Stegmayer C, Kehlenbach A, Tournaviti S et al. Direct transport across the plasma membrane of mammalian cells of Leishmania HASPB as revealed by a CHO export mutant. J.Cell Sci. 2005;118:517-527.

159. Schafer T, Zentgraf H, Zehe C et al. Unconventional secretion of fibroblast growth factor 2 is mediated by direct translocation across the plasma membrane of mammalian cells. J.Biol.Chem. 2004;279:6244-6251.

160. Stoorvogel W, Kleijmeer MJ, Geuze HJ, Raposo G. The biogenesis and functions of exosomes. Traffic. 2002;3:321-330.

161. Thery C, Boussac M, Veron P et al. Proteomic analysis of dendritic cell-derived exosomes: a secreted subcellular compartment distinct from apoptotic vesicles. J.Immunol. 2001;166:7309-7318.

162. Freyssinet JM. Cellular microparticles: what are they bad or good for? J.Thromb.Haemost. 2003;1:1655-1662.

163. Chimelli L, Scaravilli F. Trypanosomiasis. Brain Pathol. 1997;7:599-611.

164. Engman DM, Leon JS. Pathogenesis of Chagas heart disease: role of autoimmunity. Acta Trop. 2002;81:123-132.

165. Waghabi MC, Keramidas M, Calvet CM et al. SB-431542, a transforming growth factor beta inhibitor, impairs *Trypanosoma cruzi* infection in cardiomyocytes and parasite cycle completion. Antimicrob.Agents Chemother. 2007;51:2905-2910.

166. Schofield CJ, Dias JC. The Southern Cone Initiative against Chagas disease. Adv.Parasitol. 1999;42:1-27.

167. Kirchhoff LV. Is *Trypanosoma cruzi* a new threat to our blood supply? Ann.Intern.Med. 1989;111:773-775.

168. Cardoso AV, Lescano SA, Amato N, V, Gakiya E, Santos SV. Survival of *Trypanosoma cruzi* in sugar cane used to prepare juice. Rev.Inst.Med.Trop.Sao Paulo 2006;48:287-289.

169. Yoshida N. *Trypanosoma cruzi* infection by oral route: how the interplay between parasite and host components modulates infectivity. Parasitol.Int. 2008;57:105-109.

170. Gascon J, Bern C, Pinazo MJ. Chagas disease in Spain, the United States and other non-endemic countries. Acta Trop. 2009

171. Vassena CV, Picollo MI, Zerba EN. Insecticide resistance in Brazilian Triatoma infestans and Venezuelan Rhodnius prolixus. Med.Vet.Entomol. 2000;14:51-55.

172. Dvorak JA, Hyde TP. *Trypanosoma cruzi*: interaction with vertebrate cells in vitro. 1. Individual interactions at the cellular and subcellular levels. Exp.Parasitol. 1973;34:268-283.

173. Rimoldi MT, Tenner AJ, Bobak DA, Joiner KA. Complement component C1q enhances invasion of human mononuclear phagocytes and fibroblasts by *Trypanosoma cruzi* trypomastigotes. J.Clin.Invest 1989;84:1982-1989.

174. Schenkman S, Andrews NW, Nussenzweig V, Robbins ES. *Trypanosoma cruzi* invade a mammalian epithelial cell in a polarized manner. Cell 1988;55:157-165.

175. Mehendale HM, Limaye PB. Calpain: a death protein that mediates progression of liver injury. Trends Pharmacol.Sci. 2005;26:232-236.

176. Beiner JM, Jokl P. Muscle contusion injury and myositis ossificans traumatica. Clin.Orthop.Relat Res. 2002S110-S119.

177. McNeil PL, Kirchhausen T. An emergency response team for membrane repair. Nat.Rev.Mol.Cell Biol. 2005;6:499-505.

178. McNeil PL, Steinhardt RA. Plasma membrane disruption: repair, prevention, adaptation. Annu.Rev.Cell Dev.Biol. 2003;19:697-731.

179. McNeil PL, Steinhardt RA. Loss, restoration, and maintenance of plasma membrane integrity. J.Cell Biol. 1997;137:1-4.

180. Swanson JA, Taylor DL. Local and spatially coordinated movements in Dictyostelium discoideum amoebae during chemotaxis. Cell 1982;28:225-232.

181. Terasaki M, Miyake K, McNeil PL. Large plasma membrane disruptions are rapidly resealed by Ca2+-dependent vesicle-vesicle fusion events. J.Cell Biol. 1997;139:63-74.

182. Laval SH, Bushby KM. Limb-girdle muscular dystrophies--from genetics to molecular pathology. Neuropathol.Appl.Neurobiol. 2004;30:91-105.

183. Bansal D, Miyake K, Vogel SS et al. Defective membrane repair in dysferlin-deficient muscular dystrophy. Nature 2003;423:168-172.

184. Lennon NJ, Kho A, Bacskai BJ et al. Dysferlin interacts with annexins A1 and A2 and mediates sarcolemmal wound-healing. J.Biol.Chem. 2003;278:50466-50473.

185. Yasuda S, Townsend D, Michele DE et al. Dystrophic heart failure blocked by membrane sealant poloxamer. Nature 2005;436:1025-1029.

186. Benz R, Zimmermann U. The resealing process of lipid bilayers after reversible electrical breakdown. Biochim.Biophys.Acta 1981;640:169-178.

187. Miyake K, McNeil PL. Vesicle accumulation and exocytosis at sites of plasma membrane disruption. J.Cell Biol. 1995;131:1737-1745.

188. Togo T, Alderton JM, Bi GQ, Steinhardt RA. The mechanism of facilitated cell membrane resealing. J.Cell Sci. 1999;112 (Pt 5):719-731.

189. McNeil PL, Vogel SS, Miyake K, Terasaki M. Patching plasma membrane disruptions with cytoplasmic membrane. J.Cell Sci. 2000;113 (Pt 11):1891-1902.

190. McNeil PL, Baker MM. Cell surface events during resealing visualized by scanning-electron microscopy. Cell Tissue Res. 2001;304:141-146.

191. Andrews NW. Lysosomes and the plasma membrane: trypanosomes reveal a secret relationship. J.Cell Biol. 2002;158:389-394.

192. Kolter T, Sandhoff K. Lysosomal degradation of membrane lipids. FEBS Lett. 2010;584:1700-1712.

193. Martinez I, Chakrabarti S, Hellevik T et al. Synaptotagmin VII regulates Ca(2+)-dependent exocytosis of lysosomes in fibroblasts. J.Cell Biol. 2000;148:1141-1149.

194. Reddy A, Caler EV, Andrews NW. Plasma membrane repair is mediated by Ca(2+)-regulated exocytosis of lysosomes. Cell 2001;106:157-169.

195. Chakrabarti S, Kobayashi KS, Flavell RA et al. Impaired membrane resealing and autoimmune myositis in synaptotagmin VII-deficient mice. J.Cell Biol. 2003;162:543-549.

196. Wang P, Chicka MC, Bhalla A, Richards DA, Chapman ER. Synaptotagmin VII is targeted to secretory organelles in PC12 cells, where it functions as a high-affinity calcium sensor. Mol.Cell Biol. 2005;25:8693-8702.

197. Jaiswal JK, Chakrabarti S, Andrews NW, Simon SM. Synaptotagmin VII restricts fusion pore expansion during lysosomal exocytosis. PLoS.Biol. 2004;2:E233.

198. Cerny J, Feng Y, Yu A et al. The small chemical vacuolin-1 inhibits Ca(2+)-dependent lysosomal exocytosis but not cell resealing. EMBO Rep. 2004;5:883-888.

199. Borgonovo B, Cocucci E, Racchetti G et al. Regulated exocytosis: a novel, widely expressed system. Nat.Cell Biol. 2002;4:955-962.

200. Bi GQ, Alderton JM, Steinhardt RA. Calcium-regulated exocytosis is required for cell membrane resealing. J.Cell Biol. 1995;131:1747-1758.

201. Schapire AL, Valpuesta V, Botella MA. Plasma membrane repair in plants. Trends Plant Sci. 2009;14:645-652.

202. Mallat Z, Benamer H, Hugel B et al. Elevated levels of shed membrane microparticles with procoagulant potential in the peripheral circulating blood of patients with acute coronary syndromes. Circulation 2000;101:841-843.

203. Nomura S, Suzuki M, Katsura K et al. Platelet-derived microparticles may influence the development of atherosclerosis in diabetes mellitus. Atherosclerosis 1995;116:235-240.

204. Omoto S, Nomura S, Shouzu A et al. Detection of monocyte-derived microparticles in patients with Type II diabetes mellitus. Diabetologia 2002;45:550-555.

205. VanWijk MJ, VanBavel E, Sturk A, Nieuwland R. Microparticles in cardiovascular diseases. Cardiovasc.Res. 2003;59:277-287.

206. Furie B, Furie BC. Role of platelet P-selectin and microparticle PSGL-1 in thrombus formation. Trends Mol.Med. 2004;10:171-178.

207. Lima LG, Chammas R, Monteiro RQ, Moreira ME, Barcinski MA. Tumor-derived microvesicles modulate the establishment of metastatic melanoma in a phosphatidylserine-dependent manner. Cancer Lett. 2009;283:168-175.

208. van Doormaal FF, Kleinjan A, Di NM, Buller HR, Nieuwland R. Cell-derived microvesicles and cancer. Neth.J.Med. 2009;67:266-273.

209. Estey E, Dohner H. Acute myeloid leukaemia. Lancet 2006;368:1894-1907.

210. Konoplev S, Bueso-Ramos CE. Advances in the pathologic diagnosis and biology of acute myeloid leukemia. Ann.Diagn.Pathol. 2006;10:39-65.

211. Fialkow PJ, Singer JW, Adamson JW et al. Acute nonlymphocytic leukemia: heterogeneity of stem cell origin. Blood 1981;57:1068-1073.

212. Birch JM, Pang D, Alston RD et al. Survival from cancer in teenagers and young adults in England, 1979-2003. Br.J.Cancer 2008;99:830-835.

213. Geraci M, Eden TO, Alston RD et al. Geographical and temporal distribution of cancer survival in teenagers and young adults in England. Br.J.Cancer 2009;101:1939-1945.

214. Kinlen LJ. Leukaemia. Cancer Surv. 1994;19-20:475-491.

215. Deschler B, Lubbert M. Acute myeloid leukemia: epidemiology and etiology. Cancer 2006;107:2099-2107.

216. Pui CH. Childhood leukemias. N.Engl.J.Med. 1995;332:1618-1630.

217. Aquino VM. Acute myelogenous leukemia. Curr.Probl.Pediatr.Adolesc.Health Care 2002;32:50-58.

218. Stone RM, O'Donnell MR, Sekeres MA. Acute myeloid leukemia. Hematology.Am.Soc.Hematol.Educ.Program. 200498-117.

219. Levine JE, Uberti JP, Ayash L et al. Lowered-intensity preparative regimen for allogeneic stem cell transplantation delays acute graft-versus-host disease but does not improve outcome for advanced hematologic malignancy. Biol.Blood Marrow Transplant. 2003;9:189-197.

220. Nakamura T, Hemmi H, Aso H, Ishida N. Variants of a human monocytic leukemia cell line (THP-1): induction of differentiation by retinoic acid, interferon-gamma, and T-lymphocyte-derived differentiation-inducing activity. J.Natl.Cancer Inst. 1986;77:21-27.

221. Ades L, Chevret S, de BS et al. Outcome of acute promyelocytic leukemia treated with all trans retinoic acid and chemotherapy in elderly patients: the European group experience. Leukemia 2005;19:230-233.

222. Daigneault M, Preston JA, Marriott HM, Whyte MK, Dockrell DH. The identification of markers of macrophage differentiation in PMA-stimulated THP-1 cells and monocyte-derived macrophages. PLoS.One. 2010;5:e8668.

223. Zimber A, Chedeville A, Abita JP, Barbu V, Gespach C. Functional interactions between bile acids, all-trans retinoic acid, and 1,25-dihydroxy-vitamin D3 on monocytic differentiation and myeloblastin gene down-regulation in HL60 and THP-1 human leukemia cells. Cancer Res. 2000;60:672-678.

224. Waclavicek M, Berer A, Oehler L et al. Calcium ionophore: a single reagent for the differentiation of primary human acute myelogenous leukaemia cells towards dendritic cells. Br.J.Haematol. 2001;114:466-473.

225. Delneste Y, Charbonnier P, Herbault N et al. Interferon-gamma switches monocyte differentiation from dendritic cells to macrophages. Blood 2003;101:143-150.

226. Brune M, Castaigne S, Catalano J et al. Improved leukemia-free survival after postconsolidation immunotherapy with histamine dihydrochloride and interleukin-2 in acute myeloid leukemia: results of a randomized phase 3 trial. Blood 2006;108:88-96.

227. Pasquet JM, chary-Prigent J, Nurden AT. Microvesicle release is associated with extensive protein tyrosine dephosphorylation in platelets stimulated by A23187 or a mixture of thrombin and collagen. Biochem.J. 1998;333 (Pt 3):591-599.

228. Camargo EP. Growth and differentiation in *Trypanosoma cruzi.* I. Origin of metacyclic trypanosomes in liquid media. Rev.Inst.Med.Trop.Sao Paulo 1964;6:93-100.

229. Eken C, Gasser O, Zenhaeusern G et al. Polymorphonuclear neutrophil-derived ectosomes interfere with the maturation of monocyte-derived dendritic cells. J.Immunol. 2008;180:817-824.

230. de Sousa MA. Surface electrical charge of bloodstream trypomastigotes of *Trypanosoma cruzi* strains. Mem.Inst.Oswaldo Cruz 1983;78:497-500.

231. Reynolds ES. The use of lead citrate at high pH as an electron-opaque stain in electron microscopy. J.Cell Biol. 1963;17:208-212.

232. Zomer A, Vendrig T, Hopmans ES et al. Exosomes: Fit to deliver small RNA. Commun.Integr.Biol. 2010;3:447-450.

233. Morgan BP, Dankert JR, Esser AF. Recovery of human neutrophils from complement attack: removal of the membrane attack complex by endocytosis and exocytosis. J.Immunol. 1987;138:246-253.

234. Roberts PA, Morgan BP, Campbell AK. 2-Chloroadenosine inhibits complement-induced reactive oxygen metabolite production and recovery of human polymorphonuclear leucocytes attacked by complement. Biochem.Biophys.Res.Commun. 1985;126:692-697.

235. Carney DF, Koski CL, Shin ML. Elimination of terminal complement intermediates from the plasma membrane of nucleated cells: the rate of disappearance differs for cells carrying C5b-7 or C5b-8 or a mixture of C5b-8 with a limited number of C5b-9. J.Immunol. 1985;134:1804-1809.

236. Sims PJ, Faioni EM, Wiedmer T, Shattil SJ. Complement proteins C5b-9 cause release of membrane vesicles from the platelet surface that are enriched in the membrane receptor for coagulation factor Va and express prothrombinase activity. J.Biol.Chem. 1988;263:18205-18212.

237. Iida K, Whitlow MB, Nussenzweig V. Membrane vesiculation protects erythrocytes from destruction by complement. J.Immunol. 1991;147:2638-2642.

238. Lopez JA, Del C, I, Shrimpton CN. Receptors, rafts, and microvesicles in thrombosis and inflammation. J.Thromb.Haemost. 2005;3:1737-1744.

239. Azevedo LC, Janiszewski M, Pontieri V et al. Platelet-derived exosomes from septic shock patients induce myocardial dysfunction. Crit Care 2007;11:R120.

240. Denzer K, Kleijmeer MJ, Heijnen HF, Stoorvogel W, Geuze HJ. Exosome: from internal vesicle of the multivesicular body to intercellular signaling device. J.Cell Sci. 2000;113 Pt 19:3365-3374.

241. Morgan BP. Complement membrane attack on nucleated cells: resistance, recovery and non-lethal effects. Biochem.J. 1989;264:1-14.

242. Hoffmann PR, deCathelineau AM, Ogden CA et al. Phosphatidylserine (PS) induces PS receptor-mediated macropinocytosis and promotes clearance of apoptotic cells. J.Cell Biol. 2001;155:649-659.

243. Wu Y, Tibrewal N, Birge RB. Phosphatidylserine recognition by phagocytes: a view to a kill. Trends Cell Biol. 2006;16:189-197.

244. Mujawar Z, Rose H, Morrow MP et al. Human immunodeficiency virus impairs reverse cholesterol transport from macrophages. PLoS.Biol. 2006;4:e365.

245. Coltel N, Combes V, Wassmer SC, Chimini G, Grau GE. Cell vesiculation and immunopathology: implications in cerebral malaria. Microbes.Infect. 2006;8:2305-2316.

246. Nomura S, Miyazaki Y, Miyake T et al. Detection of platelet-derived microparticles in patients with diabetes. Am.J.Hematol. 1993;44:213.

247. Boilard E, Nigrovic PA, Larabee K et al. Platelets amplify inflammation in arthritis via collagen-dependent microparticle production. Science 2010;327:580-583.

248. Aharon A, Brenner B. Microparticles, thrombosis and cancer. Best.Pract.Res.Clin.Haematol. 2009;22:61-69.

249. Minagar A, Jy W, Jimenez JJ et al. Elevated plasma endothelial microparticles in multiple sclerosis. Neurology 2001;56:1319-1324.

250. Bergmann C, Strauss L, Wieckowski E et al. Tumor-derived microvesicles in sera of patients with head and neck cancer and their role in tumor progression. Head Neck 2009;31:371-380.

251. Dimberg A, Bahram F, Karlberg I et al. Retinoic acid-induced cell cycle arrest of human myeloid cell lines is associated with sequential down-regulation of c-Myc and cyclin E and posttranscriptional up-regulation of p27(Kip1). Blood 2002;99:2199-2206.

252. Daniel L, Fakhouri F, Joly D et al. Increase of circulating neutrophil and platelet microparticles during acute vasculitis and hemodialysis. Kidney Int. 2006;69:1416-1423.

253. Ramachandra L, Qu Y, Wang Y et al. Mycobacterium tuberculosis synergizes with ATP to induce release of microvesicles and exosomes containing major histocompatibility complex class II molecules capable of antigen presentation. Infect.Immun. 2010;78:5116-5125.

254. Garay E, Donnelly R, Wang X, Studzinski GP. Resistance to 1,25D-induced differentiation in human acute myeloid leukemia HL60-40AF cells is associated with reduced transcriptional activity and nuclear localization of the vitamin D receptor. J.Cell Physiol 2007;213:816-825.

255. Champelovier P, Pautre V, Elatifi M et al. Resistance to phorbol ester-induced differentiation in human myeloid leukemia cells: a hypothetic role for the mRNA stabilization process. Leuk.Res. 2006;30:1407-1416.

256. Kehrl JH, Wakefield LM, Roberts AB et al. Production of transforming growth factor beta by human T lymphocytes and its potential role in the regulation of T cell growth. J.Exp.Med. 1986;163:1037-1050.

257. Garcia BA, Smalley DM, Cho H et al. The platelet microparticle proteome. J.Proteome.Res. 2005;4:1516-1521.

258. Jennings MT, Pietenpol JA. The role of transforming growth factor beta in glioma progression. J.Neurooncol. 1998;36:123-140.

259. Grotendorst GR, Smale G, Pencev D. Production of transforming growth factor beta by human peripheral blood monocytes and neutrophils. J.Cell Physiol 1989;140:396-402.

260. Rizzino A. Transforming growth factor-beta: multiple effects on cell differentiation and extracellular matrices. Dev.Biol. 1988;130:411-422.

261. Ignotz RA, Massague J. Cell adhesion protein receptors as targets for transforming growth factor-beta action. Cell 1987;51:189-197.

262. Massague J, Cheifetz S, Endo T, Nadal-Ginard B. Type beta transforming growth factor is an inhibitor of myogenic differentiation. Proc.Natl.Acad.Sci.U.S.A 1986;83:8206-8210.

263. Ohta M, Greenberger JS, Anklesaria P, Bassols A, Massague J. Two forms of transforming growth factor-beta distinguished by multipotential haematopoietic progenitor cells. Nature 1987;329:539-541.

264. Choy L, Skillington J, Derynck R. Roles of autocrine TGF-beta receptor and Smad signaling in adipocyte differentiation. J.Cell Biol. 2000;149:667-682.

265. Kurokowa M, Lynch K, Podolsky DK. Effects of growth factors on an intestinal epithelial cell line: transforming growth factor beta inhibits proliferation and stimulates differentiation. Biochem.Biophys.Res.Commun. 1987;142:775-782.

266. Liang F, Seyrantepe V, Landry K et al. Monocyte differentiation up-regulates the expression of the lysosomal sialidase, Neu1, and triggers its targeting to the plasma membrane via major histocompatibility complex class II-positive compartments. J.Biol.Chem. 2006;281:27526-27538.

267. Schatz G, Dobberstein B. Common principles of protein translocation across membranes. Science 1996;271:1519-1526.

268. Mehul B, Hughes RC. Plasma membrane targetting, vesicular budding and release of galectin 3 from the cytoplasm of mammalian cells during secretion. J.Cell Sci. 1997;110 (Pt 10):1169-1178.

269. MacKenzie A, Wilson HL, Kiss-Toth E et al. Rapid secretion of interleukin-1beta by microvesicle shedding. Immunity. 2001;15:825-835.

270. Hirai Y, Nelson CM, Yamazaki K et al. Non-classical export of epimorphin and its adhesion to alphav-integrin in regulation of epithelial morphogenesis. J.Cell Sci. 2007;120:2032-2043.

271. Flieger O, Engling A, Bucala R et al. Regulated secretion of macrophage migration inhibitory factor is mediated by a non-classical pathway involving an ABC transporter. FEBS Lett. 2003;551:78-86.

272. Gregory JL, Morand EF, McKeown SJ et al. Macrophage migration inhibitory factor induces macrophage recruitment via CC chemokine ligand 2. J.Immunol. 2006;177:8072-8079.

273. Abedin MJ, Kashio Y, Seki M, Nakamura K, Hirashima M. Potential roles of galectins in myeloid differentiation into three different lineages. J.Leukoc.Biol. 2003;73:650-656.

274. Valenti R, Huber V, Filipazzi P et al. Human tumor-released microvesicles promote the differentiation of myeloid cells with transforming growth factor-beta-mediated suppressive activity on T lymphocytes. Cancer Res. 2006;66:9290-9298.

275. Mesri M, Altieri DC. Endothelial cell activation by leukocyte microparticles. J.Immunol. 1998;161:4382-4387.

276. Al-Nedawi K, Meehan B, Micallef J et al. Intercellular transfer of the oncogenic receptor EGFRvIII by microvesicles derived from tumour cells. Nat.Cell Biol. 2008;10:619-624.

277. Li MO, Wan YY, Sanjabi S, Robertson AK, Flavell RA. Transforming growth factor-beta regulation of immune responses. Annu.Rev.Immunol. 2006;24:99-146.

278. Lira AA, Rossetti FC, Nanclares DM et al. Preparation and characterization of chitosan-treated alginate microparticles incorporating all-trans retinoic acid. J.Microencapsul. 20081-8.

279. Messer L, Alsaleh G, Freyssinet JM et al. Microparticle-induced release of B-lymphocyte regulators by rheumatoid synoviocytes. Arthritis Res.Ther. 2009;11:R40.

280. Bombara C, Ignotz RA. TGF-beta inhibits proliferation of and promotes differentiation of human promonocytic leukemia cells. J.Cell Physiol 1992;153:30-37.

281. Turley JM, Falk LA, Ruscetti FW et al. Transforming growth factor beta 1 functions in monocytic differentiation of hematopoietic cells through autocrine and paracrine mechanisms. Cell Growth Differ. 1996;7:1535-1544.

282. Fiorelli G, Ballock RT, Wakefield LM et al. Role for autocrine TGF-beta 1 in regulating differentiation of a human leukemic cell line toward osteoclast-like cells. J.Cell Physiol 1994;160:482-490.

283. Lehmann LE, Weber SU, Fuchs D et al. Intracellular detection of macrophage migration inhibitory factor in peripheral blood leukocytes. Free Radic.Biol.Med. 2005;38:1170-1179.

284. Engling A, Backhaus R, Stegmayer C et al. Biosynthetic FGF-2 is targeted to non-lipid raft microdomains following translocation to the extracellular surface of CHO cells. J.Cell Sci. 2002;115:3619-3631.

285. Thery C, Boussac M, Veron P et al. Proteomic analysis of dendritic cell-derived exosomes: a secreted subcellular compartment distinct from apoptotic vesicles. J.Immunol. 2001;166:7309-7318.

286. Jenkins G. The role of proteases in transforming growth factor-beta activation. Int.J.Biochem.Cell Biol. 2008;40:1068-1078.

287. Sarkar A, Mitra S, Mehta S, Raices R, Wewers MD. Monocyte derived microvesicles deliver a cell death message via encapsulated caspase-1. PLoS.One. 2009;4:e7140.

288. Halder SK, Beauchamp RD, Datta PK. A specific inhibitor of TGF-beta receptor kinase, SB-431542, as a potent antitumor agent for human cancers. Neoplasia. 2005;7:509-521.

289. Cao Z, Flanders KC, Bertolette D et al. Levels of phospho-Smad2/3 are sensors of the interplay between effects of TGF-beta and retinoic acid on monocytic and granulocytic differentiation of HL-60 cells. Blood 2003;101:498-507.

290. Berckmans RJ, Neiuwland R, Boing AN et al. Cell-derived microparticles circulate in healthy humans and support low grade thrombin generation. Thromb.Haemost. 2001;85:639-646.

291. van Beers EJ, Schaap MC, Berckmans RJ et al. Circulating erythrocyte-derived microparticles are associated with coagulation activation in sickle cell disease. Haematologica 2009;94:1513-1519.

292. Aupeix K, Hugel B, Martin T et al. The significance of shed membrane particles during programmed cell death in vitro, and in vivo, in HIV-1 infection. J.Clin.Invest 1997;99:1546-1554.

293. Pap E, Pallinger E, Pasztoi M, Falus A. Highlights of a new type of intercellular communication: microvesicle-based information transfer. Inflamm.Res. 2009;58:1-8.

294. Losche W, Scholz T, Temmler U, Oberle V, Claus RA. Platelet-derived microvesicles transfer tissue factor to monocytes but not to neutrophils. Platelets. 2004;15:109-115.

295. Tailleux L, Pham-Thi N, Bergeron-Lafaurie A et al. DC-SIGN induction in alveolar macrophages defines privileged target host cells for mycobacteria in patients with tuberculosis. PLoS.Med. 2005;2:e381.

296. Fadok VA, Bratton DL, Konowal A et al. Macrophages that have ingested apoptotic cells in vitro inhibit proinflammatory cytokine production through autocrine/paracrine mechanisms involving TGF-beta, PGE2, and PAF. J.Clin.Invest 1998;101:890-898.

297. Gasser O, Schifferli JA. Activated polymorphonuclear neutrophils disseminate anti-inflammatory microparticles by ectocytosis. Blood 2004;104:2543-2548.

298. Inman GJ, Nicolas FJ, Callahan JF et al. SB-431542 is a potent and specific inhibitor of transforming growth factor-beta superfamily type I activin receptor-like kinase (ALK) receptors ALK4, ALK5, and ALK7. Mol.Pharmacol. 2002;62:65-74.

299. Yingling JM, Blanchard KL, Sawyer JS. Development of TGF-beta signalling inhibitors for cancer therapy. Nat.Rev.Drug Discov. 2004;3:1011-1022.

300. Wahl SM, Chen W. Transforming growth factor-beta-induced regulatory T cells referee inflammatory and autoimmune diseases. Arthritis Res.Ther. 2005;7:62-68.

301. Nakamura K, Kitani A, Strober W. Cell contact-dependent immunosuppression by CD4(+)CD25(+) regulatory T cells is mediated by cell surface-bound transforming growth factor beta. J.Exp.Med. 2001;194:629-644.

302. Baker K, Raut P, Jass JR. Colorectal cancer cells express functional cell surface-bound TGFbeta. Int.J.Cancer 2008;122:1695-1700.

303. Johansson C, Ingman M, Jo WM. Elevated neutrophil, macrophage and dendritic cell numbers characterize immune cell populations in mice chronically infected with Salmonella. Microb.Pathog. 2006;41:49-58.

304. Buscaglia CA, Campo VA, Frasch AC, Di Noia JM. *Trypanosoma cruzi* surface mucins: host-dependent coat diversity. Nat.Rev.Microbiol. 2006;4:229-236.

305. Lambris JD, Ricklin D, Geisbrecht BV. Complement evasion by human pathogens. Nat.Rev.Microbiol. 2008;6:132-142.

306. Cestari I, Ramirez MI. Inefficient complement system clearance of *Trypanosoma cruzi* metacyclic trypomastigotes enables resistant strains to invade eukaryotic cells. PLoS.One. 2010;5:e9721.

307. Yoshida N. Molecular basis of mammalian cell invasion by *Trypanosoma cruzi*. An.Acad.Bras.Cienc. 2006;78:87-111.

308. Andrade LO, Andrews NW. Lysosomal fusion is essential for the retention of *Trypanosoma cruzi* inside host cells. J.Exp.Med. 2004;200:1135-1143.

309. Tardieux I, Webster P, Ravesloot J et al. Lysosome recruitment and fusion are early events required for trypanosome invasion of mammalian cells. Cell 1992;71:1117-1130.

310. Ming M, Ewen ME, Pereira ME. Trypanosome invasion of mammalian cells requires activation of the TGF beta signaling pathway. Cell 1995;82:287-296.

311. Hall BS, Pereira MA. Dual role for transforming growth factor beta-dependent signaling in *Trypanosoma cruzi* infection of mammalian cells. Infect.Immun. 2000;68:2077-2081.

312. Woolsey AM, Burleigh BA. Host cell actin polymerization is required for cellular retention of *Trypanosoma cruzi* and early association with endosomal/lysosomal compartments. Cell Microbiol. 2004;6:829-838.

313. Burleigh BA, Andrews NW. The mechanisms of *Trypanosoma cruzi* invasion of mammalian cells. Annu.Rev.Microbiol. 1995;49:175-200.

314. Cestari IS, Evans-Osses I, Freitas JC, Inal JM, Ramirez MI. Complement C2 receptor inhibitor trispanning confers an increased ability to resist complement-mediated lysis in *Trypanosoma cruzi*. J.Infect.Dis. 2008;198:1276-1283.

315. Tomlinson S, Pontes de Carvalho LC, Vandekerckhove F, Nussenzweig V. Role of sialic acid in the resistance of *Trypanosoma cruzi* trypomastigotes to complement. J.Immunol. 1994;153:3141-3147.

316. Faille D, Combes V, Mitchell AJ et al. Platelet microparticles: a new player in malaria parasite cytoadherence to human brain endothelium. FASEB J. 2009;23:3449-3458.

317. Pilzer D, Gasser O, Moskovich O, Schifferli JA, Fishelson Z. Emission of membrane vesicles: roles in complement resistance, immunity and cancer. Springer Semin.Immunopathol. 2005;27:375-387.

318. Combes V, Taylor TE, Juhan-Vague I et al. Circulating endothelial microparticles in malawian children with severe falciparum malaria complicated with coma. JAMA 2004;291:2542-2544.

319. Redman CW, Sargent IL. Circulating microparticles in normal pregnancy and pre-eclampsia. Placenta 2008;29 Suppl A:S73-S77.

320. Baran J, Baj-Krzyworzeka M, Weglarczyk K et al. Circulating tumour-derived microvesicles in plasma of gastric cancer patients. Cancer Immunol.Immunother. 2010;59:841-850.

321. Baj-Krzyworzeka M, Szatanek R, Weglarczyk K, Baran J, Zembala M. Tumour-derived microvesicles modulate biological activity of human monocytes. Immunol.Lett. 2007;113:76-82.

322. Costa VM, Torres KC, Mendonca RZ et al. Type I IFNs stimulate nitric oxide production and resistance to *Trypanosoma cruzi* infection. J.Immunol. 2006;177:3193-3200.

323. Raujo-Jorge TC, Waghabi MC, Soeiro MN et al. Pivotal role for TGF-beta in infectious heart disease: The case of *Trypanosoma cruzi* infection and consequent Chagasic myocardiopathy. Cytokine Growth Factor Rev. 2008;19:405-413.

324. Waghabi MC, Keramidas M, Bailly S et al. Uptake of host cell transforming growth factor-beta by *Trypanosoma cruzi* amastigotes in cardiomyocytes: potential role in parasite cycle completion. Am.J.Pathol. 2005;167:993-1003.

325. Waghabi MC, Coutinho CM, Soeiro MN et al. Increased *Trypanosoma cruzi* invasion and heart fibrosis associated with high transforming growth factor beta levels in mice deficient in alpha(2)-macroglobulin. Infect.Immun. 2002;70:5115-5123.

326. Raujo-Jorge TC, Waghabi MC, Hasslocher-Moreno AM et al. Implication of transforming growth factor-beta1 in Chagas disease myocardiopathy. J.Infect.Dis. 2002;186:1823-1828.

327. Comis A, Easterbrook-Smith SB. Inhibition of serum complement haemolytic activity by lipid vesicles containing phosphatidylserine. FEBS Lett. 1986;197:321-327.

328. Gonzalez LJ, Gibbons E, Bailey RW et al. The influence of membrane physical properties on microvesicle release in human erythrocytes. PMC Biophys. 2009;2:7.

329. Allan D, Thomas P. Ca2+-induced biochemical changes in human erythrocytes and their relation to microvesiculation. Biochem.J. 1981;198:433-440.

330. Song HO, Ahn MH, Ryu JS et al. Influence of calcium ion on host cell invasion and intracellular replication by *Toxoplasma gondii*. Korean J.Parasitol. 2004;42:185-193.

331. Kalra A, Dubey ML, Ganguly NK, Mahajan RC. Effect of nifedipine on calcium status and chemiluminescence response of phagocytes during *Plasmodium berghei* infection in mice. J.Pharm.Pharmacol. 1993;45:540-544.

332. Zhou D, Mooseker MS, Galan JE. Role of the *S. typhimurium* actin-binding protein SipA in bacterial internalization. Science 1999;283:2092-2095.

333. Cossart P. Host/pathogen interactions. Subversion of the mammalian cell cytoskeleton by invasive bacteria. J.Clin.Invest 1997;99:2307-2311.

334. Finlay BB, Cossart P. Exploitation of mammalian host cell functions by bacterial pathogens. Science 1997;276:718-725.

335. Isberg RR, Tran Van NG. Binding and internalization of microorganisms by integrin receptors. Trends Microbiol. 1994;2:10-14.

336. Dramsi S, Cossart P. Intracellular pathogens and the actin cytoskeleton. Annu.Rev.Cell Dev.Biol. 1998;14:137-166.

337. Sansonetti PJ. Rupture, invasion and inflammatory destruction of the intestinal barrier by Shigella, making sense of prokaryote-eukaryote cross-talks. FEMS Microbiol.Rev. 2001;25:3-14.

338. Watarai M, Makino S, Michikawa M et al. Macrophage plasma membrane cholesterol contributes to *Brucella abortus* infection of mice. Infect.Immun. 2002;70:4818-4825.

339. Gatfield J, Pieters J. Essential role for cholesterol in entry of mycobacteria into macrophages. Science 2000;288:1647-1650.

340. Costa MJ, Song Y, Macours P et al. Sphingolipid-cholesterol domains (lipid rafts) in normal human and dog thyroid follicular cells are not involved in thyrotropin receptor signaling. Endocrinology 2004;145:1464-1472.

341. Manes S, del RG, Martinez A. Pathogens: raft hijackers. Nat.Rev.Immunol. 2003;3:557-568.

342. Vieira FS, Correa G, Einicker-Lamas M, Coutinho-Silva R. Host-cell lipid rafts: a safe door for micro-organisms? Biol.Cell 2010;102:391-407.

343. Hartlova A, Cerveny L, Hubalek M, Krocova Z, Stulik J. Membrane rafts: a potential gateway for bacterial entry into host cells. Microbiol.Immunol. 2010;54:237-245.

344. Alfsen A, Iniguez P, Bouguyon E, Bomsel M. Secretory IgA specific for a conserved epitope on gp41 envelope glycoprotein inhibits epithelial transcytosis of HIV-1. J.Immunol. 2001;166:6257-6265.

345. Manes S, del RG, Lacalle RA et al. Membrane raft microdomains mediate lateral assemblies required for HIV-1 infection. EMBO Rep. 2000;1:190-196.

346. Peterlin BM, Trono D. Hide, shield and strike back: how HIV-infected cells avoid immune eradication. Nat.Rev.Immunol. 2003;3:97-107.

347. Nguyen DH, Hildreth JE. Evidence for budding of human immunodeficiency virus type 1 selectively from glycolipid-enriched membrane lipid rafts. J.Virol. 2000;74:3264-3272.

348. Liu NQ, Lossinsky AS, Popik W et al. Human immunodeficiency virus type 1 enters brain microvascular endothelia by macropinocytosis dependent on lipid rafts and the mitogen-activated protein kinase signaling pathway. J.Virol. 2002;76:6689-6700.

349. Fullekrug J, Simons K. Lipid rafts and apical membrane traffic. Ann.N.Y.Acad.Sci. 2004;1014:164-169.

350. Krauss K, Altevogt P. Integrin leukocyte function-associated antigen-1-mediated cell binding can be activated by clustering of membrane rafts. J.Biol.Chem. 1999;274:36921-36927.

351. Bodin S, Soulet C, Tronchere H et al. Integrin-dependent interaction of lipid rafts with the actin cytoskeleton in activated human platelets. J.Cell Sci. 2005;118:759-769.

352. Simons K, Toomre D. Lipid rafts and signal transduction. Nat.Rev.Mol.Cell Biol. 2000;1:31-39.

353. van KY, Weder P, Heije K, Figdor CG. Extracellular Ca2+ modulates leukocyte function-associated antigen-1 cell surface distribution on T lymphocytes and consequently affects cell adhesion. J.Cell Biol. 1994;124:1061-1070.

354. Scibelli A, Roperto S, Manna L et al. Engagement of integrins as a cellular route of invasion by bacterial pathogens. Vet.J. 2007;173:482-491.

355. Kerr JR, Taylor GW, Rutman A et al. *Pseudomonas aeruginosa* pyocyanin and 1-hydroxyphenazine inhibit fungal growth. J.Clin.Pathol. 1999;52:385-387.

356. Agerer F, Lux S, Michel A et al. Cellular invasion by *Staphylococcus aureus* reveals a functional link between focal adhesion kinase and cortactin in integrin-mediated internalisation. J.Cell Sci. 2005;118:2189-2200.

357. Frankel G, Lider O, Hershkoviz R et al. The cell-binding domain of intimin from enteropathogenic *Escherichia coli* binds to beta1 integrins. J.Biol.Chem. 1996;271:20359-20364.

358. Evans DJ, Maltseva IA, Wu J, Fleiszig SM. *Pseudomonas aeruginosa* internalization by corneal epithelial cells involves MEK and ERK signal transduction proteins. FEMS Microbiol.Lett. 2002;213:73-79.

359. Unkmeir A, Latsch K, Dietrich G et al. Fibronectin mediates Opc-dependent internalization of *Neisseria meningitidis* in human brain microvascular endothelial cells. Mol.Microbiol. 2002;46:933-946.

360. Watarai M, Funato S, Sasakawa C. Interaction of Ipa proteins of *Shigella flexneri* with alpha5beta1 integrin promotes entry of the bacteria into mammalian cells. J.Exp.Med. 1996;183:991-999.

361. Idone V, Tam C, Goss JW et al. Repair of injured plasma membrane by rapid Ca2+-dependent endocytosis. J.Cell Biol. 2008;180:905-914.

362. Andrews NW. Lysosomes and the plasma membrane: trypanosomes reveal a secret relationship. J.Cell Biol. 2002;158:389-394.

363. Burleigh BA, Andrews NW. Signaling and host cell invasion by *Trypanosoma cruzi*. Curr.Opin.Microbiol. 1998;1:461-465.

364. Silva-Monteiro E, Reis LL, Kenji NO et al. Altered expression of galectin-3 induces cortical thymocyte depletion and premature exit of immature thymocytes during *Trypanosoma cruzi* infection. Am.J.Pathol. 2007;170:546-556.

365. Fernandes MC, Cortez M, Geraldo Yoneyama KA et al. Novel strategy in *Trypanosoma cruzi* cell invasion: implication of cholesterol and host cell microdomains. Int.J.Parasitol. 2007;37:1431-1441.

366. Wary KK, Mariotti A, Zurzolo C, Giancotti FG. A requirement for caveolin-1 and associated kinase Fyn in integrin signaling and anchorage-dependent cell growth. Cell 1998;94:625-634.

367. Rankin S, Isberg RR, Leong JM. The integrin-binding domain of invasin is sufficient to allow bacterial entry into mammalian cells. Infect.Immun. 1992;60:3909-3912.

368. Laucella SA, Riarte A, Prado N, Zapata J, Segura EL. alpha 4 Integrins and sialyl Lewis x modulation in chronic Chagas disease: further evidence of persistent immune activation. Scand.J.Immunol. 2001;53:514-519.

369. Miyake K, Tanaka T, McNeil PL. Lectin-based food poisoning: a new mechanism of protein toxicity. PLoS.One. 2007;2:e687.

370. Rodriguez A, Webster P, Ortego J, Andrews NW. Lysosomes behave as Ca2+-regulated exocytic vesicles in fibroblasts and epithelial cells. J.Cell Biol. 1997;137:93-104.

371. Rodriguez A, Samoff E, Rioult MG, Chung A, Andrews NW. Host cell invasion by trypanosomes requires lysosomes and microtubule/kinesin-mediated transport. J.Cell Biol. 1996;134:349-362.

372. Lin GC, Rurangirwa JK, Koval M, Steinberg TH. Gap junctional communication modulates agonist-induced calcium oscillations in transfected HeLa cells. J.Cell Sci. 2004;117:881-887.

373. sazuma-Nakamura Y, Dai P, Harada Y et al. Cx43 contributes to TGF-beta signaling to regulate differentiation of cardiac fibroblasts into myofibroblasts. Exp.Cell Res. 2009;315:1190-1199.

374. Dai P, Nakagami T, Tanaka H, Hitomi T, Takamatsu T. Cx43 mediates TGF-beta signaling through competitive Smads binding to microtubules. Mol.Biol.Cell 2007;18:2264-2273.

375. Andrade LO, Andrews NW. The *Trypanosoma cruzi*-host-cell interplay: location, invasion, retention. Nat.Rev.Microbiol. 2005;3:819-823.

376. Woolsey AM, Sunwoo L, Petersen CA et al. Novel PI 3-kinase-dependent mechanisms of trypanosome invasion and vacuole maturation. J.Cell Sci. 2003;116:3611-3622.

377. Silva JS, Aliberti JC, Martins GA et al. The role of IL-12 in experimental *Trypanosoma cruzi* infection. Braz.J.Med.Biol.Res. 1998;31:111-115.

378. Medina FA, Cohen AW, de Almeida CJ et al. Immune dysfunction in caveolin-1 null mice following infection with *Trypanosoma cruzi* (Tulahuen strain). Microbes.Infect. 2007;9:325-333.

379. Roffe E, Oliveira F, Souza AL et al. Role of CCL3/MIP-1alpha and CCL5/RANTES during acute *Trypanosoma cruzi* infection in rats. Microbes.Infect. 2010

380. Lima MF, Zhang Y, Villalta F. Beta-chemokines that inhibit HIV-1 infection of human macrophages stimulate uptake and promote destruction of *Trypanosoma cruzi* by human macrophages. Cell Mol.Biol.(Noisy.-le-grand) 1997;43:1067-1076.

381. McNeil PL. Repairing a torn cell surface: make way, lysosomes to the rescue. J.Cell Sci. 2002;115:873-879.

382. Nomura S, Ozaki Y, Ikeda Y. Function and role of microparticles in various clinical settings. Thromb.Res. 2008;123:8-23.

383. Iida K, Whitlow MB, Nussenzweig V. Membrane vesiculation protects erythrocytes from destruction by complement. J.Immunol. 1991;147:2638-2642.

384. Miyoshi H, Umeshita K, Sakon M et al. Calpain activation in plasma membrane bleb formation during tert-butyl hydroperoxide-induced rat hepatocyte injury. Gastroenterology 1996;110:1897-1904.

385. Viaud S, Thery C, Ploix S et al. Dendritic cell-derived exosomes for cancer immunotherapy: what's next? Cancer Res. 2010;70:1281-1285.

386. Dimberg A, Oberg F. Retinoic acid-induced cell cycle arrest of human myeloid cell lines. Leuk.Lymphoma 2003;44:1641-1650.

387. Chakrabarti S, Andrade LO, Andrews NW. *Trypanosoma cruzi* invades synaptotagmin VII-deficient cells by a PI-3 kinase independent pathway. Mol.Biochem.Parasitol. 2005;141:125-128.

388. Jaiswal JK, Andrews NW, Simon SM. Membrane proximal lysosomes are the major vesicles responsible for calcium-dependent exocytosis in nonsecretory cells. J.Cell Biol. 2002;159:625-635.

389. Waghabi MC, Keramidas M, Feige JJ, raujo-Jorge TC, Bailly S. Activation of transforming growth factor beta by *Trypanosoma cruzi*. Cell Microbiol. 2005;7:511-517.

Trypanosoma cruzi utilization of host cell vesicle release aids invasion

Ephraim A. Ansa-Addo,[1] Igor Cestari,[2,*] Paras Pathak,[1,3] Marcel I. Ramirez,[2] Jameel M. Inal[1]†

[1]Cellular and Molecular Immunology Research Centre, School of Human Sciences, Faculty of Life Sciences, London Metropolitan University, 166-220 Holloway Road, London, N7 8DB, UK.

[2]Instituto Oswaldo Cruz - Fiocruz, Laboratório de Biologia Molecular de Parasitas e Vetores, Rio de Janeiro, 21040-900, Brazil.

[3]MRC Harwell, Harwell Science and Innovation Campus, Oxfordshire, OX11 0RD, UK.

*Present address: Seattle Biomedical Research Institute, Seattle-WA 98109, USA.

†To whom correspondence should be addressed. Email: j.inal@londonmet.ac.uk

Abstract

In addition to their pivotal role in immune evasion and inflammatory responses, plasma membrane-derived vesicles (PMVs) participate in pathogen invasion. We investigated the role of PMVs in *Trypanosoma cruzi* invasion of cells. We identified that *T. cruzi*-mediated increase in host cell intracellular calcium ($[Ca^{2+}]_i$), resulting in depolymerization of the actin cytoskeleton and PMV release, is a necessary precursor for parasite invasion. Furthermore, we show that *T. cruzi* triggers the release of PMVs through lipid raft domains, integrins, phosphoinositol 3-kinases and Ca^{2+} channels including stretch-activated channels (SACs). We present evidence that *T. cruzi*-elicited release of PMVs causes damage to the integrity of the host plasma membrane, which is then exploited by the parasite for entry before lysosomal repair. Thus, these findings demonstrate a previously unappreciated role for PMVs, induced by the parasite during invasion of cells.

Trypanosoma cruzi is a flagellated, intracellular, protozoan parasite of mammals and the aetiological agent of the debilitating Chagas disease in humans. In order to survive in the host, *T. cruzi* has to invade and replicate in a variety of cell types. Parasite invasion of non-professional phagocytic cells is a complex process with many factors involved, nonetheless, two distinct entry mechanisms, both coinciding with the formation of a tight membranous vacuole in which the parasite transiently resides, have been described *(1, 2)*. *T. cruzi*-elicited $[Ca^{2+}]_i$ -elevations occur in host cells upon exposure to the parasite and this is reported as a prerequisite for cell invasion, since it is detected prior to internalization of the parasite (*3*).

An increase in host cell $[Ca^{2+}]_i$ also results in the release of plasma membrane-derived vesicles from the surface membrane of most cells (*4*). PMVs, also known as microparticles (*5*), microvesicles (*6*) or ectosomes (*7*), are small (0.1-≤1 μm in diameter), intact, membrane vesicles released constitutively or upon stimulation. The process is dependent on an increase in cytosolic Ca^{2+}, which activates calpain, leading to depolymerization of the actin cytoskeleton and release of the vesicles. PMVs have been demonstrated to be involved in several diseases including cancer (*8*), inflammatory conditions (*9*) and HIV infection (*10*). The ability of *T. cruzi* to stimulate PMV release during infection and various reports, which linked the depolymerization of the host cell cytoskeleton to invasion (*11, 12*), prompted us to investigate the role of PMV production during parasite entry.

Whereas *T. cruzi*, an intracellular parasite, induced PMV release from HeLa cells that could be inhibited by Ca^{2+} chelation, the extracellular trypanosomatid, *T. brucei* (Fig. 1A) did not. Interestingly, *Salmonella enterica serovar typhimurium* (ST), which also causes a Ca^{2+}-mediated depolymerization of the actin cytoskeleton (*13*), stimulated the release of PMVs from HeLa cells; however, this was not the case with the non-invasive mutant strain, SPI1 (SL1344, SPI1) (fig. S1). *T. cruzi* induction of PMVs was dose-dependent (Fig. 1B).

Transmission electron microscopy of HeLa cell-derived PMVs ranged from 0.1 to 1 μm in diameter (Fig. 1C and D), and as such cannot be apoptotic blebs, which would be larger; respective inset panels show PMVs and exosomes purified separately by differential centrifugation.

As other vesicles including exosomes, released when multivesicular bodies fuse with the plasma membrane (PM) (Fig. 1E), are secreted from cells including monocytes (*14*) in a Ca^{2+}-dependent manner, we wanted to confirm that PMVs were being isolated. We recently showed that stimulation of THP-1 cells with 10% normal human serum (NHS) causes the release of PMVs due to sublytic complement deposition and membrane attack complex formation with subsequent influx of Ca^{2+} (*15*). Moreover, these PMVs detected were not from the NHS stimulus itself, as PMV levels in commercial NHS were negligible (*15*). Such 'constitutive' release of PMVs from cells in culture can be inhibited by Ca^{2+}-chelation (EGTA), or with classic inhibitors of PMV release including the Rho-

associated kinase (ROCK) inhibitor, Y-27632 and the calpain inhibitor, calpeptin (fig. S2A). Isolated PMVs also displayed the typical dot plot distribution after flow cytometry analysis, and were positive for Annexin V (AnV)-PE (a hallmark characteristic) binding (fig. S2B and inset), indicating surface phosphatidylserine (PS) as reported previously (*15, 16*). We also detected by immunoblotting that PMVs were characteristically enriched for actin and other surface molecules (fig. S2C).

Expression of PS on the cell surface was also observed by immunofluorescence microscopy upon activation with *T. cruzi* metacyclic trypomastigotes (Fig. 1F) as well as the release of PS-positive PMVs (Fig. 1G). Although our PMVs isolated by the conventional differential centrifugation of cell culture supernatants produced vesicles with the expected properties, to avoid contamination with other types of vesicles, a conventional sucrose gradient was used to purify exosomes and PMVs (fig. S3) and ascertain for ourselves their respective properties. LAMP-1-positive exosomes, which were cup-shaped as seen by electron microscopy (≤100 nm diameter), of limited size distribution in forward scatter/side scatter cytometry plots and sedimenting at a peak sucrose density of 1.04-1.05 g/ml were distinguished as were the more highly PS-positive, larger PMVs. Based on the size difference between PMVs and exosomes, we developed a more convenient filtration method of isolation (fig. S4).

We investigated the possibility that PMV release plays an early role in *T. cruzi* invasion. We studied the role of lipid rafts, membrane domains consisting mainly of cholesterol and sphingolipids; also integrins, phosphoinositol 3-kinases (PI3K) and Ca^{2+} channels, since these signalling pathways activated by the parasite, are involved in the processes leading to Ca^{2+} mobilisation from intracellular compartments.

We were able to show inhibition with the cholesterol-depleting agent, methyl-β-cyclodextrin (MβCD), but not filipin, which sequesters cholesterol. The inhibition of PMV release with MβCD was regardless of whether the stimulus was *T. cruzi* (Fig. 2A) or 10% NHS (sublytic complement) (Fig. 2B). Integrin binding induced by raft clustering is proposed to modulate cytoskeleton rearrangement (*17*). During invasion, trypanosomes can interact via RGD-containing proteins with host cell integrins, resulting in increased $[Ca^{2+}]_i$ and actin depolymerization. This invasion can be blocked in the case of trypanosomal entry into macrophages (*18*), by the use of integrin antibodies, such as anti-β1 or to a lesser degree anti-α4. RGD-containing peptides, which block integrin-ligand interaction, have also been used to reduce trypomastigote invasion of cardiomyocytes (*19*), probably by competing with RGD-containing parasite proteins such as DGF-1 (*20*) or Lmsp1 (*21*). Here, we show that the RGD peptide and anti-CD49d could reduce PMV production most likely by inhibiting parasite-integrin interaction, and so limiting any resulting increase in $[Ca^{2+}]_i$/actin depolymerization. However, RGD and anti-CD49d only reduced PMV production when the stimulus was *T. cruzi*

(Fig. 2D) and not when it was sublytic complement (10% NHS) (Fig. 2E), thereby confirming that the parasite requires activation of the receptor to stimulate PMV release.

Another signalling route reported as important for *T. cruzi* invasion is PI3K (*22, 23*) and here, we show that blocking activation of this kinase with wortmannin abrogates parasite induction of PMVs (Fig. 2G), as well as NHS vesicle stimulation (Fig. 2H). Activation of the PI3K signalling pathway and subsequent depolymerization of the actin cytoskeleton, which as described here leads to PMV production, were recently suggested as necessities for *T. cruzi* invasion (*24*). Thus, wortmannin inhibition of *T. cruzi*-mediated PMV release affirms that in order to stimulate PMV production, parasites have to activate this pathway.

We also investigated whether Ca^{2+} channels and in particular stretch-activated calcium channels (SACs) are involved in the increased $[Ca^{2+}]_i$ that the *T. cruzi*-mediated PMV release causes. We employed the L-type calcium channel blockers, verapamil and nifedipine and the SACs inhibitor, gadolinium chloride ($GdCl_3$). The former two reduced PMV release significantly by ~30% and $GdCl_3$ by ~80% (Fig. 2J). No such reduction was observed when PMV release was stimulated by sublytic complement (Fig. 2K). Questions about the specificity of $GdCl_3$ as an inhibitor of membrane SAC, prompted us to use GsMTx-4, a peptide derived from the tarantula toxin, which is a potent inhibitor of SAC, specifically,

TRPC6 (*25*). We observed the inhibition of PMV release to correspond to that with $GdCl_3$ (Fig. 2J).

As blocking these receptors/domains has been shown to reduce *T. cruzi* invasion (*18, 26, 27*), and since we have shown here that they also inhibit PMV release, we wondered whether invasion and host cell PMV production could be connected. Indeed, *T. cruzi* entry was reduced upon pretreatment of HeLa cells with MβCD (Fig. 2C). Moreover, RGD, but not the control peptide, RGE, inhibited parasite entry (Fig. 2F), in a dose-dependent manner (fig. S5A). Also blocking PI3K activation inhibited *T. cruzi* entry (Fig. 2I) as, interestingly, did SAC inhibition with GsMTx-4 (Fig. 2L).

We wanted to understand whether the Ca^{2+}-mediated disruption of the actin cytoskeleton and PMV release following parasite interaction with the PM could enhance invasion. This is because rearrangement of the actin cytoskeleton in host cells caused by elevated $[Ca^{2+}]_i$ and thus the release of PMVs, have been proposed as essential for the recruitment and fusion of lysosomes required for *T. cruzi* invasion (*28*). We also report here that PMV release continued unabated after pretreatment with the actin filament disruptor, cytochalasin D (CytD) (fig. S5B) and that *T. cruzi* entry was enhanced (fig. S5C). Also since Ca^{2+}-triggered lysosomal exocytosis has been reported in the repair of PM lesions (*29*), we wondered whether PMV release elicited by *T. cruzi*, causes damage to the host PM which is then utilized by the parasite for entry before lysosomal repair. This

rationale is supported by earlier suggestions that *T. cruzi* haemolysin causes elevations in $[Ca^{2+}]_i$ so activating a lysosome-mediated PM resealing process, which parasites might then take advantage of for gaining access to the intracellular environment (*28*). The resealing mechanism which repairs lesions, occurs within seconds (*30*) primarily for survival of the host cell. Activated lysosomes fuse together and patch-up the site of damage (*29*), but other organelles may also function in a similar manner (*31, 32*). Lysosomal exocytosis can be measured after translocation to and fusion with the PM, by the appearance on the surface of wounded cells of luminal epitopes of the lysosomal glycoprotein LAMP-1 (*33*).

Sublytic complement can injure cells through the deposition of pore-forming proteins (*34*), resulting in Ca^{2+} influx and associated PMV release (*35*) leading to membrane repair (*36*). We first showed that under these conditions, a resealing inhibitor, concanavalin A (conA) (*37*) could reduce LAMP-1 surface expression from ~68% to 10% (fig. S6A) without any concomitant decrease in PMV production (fig. S6B). Subsequent experiments with *T. cruzi* in the absence of resealing inhibitors resulted in PMV release (fig. S6C) and recruitment of lysosomes to the cell surface, seen here by increased LAMP-1 fluorescence (fig. S6D). As the mechanism of PMV release (due to parasite-host interaction), which requires Ca^{2+} influx and actin rearrangement, is also the mechanism that triggers lysosomal exocytosis, we believe that inhibition of PMV release must inhibit resealing. Thus, we set up experiments to ascertain whether PMV release,

triggered by *T. cruzi* causes damage to the host cell PM that leads to lysosomal exocytosis. Calpeptin, also described as a resealing inhibitor (*38*) caused a marked reduction in PMV release (fig. S6E) and abrogated LAMP-1 surface expression (fig. S6F). This implies that by inhibiting PMV release, the host cell PM sustains less damage and so fewer lysosomes are recruited for repair.

Interestingly, conA treatment did not inhibit PMV production (due to parasite-host interaction) (fig. S6G), but nonetheless, LAMP-1 expression was reduced to 20% (fig S6H), thus confirming the specificity of conA as a potent inhibitor of lysosomal exocytosis (*37*). This suggests that the enhanced invasion after conA treatment (fig. S7A-10'), also observed with trypomastigote entry into conA-treated macrophages (*39*), was due to the reduced membrane repair. It is noteworthy, that when cells were pretreated with conA for 30 min as opposed to 10 min, invasion was reduced by 90% (fig. S7A), because most cells had lost a large part of the cytoplasm (fig. S7B). PMVs isolated after the invasion experiment were positive for Annexin V and CD63 (fig. S7C and D respectively), thus confirming that the vesicles were released from the cells and not from *T. cruzi*. Furthermore, the increase in invasion following inhibition of membrane repair, in addition to increasing infection of cells with a single parasite, also resulted in an increase in superinfection (fig. S7E). A contributing factor to the previously described decrease in invasion following wortmannin treatment (*22*), which inhibited membrane repair, may have been the reduction in PMV release which we observed (Fig. 2I), and which was not considered at the time.

To further ascertain the relationship between PMV release, parasite invasion and lysosome exocytosis, flow cytometry experiments were set up to detect host cell expression of LAMP-1 after *T. cruzi* activation, in the presence or absence of known inhibitors of PMV production. Detection of LAMP-1 fluorescence suggests the recruitment of lysosomes to the damage site and PM resealing. Cells were also labelled with propidium iodide (PI) so that the uptake of this dye would suggest an unrepaired PM breakage caused by *T. cruzi*-triggered PMV release. In the absence of inhibitors, *T. cruzi* triggered the release of PMVs (Fig. 3A) and invaded the cells (Fig. 3B). However, an increase in the LAMP-1 fluorescence (93%, lysosome exocytosis) (Fig. 3C) and the low PI uptake (10.8%) measured after 30 min (Fig. 3D), suggested damage repair. In contrast, pretreatment with $GdCl_3$ inhibited PMV release (Fig. 3E), as well as *T. cruzi* entry (Fig. 3F). Also fewer lysosomes (Fig. 3G) were recruited (LAMP-1 expression, 11%), since cells sustained limited damage (Fig. 3H). Here the reduced LAMP-1 fluorescence was not due to lysosome-mediated PM resealing, but the lack of damage due to limited PMV production.

As for $GdCl_3$, calpeptin treatment also reduced PMV production (Fig. 3I) and prevented parasite entry (Fig. 3J). Lysosome recruitment was significantly reduced (Fig. 3K, low LAMP-1 fluorescence) and PI analysis revealed an intact PM (Fig. 3L). As previously observed, pretreatment with conA failed to inhibit PMV production (Fig. 3M) after inducing cells with *T. cruzi* and parasite entry progressed unabated (Fig. 3N). However, analysis of LAMP-1 fluorescence

revealed abrogation of lysosome exocytosis (Fig. 3O) and a severely damaged PM shown by an increased (35.9%) PI uptake (Fig. 3P). This result agrees with previous findings, which suggested that conA is a specific inhibitor of lysosomal exocytosis (*37*). It also confirms that PMV production results in damage to the integrity of the host PM, which the parasite takes advantage of for entry.

Earlier reports which showed the involvement of PI3K activation in *T. cruzi* invasion and lysosomal exocytosis (*22*), prompted us to confirm this in our study. In addition to showing that PMV production is reduced after blocking PI3K activation with wortmannin (Fig. 3Q) and thus results in decreased *T. cruzi* entry (Fig. 3R), we also confirmed that fewer lysosomes (27% LAMP-1 fluorescence) are recruited (Fig. 3S) to the surface membrane due to reduced damage (5.7% PI uptake) sustained by the host PM (Fig. 3T) following pretreatment with the agent.

Further analysis revealed a positive correlation between PMV release and parasite invasion (Fig. 3U), but a negative correlation between invasion and the PM integrity (Fig. 3V). However, there was no correlation between *T. cruzi* invasion and lysosome exocytosis (Fig. 3W). These data imply that *T. cruzi* entry is highest when PMV release is at maximum and host PM integrity is severely damaged. A direct correlation was measured between PMV production and lysosome exocytosis (fig. S8A), however, PMV release and PM integrity (fig. S8B) had an inverse relationship. Likewise lysosome exocytosis negatively

correlated with PM integrity (fig. S8C). These data imply that an increase in PMV release elicited by the parasite severely damages the integrity of the host PM, which leads to lysosome exocytosis for repair.

Kinetic analysis of *T. cruzi* invasion showed that parasites invade, taking advantage of PMV release during the early stages of infection, when host cells can respond to external stress and microvesiculate (Fig. 4A). Although parasites continued to invade beyond 30 min, this invasion was independent of host PMV production; thus, additional lysosomes were not being recruited (Fig. 4B) and image (Fig. 4C a), shows reduced LAMP-1 fluorescence after 1 h. In contrast, lysosomes were recruited to the surface after 30 min incubation of HeLa cells with *T. cruzi* (Fig. 4C b). Addition of previously isolated PMVs from HeLa cell culture supernatants failed to restore *T. cruzi* invasion in presence of agents, which inhibit PMV production (Fig. 4D-F). This implies that it is the release of PMVs from the host cell that aids parasite entry, and not just the presence of PMVs. As others have also reported that *T. cruzi* invades cells via activation of TGF-β signalling (*40*), we speculate that another possible reason why HeLa cell-derived PMVs failed to enhance invasion even via the TGF-β route, could be because these cells do not express connexin43 (Cx43), a gap-junctional protein reported to mediate TGF-β signalling (*41*). It is noteworthy that although this entry strategy is independent of lysosomal exocytosis, the recruitment and fusion of lysosomes is essential for parasite retention inside the host (Fig. 4G) in order to establish an effective infection as reported previously (*22*). Here, we report a

novel entry strategy involving an early host cell response to *T. cruzi* trypomastigotes. Parasite-directed PMV production is an essential early step in the invasion process.

These observations reported here provide the basis of a model (Fig. 4H), where the active movement and the application of force exerted by *T. cruzi* to gain entry into cells, causes activation of lipid rafts, integrins, PI3K and Ca^{2+} channels, thus leading to the release of PMVs. PMV release causes a breach of the host PM integrity, which activates the exocytosis of lysosomes for resealing. However, in the presence of damaged host PM, *T. cruzi* exploits this breach for entry before lysosomal repair. Invading parasites coincide with activated lysosomes and fuse to form the parasitophorous vacuole in which they reside and initiate differentiation into amastigotes. Parasites break out of the vacuole, using a protein, Tc Tox (*42*), and complete their differentiation into amastigotes in the cytoplasm. After multiple rounds of binary division, amastigotes differentiate into trypomastigotes and break out to infect other cells. Our results provide compelling evidence of a *T. cruzi* invasion strategy involving parasite-mediated release of PMVs from host cells. It also shows that the parasite takes advantage of a host cell mechanism for gaining access to the intracellular environment and provides possible pathways that could be therapeutically targeted.

References and Notes

1. N. W. Andrews, C. K. Abrams, S. L. Slatin, G. Griffiths, *Cell* **61**, 1277 (1990).

2. M. Lopez, C. Huynh, L. O. Andrade, M. Pypaert, N. W. Andrews, *Mol. Biochem. Parasitol.* **119**, 141 (2002).

3. I. Tardieux, M. H. Nathanson, N. W. Andrews, *J. Exp. Med.* **179**, 1017 (1994).

4. J. Ratajczak, M. Wysoczynski, F. Hayek, A. Janowska-Wieczorek, M. Z. Ratajczak, *Leukemia* **20**, 1487 (2006).

5. M. C. Martinez, A. Tesse, F. Zobairi, R. Andriantsitohaina, *Am. J. Physiol. Heart Circ. Physiol* **288**, H1004 (2005).

6. K. Al-Nedawi *et al.*, *Nat. Cell Biol.* **10**, 619 (2008).

7. C. Eken *et al.*, *J. Immunol.* **180**, 817 (2008).

8. M. Wysoczynski, M. Z. Ratajczak, *Int. J. Cancer* **125**, 1595 (2009).

9. E. Boilard *et al.*, *Science* **327**, 580 (2010).

10. M. Mack *et al.*, *Nat. Med.* **6**, 769 (2000).

11. A. M. Woolsey, B. A. Burleigh, *Cell Microbiol.* **6**, 829 (2004).

12. A. Rodriguez, E. Samoff, M. G. Rioult, A. Chung, N. W. Andrews, *J. Cell Biol.* **134**, 349 (1996).

13. D. Zhou, M. S. Mooseker, J. E. Galan, *Science* **283**, 2092 (1999).

14. C. Thery *et al.*, *Nat. Immunol.* **3**, 1156 (2002).

15. E. A. Ansa-Addo *et al.*, *J. Immunol.* **185**, 5236 (2010).

16. E. Hind *et al.*, *Biochem. Biophys. Res. Commun.* **399**, 465 (2010).

17. S. Bodin *et al.*, *J. Cell Sci.* **118**, 759 (2005).

18. M. A. Fernandez, M. A. Munoz-Fernandez, M. Fresno, *Eur. J. Immunol.* **23**, 552 (1993).

19. C. M. Calvet, M. Meuser, D. Almeida, M. N. Meirelles, M. C. Pereira, *Exp. Parasitol.* **107**, 20 (2004).

20. S. Y. Kawashita, C. V. da Silva, R. A. Mortara, B. A. Burleigh, M. R. Briones, *Mol. Biochem. Parasitol.* **165**, 19 (2009).

21. A. Campos-Neto *et al.*, *Infect. Immun.* **71**, 5065 (2003).

22. L. O. Andrade, N. W. Andrews, *J. Exp. Med.* **200**, 1135 (2004).

23. A. M. Woolsey *et al.*, *J. Cell Sci.* **116**, 3611 (2003).

24. A. G. Todorov, M. Einicker-Lamas, S. L. de Castro, M. M. Oliveira, A. Guilherme, *J. Biol. Chem.* **275**, 32182 (2000).

25. N. Alessandri-Haber, O. A. Dina, X. Chen, J. D. Levine, *J. Neurosci.* **29**, 6217 (2009).

26. M. C. Fernandes *et al.*, *Int. J. Parasitol.* **37**, 1431 (2007).

27. A. Rodriguez, M. G. Rioult, A. Ora, N. W. Andrews, *J. Cell Biol.* **129**, 1263 (1995).

28. N. W. Andrews, *J. Cell Biol.* **158**, 389 (2002).

29. P. L. McNeil, *J. Cell Sci.* **115**, 873 (2002).

30. P. L. McNeil, T. Kirchhausen, *Nat. Rev. Mol. Cell Biol.* **6**, 499 (2005).

31. B. Borgonovo *et al.*, *Nat. Cell Biol.* **4**, 955 (2002).

32. J. Cerny *et al.*, *EMBO Rep.* **5**, 883 (2004).

33. A. Reddy, E. V. Caler, N. W. Andrews, *Cell* **106**, 157 (2001).

34. B. P. Morgan, A. K. Campbell, *Biochem. J.* **231**, 205 (1985).

35. P. J. Sims, E. M. Faioni, T. Wiedmer, S. J. Shattil, *J. Biol. Chem.* **263**, 18205 (1988).

36. V. Idone *et al.*, *J. Cell Biol.* **180**, 905 (2008).

37. K. Miyake, T. Tanaka, P. L. McNeil, *PLoS. One.* **2**, e687 (2007).

38. R. L. Mellgren *et al.*, *Biochim. Biophys. Acta* **1793**, 1886 (2009).

39. M. N. Meirelles, A. Martinez-Palomo, T. Souto-Padron, S. W. De, *J. Cell Sci.* **62**, 287 (1983).

40. M. C. Waghabi *et al.*, *Antimicrob. Agents Chemother.* **51**, 2905 (2007).

41. P. Dai, T. Nakagami, H. Tanaka, T. Hitomi, T. Takamatsu, *Mol. Biol. Cell* **18**, 2264 (2007).

42. L. O. Andrade, N. W. Andrews, *Nat. Rev. Microbiol.* **3**, 819 (2005).

43. We thank the following individuals for helpful discussions, access to facilities and instruments or providing reagents: A. Kidger, K. Sullivan, Y. Gu, S. Lange, M. McCrossan, A Anyogu, S. Kaur and J. Sutherland. Support was provided to J.M.I. and M.I.R. (Royal Society Grant IV0871706/ LMU, UK), E.A.A. (LMU Graduate Assistantship) and I.C. (Brazilian Ministry of Education Scholarship).

Supporting Online Material

Figure Legends

Fig. 1. *Trypanosoma cruzi* induces Annexin V-positive PMVs from mammalian cells. (**A**) *T. cruzi* 5:1 (parasites to cell) ratio induces the release of PMVs from HeLa cells ($1x10^6$/well in triplicate), but *T. brucei*, an extracellular trypanosomatid, does not. (**B**) *T. cruzi* induces cells to release PMVs in a dose-dependent manner. (**C**) Electron microscopy of HeLa cell-derived PMVs after stimulation with *T. cruzi* 5:1 (parasites to cell) ratio at 37°C for 30 min. Cells release both PMVs (arrows) and exosomes (arrowheads) after stimulation – insets show purified PMVs. Scale bar= 500 nm and 100 nm (insets). (**D**) Released PMVs (arrows) and exosomes (arrowheads) from activated cells – inset shows cup-shaped exosomes. Scale bar= 100 nm. (**E**) Fusion of multivesicular body (MVB) with plasma membrane and release of exosomes by exocytosis. Asterisk indicates intravesicular lumen of fused the MVB. Bar = 200 nm. (**F and G**) HeLa cells release PMVs observed by immunofluorescence microscopy after labelling with Annexin V Alexafluor 488. PS-positive PMVs (green dots) are released after stimulating with *T. cruzi*. Scale bar= 20 µm. Data represents the mean ± SD of duplicate experiments performed in triplicate. $^*p < 0.01$ was considered statistically significant.

Fig. 2. *T. cruzi* elicit PMV release via signalling pathways activated by Ca^{2+} mobilization from intracellular compartments. (**A**) Disruption of lipid rafts with the cholesterol-depleting agent, MβCD (5 mM), reduces PMV release after stimulating with *T. cruzi*. (**B**) PMV release due to NHS induction also reduces

when cholesterol is depleted; however, no such reduction occurs when cells are pretreated with cholesterol-sequestering agent, filipin. (**C**) Pretreatment with MβCD but not filipin inhibits parasite entry. (**D-F**) Blocking integrin activation prevents *T. cruzi*-elicited release of PMVs. However, PMV release due to sublytic complement (10% NHS) continues unabated and parasite entry is abrogated. (**G-I**) Pretreatment of cells with wortmannin (40 nM) reduces PMV release regardless of whether the stimulus is *T. cruzi* or sublytic complement and also inhibits parasite invasion of cells. (**J-L**) Blocking activation of calcium channels, including stretch-activated channels, inhibits PMV release after *T. cruzi* stimulation for 30 min at 37°C, but not after inducing cells with NHS. Data represents the mean ± SD of triplicate experiments performed in triplicate. $^{*}p < 0.05$, $^{**}p < 0.01$ and $^{***}p < 0.001$ were considered statistically significant.

Fig. 3. *T. cruzi* exploits damage to the host cell PM integrity, caused by PMV release. **(A-D)** In the absence of inhibitors of microvesiculation, *T. cruzi* triggers (37°C for 30 min) PMV release and invades cells. PMV release activates lysosomal exocytosis to the plasma membrane (PM), detected as LAMP-1 fluorescence. Recruited lysosomes reseal any damage sustained by the host PM, leading to a low propidium iodide (PI) uptake. Pretreatment (37°C for 30 min) with $GdCl_3$ (200 μM) inhibits PMV release (**E**) and parasite invasion (**F**). The reduction in LAMP-1 fluorescence (**G**) is due to the lack of PMV release, thus, the host cells' PM integrity is relatively intact, hence the low PI uptake (**H**). Calpeptin (20 μM) also inhibits PMV release (**I**), and abrogates parasite entry (**J**).

Reduction in LAMP-1 fluorescence (**K**) implies recruitment of fewer lysosomes and low PI uptake (**L**) indicates an intact PM. (**M**) PMV release continues unabated after pretreatment with conA and *T. cruzi* invades successfully (**N**). Detection of a low LAMP-1 fluorescence (**O**) indicates an unrepaired PM lesion, thus, leading to an increase in PI uptake (**P**). Wortmannin reduces PMV release (**Q**) and abrogates *T. cruzi* invasion (**R**). Reduction in PMV release means fewer lysosomes are recruited for repair (**S**) and host PM integrity remains relatively intact (**T**). (**U**) Correlation analysis shows that *T. cruzi* invasion is maximal, when host PMV release is highest. (**V**) *T. cruzi* invasion is inversely proportional to the integrity of the host PM, such that more parasites invade when the host PM integrity is severely damaged. (**W**) However, *T. cruzi* invasion and lysosome exocytosis are not directly proportional. Data represents the mean ± SD of duplicate experiments performed in triplicate. $^{**}p < 0.01$ and $^{***}p < 0.001$ were considered statistically significant.

Fig. 4. *T. cruzi* invasion via the PMV release mechanism occurs early during infection. (**A**) Kinetic analysis of PMV release (lines) and *T. cruzi* invasion (bars) before and after pretreatment (37°C for 30 min) with calpeptin (20 μM). Without treatment (green), *T. cruzi*-elicited release of PMVs increases over the first 30 min, but parasite invasion continues beyond this point. However, calpeptin (red) inhibits PMV release and abrogates parasite entry. (**B**) Kinetic analysis shows that *T. cruzi* activation of lysosome exocytosis occurs early (within 30 min) during infection when PMVs are released. (**C**) *T. cruzi* invasion after 1 h (**a**) did not

cause further LAMP-1 activation. In contrast, high LAMP-1 fluorescence (**b**) was detected where the parasite invades during PMV release (30 min). (**D-F**) Addition of HeLa cell-derived PMVs did not enhance *T. cruzi* invasion of cells. (**G**) After 5 h incubation with parasites, cells were permeabilised with 0.1% Triton X-100 and stained with anti-LAMP-1 Alexafluor 488 to observe *T. cruzi* inside parasitophorous vacuoles. (**H**) Model of *T. cruzi* invasion of cells. Scale bar= 20 µm. Data represents the mean ± SD of triplicate experiments performed in triplicate. ***$p < 0.001$ was considered statistically significant. Parasites are not drawn to scale.

Supporting Online Material

Materials and Methods

Antibodies and Reagents

GsMTx-4 was purchased from Peptide Int. Inc., and $GdCl_3$ was obtained from Reaction Product, Cheshire, UK. Calpeptin was obtained from Merck Biosciences and anti-LAMP-1 Alexafluor 488 was purchased from Santa Cruz Biotechnology, Inc. The anti-Annexin V Alexafluor 488 was purchased from Invitrogen. All other chemical agents were purchased from Sigma-Aldrich (St. Louis, MO) and Fisher Scientific (Pittsburgh, PA) unless otherwise stated.

Cell culture

All cells used in the study were maintained in growth medium (GM) containing RPMI 1640 supplemented with 10% FBS, 100 U/ml penicillin, and 100 mg/ml streptomycin. In addition, cells were occasionally maintained for a week in GM supplemented with 1% kanamycin at 37°C in a humidified atmosphere of 5% CO_2. Exponentially growing cells were counted and viability was determined using the Guava EasyCyte flow cytometer (ViaCount assay; Guava Technologies, Hayward, CA). Throughout, after three days in culture, cells were split 1:4 and only cultures with at least 95% viability were used.

T. cruzi culture and purification of metacyclic trypomastigote forms

T. cruzi epimastigotes, strain Silvio X10/6, were cultured to exponential growth phase in liver infusion tryptose (LIT) liquid medium *(S1)* with 10% heat-

inactivated (HI) FBS at 28°C. Metacyclic trypomastigote forms were obtained and purified with slight modifications, according to the method of Sousa *et al* (1983) *(S2)*. Briefly, epimastigotes in the stationary phase were incubated at 28°C for 2 h in triatomine urine medium (TAU; 190 mM NaCl, 17 mM KCl, 2 mM $CaCl_2$, 2 mM $MgCl_2$, 8 mM phosphate buffer pH 6.0) and subsequent incubation in TAU3AAG medium (TAU supplemented with 10 mM L-proline, 50 mM L-glutamate, 2 mM L-aspartate, 10 mM glucose) for 3 days. In some experiments epimastigotes in the late stationary phase differentiated into metacyclic trypomastigote forms after incubation at 28°C for five days in LIT medium. Metacyclic forms were identified under the light microscope, and by DAPI-staining to observe the position of the nucleus and kinetoplast. Once confirmed, metacyclic forms were purified on the day of the experiment. Parasites were harvested by centrifugation (4,000 rpm, 10 min; A-4-62 swing-out rotor, using 5810R centrifuge, Eppendorf) and resuspended in PSG (73 mM NaCl, 1% glucose, 5 mM sodium phosphate, pH 8.0). Metacyclic forms were separated in diethylaminoethyl (DEAE)-52-cellulose, resuspended in PSG after centrifugation and counted using a haemocytometer. The required number of parasites was obtained and stained with PKH27 dye (Sigma-Aldrich) according to the manufacturer's instructions.

Cell treatments

HeLa cells were plated at $1x10^5$ cells/well in GM into 12-well plates containing sterilized 18-mm round coverslips and incubated at 37°C and 5% CO_2 for 24 h.

Cells were washed twice with serum-free RPMI 1640 (SFR) without phenol red and preincubated at 37°C for 30 min with various agents including the lipid raft inhibitors (MβCD, 5 mM; filipin, 5 µg/ml; chlorpromazine, 25 µg/ml), PI3K inhibitor (Wortmannin, 40 nM), calcium channel blockers (GsMTx-4, 20 µg/ml; $GdCl_3$, 200 µM; Verapamil, 200 µM and Nifedipine, 200 µM) and integrin inhibitors (RGD peptide, 100-500 µg/ml; RGE peptide, 200 µg/ml; α-CD49d, 10 µg/ml). The latter was preincubated with cells at 37°C for 10 min. In some experiments HeLa cells were pretreated separately with the calpain inhibitor, calpeptin (20 µM; 37°C, 30 min), concanavalin A (20 µg/ml) [room temperature (RT), 10 min], Wheat gelatine agglutinin (WGA, 20 µg/ml; RT, 10 min) and cytochalasin D (10 µM; 37°C, 10 min). All agents were removed by washing cells twice with SFR prior to the addition of parasites or normal human serum (NHS). In addition, EGTA (5 mM) was used in most induction experiments as a negative control.

In vitro invasion assays

Semiconfluent HeLa cells in SFR were infected *in vitro* with metacyclic trypomastigotes using a modification of a method described earlier *(S3)*. HeLa cells pretreated or not with the agents mentioned earlier, were infected by the addition of metacyclic trypomastigotes at a 5:1 (parasites to cell) ratio for 3 h or 30 min in some experiments and incubated at 37°C in a humidified atmosphere of 5% CO_2. Cells were then washed three times with PBS, fixed for 10 min at RT with 4% paraformaldehyde (PFA) and washed a further three times with PBS. Coverslips were mounted on microscope slides with DAPI-Vectashield medium

(Vector Laboratories, Burlingame, CA), and images were collected using a fluorescence microscope (Bright field, IX81 motorized, inverted fluorescence microscope; Olympus). The number of intracellular parasites was determined by counting at least 300 cells in all coverslips. Also to check for multiple infections by the parasites, the number of infected cells was also counted. Data was normalised to 100.

Flow cytometry analysis

Trypsinized HeLa cells ($1x10^6$/well in triplicate) resuspended in SFR were left untreated or pretreated with calpeptin, conA, $GdCl_3$, WGA and wortmannin, and washed twice with PBS as described. Cells were resuspended in Ringer's solution (138 mM NaCl, 2.7 mM KCl, 1.06 mM $MgCl_2$, 1.8 mM $CaCl_2$, 12.4 mM HEPES and 5.6 mM D-glucose [pH 7.4]) and stimulated by addition of metacyclic trypomastigotes at a 5:1 (parasites to cells) ratio or 10% NHS, and incubated at 37°C for 30 min. Cells were immediately fixed with 4% PFA after 30 min and stained in the dark with 10 µg/ml anti-LAMP-1 Alexafluor 488 diluted in PBS with 3% BSA, at 4°C for 1 h with shaking. Samples were washed three times with PBS and labelled with 50 µg/ml of propidium iodide (PI) at RT for 1 min. After washing, cells were resuspended in PBS with 1% BSA and analysed by flow cytometry (ExpressPlus, EasyCyte, Guava Technologies) for lysosome exocytosis.

Purification and characterization of PMVs from conditioned medium

Conditioned medium from cells not stimulated (control) or stimulated with 10% NHS, *T. cruzi* (5:1, parasites to cell) or *S. typhimurium* (5:1, bacteria per cell), after pretreatment or not with various inhibiting agents was collected, and PMVs were isolated as described previously *(S4)*. Briefly, cells were pelleted at 200 *g* for 5 min and the resulting supernatant was centrifuged twice at 4,000 *g* for 30 min to remove cell debris. The supernatant was sonicated for 5 x 1 min in a sonicating water bath (Townson and Mercer Ltd, Croydon) to disperse aggregated exosomes and centrifuged at 25,000 *g* for 2 h to pellet PMVs. Pelleted PMVs were washed once by resuspending in PBS and centrifuging at 25,000 *g* for 2 h. The PMV pellet was resuspended in PBS and quantified on a flow cytometer (ExpressPlus, EasyCyte, Guava Technologies). For some experiments, PMVs were stained with Annexin V-FITC (R&D Systems, UK) for PS expression and anti-CD63-PE antibody. In some experiments PMVs and exosomes were isolated by a reverse filtration method.

Isolation of PMVs and exosomes by reverse filtration method

Cell-free and debris-free culture supernatants were filtered through a 0.22 µm pore size membrane filter. After filtration of the supernatant, the membrane filter was reversed and PMVs bound to the surface were removed by washing with PBS. Isolated PMVs were pelleted by centrifugation at 25,000 *g* for 30 min and where exosomes were required, the resultant filtrate was ultracentrifuged at

160,000 *g* for 16 h. Isolated exosomes and PMVs were analysed by flow cytometry and their dot plot distributions compared.

Sucrose gradient

Cell-free and debris-free conditioned medium was sonicated in a sonicating water bath for 5 x 1 min and ultracentrifuged at 160,000 *g* for 16 h to pellet all microvesicles (PMVs and exosomes). In order to isolate PMVs and exosomes, samples were subjected to sucrose equilibrium centrifugation. Briefly, microvesicle pellets were resuspended in 2 ml of PBS and transferred to the bottom of a SW41 centrifugation tube (Beckman Coulter, Fullerton, CA). A 10-40% (w/v) discontinuous sucrose density gradient was layered on top, and the gradient was centrifuged at 30,000 *g* for 1 h. Fractions of 1 ml were collected from the bottom of the tube, and the density of each fraction was determined using a refractometer (Schmidt and Haensch, Berlin, Germany).

Transmission electron microscopy

Trypsinized HeLa cells ($5x10^6$/ml) were resuspended in prewarmed (37°C) SFR supplemented with 0.5 mM $CaCl_2$. Cells either stimulated (5% NHS or *T. cruzi*, 5:1 ratio) or not (control) were fixed with 0.1 M fixative solution (3% glutaraldehyde in 0.1 M sodium cacodylate buffer [pH 7.2]). Samples were post-fixed by incubation at 0°C for 1 h in 1% osmium tetroxide solution (2% osmium tetroxide (Sigma-Aldrich) 1:1 0.2 M sodium cacodylate buffer) and block stained by resuspending in 1% aqueous uranyl acetate (overnight on a rocker). Samples

were resuspended in 1% hot agarose, dehydrated in an ascending ethanol series (from 70% to 100% absolute ethanol, v/v, 30 min each time) and washed twice (30 min each) with propylene oxide (Agar Scientific, Essex, UK). Sample was infiltrated with a 1:1 mixture of propylene oxide: Agar resins (mixture of 4.8 g agar resin, 3.6 g MNA, 1.9 g DDSA and 0.2 g BDMA, Agar Scientific) and left rocking overnight at room temperature. Infiltrated samples were embedded in capsules using applicators and polymerized at 60°C for 24 h.

In other experiments, pure isolated PMVs and exosomes were separately fixed and infiltrated with agar resin. Ultra thin sections were cut on a Leica Ultracut R ultra microtome (Leica Microsystems, Deerfield, IL) and stained for 10 minutes in Reynolds lead citrate stain *(S5)*. The sections were examined on a Jeol JEM – 1200 Ex II electron microscope (JOEL, Peabody, MA).

For negative staining, microvesicles isolated using the reverse filtration or sucrose gradient method were stained with 2% aqueous uranyl acetate or 2% phosphotungstic acid (pH 6.8) plus aqueous bacitracin. Samples were placed on 400 mesh copper grids with a Pioloform support film (grids and Pioloform powder from Agar Scientific) and pretreated with 1% aqueous Alcian Blue 8GX for 10 min. Digital images were recorded using the AMT Digital camera (Advanced Microscopy Techniques Corp. 3 Electronics Ave., Danvers, MA 01923 USA, supplied by Deben UK limited, IP30 9QS).

Immunostaining and Fluorescent microscopy analysis

HeLa cells ($1x10^5$/well) were seeded overnight into 12-well plates containing 18-mm coverslips. After washing twice with PBS, cells were placed into Ringer's solution and either left untreated, or pretreated with calpeptin or conA and stimulated with *T. cruzi* (5:1 ratio) at 37°C for 30 min or 1 h for some experiments. Cells were immediately fixed with 4% PFA and washed several times with PBS, before labelling with anti-LAMP-1 Alexafluor 488 or Annexin V-Alexafluor 488 diluted in PBS with 3% BSA or in Annexin V binding buffer (10 mM HEPES/NaOH, 140 mM NaCl and 2.5 mM $CaCl_2$ [pH 7.4]) respectively. Plates were gently washed twice with PBS, and coverslips were mounted on microscope slides with DAPI-Vectashield medium. In order to observe *T. cruzi* inside LAMP-1 positive parasitophorous vacuole, parasites were incubated with cells for 5 h prior to fixation. Fixed cells were then permeabilised with 0.1% Triton X-100 for 10 min at room temperature prior to staining with anti-LAMP-1 Alexafluor 488. Images were collected using an Olympus IX81 inverted microscope, equipped with a monochromatic camera U-CMAD3 and subsequently coloured using the Cell^M imaging software (Olympus).

Immunoblotting analysis

Purified PMVs were lysed with lysis buffer (100 mM HEPES/KOH, 2 mM $CaCl_2$, 0.5% Triton X-100 plus cocktail protease inhibitor). The protein content of the lysates was quantified using the BCA assay kit (Pierce Biosciences) and 30 µg was resolved by SDS-PAGE on a 12% acrylamide gel. Murine antibodies were

used to detect actin, decay accelerating factor (DAF) and complement receptor 1 (CR1). The latter two were purchased from Complement Tech (Complement Technology, CA)

Quantification of cytokines/growth factors by ELISA

PMVs and exosomes were isolated from HeLa cells stimulated with *T. cruzi* 5:1 (parasites to cell) ratio at 37°C for 30 min. The concentrations of transforming growth factor (TGF)-β1 and macrophage migration inhibitory factor (MIF) were measured by using 30 µg proteins in ELISA kits (R&D Systems) according to the manufacturer's instructions.

Statistical analysis

Statistical analysis (unpaired *t* test) was performed using GraphPad Prism software, version 5.0 (GraphPad Software, San Diego, CA). Differences giving a value of $p < 0.05$ were considered statistically significant.

Supporting Figure Legends

fig. S1. Wild-type *Salmonella typhimurium* (ST) induces PMV release from cells

Trypsinized HeLa cells ($1x10^6$/well in triplicate) were stimulated with ST SL1-344 (wild-type, wt) or SP11 (non-invasive mutant strain, mut) in 5:1 bacteria to cell ratio in the presence (black bars) or absence (white bars) of EGTA (5 mM). Enhanced PMV release was measured in cells induced with wild-type ST, in contrast to the knockout mutant strain, which failed to stimulate significant PMV release. PMVs released from cells left non-induced (NI), or induced with 10% NHS in presence or absence of EGTA were used as controls. Data represents the means ± SD of two independent experiments performed in triplicate. $^{**}p < 0.01$ were considered statistically significant.

fig. S2. Characterization of PMVs by flow cytometry and immunoblotting analysis (**A**) PMV release after NHS induction is inhibited after pretreatment of cells with the Rho-kinase inhibitor, Y-27632 (10 μM), the calpain inhibitor, calpeptin (20 μM) or with both. (**B**) Isolated PMVs were analysed for PS expression by staining with Annexin V (AnV); the resulting histogram shows ~57% of labelled PMVs to be AnV-FITC positive. Representative dot plot distribution of PMVs on a flow cytometer (inset), showing FSC (size) and SSC (granularity) of PMVs heterogeneous in size. (**C**) Isolated PMVs are enriched for actin and carry the complement regulatory proteins, decay accelerating factor (DAF) and complement receptor 1 (CR1) as detected by immunoblotting

analysis. Data represents the means ± SD of two independent experiments performed in triplicate (**A**) or from one representative of two (**B, C**) independent experiments. *$p < 0.05$ was considered statistically significant.

fig. S3. Sucrose gradient separation, and flow cytometry distribution of PMVs and exosomes

A mixture of exosomes and PMVs were applied to a 10-40% sucrose gradient and spun at 30,000 *g* for 1 h. (**A**) The first six fractions (1 ml) were pooled (pool 1) and found to be highly positive for LAMP-1 expression after antibody labelling. (**B**) Pool 2 fractions (7-11), were in contrast more positive for Annexin V binding. Pool 1 fractions show an average density of 1.04 g/ml; in contrast to pool 2 fractions, which has a mean density of 1.14 g/ml. (**C**) Electron microscopy (EM) examinations showed that fractions in pool 1 are mainly exosomes and those contained in pool 2 (**D**), are PMVs. Scale bar= 500 nm.

fig. S4. Reverse filtration method for isolation of PMVs and exosomes, and analysis of their cytokine content

(**A**) PMVs (inset) isolated by differential centrifugation from conditioned medium as described in 'materials and methods' were positive for AnV staining (41%) after flow cytometry analysis. (**B**) Microvesicles isolated by the reverse filtration method are confirmed as PMVs by EM (inset), and also AnV positive (47%). (**C**) The filtrate was less positive (18%) for AnV and EM examination shows cup-shaped exosomes (inset). (**D**) Representative dot plot distribution of PMVs and

exosomes isolated by the reverse filtration method and analysed by flow cytometry. PMVs are identified by their typical heterogeneous distribution, but exosomes exhibit a dot plot more homogeneous in size (FSC) and granularity (SSC). Right - dot plot distribution of a mixture of PMVs and exosomes. ELISA analysis showed that TGF-β1 (**E**) and MIF (**F**) are present at about four-fold higher levels in PMVs than in exosomes. Data represent mean ± SD of two independent experiments performed in triplicate. $^{**}p < 0.01$ was considered statistically significant.

fig. S5. Blocking *T. cruzi*-triggered release of PMVs, reduces parasite entry into cells, but actin depolymerization enhances invasion

(**A**) The integrin-interacting peptide, RGD, reduces *T. cruzi* invasion of cells in a dose-dependent manner. HeLa cells ($1x10^5$/well) in duplicate were pretreated with RGD peptide (100-500 µg/ml) at 37°C for min and the agent was washed-off three times with PBS. *T. cruzi* metacyclics were added at 5:1 (parasites to cell) ratio and incubated at 37°C for 3 h. (**B**) Pretreatment of cells with cytochalasin D (CytD, 10 µM) at 37°C for 10 min increases parasite-mediated PMV release and (**C**) subsequently enhances *T. cruzi* entry into cells. Trypsinized HeLa cells ($1x10^6$/well in triplicate) for PMV induction and semiconfluent cells, $1x10^5$/well in duplicate for invasion assay, were infected with 5:1 ratio of parasites at 37°C for 30 min and 3 h respectively. Cells were washed with PBS, fixed with 4% paraformaldehyde and mounted on microscope slide using DAPI-Vectashield.

Images were collected using an Olympus IX81 inverted microscope. $^{*}p < 0.05$, $^{**}p < 0.01$, $^{***}p < 0.001$ were considered statistically significant.

fig. S6. *T. cruzi*-elicited PMV release activates LAMP-1 translocation to the plasma membrane (PM)

(**A**) Stimulation of HeLa cells ($1x10^6$/well in triplicate) with 10% NHS causes PM lesions, which result in LAMP-1 translocation to the surface membrane for repair. However, pretreatment of cells with known inhibitors of lysosome exocytosis, concanavalin A (ConA) or wheat gelatine agglutinin (WGA), both at 20 µg/ml for 10 min at room temperature (RT) prior to addition of NHS, abrogated LAMP-1 translocation. (**B**) HeLa cells release PMVs following induction with 10% NHS in the absence of inhibitors. Surprisingly, PMV release continued unabated following pretreatment with inhibitors of lysosomal exocytosis. (**C**) As for NHS induction, stimulation of HeLa cells with *T. cruzi* 5:1 (parasites to cell) ratio causes PM lesions through PMV release, which is repaired by migration of lysosomes to the surface membrane. (**D**) Lysosome recruitment is detected by LAMP-1 translocation, analysed by flow cytometry and immunofluorescence microscopy. (**E**) Pretreatment of cells with the calpain inhibitor, calpeptin (20 µM) reduces *T. cruzi*-triggered PMV release, and the host PM thus sustains less damage. This leads to fewer lysosomes being recruited to the surface membrane (**F**). (**G**) Unlike calpeptin, pretreatment with ConA does not reduce parasite-triggered PMV release. Nonetheless, LAMP-1 translocation is severely reduced (**H**), confirming that ConA is a potent inhibitor of lysosome exocytosis. Data

presented is the mean ± SD of two independent experiments performed in triplicate. $^{**}p < 0.01$ and $^{***}p < 0.001$ were considered statistically significant.

fig. S7. *T. cruzi*-triggered PMV release from host cells is exploited by the parasite for entry

(**A**) Pretreatment of HeLa cells ($1x10^5$/well) in triplicate with ConA (20 µg/ml at RT for 10 min), which inhibits membrane repair, but not PMV release, enhances parasite entry into cells. In contrast, pretreatment with calpeptin reduces *T. cruzi* entry into cells. However, prolonged incubation (30 min at RT) with ConA prevents parasite entry due to the loss of cell cytoplasm (**B**), caused by unrepaired PM lesions. (**C**) PMVs isolated from the conditioned medium of cells infected with *T. cruzi* stained positive for AnV binding and anti-CD63 labelling (**D**) analysed by flow cytometry. These further confirm that the cells and not the parasite release the PMVs. (**E**) Pretreatment of cells with ConA enhance the overall invasion by *T. cruzi* and slightly increase parasite superinfection.

fig. S8. Correlation analysis between PMV release, lysosome exocytosis and parasite invasion

(**A**) PMV release is directly proportional to lysosome exocytosis, meaning, more lysosomes migrate to the plasma membrane (PM) to repair damage caused by parasite-triggered PMV release. (**B**) The release of PMVs compromises the integrity of the host plasma membrane. This implies that the integrity of the host PM is most intact (> 90%) when PMV release is low (< 50% of control). (**C**) The

relationship between PM integrity and lysosome exocytosis was negatively correlated. This implies that when the PM integrity is most intact, only fewer lysosomes are recruited to for repair. However, more lysosomes migrate to the surface when the host cell PM integrity is severely damaged. $^{*}p < 0.05$ and $^{**}p < 0.01$ were considered statistically significant.

Supporting References

S1. E. P. Camargo, *Rev. Inst. Med. Trop. Sao Paulo* **6,** 93 (1964).

S2. M. A. de Sousa, *Mem. Inst. Oswaldo Cruz* **78,** 497 (1983).

S3. I. Cestari, M. I. Ramirez, *PLoS. One* **5**, e9721 (2010).

S4. E. A. Ansa-Addo *et al.*, *J. Immunol.* **185**, 5236 (2010).

S4. E. S. Reynolds, *J. Cell Biol.* **17,** 208 (1963).

Fig. 1

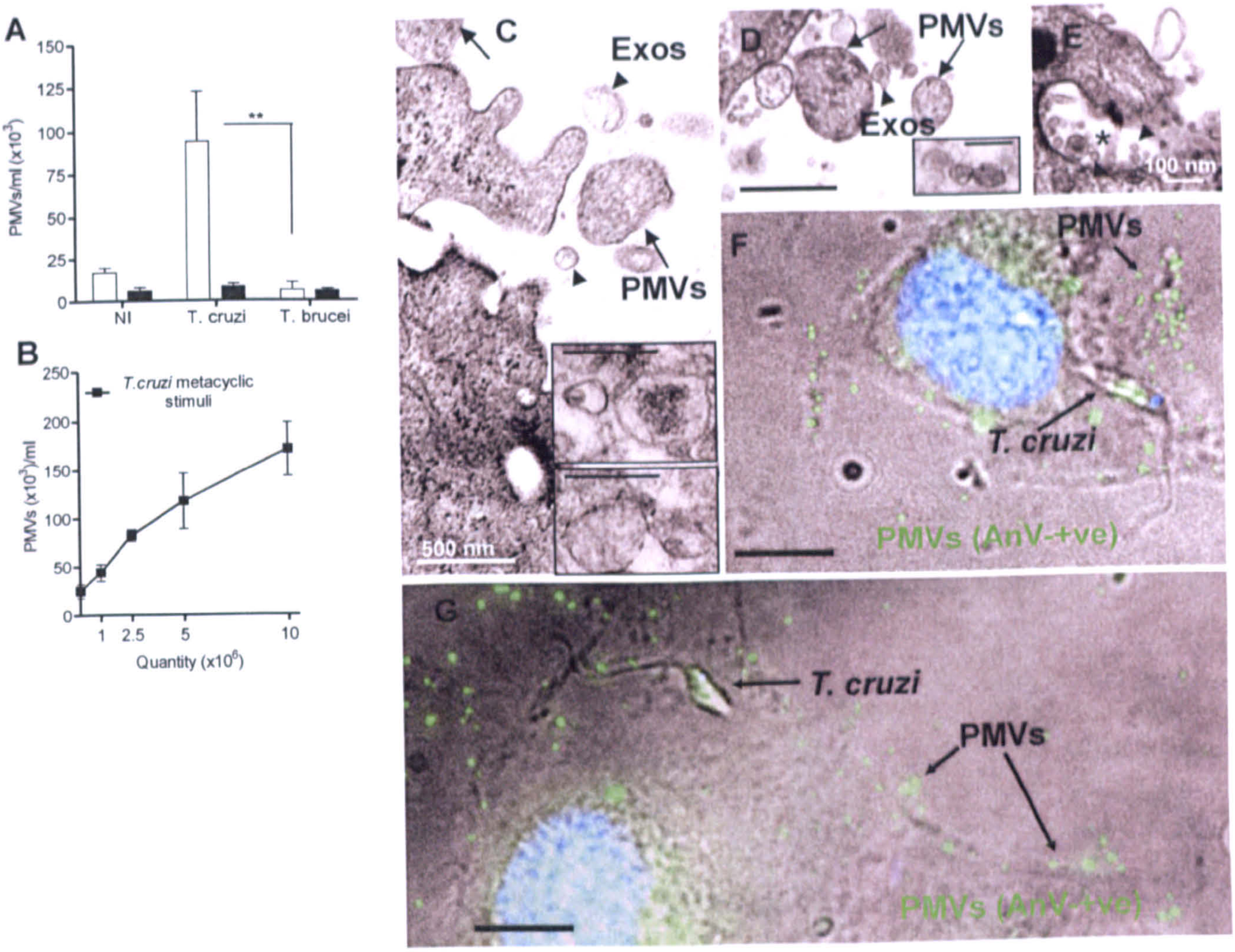
A
PMVs/ml (x10³)
150
125
100
75
50
25
0
**
NI
T. cruzi
T. brucei
B
T.cruzi metacyclic stimuli
PMVs (x10³)/ml
250
200
150
100
50
0
1
2.5
5
10
Quantity (x10⁶)
C
Exos
PMVs
500 nm
D
PMVs
Exos
E
*
100 nm
F
PMVs
T. cruzi
PMVs (AnV-+ve)
G
T. cruzi
PMVs
PMVs (AnV-+ve)

Fig. 2

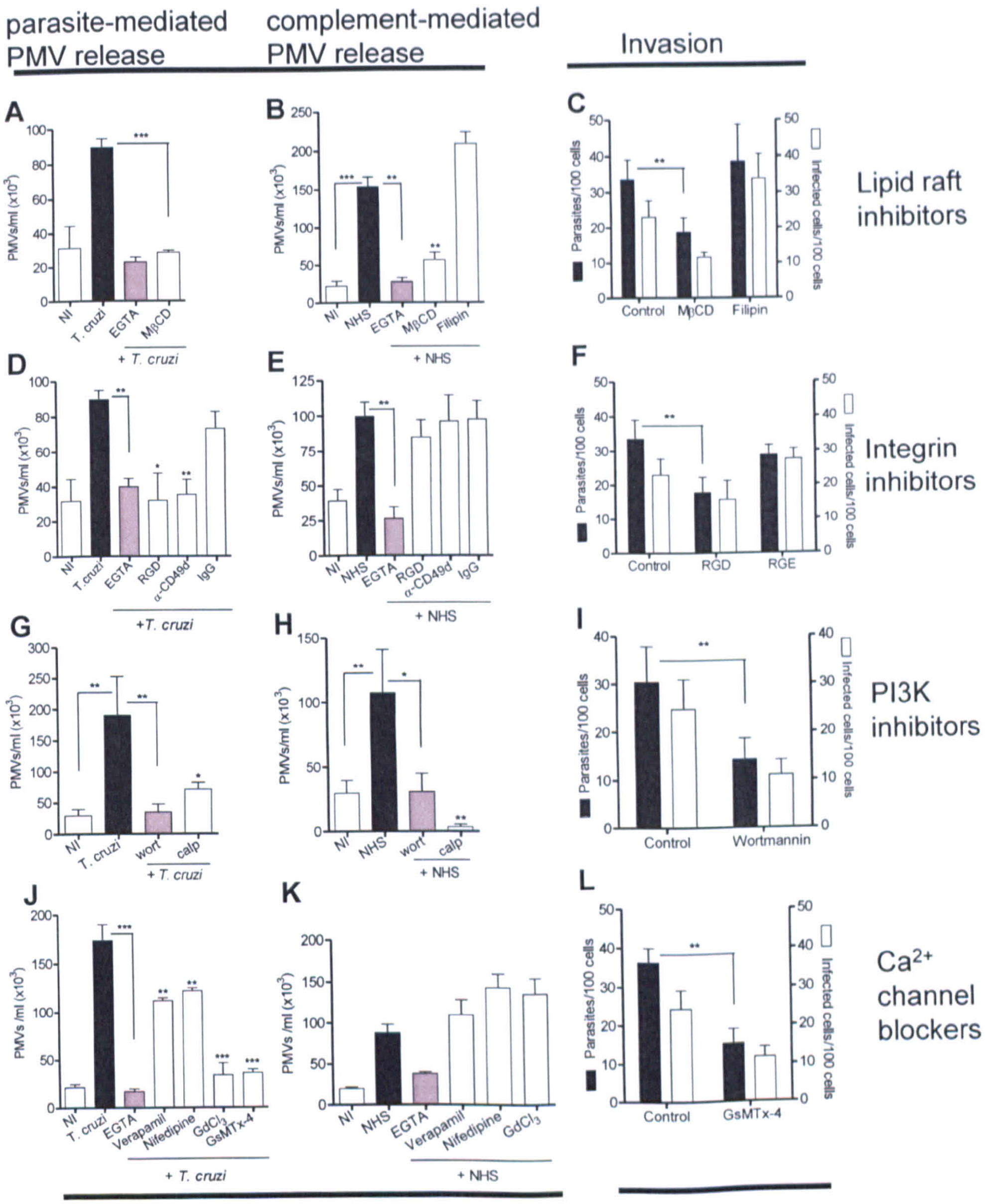
parasite-mediated PMV release
complement-mediated PMV release
Invasion
A
B
C
PMVs/ml (x10³)
NI
T. cruzi
EGTA
MβCD
+ T. cruzi
NHS
Filipin
+ NHS
Parasites/100 cells
Infected cells/100 cells
Control
Lipid raft inhibitors
D
E
F
T.cruzi
RGD
α-CD49d
IgG
RGE
Integrin inhibitors
G
H
I
wort
calp
Wortmannin
PI3K inhibitors
J
K
L
PMVs /ml (x10³)
Verapamil
Nifedipine
GdCl3
GsMTx-4
Ca2+ channel blockers

Fig. 3

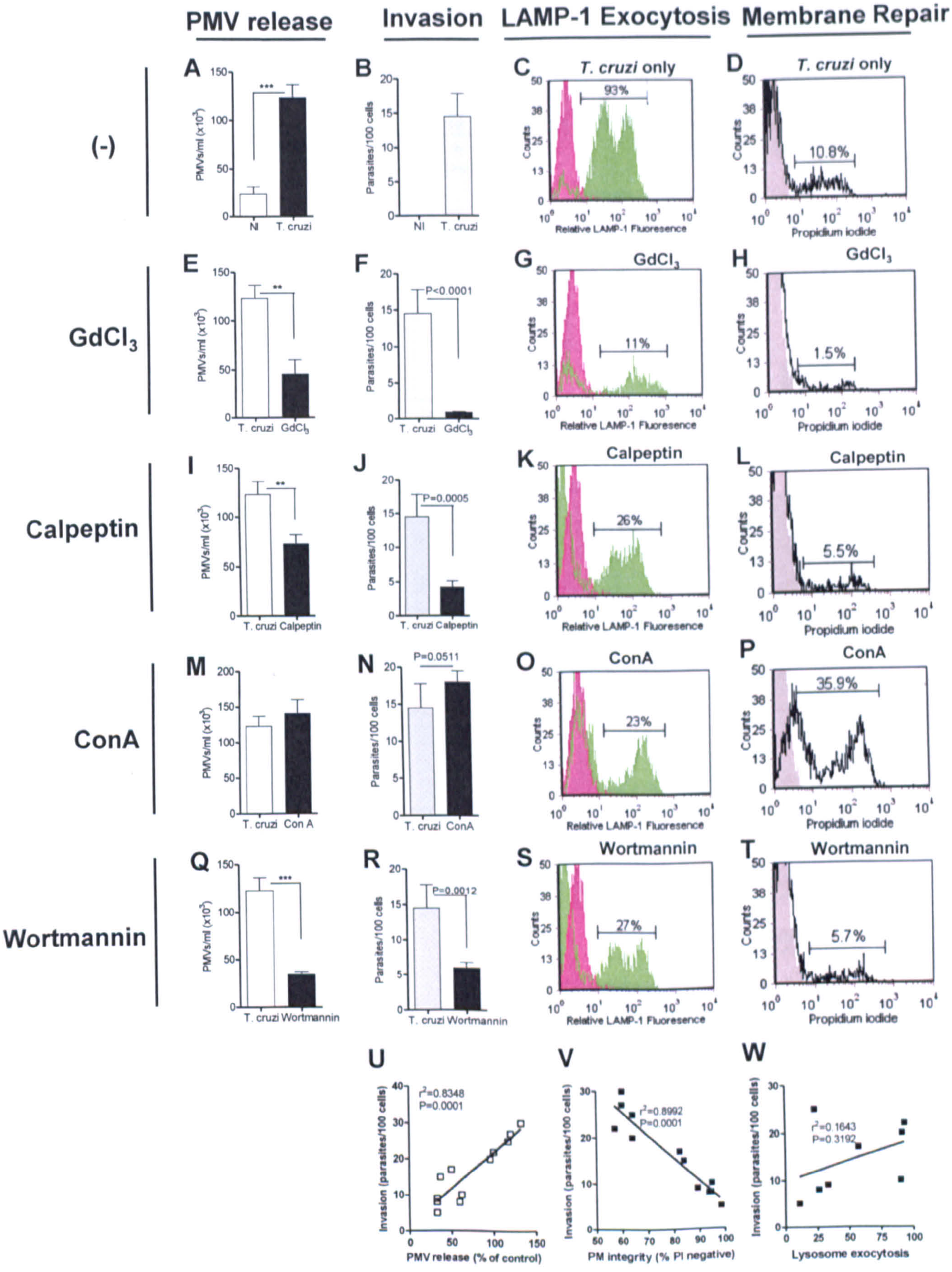
PMV release
Invasion
LAMP-1 Exocytosis
Membrane Repair
(-)
A
B
C
D
T. cruzi only
PMVs/ml (x10³)
Parasites/100 cells
Counts
93%
10.8%
Relative LAMP-1 Fluorescence
Propidium iodide
NI
T. cruzi
GdCl3
E
F
G
H
11%
1.5%
P<0.0001
Calpeptin
I
J
K
L
26%
5.5%
P=0.0005
ConA
M
N
O
P
23%
35.9%
P=0.0511
Wortmannin
Q
R
S
T
27%
5.7%
P=0.0012
U
V
W
r²=0.8348
P=0.0001
r²=0.8992
P=0.0001
r²=0.1643
P=0.3192
Invasion (parasites/100 cells)
PMV release (% of control)
PM integrity (% PI negative)
Lysosome exocytosis

Fig. 4

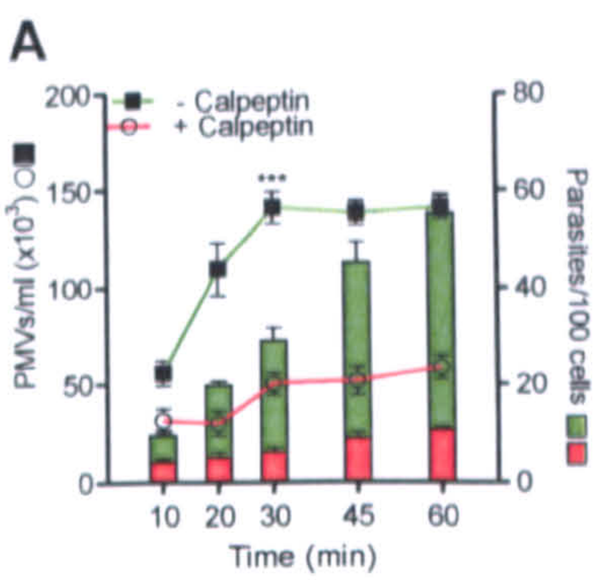
A
- Calpeptin
+ Calpeptin
PMVs/ml (x10³)
Parasites/100 cells
Time (min)

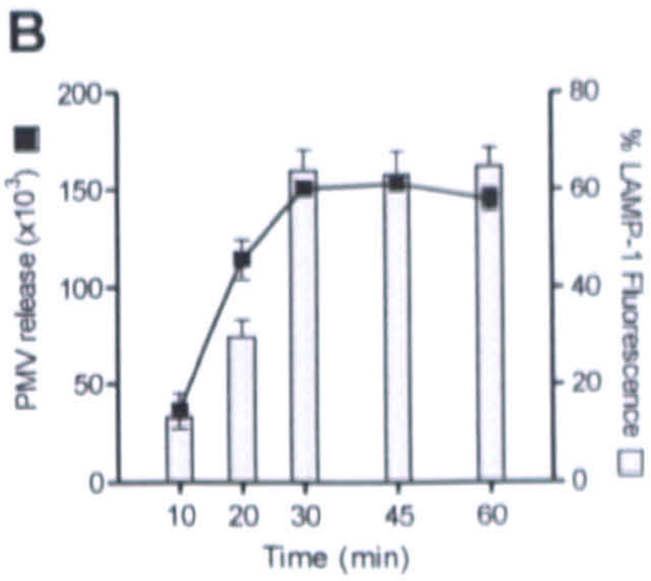
B
PMV release (x10³)
% LAMP-1 Fluorescence
Time (min)

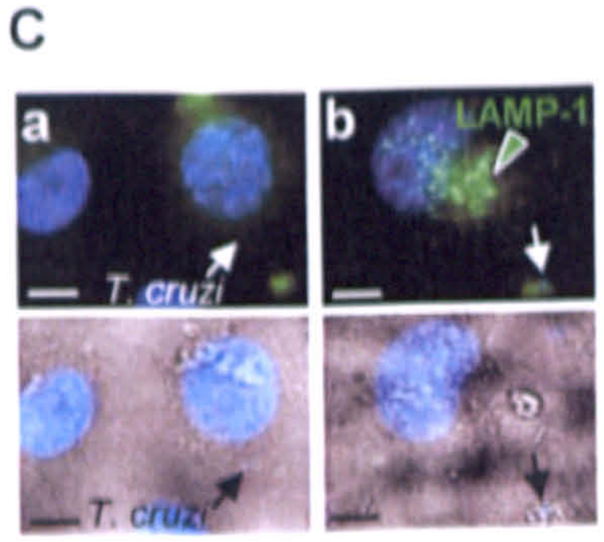
C
a
b
LAMP-1
T. cruzi
T. cruzi

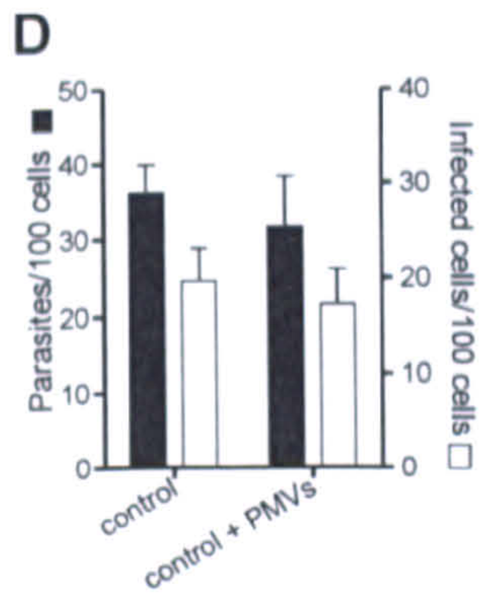
D
Parasites/100 cells
Infected cells/100 cells
control
control + PMVs

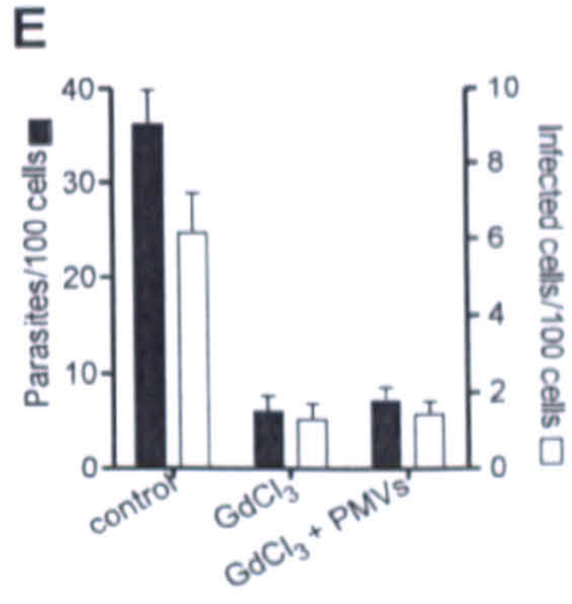
E
Parasites/100 cells
Infected cells/100 cells
control
GdCl3
GdCl3 + PMVs

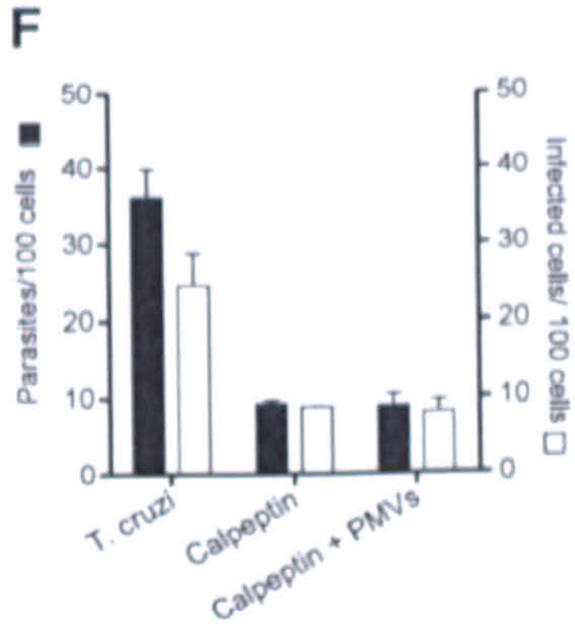
F
Parasites/100 cells
Infected cells/ 100 cells
T. cruzi
Calpeptin
Calpeptin + PMVs

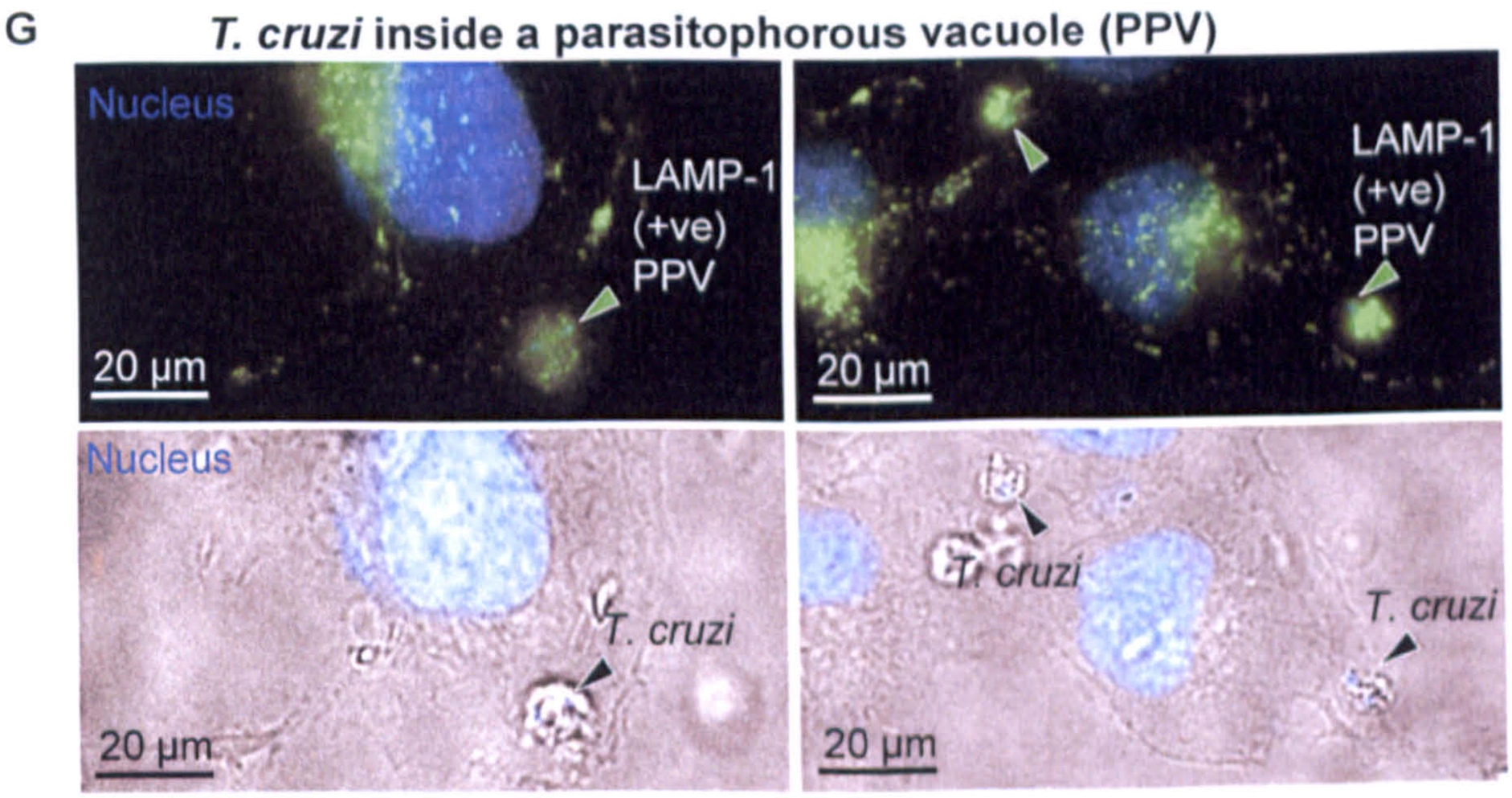
G
T. cruzi inside a parasitophorous vacuole (PPV)
Nucleus
LAMP-1
(+ve)
PPV
20 µm
Nucleus
LAMP-1
(+ve)
PPV
20 µm
Nucleus
T. cruzi
20 µm
T. cruzi
T. cruzi
20 µm

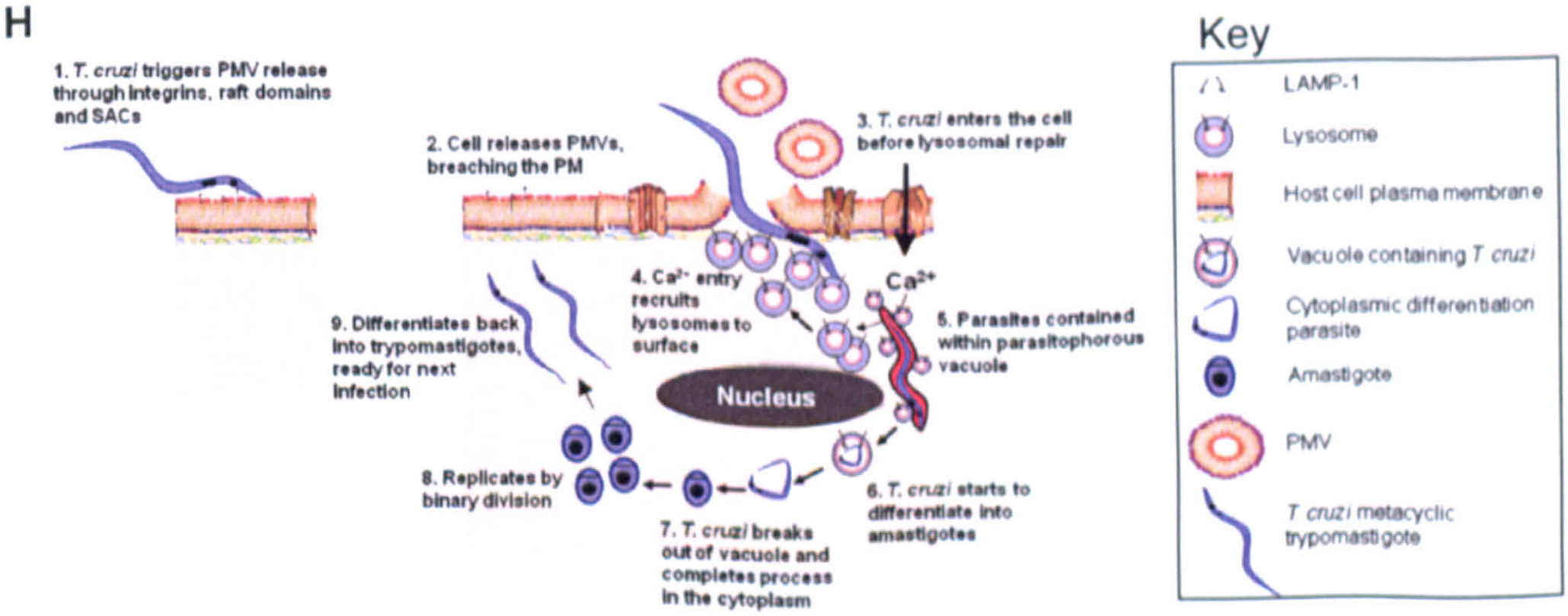
H
1. T. cruzi triggers PMV release through integrins, raft domains and SACs
2. Cell releases PMVs, breaching the PM
3. T. cruzi enters the cell before lysosomal repair
4. Ca2+ entry recruits lysosomes to surface
Ca2+
5. Parasites contained within parasitophorous vacuole
6. T. cruzi starts to differentiate into amastigotes
7. T. cruzi breaks out of vacuole and completes process in the cytoplasm
8. Replicates by binary division
9. Differentiates back into trypomastigotes, ready for next infection
Nucleus
Key
LAMP-1
Lysosome
Host cell plasma membrane
Vacuole containing T cruzi
Cytoplasmic differentiation parasite
Amastigote
PMV
T cruzi metacyclic trypomastigote

Supporting figures

Fig. S1

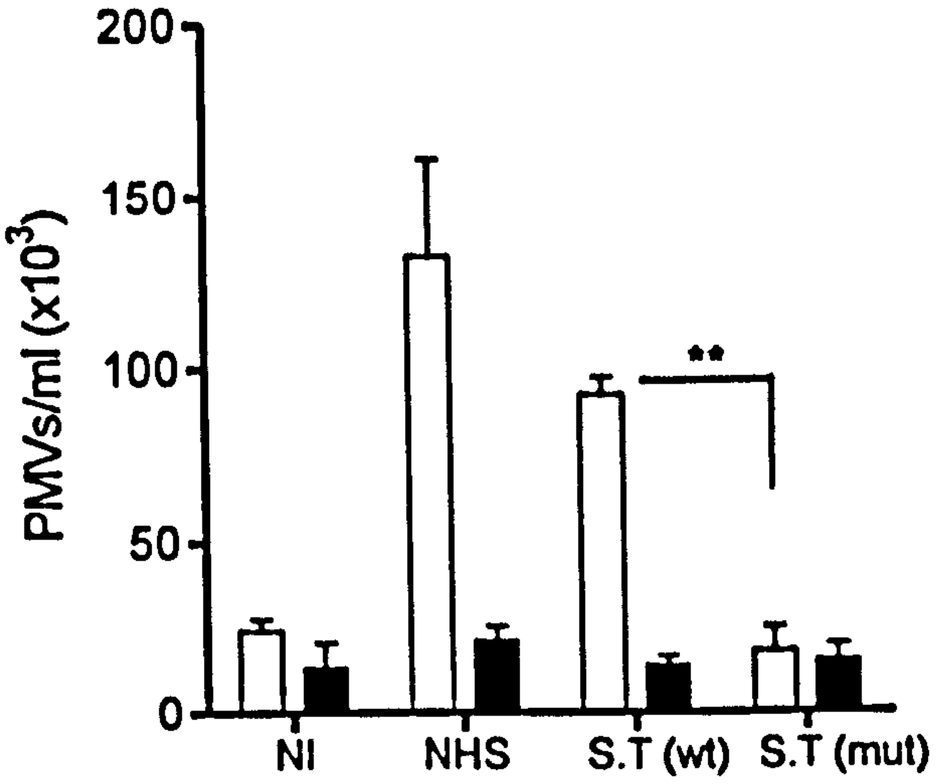

Fig. S2

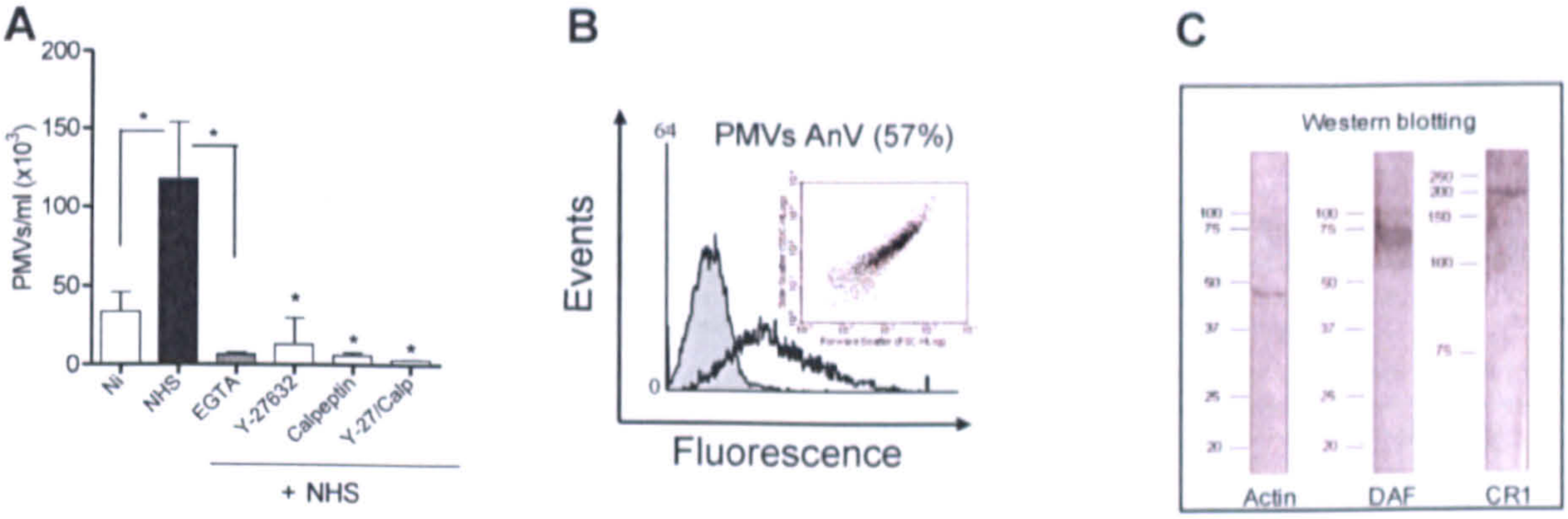
A
200
150
100
50
0
PMVs/ml (x10³)
*
*
*
*
*
Ni
NHS
EGTA
Y-27632
Calpeptin
Y-27/Calp
+ NHS
B
64
PMVs AnV (57%)
Events
0
Fluorescence
C
Western blotting
100
75
50
37
25
20
Actin
DAF
CR1

Fig. S3

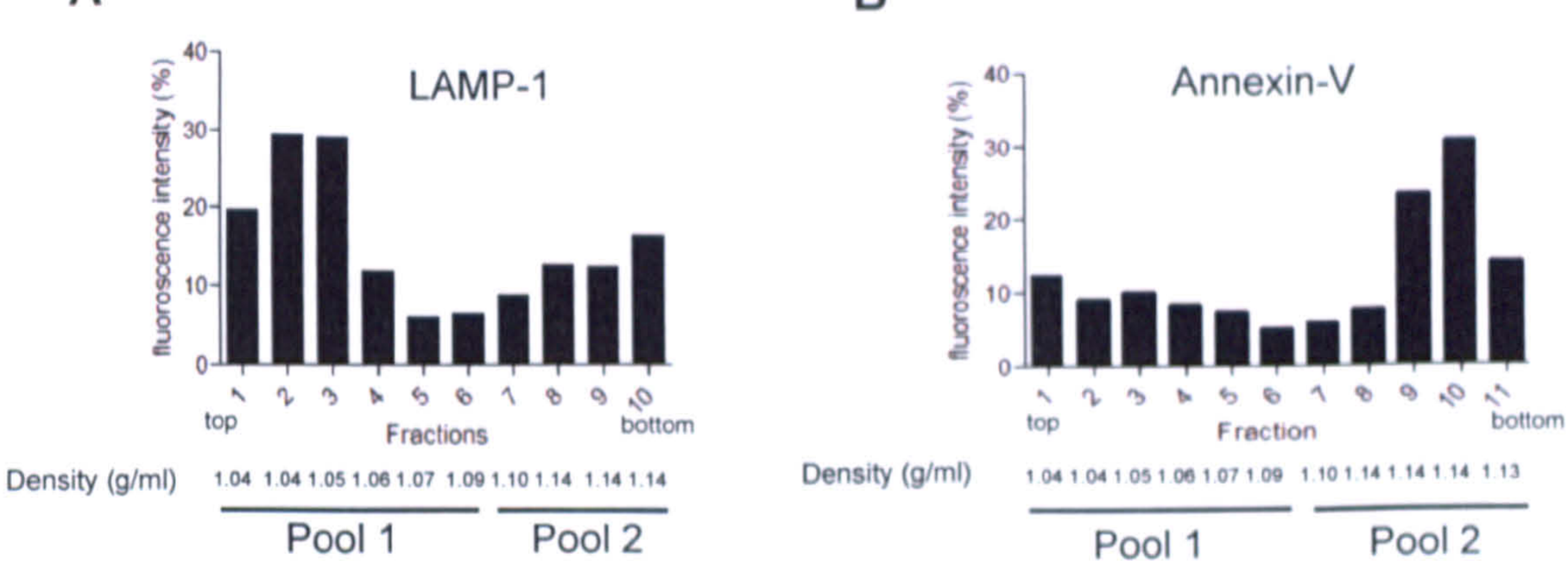
A
LAMP-1
fluoroscence intensity (%)
0
10
20
30
40
1 2 3 4 5 6 7 8 9 10
top
bottom
Fractions
Density (g/ml)
1.04 1.04 1.05 1.06 1.07 1.09 1.10 1.14 1.14 1.14
Pool 1
Pool 2
B
Annexin-V
fluoroscence intensity (%)
0
10
20
30
40
1 2 3 4 5 6 7 8 9 10 11
top
bottom
Fraction
Density (g/ml)
1.04 1.04 1.05 1.06 1.07 1.09 1.10 1.14 1.14 1.14 1.13
Pool 1
Pool 2

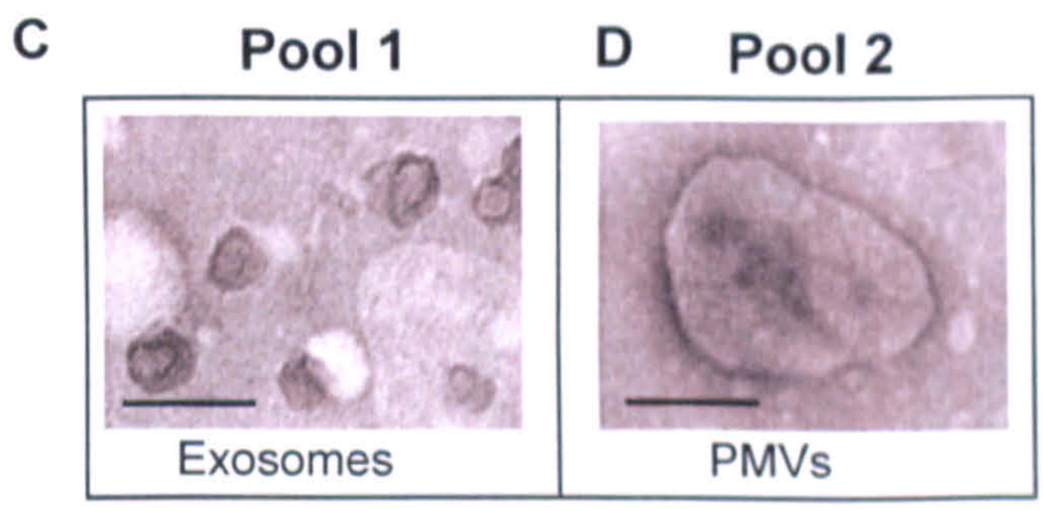
C
Pool 1
D
Pool 2
Exosomes
PMVs

Fig. S4

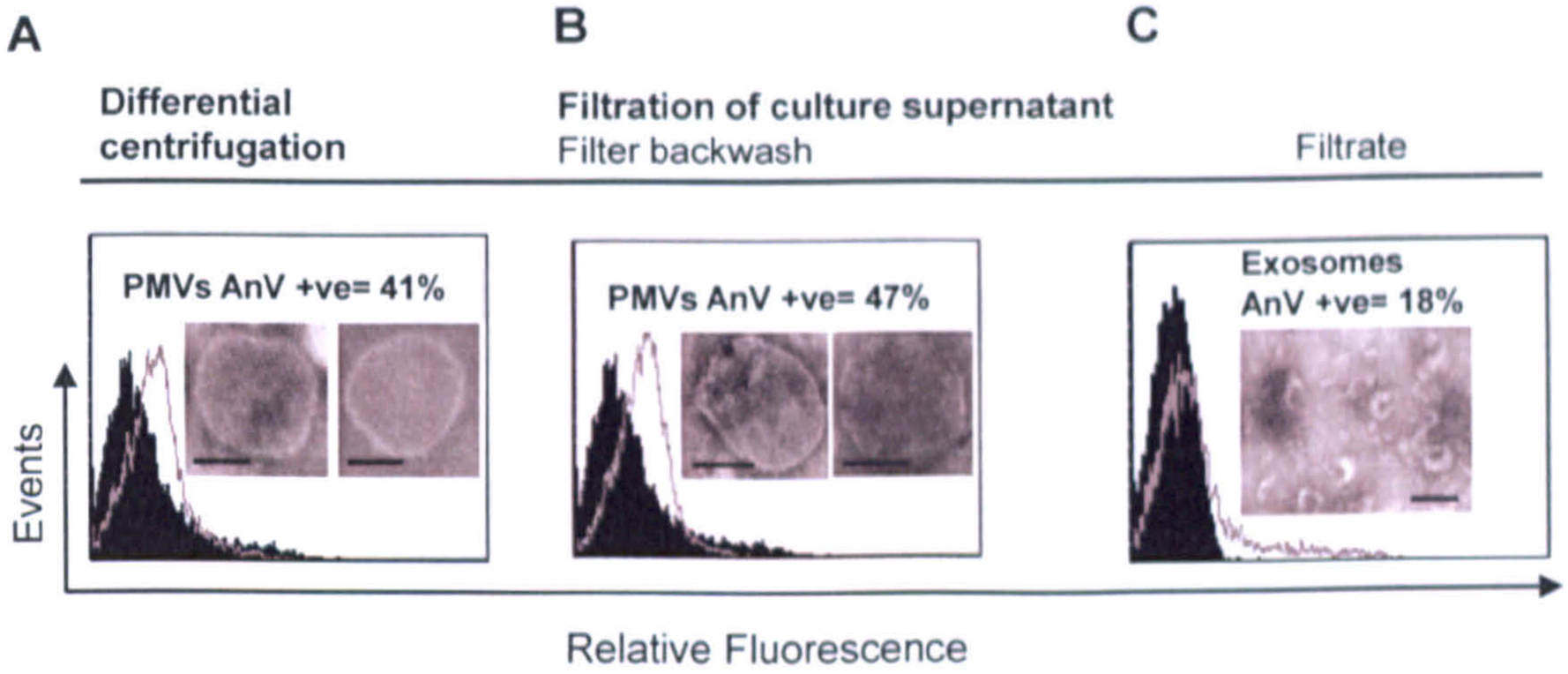
A
B
C
Differential centrifugation
Filtration of culture supernatant
Filter backwash
Filtrate
PMVs AnV +ve= 41%
PMVs AnV +ve= 47%
Exosomes AnV +ve= 18%
Events
Relative Fluorescence
D
PMVs
Exosomes
Exosomes + PMVs
SSC-HLog
FSC-HLog
E
TGF-β1 (ng/ml)
1.5
1.0
0.5
0.0
**
Exo
PMVs
F
MIF (ng/ml)
6
4
2
0
**
Exo
PMVs

Fig. S5

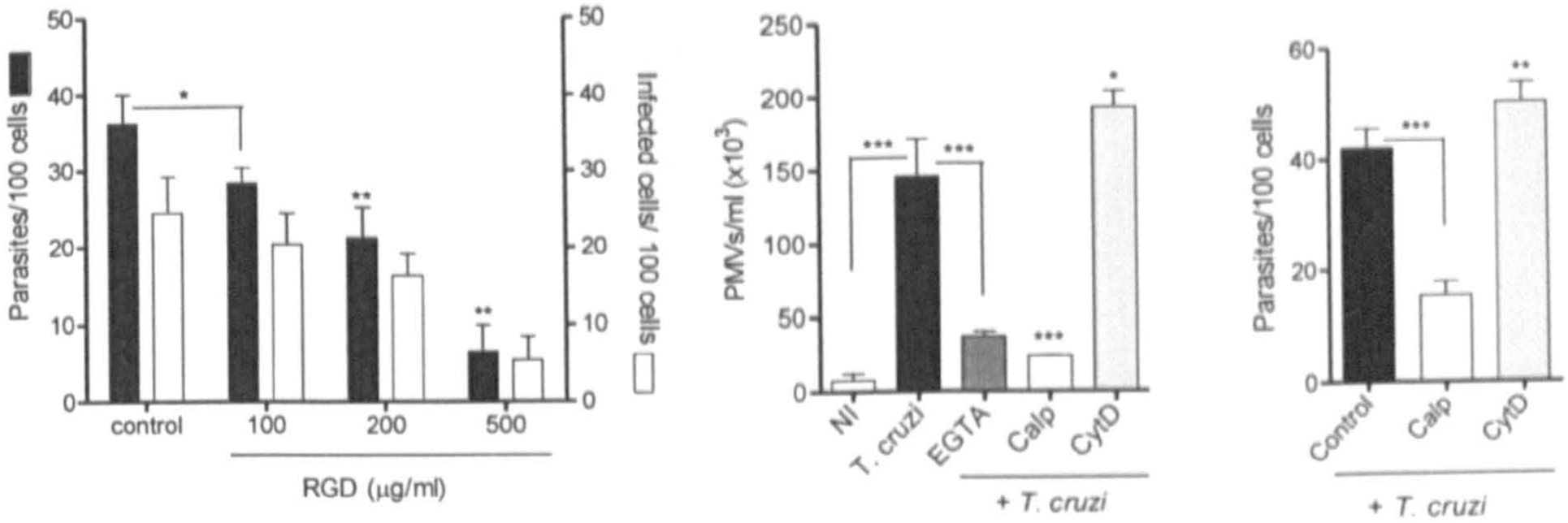
A
Parasites/100 cells
Infected cells/ 100 cells
control
100
200
500
RGD (µg/ml)
B
PMVs/ml (x10³)
NI
T. cruzi
EGTA
Calp
CytD
+ T. cruzi
C
Parasites/100 cells
Control
Calp
CytD
+ T. cruzi

Fig. S6

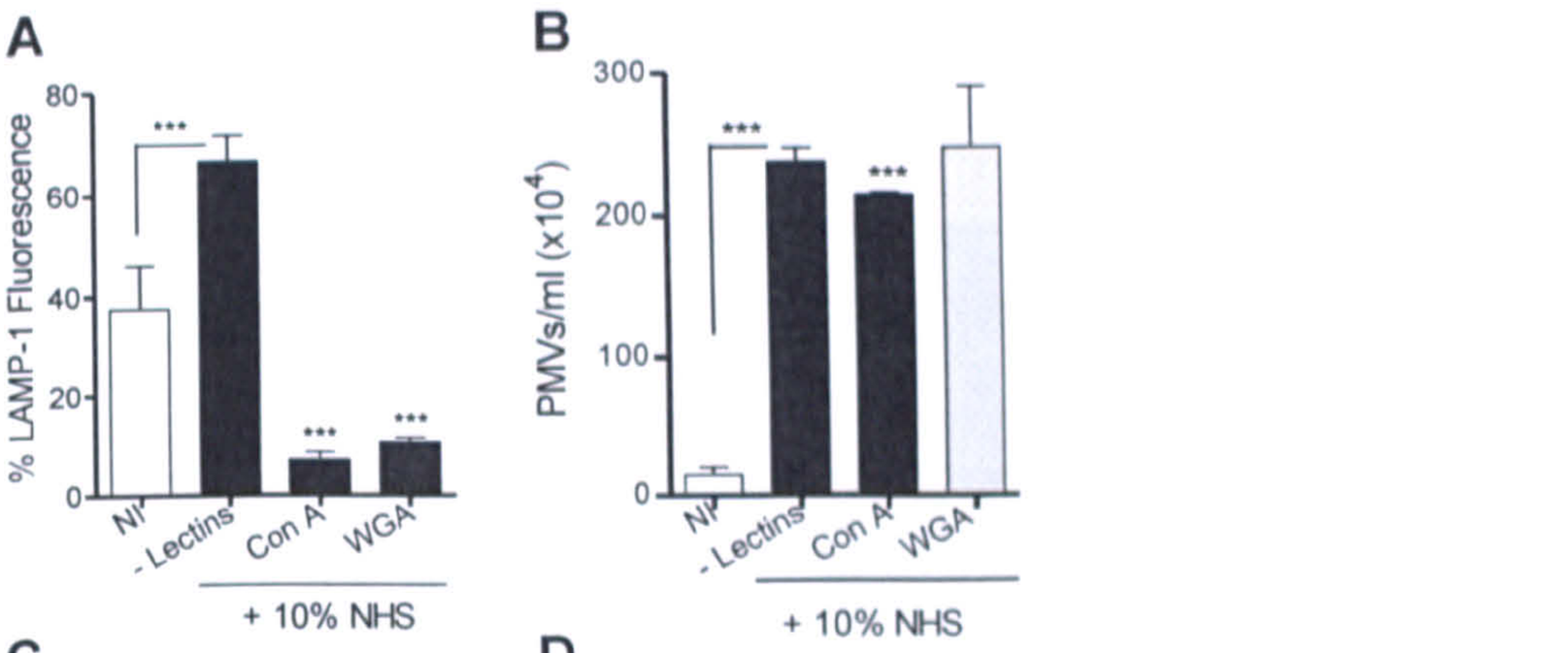
A
% LAMP-1 Fluorescence
80
60
40
20
0
***
***
***
NI
- Lectins
Con A
WGA
+ 10% NHS
B
PMVs/ml (x10^4)
300
200
100
0
***
***
NI
- Lectins
Con A
WGA
+ 10% NHS
C
PMVs/ml (x10^3)
200
150
100
50
0
**
HeLa only
+ T. cruzi
D
(-) inhibitor= 79%
Events
64
0
10^0 10^1 10^2 10^3 10^4
Anti-LAMP 1 Fluorescence
LAMP-1
20 µm
E
PMVs/ml (x10^3)
200
150
100
50
0
***
HeLa
+ calpeptin
+ T. cruzi
F
calpeptin= 17.4%
Events
64
0
10^0 10^1 10^2 10^3 10^4
Anti-LAMP 1 Fluorescence
LAMP-1
20 µm
G
PMVs/ml (x10^3)
200
150
100
50
0
HeLa
+ con A
+ T. cruzi
H
conA= 20.4%
Events
64
0
10^0 10^1 10^2 10^3 10^4
Anti-LAMP 1 Fluorescence
LAMP-1
20 µm

Fig. S7

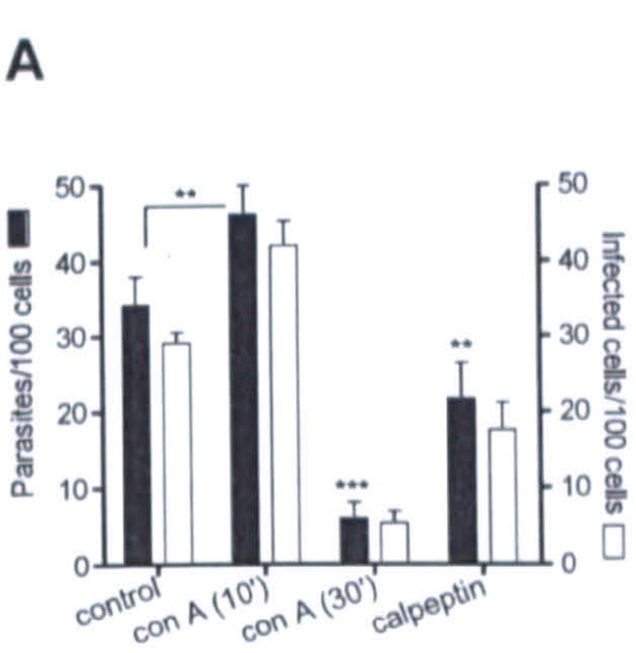
A
Parasites/100 cells
Infected cells/100 cells
**
***
**
control
con A (10')
con A (30')
calpeptin

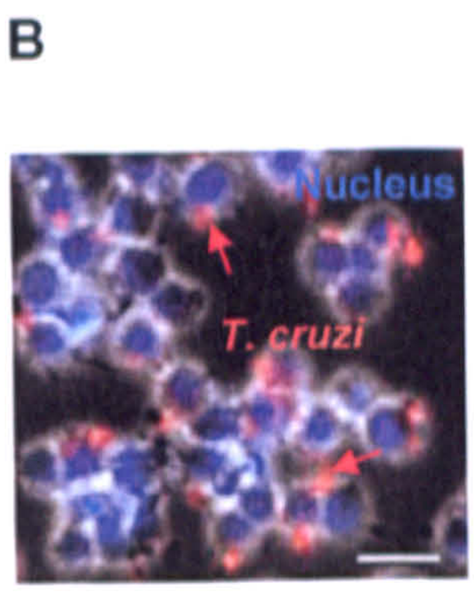
B
Nucleus
T. cruzi

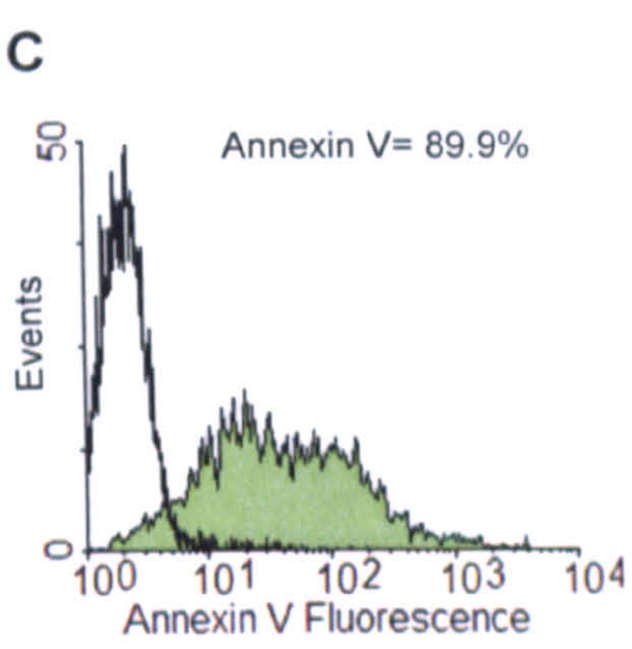
C
Annexin V= 89.9%
Events
Annexin V Fluorescence

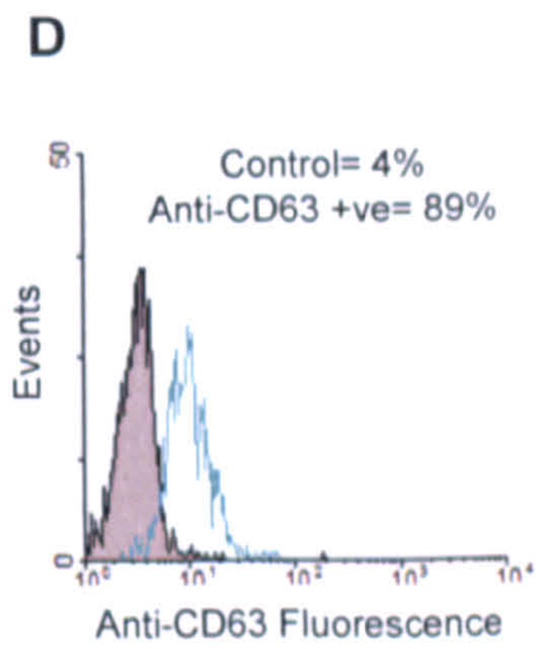
D
Control= 4%
Anti-CD63 +ve= 89%
Events
Anti-CD63 Fluorescence

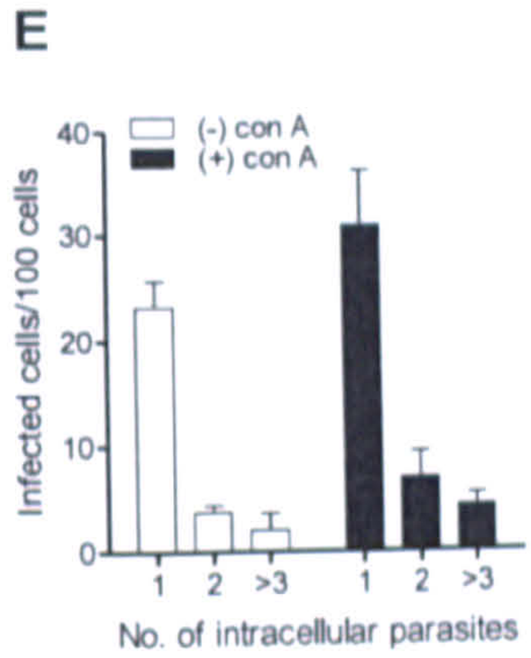
E
(-) con A
(+) con A
Infected cells/100 cells
1
2
>3
1
2
>3
No. of intracellular parasites

Fig. S8

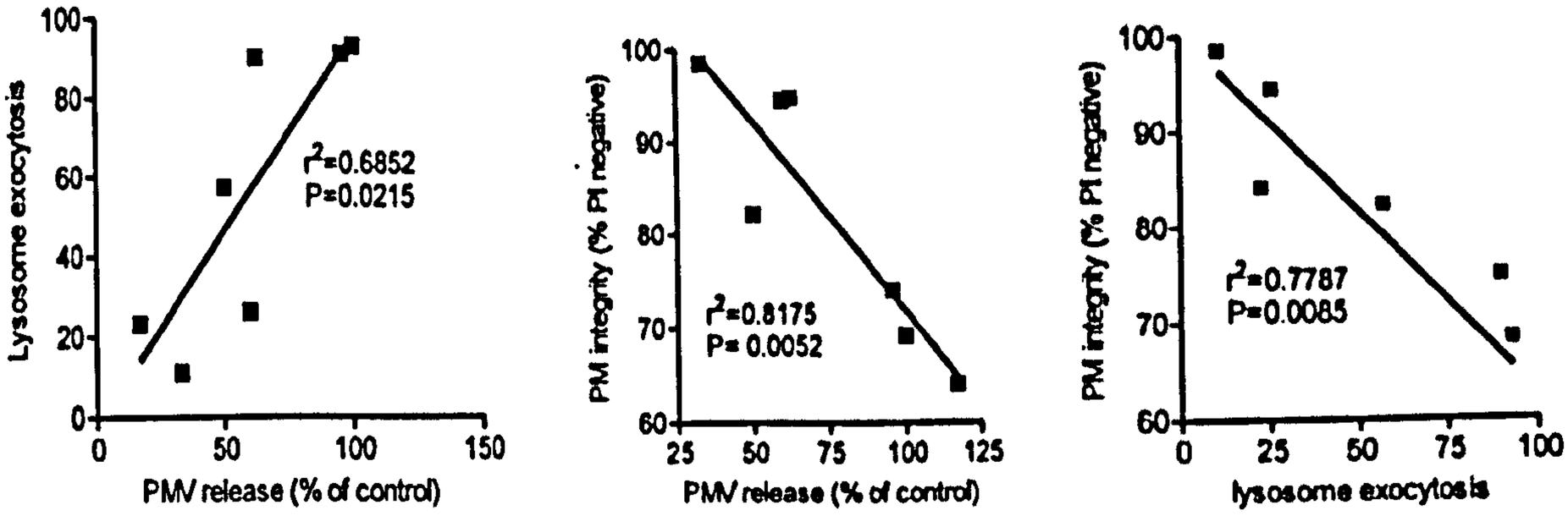
A
Lysosome exocytosis
PMV release (% of control)
r²=0.6852
P=0.0215
B
PM integrity (% PI negative)
PMV release (% of control)
r²=0.8175
P= 0.0052
C
PM integrity (% PI negative)
lysosome exocytosis
r²=0.7787
P=0.0085

The Journal of Immunology

Human Plasma Membrane-Derived Vesicles Halt Proliferation and Induce Differentiation of THP-1 Acute Monocytic Leukemia Cells

Ephraim A. Ansa-Addo, Sigrun Lange, Dan Stratton, Samuel Antwi-Baffour, Igor Cestari, Marcel I. Ramirez, Maria V. McCrossan and Jameel M. Inal

J. Immunol. 2010;185;5236-5246; originally published online Oct 4, 2010;
doi:10.4049/jimmunol.1001656
http://www.jimmunol.org/cgi/content/full/185/9/5236

The Journal of Immunology is published twice each month by The American Association of Immunologists, Inc., 9650 Rockville Pike, Bethesda, MD 20814-3994.

Print ISSN: 0022-1767 Online ISSN: 1550-6606.

Human Plasma Membrane-Derived Vesicles Halt Proliferation and Induce Differentiation of THP-1 Acute Monocytic Leukemia Cells

Ephraim A. Ansa-Addo,* Sigrun Lange,† Dan Stratton,* Samuel Antwi-Baffour,* Igor Cestari,*,‡,1 Marcel I. Ramirez,*,‡ Maria V. McCrossan,§ and Jameel M. Inal*

Plasma membrane-derived vesicles (PMVs) are small intact vesicles released from the cell surface that play a role in intercellular communication. We have examined the role of PMVs in the terminal differentiation of monocytes. The myeloid-differentiating agents all-*trans* retinoic acid/PMA and histamine, the inflammatory mediator that inhibits promonocyte proliferation, induced an intracellular Ca^{2+}-mediated PMV (as opposed to exosome) release from THP-1 promonocytes. These PMVs cause THP-1 cells to enter G_0–G_1 cell cycle arrest and induce terminal monocyte-to-macrophage differentiation. Use of the TGF-β receptor antagonist SB-431542 and anti–TGF-β1 Ab showed that this was due to TGF-β1 carried on PMVs. Although TGF-β1 levels have been shown to increase in cell culture supernatants during macrophage differentiation and dendritic cell maturation, the presence of TGF-β1 in PMVs is yet to be reported. In this study, to our knowledge we show for the first time that TGF-β1 is carried on the surface of PMVs, and we confirm the presence within PMVs of certain leaderless proteins, with reported roles in myeloid cell differentiation. Our in vitro findings support a model in which TGF-β1–bearing PMVs, released from promonocytic leukemia cells (THP-1) or primary peripheral blood monocytes on exposure to sublytic complement or after treatment with a differentiation therapy agent, such as all-*trans* retinoic acid, significantly reduce proliferation of THP-1 cells. Such PMVs also induce the terminal differentiation of primary peripheral blood monocytes as well as THP-1 monocytes. *The Journal of Immunology*, **2010, 185: 5236–5246.**

Microvesiculation is a ubiquitous cellular mechanism that occurs as a result of exocytosis, releasing exosomes (between 50 and 100 nm) (1) or directly releasing vesicles from the cell surface membrane, which we refer to in this study as plasma membrane-derived vesicles (PMVs) (0.1–1 μm) (2). Various changes in cell physiology are involved in the release of cellular PMVs (reviewed in Ref. 3), but microvesiculation is always initiated by an increase in intracellular calcium and a loss of lipid asymmetry in the plasma membrane (3). In vitro, PMV release can be initiated by sublytic complement deposition and the fungal calcium ionophore A23187 (calcimycin). Unlike apoptotic bodies, which are derived from damaged cells, PMVs, released from healthy viable cells, are smaller in size and do not contain damaged DNA. Instead, PMVs carry microRNA (4), mRNA, numerous membrane proteins, lipids, and cytoplasmic constituents, characteristic of their parental cell (5), and, being able to transmit such proteins between cells, they are important mediators of intercellular communication.

As an alternative to conventional protein export, an important function of microvesiculation involves the export of proteins lacking a signal peptide (6, 7). Among these, epimorphin, fibroblast growth factor (FGF)-1, FGF-2, macrophage migration inhibitory factor (MIF), and galectin (Gal)-3 are all transported to the plasma membrane via the adenosine triphosphate cassette transport channel (ABCA1) needed for the release of PMVs or by exocytosis of exosomes (8). In this study we show the presence in PMVs of leaderless proteins MIF, FGF-1, and Gal-3. Although we cannot comment on their specific function in PMVs or in intercellular communication and induction of THP-1 cell differentiation, these proteins have been reported to function during the differentiation of myeloid cells. For example, MIF was reported to induce the migration of monocytes into tissues, while changes in Gal-3 expression are important for myeloid cell differentiation into specific lineages (9, 10).

In experiments using THP-1 cells, microRNAs have been shown to be involved in monocytic differentiation (11), and thus it may be pertinent for THP-1 differentiation that PMVs carry microRNAs (4). In other studies involving the chronic myeloid leukemia cell line K-562, PMVs carrying hedgehog proteins could induce the differentiation toward the megakaryocytic lineage (12). Most recently, PMVs derived from embryonic stem cells were found to

*Cellular and Molecular Immunology Research Centre, School of Human Sciences, Faculty of Life Sciences, London Metropolitan University; †University College of London Institute for Women's Health, Maternal and Fetal Medicine, Perinatal Brain Repair Group; ‡Immunology Unit, London School of Hygiene and Tropical Medicine, London, United Kingdom; and §Instituto Oswaldo Cruz-Fiocruz, Rio de Janeiro, Brazil

1Current address: Department of Global Health, Seattle Biomedical Research Institute, University of Washington, Seattle, WA.

Received for publication May 19, 2010. Accepted for publication August 26, 2010.

This work was supported in part by a Graduate Assistantship to E.A.A. from the Faculty of Life Sciences at London Metropolitan University/Cellular and Molecular Immunology Research Centre (CMIRC). The work was also funded in part by the Royal Society Grant IV0871706 (to J.M.I. for visit of M.I.R. to CMIRC), funding from London Metropolitan University/ Cellular and Molecular Immunology Research Centre (Faculty of Life Sciences), and a one-year Brazilian Ministry of Education Scholarship (for I.C. to visit CMIRC).

Address correspondence and reprint requests to Prof. Jameel M. Inal, Cellular and Molecular Immunology Research Centre, School of Human Sciences, Faculty of Life Sciences, London Metropolitan University, 166-220 Holloway Road, London N7 8DB, U.K. E-mail address: j.inal@londonmet.ac.uk

Abbreviations used in this paper: 7-AAD, 7-aminoactinomycin D; AnV, annexin V; APL, acute promyelocytic leukemia; ATRA, all-*trans* retinoic acid; BF, bright field; $[Ca^{2+}]_i$, intracellular Ca^{2+} concentration; FGF, fibroblast growth factor; FSC, forward light scatter; Gal, galectin; HI, heat-inactivated; MIF, migration inhibitory factor; NHS, normal human serum; PB mono, peripheral blood monocytes; PMV, plasma membrane-derived vesicle; PS, phosphatidylserine; R18, octadecyl rhodamine chloride; SSC, side light scatter.

www.jimmunol.org/cgi/doi/10.4049/jimmunol.1001656

carry Wnt-3, which is involved in hematopoietic differentiation, and such PMVs were shown to reprogram hematopoietic progenitor cells (13). This evidence, that PMVs, albeit from embryonic stem cells, are involved in differentiation in the hematopoietic environment in the bone marrow suggests possible PMV involvement in leukemia myeloid development and possibly monocytic hematopoiesis, all of which need to be investigated further.

In addition to PMA and all-*trans* retinoic acid (ATRA), inflammatory mediators, such as histamine (this study), and bacterial products fMLP and LPS can also induce microvesiculation, providing that cells have the cognate receptors. Because inducers of PMV release have been described in connection with possible therapies for acute monocytic leukemia, we wanted to see whether PMVs themselves could induce cell cycle arrest/terminal differentiation (the hallmark of differentiation therapy) in the monocytic leukemia cell line THP-1. This was important in view of the recent findings that microvesicles, albeit from neutrophils (termed ectosomes), were shown to interfere with the maturation of immature dendritic cells (14). Furthermore, early success of ATRA in acute promyelocytic leukemia (APL) has not been followed up with new drugs, and resistance can develop with all existing therapies (15, 16).

This study aims to show principally whether PMVs can initiate differentiation/stop proliferation of THP-1 cells. From surveying the literature, such PMV-mediated differentiation would likely be a multifactorial process involving several proteins and microRNAs. Among the many factors that PMVs harbor and the numerous PMV-associated cytokines revealed by proteomics studies is the multifunctional TGF-β1, which is found principally associated with platelet PMVs (17) and that inhibits the proliferation of various cell types in vitro (18). To our knowledge, we describe for the first time the presence of surface-bound TGF-β1 on PMVs. Given the important role that TGF-β1 plays in the regulation of cellular proliferation, as well as its autocrine inhibition of proliferation in APL cell line HL-60, we asked whether any growth regulation and differentiation of promonocytic leukemia cells could in part be influenced by PMVs bearing TGF-β1, which are released from cells by the action of known differentiation therapeutics. If so, this would be the first report of TGF-β1 carried on the surface of a PMV that was deliverable as a functional signaling molecule.

Materials and Methods

Cell culture and peripheral blood monocyte isolation

All cells used in this study were maintained in growth medium containing RPMI 1640 supplemented with 10% FBS, 100 U/ml penicillin, and 100 mg/ml streptomycin. Cells were occasionally maintained for a week in growth medium supplemented with 1% kanamycin at 37°C in a humidified atmosphere of 5% CO_2 (all reagents were purchased from Sigma-Aldrich, St. Louis, MO). Exponentially growing cells were counted and viability was determined using the Guava EasyCyte flow cytometer (ViaCount assay; Guava Technologies, Hayward, CA). Throughout, after 3 d in culture, cells were split 1:4 and only cultures with at least 95% viability were used. After 3 mo, cells were recovered from original frozen stocks. For experiments, THP-1 cells were grown in a similar growth medium supplemented with 5% FBS. Throughout, cell morphology was monitored and images were collected using a 1X81 motorized inverted fluorescence microscope (Olympus, Melville, NY). Peripheral blood monocytes (PB mono) were isolated from whole blood using a two-step technique (19) with Ficoll-Hypaque of density 1.070 g/ml and then a Percoll gradient of density 1.064 g/ml. This technique gave a high yield of monocytes with a minimum contamination with platelets and RBCs.

Purification and characterization of PMVs from conditioned medium

PMVs were isolated by a modification of the method of Eken et al. (14). Briefly, conditioned medium from cells (1×10^6) stimulated with 10% normal human serum (NHS), 0.1 μM PMA, 10 μM histamine, or 1 μM ATRA at 37°C for 30 min, unless otherwise stated, was first centrifuged at $160 \times g$ for 5 min to remove cells. The supernatant was then centrifuged twice at $4000 \times g$ for 30 min to remove cell debris. The resultant supernatant was sonicated in a sonicating water bath (Townson and Mercer, Croydon, U.K.) for 5×1 min prior to centrifugation to disperse aggregated exosomes. Supernatant was centrifuged at $25,000 \times g$ for 90 min to pellet PMVs, which were then washed once by resuspending in PBS and centrifuging at $25,000 \times g$ for 90 min. The PMVs were then resuspended in PBS and quantified on a Guava EasyCyte flow cytometer using ExpressPlus software, or stained with annexin V (AnV)-FITC to determine surface phosphatidylserine (PS). The protein concentration of isolated PMVs was determined using the BCA protein assay kit (Pierce, Rockford, IL), according to the manufacturer's instructions, and PMVs were then used immediately. To confirm the size range of PMVs isolated, and to standardize the flow cytometer (Guava EasyCyte) settings for counting THP-1–derived PMVs, Megamix fluorescent sizing beads (Biocytex, Marseille, France) calibrated to 0.5 and 0.9 μm were used, according to the manufacturer's instructions.

Growth inhibition assays

Human THP-1 cells in the exponential phase were washed twice with RPMI 1640 and resuspended in growth medium containing 5% FBS. Cells were seeded into 12-well plates at 1×10^5 cells/well in triplicate. Different concentrations of PMVs, or a range of differentiation/proliferation-inhibiting agents (PMA, ATRA, histamine), were added to each well (except controls) and plates were incubated at 37°C for 3 d. On the days indicated, nonadherent cells were removed and counted by ViaCount assay on a Guava EasyCyte flow cytometer. In some experiments, THP-1 cells were incubated with 30 μg PMVs alone or in the presence of the TGF-β receptor antagonist SB-431542 (10 μM) or with 25 μg/ml affinity-purified, neutralizing rabbit anti–TGF-β1 (GenWay Biotech, San Diego, CA).

Measurement of intracellular calcium

Measurements of intracellular calcium were made before and after addition of histamine, ATRA, and PMA with or without 25 μM calcium chelator BAPTA-AM (Sigma-Aldrich). After 30 min of pretreatment with the agents in phenol red-free RPMI 1640 (Invitrogen, Carlsbad, CA), cells (1×10^6/ml) were resuspended in physiological salt solution containing 130 mM NaCl, 5 mM KCl, 1 mM $MgCl_2$, 1 mM $CaCl_2$, 10 mM HEPES, and 1% BSA. The procedure was carried out as described previously (20), but essentially the cells were loaded with 2 μM fura 2-AM (Sigma-Aldrich) with continual stirring, and fluorescence was monitored on a spectrofluorimeter at 505 nm upon excitation at 340 and 380 nm every second. Intracellular Ca^{2+} concentration ($[Ca^{2+}]_i$) was calculated using the equation $[Ca^{2+}]_i = K_d[(R - R_{min})/(R_{max} - R)]$, where R is the ratio of the emission intensities measured at 505 nm on excitation at 340 and 380 nm. R_{min} was obtained at $[Ca^{2+}]_i$ of 0 (by addition of 10 mM EGTA), and R_{max} was obtained by lysing the cells with 0.1% Triton X-100, thus allowing Fura-2 measurement in the maximum external calcium concentration of 1 mM. The temperature of the experiment was 37 ± 1°C, and K_d for Fura-2 is 224 nM.

Cell cycle analysis

THP-1 cells (1×10^6) in cold PBS were fixed in cold 70% ethanol. After washing in PBS, cells were stained with propidium iodide (50 μg/ml) for 1 h at 4°C and analyzed using a FACSCalibur flow cytometer (BD Biosciences, San Jose, CA) according to the manufacturer's instructions. The percentage of the population in G_0–G_1, S, and G_2–M phases of the cell cycle was determined using CellQuest software (BD Biosciences) and represented in GraphPad Prism 5.0 (Graphpad Software, San Diego CA).

Differentiation assays

Adherence of cells was determined following treatment with 30 μg PMVs. On the day of the experiment, 1×10^5 cells/well were seeded into 12-well culture plates in triplicate. On each of the indicated days, the nonadherent cells were transferred into new plates and incubated at 37°C in a 5% CO_2 incubator. The wells were then washed twice with serum-free RPMI 1640 and the attached cells released with trypsin/EDTA (Sigma-Aldrich). The trypsinized cells, now in suspension, were collected by centrifugation ($200 \times g$, 5 min), stained with ViaCount reagent, and counted by flow cytometry.

To investigate differentiation, THP-1 cells or PB mono were seeded into 12-well plates in triplicate. Cells were left untreated (control) or treated either with 30 μg PMVs or with PMA (0.1 μM) and incubated at 37°C in a humidified atmosphere of 5% CO_2 for 3 d. After this time, cells still in suspension were removed and the plates washed three times with RPMI

1640. Cells attached to the bottom of the plates were immunolabeled at 4°C for 1 h with the Abs anti–CD14-FITC, anti–CD11b-PE, and anti–DC-SIGN-FITC, with IgG-FITC and IgG-PE isotypes being used as controls. After three washes with PBS, cells were placed in PBS, 1% BSA and relative fluorescence was determined using the FLUOstar Omega microplate reader (BMG Labtech, Ayelsbury, U.K.).

NBT (Sigma-Aldrich) was used to determine intracellular O^{2-} as a measure of differentiation. For this assay, cells seeded at ~5 × 10^5 cells/ml in 24-well plates were treated for 1 h at 37°C with 1 mg/ml NBT and 4 μg/ml PMA. After washing in PBS the cell pellet was dissolved in 100 μl DMSO and the absorbance read at 570 nm on a spectrophotometer.

SDS-PAGE and Western blotting

Protein extracts were prepared and either analyzed by SDS-PAGE (for identification by mass spectrometry) or by Western blotting as described previously (21).

Immunofluorescence staining for cytokines/growth factors

Cell surface expression of TGF-β1, MIF, FGF-1, and Gal-3 molecules was analyzed by flow cytometry (EasyCyte; Guava Technologies). THP-1 cells (2 × 10^6) were washed twice (200 × *g*, 5 min each) with PBS and resuspended in cold PBS containing 10% FBS and 1% NaN_3. Cells were incubated in the dark with primary Abs (2 μg/million cells; R&D Systems, Abingdon, U.K.) at 4°C for 1 h with shaking. After three washes (400 × *g*, 5 min), cells were stained with the isotype-matched controls (anti-mouse or anti-rabbit IgG-FITC; R&D Systems) diluted 1/320 in PBS with 3% BSA and incubated with shaking, in the dark, at 4°C for 1 h. Cells were again washed three times with cold PBS, resuspended in 200 μl PBS containing 3% BSA, 1% NaN_3, and analyzed immediately using flow cytometry and the ExpressPlus assay program.

For staining of intracellular cytokines, THP-1 cells (2 × 10^6/reaction) in triplicate were resuspended in permeabilization buffer (0.5% Tween 20 in PBS) at room temperature for 20 min. Cells were permeabilized by washing three times with permeabilization buffer and incubated with 2 μg primary Abs at 4°C for 1 h in PBS with 10% FBS/1% NaN_3. Cells were washed three times and incubated with IgG-FITC–labeled secondary Abs (4°C, 1 h) and again washed three times with PBS. Samples were finally resuspended in 200 μl PBS containing 3% BSA, 1% NaN_3, and analyzed immediately by flow cytometry.

Flow cytometric analysis of apoptosis

To see whether PMV-releasing THP-1 cells were undergoing apoptosis, cells were stained with annexin V (AnV) and 7-aminoactinomycin D (7-AAD) (Guava Nexin Reagent). AnV and 7-AAD-positive cells were then quantified using a Guava EasyCyte flow cytometer over the course of 1 h. To see if adding PMVs to cells rendered them apoptotic, these measurements were made 24, 48, and 72 h after addition of PMVs.

Fluorescent microscopy analysis

For fluorescent microscopy, all experimental samples were placed into plates containing coverslips by centrifugation (200 × *g*, 5 min, using an A-2-DWP rotor in a 5804R centrifuge; Eppendorf, Cambridge, U.K.) and fixed with 4% paraformaldehyde at 37°C for 10 min. Plates were gently washed twice with PBS, and coverslips were mounted on microscope slides with DAPI-Vectashield medium (Vector Laboratories, Burlingame, CA) for fixed cells and mounting medium (Agar Scientific, Essex, U.K.) for PMVs. Images were collected using a fluorescence microscope (1X81 motorized, inverted fluorescence microscope; Olympus).

Fluorescence microscopy of PMV-cell interaction using octadecyl rhodamine-labeled PMVs

THP-1–derived PMVs were labeled with octadecyl rhodamine chloride (R18) by treating PMVs with 1.37 mM ethanolic solution of R18 (containing a final concentration ≤1% v/v) for 1 h at room temperature in the dark. R18-labeled PMVs were separated from unincorporated R18 by ultracentrifugation at 100,000 × *g* for 1 h followed by dialysis in 14-kDa dialysis tubes at 4°C in HEPES/NaCl buffer. The ratio of R18 to PMVs was estimated measuring the fluorescence before and after removal of the unincorporated probe. THP-1 cells were incubated with R18-labeled PMVs for 10 min at 37°C, followed by three washes in PBS. The cells were fixed in 4% paraformaldehyde in PBS for 15 min. The cells were then washed five times and mounted on slides with Vectashield mounting medium (Vector Laboratories). For fluorescence microscopy, an Olympus IX81 inverted microscope, equipped with a monochromatic camera U-CMAD3, was used. Images were subsequently colored using the Cell^M imaging software (Olympus).

Quantitation of cytokines/growth factors by ELISA

PMVs were isolated from THP-1 cells stimulated with 10% NHS at 37°C for 30 min (22). The concentrations of TGF-β1, MIF, FGF-1, and Gal-3 were measured by using 30 μg protein in ELISA kits (R&D Systems) according to the manufacturer's instructions. In some experiments, PMVs (1 × 10^6/reaction), in triplicate, from THP-1, Jurkat, and MCF-7 cells were lysed before measuring cytokine levels.

Transmission electron microscopy and negative staining

THP-1 cells (5 × 10^6/ml) either stimulated (5% NHS) or not (control) were fixed in 0.1 M fixative solution (3% glutaraldehyde in 0.1 M sodium cacodylate buffer [pH 7.2]) and incubated at room temperature for 1 h. Samples were postfixed by incubation at 0°C for 1 h in 1% osmium tetroxide solution (1:1 mixture of 2% osmium tetroxide [Sigma-Aldrich] and 0.2 M sodium cacodylate buffer) and block stained in 1% aqueous uranyl acetate. Samples were resuspended in 1% hot agarose and dehydrated in an ascending ethanol series (from 70 to 100%, absolute ethanol [v/v]; Sigma-Aldrich) and washed twice with propylene oxide (Agar Scientific). Sample was infiltrated with a 1:1 mixture of propylene oxide/Agar resins (mixture of 4.8 g Agar resin, 3.6 g methyl nadic anhydride, 1.9 g dodecenyl succinic anhydride, and 0.2 g benzyldimethylamine; Agar Scientific) and left rocking overnight at room temperature. Infiltrated samples were embedded in capsules using applicators and polymerized at 60°C for 24 h. Ultrathin sections were cut on a Leica Ultracut R ultramicrotome (Leica Microsystems, Deerfield, IL) and stained in Reynolds lead citrate. The sections were examined on a JEOL JEM-1200 EX II electron microscope (JEOL, Peabody, MA).

For negative staining, microvesicles isolated without prior sonication were stained with 2% aqueous uranyl acetate or 2% phosphotungstic acid (pH 6.8) plus aqueous bacitracin. Samples were placed on 400-mesh copper grids with a Pioloform support film (grids and Pioloform powder from Agar Scientific) and pretreated with 1% aqueous Alcian blue 8GX for 10 min. Digital images were recorded using the AMT digital camera previously described for the examination of stained ultrathin sections.

Statistical analysis

Statistical analysis (unpaired *t* test) was performed using GraphPad Prism software, version 5.0 (GraphPad Software, San Diego, CA). Differences giving a value of $p < 0.05$ were considered statistically significant.

Results

Characterization of PMVs isolated from THP-1 monocytes

PMVs were isolated by differential centrifugation of THP-1 cell-depleted conditioned medium after stimulation of THP-1 cells, and they were quantified using the Guava EasyCyte flow cytometer. The stimulus was sublytic complement (5% NHS), as heat inactivation (Fig. 1*A*) and C9 depletion of NHS (Fig. 1*B*) abrogated PMV release. The NHS as a source of complement itself had a negligible quantity of PMVs (Fig. 1*C*). Quantified PMVs were identifiable by their typical, heterogeneous size and granularity profile, R1, in Fig. 1*D*, as assessed by the logarithmic amplification of forward light scatter (FSC) and side light scatter (SSC) signals. PS expression on the membrane surface indicates the loss of lipid membrane asymmetry and, as well as being a distinguishing characteristic of cells undergoing very early apoptosis (23), it is found on the external leaflet of PMVs. Using flow cytometry, isolated PMVs were found to be PS-positive by staining with AnV (Fig. 1*E*), to be enriched for actin (Fig. 1*F*), and to fall within the expected size range, 0.5–0.9 μm diameter (Fig. 1*G*).

After stimulation, the release of PMVs increased over a 20-min period, without any further increase up to 1 h (Fig. 1*H*). During this time and coincident with the increased numbers of released PMVs, the increase in the percentage of early apoptotic cells almost doubled (from 4.5 to 10% AnV-positive) and of late apoptotic cells also increased significantly (from 1 to 3% AnV plus 7-AAD-positive cells) compared with unstimulated controls.

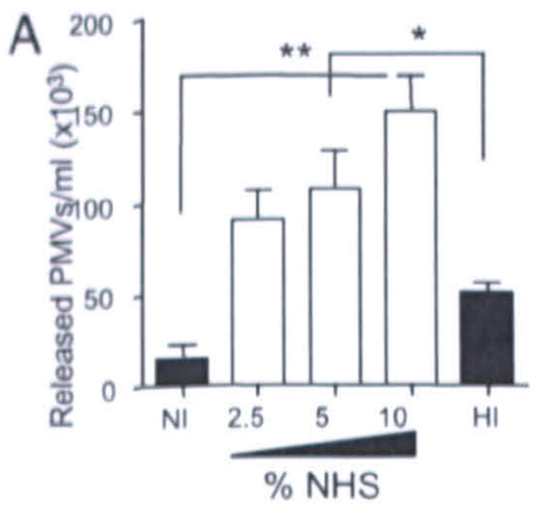

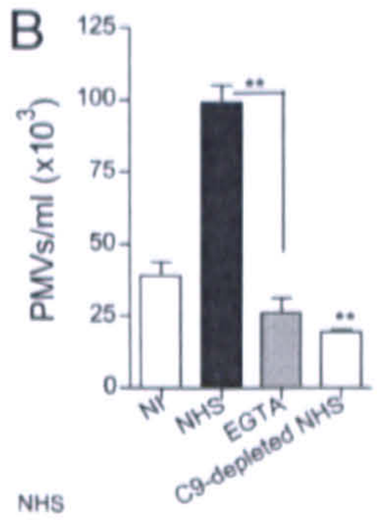

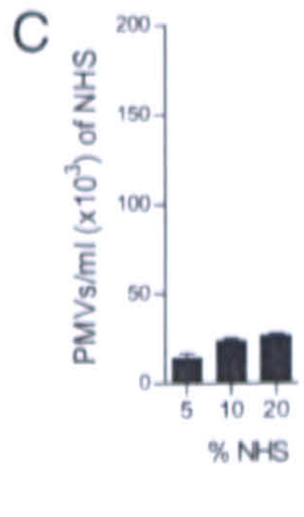

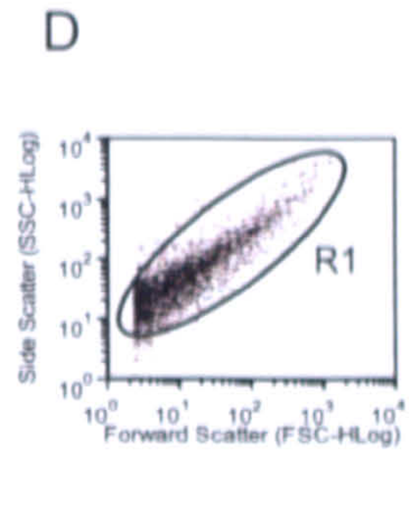

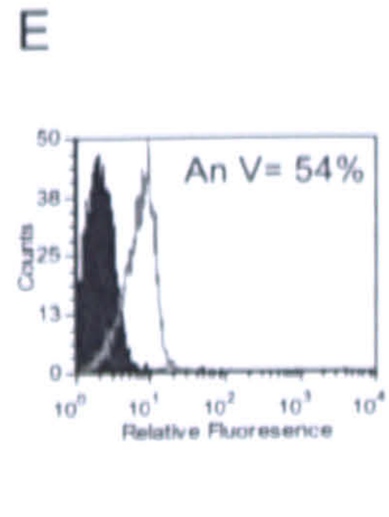

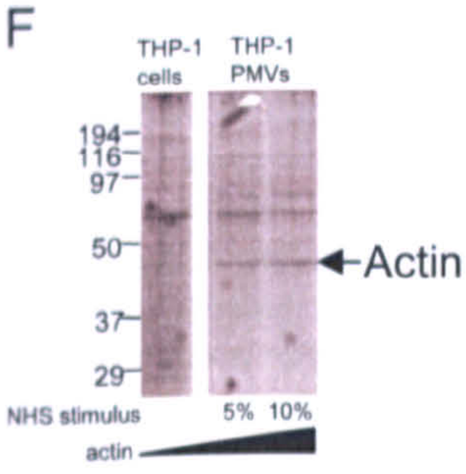

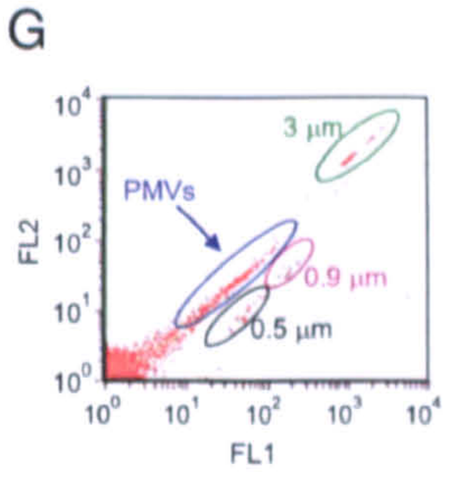

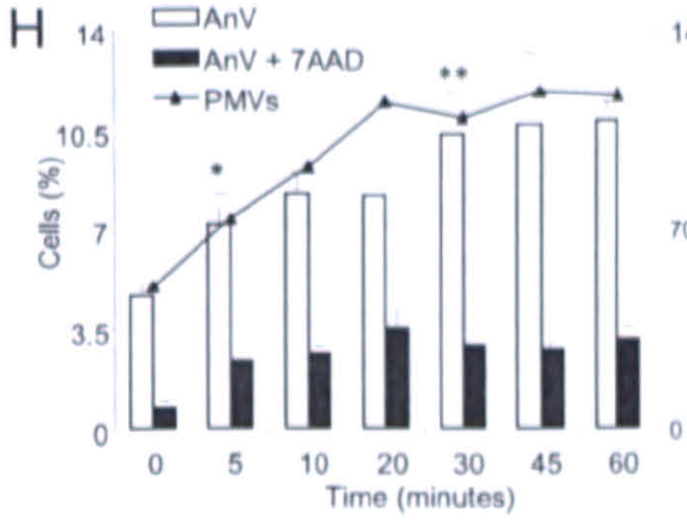

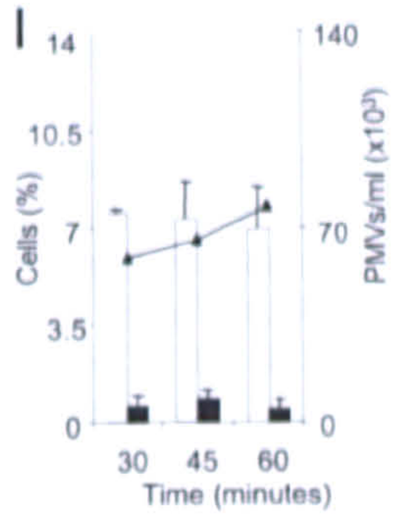

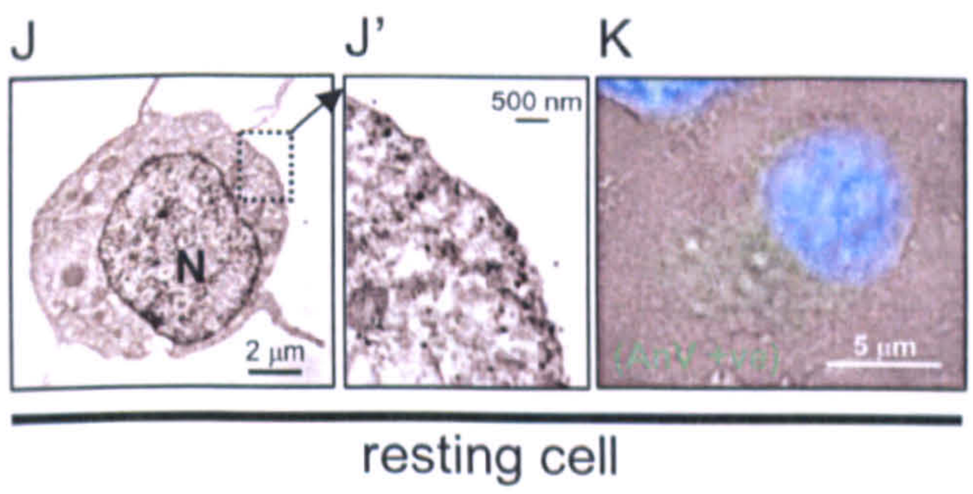

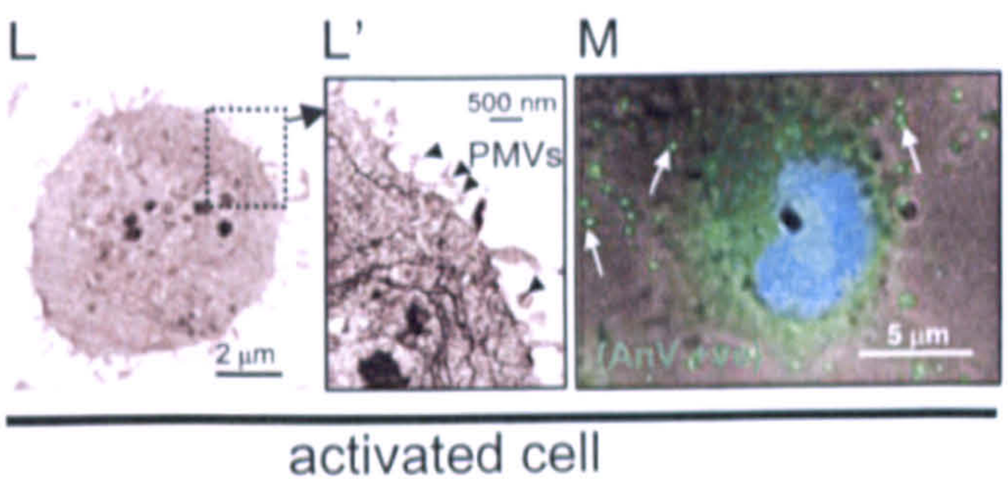

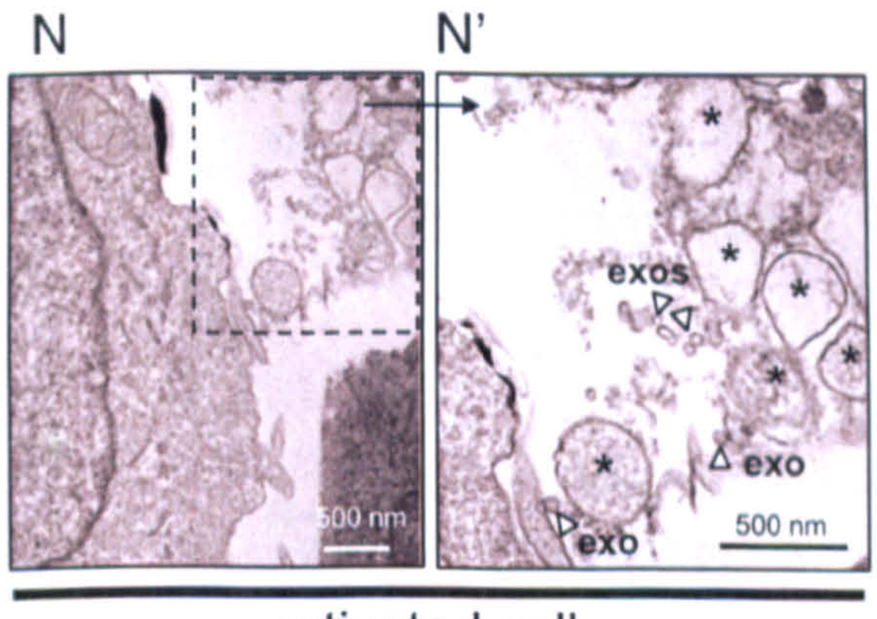

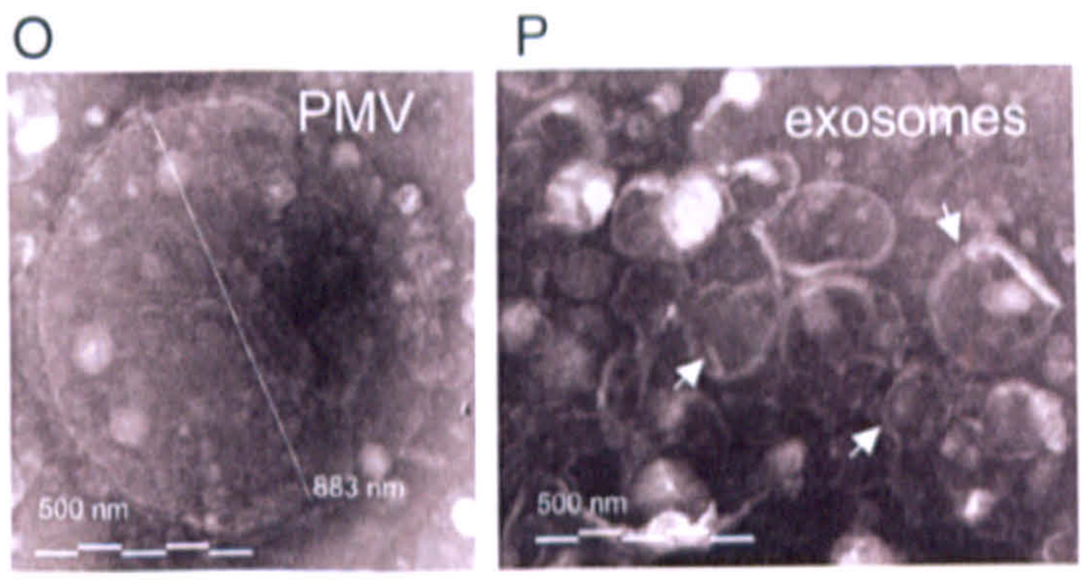

FIGURE 1. Analysis of isolated PMVs. *A*, Dose response of PMVs released from THP-1 cells with increasing NHS but not heat-inactivated (HI) NHS. *B*, PMV release is inhibited by incubating cells with 10 mM EGTA and by depletion of complement C9 from NHS. The amount of PMVs in the stimulating 5 and 10% NHS itself is negligible, *C*, A representative dot plot distribution of PMVs on a flow cytometer in *D* showing FSC (size) and SSC (granularity). PMVs are heterogeneous in size, and the region, R1, represents the FSC/SSC scatter gate of the vesicles. *E*, Isolated PMVs were analyzed for PS expression by staining with AnV; the resulting histogram shows ~54% of labeled PMVs to be AnV-FITC–positive. In *F*, the feature that PMVs are enriched for actin, identified by mass spectrometry, is confirmed in SDS-PAGE of equal loadings of THP-1 lysate compared with released PMVs. Using fluorescent sizing beads, *G* shows most released PMVs to be in the size range 0.5–0.9 μm diameter. *H*, After stimulation to vesiculate, PMV release increased over the first 20 min only, during which time there was an insignificant rise of early apoptotic cells (from 4 to 10%) and of late apoptotic cells (from 1 to 3%). *I*, One hour later cells were placed in complete growth medium lacking vesiculation stimulus and returned back to almost basal levels of apoptosis (7% early, 1% late). The release of PMVs from THP-1 cells, by electron or immunofluorescent microscopy, was observed for cells either left uninduced (resting) (*J*, *J'*, *K*) or stimulated with 5% NHS (*L*, *L'*, *M*) and in higher magnification (*N*, *N'*). Annexin V Alexafluor 488 and DAPI-VECTASHIELD, original magnification ×10,000 (*J*, *J'*, *L*, *L'*), ×60 (*K*, *M*), ×20,000 (*N*, *N'*). Magnified image *N'*, *inset*, show details of PMV release close to the cells (asterisks indicate released PMVs; white arrowheads point to exosomes). *O*, Image, prepared by negative staining, of purified PMVs isolated after sonication of supernatant and centrifugation at 25,000 × *g* for 90 min. Original magnification ×100,000. *P*, Negative staining image of purified exosomes isolated from PMV-depleted supernatant by ultracentrifugation at 160,000 × *g* for 16 h. Original magnification ×100,000. $*p < 0.05$; $**p < 0.01$; $***p < 0.001$.

When the stimulus was removed and cells were assessed 30–60 min later (Fig. 1*I*), the percentage apoptosis levels returned to initial levels (7% early and 1% late). This suggests the PS exposition on the outer leaflet of the plasma membrane, detected by AnV binding, to be an early feature of PMV release (7) that does not induce cell death. In fact, upon returning the cells to

non-microvesiculation conditions, the raised PS levels are found to be only transient, as described for IL-1–containing PMVs (7), with the level of late apoptotic cells being only 1%.

THP-1 cells left untreated (Fig. 1*J*, 1*J'*, 1*K*) or stimulated with 5% NHS at 37°C for 30 min (Fig. 1*L*, 1*L'*, 1*M*) were fixed immediately and processed either for transmission electron microscopy or immunofluorescence microscopy. Compared to control cells (Fig. 1*J*, 1*J'*), the cells activated with sublytic complement showed increased levels of pseudopodia (Fig. 1*L*, 1*L'*) and the release of AnV-FITC–labeled PMVs (Fig. 1*M* compared with control in Fig. 1*K*). Arrowheads indicate PMVs detached from the plasma membrane (Fig. 1*L'*, *inset*) and noted with asterisks under higher magnification (Fig. 1*N*, 1*N'*). Ultracentrifugation of samples depleted of debris at 160,000 × *g* for 90 min without prior water sonication resulted in aggregated exosomes being pelleted together with the PMVs (not shown). This is consistent with earlier reports, which suggested that exosomes are able to form clusters by binding with other exosomal vesicles (24). We show electron microscopy images of more pure PMVs (Fig. 1*O*) isolated, after sonication of supernatant (five times at 1 min) in a sonicating water bath, by centrifugation at 25,000 × *g* for 90 min. To obtain pure exosomes, supernatant depleted of PMVs was ultracentrifuged at 160,000 × *g* for 16 h, resulting in vesicles with the typical cup-shaped morphology of exosomes (Fig. 1*P*).

Monocyte-differentiating agent PMA, proliferation inhibitor histamine, and differentiating therapeutic ATRA induce PMV release and reduce proliferation

To confirm that ATRA, used in differentiation therapy for APL, limits proliferation of THP-1 monocytes, cell counts were determined for 3 d following addition of ATRA. Histamine and PMA were also used (Fig. 2*A*). By day 3, the significantly decreased proliferation levels with histamine, ATRA, and PMA correlated inversely with increasing levels of PMV release (Fig. 2*B*, 2*C*), and all three caused a marked increase in $[Ca^{2+}]_i$ (400 nM in 20 s) in THP-1 cells (Fig. 2*D*).

PMVs reduce the proliferation of THP-1 cells, alter cell morphology, increase adherence, and induce terminal differentiation

To investigate the effect of PMVs per se, we looked at the effect of separately isolated THP-1 PMVs on the growth of THP-1 cells in culture. Current estimates of microvesicle concentration in the peripheral blood of healthy individuals range from 5 to 50 μg/ml. According to our calculations, this equates to 2×10^5 to 2×10^6 PMVs/ml for PMVs ranging in size from 0.5 to 0.9 μm in diameter. Furthermore, we have found the quantity of PMVs/ml in plasma (from 25 fasting subjects) to range from 2.8×10^5 to 5.8×10^5 PMVs/ml (R. Grant, D. Stratton, S. Lange, S. Antwi-Baffour, E. Ansa-Addo, S. Kholia, J. Naveda, and J. Inal, manuscript

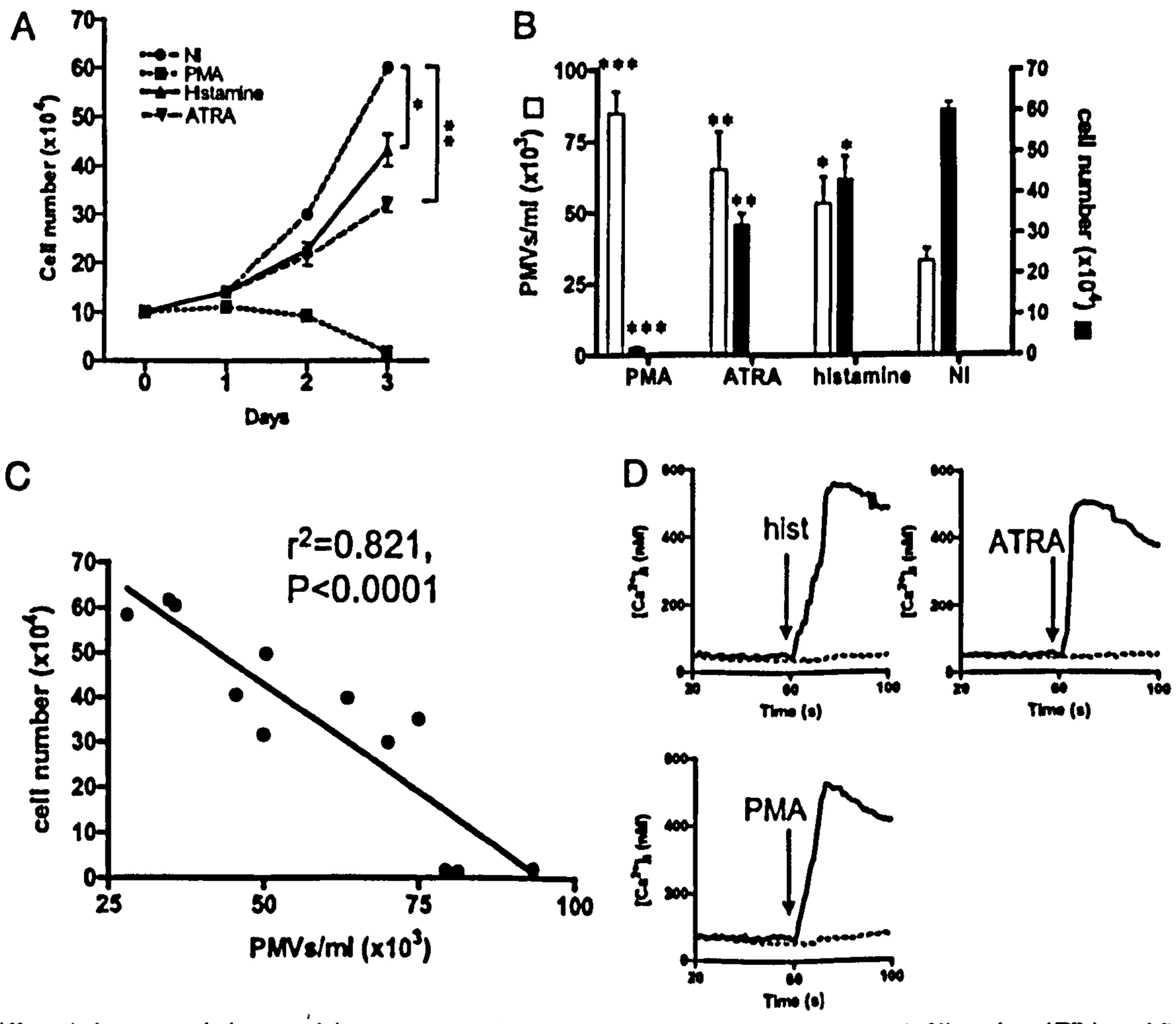

FIGURE 2. Differentiating agents induce a calcium-mediated release of PMVs from THP-1 monocytes. *A*, Histamine, ATRA, and PMA result in increasingly significant reductions in cell growth after 3 d. ATRA, PMA, and histamine induce PMV release. THP-1 cells (1×10^5 cells/ml) in triplicate wells of a 24-well plate were incubated with 0.1 μM PMA, 10 μM histamine, and 1 μM ATRA. Cell numbers were determined using a ViaCount assay on the Guava EasyCyte flow cytometer on days 1, 2, and 3 after addition of these agents. In *B*, for the day 3 results presented, there is an apparent inverse correlation between cell number and PMVs/ml released after treating with histamine, ATRA, or PMA. This is confirmed in *C*, which shows a significant negative correlation between cell number on the third day and the released PMVs/ml upon treatment with PMA/ATRA/histamine. To show that these differentiating/proliferation-inhibiting agents are inducing PMV release mediated after a rise in $[Ca^{2+}]_i$, spectrophotometric measurements of $[Ca^{2+}]_i$ using fura 2-AM were made after addition of ATRA, PMA, or histamine (dotted line represents control, untreated cells) (*D*). $*p < 0.05$; $**p < 0.01$; $***p < 0.001$.

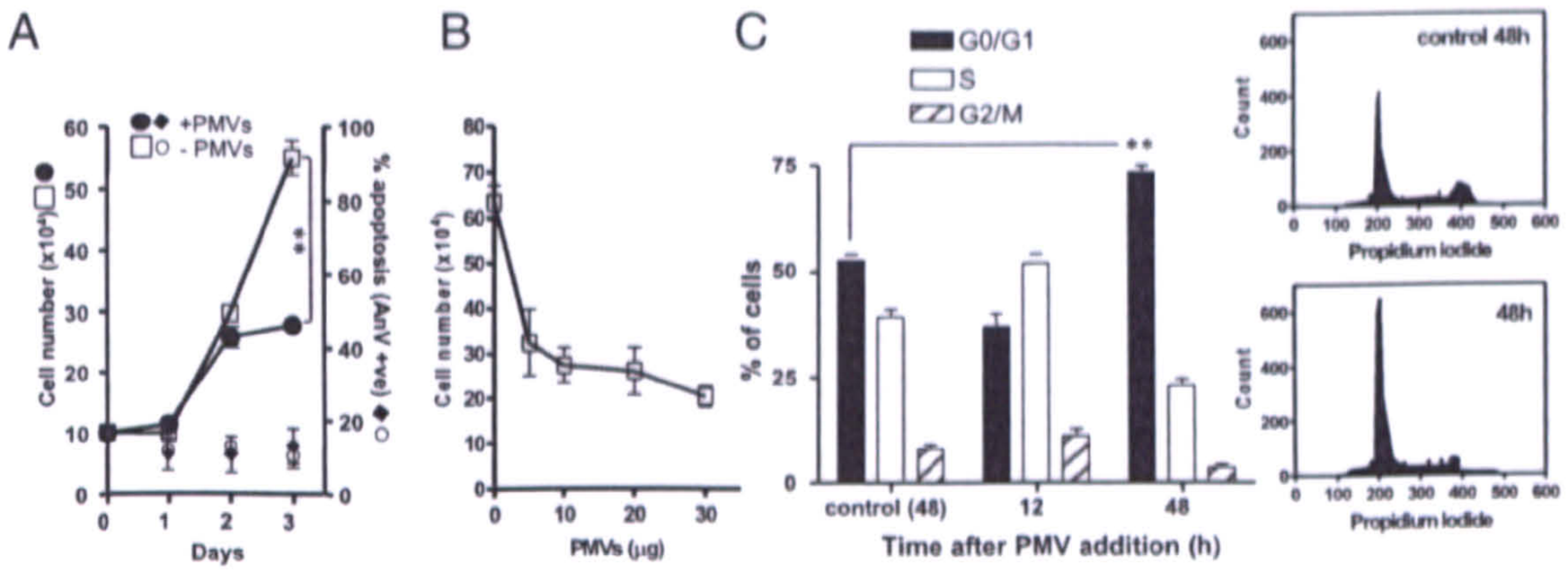

FIGURE 3. PMVs stop the proliferation of THP-1 monocytes and induce their terminal differentiation as well as that of primary monocytes. *A*, THP-1 cells were seeded at 1×10^5 cells/well in triplicate in RPMI 1640 supplemented with 5% FBS. Wells were incubated without (□) or with (●) 10 μg of PMVs. At 24-h intervals, cells were harvested and the number was determined by flow cytometry. On days 1, 2, and 3, the percentage apoptosis (AnV-positive) was determined to be ~15% whether PMVs had been added (♦) or not (○). Addition of PMVs appeared to have halted proliferation by 48h. *B*, The number of viable cells 3 d after exposure to PMVs did not reduce substantially with amounts of PMVs ≥10 μg. Each point represents the mean of triplicate cultures. *C*, Cell cycle analysis shows a large increase in the percentage of cells in cell cycle arrest G_0–G_1, from 32% after 12 h to 72% at 48 h, compared with control without PMVs (52% after 48 h). *D*, THP-1 monocytes and PB mono (1×10^6 each) are stimulated to release PMVs after incubation with 5% NHS at 37°C for 20 min. This release is inhibited upon calcium chelation with 10 mM EGTA. *E*, Human THP-1 and PB mono (1×10^5/well) were seeded in triplicate into 24-well plates with or without PMVs. Cell morphology (unstained) was assessed daily using an inverted light microscope. Arrows

in preparation). In the absence of such figures for the hematopoietic environment, THP-1 cells were seeded into 24-well plates (1×10^5 cells/well containing 1 ml of medium) with or without 30 μg or 1.2×10^6 PMVs (released from ~1×10^7 THP-1 cells), in triplicate. Plates were incubated at 37°C in a humidified atmosphere of 5% CO_2 for 3 d. On each of the days indicated, cells were stained with ViaCount reagent, a DNA-binding dye (Guava Technologies), and the number of viable and apoptotic cells per well was determined using the ViaCount assay by flow cytometry.

After a lag phase of ~24 h, the increase in cell number of the cultures treated with PMVs, over the following 48 h, was markedly less than that of cells without added PMVs (Fig. 3*A*), and at no point was there an increase in the level of apoptotic cells (≤15%). Neither PMVs added nor the ViaCount reagent used was cytotoxic to the cultures, as the percentage of apoptosis was similar between untreated and PMV-treated (Fig. 3*A*). This PMV-induced reduction in growth rate was significant by day 3 (Fig. 3*A*), with 10 μg providing a saturating amount of PMVs (Fig. 3*B*). These results are broadly similar to earlier observations made on addition of TGF-β1 to THP-1 cells (25) and by an autocrine/paracrine mechanism described in APL HL60 cells (26). The THP-1 cells were found to apparently exit the cell cycle after 48 h, with the percentage of the population in G_0–G_1 increasing from 53 to 73% (Fig. 3*C*).

Having shown that THP-1 cell proliferation is inhibited by PMVs, and because primary monocytes, as well as the THP-1 monocyte cell line, are able to release PMVs (Fig. 3*D*), we measured the effect of PMVs on monoyctes (primary and continuous cell line) in terms of their capacity to induce differentiation. When monocytes are cultured, they grow in suspension as round cells. However, compared with control cells, we observed distinct changes in morphology within 24 h of addition of PMVs, which became more marked by day 3 with the appearance of membrane protrusions (Fig. 3*E*). To look for changes in adherence, THP-1 cells and PB mono were seeded into 12-well plates in RPMI 1640 containing 5% FBS and left untreated or treated with PMVs (30 μg). Consistent with the changes in morphology, increased numbers of cells attached to the culture plates after 3 d (Fig. 3*F*, black bars) in the presence of PMVs, and only a few cells attached without any treatment.

These observations further suggested that PMVs might be inducing the expression of a macrophage-like phenotype in the cells. To investigate this, THP-1 cells and PB mono were treated with 30 μg of PMVs and, after 3 d of incubation, were found to have increased expression of CD14 (Fig. 3*G*, 3*J*) and CD11b (Fig. 3*H*, 3*K*) (typical for macrophages), but not DC-SIGN (dendritic cells) (Fig. 3*I*, 3*L*). Untreated cells expressed low levels of these surface receptors, and PMA (0.1 μM)-treated cells were used as a positive control for differentiation into macrophages (Fig. 3*G–I*) (27). As a marker of more mature phagocytes, we found the ability to generate reactive oxygen species, using the NBT reduction assay, to be significantly increased 24 and 72 h after addition of PMVs (Fig. 3*M*, 3*N*).

PMVs released from THP-1 monocytes carry extravesicular TGF-β1 and intravesicular proteins MIF, FGF-1, and Gal-3, which are involved in monocyte-to-macrophage differentiation

In a preliminary study, we applied isolated THP-1 PMVs to a human Ab cytokine microarray (R&D Systems) and found the PMVs to carry a range of cytokines, acute phase proteins, and chemokines, including IL-12 p70, IL-13, I-TAC, IL-16, IL-17E, MIF, MIP-1α, and Serpin E1. Given the wide range of cytokines carried by the PMVs, we decided to focus on TGF-β1, which if present on the surface of released PMVs, we surmised, could potentially bind in an autocrine/paracrine-like manner to its cognate receptor on myeloid cells and initiate differentiation. Since TGF-β1 has a signal peptide, we also examined whether cytokines, such as MIF, FGF-1, and Gal-3, which lack a signal sequence (28–30), are transported in PMVs. Although it has previously been shown that such leaderless cytokines are transported via a nonconventional secretory process (6, 7), note that most of these studies are based on exosomes, which, unlike PMVs, which are released through a budding process from the cell's plasma membrane, are released upon fusion of multivesicular bodies with the plasma membrane (31).

By flow cytometry we found THP-1 cells to strongly express TGF-β1 on the surface (Fig. 4*A*). This has been described for the propeptide part of the large latent TGF-β complex, often tethered to fibronectin in the extracellular matrix (32). MIF, FGF-1, and Gal-3 are expressed on the surface at lower levels (Fig. 4*A*). Upon stimulation of these labeled cells with 10% NHS, the PMVs released showed surface expression of TGF-β1, but not of MIF, FGF-1, and Gal-3 (Fig. 4*B*). When the cells were permeabilized with 0.5% Tween 20, there was an increased labeling of MIF, FGF-1, and Gal-3 (Fig. 4*C* compared with Fig. 4*B*), which implies their greater intracellular expression.

The appearance of TGF-β1 on PMVs after stimulation of release from THP-1 cells coincided with a removal of the TGF-β1 signal as detected by Western blot on THP-1 cells (Fig. 4*D*). We also showed extravesicular expression of TGF-β1 by immunofluorescence microscopy (Fig. 5*A*). Although no significant difference was observed in TGF-β1 levels by ELISA, regardless of whether the PMVs were lysed (Fig. 5*B*), levels of MIF, FGF-1, and Gal-3 were significantly higher when PMVs were lysed before measurement (Fig. 5*B*), suggesting that TGF-β1 is predominantly expressed on the cell/PMV surface, whereas MIF, FGF-1, and Gal-3, for the most part, have an intracellular/vesicular location.

TGF-β1 carried by PMVs inhibits proliferation of THP-1 monocytes

To determine whether THP-1 PMVs can interact with THP-1 cells, we were able to show the appearance of the fluorescent lipid R18 on THP-1 cells after incubation for 10 min at 37°C with R18-labeled PMVs (Fig. 6*A*). The punctuate fluorescence indicates association or attachment of PMVs. To confirm that the surrounding limited diffuse staining in Fig. 6*A3* could be due to lipid mixing, we were able to demonstrate R18 dequenching spectrophotometrically within 4 s of adding R18-labeled PMVs (Fig. 6*B*). This was indicative of lipid mixing and so potentially of membrane fusion and could be blocked by preincubation of recipient THP-1 cells with AnV.

We also investigated whether the ability to inhibit the rate of cell growth was only characteristic of PMVs released from THP-1 cells. When 30 μg of PMVs (equivalent to ~1×10^6 PMVs) from other cell lines, such as MCF-7 (breast cancer), Jurkat (T cell), as

in cultures treated with PMVs indicate attached cells with pseudopodia-like processes after 3 d of incubation. *F*, After 3 d, increased numbers of cells (THP-1 promonocytes and primary cells) were found attached to the plates in PMV-treated wells (filled bars), but very few cells adhered to the culture plates in the absence of PMVs (open bars). Mean fluorescence intensity, indicative of surface expression levels, showed THP-1 monocytes (*G–I*) and PB mono (*J–L*) treated with PMVs to be significantly positive for CD14 and CD11b, but not DC-SIGN (CD209), as compared with untreated control. PMA-treated cells used as control for monocyte-derived macrophages were also shown to be highly positive for CD14 and CD11b. The NBT reduction assay shows an increase in superoxide activity in THP-1 monocytes and primary monocytes (*M* and *N*, respectively) treated with PMVs, indicative of their differentiation. Data represent the mean ± SD of two experiments performed in triplicate. $*p < 0.05$; $**p < 0.01$; $***p < 0.001$.

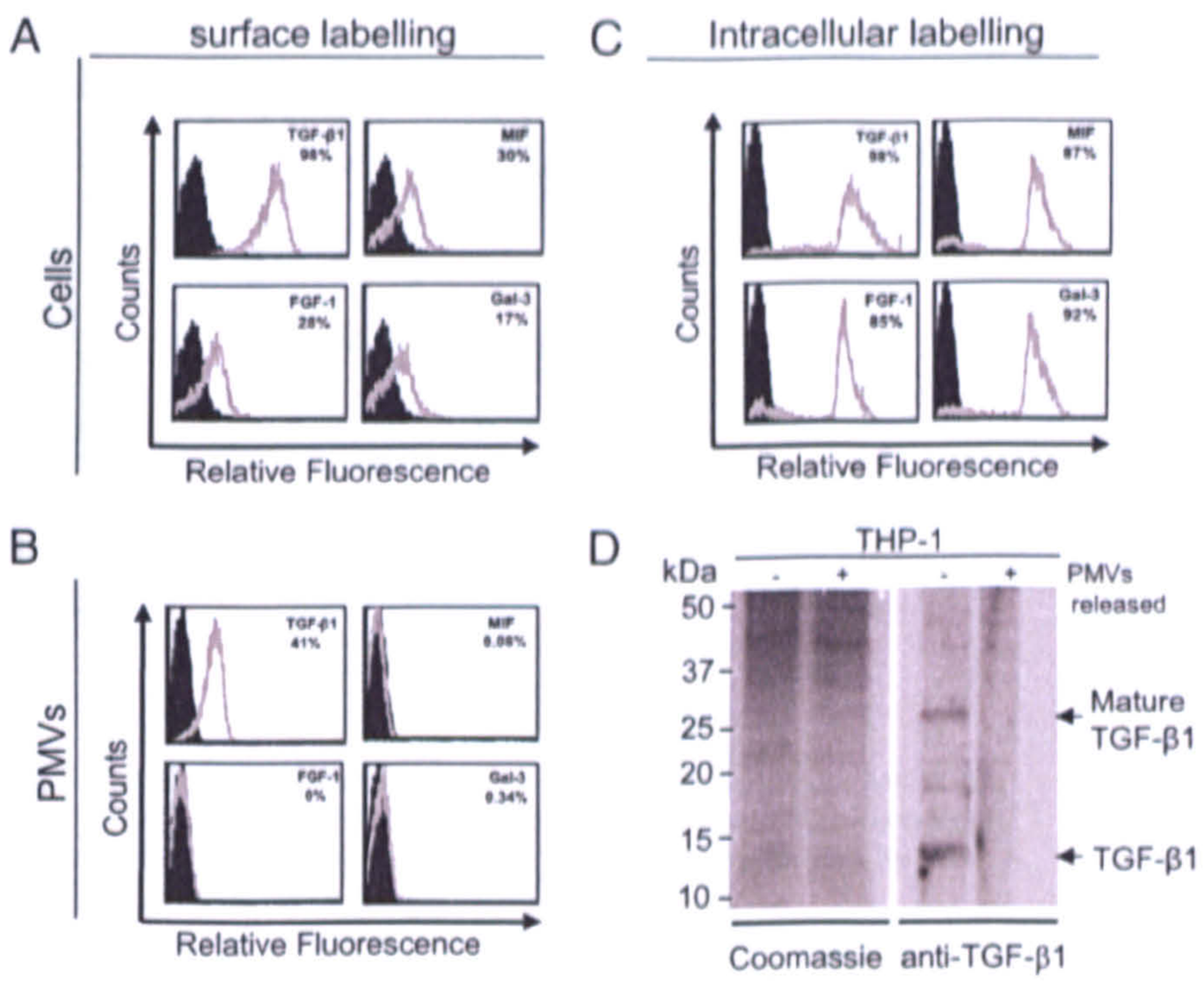

FIGURE 4. Flow cytometry of PMVs for TGF-β1, MIF, FGF-1, and Gal-3. *A*, Flow cytometric analysis of THP-1 cells (2×10^6) and of released PMVs (*B*) after surface labeling with Abs against TGF-β1 and proteins, which lack a signal peptide (MIF, FGF-1, and Gal-3). Intracellular staining after permeabilization with 0.5% Tween 20 in THP-1 cells for the above-mentioned proteins (*C*). Western blotting of THP-1 cells after stimulating PMV release (+) shows a dramatic reduction of TGF-β1 compared with unstimulated cells (−) (*D*). In all experiments, PMVs were released by providing THP-1 cells with sublytic complement (5% NHS) for 30 min at 37°C.

well as those from THP-1 (monocytic leukemia), was added to THP-1 cells, only those from Jurkat and THP-1 cells, which carried higher levels of TGF-β1 (Fig. 6*C*; 1900 pg by the 1×10^6 [30 μg] THP-1 cells and 2600 pg by the 1×10^6 [30 μg] Jurkat PMVs), significantly reduced proliferation (Fig. 6*D*), a known prerequisite for differentiation (33). In contrast, MCF-7 PMVs, which carry less TGF-β1 (250 pg by the 1×10^6 [30 μg] PMVs added), only reduced proliferation marginally compared with untreated control. With increasing amounts of MCF-7 PMVs (90 μg [carrying 750 pg of TGF-β1] or 210 μg [carrying 1750 pg of TGF-β1]), a growth reduction equivalent to the level achieved with 30 μg of THP-1 PMVs (carrying 1900 pg of TGF-β1) was achieved. This apparent correlation between levels of TGF-β1 and growth reduction suggests the involvement of TGF-β1 present on the PMVs.

This was further implied by showing that inhibition of growth rate after PMV addition could be restored to near control rates with SB-431542 (Fig. 6*E*). This is a specific small molecule inhibitor of TGF-βRI kinase and the associated intracellular mediators, such as Smad, with both being central to TGF-β1–mediated differentiation of myeloid cells (34). As TGF-βRI could also be activated

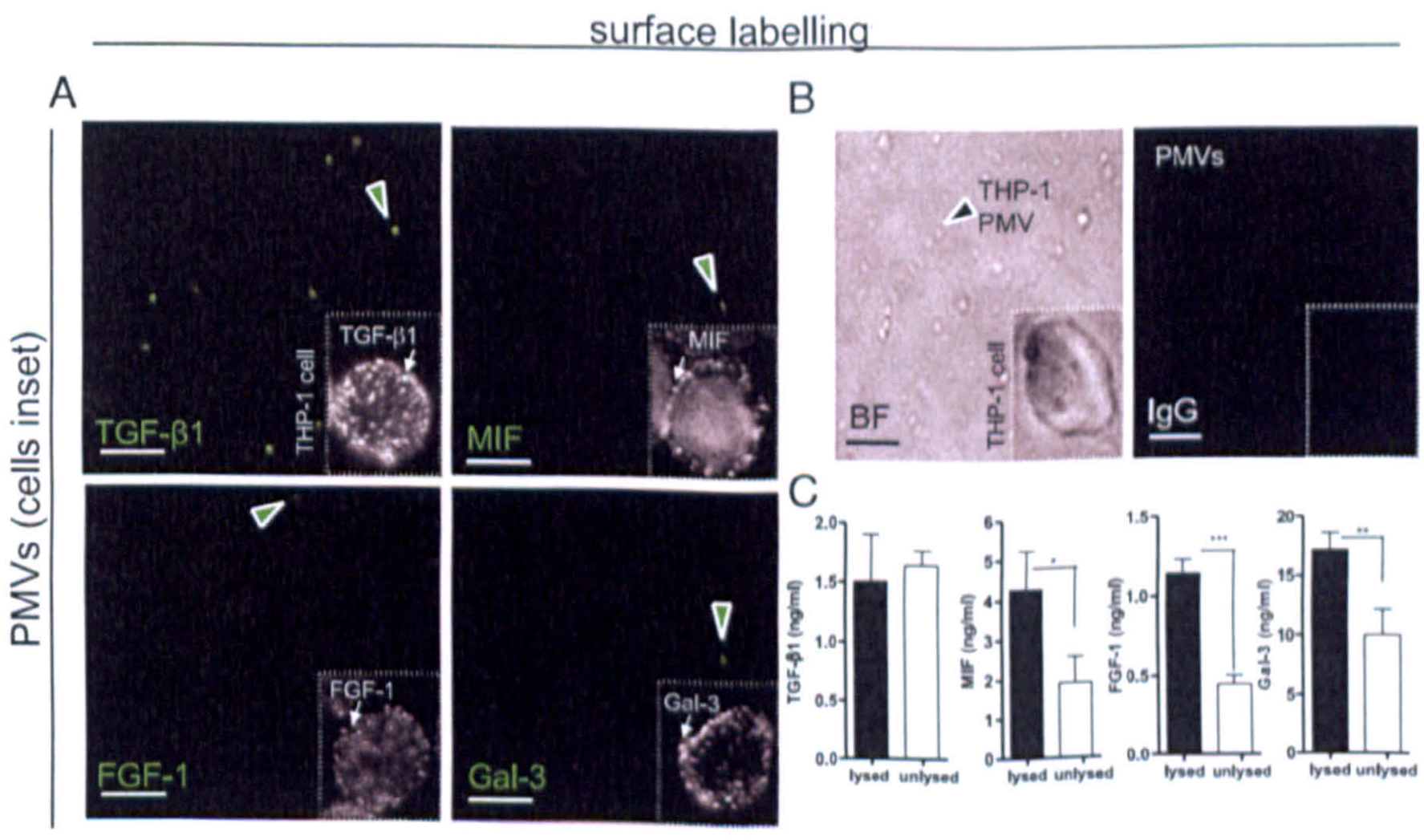

FIGURE 5. Extravesicular expression of TGF-β1 and intravesicular expression of MIF, FGF-1, and Gal-3 by immunofluorescence microscopy. *A*, Surface labeling of TGF-β1 on THP-1–derived PMVs but low levels of MIF, FGF-1, and Gal-3. Original magnification ×60; *inset*, ×20. *Inset*, Highest expression of TGF-β1 on cell surface. Bright field (BF) and representative IgG are shown. Isotype control images are shown in *B*. Original magnification ×60, *inset*, ×20. Scale bar, 10 μm. *C*, ELISA measurements of selected proteins in lysed and intact PMVs released from THP-1 cells. PMVs (30 μg) from stimulated cells (10% NHS at 37°C for 30 min) were either lysed or left unlysed and cytokine/growth factor levels were measured. There was no significant difference between TGF-β1 levels in lysed or intact PMVs. Increased levels of MIF, FGF-1, and Gal-3, however, were measured by ELISA after lysis of PMVs. $*p < 0.05$; $**p < 0.01$; $***p < 0.001$.

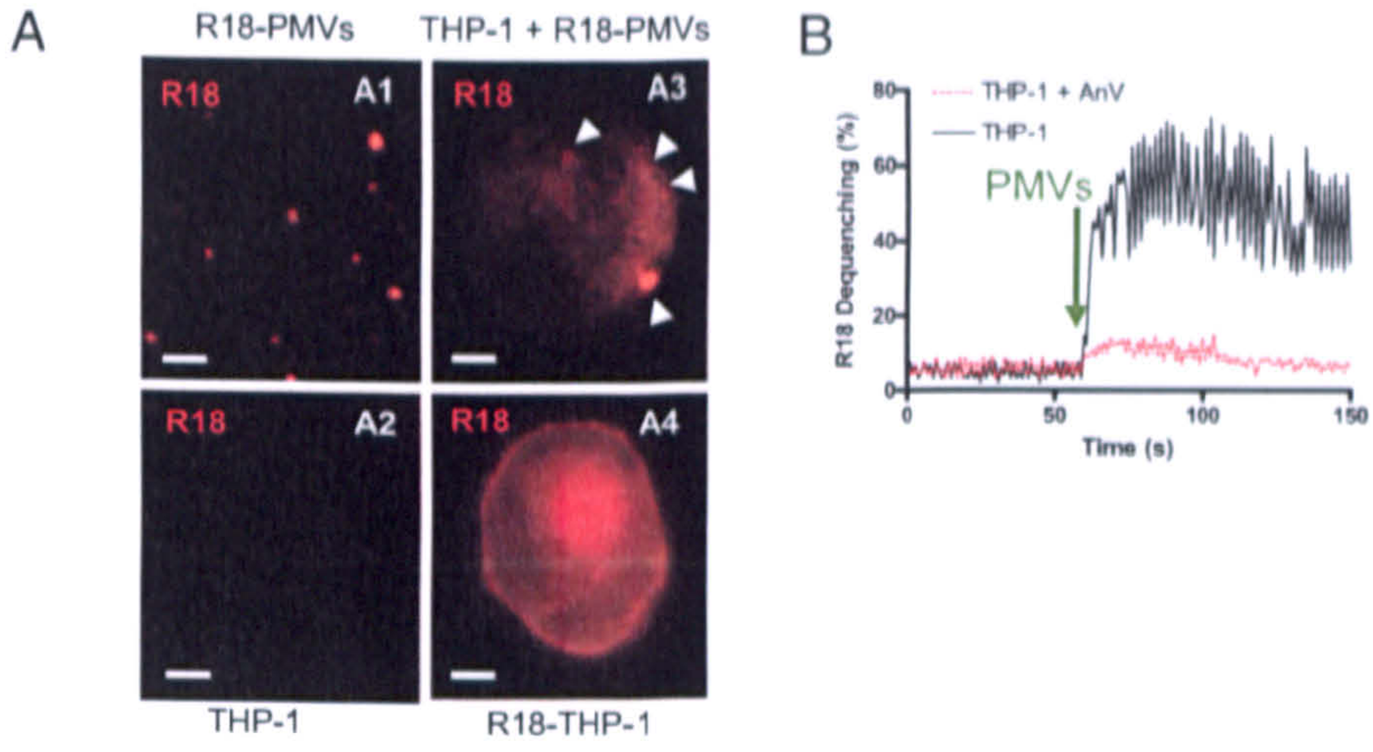

FIGURE 6. PMVs carrying surface TGF-β1 interact with THP-1 monocytes and reduce their proliferation. *A*, Transfer of R18 from R18-labeled THP-1 PMVs (*A1*) to recipient unlabeled THP-1 cells (*A2*, control, and *A3*) suggests contact, although not necessarily membrane fusion (lipid mixing). Control R18-labeled THP-1 cells have uniform, strong surface labeling with R18 (*A4*). Original magnification ×60. Scale bar, 2 μm. *B*, Lipid mixing upon addition of R18-labeled PMVs to THP-1 monoyctes is indicated by rapid dequenching as determined spectrophotometrically. This is probably mediated through PS interactions, as preincubation of THP-1 cells with AnV abrogated fusion. *C*, ELISA measurements of TGF-β1 isolated from THP-1 and Jurkat cells, unlike those from MCF-7 cells, show that they carry higher levels of TGF-β1. *D*, THP-1 cells (1×10^5/well) were left untreated or treated with Jurkat or THP-1 PMVs (30 μg) as well as MCF-7 PMVs (30, 90, and 120 μg). The cells were incubated at 37°C and quantified each day by flow cytometry. PMVs from THP-1 and Jurkat cells were more effective ($p < 0.01$) at reducing the growth rate than were MCF-7 PMVs. *E*, Addition of the TGF-β1 receptor antagonist SB-431542 or of anti–TGF-β1, but not control Rb IgG, abolished the inhibitory effect of PMVs (30 μg) significantly ($p < 0.05$) and restored the growth rate of the cells to almost control levels. Data represent mean ± SD of two separate experiments performed in triplicate. $*p < 0.05$; $**p < 0.01$; $***p < 0.001$.

by TGF-β1, 2, or 3, we further used anti–TGF-β1 as a blocking Ab, with similar results (Fig. 6*E*).

Discussion

The release of PMVs by various cells has been implicated in a wide range of biological activities in both in vitro and in vivo studies (5), with the most characterized function being that of intercellular communication (3, 35). We have shown that PMVs are released from cells stimulated through deposition with either sublytic complement or upon treatment with agents used in differentiation therapy. In the present study, to our knowledge we demonstrate for the first time that PMVs (isolated from THP-1 cells) carry TGF-β1 on their membrane surface. These TGF-β1–bearing PMVs can modulate the growth rate of THP-1 monocytes in vitro, without inducing apoptosis, the cells exiting the cell cycle at G_0–G_1. Additionally, we observed dramatic changes in the morphology of PMV-treated THP-1 monocytes and PB mono as they became increasingly irregular in shape, with membrane extensions resembling pseudopodia. By day 3 they became completely attached to the culture plate and expressed significantly higher levels of typical macrophage markers, such as CD14 and CD11b, but not the dendritic cell specific marker DC-SIGN (CD209). We also showed that PMVs isolated from Jurkat and THP-1 cells carrying high levels of TGF-β1 (≥200 pg TGF-β1/10^5 PMVs) caused significantly greater reductions in the growth rate of THP-1 cells as compared with PMVs from MCF-7 breast cancer cells, expressing lower levels (~30 pg of TGF-β1/10^5 PMVs). Because differentiation experiments with freshly isolated, human peripheral blood monocytes, as opposed to a leukemic promonocytic cell line, gave similar results, the possible involvement of PMVs in terminal monocyte-to-macrophage differentiation warrants further study.

Others have previously shown that rTGF-β1 can inhibit proliferation and promote differentiation of human promonocytic leukemic cells into macrophages (31). Our results are in agreement, but we go on to show the source of macrophage-inducing TGF-β1 to be that bound to the PMV surface. We also showed that attachment of PMVs to THP-1 cells is PS-mediated, similar to contact (and fusion) of monocyte-derived PMVs with platelets (36), but we did not show that such attachment/fusion was a prerequisite for the observed differentiation. Although contact with or phagocytosis of apoptotic cells and PMVs by macrophages has

been shown to release TGF-β1 at levels of 80 pg/ml (37) and 350 pg/ml (38), respectively, importantly, such release and autocrine-like action of TGF-β1 on the THP-1 cells, resulting in the observed reduction in proliferation (and consequent differentiation), is unlikely to have occurred in our study, as low TGF-β1–carrying MCF-7–derived PMVs were unable to elicit significant reductions in proliferation.

PMVs carry the majority of nonconventionally secreted proteins released into culture supernatants, and potentially carry them within the PMVs themselves. We have confirmed that the leaderless, intracellular proteins MIF, FGF-1, and Gal-3 are present within PMVs, and thus they are secreted nonconventionally. As reported for TGF-β1, and as described earlier, these leaderless proteins have also been shown to play important roles during the differentiation of myeloid cells. Although PMVs are known to deliver intravesicular proteins and surface receptors to recipient cells (39), this has not hitherto been demonstrated for a surface-bound cytokine, as we describe in this study, for TGF-β1.

The concept that surface TGF-β1 can stimulate TGF-β–mediated signaling on cell-to-cell contact, or by implication in this study by PMV–cell contact, is not new and has been described in T cells. Regulatory T cells ($CD4^+CD25^+$) express active TGF-β1 (40), which interacts with TGF-β receptor on effector cells, thereby mediating immunosuppression (41). Similarly, surface-bound, albeit latent TGF-β on the surface of colorectal cancer cells has also been implicated in immunosuppression following cell-to-cell contact (42). Although activation may occur through various mechanisms upon cell contact, latent TGF-β may be activated by α_V integrins, then mediating Smad signaling through TGF-βRI and TGF-βRII; MAPK and PI3K/Akt pathways may also be modulated.

Several inhibitors of TGF-β1 signaling have been reported as potential therapeutics in cancer immunotherapy. Among these is the TGF-β receptor type I antagonist SB-431542, a selective inhibitor of endogenous activin, of TGF-β1 signaling (43), and of resulting phosphorylation of Smads. The tumor-suppressive functions of TGF-β1 have also been reversed using SB-431542 in studies using the colon cancer-derived FET cells (34), and the antagonist has been shown to inhibit the ligand-dependent growth of HT-29 colon cancer cells (34). We demonstrated TGF-β1–mediated involvement in this study by showing that SB-431542 almost completely abrogated the growth inhibition due to PMV treatment of cells. That TGF-β1, on the surface of PMVs, could mediate such a change was confirmed by also reversing growth inhibition in the presence of anti–TGF-β1.

To ascertain the relative importance of PMV release after stimulation with ATRA, PMA, or histamine, in terms of limiting proliferation, it would be interesting to treat promonocytic cell lines with these agents following pretreatment with calpeptin, which specifically blocks calpain-mediated PMV release. TGF-β1 is unlikely to be the only factor that PMVs from THP-1 cells convey to induce differentiation. By using lentivirus-mediated short hairpin RNA expression, we have now generated a THP-1 cell line knocked down for expression of TGF-β1, which we can use in a repeat of the above experiments. Other factors carried by PMVs with the potential to induce differentiation should now also be studied, including Gal-3 and monocyte microRNAs, such as miRNA-155, shown to be involved in myeloid differentiation (11). In view of the need to expand the limited range of therapies in monocytic leukemia, it might be prudent to look at other PMV-releasing agents as potential alternative drugs in differentiation therapy against acute myeloid leukemia.

Acknowledgments

We thank V. Hornhoffer for protein identification by mass spectrometry.

Disclosures

The authors have no financial conflicts of interest.

References

1. Simons, M., and G. Raposo. 2009. Exosomes: vesicular carriers for intercellular communication. *Curr. Opin. Cell Biol.* 21: 575–581.
2. Hugel, B., M. C. Martínez, C. Kunzelmann, and J. M. Freyssinet. 2005. Membrane microparticles: two sides of the coin. *Physiology (Bethesda)* 20: 22–27.
3. Ratajczak, J., M. Wysoczynski, F. Hayek, A. Janowska-Wieczorek, and M. Z. Ratajczak. 2006. Membrane-derived microvesicles: important and underappreciated mediators of cell-to-cell communication. *Leukemia* 20: 1487–1495.
4. Hunter, M. P., N. Ismail, X. Zhang, B. D. Aguda, E. J. Lee, L. Yu, T. Xiao, J. Schafer, M. L. Lee, T. D. Schmittgen, et al. 2008. Detection of microRNA expression in human peripheral blood microvesicles. *PLoS ONE* 3: e3694.
5. Piccin, A., W. G. Murphy, and O. P. Smith. 2007. Circulating microparticles: pathophysiology and clinical implications. *Blood Rev.* 21: 157–171.
6. Nickel, W. 2005. Unconventional secretory routes: direct protein export across the plasma membrane of mammalian cells. *Traffic* 6: 607–614.
7. MacKenzie, A., H. L. Wilson, E. Kiss-Toth, S. K. Dower, R. A. North, and A. Surprenant. 2001. Rapid secretion of interleukin-1β by microvesicle shedding. *Immunity* 15: 825–835.
8. Flieger, O., A. Engling, R. Bucala, H. Lue, W. Nickel, and J. Bernhagen. 2003. Regulated secretion of macrophage migration inhibitory factor is mediated by a non-classical pathway involving an ABC transporter. *FEBS Lett.* 551: 78–86.
9. Gregory, J. L., E. F. Morand, S. J. McKeown, J. A. Ralph, P. Hall, Y. H. Yang, S. R. McColl, and M. J. Hickey. 2006. Macrophage migration inhibitory factor induces macrophage recruitment via CC chemokine ligand 2. *J. Immunol.* 177: 8072–8079.
10. Abedin, M. J., Y. Kashio, M. Seki, K. Nakamura, and M. Hirashima. 2003. Potential roles of galectins in myeloid differentiation into three different lineages. *J. Leukoc. Biol.* 73: 650–656.
11. Forrest, A. R. R., M. Kanamori-Katayama, Y. Tomaru, T. Lassmann, N. Ninomiya, Y. Takahashi, M. J. de Hoon, A. Kubosaki, A. Kaiho, M. Suzuki, et al. 2010. Induction of microRNAs, mir-155, mir-222, mir-424 and mir-503, promotes monocytic differentiation through combinatorial regulation. *Leukemia* 24: 460–466.
12. Martínez, M. C., F. Larbret, F. Zobairi, J. Coulombe, N. Debili, W. Vainchenker, M. Ruat, and J.-M. Freyssinet. 2006. Transfer of differentiation signal by membrane microvesicles harboring hedgehog morphogens. *Blood* 108: 3012–3020.
13. Ratajczak, J., K. Miekus, M. Kucia, J. Zhang, R. Reca, P. Dvorak, and M. Z. Ratajczak. 2006. Embryonic stem cell-derived microvesicles reprogram hematopoietic progenitors: evidence for horizontal transfer of mRNA and protein delivery. *Leukemia* 20: 847–856.
14. Eken, C., O. Gasser, G. Zenhaeusern, I. Oehri, C. Hess, and J. A. Schifferli. 2008. Polymorphonuclear neutrophil-derived ectosomes interfere with the maturation of monocyte-derived dendritic cells. *J. Immunol.* 180: 817–824.
15. Garay, E., R. Donnelly, X. Wang, and G. P. Studzinski. 2007. Resistance to 1,25D-induced differentiation in human acute myeloid leukemia HL60-40AF cells is associated with reduced transcriptional activity and nuclear localization of the vitamin D receptor. *J. Cell. Physiol.* 213: 816–825.
16. Champelovier, P., V. Pautre, M. Elatifi, I. Dupré, B. Rostaing, A. Michoud, F. Berger, and D. Seigneurin. 2006. Resistance to phorbol ester-induced differentiation in human myeloid leukemia cells: a hypothetic role for the mRNA stabilization process. *Leuk. Res.* 30: 1407–1416.
17. Garcia, B. A., D. M. Smalley, H. Cho, J. Shabanowitz, K. Ley, and D. F. Hunt. 2005. The platelet microparticle proteome. *J. Proteome Res.* 4: 1516–1521.
18. Li, M. O., Y. Y. Wan, S. Sanjabi, A.-K. L. Robertson, and R. A. Flavell. 2006. Transforming growth factor-β regulation of immune responses. *Annu. Rev. Immunol.* 24: 99–146.
19. de Almeida, M. C., A. C. Silva, A. Barral, and M. Barral Netto. 2000. A simple method for human peripheral blood monocyte isolation. *Mem. Inst. Oswaldo Cruz* 95: 221–223.
20. Sham, R. L., P. D. Phatak, K. A. Belanger, C. Braggins, and C. H. Packman. 1995. Functional characteristics of mature granulocytes in a patient with acute promyelocytic leukemia treated with all-*trans* retinoic acid. *Leuk. Res.* 19: 505–511.
21. Inal, J. M., K.-M. Hui, S. Miot, S. Lange, M. I. Ramirez, B. Schneider, G. Krueger, and J. A. Schifferli. 2005. Complement C2 receptor inhibitor trispanning: a novel human complement inhibitory receptor. *J. Immunol.* 174: 356–366.
22. Morgan, B. P., and A. K. Campbell. 1985. The recovery of human polymorphonuclear leucocytes from sublytic complement attack is mediated by changes in intracellular free calcium. *Biochem. J.* 231: 205–208.
23. Kuypers, F. A., and K. de Jong. 2004. The role of phosphatidylserine in recognition and removal of erythrocytes. *Cell. Mol. Biol. (Noisy-le-grand)* 50: 147–158.
24. Azevedo, L. C. P., M. Janiszewski, V. Pontieri, Mde. A. Pedro, E. Bassi, P. J. Tucci, and F. R. Laurindo. 2007. Platelet-derived exosomes from septic shock patients induce myocardial dysfunction. *Crit. Care* 11: R120.
25. Bombara, C., and R. A. Ignotz. 1992. TGF-β inhibits proliferation of and promotes differentiation of human promonocytic leukemia cells. *J. Cell. Physiol.* 153: 30–37.
26. Turley, J. M., L. A. Falk, F. W. Ruscetti, J. J. Kasper, T. Francomano, T. Fu, O. S. Bang, and M. C. Birchenall-Roberts. 1996. Transforming growth factor β1

functions in monocytic differentiation of hematopoietic cells through autocrine and paracrine mechanisms. *Cell Growth Differ.* 7: 1535–1544.
27. Hmama, Z., D. Nandan, L. Sly, K. L. Knutson, P. Herrera-Velit, and N. E. Reiner. 1999. 1α,25-Dihydroxyvitamin D_3-induced myeloid cell differentiation is regulated by a vitamin D receptor–phosphatidylinositol 3-kinase signaling complex. *J. Exp. Med.* 190: 1583–1594.
28. Lehmann, L. E., S. U. Weber, D. Fuchs, S. Klaschik, J. C. Schewe, M. Book, A. Hoeft, and F. Stüber. 2005. Intracellular detection of macrophage migration inhibitory factor in peripheral blood leukocytes. *Free Radic. Biol. Med.* 38: 1170–1179.
29. Mizukoshi, E., M. Suzuki, A. Loupatov, T. Uruno, H. Hayashi, T. Misono, S. C. Kaul, R. Wadhwa, and T. Imamura. 1999. Fibroblast growth factor-1 interacts with the glucose-regulated protein GRP75/mortalin. *Biochem. J.* 343: 461–466.
30. Liu, F. T. 2005. Regulatory roles of galectins in the immune response. *Int. Arch. Allergy Immunol.* 136: 385–400.
31. Théry, C., M. Boussac, P. Véron, P. Ricciardi-Castagnoli, G. Raposo, J. Garin, and S. Amigorena. 2001. Proteomic analysis of dendritic cell-derived exosomes: a secreted subcellular compartment distinct from apoptotic vesicles. *J. Immunol.* 166: 7309–7318.
32. Jenkins, G. 2008. The role of proteases in transforming growth factor-β activation. *Int. J. Biochem. Cell Biol.* 40: 1068–1078.
33. Zhu, L., and A. I. Skoultchi. 2001. Coordinating cell proliferation and differentiation. *Curr. Opin. Genet. Dev.* 11: 91–97.
34. Halder, S. K., R. D. Beauchamp, and P. K. Datta. 2005. A specific inhibitor of TGF-β receptor kinase, SB-431542, as a potent antitumor agent for human cancers. *Neoplasia* 7: 509–521.
35. Pap, E., E. Pállinger, M. Pásztói, and A. Falus. 2009. Highlights of a new type of intercellular communication: microvesicle-based information transfer. *Inflamm. Res.* 58: 1–8.
36. Del Conde, I., C. N. Shrimpton, P. Thiagarajan, and J. A. López. 2005. Tissue-factor-bearing microvesicles arise from lipid rafts and fuse with activated platelets to initiate coagulation. *Blood* 106: 1604–1611.
37. Fadok, V. A., D. L. Bratton, A. Konowal, P. W. Freed, J. Y. Westcott, and P. M. Henson. 1998. Macrophages that have ingested apoptotic cells in vitro inhibit proinflammatory cytokine production through autocrine/paracrine mechanisms involving TGF-β, PGE_2, and PAF. *J. Clin. Invest.* 101: 890–898.
38. Gasser, O., and J. A. Schifferli. 2004. Activated polymorphonuclear neutrophils disseminate anti-inflammatory microparticles by ectocytosis. *Blood* 104: 2543–2548.
39. Al-Nedawi, K., B. Meehan, J. Micallef, V. Lhotak, L. May, A. Guha, and J. Rak. 2008. Intercellular transfer of the oncogenic receptor EGFRvIII by microvesicles derived from tumour cells. *Nat. Cell Biol.* 10: 619–624.
40. Wahl, S. M., and W. Chen. 2005. Transforming growth factor-β-induced regulatory T cells referee inflammatory and autoimmune diseases. *Arthritis Res. Ther.* 7: 62–68.
41. Nakamura, K., A. Kitani, and W. Strober. 2001. Cell contact-dependent immunosuppression by $CD4^+CD25^+$ regulatory T cells is mediated by cell surface-bound transforming growth factor β. *J. Exp. Med.* 194: 629–644.
42. Baker, K., P. Raut, and J. R. Jass. 2008. Colorectal cancer cells express functional cell surface-bound TGFβ. *Int. J. Cancer* 122: 1695–1700.
43. Yingling, J. M., K. L. Blanchard, and J. S. Sawyer. 2004. Development of TGF-β signalling inhibitors for cancer therapy. *Nat. Rev. Drug Discov.* 3: 1011–1022.

Biochemical and Biophysical Research Communications 399 (2010) 465–469

Contents lists available at ScienceDirect

Biochemical and Biophysical Research Communications

journal homepage: www.elsevier.com/locate/ybbrc

Mini Review

Red cell PMVs, plasma membrane-derived vesicles calling out for standards

Elliott Hind [a], Sheelagh Heugh [a], Ephraim A. Ansa-Addo [a], Samuel Antwi-Baffour [a], Sigrun Lange [b], Jameel Inal [a,*]

[a] Cellular and Molecular Immunology Research Centre, School of Human Sciences, Faculty of Life Sciences, London Metropolitan University, 166-220 Holloway Road, London, N7 8DB, UK
[b] UCL Institute for Women's Health, Maternal & Foetal Medicine, Perinatal Brain Repair Group, 86-96 Chenies Mews, London WC1E 6HX, UK

ARTICLE INFO

Article history:
Received 30 June 2010
Available online 30 July 2010

Keywords:
Red cell
Plasma membrane-derived vesicles
Standardization

ABSTRACT

Plasma membrane-derived vesicles (PMVs) or microparticles are vesicles (0.1–1 μm in diameter) released from the plasma membrane of all blood cell types under a variety of biochemical and pathological conditions. PMVs contain cytoskeletal elements and some surface markers from the parent cell but lack a nucleus and are unable to synthesise macromolecules. They are also defined on the basis that in most cases PMVs express varying amounts of the cytosolic leaflet lipid phosphatidylserine, which is externalised during activation on their surface. This marks the PMV as a biologically distinct entity from that of its parent cell, despite containing surface markers from the original cell, and also explains its role in events such as phagocytosis and thrombosis. There is currently a large amount of variation between investigators with regard to the pre-analytical steps employed in isolating red cell PMVs or RPMVs (which are slightly smaller than most PMVs), with key differences being centrifugation and sample storage conditions, which often leads to result variability. Unfortunately, standardization of preparation and detection methods has not yet been achieved. This review highlights and critically discusses the variables contributing to differences in results obtained by investigators, bringing to light numerous studies of which RPMVs have been analysed but have not yet been the subject of a review.

1. Introduction

In recent years there has been a surge of scientific interest in PMVs or microparticles and extracellular vesicles [1] and in particular, red cell-derived PMVs (RPMVs). However, researchers often state that interpreting results is difficult due to a lack of standardization in the pre- and post-analytical context [2]. Despite these concerns, no papers have been published on standardization of assays for RPMVs, with only minimal investigation into platelet-derived PMVs (PPMVs) [3]. Also, a strict definition of PMVs has not yet been fully established [4]. This review will be adopting the International Society on Thrombosis and Haemostasis (ISTH) definition of PMVs as although this definition is mainly consensus driven, it best describes RPMVs, the focus of this review.

RPMVs, like other PMV subpopulations, are extracellular vesicles released from the plasma membrane of the mature red cell and have been reported to be smaller than other PMV subtypes ranging in size from 0.1 to 0.4 μm [5] although we have routinely found PMVs of the same size range from monocytes (Fig. 1) and T lymphocytes [6]. RPMVs are released following a rise in cytosolic Ca^{2+} levels, causing transaminase-mediated membrane protein aggregation and cytoskeletal changes due to the breakdown of major cytoskeletal proteins such as band 4.1 [7]. As well as proteolysis, phospholipid redistribution also occurs, with phosphatidylserine (PS) being externalised [8]. It has been suggested that PS exposure on RPMVs is a signal for their removal by the reticuloendothelial system as it was found that almost 50% of RPMVs were rapidly removed from the circulation by liver Kupffer cells in a PS-dependent manner in rat models [9]. RPMV release has also been associated with cell ageing [10], numerous disease states [11] and *in vitro* mechanisms such as a spectrin oxidation [12] and Adenosine triphosphate (ATP) depletion [13].

The purpose of this review is to provide an introduction to RPMV research, and to draw attention to the challenge of standardization whilst highlighting a subset of PMVs that has not yet had a central role in studies despite RPMVs being the most abundant source of PMVs in certain pathological states, such as sickle cell disease and in atherosclerotic plaques [14]. This review also aims to familiarise the reader with historical landmarks in RPMV research, coupled with an overview of the possible roles of RPMVs in disease. It does not focus on other PMV subpopulations, although the issue of standardization is relevant to the study of all cell-derived PMVs. The main aim however, is to provide evidence as to why standardization is so important [15] and will be highlighted by reviewing the factors contributing to result variability and the technical hurdles that need

* Corresponding author. Fax: +44 20 71334149.
E-mail address: j.inal@londonmet.ac.uk (J. Inal).

0006-291X/$ - see front matter © 2010 Elsevier Inc. All rights reserved.
doi:10.1016/j.bbrc.2010.07.095

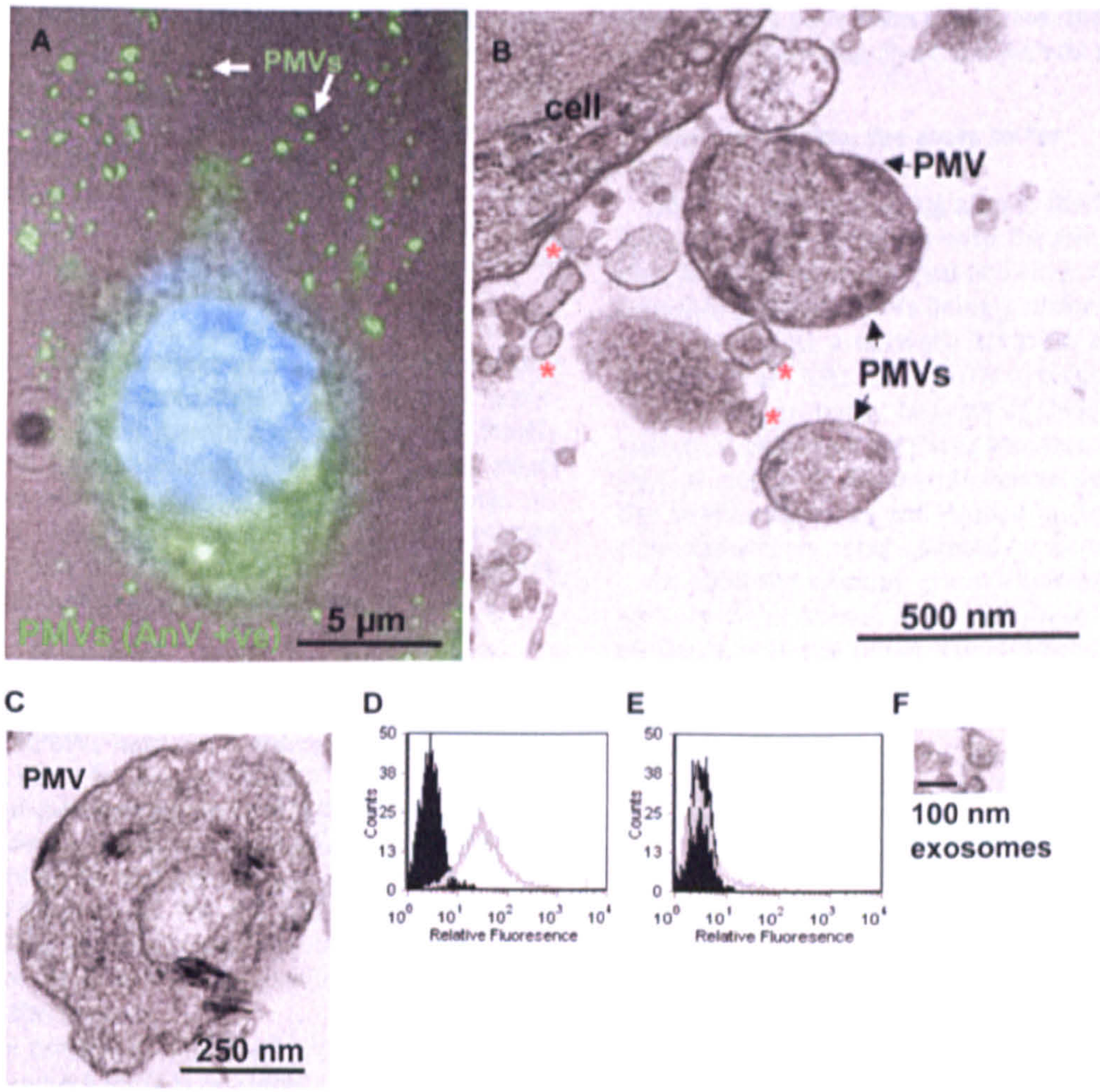

Fig. 1. PMV release from the cell surface. (A) PMVs released from the surface of a monocyte, following exposure to sublytic complement and increased $[Ca^{2+}]_i$ in which exposed phosphatidylserine on released PMVs has been detected with Annexin V-FITC. (B) Electron microscope image of released PMVs, also showing the smaller released exosomes (asterisked) with their characteristic saucer-shape morphology. (C) Representative PMV isolated by differential centrifugation (500 nm diameter) and (D) flow cytometry showing 60% positive AnV labelling for PMVs and only 10% for exosomes (~100 nm diameter), (E) and by electron microscopy (F).

to be overcome in order to establish standardised reagents and assays for RPMVs and other cell-derived PMVs. A critical approach will be adopted, with possible methodological pitfalls being highlighted and discussed when necessary.

Hopefully, in the coming years, as more work is done on RPMVs and as this exciting field continues to grow, investigators will adopt a more collaborative effort. Despite efforts by many [16], including the Working Group on Vascular Biology of the SSC (Scientific and Standardization Committee) investigators of RPMVs continue to adopt a wide range of methods to isolate and quantify RPMVs.

2. Red cell plasma membrane-derived vesicles: highlights from over 30 years of research

The initial papers reporting the release of RPMVs that made a significant impact were published between 1976 and 1980 [17]. Initial studies focused on PMV production in storage and found that when the intracellular Ca^{2+} concentration was increased by the addition of calcium ionophore A23187 or when the red cells were ATP deficient, PMVs budded from the cell membrane. The PMVs were depleted in the internal membrane lipid phosphatidylcholine and cytoskeletal proteins spectrin and actin. Glycophorin, band 3 and acetylcholinesterase PMV expression levels were found to be the same as in the intact cell membranes [18].

In the early 1980's, the viability of red cells during storage for transfusion was an area being studied in detail [19]. This, coupled with the accumulating knowledge of PMVs in transfusion products, made the era a particularly successful one in the area of RPMV research. For example, it was reported in 1980 that RPMVs accumulated during storage of RBCs for 21 days in citrate phosphate dextrose did not contain the 240-kDa cytoskeletal protein spectrin [20]. This characteristic was later studied in more detail and it was found that spectrin oxidation strongly correlated with PMV release [12]. The authors also suggested that as their findings supported the hypothesis that oxidation of membrane components contributes to the storage lesion, antioxidants may be of use in prolonging the life of blood for transfusion. Interestingly, another group's research also lent support to this hypothesis by finding that supplementing blood donors with antioxidants 10 days prior to donation can improve red cell storage by reducing free radical induced cell damage [21].

In 1992 it was demonstrated that epitopes of the A, B, D, Fya, M, N, S, s, and K blood group antigens are present on RPMVs [22]. Recently, another group also demonstrated the presence of rhesus antigens on the surface of RPMVs by the use of flow cytometry and suggested that they are likely to be immunogenic and could therefore be a key factor in red cell alloimmunization post-transfusion [23]. Also in 1992, a study looked at the red blood cells of a patient with Scott Syndrome. Interestingly, it found that the release of RPMVs was significantly less than that of normal cells [24]. Scott Syndrome is a rare bleeding disorder in which platelets and red cells cannot expose PS on the outer membrane surface, leading to a decrease in membrane vesiculation [25]. The discovery of a reduction in the number of RPMVs being released into the circulation illustrates the multi-faceted role PMVs are thought to play

in haemostasis and supports an hypothesis that was explored recently claiming that there are both "good" and "bad" PMVs [26].

The last decade has seen numerous quantitative studies published on RPMVs in both healthy subjects and pathological states (see Table 1). This is laying the groundwork for PMV testing to enter the mainstream of clinical testing, which some investigators believe could occur in the not too distant future [27]. Currently however, a normal physiological range for PMVs has yet to be established.

Last year, a new and exciting possible role of RPMVs was brought to light. A team of investigators studied RPMVs isolated from umbilical cord blood and demonstrated that PS may be transferred to healthy nucleated cell membranes, possibly and falsely indicating that the cell is undergoing apoptosis [28]. This novel finding of the transference of surface markers has also been reported in PPMVs with CD41 integrin and CXCR4 receptors being transferred to nucleated cells, resulting in enhanced binding to fibrinogen and endothelium as a result of CD41 transfer [29].

3. Red cell plasma membrane-derived vesicles and disease

Increased levels of RPMVs have been observed in systemic diseases such as chronic renal failure and clinical conditions such as sickle cell disease and β-thalassaemia [30–32]. However, at this stage there is only evidence to support a circumstantial association of raised plasma RPMV levels and systemic disease, as studies are only quantitative and do not look into the specific role of RPMVs in disease states nor their contribution to pathogenesis. Hopefully, more experiments that focus on the function of RPMVs in disease states will emerge in the future.

Increased levels are not always observed in disease states, as in meningococcal sepsis, where there is no significant difference with healthy controls. In patients with paroxysmal nocturnal haemoglobinuria (PNH) and Scott syndrome (SS) RPMV-associated vesiculation is significantly decreased (Table 1) [24,33]. Research carried out on PNH blood samples that looked at the ability of red cells to vesiculate and externalise PS via a prothrombinase assay, found that RPMV vesiculation was reduced. Vesiculation was also reduced in some samples compared to controls when flow cytometry was used for detection, but appeared normal when the prothrombinase assay was employed. This is because flow cytometry estimates the number of vesicles in a sample whereas the prothrombinase assay is a measure of the procoagulant activity of PMVs [33]. In SS where red cell vesiculation is also impaired, SS red cells show a lower proportion of binding sites for factor Va compared to controls, resulting in an inability to assemble the prothombinase VaXa enzyme complex. These findings led investigators to conclude that there is a specific membrane component required for the expression of a procoagulant cell surface and that PMV formation is a key part of maintaining haemostasis [24]. It was also suggested that a stem cell mutation could possibly be responsible for the membrane defects observed in SS but as only three studies have been conducted, there is currently insufficient data to indicate that there is a genetic link [24,25].

Table 1
RPMV levels in various pathological states compared to healthy controls. A brief review of red cell PMV (RPMV) levels in plasma, in a range of diseases, showing increases (↑), decreases (↓), or no change (-) compared to healthy controls.

Disease	RPMV level	Reference
Atherosclerotic plaque	↑	[44]
β-Thalassaemia	↑	[32]
Chronic renal failure	↑	[30]
Falciparum malaria	↑	[39]
Sickle cell disease	↑	[14]
Meningococcal sepsis	-	[45]
Paroxysmal nocturnal haemoglobinuria	↓	[35]
Scott syndrome	↓	[24]

4. Standardisation, the story so far

In 2003 leading investigators in the field, established a working group on vascular biology with the aim of investigating the detection, function, measurement and clinical significance of PMVs, with standardization of PMVs being a prime objective.

Subsequently a network has been established, aimed at standardising PMV detection, partly in response to the increase in publication but primarily because of their potential as a pathogenic marker. A definition for PMVs has been adopted in a recent review [16], as well as in this one. However, defining PMVs is challenging due to their diversity and is open to debate, with different definitions sometimes being adopted by different groups [2,31].

In 2008 the working group implemented the use of calibrated microbeads of known sizes, distributed by the manufacturer free of charge, with the aim of standardising flow cytometer instrument settings. It was also proposed that biological samples should be distributed from a core laboratory to minimise variability. The calibrated beads have been deemed a useful tool for standardization of PMV counts from one manufacturer with a coefficient of variation >20%.

5. Analytical variables and storage/processing time

There is a general consensus that citrate is the preferred anticoagulant in both RPMVs and other PMV studies [34]. This is because of the ability of citrate to chelate calcium [35], a necessary prerequisite for PMV release [36].

Recent reviews have questioned the suitability of EDTA as an anti-coagulant for PMV analysis because of its ability to extract calcium which is necessary for the structural integrity of surface markers and to induce platelet activation through CD62P, which could result in higher PMV counts [16]. Despite citrate being the most commonly used anti-coagulant, a study on its effect on platelets however found different levels of soluble enzyme markers of activation, β-thromboglobulin and platelet factor 4 depending on which tubes were used and the tube manufacturer [37].

Another issue is the effect of storage temperature and duration on PMV numbers. One group quantified RPMVs in stored red cell concentrates and reported a 20-fold increase from 3371 ± 1181 PMV/μl at day 5 to 64,858 ± 37,846 PMV/μl at day 50 [23]. By contrast, another group found that PMV counts decrease during storage. When PMVs were aliquoted and stored overnight at 4 °C, at −20 °C and after storage for 1 month at −80 °C, lower PMV concentrations were observed [2].

Centrifugation conditions are not standardised. Without having a comparable standard, conflicting PMV counts are common [27]. A recent study on RPMVs and other circulating PMV subtypes in sickle cell disease found that they did not detect Tissue Factor$^+$ (TF$^+$) PMVs, monocyte PMVs (MPMVs) (CD14$^+$), or EPMVs (CD 144$^+$, CD146$^+$, CD62E$^+$) in their samples [14]. Contrastingly, others have not just detected TF$^+$ PMVs, MPMVs and EPMVs, but concluded that the observed increase strengthened the hypothesis that sickle cell disease is an inflammatory state with endothelial cell and monocyte activation along with abnormal vessel wall activity [31]. Unsurprisingly, both groups used different methods for PMV isolation, and it appears therefore, that centrifugation conditions are a possible reason for the difference in PMV subtypes detected.

The centrifugation conditions employed to obtain platelet poor plasma (PPP) also differ between groups. A method consisting of two successive 1500*g*, 15 min centrifugations has been recom-

mended for obtaining PPP for PMV analysis [38]. However, the same authors also highlight a possible limitation, being that detection of RPMVs may be compromised due to their small size. As a result, RPMVs may be indistinguishable by flow cytometry.

Not all PMVs are positive for annexin V binding but despite this fact, some investigators define PMVs in terms of annexin V binding externalized PS [2]. Investigators could therefore be underestimating the total number of PMVs. The majority of RPMVs do however, express PS [39], with one study finding that 87% of RPMVs bound annexin V.

Flow cytometry is the most commonly used technique to detect RPMVs. Some investigators identify PMVs with a forward angle light scatter smaller than the 1–1.5 μm latex beads used as an internal standard [31]. Other investigators also employ a lower size limit of 100 nm. However, any particles detected by the flow cytometer under this size are not considered true PMVs [40]. Using the upper size limit criteria could also lead to an underestimation of true PMV numbers as some investigators consider PMVs to be up to 2 μm in size [41]. As several different flow cytometers have been used to analyse PMVs, it may be possible that the flow technology and instrument settings as well as interpretation of results could impact on PMV measurement. Flow cytometry methods and settings need to be presented in full in publications to make results both reproducible and easier to interpret; the manufacturer and model should be declared along with the fluidics configuration, optical configuration and electronic configuration.

6. New developments in detecting PMVs

A flow rate based assay that uses direct immunostaining on whole blood samples has been suggested as an alternative for detection [39]. In this novel assay, the exact volume per unit time is measured alongside a known number of red cell beads that flow through the flow cytometer detector within 2 min. The number of RPMVs in the sample is then calculated by counting RPMVs over that time period with reference to the known volume.

Whilst development of novel assays is welcome, without a body of work defining the optimum analytical conditions, their suitability will continue to be determined via consensus as opposed to a standard based on scientific evidence, making any results obtained difficult to interpret unless reference standard methods are developed [15,27].

7. Concluding remarks

More collaborative effort is needed to establish reliable and reproducible standards. Whilst consistent RPMV counts have been obtained by disparate groups [42,43], the centrifugation conditions in the case of Shah et al. [2] were probably responsible for the low count obtained.

On a positive note, the SSC 2010 meeting announced the validation of numerous flow cytometers, which is a huge step in the right direction. This, coupled with a recent study providing guidelines for the correct reporting of flow methods is evidence that good progress is being made. However, researchers focusing on the study of RPMVs need to come to a consensus regarding sample processing and analysis to make interpreting results less of a challenge, as the differences in methods and results presented are numerous and clear.

Acknowledgments

Thanks to Drs Jean-Marie Freyssinet and Stephane Robert for helpful guidance at the inception of this work.

References

[1] B. Toth, C.A. Lok, A. Boeing, M. Diamant, J.A. van der Post, K. Friese, R. Nieuwland, Microparticles and exosomes: impact on normal and complicated pregnancy, Am. J. Reprod. Immunol. 58 (2007) 389–402.
[2] M.D. Shah, A.L. Bergeron, D. Jing-Fei, J.A. López, Flow cytometric measurement of microparticles: pitfalls and protocol modifications, Platelets 19 (2008) 365–372.
[3] S. Robert, P. Poncelet, R. Lacroix, L. Arnaud, L. Giraudo, A. Hauchard, J. Sampol, F. Dignat-George, Standardization of platelet-derived microparticle counting using calibrated beads and a Cytomics FC500 routine flow cytometer: a first step towards multicenter studies?, J Thromb. Haemost. 7 (2008) 190–197.
[4] L. Burnier, P. Fontana, B.R. Kwak, A. Angelillo-Scherrer, Cell-derived microparticles in hemostasis and vascular medicine, J. Thromb. Haemost. 101 (2009) 439–451.
[5] A.S. Lawrie, P. Harrison, R.A. Cardigan, I.J. Mackie, The characterization and impact of microparticles on hemostasis within fresh-frozen plasma, Vox Sang. 95 (2008) 197–204.
[6] S. Antwi-Baffour, S. Kholia, Y.K.-D. Yushau, E.A. Ansa-Addo, D. Stratton, S. Lange, J.M. Inal, Human plasma membrane-derived vesicles inhibit the phagocytosis of apoptotic cells – possible role in SLE, Biochem. Biophys. Res. Commun. (2010), doi:10.1016/j.bbrc.2010.06.079.
[7] U. Salzer, P. Hinterdorfer, U. Hunger, C. Borken, R. Prohaska, Ca(++)-dependent vesicle release from erythrocytes involves stomatin-specific lipid rafts, synexin (annexin VII) and sorcin, Blood 99 (2002) 2569–2577.
[8] R. Bucki, C. Bachelot-Loza, A. Zachowsk, F. Giraud, J.-C. Sulpice, Calcium induces phospholipid redistribution and microvesicles release in human erythrocyte membranes by independent pathways, Biochemistry 37 (1998) 15383–15391.
[9] F.L. Willekens, J.M. Were, J.K. Kruist, B. Roerdinkholder-Stoelwinder, Y.A. Groenen-Döpp, A.B. Van den Bos, G.J. Bosman, T.J. van Berkel, Liver kupffer cells rapidly remove red blood cell-derived vesicles from the circulation by scavenger receptors, Blood 105 (2005) 2141–2145.
[10] M.G. Rumsby, J. Trotter, D. Allan, R.H. Michell, Recovery of membrane microvesicles from human erythrocytes stored for transfusion: a mechanism for the erythrocyte discocyte-to-spherocyte shape transformation, Biochem. Soc. Trans. 5 (1977) 126–128.
[11] D.W. Knowles, L. Tilley, N. Mohandas, J.A. Chasis, Erythrocyte membrane vesiculation: model for the molecular mechanism of protein sorting, Proc. Natl. Acad. Sci. USA 94 (1997) 12969–12974.
[12] G.M. Wagner, D.T. Chiu, J.H. Qju, R.H. Heath, B.H. Lubin, Spectrin oxidation correlates with membrane vesiculation in stored RBCs, Blood 69 (1987) 1777–1781.
[13] H.U. Lutz, S.C. Liu, J. Palek, Release of spectrin-free vesicles from human erythrocytes during ATP depletion. I. Characterization of spectrin-free vesicles, J. Cell Biol. 73 (1977) 548–560.
[14] E.J. van Beers, M. Schaap, J. Berckmans, R. Nieuwland, A. Sturk, F.F. van Doormaal, J.C. Meijers, B.J. Biemond, Circulating erythrocyte-derived microparticles are associated with coagulation activation in sickle cell disease, Haematologica 94 (2009) 1513–1519.
[15] F. Dignat-George, J.-M. Freyssinet, N.S. Key, Centrifugation is a crucial step impacting microparticle measurement, Platelets 20 (2009) 225–226.
[16] A.K. Enjeti, L.F. Lincz, M. Seldon, Detection and measurement of microparticles: an evolving research tool for vascular biology, Semin. Thromb. Hemost. 33 (2007) 771–779.
[17] D. Allan, R.H. Michell, Calcium ion-dependent diacylglycerol accumulation in erythrocytes is associated with microvesiculation but not with efflux of potassium ions, Biochem. J. 166 (1977) 495–499.
[18] W.F. Cole, M.G. Rumsby, G.H. Langster, L.A. Tovey, The release of erythrocyte membrane antigens to the plasma as membrane microvesicles during the storage of human blood for transfusion, Biochem. Soc. Trans. 6 (1978) 1375–1378.
[19] R.T. Card, N. Mohandas, P.L. Mollison, Relationship of post-transfusion viability to deformability of stored red cells, Br J. Haematol. 53 (1983) 237–240.
[20] T.J. Greenwalt, The how and why of exocytic vesicles, Transfusion 46 (2006) 143–152.
[21] J. Racek, R. Herynková, V. Holecek, Z. Jerábek, V. Sláma, Influence of antioxidants on the quality of stored blood, Vox Sang. 72 (1997) 6–19.
[22] R.T. Oreskovic, U.J. Dumaswala, T.J. Greenwalt, Expression of blood group antigens on red cell microvesicles, Transfusion 32 (1992) 848–849.
[23] O. Rubin, D. Crettaz, G. Canellini, J.-D. Tissot, N. Lion, Microparticles in stored red blood cells: an approach using flow cytometry and proteomic tools, Vox Sang. 95 (2008) 288–297.
[24] E.M. Bevers, T. Wiedmer, P. Comfurius, S.J. Shattil, H.J. Weiss, R.F. Zwaal, P.J. Sims, Defective Ca(2+)-induced microvesiculation and deficient expression of procoagulant activity in erythrocytes from a patient with a bleeding disorder: a study of the red blood cells of Scott syndrome, Blood 79 (1992) 380–388.
[25] F. Toti, J.M. Freyssinet, An ABC for Scott syndrome?, Blood 106 (2005) 396–397
[26] J.M. Freyssinet, Cellular microparticles: what are they bad or good for?, J Thromb. Haemost. 1 (2003) 655–1662.
[27] L.L. Horstman, W. Jy, J.J. Jimenez, C. Bidot, Y.S. Ahn, New horizons in the analysis of circulating cell-derived microparticles, Keio J. Med. 53 (2004) 210–230.
[28] R. Liu, I. Klich, J. Ratajczak, M.Z. Ratajczak, E.K. Zuba-Surma, Erythrocyte-derived microvesicles may transfer phosphatidylserine to the surface of nucleated cells and falsely 'mark' them as apoptotic, Eur. J. Haematol. 83 (2009) 220–229.

[29] T. Rozmyslowicz, M. Majka, J. Kijowski, S.L. Murphy, D.O. Conover, M. Poncz, J. Ratajczak, G.N. Gaulton, M.F. Ratajczak, Platelet- and megakaryocyte-derived microparticles transfer CXCR4 receptor to CXCR4-null cells and make them susceptible to infection by X4-HIV, AIDS 17 (2003) 33–42.
[30] V. Faure, L. Dou, F. Sabatier, C. Cerini, J. Sampol, Y. Berland, P. Brunet, F. Dignat-George, Elevation of circulating endothelial microparticles in patients with chronic renal failure, J. Thromb. Haemost. 4 (2005) 566–573.
[31] A.S. Shet, Characterizing blood microparticles: technical aspects and challenges, Vasc. Health Risk Manag. 4 (2008) 769–774.
[32] K. Pattanapanyasat, E. Noulsri, S. Fucharoen, S. Lerdwana, P. Lamchiagdhase, N. Siritanaratkul, H.K. Webster, Flow cytometric quantitation of red blood cell vesicles in thalassemia, Cytometry B Clinical Cytom. 57 (2004) 23–31.
[33] B. Hugel, G. Socié, T. Vu, F. Toti, E. Gluckman, J.M. Freyssinet, M.L. Scrobohaci, Elevated levels of circulating procoagulant microparticles in patients with paroxysmal nocturnal hemoglobinuria and aplastic anemia, Blood 93 (1999) 3451–3456.
[34] W. Jy, L.L. Horstmann, J.J. Jimenez, Y.S. Ahn, Measuring circulating cell-derived microparticles, J. Thromb. Haemost. 2 (2004) 1842–1843.
[35] M. Gritters M, M.P. Grooteman, M. Schoorl, M. Schoorl, P.C. Bartels, P.G. Scheffer, T. Teerlink, C.G. Schalkwijk, M. Spreeuwenberg, M.J. Nubé, Citrate anticoagulation abolishes degranulation of polymorphonuclear cells and platelets and reduces oxidative stress during haemodialysis, Nephrol. Dial. Transplant. 21 (2006) 153–159.
[36] D. Allan, P. Thomas, R. Limbrick, The isolation and characterization of 60 nm vesicles ('nanovesicles') produced during ionophore A23187-induced budding of human erythrocytes, Biochem. J. 188 (1980) 881–887.
[37] J. Philippé, E. De Logi, G. Baele, Comparison of five different citrated tubes and their in vitro effects on platelet activation, Clin. Chem. 50 (2004) 656–658.
[38] D. Nantakomol, M. Imwong, I. Soontarawirat, D. Kotjanya, C. Khakhai, J. Ohashi, P. Nuchnoi, The absolute counting of red cell-derived microparticles with red cell bead by flow rate based assay, Cytometry B Clin. Cytom. 76 (2009) 191–198.
[39] D. Nantakomol, P. Chimma, N.P. Day, A.M. Dondorp, V. Combes, S. Krudsood, S. Looareesuwan, N.J. White, K. Pattanapanyasat, K. Chotivanich, Quantitation of cell-derived microparticles in plasma using flow rate based calibration, Southeast Asian J. Trop. Med. Public Health 39 (2008) 146–153.
[40] C.M. Boulanger, N. Amabile, A. Tedgui, Circulating microparticles: a potential prognostic marker for atherosclerotic vascular disease, Hypertension 48 (2006) 180–186.
[41] A. Piccin, W.G. Murphy, O.P. Smith, Circulating microparticles: pathophysiology and clinical implications, Blood Rev. 21 (2007) 157–171.
[42] R.J. Berckmans, R. Neiuwland, A.N. Boeing, F.P. Romijn, C.E. Hack, A. Sturk, Cell-derived microparticles circulate in healthy humans and support low grade thrombin generation, J. Thromb. Hemost. 85 (2001) 639–646.
[43] G. Hron, M. Kollars, H. Weber, V. Sagaster, P. Quehenberger, S. Eichinger, P.A. Kyrle, A. Weltermann, Tissue factor-positive microparticles: cellular origin and association with coagulation activation in patients with colorectal cancer, J. Thromb. Haemost. 97 (2007) 119–123.
[44] A.S. Leroyer, H. Isobe, G. Lesèche, Y. Castier, M. Wassef, Z. Mallat, B.R. Binder, A. Tedgui, C.M. Boulanger, Cellular origins and thrombogenic activity of microparticles isolated from human atherosclerotic plaques, J. Am. Coll. Cardiol. 49 (2007) 772–777.
[45] R. Nieuwland, R.J. Berckmans, S. McGregor, A.N. Böing, F.P. Romijn, R.G. Westendorp, C.E. Hack, A. Sturk, Cellular origin and procoagulant properties of microparticles in meningococcal sepsis, Blood 95 (2000) 930–935.

Biochemical and Biophysical Research Communications 398 (2010) 278–283

Contents lists available at ScienceDirect

Biochemical and Biophysical Research Communications

journal homepage: www.elsevier.com/locate/ybbrc

Human plasma membrane-derived vesicles inhibit the phagocytosis of apoptotic cells – Possible role in SLE

Samuel Antwi-Baffour [a], Sharad Kholia [a], Yushau K.-D. Aryee [a,1], Ephraim A. Ansa-Addo [a], Dan Stratton [a], Sigrun Lange [b], Jameel M. Inal [a,*]

[a] Cellular and Molecular Immunology Research Centre, School of Human Sciences, Faculty of Life Sciences, London Metropolitan University, 166-220 Holloway Road, London N7 8DB, UK
[b] Developmental Biology Unit, Institute of Child Health, U.C.L., Guilford St., London, UK

ARTICLE INFO

Article history:
Received 14 June 2010
Available online 23 June 2010

Keywords:
Plasma membrane-derived vesicles
Phagocytosis
Apoptotic cells
Autoimmune disease
Systemic lupus erythematosus

ABSTRACT

Plasma membrane-derived vesicles (PMVs) also known as microparticles, are small membrane-bound vesicles released from the cell membrane via blebbing and shedding. PMVs have been linked with various physiological functions as well as pathological conditions such as inflammation, autoimmune disease and cardiovascular disease. PMVs are characterised by the expression of phosphatidylserine (PS) on the plasma membrane. PS, also expressed on apoptotic cells (ACs) enables macrophages to phagocytose ACs. As it is widely known that PMV production is increased during apoptosis, we were able to show that PMVs could compete dose dependently with ACs for the PS receptor on macrophages, so reducing phagocytosis of ACs. In a clinical setting this may result in secondary necrosis and further pathological conditions. In SLE in which there are raised PMV levels, there is an anti-phospholipid-mediated increase in PMV release, which can be abrogated by depletion of IgG. Our work provides an insight into how PMVs may play a role in the aetiology of autoimmune disease, in particular SLE.

1. Introduction

Apoptotic cells (ACs) are taken up in a phagocytic process called efferocytosis, ('burying of dead cells') [1], a mechanism which does not provoke inflammatory or immune reactions. By contrast necrotic and secondary necrotic cells, derived from uncleared ACs are proinflammatory and associated with autoimmune disease [2].

Plasma membrane-derived vesicles (PMVs) are vesicles released from the plasma membrane (PM) of most cells with an average diameter of 0.1–1 μm [3]. They carry PM-associated proteins and a host of intravesicular proteins including cytokines, growth factors and acute phase proteins, as well as messenger RNA (mRNA) and microRNA (miRNA) [4]. There is a range of stimuli that result in PMV release but key amongst these is an increase in intracellular calcium and the exposition of phosphatidylserine on the outer leaflet of the releasing cell and the resultant PMV.

The presence of basal levels of PMVs is common in healthy individuals, and is estimated, in peripheral blood, to range between 5 and 50 μg/ml (10^5–10^6 PMVs/ml). PMVs play a role in various physiological functions such as thrombosis, inflammation, angiogenesis and vasoconstriction [5–8]. They have also been linked with a wide range of clinical conditions [9] such as diabetes, cardiovascular diseases, inflammatory diseases as well as autoimmune diseases such as multiple sclerosis, particularly where there is persistent apoptosis coupled with defective clearance of apoptotic cells (ACs), and atherosclerosis [10–12]. Whether PMVs are direct contributors to such diseases or are a reflection of disease, a knowledge of their level in plasma may serve as an indicator of cell stress and injury and thus, in the future, help monitor disease treatment.

Systemic lupus erythematosus (SLE) is a prototypic autoimmune disease in which there is a deficient phagocytosis of ACs. The resulting secondary necrosis results in autoantibodies such as anti-phospholipid antibodies (aPLA) which can further block phagocytosis and enhance disease progression. In SLE patients with secondary APS (anti-phospholipid syndrome) there are increased numbers of plasma PMVs [13]. Similarly, in patients with aPLA it is believed that aPLA-mediated endothelial injury or activation leads to increased PMV release [14].

Because both PMVs and ACs express phosphatidylserine (PS) on the outer leaflet of the plasma membrane, and as PS is a marker for phagocytosis of ACs by macrophages, we set out to ascertain if the PMVs have any significant effect on this process, essentially to see

Abbreviations: PMV, plasma membrane-derived vesicle; aPLA, anti-phospholipid antibody; PSR, phosphatidylserine receptor; AC, apoptotic cell.

* Corresponding author. Fax: +44 20 7133 4149.
E-mail address: J.Inal@londonmet.ac.uk (J.M. Inal).
[1] Present address: Cambridge University Hospital NHS Foundation Trust, Department of Biochemistry and Immunology, Addenbrookes Hospital, Cambridge, UK.

0006-291X/$ - see front matter © 2010 Elsevier Inc. All rights reserved.
doi:10.1016/j.bbrc.2010.06.079

whether the PMVs inhibit the phagocytosis of ACs by competing for the PS receptor on macrophages.

2. Materials and methods

2.1. Cell culture and monocyte-to-macrophage differentiation

THP-1 (monocytic leukaemia) and Jurkat (T lymphocyte) cell lines were cultured in the same complete growth medium, in RPMI 1640, containing 2 mM L-glutamine, 10% foetal bovine serum and 100 U/ml penicillin/streptomycin as described before [15]. To induce differentiation of THP-1 monocytes into macrophages, THP-1 cells with a viability of ⩾94%, were treated with 0.1 μM of PMA at 37 °C for 3 days. Macrophages were then washed three times in PBS to remove PMA. Differentiation was confirmed by expression of surface markers CD11b/CD14, and the ability to generate reactive oxygen species (ROS) via NADP oxidase using the nitro blue tetrazolium (NBT) (Sigma–Aldrich) assay. Cells seeded at a concentration of 5×10^5 cells/ml in a 12- or 24-well plates were treated with 1 mg/ml NBT and 4 μg/ml PMA for 1 h at 37 °C. The pellet after washing was dissolved in 100 μl DMSO and the absorbance read at 570 nm.

2.2. Fluorescence microscopy

For fluorescent microscopy of PMV release, cells were labelled with annexin V AlexFluor 488 (1 μg/10^6 cells) and washed three times with RPMI. After stimulation for 30 min, the cells on coverslips were fixed with 4% paraformaldehyde at 37 °C for 10 min. The cells were then gently washed in PBS and the coverslips mounted on microscope slides with DAPI-VECTASHIELD medium (Vector Laboratories Inc., Burlingame, CA). Images were collected using a fluorescence microscope (1X81 motorized, inverted fluorescence microscope, Olympus Corporation).

2.3. PMV induction from Jurkat cells

In experiments to induce PMV release, either Jurkat cells with a viability of ⩾95% or else cells specifically rendered early apoptotic (see below) were used. Cells (1×10^6) were washed twice at 160*g* for 5 min and re-suspended in 1 ml of fresh pre-warmed RPMI 1640. Two millimolar $CaCl_2$ was then added to the cell suspension. The requisite amount of the various inducing agents (10% normal human serum [NHS], aPLA plasma or SLE plasma) were then added and the cell preparation incubated at 37 °C in a water bath (with shaking) for 30 min. After incubation, the reaction was stopped by placing the tubes on ice. In order to remove cells, the cell suspension was centrifuged at a low speed of 160*g* for 5 min. The supernatant was then collected and transferred to another tube and centrifuged at a higher speed (4000*g*, 60 min) to remove any cell debris.

After centrifugation, the supernatant was sonicated (in a water sonicator) for 5 min followed by centrifugation (25,000*g* for 90 min). The supernatant was discarded and the pellet containing the PMVs re-suspended in 200 μl PBS. The PMV samples (diluted 1:40 in PBS) were then quantified using Guava Express plus as described by the manufacturer (Guava, Millipore). This study was approved by the local Ethics committee.

2.4. Flow cytometry

All the experiments that involved flow cytometry were carried out on a Guava EasyCyte. To measure cell counts and determine viability, 50 μl of cell suspension to be analysed was added to 150 μl of Guava Viacount reagent in three separate wells of a 96 well plate. One well was used to adjust the settings, the other three, for the count. The plate was then loaded into the Guava EasyCyte flow cytometer and PMVs in PBS quantified using ExpressPlus software. To confirm expression of external PS, PMVs were stained with annexin-V-FITC. Fluorescent sizing beads calibrated to 0.5 and 0.9 μm were used, according to the manufacturer's instructions (Biocytex, France).

2.5. FITC labelling Jurkat cells and induction of apoptosis

FITC dye (prepared as per the manufacturer's protocol [Sigma-Aldrich]) was added (1 μg/10^6 cells) to the cell suspension and incubated on a shaker at room temperature for 90 min in the dark. After incubation the cells were washed three times with PBS at 400*g* for 5 min and re-suspended in RPMI ready for use. A small sample of the labelled cells was then tested for FITC staining by FACS analysis. The cells were only used after obtaining fluorescence greater than 70%. Fifteen micromolar of PMA was then added to a 1 ml cell suspension containing 7×10^6 FITC-labelled Jurkat cells in RPMI which was incubated at 37 °C for 1 h in the dark. After three washes with PBS and re-suspension in 2 ml PBS, flow cytometry (Guava Nexin® assay) was carried out to confirm apoptosis.

2.6. Apoptosis detection using annexin V-PE and 7-AAD

This assay was used primarily to detect and measure percentage apoptosis of PMA-induced Jurkat cells. Apoptotic cells or viable cells were stained with Guava Nexin® reagent (containing annexin V-PE to detect externalised phosphatidylserine and 7-AAD, a cell impermeant dye, as an indicator of late stage apoptosis) according to the manufacturer's instructions (Guava, Millipore). After incubation at RT for 30 min with mixing in the dark, the cells were analysed on the Guava EasyCyte flow cytometer.

2.7. Phagocytosis assay

FITC-labelled ACs (7×10^6 in 2 ml PBS) were opsonised with 20% NHS for 30 min at 37 °C and then washed three times in PBS. The 24-well plates containing macrophages (1×10^5) were kept on ice during addition of the various combinations of ACs and PMVs and then incubated at 37 °C for 18 h in a CO_2 incubator.

After incubation, the plates were placed on ice for 2 min and coverslips with adherent macrophages washed three times to remove non-phagocytosed cells. Hoescht dye (0.2 μg/ml final concentration) was added to wells designated for fluorescence microscopy and 5 mM EDTA added to detach macrophages where they were needed for flow cytometry using the Guava EasyCyte flow cytometer (Guava Express Plus). The plate was then incubated at 37 °C for a further 30 min. After washing to remove unbound excess dye, 100 μl of methanol was added for 5 min at room temperature to fix the cells for microscopy. The wells were then washed once with PBS to remove excess methanol and then refilled with 250 μl of PBS for microscopy.

For determining phagocytosis by microscopy, 500 macrophages were counted per well, noting the number of macrophages that had internalised at least one AC. The average was then taken and a phagocytic index calculated (expressed as a mean percentage of macrophages that had phagocytosed at least one AC). The fluorescence microscope was equipped with a UCMAD3 monochromatic camera, and images taken for fluorescence were coloured with the Cell^M software (Olympus).

2.8. Spin-column procedure for IgG antibody purification from plasma

This was carried out as described in the manufacturer's instructions. Briefly, after equilibrating the Gel IgG Purification Support in Purification Buffer (PB), the Purification Support slurry was washed

with PB in a spin column twice. With the bottom cap in place, 100–500 μl serum was added with mixing and the purified antibody collected by centrifugation.

2.9. IgG removal from plasma

A spin column containing 170 μl of a slurry of immobilized Cibacron Blue/Protein A gel was prepared. The SLE plasma was diluted to 75 μl with Binding/Wash buffer, added to the column with vortexing and left on a mixer for 10 min. Filtrate was then collected from the column by removing the bottom plug and then 75 μl Binding/Wash buffer collected in the same tube by centrifuging at 10,000g for 1 min. The sample obtained was now free of albumin and IgG.

2.10. Statistical analysis

Students's *t*-test was performed using GraphPad Prism software, version 5.0 (San Diego, CA, USA). Where $p < 0.05$, differences are considered statistically significant. All experiments were carried out in triplicate. The results from three experiments are represented as means ± SD.

3. Results

3.1. Characterisation of plasma membrane-derived vesicles from Jurkat cells

PMVs, for the purpose of adding to phagocytosis assays were induced from Jurkat cells by treating cells with sublytic complement in the form of 10% NHS for 30 min. Cells so treated were confirmed to be releasing PMVs by electron microscopy (Fig. 1A) showing released PMVs (~500 nm in diameter) and exosomes showing a typical saucer-shaped morphology (⩽100 nm). By flow cytometry in a forward/side scatter plot they present as the characteristic heterogeneous plot of PMVs (Fig. 1B) ranging in size from 0.5 to 0.9 μm in diameter (Fig. 1C) which are positive for PS as revealed by AnV-FITC binding (Fig. 1D) and in immunofluorescence microscopy (Fig. 1E).

3.2. Plasma membrane-derived vesicles from Jurkat cells inhibit the phagocytosis of apoptotic cells by THP-1 macrophages

Viable Jurkat cell cultures (7% early apoptosis, Fig. 2A) as judged by AnV-PE/7-AAD labelling, became 93.4% early apoptotic (Fig. 2A) upon treatment with 0.1 μM PMA for 24 h. These ACs were 88% FITC-labelled (Fig. 2B) and used in preliminary phagocytosis assays to confirm phagocytosis of ACs (42%) as opposed to 10% for viable cells, VC (Fig. 2C). This phagocytosis was unable to proceed at 4 °C, in the presence of 50 μg/ml anti-phosphatidyl serine receptor (PSR) antibody (Sigma–Aldrich) or with ACs preincubated with 50 μg of AnV/10^5 cells (Fig. 2E and F). When phagocytosis of 5×10^5 ACs was carried out in the presence of Jurkat PMVs, they were found to dose-dependently inhibit phagocytosis (Fig. 2G and H) (with ratios of ACs: PMVs ranging from 1:10 to 1:16 and 1:20).

3.3. Plasma membrane-derived vesicles levels are raised in SLE; role of anti-phospholipid antibodies in their release from apoptotic cells

If defective phagocytosis in SLE might be associated with increased PMV levels, then anti-phospholipid antibody (aPLA) or SLE plasma samples would be expected to have elevated levels of PMVs. Such raised levels of PMVs could themselves be due to the presence of increasing levels of sensitizing autoantibodies such as aPLA and sublytic complement [16]. In general, as expected,

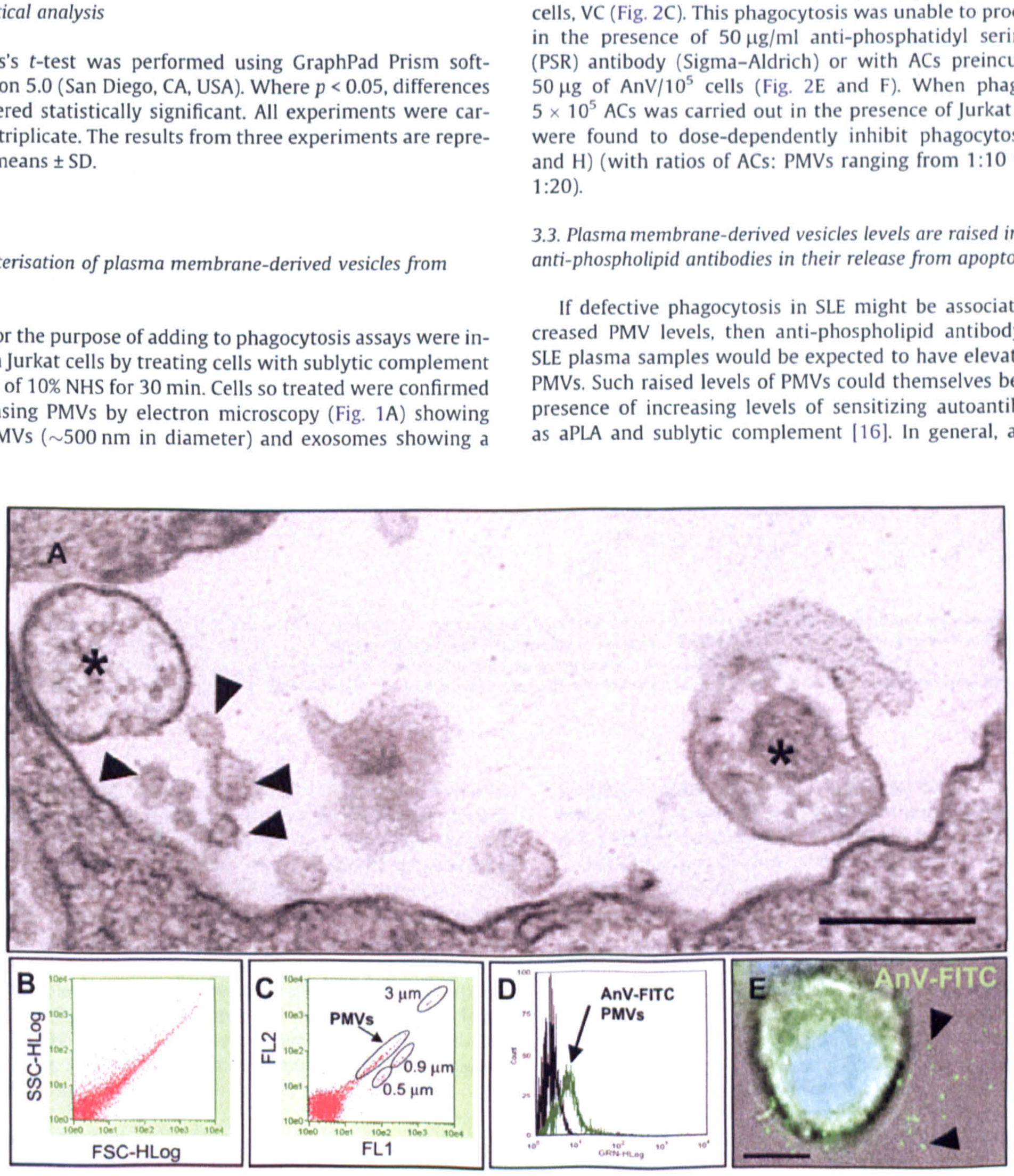

Fig. 1. PMVs released from Jurkat cells are PS^+, and ranging in size between 0.5 and 0.9 μm. (A) Transmission electron microscopy of a stimulated Jurkat cell releasing PMVs (asterisked) and exosomes (arrowheads). (B) Typical flow cytometer forward/side scatter plot for PMVs. (C) Magimix fluorescent sizing beads (0.5, 0.9 and 3 μm) show the PMVs to range between 0.5 and 0.9 μm in diameter. (D) PMVs are PS^+ as revealed by AnV-FITC staining using flow cytometry. (E) Immunofluorescence microscopy showing the release of AnV-FITC-positive PMVs. Scale bars represent the following sizes: (A), 400 nm; (E), 5 μm.

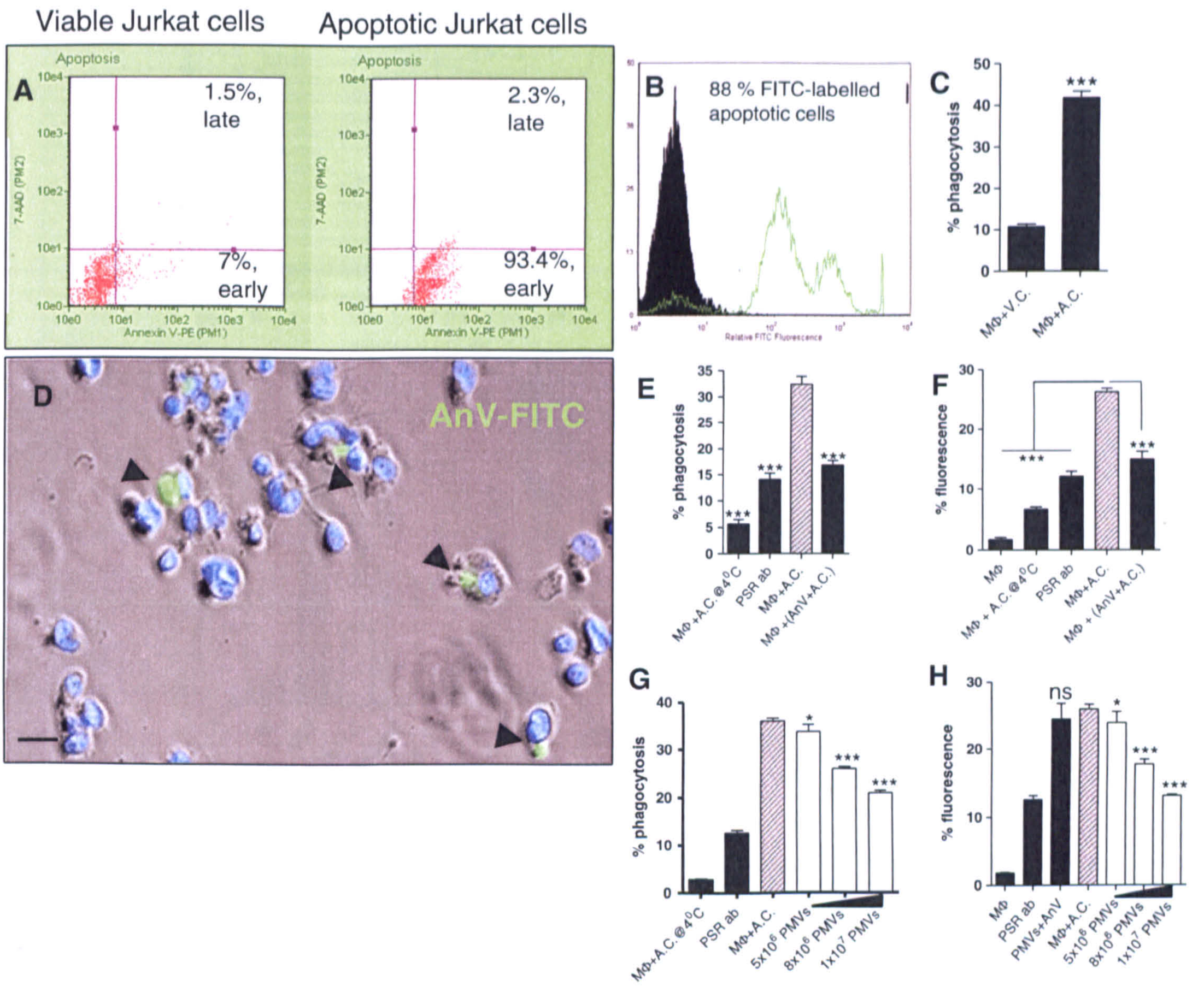

Fig. 2. PMVs inhibit the phagocytosis of Jurkat apoptotic cells by THP-1 macrophages. (A) PMA treatment (0.1 μM for 3 days) generates 93.4% early apoptotic (AnV^+, $7\text{-}AAD^-$) Jurkat cells. Using 88% FITC-labelled ACs (B), THP-1 macrophages phagocytose FITC-labelled ACs as opposed to viable cells, VCs (C, D). Phagocytosis at 4 °C, or in the presence of phosphatidylserine receptor-blocking antibody, or using AnV to block PS on ACs abrogates phagocytosis (E, F). PMVs (5×10^6, 8×10^6 and 1×10^7) added to 5×10^5 ACs in a ratio to 1:10, 1:16 or 1:20, respectively (G, H) dose-dependently inhibit phagocytosis of ACs. $^*p < 0.05$, $^{**}p < 0.01$ and $^{***}p < 0.001$ were considered statistically significant. Scale bar in (D) represents 10 μm.

we found raised PMV levels in both aPLA plasma (Fig. 3A, $n = 13$) and SLE plasma (Fig. 3B, $n = 20$) compared to normal controls. To test whether the aPLA component of SLE plasma samples was able to stimulate PMV release from early ACs through the stimulation of sublytic complement, we were able to show that removal of aPLA reduced PMV production, which was then only partially replenished with 1 mg/ml human IgG (Fig. 3C). That the SLE-induced PMV release from ACs was due to complement activation was confirmed by depletion of complement C9 (Fig. 3C). In IgG-depleted NHS, PMV release was also reduced, and when aPLA added (1 mg/ml), PMV release was almost restored to the level achieved with NHS (Fig. 3D). C9 depletion once more significantly reduced PMV production.

4. Discussion

The effective removal of ACs by phagocytes is not just limited to safe removal of injured, aged or infected cells but is crucial to processes ranging from embryogenesis, tissue homeostasis, and cellular immunity to the resolution of inflammation [2]. It has also been well established that in certain clinical conditions such as cystic fibrosis [17], as well as chronic autoimmune diseases [18,19] there is a defect in the clearance of apoptotic cells (ACs).

Recently there has been a rise in the interest of the role of PMVs in helping maintain the delicate balance between health and disease [20]. On this basis, this investigation reports that PMVs may play a role in the reduction of phagocytosis of ACs by macrophages. Various studies have shown that PMVs express high concentrations of PS on the outer leaflet of the plasma membrane when they are released via blebbing and shedding following the loss of phospholipid membrane asymmetry on the parent cell [21]. ACs also express PS on the outer leaflet, this being one of the primary phospholipids through which ACs are phagocytosed by macrophages [20]. Inhibition of PS on ACs, therefore, inhibits phagocytosis significantly [22,23] and enrichment of cell membranes with exogenous PS results in the phagocytic clearance of Jurkat cells [24]. We also observed a significant reduction in phagocytosis of ACs after incubating macrophages with a PS receptor antibody. On the basis of these findings, an explanation for the dose-dependent reduction in phagocytosis by PMVs observed, could be that PS

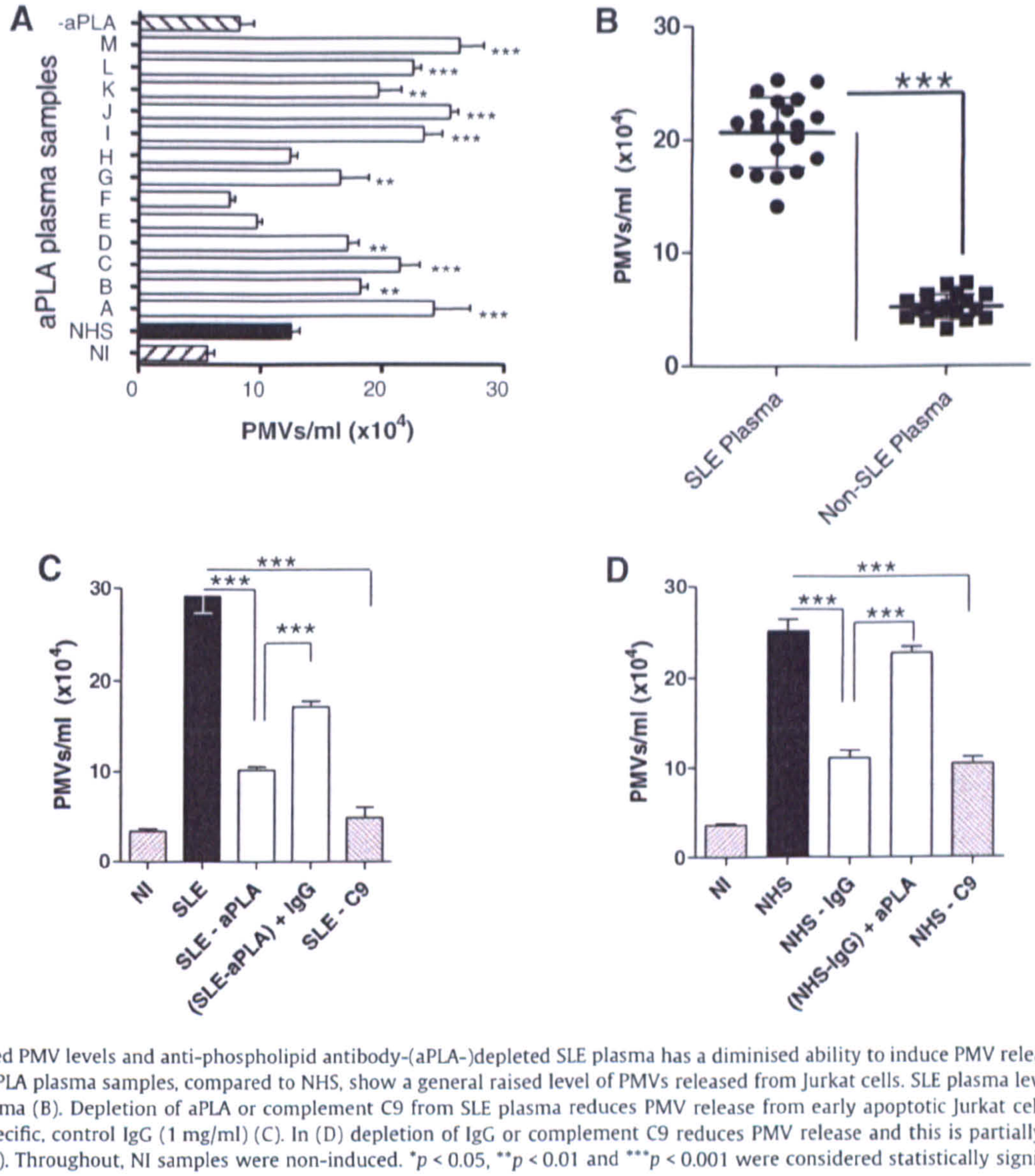

Fig. 3. SLE plasma has raised PMV levels and anti-phospholipid antibody-(aPLA-)depleted SLE plasma has a diminised ability to induce PMV release from apoptotic cells. (A) PMV levels in a cohort of aPLA plasma samples, compared to NHS, show a general raised level of PMVs released from Jurkat cells. SLE plasma levels of PMVs are also higher than those of non-SLE plasma (B). Depletion of aPLA or complement C9 from SLE plasma reduces PMV release from early apoptotic Jurkat cells and this is only partially restored by adding non-specific, control IgG (1 mg/ml) (C). In (D) depletion of IgG or complement C9 reduces PMV release and this is partially restored upon addition of purified aPLA (1 mg/ml) (D). Throughout, NI samples were non-induced. $^{*}p < 0.05$, $^{**}p < 0.01$ and $^{***}p < 0.001$ were considered statistically significant.

on PMVs in binding to PS receptors (PSRs) on macrophages, directly competes with PS on ACs. This was confirmed by blocking the PS on PMVs with annexin V which abrogated PMVs' inhibition of AC phagocytosis.

Our findings do have certain clinical implications. It has been well established that increased apoptosis occurs in a variety of clinical settings such as during chemotherapy, and radiation therapy [25,26] as well as certain autoimmune diseases such as rheumatoid arthritis, and SLE mainly due to a defect in apoptosis [18]. In addition to this, ACs have been shown to themselves produce PMVs which in turn can induce further PMV production [27]. In these cases, the already high level of ACs would rise still further as more AC-derived PMVs would reduce the phagocytosis of ACs leading to their secondary necrosis, thereby intensifying inflammation, cell injury and worsening the disease prognosis.

In summary this study has shown firstly that high concentrations of PMVs significantly reduce the phagocytosis of ACs by competing with the normal PSR-PS mediated phagocytosis of ACs. Secondly raised plasma PMV levels are symptomatic of SLE and may well play a role in disease progression. Whilst autoantibodies such as aPLA may help stimulate PMV release through sublytic complement, this will need further investigation. Where other particular cell types, undergoing apoptosis and needing appropriate and efficient removal to avoid inflammatory damage occur, our findings on the role of PMVs in the PS-dependent removal of ACs become pertinent. For example, in neural circuit development, axon pruning is essential because apoptotic neurons need to be efficiently removed by glial phagocytes [28]. Together our findings add to the novel roles being described for PMVs in normal cell physiology and disease.

Acknowledgments

We thank Maria McCrossan, of the London School of Hygiene and Tropical Medicine for assistance with electron microscopy. This work was supported by: NHS and Sir Richard Stapley Educational Trust part-funding of S. Antwi-Baffour; a Graduate Assistantship to E. A. Ansa-Addo and a VC scholarship to S. Kholia (from the Faculty of Life Sciences (FoLS) at London Metropolitan University); funding from the Cellular and Molecular Immunology Research Centre.

References

[1] J. Savill, V. Fadok, P. Henson, C. Haslett C, Phagocyte recognition of cells undergoing apoptosis, Immunol. Today 14 (1993) 131–136.
[2] S. Nagata, R. Hanayama, K. Kawane, Autoimmunity and the clearance of dead cells, Cell 140 (2010) 619–630.
[3] B. Hugel, M.C. Martinez, C. Kunzelmann, J.M. Freyssinet, Membrane microparticles: two sides of the coin, Physiology 20 (2005) 22–27.
[4] C.F. Reich 3rd, D.S. Pisetsky, The content of DNA and RNA in microparticles released by Jurkat and HL-60 cells undergoing in vitro apoptosis, Exp. Cell. Res. 315 (2009) 760–768.
[5] B. Toth, C.A. Lok, A. Boing, M. Diamant, J.A. van der Post, K. Friese, R. Nieuwland, Microparticles and exosomes: impact on normal and complicated pregnancy, Am. J. Reprod. Immunol. 58 (2007) 389–402.

[6] R.J. Berckmans, R. Nieuwland, M.C. Kraan, M.C. Schaap, C. Pots, T.J. Smeets, A. Sturk, P.P. Tak, Synovial microparticles from arthritic patients modulate chemokine and cytokine release by synoviocytes, Arthritis Res. Ther. 7 (2005) R536–R544.
[7] H.K. Kim, K.S. Song, J.H. Chung, K.R. Lee, S.N. Lee, Platelet microparticles induce angiogenesis in vitro, Br. J. Haematol. 124 (2004) 376–384.
[8] C.M. Boulanger, A. Scoazec, T. Ebrahimian, P. Henry, E. Mathieu, A. Tedgui, Z. Mallat, Circulating microparticles from patients with myocardial infarction cause endothelial dysfunction, Circulation 104 (2001) 2649–2652.
[9] S. Nomura, Y. Ozaki, Y. Ikeda, Function and role of microparticles in various clinical settings, Thromb. Res. 123 (2008) 8–23.
[10] G. Chironi, A. Simon, B. Hugel, P.M. Del, J. Gariepy, J.M. Freyssinet, A. Tedgui, Circulating leukocyte-derived microparticles predict subclinical atherosclerosis burden in asymptomatic subjects, Arterioscler. Thromb. Vasc. Biol. 26 (2006) 2775–2780.
[11] Z. Mallat, B. Hugel, J. Ohan, G. Leseche, J.M. Freyssinet, A. Tedgui A, Shed membrane microparticles with procoagulant potential in human atherosclerotic plaques: a role for apoptosis in plaque thrombogenicity, Circulation 99 (1999) 348–353.
[12] D.M. Schrijvers, G.R. De Meyer, M.M. Kockx, A.G. Herman, W. Martinet, Phagocytosis of apoptotic cells by macrophages is impaired in atherosclerosis, Arterioscler. Thromb. Vasc. Biol. 25 (2005) 1256–1261.
[13] C. Beyer, D.S. Pisetsky, The role of micoparticles in the pathogenesis of rheumatic diseases, Nat. Rev. Rheumatol. 6 (2010) 21–29.
[14] W. Jy, M. Tiede, C.J. Bidot, L.L. Horstman, J.J. Jimenez, J. Chirinos, Y.S. Ahn, Platelet activation rather than endothelial injury identifies risk of thrombosis in subjects positive for antiphospholipid antibodies, Thromb. Res. 121 (2007) 319–325.
[15] J.M. Inal, K.-M. Hui, S. Miot, S. Lange, M.I. Ramirez, B. Schneider, G. Krueger, J.A. Schifferli, Complement C2 receptor inhibitor trispanning: a novel human complement inhibitory receptor, J. Immunol. 174 (2005) 356–366.
[16] B.P. Morgan, A.K. Campbell, The recovery of human polymorphonuclear leucocytes from sublytic complement attack is mediated by changes in intracellular free calcium, Biochem. J. 231 (1985) 205–208.
[17] S.M. Bianchi, L.R. Prince, K. McPhillips, L. Allen, H.M. Marriott, G.W. Taylor, P.G. Hellewell, I. Sabroe, D.H. Dockrell, P.W. Henson, M.K. Whyte, Impairment of apoptotic cell engulfment by pyocyanin, a toxic metabolite of *Pseudomonas aeruginosa*, Am. J. Respir. Crit. Care Med. 177 (2008) 35–43.
[18] M. Herrmann, R.E. Voll, O.M. Zoller, M. Hagenhofer, B.B. Ponner, J.R. Kalden, Impaired phagocytosis of apoptotic cell material by monocyte-derived macrophages from patients with systemic lupus erythematosus, Arthritis Rheum. 41 (1998) 1241–1250.
[19] I. Baumann, W. Kolowos, R.E. Voll, B. Manger, U. Gaipl, W.L. Neuhuber, T. Kirchner, J.R. Kalden, M. Herrmann, Impaired uptake of apoptotic cells into tingible body macrophages in germinal centers of patients with systemic lupus erythematosus, Arthritis Rheum. 46 (2002) 191–201.
[20] E. Cocucci, G. Racchetti, J. Meldolesi, Shedding microvesicles: artefacts no more, Trends Cell Biol. (2010) 43–51.
[21] A. Piccin, W.G. Murphy, O.P. Smith, Circulating microparticles: pathophysiology and clinical implications, Blood Rev. 21 (2007) 157–171.
[22] M. Tanaka, Apoptotic cell clearance by phagocytes, Int. Congr. Ser. 1285 (2005) 55–59.
[23] G. Liu, J. Wang, Y.J. Park, Y. Tsuruta, E.F. Lorne, X. Zhao, E. Abraham, High mobility group protein-1 inhibits phagocytosis of apoptotic neutrophils through binding to phosphatidylserine, J. Immunol. 181 (2008) 4240–4246.
[24] V.E. Kagan, B. Gleiss, Y.Y. Tyurina, V.A. Tyurin, C. Elenstrom-Magnusson, S.X. Liu, F.B. Serinkan, A. Arroyo, J. Chandra, S. Orrenius, B. Fadeel, A role for oxidative stress in apoptosis: oxidation and externalization of phosphatidylserine is required for macrophage clearance of cells undergoing Fas-mediated apoptosis, J. Immunol. 169 (2002) 487–499.
[25] S. Jeha, Tumor lysis syndrome, Semin. Hematol. 38 (2001) 4–8.
[26] A. Altman, Acute tumor lysis syndrome, Semin. Oncol. 28 (2001) 3–8.
[27] J.H. Distler, L.C. Huber, A.J. Hueber, C.F. Reich III, S. Gay, O. Distler, D.S. Pisetsky, The release of microparticles by apoptotic cells and their effects on macrophages, Apoptosis 10 (2005) 731–741.
[28] T. Awasaki, R. Tatsumi, K. Takahashi, K. Arai, Y. Nakanishi, R. Ueda, K. Ito, Essential role of the apoptotic cell engulfment genes draper and ced-6 in programmed axon pruning during Drosophila metamorphosis, Neuron 50 (2006) 855–867.

Biochemical and Biophysical Research Communications 395 (2010) 382–386

Contents lists available at ScienceDirect

Biochemical and Biophysical Research Communications

Journal homepage: www.elsevier.com/locate/ybbrc

Involvement of lectin pathway activation in the complement killing of *Giardia intestinalis*

Ingrid Evans-Osses [a,b], Ephraim A. Ansa-Addo [c], Jameel M. Inal [c], Marcel I. Ramirez [a,*]

[a] *Laboratório de Biologia Molecular de Parasitas e Vetores-Instituto Oswaldo Cruz-Fiocruz, Rio de Janeiro 21040-900, Brazil*
[b] *Laboratório Interdisciplinar de Pesquisas Médicas–LIP Med-Instituto Oswaldo Cruz-Fiocruz, Av. Brasil 43475, Rio de Janeiro 21040-900, Brazil*
[c] *Cellular and Molecular Immunology Research Centre, Faculty of Life Sciences, London Metropolitan University, London N7 8DB, UK*

ARTICLE INFO

Article history:
Received 25 March 2010
Available online 9 April 2010

Keywords:
Giardia intestinalis
Lectin pathway
Trophozoites
Complement-mediated killing
Intestinal disease
Mannose
GlcNAc

ABSTRACT

Giardia intestinalis (syn. *G. lamblia, G. duodenalis*) is a flagellated unicellular eukaryotic microorganism that commonly causes diarrheal disease throughout the world. In humans, the clinical effects of *Giardia* infection range from the asymptomatic carrier state to a severe malabsorption syndrome possibly due to different virulence of the *Giardia* strain, the number of cysts ingested, the age of the host, and the state of the host immune system at the time of infection.

The question about how *G. intestinalis* is controlled by the organism remains unanswered. Here, we investigated the role of the complement system and in particular, the lectin pathway during *Giardia* infections. We present the first evidence that *G. intestinalis* activate the complement lectin pathway and in doing so participate in eradication of the parasite. We detected rapid binding of mannan-binding lectin, H-ficolin and L-ficolin to the surface of *G. intestinalis* trophozoites and normal human serum depleted of these molecules failed to kill the parasites. Our finding provides insight into the role of lectin pathway in the control of *G. intestinalis* and about the nature of surface components of parasite.

1. Introduction

Giardia intestinalis (syn. *G. lamblia, G. duodenalis*) is a flagellated unicellular eukaryotic microorganism that commonly causes diarrheal disease worldwide. The protozoan inhabits in the upper part of the small intestine and has a direct life cycle. When the cysts are ingested to the host, trophozoites are release from the cysts into the duodenum and these attach to the mucosa of the small intestine. Some trophozoites remain encyst and are eliminated from the host into feces. If the immune system of the host is fully developed and healthy, the acute phase usually resolves spontaneously and the symptoms will disappear. In humans, the clinical effects of *Giardia* infection range from the asymptomatic carrier state to a severe malabsorption syndrome. These variations are possibly due to different conditions: the virulence of the *Giardia* strain [1,2], the number of cysts ingested, the age of the host, and the state of the host immune system at the time of infection. All these play important roles in susceptibility to infection or in the duration and severity of the disease.

1.1. How *G. intestinalis* is controlled by the organism?

In the host organism, natural barriers in the intestine (duodenum and jejunum), mucus layer, proteases, lipases and bile present in the upper part of the small intestine, are factors that contribute in controlling *Giardia* infections. In humans, the defense mechanism against *G. intestinalis* infections is probably activated locally, because there is little or no mucosal inflammation present in the intestine. Although access by most pathogens to the intestinal mucosa in humans requires an invasive procedure, our knowledge about the mucosa pathology in *Giardia* infection, is limited.

During the course at the infection the immunological and non-immunological factors play a role at different stages. Since *G. intestinalis* reside in the lumen of the intestine, it's unlikely that the above mechanisms play a role in controlling parasite numbers within the intestine. However, lysis of trophozoites by specific antibodies in the presence of complement may play an important role in limiting parasite invasion of tissues by trophozoites [3]. We asked whether the complement system participates during host eradication of the parasite.

The complement system is the first line of vertebrate host defense against pathogenic infections and the principal components include, serine protease enzymes, which active each other in a cascade-like manner culminating in the formation of a membrane attack complex and pathogen lysis [4]. The complement system can

* Corresponding author. Fax: +55 (21) 2590 3495.
E-mail addresses: marcelr@ioc.fiocruz.br, marcelramirez4@hotmail.com (M.I. Ramirez).

0006-291X/$ - see front matter © 2010 Elsevier Inc. All rights reserved.
doi:10.1016/j.bbrc.2010.04.025

be activated by three distinct pathways including, the classical, lectin, and alternative pathways. In 1984, Hill et al. [5] showed that the lethal effect of human serum against for *G. intestinalis* was dependent on the presence of an intact classical pathway of complement. Studies performed *in vitro* with normal human serum (NHS) containing anti-*G. intestinalis* trophozoite antibodies killed more than 98% of the parasites. When the NHS was chelated with EDTA or heat-inactivated at 56 °C for 30 min, the killing effect of the NHS was eliminated. These results were confirmed in another study using NHS from infected humans, containing anti-*G. intestinalis* trophozoite IgM antibodies. The authors showed complement-mediated lyses of trophozoites [6].

However, these early investigations did not consider the lectin pathway (LP), a recently described complement pathway, which is activated when mannan-binding lectin (MBL), L-ficolin, or H-ficolin bind to target molecules, often glycans on the pathogen surface. The protease associated with them, MBL-associated serine protease 2 (MASP2), autoactivates or cleaves C2 and C4 and subsequently, generates C3 convertase as in the classical pathway (CP) [7]. Here, we describe activation of the LP by *G. intestinalis* trophozoites and give insights into the poor constitutive repertoire of glycoprotein on the surface membrane of this parasite.

2. Material and methods

2.1. Parasites and reagents

Giardia intestinalis strains WB (genome project strain) were grown axenically in TYI-S-33 medium supplemented with bile salts. Trophozoites were kept in a 37 °C incubator and sub-cultured every 72 h when adherent parasites reach complete populations.

The depletion of MBL, L-ficolin and C1q from human serum was adapted from previously described methods [21] and prepared in our lab [22].

2.2. Complement-mediated lysis assay

Giardia intestinalis (trophozoites, $5.0 \times 10^{5)}$ from the exponential phase were resuspended in 100 μl of fresh RPMI without fetal bovine serum (FBS) and mixed with 100 μl normal human serum (NHS) diluted in serum-free RPMI at 37 °C in microfuge tubes. Reaction was performed in triplicate and incubation between 30 s and 30 min, after which 800 μl of cold serum-free RPMI was added and tubes were placed on ice to stop the reaction. Surviving parasites were stained with vital colorant (Trypan blue) and quantified with a haemocytometer (Neubauer, Germany) under a light microscope. Assays were performed under varying conditions using different concentrations of NHS. Also various incubations were performed in the presence or absence of CP and LP inhibitors.

(I) *Serum Lethal Concentration-50 (SLC-50):* 5.0×10^5 logarithmic trophozoites forms of WB *G. intestinalis* strain were resuspended in 100 μl of fresh RPMI without FBS and mixed with 100 μl of NHS at concentrations of 6.25%, 12.5%, 25%, 50% and incubated for 30 min at 37 °C. Heated-inactivated NHS (56 °C for 30 min) was used as a negative control.

(II) *Kinetics of C-mediated killing:* 5.0×10^5 logarithmic trophozoites forms of WB *G. intestinalis* were resuspended in 100 μl of fresh serum-free RPMI, mixed with 100 μl of 25% NHS and incubated for 5, 15 and 30 min. Experiments in which required inhibition of CP and LP activation, were performed by incubating the NHS with 10 mM EGTA and 7 mM $MgCl_2$. Heated-inactivated NHS (56 °C for 30 min) was used as a negative control.

In some experiments NHS depleted of MBL and ficolins was used to inhibit serum activation of the LP.

(III) *Sugar inhibition assays:* Parasites (5.0×10^5 in 100 μl of veronal buffer, VB) were incubated at 37 °C for 15 min in 100 μl of 12.5% NHS (diluted in VB) previously pre-incubated at 4 °C with different concentrations of glucosamine, L-fucose, *N*-acetyl-glucosamine, *N*-acetyl-galactosamine, D(+)-mannose, D(+)-galactose and mannitol. Reactions were stopped as described above and surviving parasites were stained with vital colorant (Trypan blue) and quantified using a haemocytometer under a light microscope.

2.3. Flow cytometry analysis

Giardia intestinalis WB strain (1.0×10^6 in 900 μl of VB) were incubated with 100 μl of NHS to give 10% final concentration for 5 min at room temperature (unless otherwise stated). Parasites were washed by centrifugation (2000 rpm, 5 min) with PBS and incubated with anti-MBL (1:500), anti-L-ficolin (1:500), anti-H-ficolin (1:500) and anti-C3 (1:1000) antibodies diluted in PBS 1% BSA at 4 °C for 1 h with shaking. Parasites were washed again and incubated with anti-rabbit IgG-FITC (1:500) antibodies for 1 h at 4 °C with shaking. After washing with PBS, parasites were analyzed on a Guava EasyCyte flow cytometer using ExpressPlus software (Guava Technologies). Anti-IgG-FITC antibodies were used as an isotype control.

2.4. Data presentation and statistical analysis

All data are shown as mean ± SD. Comparisons among groups were made by the unpaired *t*-test for repeated measures using GraphPad Prism version 4.00 for Windows (GraphPad Software, San Diego, California, USA). Values of $p < 0.05$ with confidence interval of 99% were considered statistically significant unless otherwise specified.

3. Results

3.1. Complement activation by trophozoites of G. intestinalis in NHS

To determine whether complement pathways are activated by *G. intestinalis*, lysis assays were carried out *in vitro* by briefly incubating parasites with NHS. Kinetic assays were performed with different dilutions of NHS after incubation at 37 °C for 30 min. At physiological serum concentration (50%) parasite killing was close to 95% in 30 min. However, when NHS was diluted to 25%, 12.5% and 6.25%, the percentage of killing was reduced 62%, 55% and 38% respectively. These results suggest that the efficiency of NHS in killing trophozoites is dependent on components present in the serum.

3.2. Ficolins and MBL bind to the surface of G. intestinalis trophozoites

In order to investigate the role of LP in triggering the complement killing of *G. intestinalis*, trophozoites were incubated with NHS and then subjected to flow cytometry analysis with antibodies against MBL, L-ficolin, H-ficolin and C3. MBL (30%) (Fig. 2A), L-ficolin (61%) (Fig. 2B) and H-ficolin (41%) (Fig. 2C) were detected on the surface of the parasite. Also C3 a molecule that bind trophozoites had 55% of binding (Fig. 2D). Parasites treated with tunicamycin, an inhibitor of N-glycosylation, failed to inhibit deposition of the complement factors to the membrane surface (not showed). These results suggest that LP participates in the binding and activation of the complement system by *G. intestinalis* and also confirms a poor N-glycosylated plasma membrane surface.

3.3. Inhibition of complement killing with sugars showed that glucosamine, N-acetyl-glucosamine (GlcNAC) and mannose predominate during complement activation

NHS was incubated with different concentrations of various sugars for 10 min and killing assays were performed with

trophozoite forms of *G. intestinalis*. Results obtained indicate a dose dependent killing of parasites in the presence of mannose, glucosamine and GlcNAC, reaching inhibitions higher than 40% when the NHS was incubated with 40–80 mM of each sugars.

3.4. MBL and ficolins are required for the complement-mediated killing of G. intestinalis

Killing assays were performed using 50% NHS depleted of MBL, L-ficolin and H-ficolin (this measures activation CP + AP). Also 50% NHS treated with EGTA/Mg^{2+} (measuring AP), 50% NHS (measuring CP + AP + LP) were used.

As shown in Fig. 4, 5 min incubation with 50% NHS (CP + AP + LP) killed more than 60% of parasites, in contrast to AP (50% EGTA/Mg^{2+}), which killed 15% of the population in 5 min and reached only 30% after 30 min. NHS depleted of MBL, L-ficolin and H-ficolin was poorly efficient, killing only 30% of parasites after 5 min incubation and reaching a plateau of 45% within 30 min. This result indicates that LP contributes markedly to the killing of *G. intestinalis* during the first 5 min of parasite contact with NHS.

4. Discussion

4.1. MBL, H-ficolin and L-ficolin bind trophozoites and activate lectin pathway

The role of carbohydrates in the host–parasite interaction of *G. intestinalis* has been associated with the mechanism of adhesion to the intestinal mucosa. After cyst ingestion and passage through the stomach, trophozoites colonize the small intestine. There is very little knowledge about cell surface components or secretory products of *G. intestinalis* that could participate in differential mechanisms or in mucosal alterations during giardiasis.

Two articles recently reported shows how the surface membrane of *G. intestinalis* trophozoites is characterized. Samuelson et al. [8] showed through genome databases analysis by bioinformatics that *G. intestinalis* make a very short N-glycan and that it is also missing the N-glycan dependent QC system for protein folding. *Giardia* has only two GlcNAC which are added to Asn-linked glycans rather than the dolichol-linked precursor with 14 sugars present in higher eukaryotes. However, the report by Morelle et al. [9] gives a different interpretation about the components of the surface membrane. They showed with structural strategies based on MALDI-TOF and electrospray mass spectrometry, the N-glycan content of excreted/secreted molecules. The major oligosaccharides are complex-type structures and correspond to bi and triantennary structures without core fucosylation, including GlcNAC, mannose and sialic acid as main components.

Activation of LP has never been previously described in *G. intestinalis*. The pathway depends on the recognition of mannose or acetylated monosugars, especially GlcNAC, available on the surface of the membrane by MBL and ficolins presents in NHS. We show in the present study two pieces of evidence, which suggest that mannose and GlcNAC are present on the membrane surface of trophozoites, thus, enable LP activation.

First, we showed by flow cytometry analysis that components of NHS bind to the surface of trophozoites and anti-MBL, anti H-ficolin and anti L-ficolin are present in 30%, 41% and 61% of the parasite population (Fig. 2).

Secondly, lysis experiments performed using NHS pre-incubated with different concentrations of sugars, indicated a dose dependent inhibition in the killing of trophozoites. Higher inhibitions of complement-mediated killing were observed when NHS was incubated with mannose, GlcNAC or glucosamine prior to contact with *G. intestinalis* (Fig. 3).

Ficolins are oligomeric lectins, which comprises of collagen-like and a fibrinogen-like domains with a binding specificity for GlcNAC. It was reported that L-ficolin/p35 associate with MBL-associated serine proteases (MASP 1 and 2) and MBL-associated protein-19 (Map-19) in serum and forms complexes able to activate complement system. MBL is a soluble pattern-recognition receptor that binds to mannose and GlcNAC groups present on the surface of pathogens and initiates activation of the LP through cleavage of C4 and C2.

MBL and ficolins are able to recognize GlcNAC present on the surface of the parasite and so support the hypothesis about their poor membrane components. However, inhibition of parasite lyses with dose dependent concentrations of mannose suggest MBL and ficolin interactions are affected in the presence of high mannose. Thus, stimulating agglomeration of the molecules and decreasing normal recognition of GlcNAC. Another possibility is an incomplete annotation of the *Giardia* genome, hence, the parasite lack genes, which would otherwise enable the expression of mannose transferases and other useful enzymes.

4.2. Innate and acquired immune response participates as parasite clearance in Giardiasis

Our results have showed the participation of the innate immune response during clearance of *G. intestinalis*. Activation of complement pathways was efficient in killing parasites after a short contact with NHS (Fig. 1). Moreover, experiments with MBL and ficolins indicated that these serum components (Fig. 2) trigger activation of the LP and subsequently, mediate killing of trophozoites at the earliest contact with NHS (Figs. 3 and 4). In addition, the antimicrobial peptides defensin and lactoferrin possess antigiardial activity *in vitro* and could participate in the defensing against *Giardia* infections [10]. Paneth cells secrete defensins and murine *Giardia* is killed by mouse Paneth cells [11].

In human, Giardiasis has been described to occur via both humoral and cell mediated responses [12]. Immunity to *Giardia* has been shown to occur via two phases, the early B cell independent phase (which occurs within the first 2 weeks) followed by and antibody-dependent phase [10,13]. However, our knowledge of the immune response in *Giardia* infection is based on the mouse model of the disease carrying a rodent form source of *Giardia* (*G. muris*).

Some results also suggest a role for T cells during clearance of the parasites: (i) reconstitution of infected athymic mice with T

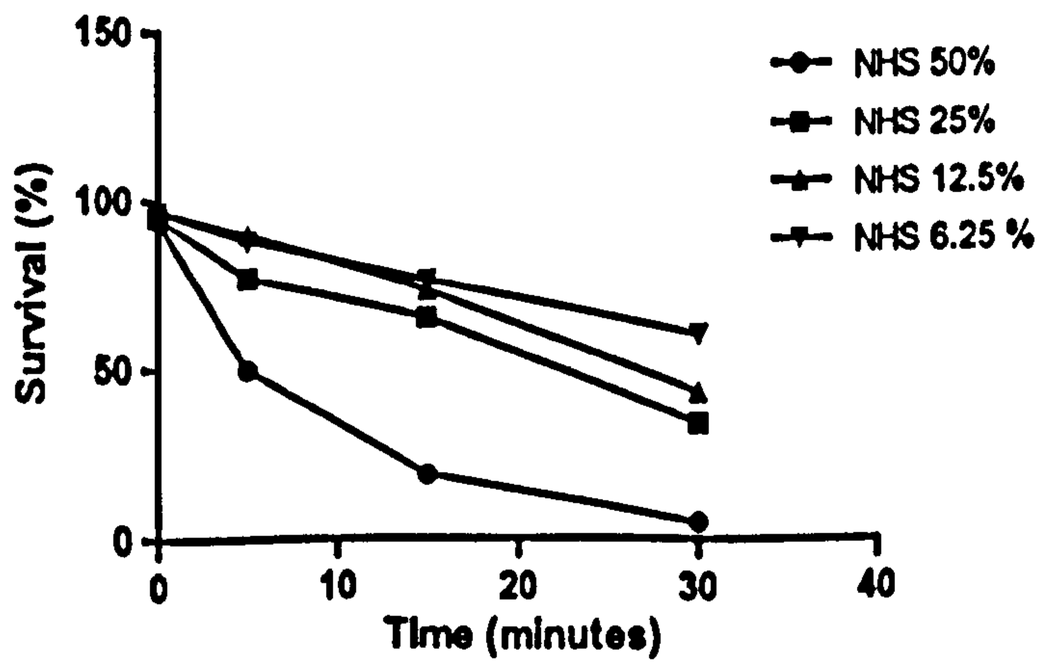

Fig. 1. C-mediated lysis assay in different concentrations of NHS. Trophozoites of *G. intestinalis* (5.0×10^5 from the logarithmic phase) were resuspended in 100 μl of fresh RPMI 1640 and mixed with 100 μl of diluted normal human serum (NHS) in RPMI 1640. Parasites were incubated in fold serial dilutions, ranging from undiluted to 6.25% NHS at 37 °C in microcentrifuge tubes for 30 min. Surviving parasites were stained with Trypan blue and counted using a haemocytometer under a light microscope.

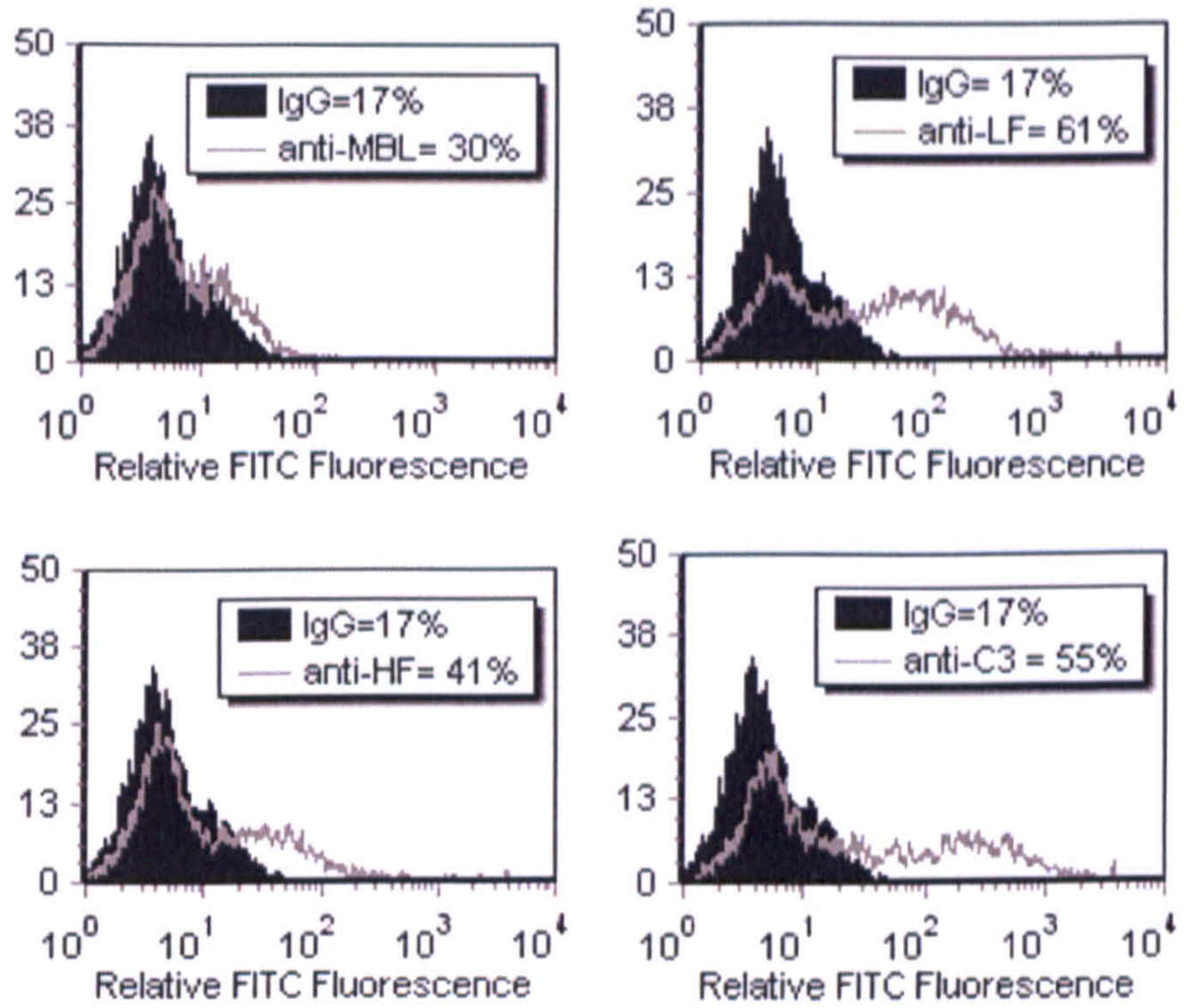

Fig. 2. Ficolins and MBL bind to the surface of *G. intestinalis* trophozoites forms. Flow cytometry analyze MBL, H-ficolin, L-ficolin and C3 binding to trophozoites to *G. intestinalis*. (A) 1.0×10^6 parasites were incubated with 1 ml of 10% NHS in VB at room temperature for 5 min and then incubated with anti-MBL antibodies. IgG-FITC antibodies were used for detection. Non-serum-treated parasites incubated with antibodies were used as negative controls. (B) As in (A), but with anti-L-ficolin antibodies. (C) As in (A), but with anti-H-ficolin antibodies. (D) As in (A) but with anti-C3 antibodies. Results presented are the averages of two independent experiments, each performed in duplicate.

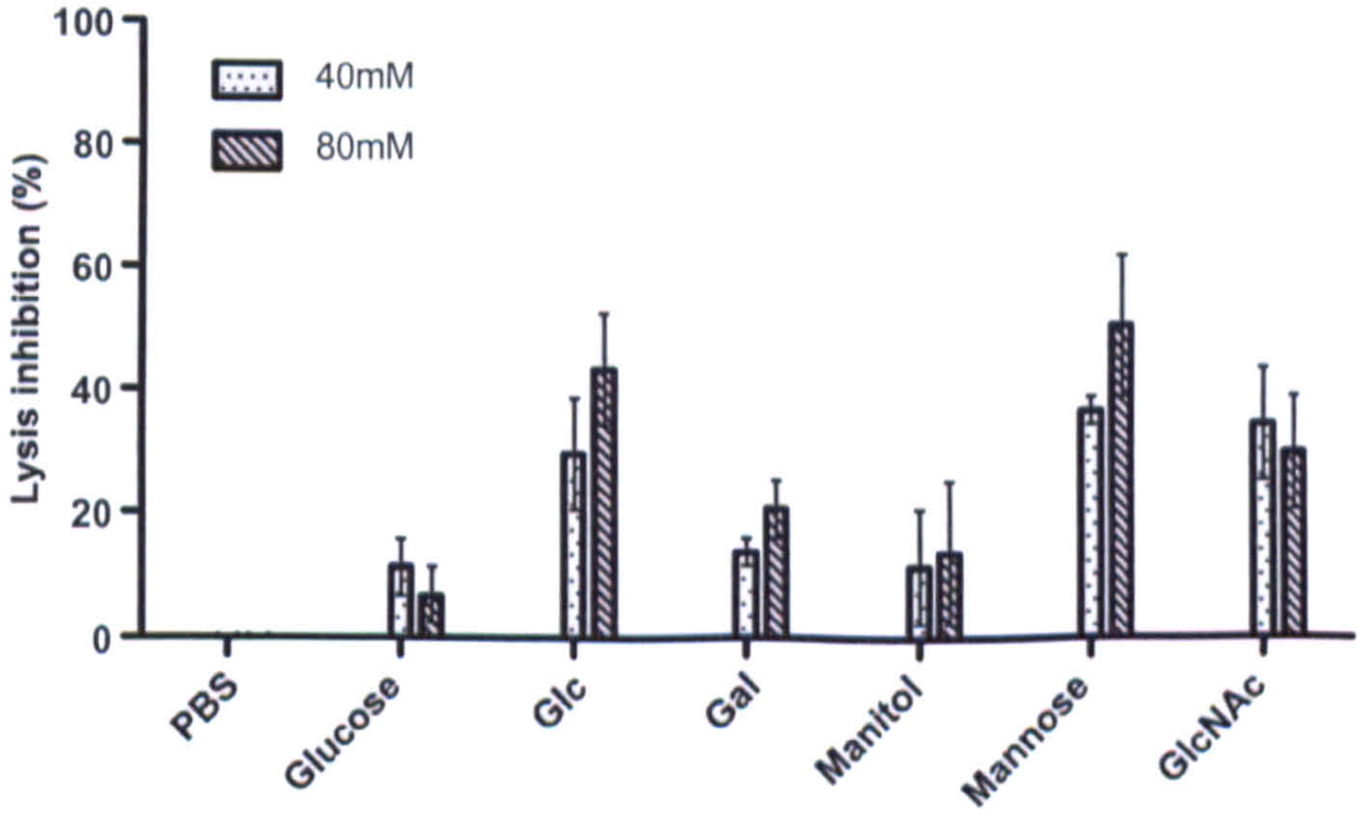

Fig. 3. Inhibition of complement-mediated killing with sugars. One hundred microliters of 25% NHS was pre-incubated in VB at 4 °C for 1 h with increasing concentrations of carbohydrates (as indicated in the figure). This serum was incubated with 100 μl of trophozoites forms of *G. intestinalis* (5.0×10^5 parasites) in VB at 37 °C for 15 min. Data are presented as percentage of lysis inhibition, with parasite survival in the absence of added sugars set as zero (control PBS). Increasing concentrations (40–80 mM) of carbohydrates, glucose, Gal (galactose), mannose, GlcNAc (*N*-acetyl-glucosamine), Glc (glucosamine) and mannitol. % Lysis inhibition was estimated comparing lysis of NHS/sugars with the lysis of NHS/PBS. Results presented are the averages of two experiments, each performed in duplicate. Bars represent the standard deviation of two individual experiments performed in triplicate.

cells resulted in decreased parasite load [14]. (ii) Moreover, specific depletion of CD4 T cells allows the development of chronic giardiasis in mice [15,16].

T cells have also been implicated in the pathogenesis of mucosal epithelial injury [17,18]. Previous studies using athymic nude mice have shown that activated T cells mediate villous atrophy and crypt cell hyperplasia in giardiasis. Moreover, reconstitution of T cells in athymic infected mice causes crypt-villous abnormalities [14,19]. Similarly, villous atrophy and crypt cell hyperplasia may be induced in T cells stimulated with either pokeweed mitogen or anti-CD3 antibody [20].

Together, these observations suggest the involvement of complement system, especially LP during the early clearance of *G. intestinalis*. Thus, reinforces the role of both innate and acquired immune responses in controlling the infection. The host defense against *Giardia* infections involves immunological and non-immunological mucosal processes, but many questions are still unanswered. Using informatics from *Giardia* genome project, together

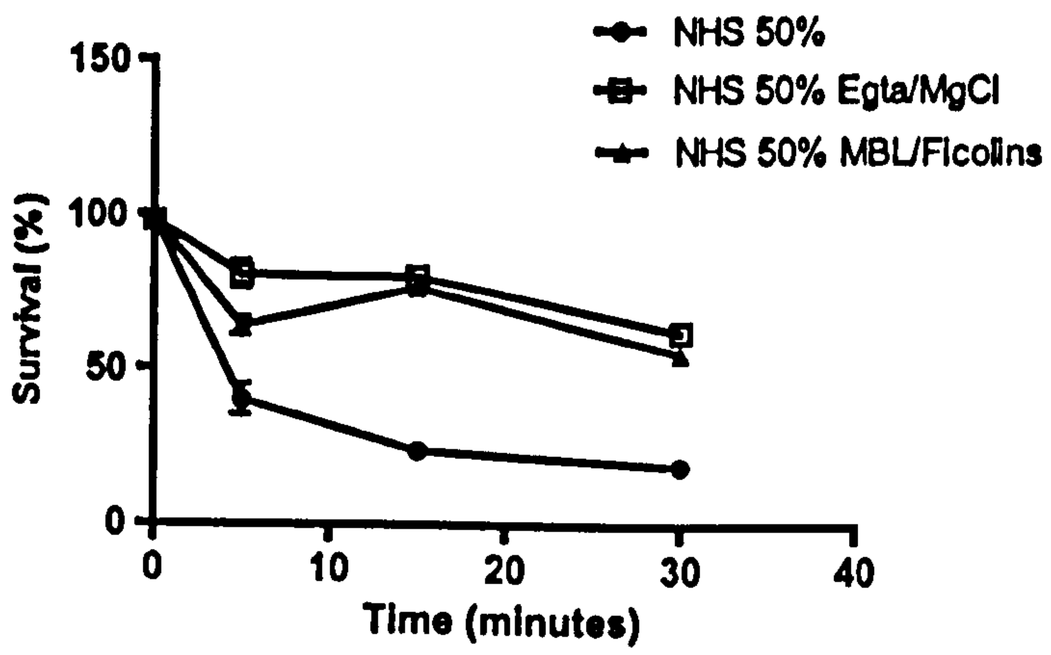

Fig. 4. Kinetics of complement activation. *G. intestinalis* WB strain were incubated with 50% NHS (CP + LP + AP) or with 50% NHS treated with 10 mM EGTA and 7 mM $MgCl_2$ (AP) or with 50% ΔMBL/ficolins NHS (C + A P) at 37 °C from between 0 and 30 min. Surviving parasites were stained with Trypan blue and quantified using a haemocytometer under a light microscope. Bars represent the standard deviation of three individual experiments performed in triplicate.

with relevant *in vivo* infection experiments could help elucidate specific host and parasite genes that affect the outcome of *Giardia* infection.

Acknowledgments

We are very grateful to Prof. R.B. Sim for antiserum against L-ficolins, H-ficolins, C1q and C3, Dr. Igor Cestari for providing NHS depleted of MBL/ficolins. I.E.-O. is a fellowship recipient from FAPERJ. M.I.R. received a traveling fellowship from Royal Society. This work was supported by CNPq (476737/2004-4, and funding from Cellular & Molecular Immunology Research Centre.

References

[1] A. Aggarwal, T.E. Nash, Comparison of two antigenically distinct *Giardia lamblia* isolates in gerbils, Am. J. Trop. Med. Hyg. 36 (1987) 325–332.
[2] T.E. Nash, D.A. Herrington, G.A. Losonsky, M.M. Levine, Experimental human infections with *Giardia lamblia*, J. Infect. Dis. 156 (1987) 974–984.
[3] S.C. Kraft, The intestinal immune response in giardiasis, Gastroenterology 76 (1979) 877–879.
[4] J.D. Lambris, D. Ricklin, B.V. Geisbrecht, Complement evasion by human pathogens, Nat. Rev. Microbiol. 6 (2008) 132–142.
[5] D.R. Hill, J.J. Burge, R.D. Pearson, Susceptibility of *Giardia lamblia* trophozoites to the lethal effect of human serum, J. Immunol. 132 (1984) 2046–2052.
[6] M. Deguchi, F.D. Gillin, I. Gigli, Mechanism of killing of *Giardia lamblia* trophozoites by complement, J. Clin. Invest. 79 (1987) 1296–1302.
[7] A. Roos, L.H. Bouwman, J. Munoz, T. Zuiverloon, M.C. Faber-Krol, F.C. Fallaux-van den Houten, N. Klar-Mohamad, C.E. Hack, M.G. Tilanus, M.R. Daha, Functional characterization of the lectin pathway of complement in human serum, Mol. Immunol. 39 (2003) 655–668.
[8] J. Samuelson, S. Banerjee, P. Magnelli, J. Cui, D.J. Kelleher, R. Gilmore, P.W. Robbins, The diversity of dolichol-linked precursors to Asn-linked glycans likely results from secondary loss of sets of glycosyltransferases, Proc. Natl. Acad. Sci. USA 102 (2005) 1548–1553.
[9] W. Morelle, J.C. Jimenez, C. Cleniewski-Bernard, E. Dei-Cas, J. Michalski, Characterization of the N-linked glycans of *Giardia intestinalis*, Glycobiology 15 (5) (2005) 549–559.
[10] L. Eckmann, Mucosal defences against Giardia, Parasite Immunol. 25 (2003) 259–270.
[11] K.A. El-Shewy, R.A. Eid, In vivo killing of Giardia trophozoites harbouring bacterial endosymbionts by intestinal Paneth cells: an ultrastructural study, Parasitology 130 (2005) 269–274.
[12] R.D. Adam, The biology of Giardia spp., Microbiol. Rev. 55 (1991) 706–732.
[13] E. Li, P. Zhou, Z. Petrin, S.M. Singer, Mast cell-dependent control of *Giardia lamblia* infections in mice, Infect. Immun. 72 (2004) 6642–6649.
[14] I.C. Roberts-Thomson, G.F. Mitchell, Giardiasis in mice: I. Prolonged infections in certain mouse strains and hypothymic (nude) mice, Gastroenterology 75 (1978) 42–46.
[15] B.M. Chung, L.E. Wallace, J.A. Hardin, D.G. Gall, The effect of epidermal growth factor on the distribution of SGLT-1 in rabbit jejunum, Can. J. Physiol. Pharmacol. 80 (2002) 872–878.
[16] S.M. Singer, T.E. Nash, T-cell-dependent control of acute *Giardia lamblia* infections in mice, Infect. Immun. 68 (2000) 170–175.
[17] M.J. Farthing, Diarrhoeal disease: current concepts and future challenges. Pathogenesis of giardiasis, Trans. R. Soc. Trop. Med. Hyg. 87 (Suppl. 3) (1993) 17–21.
[18] L.C.H. Yu, M.H. Perdue, Immunologically mediated transport of ions and macromolecules, Ann. N. Y. Acad. Sci. 915 (2001) 247–259.
[19] R.C. Ferreira, L.E. Forsyth, P.I. Richman, C. Wells, J. Spencer, T.T. MacDonald, Changes in the rate of crypt epithelial cell proliferation and mucosal morphology induced by a T-cell-mediated response in human small intestine, Gastroenterology 98 (1990) 1255–1263.
[20] T.T. McDonald, J. Spencer, Evidence that activated mucosal T cells play a role in the pathogenesis of enteropathy in human small intestine, J. Exp. Med. 167 (1988) 1341–1349.
[21] A. Krarup, S. Thiel, A. Hansen, T. Fujita, J.C. Jensenius, L-ficolin is a pattern recognition molecule specific for acetyl groups, J. Biol. Chem. 279 (2004) 47513–47519.
[22] S. Cestari Idos, A. Krarup, R.B. Sim, J.M. Inal, M.I. Ramirez, Role of early lectin pathway activation in the complement-mediated killing of *Trypanosoma cruzi*, Mol. Immunol. 47 (2009) 426–437.